Towards a mechanistic understanding of PBP-mediated beta-lactam resistance in *Streptococcus pneumoniae*

Catherine Emily Rowland
BSc. (Hons)

A thesis submitted in partial fulfilment
of the requirements for the degree of

Doctor of Philosophy in Life Sciences

University of Warwick, School of Life Sciences

August 2019

Table of Contents

List of Tables

List of Figures

Acknowledgements

I would like to thank the members of the Dowson, Roper and Lloyd groups, past and present, with whom it was an absolute pleasure to spend 3 years! In particular thank you to Julie Tod and Anita Catherwood, who taught me their craft and contributed some of the substrates and enzymes for this work.

I acknowledge the well-appreciated support of Ricky Cain and David Fox in the chemical synthesis part of this work.

Thank you to Micropathology Ltd. for funding this work and giving me the opportunity to work on this project.

Thank you to my supervisors, Chris Dowson and Adrian Lloyd, for your support and patience throughout the project. Thanks also to David Roper for your advice and humour in the lab.Thank you to Chris for having me in your group, and for the brilliant opportunities I've had thanks to your encouragement. Thank you to Adrian for the Friday-morning coffees, for dreaming about science with me, and everything else from when I arrived at Warwick 8 years ago.

To the most special of all the special friends, Anna – may we always inspire and encourage each other, and may there always be a hot chocolate on hand when things get tough. I'm so grateful to have shared this experience with you!

Thank you to my family who have supported (and tolerated!) me throughout this journey. Thank you for listening to my presentations, calming me down, and cheering me on.

Finally, thank you to my fiancé, my best friend, Coxy. Your endless patience and thoughtfulness have meant the world to me. I couldn't have made it this far without you. This thesis is dedicated to you.

Declaration

I hereby declare that I personally have carried out the work submitted in this thesis, under the supervision of Professor Christopher Dowson and Dr Adrian Lloyd at the School of Life Sciences, University of Warwick. Where work has been contributed to by other individuals, it is specifically stated in the text.

This thesis is submitted to the University of Warwick in support of my application for the degree of Doctor of Philosophy. It has been composed by myself and has not been submitted in any previous application for any degree. All sources of information are specifically acknowledged in the form of references.

Abstract

Cell wall biosynthesis is a crucial process for bacterial growth and a well-validated source of targets for existing antimicrobials. Among such targets are the penicillin-binding proteins (PBPs), which act within multiprotein complexes to assemble peptidoglycan from Lipid II, catalysing both glycosyltransferase (GT) and transpeptidase (TP) activities. This work focussed on the PBPs of *Streptococcus pneumoniae*, a key pathogen in terms of its healthcare burden and the prevalence of pneumococcal resistance to β-lactams.

The requirement for both PBP modification and branched muropeptides in the pneumococcal β-lactam resistance mechanism has been well documented. Progress in demonstrating the mechanistic link between these two factors has historically been limited by availability of the native substrates. We aimed to address the hypothesis that branching of precursors is beneficial for competition of PG substrates against β-lactams, and also to explore the impact of lipid environment on PBP1a activity, based upon previous observations with the MurM protein that generates branched Lipid II precursors.

We used chemoenzymatic methods to demonstrate the first synthesis of potential donor- and acceptor-only amidated substrates, in addition to branched precursors, for pneumococcal PBPs. These substrates will provide valuable tools for study of pneumococcal PBP function with natural substrates, which is key for addressing pneumococcal β-lactam resistance.

A novel spectrophotometric assay for transpeptidation was used to attempt observation of *in vitro* transpeptidase activity by PBP1a. Mass spectrometry revealed that D,D-carboxypeptidase activity alone occurred under the current reaction conditions. We discuss possible further work to establish *in vitro* transpeptidase activity.

Established assays for GT activity were used to identified a novel link between pneumococcal membrane phospholipids and the activity of PBP1a. This is the first observation of the impact of cardiolipin on the activity of a PBP, and corresponds with growing evidence in support of a role for cardiolipin in regulation of cell division proteins.

List of Abbreviations

All abbreviations are used in accordance with the Journal of Biological Chemistry abbreviations list. Any additional abbreviations have been detailed below.

Abbreviation	Meaning
ADP	Adenosine 5'-diphosphate
APS	Ammonium persulfate
ATP	Adenosine 5'-triphosphate
A_{xnm}	Absorbance at xnm
$C_{55}P$	Undecaprenyl phosphate
CDI	1,1'-carbonyldiimidazole
CENTA	7-β-thien-2-yl-acetamido-3-[(4-nitro-3-carboxyphenyl)thiomethyl]-3-cephem-4-carboxylic acid
CMC	Critical micelle concentration
CV	Column volumes
DDM	*N*-dodecyl β-D-maltoside
D-iGln	D-isoglutamine
DIPEA	*N,N*-Diisopropylethylamine
DMF	Dimethylformamide
DMSO	Dimethyl sulfoxide
EDC	1-ethyl-3-(3-dimethylaminopropyl) carbodiimide
FBLA	FRET-based Lipid II Analogue
Fmoc	9-fluorenylmethyloxycarbonyl
FRET	Förster resonance energy transfer
GDH	Glucose dehydrogenase
Glc*N*Ac	*N*-acetyl glucosamine
GT	glycosyltransferase
h	Hours
HATU	*N*-[(Dimethylamino)-1*H*-1,2,3-triazolo-[4,5-*b*]pyridin-1-ylmethylene]-*N*-methylmethanaminium hexafluorophosphate *N*-oxide
HEPES	4-(2-Hydroxyethyl)piperazine-1-ethanesulfonic acid
HOSu	*N*-hydroxysuccinimide
HPLC	High pressure liquid chromatography
IDH	Isocitrate dehydrogenase
IMAC	Immobilised metal ion affinity chromatography
IPTG	Isopropyl-β-D-thiogalactopyranoside
MBL	Metallo-β-lactamase
mins	Minutes
MOPS	3-(*N*-morpholino)propanesulfonic acid
Mur*N*Ac	*N*-acetylmuramic acid

MWCO	Molecular weight cut-off
$NADP^+$	Nicotinamide adenine dinucleotide phosphate
NADPH	Dihydronicotinamide adenine dinucleotide phosphate
OD_{600nm}	Absorbance at 600 nm
PBP	Penicillin binding protein
PBS	Phosphate buffered saline
PEP	Phospho-*enol* pyruvate
P_i	Inorganic phosphate
PK	Pyruvate kinase
SDS	Sodium dodecyl sulfate
SEDS proteins	Shape, elongation, division and sporulation (proteins)
SPPS	Solid phase peptide synthesis
TEMED	*N,N,N′,N′*-tetramethylethane-1,2-diamine
TLC	Thin-layer chromatography
TFA	Trifluoroacetic acid
TOF	Time of flight
UDP	Uridine 5’-diphosphate
UDP MurNAc 5P (iGln)	Uridine diphosphate *N*-acetyl-muramyl pentapeptide intermediate, with amidation of the second residues of the pentapeptide stem (i.e. D-glutamine in place of D-glutamate)
UMP	Uridine 5’-monophosphate
UTP	Uridine 5’-triphosphate

Chapter 1: Introduction

1.1 Antibiotic resistance

1.1.1 The history and current use of antibiotics

Antibiotics are the drugs used to kill or arrest the growth of bacteria. Antibiotics have been unknowingly used by humans for thousands of years prior to the development of industrial chemical processes for their manufacture, such as by the use of extracts from moulds in ancient civilisations (Mohr, 2016).

Whilst the early 1900s yielded several treatments for infection including salvarsan and neosalvarsan, the application of these was limited by their severe side effects and narrow spectrum of activity (Kardos & Demain, 2011). Multiple reports emerged in the 19th Century of antibiotic effects by moulds, including that of Ernest Duchesne, who described the treatment of *Escherichia coli* and *Salmonella typhi* infection of guinea pigs by use of a mould suspension (Duchesne, 1897; as reviewed by Mohr (2016)). Penicillin, one compound responsible for such observations, was famously discovered in 1928 by Alexander Fleming (Fleming, 1929; Chain *et al.*, 1940), and subsequent work by Chain, Florey and others resulted in the development of methods for the mass production of penicillin. Penicillin thus was a key contributor to the treatment of infections during and after World War II, made possible by the cheap cost, safety and wide spectrum of the drug (Kardos & Demain, 2011).

In addition to infectious disease management, antibiotics are crucial in the management of a number of other conditions, to prevent and treat complications caused by infections. These include cancer, surgical interventions including joint replacement and organ transplants, and conditions such as diabetes and renal failure (Centers for Disease Control and Prevention, 2013).

1.1.2 The threat of antibiotic resistance

1.1.2.1 Definition of resistance, statistics on worldwide burdens

The essentiality of antibiotics to modern healthcare highlights the severity of the threat posed by antibiotic resistance. Antibiotic resistance refers to the development of tolerance in bacteria to antibiotic drugs. Whilst some bacteria exhibit primary (or 'natural') resistance to particular antibiotics, the development of secondary (or 'acquired') resistance has frequently been observed for many clinically important pathogens.

Antimicrobial susceptibility is assessed by interpretation of minimal inhibitory concentration (MIC) according to breakpoint values. Breakpoints are devised from data including the distribution of susceptibilities, the pharmacological properties of the drug, and clinical outcomes (MacGowan & Wise, 2001; Turnidge & Paterson, 2007). Treatment failure under standard dosage would be expected for an isolate designated as 'resistant' to an antibiotic by evaluation of breakpoints (Turnidge & Paterson, 2007).

Antibiotic resistance, whilst a natural phenomenon, has developed at an accelerated rate, due in part to the misuse of antibiotics. Such misuse includes inappropriate and empirical prescribing, and poor regulation of access to antibiotics (Aminov, 2010). Antibiotic resistance limits the available treatment options, and resistant infections are associated with higher healthcare costs and higher mortality (World Health Organisation, 2018). It is currently estimated that without significant prevention efforts, deaths resulting from antibiotic resistant infections could reach 10 million a year worldwide by 2050 (O'Neill, 2014). This figure was drawn from commissioned reports modelling the rise in morbidity and mortality due to resistant infections by a subset of medically important pathogens, using different projected resistance rates (Taylor *et al.*, 2014; KPMG, 2014). The accuracy of these projections was limited by the available data on current incidences of infection and resistance rates in each case (de Kraker *et al.*, 2016).

1.1.2.2 Key pathogens in antibiotic resistance: WHO priority pathogens and ESKAPES

Among the various bacteria which have been observed to be decreasing in susceptibility to key antibiotics, the World Health Organisation (WHO) have designated a subset of priority pathogens for research and development of new antimicrobials (Tacconelli *et al.*, 2018). Among the criteria for inclusion were their treatability, the prevalence of resistance, and the current pipeline for new agents. The chosen priority pathogens were itemised (with the exception of *Mycobacterium tuberculosis*, as this was an existing global health priority) into categories of critical, high and medium priority for research and development of new antibiotics (Figure 1.1).

In addition, the ESKAPE pathogens panel notes the most common pathogens associated with nosocomial infections, which show worldwide prevalence of antibiotic resistance. The panel includes *Enterococcus faecium, Staphylococcus aureus, Klebsiella pneumoniae, Acinetobacter baumanii, Pseudomonas aeruginosa*, and *Enterobacter* species (Boucher *et al.*, 2009).

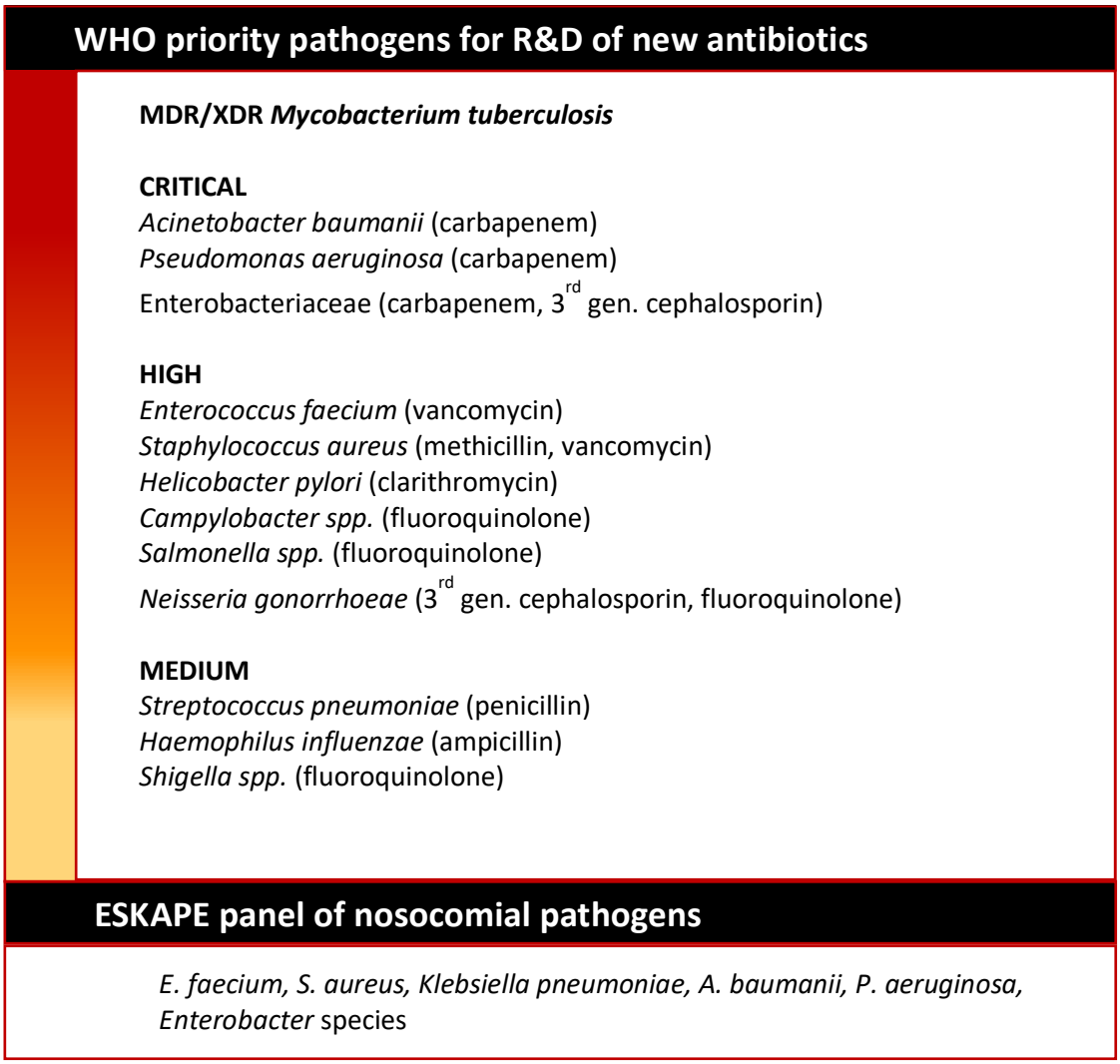

Figure 1.1 Organisms included in the WHO priority pathogens and ESKAPE panel. The WHO priority pathogens (listed with the most significant resistance phenotypes) were chosen based on criteria of treatability, pipeline for new antimicrobials, and the prevalence of resistance (Tacconelli *et al.*, 2018). The ESKAPE panel includes those pathogens most commonly associated with nosocomial infections and which show notable worldwide prevalence of antibiotic resistance (Boucher *et al.,* 2009).

1.1.2 *Streptococcus pneumoniae* as a key pathogen for new antimicrobial research and development

Penicillin non-susceptible *S. pneumoniae* is one important target for research and development of new antibiotics (World Health Organization, 2017). *S. pneumoniae* is a Gram-positive opportunistic pathogen. Pneumococci asymptomatically colonise the nasopharynx, with carriage rates in young children reported between 30 and 70 % (Regev-Yochay *et al.*, 2004). Such asymptomatic carriage is the precursor to development of invasive pneumococcal disease, and has enabled rapid dispersal of resistant strains.

Invasive pneumococcal disease is a major cause of mortality in the very young and elderly population. Invasive pneumococcal disease includes conditions such as pneumonia, meningitis and sepsis (Cartwright, 2002). *S. pneumoniae* is the second most common cause of meningitis after meningococci, and is the most common cause of bacterial pneumonia in children aged under two (Randle *et al.*, 2011). An estimated 294 000 deaths due to pneumococcal infection were reported in 2015, with an additional 8.9 million cases of pneumococcal pneumonia (Wahl *et al.*, 2018).

The greatest disease burden is observed in India, Nigeria, the Democratic Republic of Congo and Pakistan, with half of the reported deaths from these countries (Figure 1.2).

Penicillin non-susceptible pneumococcal isolates have been detected across the globe (Figure 1.3). The current European Committee on Antimicrobial Susceptibility Testing (EUCAST) clinical breakpoint is 0.06 $\mu g.mL^{-1}$ for penicillin-susceptible pneumococci (EUCAST, 2018). In isolates from meningitis cases, MICs > 0.06 $\mu g.mL^{-1}$ are designated resistant, whereas in non-meningitis cases, MICs in the range of 0.06 – 2 $\mu g.mL^{-1}$ are taken as intermediate susceptibility, with resistance if MIC > 2 $\mu g.mL^{-1}$; this difference in breakpoint according to clinical context is necessitated by the limited penetration of the blood-brain barrier by penicillin (Weinstein *et al.*, 2009).

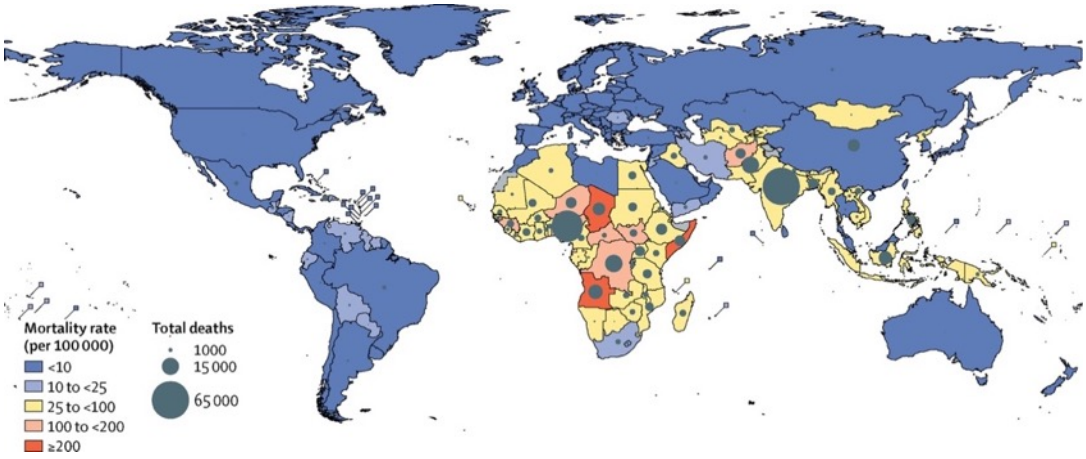

Figure 1.2 Mortality rates and deaths due to pneumococcal infection in 2015. Mortality and death rates in HIV-negative children aged 1-59 months are displayed per country, per 100 000 children in the age bracket. The greatest proportion of deaths were observed in India, Pakistan, Nigeria and the Democratic Republic of Congo.
Reproduced from Wahl *et al.* (2018). Copyright © 2018 The Author(s). Published by Elsevier Ltd.

Penicillin non-susceptible pneumococcal isolates were first detected in 1967, and subsequently emerged throughout Europe, Africa, Asia and North and South America by the late 1990s (Linares *et al.*, 2010). Analysis of pneumococcal isolates from respiratory tract infections in the course of the PROTEKT study revealed rates of penicillin non-susceptibility (with intermediate and resistant isolates respectively) at 42 % and 15.9 % in Greece; 40.4% and 15.9 % in France; and 29.4 % and 13.1 % in Spain (Felmingham *et al.*, 2007).

1.1.2.1 Vaccination against *S. pneumoniae*

More than 90 pneumococcal serotypes have been identified, based on the variation in capsular polysaccharides (Henrichsen, 1995). Prior to 2000, the pneumococcal serotypes associated with the greatest disease burden were 4, 6B, 9V, 14, 18C, 19F, and 23F, whilst those that demonstrated the highest rate of resistance to penicillin and erythromycin were 6B, 6A, 9V, 14, 15A, 19F, 19A and 23F (Linares *et al.*, 2010). The seven-valent pneumococcal conjugate

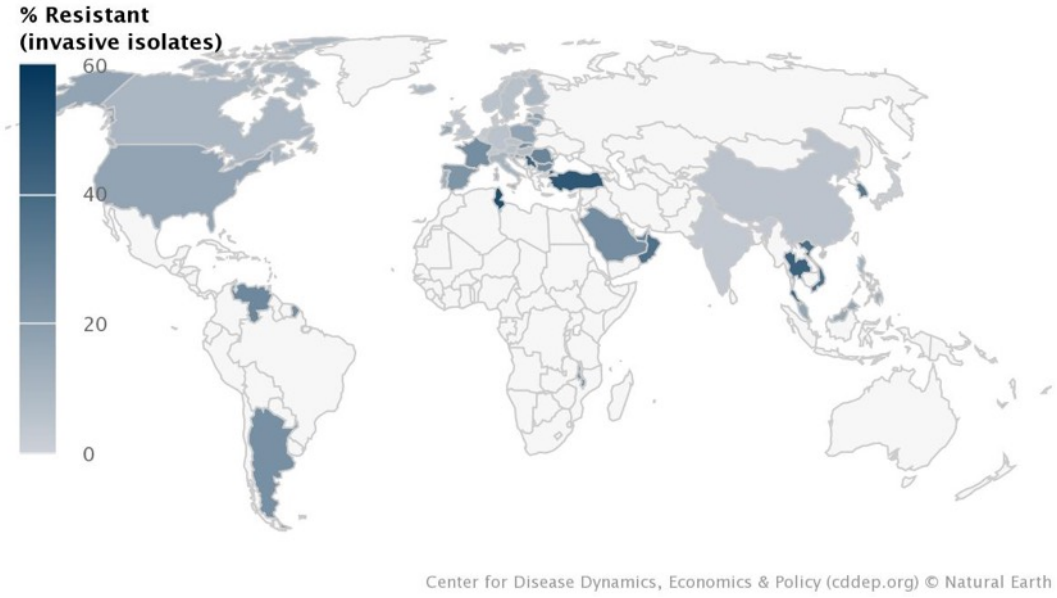

Figure 1.3 Percentage of invasive isolates of *S. pneumoniae* resistant to penicillin by country. Reported percentages refer to resistance in isolates from blood and cerebrospinal fluid from patients of all ages. Figure source: The Center for Disease Dynamics Economics & Policy. ResistanceMap: Antibiotic Resistance. 2018. https://resistancemap.cddep.org/AntibioticResistance.php. Date accessed: 28th April 2019.

vaccine against serotypes 4, 6B, 9V, 14, 18C, 19F, and 23F (PCV7) was introduced into the UK routine childhood immunisation programme in 2006 (Randle *et al.*, 2011). Whilst introduction of PCV7 was associated with a decline in pneumococcal penicillin resistance rates, serotype replacement has resulted in increasing burden of invasive pneumococcal disease (IPD) associated with non-vaccine serotypes, including multiresistant serotype 19A (Linares *et al.*, 2010). Subsequent PCVs have been marketed with coverage of 10 (PCV10: PCV7 plus serotypes 1, 5 and 7F) and 13 (PCV13: PCV10 plus serotypes 3, 6A and 19A) pneumococcal serotypes respectively, in order to

address those serotypes identified in strain replacement (Lee *et al.*, 2014). In addition, a 23-valent pneumococcal polysaccharide vaccine (PPSV23, covering serotypes 1, 2, 3, 4, 5, 6B, 7F, 8, 9N, 9V, 10A, 11A, 12F, 14, 15B, 17F, 18C, 19A, 19F, 20, 22F, 23F, and 33F) is available as a follow-up to PCV13 for particularly high-risk cases (American Academy of Pediatrics Committee on Infectious Diseases, 2010; Nuorti & Whitney, 2010).

1.1.2.2 Pneumococcal ecology

Pneumococci are aerotolerant anaerobes, although they lack the expected mechanisms for detoxifying reactive oxygen species (Pesakhov *et al.*, 2007). Pneumococci produce hydrogen peroxide as a by-product of aerobic metabolism of pyruvate (Bättig & Mühlemann, 2008). Release of hydrogen peroxide by pneumococci has been suggested to play a role in virulence, contributing to the toxicity of pneumolysin (Hirst *et al.*, 2000) and inducing DNA double-strand breaks (resulting in apoptosis) in lung cells in the context of pneumococcal pneumonia (Rai *et al.*, 2015). There has also been discussion of a role for hydrogen peroxide production by *S. pneumoniae* and viridans streptococci in inter-species competition for colonisation of the upper respiratory tract, based on inhibition of growth of *S. aureus* by pneumococcal culture supernatant (McLeod & Gordon, 1922; Regev-Yochay *et al.*, 2006). Whilst negative correlation has been reported between the upper airway colonisation rates of *S. pneumoniae* and *S. aureus* (Bogaert *et al.*, 2004; Regev-Yochay *et al.*, 2004), some studies have supported the role of hydrogen peroxide in inter-bacterial competition *in vivo* (Park *et al.*, 2008), whilst others have disputed this interaction (Margolis, 2009).

Competence-driven genetic transformation is a key component of the ecology of *S. pneumoniae*. Competence has been proposed to compensate for the lack of the ordinary SOS stress response (as seen in other bacteria), with competence stimulating peptide (CSP) mediating a stress signal to pneumococcal communities (Prudhomme *et al.*, 2006). Competence has been found to be induced by the stress of treatment of pneumococci by fluoroquinolones and mitomycin C (Prudhomme *et al.*, 2006). Horizontal gene

transfer is a key component of the pneumococcal β-lactam resistance mechanism, as further discussed in Section 1.6.3.

Pneumococcal virulence factors include the capsule, which inhibits interactions with complement and neutrophils (Hyams *et al.*, 2010); the pneumococcal exoglycosidases (such as neuraminidase and β-galactosidase) which expose host receptors and provide a carbon source; and the pore-forming toxin, pneumolysin, which has been suggested to be a key contributor to the pathology of pneumococcal pneumonia (Weiser, 2010).

1.2 Cell wall architecture and peptidoglycan

One of the major targets of antibiotics is peptidoglycan biosynthesis. This cross-linked polymer is found in bacterial cell walls and confers strength against the internal turgor of bacterial cells (Vollmer and Bertsche, 2008), in addition to providing a support for attachment of surface proteins.

1.2.1 Gram positive and Gram negative cell wall architecture

Bacteria are broadly classified according to the structure of the cell wall, with a few exceptions such as the *Mycobacteria*. Various important distinctions between the cell wall of Gram positive and Gram negative bacteria (as defined based on the Gram staining reaction (Gram, 1884)) affect the interaction of these bacteria with host cells and their environment, and the ease with which various antibiotics can gain access to the periplasm. Schematic structures of the Gram positive and Gram negative cell walls are shown in Figure 1.4.

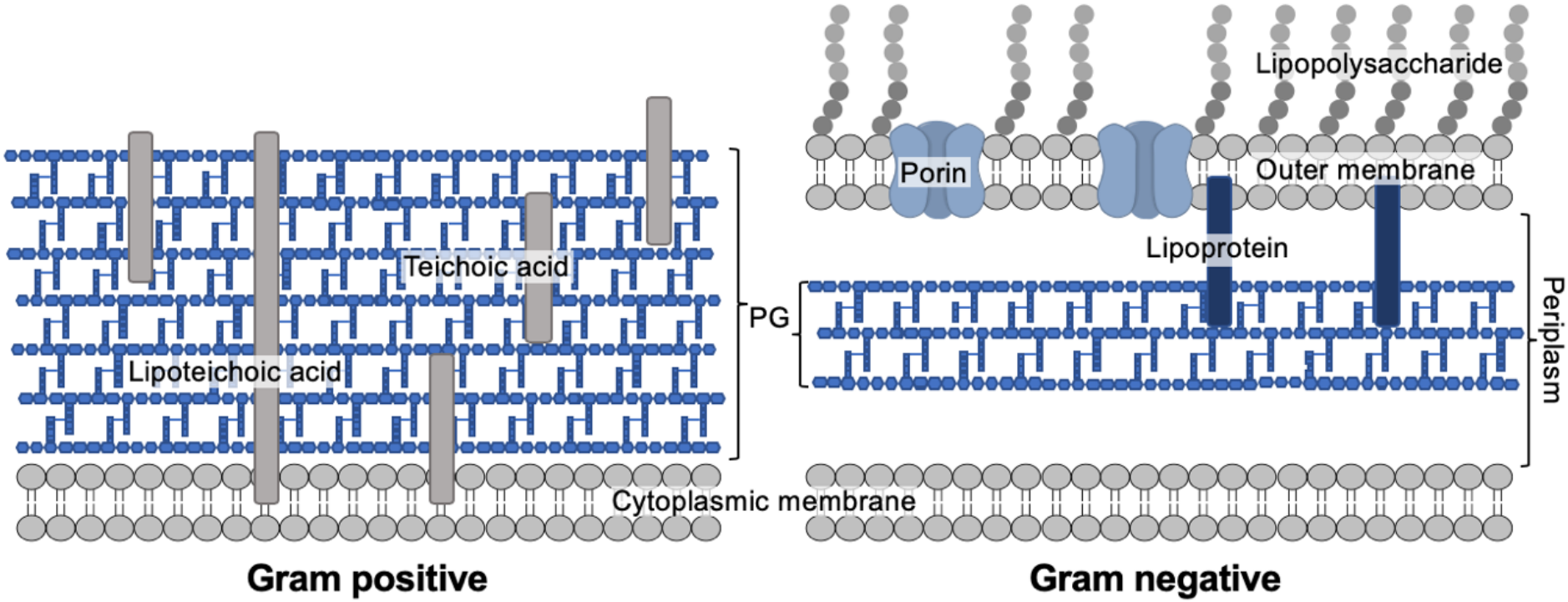

Figure 1.4 Schematic representation of the Gram positive and Gram negative cell walls. Gram positive cell walls have a thick layer of peptidoglycan that incorporates teichoic and lipoteichoic acids. Gram negative cell walls have a comparatively thinner layer of peptidoglycan, in addition to an outer membrane from which the lipopolysaccharide layer extends. Porin proteins mediate access of small molecules to the periplasm.
After Cabeen & Jacobs-Wagner (2005), and Madigan *et al.* (2010).

1.2.1.1 The Gram positive cell wall

The majority of the Gram positive cell wall consists of a thick layer of peptidoglycan (Shockman & Barren, 1983). Further molecules including teichoic acids are embedded in the peptidoglycan layer. Teichoic acids comprise polymers of glycerol phosphate or ribitol phosphate, and are distinguished based on their mode of attachment to the cell wall. Lipoteichoic acids are covalently linked to membrane phospholipids, whereas wall teichoic acids are linked to the Mur*N*Ac sugars of peptidoglycan (Weidenmaier & Peschel, 2008). Proposed functions of the teichoic acids include cation homeostasis, control of membrane permeability, and acting as a scaffold for cell wall enzymes such as hydrolases (Swoboda *et al.*, 2010). In place of the outer membrane observed in Gram negative bacterial cell walls, Gram positive bacteria may encompass a protective structure such as a capsule (Weidenmaier & Peschel, 2008). As previously described (Section 1.1.2.1), variation in the saccharide composition of the capsule defines the serotypes of pneumococci (Henrichsen, 1995).

1.2.1.2 The Gram negative cell wall

The Gram negative cell wall includes a thinner layer of peptidoglycan, in comparison to the Gram positive cell wall. In addition, the peptidoglycan layer is surrounded by an outer membrane, from which the lipopolysaccharide layer extends (Osborn, 1969). The outer membrane is anchored to the peptidoglycan layer by lipoproteins (Cabeen & Jacobs-Wagner, 2005). The outer membrane acts as a further permeability barrier to the bacterial cell (Dirienzo *et al.*, 1978), therefore posing a further impediment to antibiotic access.

1.2.2 Peptidoglycan structure

The mesh structure of the peptidoglycan polymer is created by glycan strands of alternating *N*-acetylmuramyl (Mur*N*Ac) and *N*-acetylglucosaminyl (Glc*N*Ac) sugars linked by β–(1,4)-glycosidic bonds (Figure 1.5). These glycan strands are cross-linked via stem peptides extending from the lactyl moiety of the Mur*N*Ac sugars (Vollmer and Bertsche, 2008).

In addition to the variation depicted at positions two and three of the peptide stem in Figure 1.5, variation in the peptidoglycan structure is found at the level of modifications to the sugars; to the residues of the peptide stem; and at the inclusion of direct and indirect cross links (Vollmer, Blanot*, et al.*, 2008). These modifications have known functions including modulation of immune recognition of PG fragments, and conferral of resistance to enzymes such as lysozyme (Sobhanifar *et al.*, 2013). Particular structural variations that are of interest to the pneumococcal β-lactam resistance mechanism will be discussed in Section 1.6.2.

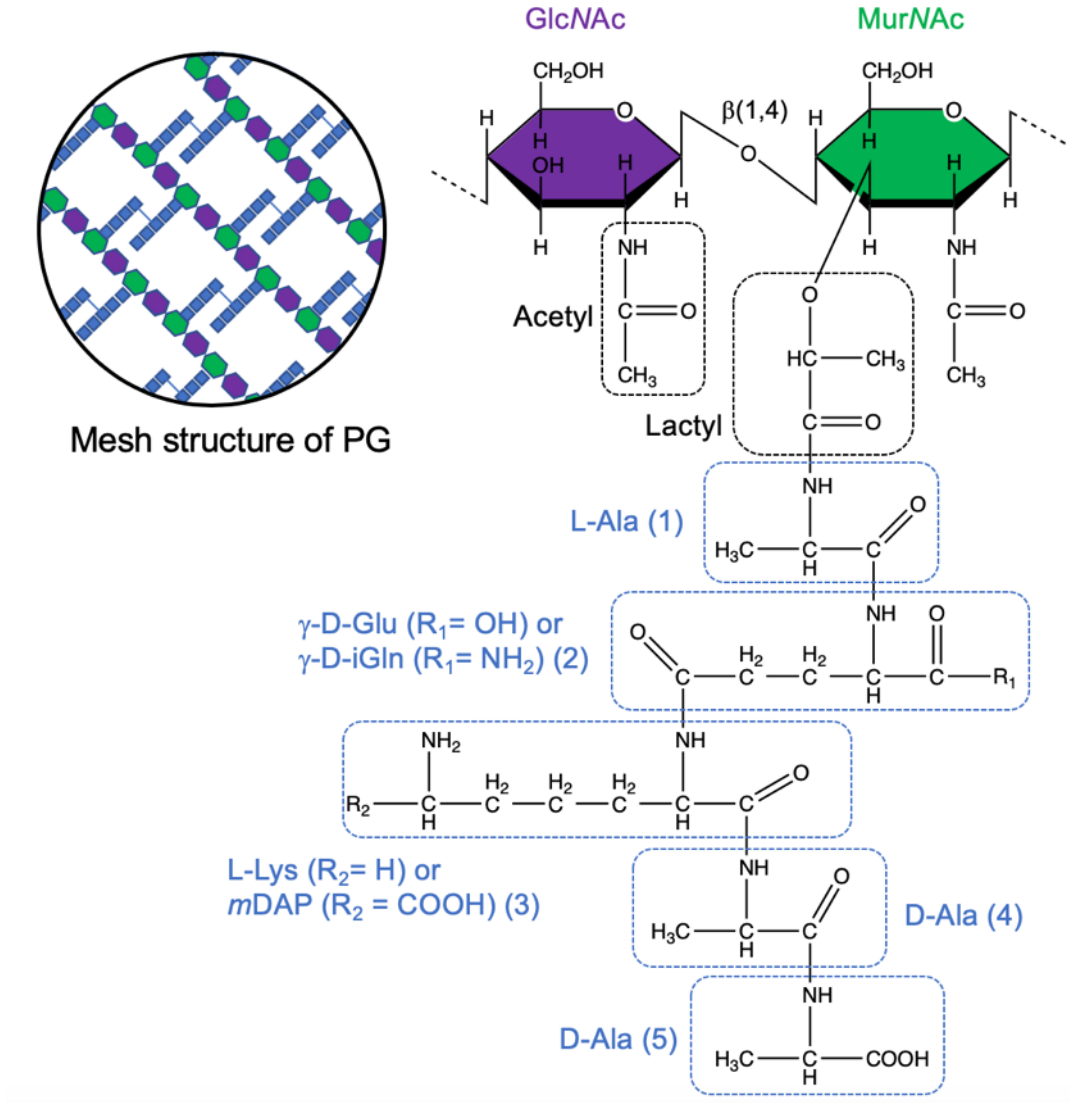

Figure 1.5 General structure of peptidoglycan. A schematic of the mesh structure is presented, demonstrating the glycan strands of alternating sugars (coloured purple to indicate *N*-acetylglucosaminyl (Glc*N*Ac) sugars, and green for *N*-acetylmuramyl (Mur*N*Ac) sugars) which are cross linked between strands via the peptide stems (shown in blue). The general chemical structure of the repeating unit in peptidoglycan is shown, with the pentapeptide stem appended to the lactyl moiety of the Mur*N*Ac sugar. Residue numbers are indicated in brackets.
Made with reference to Madigan *et al.* (2010).

1.3 Biosynthesis pathway and cell division apparatus

The biosynthesis of peptidoglycan is compartmentalised into cytoplasmic, membrane-linked and extracytoplasmic steps (Figure 1.6). In the cytoplasmic step, the Park nucleotide (UDP-Mur*N*Ac pentapeptide) is synthesised by MurA-MurF (Barreteau *et al.*, 2008). Phospho-Mur*N*Ac pentapeptide is transferred from UDP-Mur*N*Ac pentapeptide to the lipid carrier undecaprenyl monophosphate, in a reaction catalysed by MraY to form Lipid I. The muramyl sugar ring of Lipid I is glucosaminylated by MurG to furnish Lipid II. It has been suggested that the enzymes that form the Lipid II biosynthetic pathway are assembled into multi-enzyme clusters, which would allow metabolic channelling, and also mask active sites from inhibitors (Laddomada *et al.*, 2016).

The Lipid II peptidoglycan precursor is translocated across the plasma membrane by the activity of a flippase enzyme. Whilst differing experimental approaches lent support to FtsW (Mohammadi *et al.*, 2011) and MurJ (Sham *et al.*, 2014) as the candidate flippase, the current consensus supports the conclusion that MurJ coordinates the flippase activity. FtsW was subsequently found to exhibit glycosyltransferase activity (Taguchi *et al.*, 2018; see Section 1.4.1.3).

On the extracellular face of the cell membrane, Lipid II is polymerised by glycosyltransferases (with release of undecaprenyl pyrophosphate as a by-product), and the resulting polymers of Glc*N*Ac-Mur*N*Ac pentapeptide are cross-linked by transpeptidation (Vollmer and Bertsche, 2008). The attachment of nascent peptidoglycan to the sacculus in *E. coli* is similarly mediated by transpeptidation (Born *et al.*, 2006). Both glycosyltransferase (GT) and transpeptidase (TP) activities are

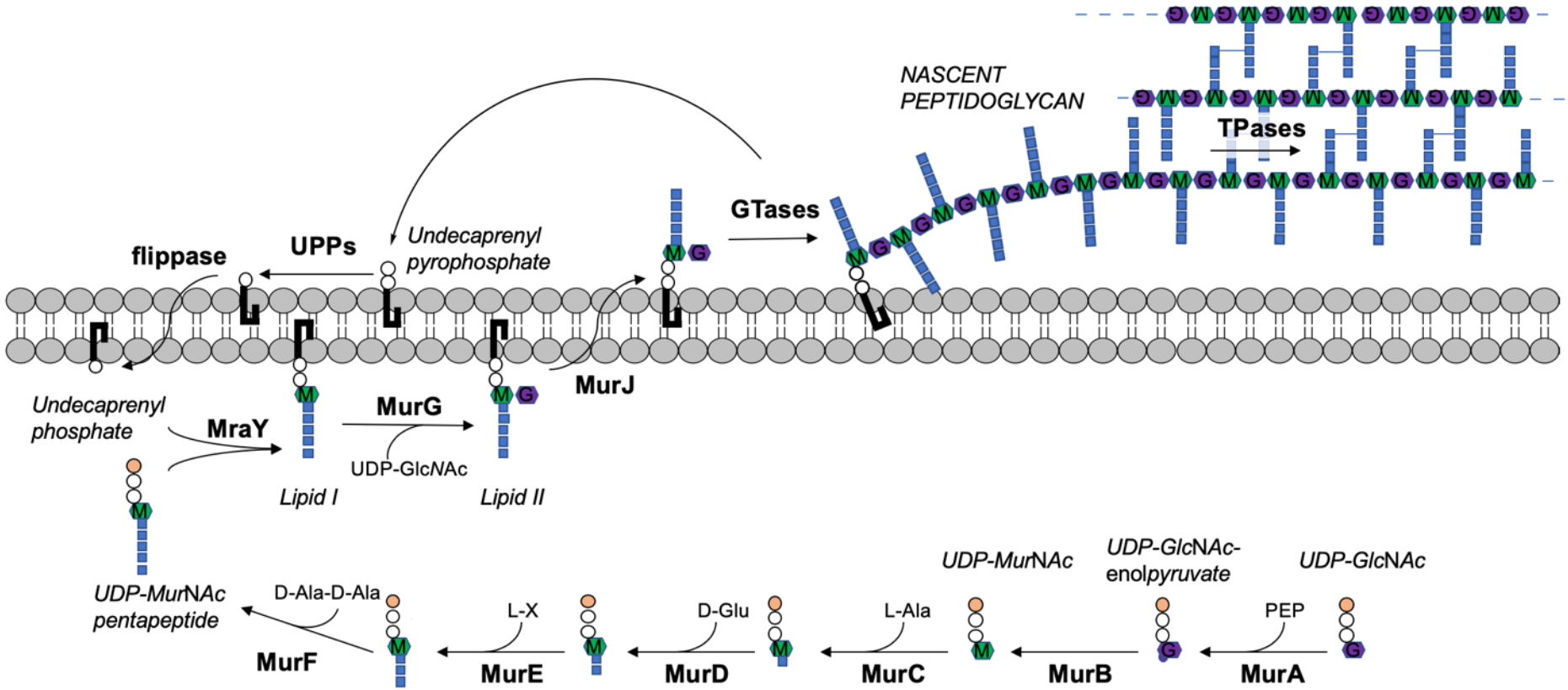

Figure 1.6 Peptidoglycan biosynthesis pathway The UDP-Mur*N*Ac sugar is synthesised from UDP-Glc*N*Ac by MurA and MurB. Amino acids are then sequentially added to UDP-Mur*N*Ac by the MurC-F, and this precursor is then linked to the lipid carrier undecaprenyl phosphate by MraY. MurG links the Glc*N*Ac sugar residue to Lipid I to generated Lipid II, the peptidoglycan precursor. This precursor is flipped across the cytoplasmic membrane by MurJ, following which the glycosyltransferases (**GTases**) generate glycan strands by formation of glycosidic bonds between Lipid II units. Finally, cross link formation between glycan strands is catalysed by transpeptidases (**TPases**). The amino acid incorporated by MurE (**L-X**) is L-Lys is Gram positives, and meso-diaminopimelic acid (**mDAP**) in Gram negatives. Undecaprenyl pyrophosphate released as a by-product of glycosyltransfer is converted to undecaprenyl phosphate by an undecaprenyl phosphatase (**UPPs** - e.g. BacA), and flipped to the cytoplasmic face of the cytoplasmic membrane by an unidentified flippase.
PEP, phospho*enol*pyruvate; **L-X**, L-Lys or meso-diaminopimelic acid (**mDAP**); **GTases**, glycosyltransferases; **TPases**, transpeptidases.

catalysed by penicillin binding proteins (PBPs), in addition to other enzyme classes catalysing glycosyltransfer (1.4.1.4).

The lipid carrier undecaprenyl phosphate is recycled. Undecaprenyl pyrophosphate is dephosphorylated to yield undecaprenyl phosphate. This activity can be catalysed by phosphatases including BacA, PgpB and YbjG (Hernández-Rocamora *et al.*, 2018). Undecaprenyl phosphate is then flipped to the cytoplasmic face of the membrane by a yet unidentified flippase (Manat *et al.*, 2014).

1.4 Penicillin-binding proteins

PBPs are classified according to function; Class A PBPs are bifunctional, i.e. with both N-terminal GT and C-terminal TP domains. Class B PBPs are monofunctional C-terminal transpeptidases with unknown N-terminal activity; and Class C PBPs are monofunctional carboxypeptidases (Sauvage *et al.*, 2008).

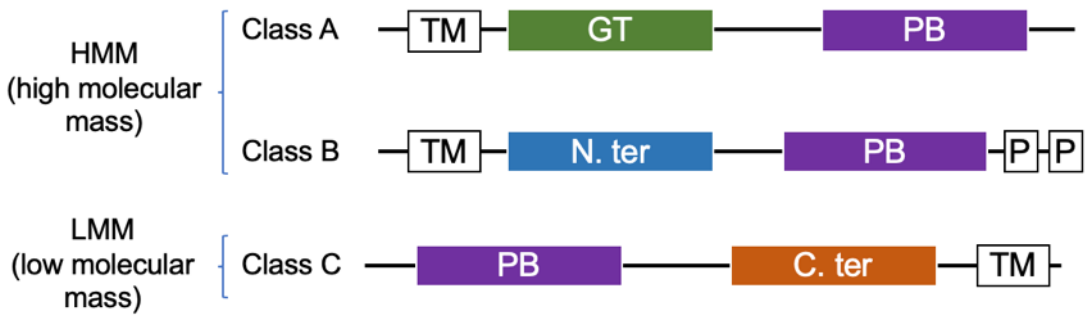

Figure 1.7 Domain structure of Class A, B and C penicillin binding proteins in *S. pneumoniae*. Schematic view of the domain structures of the Class A, B and C penicillin binding proteins of *S. pneumoniae*. The Class C domain structure can be considered to be conserved across a variety of species.
TM, transmembrane domain; **GT**, glycosyltransferase domain, **PB**, penicillin binding domain; **N. ter**, N-terminal domain; **P**, PASTA domain; **C. ter**, C-terminal domain.
Made with reference to Macheboeuf *et al.* (2006).

High molecular mass (HMM) PBPs (Class A or B) have a cytoplasmic tail, transmembrane anchor, and two domains extending from the extracellular face of the cytoplasmic membrane, with the C-terminal TP domain linked to the N-terminal domain via a □-rich linker (Sauvage *et al.*, 2008). Whilst the N-terminal domain in Class A PBPs is the GT domain, in Class B PBPs the

function of this domain is poorly characterised, although it has been suggested to participate in protein-protein interactions (Den Blaauwen *et al.*, 2008).

It has been suggested that PBPs may switch between active and inactive states (Macheboeuf *et al.*, 2006). In the case of *E. coli* PBP1a and PBP1b, activator proteins that mediate these transitions have been identified, where PBP1a and PBP1b are activated by lipoproteins LpoA and LpoB respectively. These proteins are anchored in the outer membrane and stimulate activity of their respective targets, although the mechanism of this stimulation remains unknown (Typas *et al.*, 2010). In addition, it has been suggested that a mechanism of coordination exists between the GT and TP activities in bifunctional PBPs. This is based on observations that no unattached oligomeric glycan chain intermediates are found in living cells (suggesting simultaneous polymerisation and attachment via transpeptidation of nascent glycan chains) (Goodell *et al.*, 1983). Also, GT activity has been found to predicate TP activity *in vitro* (Egan *et al.*, 2015, Bertsche *et al.*, 2005).

1.4.1 Glycosyltransferase activity

The glycan backbone of peptidoglycan is generated by GT activity, which links Lipid II units via the sugar moieties. Synthesis of glycan polymers generally follows a processive mechanism (Yuan *et al.*, 2007), though particular enzymes differ in their *in vitro* maximum glycan chain length (Wang *et al.*, 2008). Differences in the processivity of various glycosyltransferases have been demonstrated by SDS-PAGE analysis of glycan assembly, with longer glycan chains synthesised by *E. coli* PBP1b as compared to the shorter glycan chains synthesised by *Thermotoga maritima* PBP1a (Offant *et al.*, 2010); and greater processivity of *E. coli* PBP1a than *Aquifex aeolicus* PBP1a, based on the comparative lack of shorter glycan polymers with the former enzyme (Barrett *et al.*, 2007).

Usage of monomeric and oligomeric substrates has been compared to analyse the processive activity of glycosyltransferases. Zhang *et al.* (2007) demonstrated that whilst both *E. coli* PBP1a and PBP1b were able to couple a chemo-enzymatically synthesised heptaprenyl Lipid IV to heptaprenyl Lipid II, PBP1a could also ligate Lipid IV units to each other. This data thus demonstrated potential for variation in substrate usage between

glycosyltransferases. Barrett *et al.* (2007) further demonstrated, using GT domain constructs of *E. coli* and *Aquifex aeolicus* PBP1a, that use of Lipid IV as a substrate was associated with a distributive mechanism (with frequent release of short glycan polymers) compared to the processive mechanism observed with Lipid II. Longer oligomers than Lipid IV were not used as substrates in self-coupling, but could be used as substrates in the presence of Lipid II. These data supported a processive mechanism of GT activity.

A lag phase in *in vitro* GT activity was described by Schwartz *et al.* (2002), who ascribed the observation to initial slow coupling of Lipid monomers, followed by a processive extension phase. Chen *et al.* (2003) suggested that the lag was instead due to slow conformational change to the active state, as the lag could be shortened by preincubating in the appropriate detergent.

1.4.1.1 Subdomains and key motifs of the glycosyltransferase domain

The globular, all α-helical GT domain comprises two subdomains; a head subdomain; and the jaw subdomain. The groove between these subdomains contains the GT active site. The GT domain contains five conserved motifs, within which lie residues involved in binding of the Lipid II substrate, and catalysis (Figure 1.8a). Motif I contains the catalytic glutamate. Motif II creates the active site cleft, and contains residues that coordinate the pyrophosphate of the donor molecule. Motif III forms the active site pocket, containing donor site residues. Motif IV is purported to facilitate conformational changes to the jaw subdomain. Motif V contains an arginine residue that stabilises the active site glutamate.

A crystal structure of the GT domain of *A. aeolicus* PBP1a (Yuan *et al.*, 2007) revealed a hydrophobic patch adjacent to the membrane, past which the polyprenol chain of Lipid II was proposed to extend towards the membrane. Part of the active site cleft was found to be obscured by a flap created by the region linking the α2 and α3 helices.

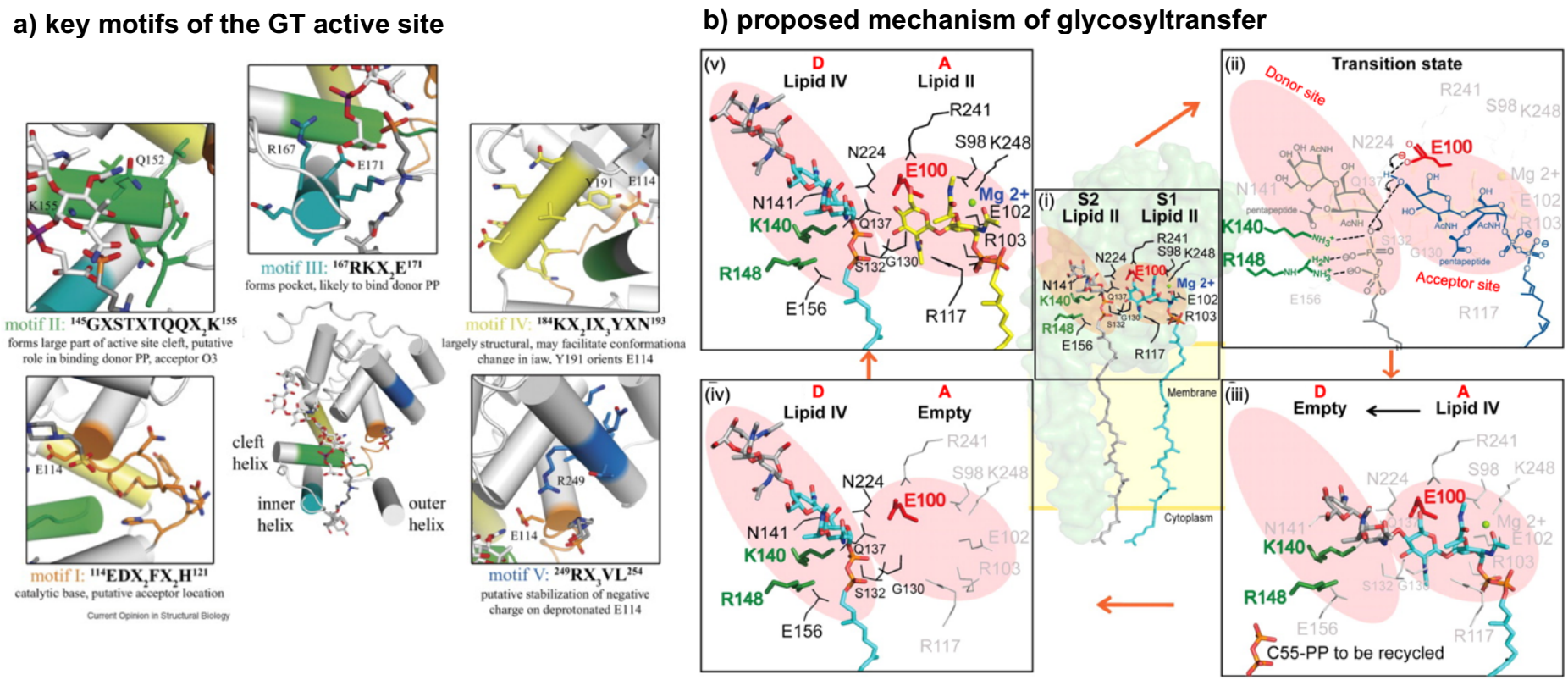

Figure 1.8 Glycosyltransferase activity: structure of the active site and mechanism. **a)** the key motifs of the glycosyltransferase active site, as seen in a crystal structure of *S. aureus* PBP2 in complex with moenomycin. Motif I contains the catalytic glutamate ($E114^{PBP2}$, $E100^{MGT}$**;** part of the acceptor site). Motif II creates the active site cleft, and contains residues that interact with the pyrophosphate of the donor molecule ($K155^{PBP2}$, $K140^{MGT}$). Motif III forms the active site pocket, containing donor site residues ($E171^{PBP2}$, $E156^{MGT}$). Motif IV is purported to facilitate conformational changes to the jaw subdomain. Motif V contains an arginine residue ($R167^{PBP2}$, $R241^{MGT}$) that stabilises the active site glutamate.
b) The proposed mechanism of glycosyltransfer, as inferred from crystal structure of *S. aureus* MGT. Two Lipid II molecules first enter the active site (**i**), one at the donor (**D**) and one at the acceptor (**A**) site. The catalytic E100 residue deprotonates the 4-OH of the acceptor Lipid II molecule (**ii**), which then reacts to form a β-1,4 glycosidic bond with the donor molecule. Interactions with K140 and R148 facilitate the departure of undecaprenyl pyrophosphate (**C55-PP**) (**iii**). The Lipid IV product is shuttled to the donor site (**iv**), and another Lipid II molecule enters the acceptor site (**v**). **A**, glycosyl acceptor site; **D**, glycosyl donor site; **C55-PP**, undecaprenyl pyrophosphate. Figure combines images modified from **(a)** Lovering *et al.* (2008); and **(b)** Huang *et al.* (2012).

The authors proposed that the flap region prevented dissociation of the nascent glycan strand from the active site cleft, and the movement of the glycan strand would then position the newly added reducing end of the glycan chain into the active site to act as a donor for the next round of glycosyltransfer.

The jaw subdomain was recently shown to bind a second molecule of moenomycin, in addition to that bound at the GT donor site, and with positive cooperativity between these two binding events (Punekar *et al.*, 2018). Further structural analysis of the jaw subdomain by Punekar *et al.* (2018) suggested that the hydrophobic properties allowed positioning of the GT active site for optimal access to lipid substrate.

1.4.1.2 Mechanism of glycosyltransfer

Glycan chain synthesis extends from the reducing end of the polymer, with the 4-OH of an incoming Lipid II acting as the acceptor for C1 of the donor polymer (Perlstein *et al.*, 2007; Ward & Perkins, 1973; Weston *et al.*, 1977). The mechanism of glycosyltransfer is illustrated in Figure 1.8b. The catalytic glutamate residue (motif I) deprotonates the 4-OH of the acceptor Lipid II, which can then react to form a β-1,4-glycosidic bond (Lovering *et al.*, 2008). The release of undecaprenyl pyrophosphate from the donor is facilitated by interactions with a lysine (of motif II) and an arginine residue in the donor site. The polymeric product is shuttled to the donor site, and the catalytic cycle repeats with binding of a new acceptor Lipid II molecule.

1.4.1.3 Non-PBP glycosyltransferases

In addition to the GT activity of Class A PBPs, glycan polymer assembly by at least two further enzyme classes has been demonstrated. Monofunctional glycosyltransferase enzymes, which structurally resemble the GT domain of Class A PBPs, have been identified in bacteria including *E. coli* and *S. aureus* (Sauvage *et al.*, 2008). In addition, activity of a monofunctional glycosyltransferase in pneumococcal membrane preparations has been identified (Park *et al.*, 1985; Wang *et al.* 2001) demonstrated *in vitro* Lipid II polymerisation by MGT of *S. aureus.*

The identification of the shape, elongation, division and sporulation (SEDS) proteins constituted a major new discovery in cell wall biosynthesis.

1.4.1.3.1 SEDS proteins

The polymerisation of Lipid II had been thought to be wholly coordinated by PBPs. However, this was disputed by observations that bifunctional PBPs could be deleted in *B. subtilis*, with no resultant loss of viability or rod morphology (McPherson & Popham, 2003). The *in vivo* activity of the unknown GT was insensitive to moenomycin inhibition. The existence of an unidentified glycosyltransferase was similarly revealed in *E. faecalis* in the course of experiments designed to identify the glycosyltransferase partner of PBP5. Despite deletion of the three class A PBPs in *E. faecalis*, cells remained viable (Arbeloa *et al.*, 2004). These observations were subsequently explained by the discovery of the GT activity of the SEDS proteins.

The SEDS proteins are required for *in vivo* peptidoglycan synthesis (Henrichfreise *et al.*, 2016), and were originally considered to function as Lipid II flippases (Mohammadi *et al.*, 2011). The Rod complex of PG synthesis in *Bacillus subtilis* was shown to be active in mutants lacking the four Class A PBPs, and the SEDS protein RodA was identified as the unknown glycosyltransferase enzyme of the Rod complex (Meeske *et al.*, 2016). RodA was further identified as the moenomycin-insensitive glycosyltransferase that conferred the intrinsic resistance of *B. subtilis* to moenomycin (Emami *et al.*, 2017). Glycosyltransferase activity by FtsW has also been demonstrated (Taguchi *et al.*, 2018).

1.4.2 The penicillin-binding domain and transpeptidase activity

The penicillin-binding domain comprises a five-stranded, antiparallel β-sheet surrounded by α-helices, with α1 and α11 on one side, opposite α8 on the other (Figure 1.9); this fold is broadly conserved among the Class A and B PBPs of a number of bacterial species (Macheboeuf *et al.*, 2006).

1.4.2.1 Mechanism

Reactions catalysed by the penicillin binding domain include transpeptidation (TP) and D,D-carboxypeptidation (CP). TP and CP activities are catalysed by Class A and B PBPs, and proceed via a common mechanism (Sauvage *et al.*, 2008). The first step is the reversible formation of an Henri-Michaelis complex between the enzyme and the donor stem peptide; followed by nucleophilic attack at the carbonyl carbon of the N-terminal D-Ala of the D-Ala-D-Ala peptide by the active site serine side chain to form an acyl-enzyme intermediate, with release of D-Ala. Finally, deacylation releases the active site serine. The identity of the acceptor for deacylation forms the distinction between TP and CP activities. For transpeptidation, nucleophilic attack of the acyl-enzyme intermediate by the amine of an additional stem peptide acts as an acceptor, thus releasing the active site serine and forming a peptide bond (Terrak *et al.*, 1999). By contrast, in CP activity the acceptor is water, and so the overall outcome of the reaction with the penicillin binding domain is hydrolytic removal of the terminal D-Ala to create a truncated stem peptide (Sauvage *et al.*, 2008). Structural data on Class A PBPs has offered explanation for apparent transition between active and inactive states, alluded to by Macheboeuf *et al.* (2006). An apo crystal structure of *S. pneumoniae* PBP1b (Macheboeuf *et al.*, 2005) revealed an apparent closed active site conformation. Comparison to the acyl-enzyme showed movement of the loop between β3 and β4. This movement resulted in blocking of the active site cleft by Asn656, with formation of a hydrogen bond with the Ala499 backbone. The catalytic serine was also in contact with β3 rather than the other catalytic residues of the penicillin binding domain. Acyl-enzyme structures obtained with nitrocefin and cefotaxime demonstrated a transition from the closed conformation, to an open conformation amenable to acylation by β-lactams.

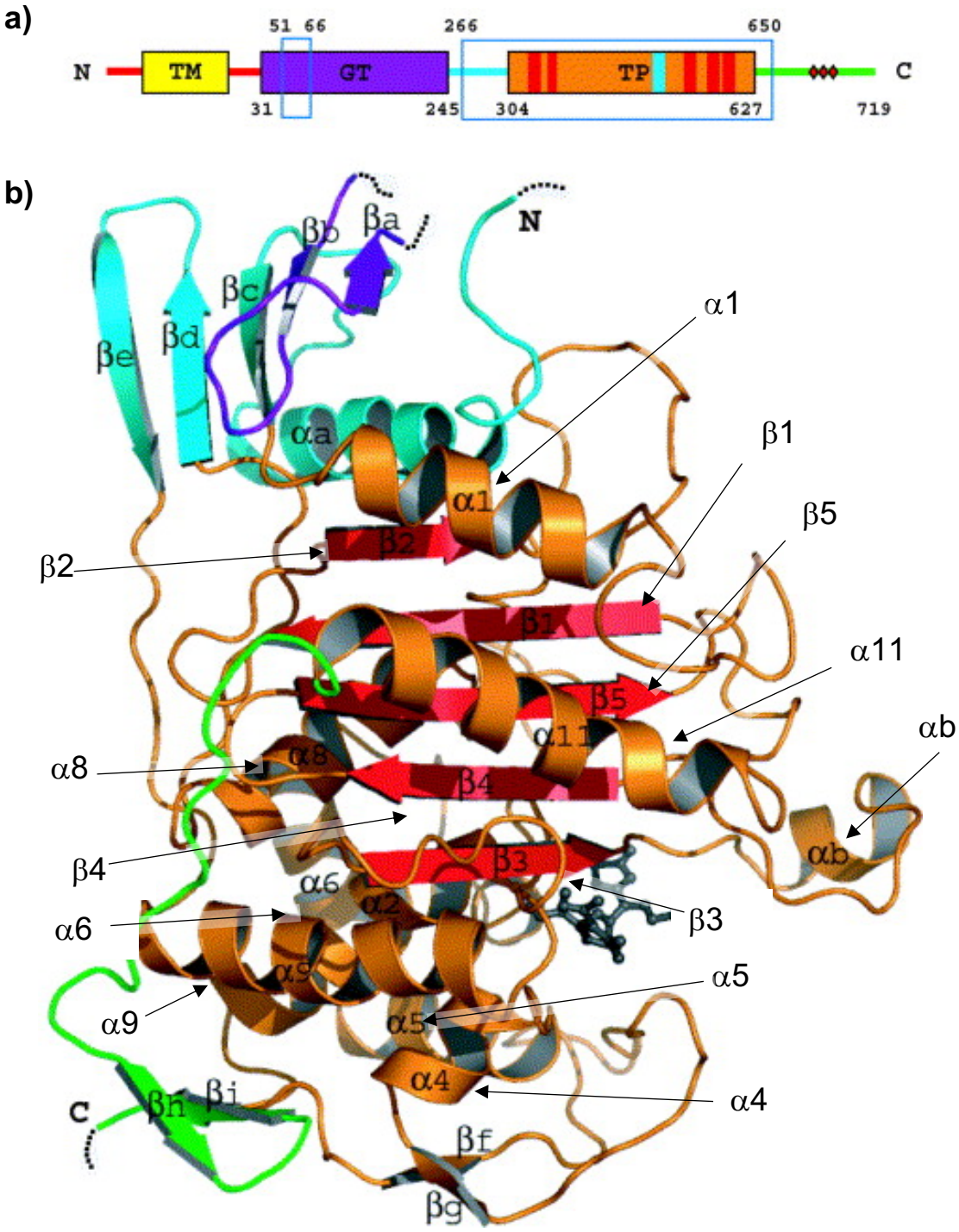

Figure 1.9 Characteristic fold of the penicillin-binding domain. A crystal structure of *S. pneumoniae* PBP1a, with domain structure **(a)** and ribbon diagram **(b)** (with colouring to indicate domains as shown in **(a)**). The penicillin-binding domain is typified by a five-stranded antiparallel β-sheet, surrounded by two alpha helices opposite a third on the other side of the β-sheet.
TM, transmembrane helix; **GT**, glycosyltransferase domain; **TP**, transpeptidase domain.
Parts a) and b) reproduced from Figure 1, Contreras-Martel *et al.* (2006) © Journal of Molecular Biology. Part c) reproduced from Figure 2, Sauvage *et al.* (2008) © 2008 Federation of European Microbiological Societies.

1.4.2.2 Conserved residues of the transpeptidase active site

There are 3 conserved motifs observed in the active site of D,D-transpeptidases. These include the SXXK tetrad, encompassing the catalytic serine and a lysine residue that activates the serine; the SXN (or YSN in *Streptomyces* R61) motif; and the KTG(T/S) motif (Sauvage *et al.*, 2008). The positioning of the transpeptidase donor stem peptide in the active site is such that the methyl group of the penultimate D-Ala is positioned in a hydrophobic pocket (Macheboeuf *et al.*, 2006), and the carbonyl oxygen is positioned in the oxyanion hole.

The conserved motifs of the transpeptidase active site participate in activation of nucleophiles for catalysis (Sauvage *et al.*, 2008). Prior to acylation of the active site serine by the donor stem peptide, a proton is abstracted by the conserved Lysine residue of the SXXK motif. For deacylation, the Lysine residue of the third motif abstracts a proton from the acceptor, to confer upon it sufficient nucleophilic character to mediate the attack of the carbonyl carbon of the acyl-enzyme.

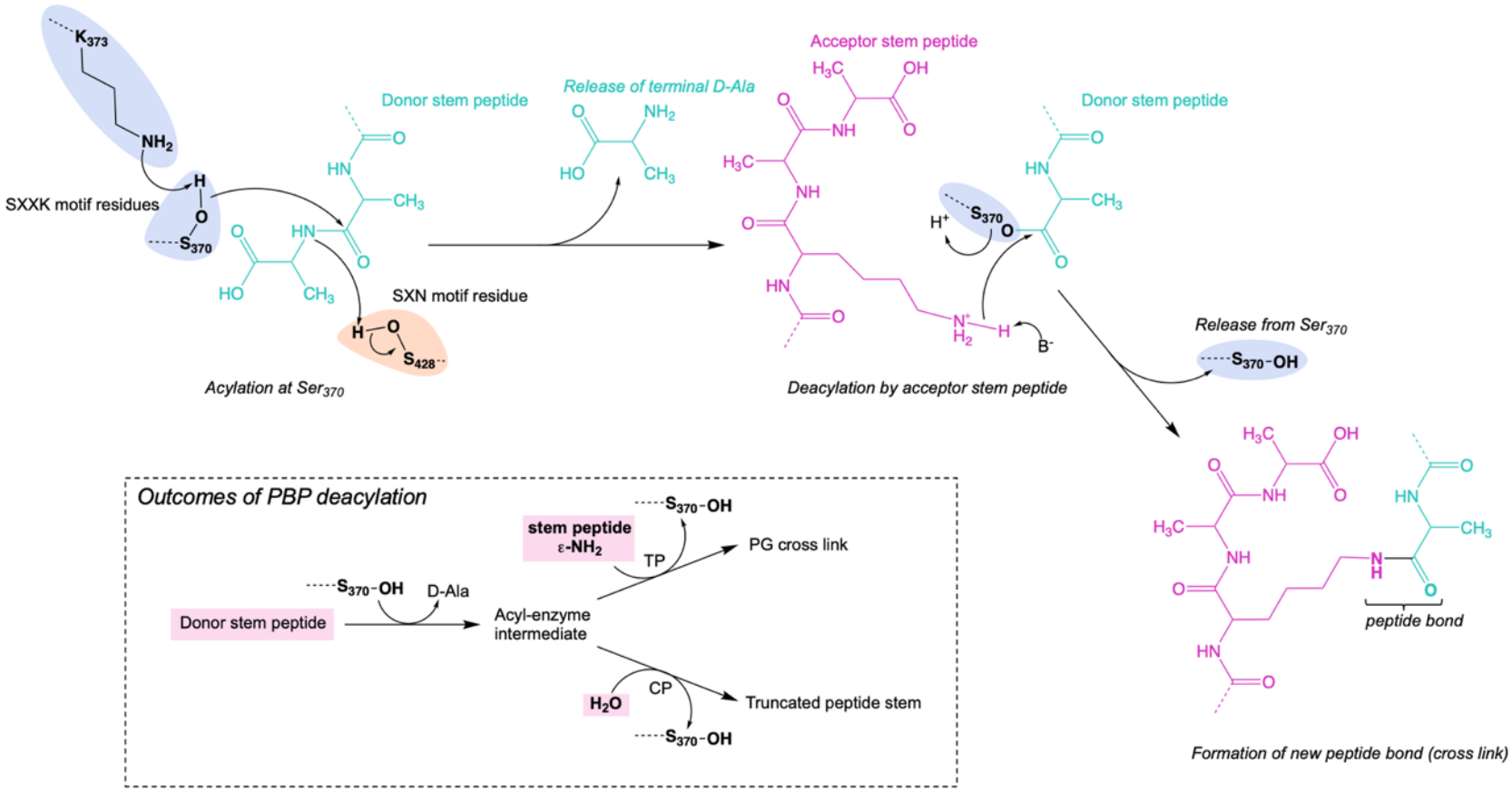

Figure 1.10 Transpeptidase mechanism as represented in *S. pneumoniae* PBP1a. The PBP forms a Michaelis complex with a Lipid II substrate or its polymeric GT product. Attack by the active site serine on the carbonyl carbon of the subterminal D-alanine residue results in formation of an acyl enzyme intermediate, with associated release of the terminal D-Ala. In *S. pneumoniae* PBP1a, the active site serine is activated by deprotonation via the lysine residue of the SXXK motif (indicated in magenta). Deacylation occurs by nucleophilic attack of the acyl enzyme intermediate by an adjacent stem peptide, releasing the active site serine and forming a peptide bond between the two stem peptides. The identity of the acceptor (pink boxes) determines the outcome of deacylation. **TP**, transpeptidase; **CP**, D,D-carboxypeptidase; **PG**, peptidoglycan.

1.4.3 Lipoprotein activators of PBPs

Lipoprotein activators have been identified for several Gram-negative, Class A PBPs. These activators were discovered on the basis of a transposon insertion screen exploiting the synthetic lethality of PBP1A and PBP1B in *E. coli* (Paradis-Bleau *et al.*, 2010). LpoA and LpoB were found to be essential for the function of *E. coli* PBP1a and PBP1b respectively. The interaction of the cognate lipoprotein:PBP pairs was demonstrated to increase the rate of glycosyltransferase activity (Paradis-Bleau *et al.*, 2010) and the extent of cross-linking (Typas *et al.*, 2010) by each of the Class A PBPs. The synthetic lethal screen was subsequently used to identify LpoP, a lipoprotein activator of *Pseudomonas aeruginosa* PBP1b (Greene *et al.*, 2018); and MacP, a phosphorylation-dependent protein activator of *S. pneumoniae* PBP2a (Fenton *et al.*, 2018).

1.5 Bacterial cell wall biosynthesis inhibitors

The essentiality of cell wall biosynthesis makes it an attractive target for antibacterials. Inhibitors of enzymes throughout the three compartmentalised stages of peptidoglycan biosynthesis have been identified. These include binders of the PG precursor, such as the glycopeptides teicoplanin and vancomycin which bind the terminal D-Ala-D-Ala moiety of the stem peptide in Lipid II (Bugg *et al.*, 2011); and substrate mimetics such as β-lactams and moenomycin, which inhibit transpeptidase and glycosyltransferase activities respectively (Schneider & Sahl, 2010). Bacitracin binds undecaprenyl pyrophosphate to prevent recycling of the lipid carrier (Winkelman & Gratton, 1989). Agents targeting the cytoplasmic steps of PG biosynthesis include fosfomycin, which inhibits MurA (Kahan *et al.*, 1974); and D-cycloserine, which inhibits both DdlB (Neuhaus & Lynch, 1964) and alanine racemase (Lambert & Neuhaus, 1972).

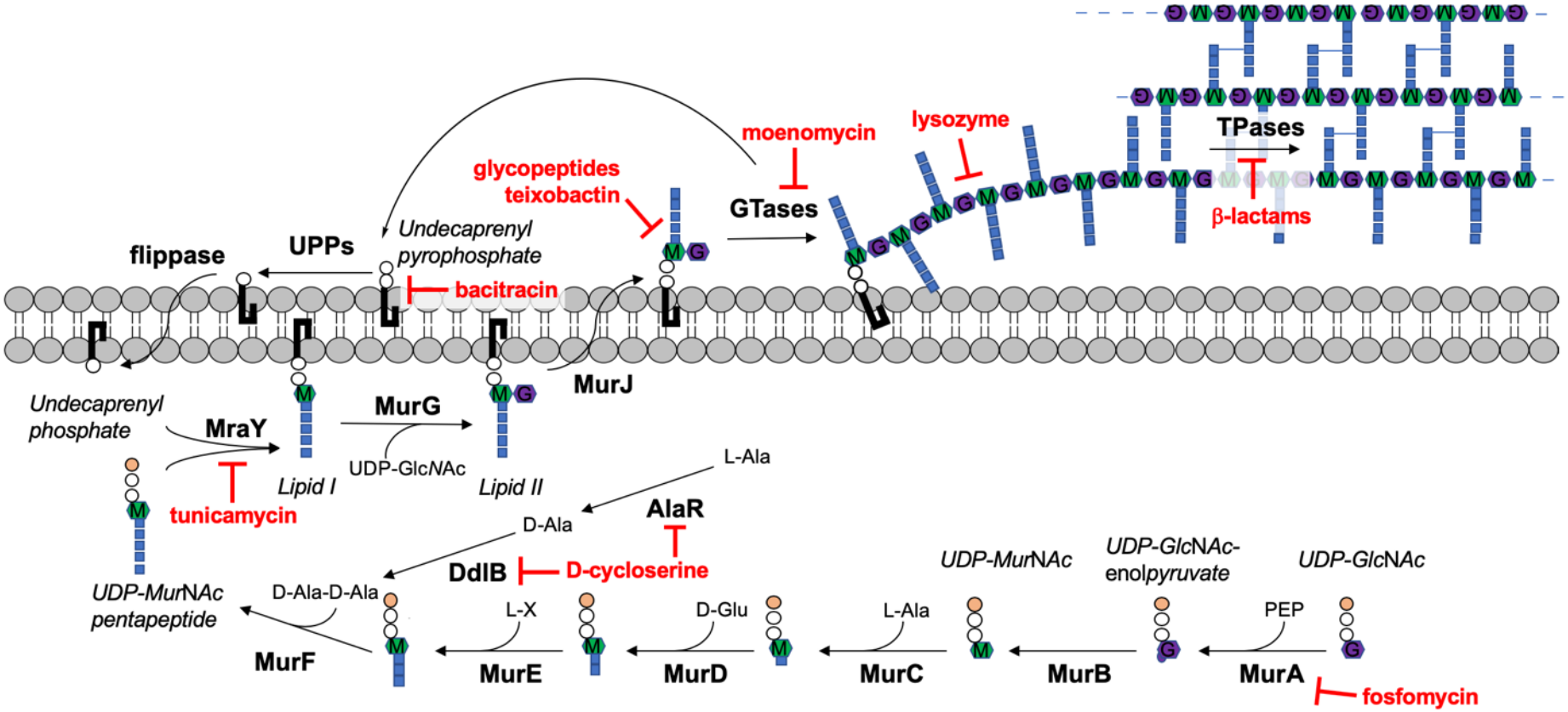

Figure 1.11 Cell wall biosynthesis inhibitors. Cell wall active compounds include enzyme inhibitors, PG-cleaving enzymes and substrate binders. Inhibitors to all three stages (cytoplasmic, membrane-associated and lipid-linked) of peptidoglycan biosynthesis have been identified. **PEP**, phospho*enol*pyruvate; **L-X**, L-Lys or meso-diaminopimelic acid (mDAP); **GTases**, glycosyltransferases; **TPases**, transpeptidases.

1.5.1 Mode of action of β-lactams

β-lactam antibiotics inhibit peptidoglycan biosynthesis; the molecule acts as a structural mimetic of the terminal D-Ala-D-Ala moiety of the donor stem peptide in transpeptidation. The β-lactam acylates the active site serine of the transpeptidase, forming an acyl-enzyme intermediate. Although this intermediate can be hydrolysed to recover the enzyme, the rate of hydrolysis is vastly slower relative to the rate of cell division, as the bulky leaving group prevents access of water to the active site to release the β-lactam (Ghuysen, 1991). The TP reaction is thus inhibited, weakening the structure of peptidoglycan due to the decreased extent of cross-linking, and culminating in cell lysis.

Key benefits of β-lactams as antibiotics include their efficacy, specificity and the accessibility of the target (Wilke *et al.*, 2005). However, the clinical use of this class of antibiotics is threatened by the development of resistance in a variety of important human pathogens.

1.5.2 Resistance mechanisms to β-lactams

Several key mechanisms of resistance to β-lactams are found among both Gram positive and Gram negative bacteria. As with other antibacterials, resistance mechanisms can be broadly categorised into drug modification, altered access to the target, and target modification.

1.5.2.1 β-lactamases

Evolutionarily linked to PBPs, the β-lactamases encompass 4 classes of enzymes which hydrolyse β-lactams (Poole, 2004). These can broadly be defined as serine β-lactamases and metallo-β-lactamases (MBLs) (which require divalent cations as cofactors) (Walsh *et al.*, 2005). Predominantly Gram negative organisms express β-lactamases, and these enzymes can be plasmid-encoded and therefore transferred between strains (Carattoli, 2013).

Serine β-lactamase inhibitors have been used to restore the efficacy of β-lactams through coadministration. For example, combination therapies such as co-amoxiclav, where the β-lactamase inhibitor clavulanic acid is coadministered with ampicillin, have restored clinical efficacy to the latter (Walsh *et al.*, 2005). Development of MBL inhibitors offers additional challenges, such as the potential for cross-reactivity with mammalian enzymes, and the variation in active site structure between MBLs (Walsh *et al.*, 2005).

Deacylation of PBPs is 6 orders of magnitude slower than β-lactamases, and crucially, takes longer than the doubling time of the bacteria (Fisher *et al.*, 2005). In class A β-lactamases, Glu_{166} at the bottom of the active site cleft coordinates a water molecule, which may participate in a proton shuttle to deprotonate the catalytic serine; or may be activated to attack the acyl-enzyme to release bound β-lactam, thus accounting for the rapid deacylation step in such β-lactamases (Macheboeuf *et al.*, 2006).

1.5.2.2 Porins and efflux pumps

Modulation of access to the periplasm is a key resistance mechanism in Gram-negative bacteria in particular. Both plasmid and chromosomally encoded efflux mechanisms have been identified. Among the five classes of efflux pumps, examples of resistance-nodulation-division (RND) and ATP-binding cassette (ABC) transporters have been identified that mediate efflux of β-lactam antibiotics (Poole, 2005). Clinical *P. aeruginosa* meropenem resistance has been linked to reduced expression of the outer membrane porin OprD, along with increased expression of the MexAB-OprM efflux pump (Köhler *et al.,* 1999; Pai *et al.*, 2001).

1.5.2.3 Target modification

In bacteria including *S. pneumoniae* (Dowson *et al.*, 1989)*, S. aureus* (Chambers, 1997) and *Neisseria gonorrhoeae* (Faruki & Sparling, 1986), resistance develops through modification of the PBPs such that affinity of the transpeptidase active site for β-lactams is decreased, whilst maintaining affinity for the natural substrate. In the case of pneumococci and *N.*

gonorrohoaea, this is a process of generation of mosaic PBP genes, through uptake and homologous recombination of exogenous DNA from oral streptococci (Dowson *et al.*, 1993) and commensal *Neisseria* species (Bowler *et al.*, 1992) respectively. The specific amino acid changes contributing to low affinity of streptococcal PBPs will be discussed in Chapter 4.

Methicillin-resistant *S. aureus* (MRSA) strains acquire β-lactam resistance via intact acquisition of the *mecA* gene, encoding PBP2a. PBP2a has low β-lactam affinity, and can therefore catalyse transpeptidation in the presence of inhibitor concentrations that would otherwise arrest growth. Lim and Strynadka (2002) concluded from structural data that decreased β-lactam susceptibility arose due to the reduced acylation rate of PBP2a, likely as a consequence of the aberrant positioning of the active-site serine (Ser_{403}) for nucleophilic attack of the β-lactam. Significant conformational changes in the transition from Michaelis complex to acyl-enzyme were proposed to slow the acylation rate, whereas in comparison to the apo and acyl-enzyme structure for β-lactam sensitive PBPs, such conformational changes were not observed (Lim & Strynadka, 2002).

1.5.2.4 L,D-transpeptidases

Enterococci have been demonstrated to exhibit intrinsic low-susceptibility to penicillin. *Enterococcus faecium* expresses Ldt_{fm}, an active site cysteine enzyme which catalyses L,D-transpeptidation (Mainardi *et al.*, 2005) and confers high-level β-lactam resistance. The TP activity of Ldt_{fm} was found to use a tetrapeptide donor stem (as generated by a D,D-carboxypeptidase), following which cross-linking was catalysed by this PBP between the α-carbonyl of the Lysyl residue in the third position of the donor stem peptide (instead of the sub-terminal D-Ala), and the α-amino group of the D-Asparaginyl moiety of the acceptor stem peptide (Mainardi *et al.*, 2000). Crystallographic data revealed putative transpeptidase donor and acceptor binding sites comprising two paths accessing the buried pocket of the transpeptidase active site of Ldt_{fm} (Biarrotte-Sorin *et al.*, 2006). Due to the structural disparity between D,D-transpeptidases and L,D transpeptidases, β-

lactams such as penicillins cannot inhibit the latter class of enzymes, although carbapenems are active against L,D transpeptidases (Ealand *et al.*, 2018).

1.6 Cell division in S. pneumoniae

Peptidoglycan is built from Lipid II by several families of peptidoglycan synthases, which participate in multiprotein complexes. Site-specific insertion of new peptidoglycan is coordinated by proteins that recruit peptidoglycan synthases to defined locations around the cell envelope, thus effecting cell division and maintaining cell shape (Cabeen & Jacobs-Wagner, 2005).

According to the two-site model of peptidoglycan biosynthesis in rod-shaped bacteria such as *E. coli*, synthesis of peptidoglycan was proposed to be coordinated by two separate machineries; the divisome, which creates the septum and divides the cell; and the elongasome, which lengthens the cell to maintain the rod shape of the sacculus (Lutkenhaus *et al.*, 2012). FtsZ forms the Z ring, to which the proteins of the divisome localize (Adams & Errington, 2009). The proteins of the divisome have been found to assemble at the septum in a defined order, with FtsZ leading, followed by FtsA, ZipA and ZapA to stabilise the Z ring; followed by further divisome proteins (Macheboeuf *et al.*, 2006).

Peptidoglycan hydrolase (autolysin) enzymes perform multiple functions including cleavage of existing peptidoglycan to enable insertion of new material; regulation of the thickness of the peptidoglycan layer; and effecting cell separation, by cleavage of glycoside and amide bonds (Vollmer, Joris*, et al.*, 2008). In Gram negative organisms, soluble peptidoglycan fragments are recycled, whereas this phenomenon has not been observed (or occurs to a much lesser extent) in Gram positive bacteria (Park & Uehara, 2008). Insertion of newly synthesised peptidoglycan into the existing sacculus has been suggested to occur by the action of bifunctional synthases participating in enzyme complexes, with simultaneous polymerisation of glycans and attachment via transpeptidation (Typas *et al.*, 2012). More recent models of peptidoglycan biosynthesis have proposed the leading action of hydrolases in

separating existing peptidoglycan for insertion of new material (H. Zhao *et al.*, 2017).

1.6.1 Divisome organisation in *S. pneumoniae*

Unlike the spatially separated divisome and elongasome complexes in rod-shaped bacteria, the pneumococcal cell wall biosynthesis proteins have been observed to cluster around the division site (Pinho *et al.*, 2013). It has been proposed that the elongasome in ovococci is responsible for synthesis of new peptidoglycan either side of the septum and between the equatorial rings. The cell is thus elongated and divided to create two daughter cells. Ovococci also differ from model rod-shaped bacteria in the division planes that are formed. In ovococci, two equatorial rings are first formed, and peripheral PG synthesis then lengthens the cell until these equatorial rings reach the distance for the midcell of the daughter cells to be formed. Septation then occurs to separate the daughter cells, culminating in cell division in parallel planes (Zapun *et al.*, 2008).

S. pneumoniae has six PBPs; five HMM PBPs, of which three are bifunctional (PBP1a, PBP1b and PBP2a) and two monofunctional (PBP2b and PBP2x); and one low molecular mass (LMM) PBP (PBP3, a D,D-carboxypeptidase) (Sauvage *et al.*, 2008). Among the bifunctional PBPs of *S. pneumoniae*, PBP1a and PBP2a form a synthetic lethal pairing (Hoskins *et al.*, 1999; Paik *et al.*, 1999).

The role of pneumococcal Class A PBPs was recently called into question by the discovery of the SEDS proteins, and the findings of Straume *et al.* (2019). These authors found that the peptidoglycan hydrolase CbpD cleaved septal peptidoglycan synthesised by PBP2x, such that preferential inhibition of PBP2x using oxacillin was associated with a ‘resistant phase’ to CbpD culture lysis. The resistance to CbpD was reasoned to result from a Class A PBP-catalysed remodelling of septal peptidoglycan, based upon the loss of resistance to CbpD when cultures were treated with moenomycin, which inhibits the glycosyltransferase activity of the Class A PBPs, but not of the

SEDS proteins. Though no structural modifications could be demonstrated to lead to the alteration in sensitivity as a consequence of Class A PBP activity, Straume *et al.* (2019) proposed that Class A PBPs were involved in creating a tightly interwoven mesh structure to create resistance to CbpD, building upon the PG structure generated by divisome synthases FtsW/PBP2x.

1.6.2 Peptidoglycan structure in *S. pneumoniae*

Species-specific modifications to the basic peptidoglycan structure are observed in pneumococci (Figure 1.12). As in several other species, the modifications found in pneumococcal peptidoglycan have important links to the β-lactam resistance mechanism.

1.6.2.1 Amidation in Gram positives

Amidation of the second position amino acid in the peptide stem (thus giving an isoglutamine at that position instead of glutamate) has been identified in the peptidoglycan of Gram positive organisms including *S. pneumoniae*, *S. aureus* and *E. faecalis* (Schleifer & Kandler, 1972). The introduction of this modification to the lipid substrate was demonstrated by Siewert and Strominger (1968) using ‘particulate’

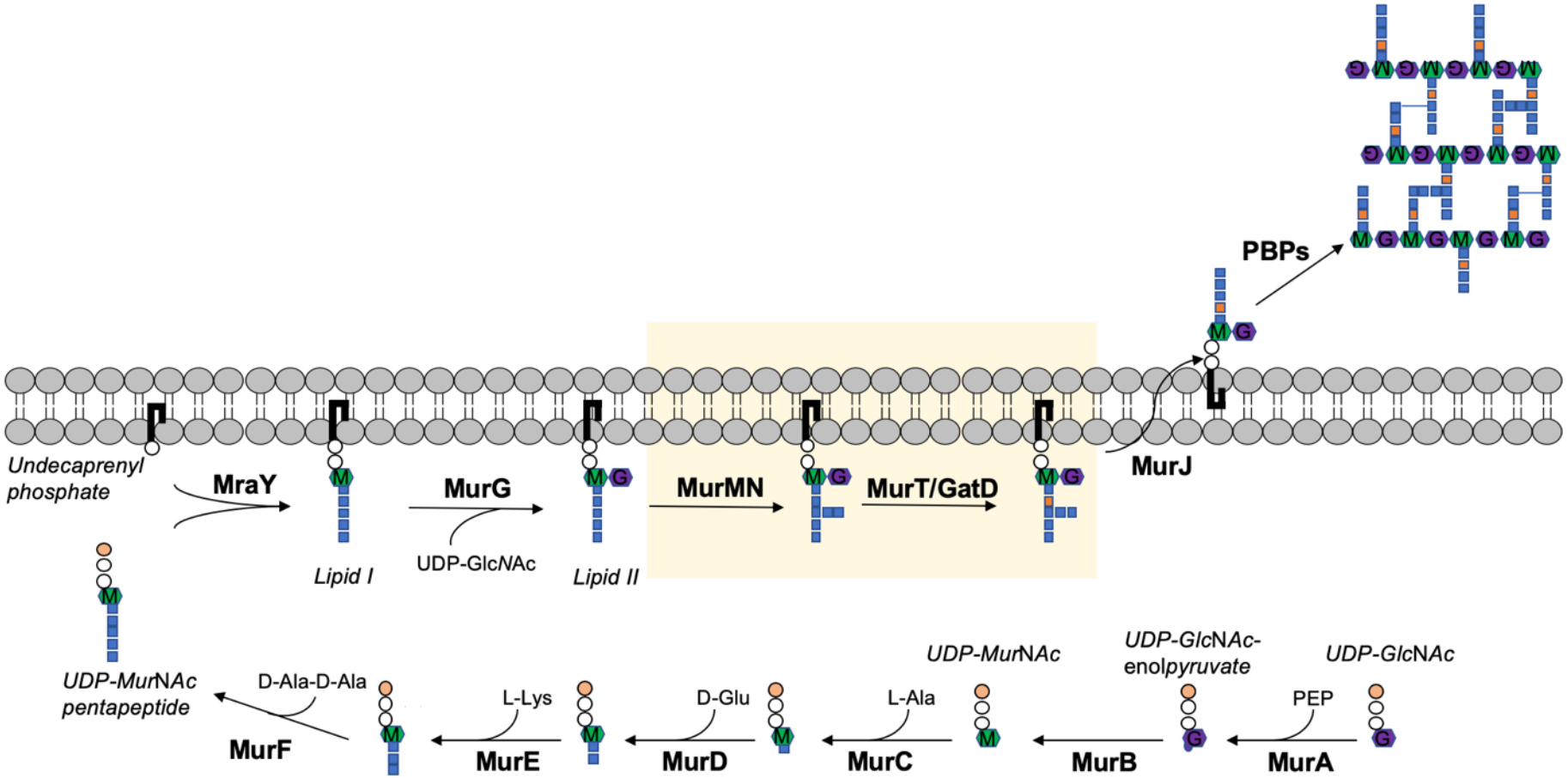

Figure 1.12 Additional stages in the peptidoglycan biosynthesis pathway of *S. pneumoniae*. Prior to the flipping of Lipid II the the extracytoplasmic face of the membrane by MurJ, two further modifications are made to Lipid II in pneumococci (yellow box). MurM and MurN catalyse addition of two further amino acids to the ε-amino group of L-Lysine in the stem peptide, and the MurT/GatD complex catalyses amidation of the D-glutamate C1 carboxylate. The order of these additional steps is currently unconfirmed. Undecaprenyl phosphate recycling is omitted for clarity.**PEP**, phospho*enol*pyruvate.

enzyme preparations. The Lipid substrate was surmised to be the acceptor of ammonia, as amidated UDP-Mur*N*Ac pentapeptide was found to be a poor substrate for MraY (Siewert & Strominger, 1968). In addition, cell wall synthesis inhibitors including vancomycin, bacitracin and penicillin G did not impact the extent of formation of amidated muropeptides, suggesting overall that amidation occurred at the lipid-linked steps of peptidoglycan synthesis.

The amidotransferase activity was identified by Munch *et al.* (2012) to be conferred in *S. aureus* by the enzyme complex MurT/GatD. The GatD amidotransferase uses L-glutamine as a nitrogen donor and transfers ammonia to the MurT active site, which catalyses the ATP-dependent amidation of the second position amino acid (Figure 1.13). The subsequently named *murT/gatD* locus was found to be a component of the β-lactam resistance mechanism on the basis of a phenotypic screen (Figueiredo *et al.*, 2012; Lee *et al.*, 2011). Zapun *et al.* (2013) identified a comparable operon in *S. pneumoniae* strain R6, and demonstrated the essentiality of the encoded amidotransferase. The structure of the amidase complex in *S. pneumoniae* was published by Morlot *et al.* (2018).

L-Glutamine is also used as a nitrogen donor by GlmS, which converts fructose-6-phosphate to glucosamine-6-phosphate in the reaction pathway that culminates in generation of UDP-Glc*N*Ac (El Khoury *et al.*, 2017). Downregulation of glutamine metabolism on treatment of *S. pneumoniae* cultures with penicillin has therefore been proposed to result from the accumulation of glutamine due to inactivity of the PG biosynthesis pathway (El Khoury *et al.*, 2017).

Amidation has been suggested to play a role in determining the capacity of the cell wall to bind divalent cations, such that these can be stored and supplied for cellular function (Kern *et al.*, 2010). NMR studies on *B. subtilis*

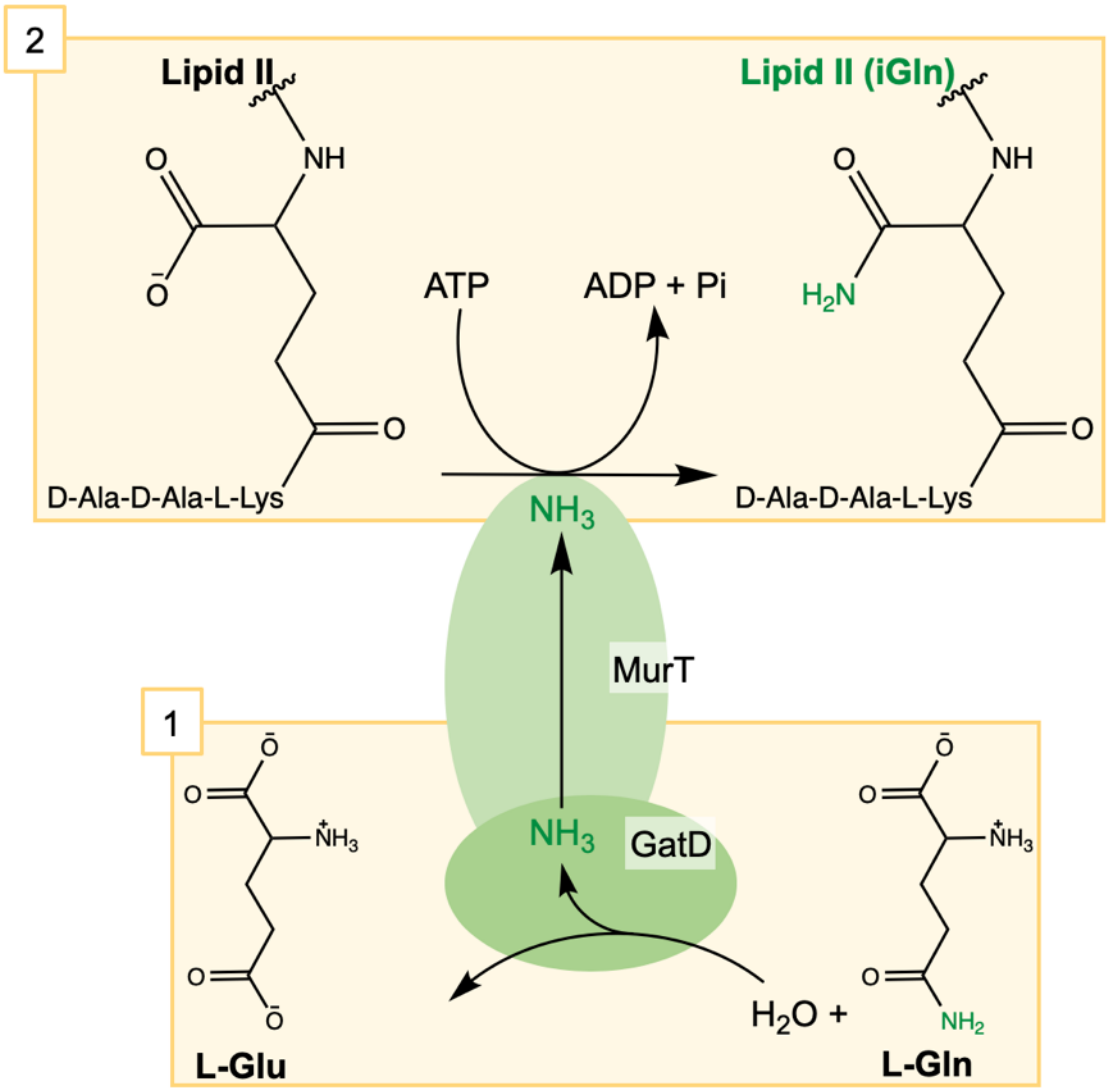

Figure 1.13 MurT/GatD amidase complex of *S. aureus* and *S. pneumoniae*. Amidation of the α-carboxylate of the stem peptide D-Glu residue is catalysed by the MurT/GatD complex, using L-glutamine as an amide donor, and ATP to activate the stem peptide Glu-carboxylate. The GatD subunit converts L-glutamine to L-glutamate and ammonia. Ammonia is then transferred to the MurT active site, for catalysis of ATP-dependent amidation. **Lipid II (iGln)**, Lipid II with γ-D-isoglutamine at the second position of the peptide stem.
Figure created with reference to Münch *et al.* (2012).

peptidoglycan by Kern *et al.* (2010) found that the carboxyl groups of D-Glu and *meso*-DAP residues in the peptide stem mediated binding of Mg^{2+} by peptidoglycan to form an intermolecular complex with teichoic acids. Amidation of *meso*-DAP in *B. subtilis* has been considered to be responsive

to growth conditions, and so Kern *et al.* (2010) suggested that this modification could be involved in allowing the supply of metal ions to be tuned to the needs of the cell.

1.6.2.2 Branched muropeptides

A second modification observed in pneumococcal PG is the linkage of additional amino acid residues to the ε-amino group of the lysyl residue of the stem peptide, yielding branched stem peptides (Severin & Tomasz, 1996; Filipe & Tomasz, 2000). When incorporated into peptidoglycan, these branched precursors generate indirect cross-links (consisting of L-Ser-L-Ala or L-Ala-L-Ala) in the PG structure (Garcia-Bustos *et al.*, 1987). Indirect cross linking has also been identified in Gram-positive bacteria including *S. aureus* and *E. faecalis* (Schleifer & Kandler, 1972; Vollmer, Blanot, *et al.*, 2008) (Figure 1.14). The composition of indirect cross links is considered a species-level characteristic, according to the diverse interpeptide bridges identified in other streptococci (Schleifer & Kandler, 1972).

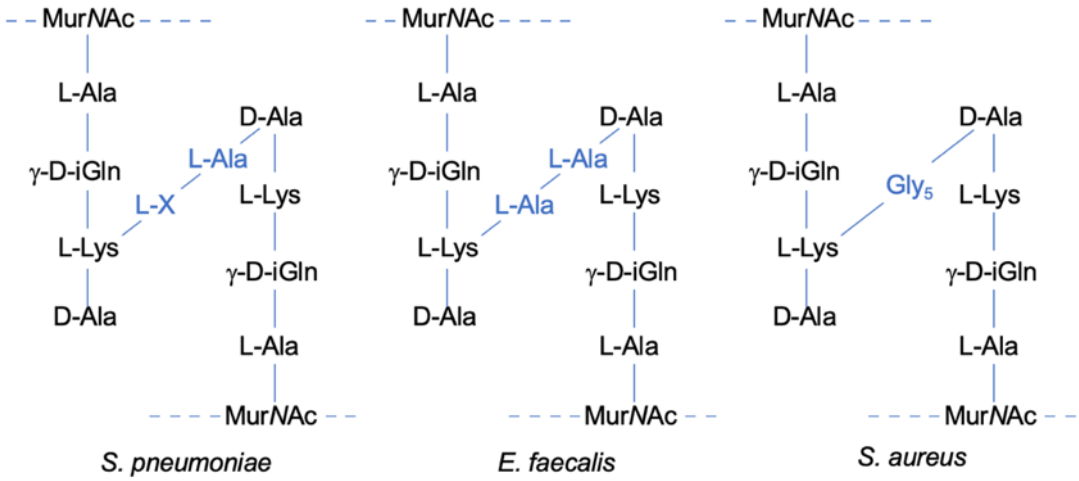

Figure 1.14 Branched muropeptides in Gram positive pathogens. The interpeptide bridge of *S. pneumoniae* is L-X-L-Ala, where **X** is L-Ala or L-Ser; in *E. faecalis* is L-Ala-L-Ala; and in *S. aureus* is an invariant pentaglycyl bridge.

The glycyl side chain on Lipid II in *S. aureus* is an essential part of the peptidoglycan precursor. FemX, the enzyme responsible for addition of the first glycine, is an essential protein, and depletion of FemX protein decreases the extent of cross linking and also sensitises the strain to methicillin (Rohrer

et al., 1999). By contrast, in pneumococci the extent and composition of indirect cross linking is variable between pneumococcal strains (Severin & Tomasz, 1996), in a manner shown to be dependent on the particular allele of MurM present (Filipe *et al.*, 2000; Filipe *et al.*, 2001). Whilst the MurMN operon is non-essential (Filipe & Tomasz, 2000), branching of muropeptides is, similarly to *S. aureus*, linked to β-lactam resistance. Both MurMN (Lloyd *et al.*, 2008) and FemXAB (Schneider *et al.*, 2004) have been demonstrated to use Lipid II and tRNAs as their substrates (Lloyd *et al.*, 2008; Schneider *et al.*, 2004). Homologues of these proteins in other organisms generate indirect cross-linking in the peptidoglycan structure, such as BppA1 and BppA2 in *Enterococcus faecalis* (generating an L-Ala-L-Ala cross-link) (Bouhss *et al.*, 2001; Bouhss *et al.*, 2002).

Whilst the physiological role of branched muropeptides in pneumococci has not been confirmed, Greene *et al.* (2015) demonstrated that the extent of branching has been shown to impact the PG hydrolase-dependent release of pneumolysin.

1.6.3 Pneumococcal β-lactam resistance

In the case of *S. pneumoniae*, high-level resistance to β-lactams involves both alteration of PBPs by homologous recombination, producing enzymes with decreased affinity for the antibiotic; and production of branched peptidoglycan intermediates.

In order for pneumococci to develop resistance to penicillin, amino acid alterations conferring low affinity to β-lactams on three of the six penicillin-binding proteins – PBP1a (a bifunctional class A PBP); and PBP2x and PBP2b (both of which are monofunctional class B PBPs) are required (Hakenbeck *et al*., 1999, Goffin and Ghuysen, 2002). This process is enabled by the natural genetic competence of pneumococci (Hakenbeck *et al.*, 1999). Transformation of pneumococci by exogeneous DNA in the pharynx has been experimentally demonstrated (Ottolenghi-Nightingale, 1972), and longitudinal study of pneumococcal isolates has also indicated that multiple horizontal gene transfer events occur between strains (Hiller *et al.*, 2010).

Particular low-affinity variants have arisen by homologous recombination of PBP alleles (Dowson *et al*., 1989), utilising exogenous DNA from related species such as *Streptococcus mitis* which the pneumococcus encounters within the oropharynx (Dowson *et al*., 1993, Dowson *et al*., 1994; Reichmann *et al.*, 1997; Chi *et al.*, 2007). Within the recombined blocks, particular mutations confer the β-lactam resistance phenotype. A genome-wide association study using large datasets of genome sequence and resistance phenotype from American and Thai pneumococcal isolates identified a common set of 71 non-synonymous single-nucleotide polymorphisms (SNPs), many within linkage blocks, associated with β-lactam non-susceptibility (Chewapreecha *et al.*, 2014). Amino acid changes were identified within the GT, TP and PASTA domains (as applicable) of each resistance-linked PBP, and those in the TP domain included previously-identified, phenotype-linked changes such as the T_{574}SQF to N_{574}TGY. In addition, amino acid alterations were identified in genes including *ciaH*, encoding a histidine kinase sensor; and *gpsB,* a cell cycle protein. The biochemical impact of particular amino acid alterations in pneumococcal PBP1a is discussed in Section 4.1.3.

The combination of asymptomatic carriage of pneumococci, and the selective pressure of β-lactam treatment, has likely contributed to the emergence of resistant pneumococcal clones (Dagan *et al.*, 1998). Nasopharyngeal colonisation in children with penicillin-resistant streptococci has been reported (Farber *et al.*, 1983; Yagupsky *et al.*, 1998; Leiberman *et al.*, 1999; Petrosillo *et al.*, 2002), which may act as a reservoir for progression to invasive pneumococcal disease (Gray *et al.*, 1980). In addition, treatment with β-lactams has been associated with selection of penicillin non-susceptible pneumococci in the nasopharyngeal flora (Dagan *et al.*, 1998; Yagupsky *et al.*, 1998).

Branched muropeptides are found in β-lactam-susceptible pneumococci, as a result of the activity of MurM and MurN. However, it has been found that the extent of peptidoglycan indirect interpeptide cross-linking generally increases in pneumococcal strains with decreased β-lactam susceptibility

(Garcia-Bustos & Tomasz, 1990), with the exception of the laboratory strain R6, which is an example of a penicillin-susceptible strain with a high degree of indirect cross linking (Smith & Klugman, 2000). In addition, the ability to synthesise branched muropeptides has been demonstrated to be an essential β-lactam resistance determinant in pneumococci; in knockout mutants of the MurMN operon, there is an increase in susceptibility to β-lactam antibiotics, as measured by minimal inhibitory concentrations (MIC) (Filipe & Tomasz, 2000; Smith & Klugman, 2000).

Based on the association of cross-linking and β-lactam resistance, J. Garcia-Bustos and Tomasz (1990) proposed that the active site remodelling that caused decreased affinity for penicillin was responsible for a shift in substrate preference for branched muropeptides. Filipe and Tomasz (2000) further suggested that branching of muropeptides was beneficial in competition for occupancy of the transpeptidase active site with β-lactams.

1.7 Aims of this thesis

Whilst the link between the requirement for both PBP modification and branched muropeptides in the pneumococcal β-lactam resistance mechanism has been well documented, it has not been possible to confirm the suspected mechanistic basis for the link between these two factors, due to challenges in obtaining the natural substrates. We aim to address the hypothesis that branching of precursors is beneficial for competition against β-lactams, by the use of a chemo-enzymatic synthesis of branched pneumococcal Lipid II variants, and the development of an *in vitro* assay for transpeptidase activity of pneumococcal PBP1a.

In order to demonstrate the impact of factors such as branching on the usage of Lipid II substrates as transpeptidase substrates, we must also analyse the impact upon glycosyltransferase activity of PBP1a. We therefore also aim to further characterise the GT activity of PBP1a under the conditions used for assays of TP activity.

Finally, key environmental factors such as the lipid environment of the enzymes could provide further links between MurMN and PBPs. An increasing body of evidence suggests that lipid environment, and particularly interaction with cardiolipin, impacts the activity of the enzymes of the peptidoglycan biosynthesis pathway. Of particular interest is the stimulation of pneumococcal MurM by cardiolipin (Dr. A.J. Lloyd, University of Warwick, unpublished). We therefore sought to compare previous observations of the impact of pneumococcal phospholipids on MurM with similar characterisation of PBP1a.

Chapter 2: Materials and Methods

2.1 Chemicals, Buffers and Solutions

Chemicals were supplied by Sigma-Aldrich (UK) or Fisher Scientific (UK) unless otherwise stated. Buffers and solutions were prepared using MilliQ purified water, and filtered using a 0.22 μm MF-Millipore Membrane Filter (Merck). Buffer solutions were adjusted to the correct pH with use of a SevenEasy pH meter (Mettler Toledo), which was calibrated at ambient temperature with pH 4.0, 7.0 and 10.01 buffer standards.

2.2 Growth and Maintenance of *Escherichia coli* strains

2.2.1 Growth Media

The following growth media were used throughout this project. All media were sterilised by autoclaving at 121 ˚C for 20 minutes (mins). Antibiotic selection was with 100 $\mu g.mL^{-1}$ ampicillin, 50 $\mu g.mL^{-1}$ kanamycin or 35 $\mu g.mL^{-1}$ chloramphenicol. Agar plates were cooled and dried in a flow cabinet, and stored at 4 ˚C. Media containing glucose were made up and sterilised by autoclaving without the glucose, and glucose was then added from a separate autoclaved stock solution, to prevent charring.

2.2.1.1 Lysogeny broth (LB) medium (Bertani, 1951)

LB medium consisted of 1 % (w/v) tryptone, 0.5 % (w/v) sodium chloride, 0.5 % (w/v) yeast extract.

2.2.1.2 LB agar plates

LB medium with 1.5 % (w/v) bacto-agar was sterilized by autoclaving at 121 ˚C for 20 mins. The solution was cooled to 50 ˚C, the appropriate antibiotics added, and plates were prepared by pouring 25 mL of the medium per sterile Petri dish.

2.2.1.3 ZY medium (Studier, 2005)

The medium was composed of 1 % (w/v) N-Z amine, 0.5 % (w/v) yeast extract.

2.2.1.4 Autoinduction medium (ZYP-5052) (Studier, 2005)

ZYP-5052 comprised ZY medium; 1 x NPS (25 mM ammonium sulfate, 50 mM potassium dihydrogen phosphate, 50 mM disodium hydrogen phosphate); and 1 x 5052 (0.5 % (v/v) glycerol, 0.05 % (w/v) D-glucose, 0.2 % (w/v) α-lactose); 1 mM magnesium sulfate. Components of the medium were mixed from autoclave-sterilised stock solutions.

2.2.1.5 Super Optimal broth with Catabolite repression (SOC) outgrowth medium

The medium was composed of 2 % (v/v) peptone, 0.5 % (w/v) yeast extract, 10 mM NaCl, 2.5 mM KCl, 10 mM $MgCl_2$, 10 mM $MgSO_4$, 20 mM glucose.

2.2.1.6 Tryptic soy broth (TSB)

The medium was composed of 17 $g.L^{-1}$ casein peptone (pancreatic), 2.5 $g.L^{-1}$ dipotassium hydrogen phosphate, 2.5 $g.L^{-1}$ glucose, 5 $g.L^{-1}$ NaCl, 3 $g.L^{-1}$ soya peptone.

2.2.1.7 TSB agar plates

TSB medium with 1.5 % (w/v) bacto-agar was sterilized by autoclaving. The solution was cooled to 50 ˚C and plates prepared by pouring 25 mL per sterile Petri dish.

2.2.1.8 Blood agar plates

Nutrient agar was sterilized by autoclaving, cooled to 50 ˚C and 5 % (v/v) defibrinated horse blood was added. Plates were prepared by pouring 25 mL per sterile Petri dish.

2.2.1.9 Cation-adjusted Mueller-Hinton Broth (Mueller et al., 1941)

The medium was composed of 17.5 $g.L^{-1}$ casein acid hydrolysate, 3.0 $g.L^{-1}$ beef extract, 1.5 $g.L^{-1}$ starch, 20-25 $mg.L^{-1}$ Ca^{2+} and 10-12.5 $mg.L^{-1}$ Mg^{2+} (both from chloride salts), pH 7.3.

2.2.2 Bacterial Strains

The strains used for DNA procedures and over-expression of proteins are given in Table 2.1.

Table 2.1 *E. coli* strains used for DNA manipulation and protein over-expression

E. coli strain	Genotype	Use in this project
NEB 5-alpha (New England BioLabs, Frankfurt, Germany)	*fhuA2 Δ(argF-lacZ)U169 phoA glnV44 Φ80Δ (lacZ)M15 gyrA96 recA1 relA1 endA1 thi-1 hsdR17*	Plasmid production
BL21 (DE3) (Studier & Moffatt, 1986)	F^- *ompT hsd*S_B (r_B^-, m_B^-) *gal dcm* (DE3)	Recombinant protein overexpression
BL21 (DE3) pRosetta (Studier and Moffatt, 1986)	F^- *ompT hsd*S_B (r_B^-, m_B^-) *gal dcm* (DE3) and pRosetta to supply tRNAs for rare codons	Recombinant protein overexpression

2.2.3 Preparation of Chemically Competent Cells for DNA Transformation

An overnight culture was prepared by inoculating 5 mL sterile LB medium (Section 2.2.1.1), plus appropriate antibiotic selection, with the required *E. coli* strain. The culture was incubated at 37 ˚C overnight with shaking at 180 rpm. 2.5 mL of the overnight culture was then used to inoculate 250 mL of sterile LB medium plus antibiotic selection and 20 mM $MgSO_4$. The 250 mL culture was incubated at 37 ˚C with shaking at 180 rpm. When the optical density (OD_{600nm}, absorbance at 600 nm) was in the range 0.4 – 0.6, the culture was

harvested by centrifugation at 4500 x g for 10 mins. The cells were washed by gentle resuspension in 100 mL ice cold TFB1 buffer (30 mM potassium acetate, 10 mM calcium chloride, 50 mM manganese chloride, 100 mM rubidium chloride, 15 % (v/v) glycerol, pH 5.8) and the suspension was incubated for 5 mins on ice, and then pelleted by centrifugation as before. The pellet was resuspended in 10 mL TFB2 buffer (10 mM MOPS pH 6.5, 75 mM calcium chloride, 10 mM rubidium chloride, 15 % (v/v) glycerol) and incubated on ice for 1 hour (h). Competent cells were stored in 50 μL aliquots flash-frozen in liquid nitrogen and subsequently stored at -80 ˚C.

2.2.4 DNA Transformation of *E. coli* strains

50 μL aliquots of competent cells were thawed on ice and then incubated with 2 μL of plasmid stock containing 50 - 100 ng of plasmid DNA for 30 mins on ice. The cells were then heat-shocked at 42 ˚C for 30 seconds (sec), and then returned to ice for 5 minutes (mins). Outgrowth was performed by addition of 950 μL SOC medium (Section 2.2.1.5), with incubation at 37 ˚C for 1 h with shaking at 180 rpm. 100 μL of the culture was then spread on an LB agar plate with the appropriate antibiotic selection, and incubated overnight at 37 ˚C.

2.3 DNA Manipulation and Cloning Techniques

2.3.1 Oligonucleotides

Oligonucleotides for cloning (Table 2.2) and for sequencing of vectors (Table 2.3) were purchased from Integrated DNA Technologies (Belgium).

2.3.2 Polymerase Chain Reaction (PCR)

PCR amplification (Mullis *et al.*, 1986) for cloning procedures was completed using Phusion High-Fidelity DNA polymerase (NEB) in accordance with the manufacturer's instructions, with use of a SureCycler 8800 thermocycler (Agilent Technologies). Annealing temperatures were determined using the NEB Tm Calculator tool (Version 1.9.13.), with further optimisation as required.

2.3.3 Agarose gel electrophoresis

1 % (w/v) agarose gels were used for separation of DNA fragments. 1 g agarose (Cleaver Scientific) per 100 mL 1 x TAE buffer (Tris-acetate EDTA: 40 mM Tris pH 8.3, 20 mM acetic acid, 1 mM EDTA) was dissolved by heating in a microwave. The solution was cooled to approximately 50 ˚C before addition of 10 μL GelRed stain (Biotium), and the solution was then poured into a gel cast to set. The gel was submerged in 1 x TAE buffer in a MultiSUB Midi Horizontal Gel System (Cleaver Scientific). 6 μL samples were made up in 1 x DNA Gel Loading Dye (NEB) and loaded into the wells. 5 μL of 1 kb or 100 bp DNA ladder (NEB) as appropriate were loaded as a size reference for sample lanes. Electrophoresis was conducted at 100 V for 1 h, and gels were visualised under ultraviolet light using a GeneSnap G:Box gel illuminator (Syngene).

2.3.4 Gel Extraction of PCR products

PCR products were purified following agarose gel electrophoresis using the Monarch DNA Gel Extraction Kit (NEB) in accordance with the manufacturer's protocol.

2.3.5 Cloning by Gibson Assembly

Primers for cloning by Gibson Assembly (Gibson *et al.*, 2009) were designed using the NEBuilder Assembly Tool (Version 1.12.13). Phusion High-Fidelity DNA polymerase (NEB, USA) was used (as previously described) for amplification of the target gene and linearization of the plasmid (see Table 2.2 for primer sequences). The NEBuilder HiFi DNA Assembly Cloning Kit (NEB, USA) was then used in accordance with the manufacturer's instructions for the assembly reaction, following which the ligated construct was transformed into NEB 5-alpha competent cells.

Table 2.2 Oligonucleotide primers used in cloning by Gibson Assembly

Primer	Sequence (5'-3')
pET46a_lin_1 (plasmid linearization)	TAAACCGGGCTTCTCCTC
pET46a_lin_2 (plasmid linearization)	ATGGTGATGGTGATGGTG
Sp_PBP1a_gibson_N (gene amplification)	TGCACCATCACCATCACCATAACAAACCAACGATTCTG
Sp_PBP1a_gibson_C (gene amplification)	TTGAGGAGAAGCCCGGTTTATTATGGTTGTGCTGGTTG

2.3.6 Preparation of plasmid DNA

NEB 5-alpha competent cells were transformed with the required plasmid (Section 2.2.4). 5 mL overnight cultures in LB medium with the appropriate antibiotic selection were inoculated with a single colony from the transformation plate. Overnight cultures were incubated at 37 ˚C with shaking at 180 rpm. Cells were pelleted by centrifugation at 1,800 x g for 10 mins (Eppendorf Centrifuge 5810R). Plasmid DNA was then purified using the Monarch Plasmid Miniprep Kit (NEB, USA) in accordance with the manufacturer's instructions.

2.3.7 Quantification of DNA

DNA samples were quantified by absorbance at 260nm using an N60 Nanophotometer (Implen), with the appropriate buffer as a blank.

2.3.8 DNA sequencing of constructs

Sanger sequencing, conducted by GATC Biotech (Germany), was used to confirm that inserts in plasmid constructs were in frame with the affinity tag, and that there were no PCR-induced mutations. Samples consisted of 500 ng plasmid DNA and 5 pmol.μL^{-1} of the relevant sequencing primer (Table 2.3). The quality of sequence reads (as shown by sequence chromatograms) was analysed using SnapGene Viewer (GSL Biotech LLC), and the clipped sequence read was translated using the ExPASy Translate tool (Artimo *et al.*, 2012). The translated sequence reads were then aligned to the desired construct amino acid sequence using the Clustal Omega Multiple Sequence Alignment program (Sievers *et al.*, 2011), to confirm the sequence of the vector and the coverage of the sequence reads.

Table 2.3. Oligonucleotide primers used for sequencing of vectors for PBP1a expression

Primer	Sequence (5'-3')
T7 promoter	TAATACGACTCACTATAGGG
T7 terminator	GCTAGTTATTGCTCAGCGG
F_upstream	ACGATGCGTCCGGCGTAGAG
Forward_1	GGGGGATTGATACCATCCG
Forward_2	GCCCAAGACCGCCGAAACTTGG
Forward_3	CTGTGGGATATTTACAATAC
Forward_4	TACTTTGGCAACATCACCTTG
Forward_5	GGGAGTGAAAAAGAGTTC
Forward_6	AAAGTTTACCGCTCTATG
Reverse_1	GGGGTTGTATTTGATTGTTG
Reverse_2	GTTGTGTTACTTGAAATG
Reverse_3	TGTTTCTACTGCTTGGTTAATTC
Reverse_4	TAAGACCAAGTTTCGGCGG
Reverse_5	GAATTGCTTTGCAGATTGCGC

2.3.9 Protein expression constructs used in this project

Details of the constructs used, and the source of each, are given in Table 2.4.

Table 2.4. Protein expression constructs used in this project

Construct	Description (strain of origin)	Selection	Source	Expression cell line
pET46a::*pbpa_D39*	N-ter. His_{12}-tagged PBP1a (*S. pneumoniae* D39)	Ampicillin	K. Abrahams (Warwick)	BL21 (DE3) pRosetta
pET46a::*pbpa_D39 S370A*	As above, but with mutation of the active site serine to alanine – S370A	Ampicillin	K. Abrahams (Warwick)	
pET46a::*pbpa_Pn16*	N-ter. His_{12}-tagged PBP1a (*S. pneumoniae* Pn16)	Ampicillin	Cloned for this project	
pET46a::*pbpa_159*	N-ter. His_{12}-tagged PBP1a (*S. pneumoniae* 159)	Ampicillin	Cloned for this project	
pET30::*pbp2a*	Untagged PBP2a (*S. pneumoniae* D39)	Kanamycin	A. Zapun (Grenoble)	
pET28::*MurA*	C-ter. His_6-tagged MurA (*E. coli*)	Kanamycin	El Zoeiby *et al.* (2001)	BL21 (DE3)
pET26a::*MurB*	C-ter. His_6-tagged MurB (*Pseudomonas aeruginosa* PAO1293)	Kanamycin	El Zoeiby *et al.* (2001)	BL21 (DE3) pRosetta
pET30a::*MurC*	C-ter. His_6-tagged MurC (*P. aeruginosa* PAO1)	Kanamycin	El Zoeiby *et al.* (2000)	
pET21b::*MurD*	C-ter. His_6-tagged MurD (*P. aeruginosa* PAO1293)	Ampicillin	El Zoeiby *et al.* (2001)	
pET21b::*MurE*	C-ter. His_6-tagged MurE (*S. pneumoniae* Pn16)	Ampicillin	Blewett *et al.* (2004)	
pPROEX-HTa::*MurF*	N-ter. His_6-tagged MurF (*S. pneumoniae* 159)	Ampicillin	Lloyd *et al.* (2008)	

2.4 Expression and Purification of Recombinant Proteins

Expression and purification of PBP1a constructs was conducted as described by Zapun *et al.* (2013), unless otherwise stated. Expression and purification of MurA-F was as described by Lloyd *et al.* (2008). MurG, IDH, and DacB proteins used in this project were kindly provided by Julie Tod and Anita Catherwood (University of Warwick).

High-speed centrifugation steps used a Beckman Coulter Avanti™ J-20 XPI centrifuge, and ultracentrifugation steps used a Beckman Coulter Optima L-90K ultracentrifuge. Both were run at 4 ˚C.

Purification columns were washed in 10 column volumes (CV) of water followed by equilibration with 10 CV of the appropriate wash buffer. For immobilised metal affinity chromatography (IMAC), the resin was washed following sample loading with 10 CV of wash buffer, to remove unbound protein (with collection of the flow-through). At completion of the purification procedure, all columns or resins were washed with 10 CV water and 10 CV 20 % (v/v) ethanol, and stored at 4 ˚C.

2.4.1 Expression by autoinduction

All PBP1a constructs were expressed by autoinduction, as described by Studier (2005). Overnight cultures in 2 mL ZYP-0.8G medium (ZY medium, 1 mM $MgSO_4$, 0.8 % (w/v) glucose, 1 x NPS) with ampicillin and chloramphenicol selection were inoculated with a single colony from a fresh transformation. Overnight cultures were incubated at 37 ˚C with shaking at 180 rpm. 1 mL of overnight culture was used to inoculate 1 L autoinduction medium (Section 2.2.1.4) plus antibiotic selection. Cultures were incubated at 25 ˚C for 22 h with shaking at 180 rpm. Cells were harvested at 10,000 x g for 20 mins and the pellet stored at -80 ˚C.

2.4.2 Expression by Isopropyl-β-D-thiogalactopyranoside (IPTG) induction

MurA-F and PBP2a were expressed by IPTG induction. 10 mL overnight cultures in LB medium plus antibiotic selection were inoculated with a single

colony from a fresh transformation. Overnight cultures were incubated at 37 ˚C with shaking at 180 rpm. The entire overnight culture was used to inoculate 1 L LB medium plus 0.8 % (w/v) glucose and antibiotic selection. Cultures were incubated at 37 ˚C with shaking at 180 rpm. Cultures were induced with 1 mM IPTG. Cultures expressing MurA-F were induced at an OD_{600nm} of 0.6 and incubated at 25 ˚C, with shaking at 180 rpm, for 4 h before harvesting. Cultures expressing PBP2a were induced at an OD_{600nm} of 2.0 and incubated overnight with shaking at 180 rpm. Cells were harvested at 10 000 x g for 20 mins and the pellet stored at -80 ˚C.

2.4.3 Purification of N-ter. His_{12}-PBP1a

2.4.3.1 Preparation of membranes containing N-ter. His_{12}-PBP1a

Cell pellets were thawed on ice and resuspended in 3 $mL.g^{-1}$ cell weight of cold phosphate buffered saline (PBS), 20 $\mu g.mL^{-1}$ DNase and 1 mM $MgCl_2$. The cell suspension was incubated with agitation at 4 ˚C for 1 h. Cells were then lysed by passing twice through a continuous cell disrupter (Constant Cell Disruption Systems) at 28 kpsi at 4 ˚C. Cell debris was pelleted by two consecutive centrifugation steps at 24,000 x g for 12 mins at 4 ˚C. Membranes were then pelleted by ultracentrifugation at 150,000 x g for 1 h at 4 ˚C. The membrane pellet was resuspended in 10 mL of cold phosphate buffered saline (PBS, pH 7.4) per litre of original culture using a glass homogeniser (Scientific Laboratory Supplies) and stored at -20 ˚C overnight.

2.4.3.2 Solubilisation of N-ter. His_{12}-PBP1a

The suspension was thawed on ice, and sodium deoxycholate added to a 1 % (w/v) final concentration to solubilise membrane proteins. This step was carried out with incubation at 4 ˚C for 3 h with agitation. The suspension was then diluted 7-fold into cold PBS with 0.1 % (w/v) *N*-dodecyl β-D-maltoside (DDM), and insoluble material was pelleted by ultracentrifugation at 150,000 x g for 30 mins at 4 ˚C.

2.4.3.3 Immobilised metal affinity chromatography (IMAC) purification

The supernatant from Section 2.4.3.2 was incubated for 3 h at 4 ˚C with 5 mL of TALON Metal Affinity Resin (Clontech) pre-equilibrated in 10 CV Buffer A (PBS with 0.1 % (w/v) DDM and 150 mM NaCl). The resin suspension was poured into an Econo-Pac Chromatography Column (BioRad) to form a column, and the unbound material washed from the resin in Buffer A, developed by gravity flow. The purification was then conducted by stepwise elution in PBS with 0.1% (w/v) DDM and 150 mM NaCl plus the relevant concentration of imidazole. The elution steps were 100 mL of 15mM imidazole, collected as 10 mL fractions; 50 mL of 50 mM imidazole, collected as 5 mL fractions; and 50 mL of 250 mM imidazole, collected as 5 mL fractions.

2.4.3.4 Gel filtration and final storage

Fractions containing PBP1a (as determined by sodium dodecyl sulfate - polyacrylamide gel electrophoresis (SDS-PAGE), Section 2.5.1) were pooled and concentrated to 20 $mg.mL^{-1}$ (see protein concentration determination Section 2.5.2.1) using a 20 mL Vivaspin 100 kDa molecular weight cut-off (MWCO) centrifugal concentrator (Sartorius) at 3,000 x g at 4 ˚C in a bench-top centrifuge (Eppendorf Centrifuge 5810R). 500 μL samples were purified by gel filtration using a Superose 6 10/300 GL column (GE Healthcare) pre-equilibrated in 1.5 CV 20 mM 4-(2-hydroxyethyl)piperazine-1-ethanesulfonic acid (HEPES) pH 7.5, 150 mM NaCl and 0.03 % (w/v) DDM, on an AKTA 10/100 system (GE Healthcare) in a cold cabinet at 4 ˚C. The column was developed in 1 CV of the same buffer at 0.4 $mL.min^{-1}$, with collection of 0.5 mL fractions. Protein elution was followed by absorbance at 280 nm, and fractions containing PBP1a at high purity (as determined by SDS-PAGE) were pooled and concentrated to 16 $mg.mL^{-1}$ using a 100 kDa MWCO centrifugal concentrator (as previous). Stocks were then diluted with equal volume 100 % glycerol to give a final stock at 8 $mg.mL^{-1}$ in 10 mM HEPES pH 7.5, 75 mM NaCl, 0.015 % (w/v) DDM and 50 % (v/v) glycerol. Aliquots of protein were stored at -20 ˚C.

2.4.4 Purification of MurA-F

Frozen cell pellets were thawed on ice and resuspended in 3 mL.g^{-1} cell weight of resuspension buffer (50 mM HEPES pH 7.5, 1 mM $MgCl_2$, 2 mM β-mercaptoethanol, 2.5 mg.mL^{-1} lysozyme, 1 μM pepstatin, 1 μM leupeptin and 0.2 mM phenylmethane sulfonyl fluoride (PMSF)). Following incubation at 4 ˚C for 10 mins, cells were lysed by sonication on ice using a Bandelin Sonoplus sonicator, with 10 bursts of 15 sec at 70 % power. Cell debris was pelleted by centrifugation at 10,000 x g for 15 mins, and the supernatant clarified by a further centrifugation step at 50,000 x g for 45 mins. The supernatant was loaded to a 5 mL HisTrap HP (GE Healthcare) IMAC column at 2 mL.min^{-1} using a P-1 peristaltic pump (Pharmacia Biotech). The column was then connected to an AKTA Pure system (GE Healthcare) and washed with 10 CV Buffer A (50 mM HEPES pH 7.5, 1 mM $MgCl_2$, 500 mM NaCl, 5 % (v/v) glycerol, 10 mM imidazole, 1 μM pepstatin, 1 μM leupeptin and 0.2 mM PMSF) at 3 mL.min^{-1} to remove unbound material. The column was then developed over a linear gradient of 10 mM to 1 M imidazole (100 % Buffer A to 100 % Buffer B. Buffer B: 50 mM HEPES pH 7.5, 1 mM $MgCl_2$, 500 mM NaCl, 5 % (v/v) glycerol, 1M imidazole, 1 μM pepstatin, 1 μM leupeptin and 0.2 mM PMSF) over 40 mins, with collection of 5 mL fractions. The A_{280nm} was continuously monitored to identify protein peaks eluted from the column. Fractions were analysed by SDS-PAGE, and those containing the protein of interest were dialysed into 50 mM HEPES pH 7.5, 1 mM $MgCl_2$, 50 mM NaCl, 3 mM DTT, 50 % (v/v) glycerol, 1 μM pepstatin, 1 μM leupeptin and 0.2 mM PMSF, overnight at 4 ˚C (dialysis tubing: 15.9 mm diameter, 12-14 kDa MWCO (Medicell International)). Protein stocks were then quantified by BioRad assay (Section 2.5.2.2) and stored as aliquots at -80 ˚C.

2.4.5 Purification of untagged *S. pneumoniae* PBP2a

2.4.5.1 Isolation of solubilised membrane proteins

PBP2a was purified based upon the method described in Helassa *et al.* (2012) with modifications. Cell pellets were thawed on ice and resuspended in 40 mL.L^{-1} original culture of resuspension buffer (50 mM HEPES pH 7.5, 100 mM

NaCl, 10 mM $MgCl_2$, 20 μg.mL^{-1} DNase and one cOmplete Protease Inhibitor Cocktail tablet (Roche)). The cell suspension was incubated at 4 ˚C with agitation for 10 mins, followed by lysis by passage twice through a continuous cell disrupter (Constant Cell Disruption Systems) at 28 kpsi at 4 ˚C. Membrane proteins were solubilised by addition of 1 % (w/v) Triton X-100, with incubation at 4 ˚C with agitation for 2 h. Insoluble material was then pelleted by centrifugation at 20,000 x g for 30 mins at 4 ˚C.

2.4.5.2 Purification of PBP2a by cation and anion exchange chromatography

A 5 mL HiTrap SP HP cation exchange column (GE Healthcare) was washed with 10 CV water, 10 CV cation-Buffer B^{PBP2a} (50 mM Tris pH 8.0, 10 mM $MgCl_2$, 0.2 % (w/v) Triton X-100, 1 M NaCl) and finally equilibrated in cation-Buffer A^{PBP2a} (50 mM Tris pH 8.0, 10 mM $MgCl_2$, 0.2 % (w/v) Triton X-100). The membrane suspension was then loaded to the column at 3 mL.min^{-1} via a 150 mL Superloop (GE Healthcare) on an AKTA 10/100 system (GE Healthcare) in a cold cabinet at 4 ˚C. The column was developed at the same flow rate on a gradient from 0 – 1 M NaCl (in the buffers previously described) over 10 CV, with collection of 2.5 mL fractions. Elution of protein was followed by A_{280nm}. Fractions containing PBP2a (as determined by SDS-PAGE) were diluted 10-fold for loading to a 6 mL RESOURCE Q anion exchange column (GE Healthcare). The column was prepared as described for the cation exchange column, though with alternative buffers (anion-Buffer A^{PBP2a}: 50 mM HEPES pH 7.5, 10 mM $MgCl_2$, 0.2 % (w/v) Triton X-100, cation-Buffer B^{PBP2a}: Buffer A plus 1 M NaCl). The sample was loaded as described previously, and the column developed using a linear gradient from 0 – 100 % cation-Buffer B^{PBP2a} (in the buffers previously described) over 10 CV at a flow rate of 6 mL.min^{-1}, with collection of 1 mL fractions. Fractions containing PBP2a (as determined by SDS-PAGE) were concentrated using a 20 mL Vivaspin 50 kDa molecular weight cut-off (MWCO) centrifugal concentrator (Sartorius) at 3000 x g in a bench-top centrifuge (Eppendorf Centrifuge 5810R). Stocks of PBP2a at 8 mg.mL^{-1} were flash-frozen in aliquots and stored at -80 ˚C.

2.5 Analysis of purified recombinant proteins

2.5.1 Sodium dodecyl sulfate - polyacrylamide gel electrophoresis (SDS-PAGE)

Protein samples were visualised under denaturing conditions by sodium dodecyl sulfate - polyacrylamide gel electrophoresis (SDS-PAGE) in a discontinuous Tris-glycine buffer system (Laemmli, 1970). Protein samples were mixed with 1 x protein loading dye (6 x stock contained 63.5 mM Tris pH 6.8, 0.4 % (w/v) sodium dodecyl sulfate (SDS), 5 % (v/v) β-mercaptoethanol, 20 % (v/v) glycerol and 2.5 % (w/v) bromophenol blue) and heat-denatured at 60 ˚C for 10 mins using an Aviso Mechatronic Systems Primus thermocycler. 12 % acrylamide:bis-acrylamide (37.5:1) gels were cast using a Mini-PROTEAN Tetra System gel kit (Bio-Rad). 5 mL resolving gel (375 mM Tris pH 8.8, 12% acrylamide:bis-acrylamide (37.5:1), 0.4 % (w/v) SDS) was polymerised with 100 μL of 10 % (w/v) ammonium persulfate (APS), and 10 μL *N,N,N′,N′*-tetramethylethane-1,2-diamine (TEMED). The gel was overlaid with 100 % ethanol to create a level top, and the ethanol was poured off once the gel had set. 2 mL stacking gel (125 mM Tris pH 6.8, 4 % acrylamide:bis-acrylamide (37.5:1), 0.1 % (w/v) SDS) was polymerised with 50 μL of 10 % (w/v) APS and 10 μL TEMED, and was then poured on top of the resolving gel, with insertion of a plastic comb to create wells.

Samples were pipetted into the wells, with a control lane containing Color Prestained Protein Standard, Broad Range (NEB) molecular weight markers to estimate molecular weight of the protein bands. Gels were run in SDS-PAGE running buffer (25 mM Tris pH 8.3, 0.19 M glycine, 0.1 % (w/v) SDS) at 180V until the dye front reached the bottom of the gel (or until the relevant protein markers showed sufficient separation). Protein bands were stained using InstantBlue Protein Stain (Expedeon), and gels were then washed in water and visualised using an ImageQuant LAS 4000 instrument (GE Healthcare).

2.5.2 Protein quantification

2.5.2.1 Quantification by A_{280nm}

Protein concentrations were quantified using an N60 Nanophotometer (Implen). The appropriate buffer was used as a blank, and then a 1 μL sample was analysed. The A_{280nm} reading (path length (l) of 1 cm) was used to calculate the protein concentration using the formula:

$$Protein\ concentration\ (mg\ .mL^{-1}) = A_{280nm} \times \varepsilon_{prot}$$

Where ε_{prot} is the protein factor, calculated by:

$$\varepsilon_{prot} = \frac{molecular\ weight\ (Da)}{Molar\ extinction\ coefficient\ at\ 280nm\ (M^{-1}cm^{-1}) \times l\ (cm)}$$

Parameters of molecular weight and extinction coefficient at 280nm were derived for each protein using the ExPASy ProtParam online tool (Artimo *et al.*, 2012).

2.5.2.2 Bio-Rad protein assay

The Bio-Rad protein assay was used for quantification of MurA-F protein stocks. In triplicate, 10 μL of protein sample was mixed with 990 μL Protein Assay Dye Reagent Concentrate (Bio-Rad) diluted to working concentration in water, and the mixture incubated at room temperature for 5 mins. The absorbance of each sample was read at 595nm using a Jenway 7305 UV-visible spectrophotometer. Protein concentration was then calculated using the formula;

$$\mu g\ .mL^{-1}\ protein = \frac{Mean\ A_{595nm}}{0.1} \times 1.95 \times \frac{1000}{sample\ volume\ (\mu L)} \times dilution\ factor$$

Where an absorbance of 0.1 was realised by 1.95 μg protein within the absorbance range of 0 – 0.6 at 595 nm, as derived from a calibration curve constructed using bovine serum albumin.

2.5.2.3 Bicinchoninic acid (BCA) assay

Protein stocks containing detergents were quantified using the Micro BCA Protein Assay Kit (Thermo Scientific) in accordance with the manufacturer's

instructions. Reactions were assembled in a clear 96-well plate, and A_{562nm} was read using a CLARIOstar plate reader (BMG LABTECH).

2.6 Synthesis of Peptidoglycan Intermediates

Dansylated lipid II variants were kindly provided by Julie Tod (University of Warwick).

2.6.1 UDP-Mur*N*Ac peptides

UDP-Mur*N*Ac peptide intermediates were synthesised enzymatically as described by Lloyd *et al.* (2008), although with inclusion of D-isoGln for incorporation into the second position of the peptide stem. This allowed generation of 100 % amidated UDP-Mur*N*Ac peptides.

2.6.1.1 Synthesis of UDP-MurNAc peptides

2 mL reactions contained 50 mM HEPES pH 7.5, 10 mM $MgCl_2$, 200 mM PEP, 1 mM dithiothreitol (DTT), 50 mM KCl, 8.22 mM uridine 5' diphospho-*N*-acetylglucosamine (UDP-Glc*N*Ac), 1.2 μM MurA, 57.3 μM MurB, 0.2 mM $NADP^+$, 1.47 units.mL^{-1} isocitrate dehydrogenase (Sigma-Aldrich), 26 mM DL-isocitrate, 6 mM ATP, 5.53 units.mL^{-1} pyruvate kinase (Sigma-Aldrich), 4.3 μM MurC, 35 mM L-Ala, 1.1 μM MurD, 105 mM D-isoGln, 4.0 μM MurE, 35 mM L-Lys, 8.5 μM MurF, 35 mM D-alanyl-D-alanine. Syntheses were incubated at 37 ˚C overnight, and then diluted with 5 mL of sterile water prior to filtration using a 20 mL Vivaspin 10 kDa MWCO centrifugal concentrator. Filtered samples were diluted into 100 mL sterile water.

2.6.1.2 Synthesis of UDP-MurNAc 3P (iGln)

UDP-Mur*N*Ac 3P (iGln) was synthesised as described for UDP-Mur*N*Ac 5P (iGln), but with omission of MurF and D-alanyl-D-alanine.

2.6.1.3 Purification of UDP-MurNAc peptides

UDP-Mur*N*Ac peptides were purified by anion exchange using a 75 mL column of Source30Q resin (GE Healthcare) on an AKTA Pure system (GE Healthcare). The column was washed with 10 CV water, cleaned with 1 M

ammonium acetate pH 7.6, and finally equilibrated in 10 mM ammonium acetate pH 7.6. The synthesis reaction was loaded on to the column and unbound material washed off with 100 mL of 10 mM ammonium acetate. The column was developed at 10 mL.min^{-1} by a linear gradient of 10 mM to 1 M ammonium acetate (both at pH 7.6) over 120 mins, with collection of 10 mL fractions. Elution of the desired products was followed by monitoring absorbance at 280 nm, 254 nm and 218 nm. Fractions containing the desired product were pooled and lyophilised 5 times in a 500 mL round-bottomed flask to remove ammonium acetate. 6 mL of sterile water was used to transfer the lyophilised, powdered product to a 15 mL falcon tube, followed by 2 further rounds of freeze drying. The product was finally resuspended in 1 mL sterile water and stored at -80 ˚C.

2.6.2 Synthesis of UDP-Mur*N*Ac 4P (iGln) using DacB

UDP-Mur*N*Ac 4P (iGln) was synthesised from UDP-Mur*N*Ac 5P (iGln) by cleavage of the terminal D-Ala using the D,D-carboxypeptidase DacB. In a final volume of 2 mL, 10 mg UDP-Mur*N*Ac 5P (iGln) was incubated with 2 mg purified recombinant DacB in 50 mM HEPES pH 7.6, 10 mM $MgCl_2$ overnight at 37 °C. Reactions were then purified as described by in Section 2.6.1.3.

2.6.3 Acid hydrolysis for synthesis of Mur*N*Ac peptides

Mur*N*Ac peptides were synthesised from UDP-Mur*N*Ac peptides by acid hydrolysis to remove the UDP group. To 10 mg of UDP-Mur*N*Ac peptide, 1 M HCl was added for 0.1 M final concentration (pH 1). The sample was boiled at 99 °C for 30 mins, and then neutralised to pH 7.5 by addition of 1M NaOH.

The reactions were purified by anion exchange chromatography using a MonoQ HR 10/10 column (GE Healthcare). The column was washed with 10 CV water, cleaned with 1 M ammonium acetate pH 7.6, and finally equilibrated in 10 mM ammonium acetate pH 7.6. Elution of the desired products was followed by monitoring absorbance at 280 nm, 254 nm and 218 nm, and 500 μL fractions were collected. The acid hydrolysis reaction was diluted to 5 mL and loaded on to the column via a 5 mL loop. Mur*N*Ac peptide compounds eluted in the column flow through. The column was then developed at 3

mL.min^{-1} by a linear gradient of 10 mM to 1 M ammonium acetate (both at pH 7.6) over 16 mins, with collection of 500 μL fractions. Fractions containing the desired product were pooled and lyophilised 5 times in a 15 mL falcon tube to remove ammonium acetate. The product was finally resuspended at 0.2 mM in sterile water and stored at -80 ˚C.

2.6.4 Synthesis of Donor-only UDP-Mur*N*Ac Pentapeptides

Donor-only UDP-Mur*N*Ac pentapeptides were made either enzymatically or chemically, and the products of both reaction schemes were purified as described in Section 2.6.1.2. Enzymatic synthesis was by the reaction described in Section 2.6.1.1, but with inclusion of 35mM L-arginine or ε-dimethyl-L-lysine for incorporation into the third position of the pentapeptide stem by MurE.

Chemical synthesis of donor-only UDP-Mur*N*Ac pentapeptide was by acetylation of iGln UDP-Mur*N*Ac pentapeptide with acetic anhydride. A stock of iGln UDP-Mur*N*Ac pentapeptide was first buffer exchanged into sodium hydrogen carbonate using a 75 mL column of Source30Q resin (GE Healthcare) on an AKTA Pure system (GE Healthcare). The column was washed with 10 CV of water, cleaned with 500 mM sodium hydrogen carbonate, and finally equilibrated in 10 mM sodium hydrogen carbonate. The iGln UDP-Mur*N*Ac pentapeptide stock was loaded to the column via a 1 mL loop, and the column was washed with 300 mL of 10 mM sodium hydrogen carbonate to ensure removal of residual ammonium acetate. The compound was eluted in a single step at 500 mM sodium hydrogen carbonate, with collection of 10 mL fractions. Fractions containing iGln UDP-Mur*N*Ac pentapeptide were distributed into 6 mL aliquots in glass bijoux tubes and incubated overnight with a 40-fold molar excess of acetic anhydride, at room temperature with stirring. Each 6 mL aliquot was diluted into 100 mL and purified as described in Section 2.6.1.2.

2.6.5 Desalting of iGln UDP-Mur*N*Ac pentapeptide

Residual ammonium acetate was removed from iGln UDP-Mur*N*Ac pentapeptide stocks by gel filtration on a Biogel P2 resin (Bio-Rad) column (89

cm length x 2.6 cm diameter). The column was equilibrated with 2 CV of sterile water at 1 mL.min^{-1}, and then the sample was loaded via a 500 μL injection loop. The column was developed over 1 CV in sterile water, with collection of 10 mL, where the eluate was monitored by absorbance at 280 nm, 254 nm and 218 nm. Fractions containing the desired product were concentrated by lyophilisation, resuspended in a small volume of sterile water and stored at -80 ˚C.

2.6.6 Synthesis of branched iGln UDP-Mur*N*Ac peptides

UDP-Mur*N*Ac (iGln) compounds with branched stem peptides were synthesized in a carbodiimide coupling reaction as described by De Pascale *et al.* (2008). 90 μmol 1-ethyl-3-(3-dimethylaminopropyl) carbodiimide (EDC), 60 μmol *N*-hydroxysuccinimide (HOSu) and 24 μmol of the relevant 9-fluorenylmethyloxycarbonyl (Fmoc)-protected amino acid or dipeptide were combined in 2 mL of 80% (v/v) acetonitrile and stirred at room temperature for 1 h. The pH was then adjusted to 10 with 0.5 M sodium bicarbonate buffer, followed by addition of 2 μmol of iGln UDP-Mur*N*Ac Lys5P. After stirring for 3 h, the product was deprotected with 100 μl piperidine with incubation for 1 h, and the reaction was then quenched by addition of 20 mL of water. The reaction mixture was filtered through a Minisart syringe filter (Sartorius), and solvents were removed by rotary evaporation using a Buchi R-210 Rotavapor. The dried product was then resuspended in 20 mL of water and freeze-dried overnight, then resuspended in 200 mL of 10 mM ammonium acetate buffer adjusted to pH 7.6 and purified on a gradient up to 1 M ammonium acetate over 80 mins at 4 mL.min^{-1} using a MonoQ HR 10/10 column (GE Healthcare), with collection of 4 mL fractions. Fractions containing the desired product were pooled and lyophilised 5 times in a 500 mL round-bottomed flask to remove ammonium acetate. 6 mL sterile water was used to transfer the lyophilised, powdered product to a 15 mL falcon tube, followed by 2 further rounds of freeze drying. The product was finally resuspended in 0.5 mL sterile water and stored at -80 ˚C.

2.6.7 Synthesis of Fmoc-dipeptides by solid-phase peptide synthesis

Dipeptides were synthesized by solid phase peptide synthesis. 500 mg Fmoc-amino acid-Wang resin (Sigma Aldrich) was swollen in 10 mL dimethylformamide (DMF) (Fisher) in an Econo-Pac Chromatography Column (BioRad) for 1 h. After removal of the DMF by vacuum, the amino acid on the resin was deprotected by addition of 10% (v/v) piperidine in DMF, with incubation for 5 mins at room temperature. The resin was washed twice with DMF, and the deprotection step repeated. Following the second deprotection, the resin was washed 4 times with 10 mL of DMF and 4 times with 10 mL dichloromethane (DCM). For coupling of L-Alanine to the amino acid of the resin, 1 mmol of Fmoc-Ala-OH (Sigma), 1 mmol of *N*-[(Dimethylamino)-1*H*-1,2,3-triazolo-[4,5-*b*]pyridin-1-ylmethylene]-*N*-methylmethanaminium hexafluorophosphate *N*-oxide **(**HATU) and 350 μL of *N,N*-Diisopropylethylamine (DIPEA) were added to the resin and incubated at room temperature overnight with agitation.

The resin was then washed with 40 mL each of DMF, DCM and methanol (using 10ml volumes at each step). The dipeptide product was cleaved from the resin by two rounds of incubation in 4.5 mL of 90 % (v/v) trifluoroacetic acid (TFA) for 1 h at room temperature with shaking, where the cleaved product was decanted after each incubation into a 50 mL round bottomed flask. The product was then precipitated (with chloroform in the case of Fmoc-L-Ala-L-Ser, and diethyl ether in the case of Fmoc-L-Ala-L-Ala), and the solvent was removed by rotary evaporation on a Buchi R-210 Rotavapor. Finally, the product was dissolved in a minimal volume of 3:1 methanol:water and transferred to a 7 mL universal tube. The stock was desiccated to yield dry product, which was stored at -20 ˚C.

2.6.8 Analysis of UDP-Mur*N*Ac Peptides

2.6.8.1 Quantification by A_{260nm}

UDP-Mur*N*Ac peptide stocks were quantified by absorbance at 260 nm, using a Jenway 7305 UV-visible spectrophotometer. 198 μL of sterile water was used as a blank, to which 2 μL of the sample, was subsequently added, mixed

by pipetting and A_{260nm} (with 1 cm path length) was determined. The mean value from triplicate readings was used to calculate the concentration of the UDP-Mur*N*Ac peptide stock using the following formula, where the molar extinction coefficient of uridine was 10,000 $M^{-1}.cm^{-1}$ at 260 nm (Dawson *et al.*, 1969).

$$Concentration\ (M) = \frac{Mean\ A_{260nm}}{\varepsilon\ (uridine)} \times \frac{Volume\ in\ cuvette}{Sample\ volume} \times dilution factor$$

2.6.8.2 Analysis of purity by analytical anion exchange chromatography

Purity of UDP-Mur*N*Ac peptides was assessed by analytical anion exchange, using a MonoQ HR 5/50 column (GE Healthcare). The column was washed with 10 CV water and 10 CV 1 M ammonium acetate pH 7.6 and then equilibrated in 10 CV 10 mM ammonium acetate pH 7.6. A 1000-fold diluted sample in 500 μL was loaded onto the column via a 1 mL loop, and chromatographed on a gradient of 10 mM to 1 M ammonium acetate buffer pH 7.6. Purity was estimated from integration of the peaks observed (using the Unicorn analysis software) by absorbance at 254 nm (the absorbance maximum corresponding to peptide bonds), with purity calculated using the formula:

$$Purity\ \ of\ UDP\ MurNAc\ peptide\ (\%) = \frac{Area\ under\ UDPMurNAc\ peptide\ peak}{Total\ area\ under\ peaks}$$

2.6.9 Synthesis of Lipid-linked Peptidoglycan Intermediates

Lipid (undecaprenyl phosphate)-linked peptidoglycan intermediates were synthesized as described by Breukink *et al.* (2003), using *Micrococcus flavus* membranes to supply MraY and MurG for assembly of Lipid II from UDP-Mur*N*Ac pentapeptide, undecaprenyl phosphate, and UDP-Glc*N*Ac.

2.6.9.1 Isolation of M. flavus membranes

A sample of *M. flavus* from a glycerol stock was streaked to allow isolation of single colonies on a TSB agar plate and incubated overnight at 37 ˚C. Cultures of 15 mL TSB medium were inoculated with a single colony each from the plate, and were incubated overnight at 37 ˚C with shaking at 180 rpm. Cultures of 800 mL TSB medium were supplemented with 4 mL of 20 % (w/v) glucose

and were inoculated with 15 mL of overnight culture and incubated at 37 ˚C with shaking at 180 rpm. Cultures were harvested at 10,000 x g for 20 mins at 4 ˚C when the OD_{600} reached 8.0, or if they appeared to be exiting log phase. Cell pellets were washed by resuspension in 100 mL of resuspension buffer (20 mM Tris.HCl pH 7.5, 1 mM $MgCl_2$, 2 mM β-mercaptoethanol) per litre of original culture, followed by a further centrifugation step at 15,000 x g for 20 mins at 4 ˚C. The cell pellets were then stored at -20 ˚C.

Cell pellets were thawed on ice and resuspended in 3 $mL.g^{-1}$ of resuspension buffer, followed by addition of 2.5 $mg.mL^{-1}$ lysozyme. The cell suspension was incubated at 4 ˚C for 20 mins with agitation. Cells were then lysed by passing twice through a continuous cell disrupter (Constant Cell Disruption Systems) at 30 kpsi at 4 ˚C. Cell debris was pelleted by centrifugation at 10,000 x g for 1 h. The membranes were then pelleted by ultracentrifugation at 75,000 x g for 1 h. Membranes were resuspended in a minimal volume of the supernatant and stored as 2 mL aliquots at -80 ˚C.

2.6.9.2 Synthesis of Lipid II

A 3.5 mL Lipid II synthesis reaction (of Lipid II (iGln) or Lipid II 3P (iGln)) contained 0.1 M Tris pH 8.0, 5 mM $MgCl_2$, 1 % (w/v) Triton X-100, 6 mM UDP-Glc*N*Ac, 4mM UDP-Mur*N*Ac peptide, 4.5 μmol undecaprenyl phosphate (Larodan), and 0.57 $mg.mL^{-1}$ MurG. Analytical scale Lipid II synthesis reactions were conducted in 200 μL. Reactions were incubated overnight at 37 ˚C.

2.6.9.3 Purification of iGln Lipid II (L-Lys)

The reaction was transferred to a test tube and mixed with 1 volume 6 M pyridinium acetate and 2 volumes *N*-butanol, followed by centrifugation at 3,000 x g for 10 mins at 4 ˚C. This resulted in partition of the suspension into organic and aqueous phases. The organic upper phase was transferred to a fresh test tube and mixed with 1 volume sterile water, followed by centrifugation at 3,000 x g for 10 mins at 4 ˚C. The organic upper phase of this separation was then transferred to a 50 mL round-bottomed flask, and solvents removed by rotary evaporation (Buchi R-210 Rota-vapor). The dried

mixture was resuspended in 6 mL of Solvent A (2:3:1 (v/v) chloroform:methanol:water).

The synthesis reaction was then chromatographed by anion exchange on a DEAE Sephacel resin (GE Healthcare) column. The column was formed in a glass burette with glass wool as a filter at the spout. A 4 mL bed volume of resin was used for 3.5 mL reactions, and this was scaled as defined in the text for smaller-scale reactions. The resin was prepared by washing with 10 CV 1 M ammonium acetate and 15 CV water, and then equilibrated in 10 CV Solvent A. The sample was then loaded to the column, followed by a wash of 3 CV Solvent A. The column was then developed over a stepwise elution in 12 mL washes of 8.3, 9.2, 10.0, 10.8, 11.7, 12.5, 13.3, 14.2, 15.0, 15.8, 16.7, 25.0, 33.3, 41.7, 50.0, 83.3 and 166.7 mM ammonium bicarbonate in Solvent A. 400 μL samples of each fraction were desiccated overnight and were then resuspended in 25 μL of fresh Solvent A. These samples were analysed by thin-layer chromatography (TLC) using silica 60-coated ALUGRAM® Xtra SIL G plates (Macherey-Nagel) run in 44:88:10:1 (v/v) chloroform:methanol:water:ammonia mobile phase at room temperature, until the solvent front was within 1 cm of the top of the plate. TLC plates were stained in iodine vapour and imaged using a scanner.

Fractions containing the desired lipid product were pooled in a 50 mL round-bottomed flask and dried by rotary evaporation (Buchi R-210 Rota-vapor), followed by 5 rounds of lyophilisation against water to remove ammonium bicarbonate. The product was then resuspended in 1.5 mL of Solvent A and stored at -80 ˚C.

2.6.9.4 Quantification of Lipid II stocks by phosphate release

Lipid II stocks were quantified based on cleavage and assay of the phosphate moiety. Two 50 μL samples were taken of the Lipid stock, and one of the Solvent A used to resuspend the Lipid II. Samples were dried in 0.5 mL low-binding Eppendorf tubes under nitrogen gas, and resuspended in 50 μL 50 mM HEPES pH 7.6, 10 mM $MgCl_2$, 30 mM KCl, 1.5 % (w/v) 3-[(3-cholamidopropyl)dimethylammonio]-1-

propanesulfonate (CHAPS). One Lipid sample was then set aside as a non-hydrolysed control. To the other Lipid sample and the Solvent A sample were added 50 μL 1 M HCl, and the samples were boiled at 100 ˚C for 30 mins. 1 M NaOH was then used to adjust the samples to pH 7.6.

The inorganic phosphate in the samples (released by acid hydrolysis) was then quantified by use of a phosphate release assay. In a crystal quartz cuvette, 200 μL reactions were assembled comprising 50 mM HEPES, 10 mM $MgCl_2$, 5 $U.mL^{-1}$ purine nucleoside phosphorylase (PNP), 5 $U.mL^{-1}$ inorganic pyrophosphatase (IPP), 200 μM 7-methyl-6-thioguanosine (MESG) (Berry and Associates) and monitored at 360nm using a Varian Cary 100 spectrophotometer at 37 ˚C. After establishing a stable baseline (3 mins), 10 μL of the sample was added and the ΔA_{360nm} was recorded until the reaction reached completion.

IPP releases phosphate from inorganic pyrophosphate generated by the acid hydrolysis of the samples. PNP catalyses the P_i-dependent conversion of MESG to ribose-1-phosphate and 7-methyl-6-thioguanine. The latter product absorbs strongly at 360nm, with a Δ molar extinction coefficient of 10,000 $M^{-1}.cm^{-1}$ relative to MESG which has a residual absorbance at this wavelength. This parameter was therefore used to convert the mean ΔA_{360nm} readings from triplicate samples into μM lipid concentrations by first calculating the phosphate concentrations in the hydrolysed and unhydrolyzed samples;

$$[P_i]\ \mu M = \frac{mean\ \Delta A_{360nm}}{10000} \times 10^6 \times \frac{Vol.\ in\ cuvette}{Sample\ vol.} \times \frac{Total\ vol.\ of\ sample}{50}$$

Where the total volume of sample refers to that following pH adjustment. The lipid concentration in the stock was then calculated, with correction for background phosphate and the presence of two P_i per Lipid II molecule, using the formula:

$$[Lipid]\ \mu M = \frac{[P_i]\ hydrolysed - [P_i]\ unhydrolysed - [P_i]\ SolA}{2}$$

2.6.10 Mass Spectrometry

All peptidoglycan intermediates were analysed by negative ion nano-spray time of flight (TOF) mass spectrometry using a SYNAPT G2-Si instrument (Waters), to verify the compounds synthesised by comparison of observed and

expected masses. The instrument was calibrated in negative ion mode with sodium iodide over a mass to charge ratio range of 200-2500. Samples were diluted into 70 % (v/v) methanol and 30 % (v/v) 25 mM ammonium acetate for lipid-linked intermediates; and 50 % (v/v) acetonitrile for UDP-Mur*N*Ac and Mur*N*Ac-peptides. Sample injection was via a thin wall nanoflow capillary (Waters) at a capillary voltage of 2.0 kV. Data were collected and analysed using Waters Mass Lynx software, by Dr. Adrian Lloyd, Julie Tod or Anita Catherwood (all University of Warwick).

2.7 Biochemical Assays

2.7.1 SDS-PAGE analysis of glycosyltransferase activity

Glycosyltransferase activity was monitored by use of gel electrophoresis as described by Galley (Thesis, 2015) whose method built upon those of Helassa *et al.* (2012) and Barrett *et al.* (2007). Assay detergent and concentrations of enzyme and substrate varied between experiments, and are described in the text. Reactions were made up in low-binding 0.5 mL eppendorf or PCR tubes, in a buffer consisting of 50 mM HEPES pH 7.6, 10 mM $MgCl_2$, 150 mM NaCl, 25 % (v/v) DMSO, and the chosen concentrations of PBP1a (from a 10 x stock), 100 % dansylated Lipid II in assay detergent (from a 100 μM stock), and assay detergent to make up the desired concentration (relative to the critical micelle concentration (CMC)). Where possible, master-mixes were used to reduce the impact of pipetting error on liquid handling. Reactions were initiated by addition of the enzyme, and incubated at 30 ˚C in an Aviso Mechatronic Systems Primus thermocycler, with the time period of incubation dictated by the experiment. Reactions were terminated by addition of 1 μL moenomycin and 1 μL 0.5 M EDTA. Samples were then mixed with loading dye (6 x stock: 100 mM Tris pH 8.8, 4 % (w/v) SDS, 40 % (v/v) glycerol, 0.05 % (w/v) bromophenol blue).

Polyacrylamide gels were made by the method of Barrett *et al.* (2007) using a Mini-PROTEAN Tetra System gel kit (Bio-Rad). 7.5 mL of 9 % Tris-Tricine gel (0.42 M Tris pH 8.45, 0.13 % (w/v) SDS, 9 % acrylamide:*bis*-acrylamide 37.5:1) was polymerised by addition of 30 μL 10 % (w/v) APS and 15 μL

TEMED, and poured into a gel casting tray with insertion of a 10 well plastic comb to form the wells. Electrophoresis was completed with anode (0.1 M Tris pH 8.8) and cathode (0.1 M Tris, 0.1 M Tricine, 0.1 % (w/v) SDS, pH 8.25) buffers at 100 V, 50 mA for 1 h 15 mins.

As specified in the text, some experiments made use of Criterion 16.5 % Tris-Tricine Precast gels (Bio-Rad). Such gels were run at 100 V, 50 mA for 3 h, in buffers as previously described.

Fluorescence was imaged using an ImageQuant LAS 4000 instrument (GE Healthcare) on the Ethidium bromide fluorescence setting (transmitted light at 312 nm, 605DF40 filter; to allow imaging of glycan strands based on dansyl group fluorescence: λ_{abs} 340 nm; λ_{em} 520 nm).

2.7.2 SDS-PAGE analysis of transpeptidase activity

Transpeptidase activity was monitored in the same gel-based system described in 2.7.1, but with use of Lipid II (iGln, Dans) and an additional substrate that could behave as a transpeptidase acceptor. Controls with 1 mM ampicillin and 200 μM moenomycin were run alongside.

Double-volume reactions were made for these experiments, such that half could be analysed by SDS-PAGE, and half by mass spectrometry as described in Section 2.7.4.

2.7.3 Amplex Red assay for D-Ala release

Transpeptidase and D,D-carboxypeptidase activity was monitored in a coupled continuous assay system developed by Dr. A. J. Lloyd (University of Warwick).

Reaction buffer, assay detergent and substrates were as dictated by the experiment, but all contained the coupling system of 33.51 $mM.min^{-1}$ *Rhodotorula gracilis* DAAO, 14.82 $mM.min^{-1}$ horseradish peroxidase and 50 μM Amplex Red, allowing D-Ala release to be followed by the generation of resorufin ($\lambda_{(max)}$ 555 nm).

Reactions were assembled, minus the initiating component, in crystal quartz cuvettes and performed in a Varian Cary 100 spectrophotometer monitoring A_{555nm} at 30 ˚C. Reactions were then initiated once a stable baseline had been reached (5 mins).

2.7.4 Mass spectrometry analysis of transpeptidase reaction products

Reactions for analysis of transpeptidase activity (by either of the methods described in Section 2.7.2 or 2.7.3) were digested with *Streptomyces globisporus* mutanolysin (prepared in 10 mM HEPES pH 7.6 and 25 mM $MgCl_2$) to allow detection of cross-linked products by mass spectrometry. Volumes are given for a 200 μL transpeptidase reaction, but these were scaled accordingly for processing of smaller reaction volumes.

To each 200 μL reaction, 20 μL 2.2 M *bis*.Tris pH 6.2 was added, followed by 20 μL of 10mg.mL^{-1} mutanolysin. The digestion was incubated for 2 h at 37 ˚C, a further 20 μL aliquot of mutanolysin added and the incubation repeated. The reaction was boiled at 100 ˚C for 10 mins, and proteins were then pelleted by centrifugation at 16,000 x g for 10 mins in a bench-top centrifuge (Eppendorf 5415 R). 150 μL was added from a fresh stock of 10 mg.mL^{-1} $NaBH_4$ followed by incubation at room temperature for 30 mins. The final step was then addition of 17.5 μL 20 % (v/v) phosphoric acid.

Mass spectrometry analysis was by liquid chromatography mass spectrometry (LCMS) using an ACQUITY UPLC Peptide BEH C_{18} column (Waters), which was equilibrated at 50 mL.min^{-1} in 99:1 water + 0.1 % (v/v) formic acid (solvent A): acetonitrile + 0.1 % (v/v) formic acid (solvent B). The column was developed over a gradient of 1 to 37 % solvent B in 30 mins; followed by a step to 90 % solvent B in 1 min, with a 3 mins wash at 90 % solvent B; and finally restoration of the original 1 % B condition over 1 min with a 6 min wash. After the first minute, the elution entered the mass spectrometer (calibrated as described in Section 2.6.7, but run in positive mode) at a capillary voltage of 2.5-3.0 kV. Further analysis of selected ions was by LCMSMS using collision-induced fragmentation, with argon flow at 2 mL.min^{-1} at a constant trap collision energy of 40 eV. Data were collected and analysed using Waters Mass Lynx software, by Dr. Adrian Lloyd, Julie Tod or Anita Catherwood (all University of Warwick).

2.7.5 Electrophoretic analysis of BOCILLIN FL binding

Interaction of PBP1a with Bocillin FL (fluorescently labelled BODIPY penicillin) was analysed by SDS-PAGE. Unless otherwise stated, 6 μM PBP1a was

incubated with 2 mM ampicillin, 200 μM moenomycin (or other test inhibitor) or water for 30 mins at room temperature. Bocillin FL was then added to give a final concentration of 60 μM (or the equivalent volume of 100 % dimethyl sulfoxide (DMSO)) and samples were incubated at 37 ˚C for 1 h in the dark. Samples were mixed with protein loading dye and run on 12 % SDS-PAGE gels (Section 2.5.1), though without the heat denaturing step to avoid disruption of the PBP-BOCILLIN FL interaction. A lane each of protein ladder (Color Prestained Protein Standard, Broad Range (NEB)) and fluorescent protein ladder (BenchMark Fluorescent Protein Standard (ThermoFisher Scientific)) were loaded for sizing of the bands. Fluorescence was detected by imaging on a Typhoon FLA 9500 laser scanner (GE Healthcare) with a Y510 filter and laser at 473 nm, and exposure setting on 100 μm pixel size. Gels were then stained using InstantBlue Protein Stain (Expedeon) and imaged using an ImageQuant LAS 4000 instrument (GE Healthcare).

2.7.6 Continuous fluorescence assay for glycosyltransferase activity

Rates of glycosyltransferase activity by pneumococcal PBPs were analysed using a continuous fluorescence assay for glycosyltransferase activity (Schwartz *et al.*, 2002), with conditions as described by Galley (2015). 50 uL reactions consisted of 50 mM HEPES pH 7.5, 10 mM $MgCl_2$, 150 mM NaCl, 25 % (v/v) DMSO, 0.0116 % (w/v) E_6C_{12}, 0.1 mg.mL^{-1} hen egg lysozyme, and concentrations of PBP1a and Lipid II (iGln, Dans) as determined by the experiment. Where cardiolipin and phosphatidylglycerol were included in the reactions, these phospholipids were dried down under N_2 gas from stocks in 2:3:1 chloroform:methanol:water, and resuspended in 0.039 % (w/v) E_6C_{12}.

Reactions were run in a FLUOTRAC^T 600 high binding 96-well plate (Greiner), and initiated by addition of 5 uL PBP1a at 10 X final concentration. Fluorescence was monitored at 30 °C for 100 mins on a Clariostar platereader (BMG Labtech) with excitation at 340 nm and emission at 521 nm.

Progress curves were exported using MARS Data Analysis Software (BMG Labtech), rates calculated in RFU.sec^{-1}, and data was plotted in GraphPad Prism.

2.8 Determination of Minimal Inhibitory Concentration (MIC) by microbroth dilution

MIC values for *S. pneumoniae* strains Pn16 and 159 were determined by microbroth dilution according to CLSI guidelines (CLSI, 2014). Cell suspensions of *S. pneumoniae* were made in PBS to match turbidity with a 0.5 McFarland standard. These cell suspensions were then diluted 100-fold in PBS to produce the working stock of *S. pneumoniae*. In a 96-well plate, 2-fold serial dilutions of antibiotics (at 2 x the required concentration for each well) were made in 100 μL per well of cation-adjusted Mueller-Hinton Broth with 5 % (v/v) lysed horse blood. Each well was then inoculated with 100 uL of the diluted cell suspension. Controls with PBS in place of inoculum and broth in place of antibiotic were included. Plates were incubated in anaerobic jars for 18 h, following which growth was assessed based on turbidity. MIC values were read as the lowest concentration of antibiotic at which no growth was observed.

MICs were determined in parallel for *S. pneumoniae* strain ATCC46919. The observed MIC values were compared to published values to validate the procedure; if values were within 1 dilution either side, the values were taken as correct.

Chapter 3: Synthesis of Pneumococcal Peptidoglycan Precursors and Substrate Analogues

3.1 Introduction

In order to address the research questions of this thesis relating to activity of pneumococcal penicillin binding proteins (PBPs), a necessary first step was the synthesis of a variety of substrates for these enzymes, to represent the naturally occurring variations in pneumococcal peptidoglycan. The necessity of different kinds of substrates for the assay systems to be used will be discussed further in Section 3.1.4.

Reviews encompassing the synthesis of peptidoglycan precursors and substrate analogues have been published by Lazar and Walker (2002), Welzel (2005), Narayan and VanNieuwenzhe (2007), and Egan *et al.* (2015). The various methodologies for obtaining or synthesising PBP substrates can be broadly categorised as the accumulation and purification of native substrates (hereafter referred to as bioaccumulation); biosynthesis with purified recombinant enzymes or bacterial membrane preparations; and chemical methods. Many published methods, however, combine a few of these approaches to reach the final product. A summary diagram of published methods for synthesis of peptidoglycan precursors is presented in Figure 3.1.

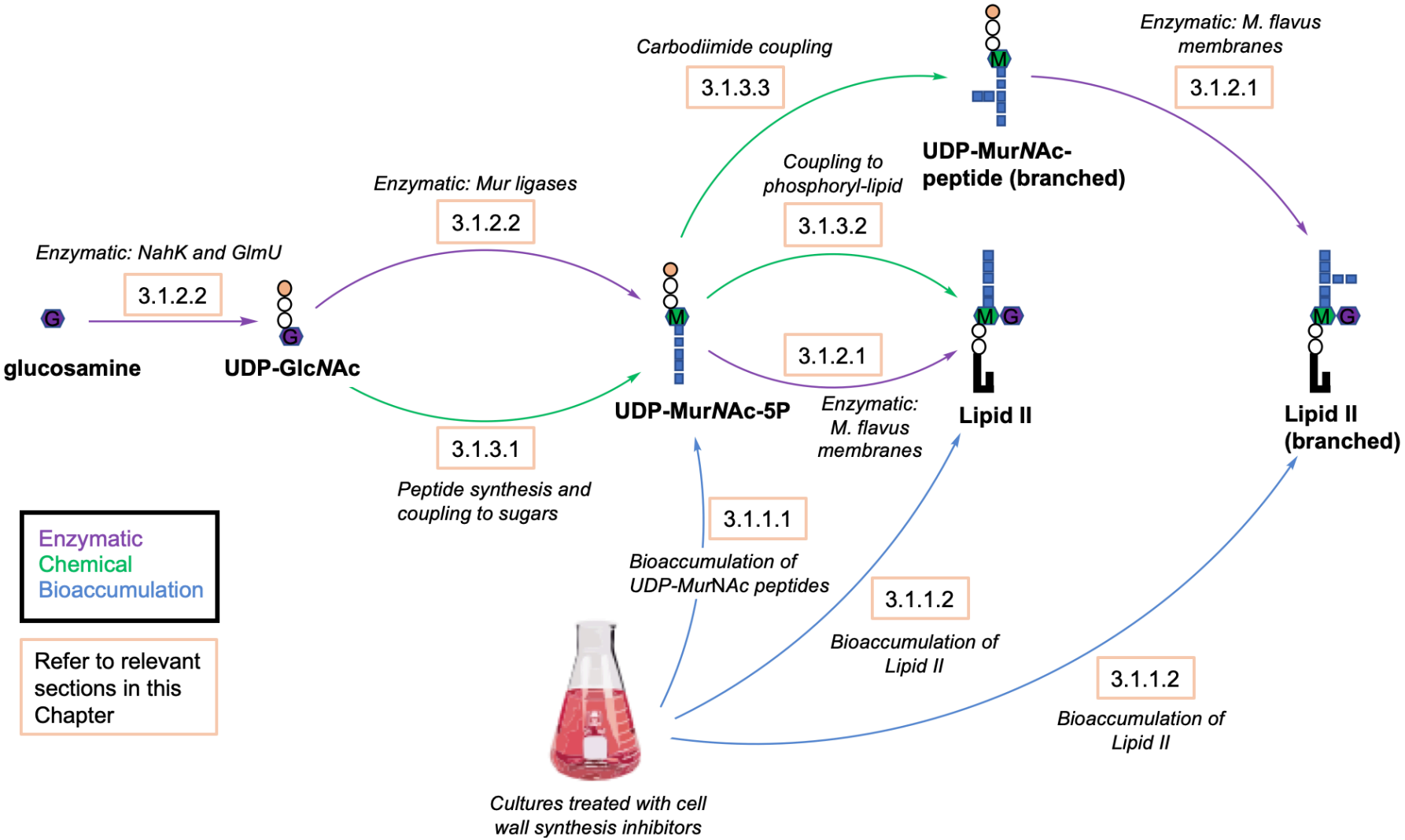

Figure 3.1: Summary of the published pathways for synthesis of peptidoglycan precursors. Chemical, enzymatic and bioaccumulation methods of various stages of peptidoglycan precursor synthesis have been described. Numbering refers to the relevant Sections of this Chapter.

3.1.1 Purification of native precursors and bioaccumulation

3.1.1.1 Bioaccumulation of UDP-Mur*N*Ac peptides

The earliest methods for obtaining peptidoglycan precursors were based on their purification from natural sources, in pursuit of chemical characterisation of the peptidoglycan precursor (Park, 1952). The estimated pool of Lipid II in *E. coli* is a maximum of 2000 molecules (Van Heijenoort *et al.*, 1992). Consequently, Park (1952) and others have used antibiotics such as penicillin (Hammes & Neuhaus, 1974), vancomycin (Reynolds, 1961) and D-cycloserine (Izaki *et al.*, 1968; Neuhaus & Struve, 1965) to accumulate UDP-Mur*N*Ac peptides *in vivo* by inhibition of peptidoglycan biosynthesis, in organisms such as *Bacillus cereus*. In general, these methods involved treatment of cultures with chloramphenicol, to increase the availability of amino acids for incorporation into the peptide stem (Ishiguro & Ramey, 1978); followed by vancomycin/penicillin or D-cycloserine to accumulate UDP-Mur*N*Ac pentapeptide or -tripeptide respectively. Kohlrausch and Höltje (1991) built upon previous methods by use of a one-step HPLC purification followed by desalting, to give high purity and yield of UDP-Mur*N*Ac pentapeptide (5P) from *B. cereus* culture. This method was adapted to supply soluble precursor for many of the enzymatic Lipid syntheses described in Section 3.1.2.

3.1.1.2 Bioaccumulation of Lipid II

Guan *et al.* (2005) isolated Lipid II from *E. coli* in sufficient yield and purity for mass spectrometry analysis. However, Qiao *et al.* (2017) were the first to publish the use of cell wall synthesis inhibition to accumulate and then purify sufficient lipid-linked peptidoglycan precursors for biochemical studies. Moenomycin treatment was used to accumulate Lipid II in *Staphylococcus aureus* cultures. Cultures were then lysed and the Lipids extracted using a chloroform:methanol mixture. This method was subsequently employed with *femA* and *femB* deletion strains, to obtain Lipids with monoglycyl- and triglycyl-branches respectively (Srisuknimit *et al.*, 2017).

3.1.1.3 Considerations for use of bioaccumulation

Bioaccumulation to obtain peptidoglycan precursors allows the generation of authentic substrates for cell wall synthesis enzymes. In addition, the methods of Qiao *et al.* (2017) and Srisuknimit *et al.* (2017) are, at the time of writing, the only published methods for generation of the pentaglycyl-Lipid II precursor of *S. aureus* peptidoglycan.

The limitations of bioaccumulation include the limit in yield unless large volumes of culture are handled; possible contamination of the product with other cellular constituents; and unsuitability for application to organisms with variation in the final peptidoglycan structure, such as the variety of interpeptide bridges found in pneumococci (Garcia-Bustos *et al.*, 1987), if a uniform final product is desired. Such a mixture may however be desired, depending on the assay system to be used. Furthermore, bioaccumulation is comparably poorer in flexibility to that afforded by biosynthetic or chemical methods, whereby altered amino acids may be incorporated or certain groups functionalized.

3.1.2 Biosynthesis methods

3.1.2.1 Bacterial membranes for linkage of UDP-Mur*N*Ac pentapeptide to undecaprenyl phosphate

The bioaccumulation method of Kohlrausch and Höltje (1991) was used by a variety of investigations seeking to synthesise and purify Lipid II. Membranes from organisms such as *S. aureus* had been used to investigate the pathway of incorporation of Mur*N*Ac 5P into the cell wall (Anderson *et al.*, 1965). These methods demonstrated the utility of membrane preparations for synthesis of lipid-linked precursors. Anderson *et al.* (1967) described the purification of Lipid II synthesised using this method, by solvent extraction followed by anion exchange chromatography. *N*-butyl alcohol was found to perform well as a quenching agent and for extraction of lipid product from the reaction mixture. Subsequent uses of similar methods include Umbreit *et al.* (1972), and van Heijenoort *et al.* (1992), who described an additional sialic acid column chromatography step.

Breukink *et al.* (2003) described synthesis of Lipid I and Lipid II intermediates with enzymatic activity provided by *M. flavus* vesicles. In this case, shorter

polyprenyl chain lipids (geranyl or farnesyl -pyrophosphate) were used in the synthesis.

3.1.2.2 Purified recombinant enzymes in synthesis of UDP-Mur*N*Ac peptides

Lipid substrates have also been synthesised from UDP-Mur*N*Ac 5P provided by enzymatic biosynthesis. Reddy *et al.* (1999) described the first preparative-scale enzymatic biosynthesis of UDP-Mur*N*Ac 5P from UDP-Glc*N*Ac by use of purified recombinant Mur-ligases. The progress of the reactions was followed by ADP accumulation, as reported by NADH consumption in a pyruvate kinase/lactate dehydrogenase coupled assay. At completion, the product of each step was purified by anion exchange chromatography. Each intermediate in the pathway could be synthesised via this enzymatic method, at quoted yields of 10 – 100 mg. Limitations of the enzymatic synthesis included the impact of substrate and product inhibition on MurB, as well as NADPH oxidase activity by this enzyme (necessitating high concentrations of MurB and NADPH to overcome respectively); and the need for multiple rounds of anion exchange chromatography to resolve ADP accumulated by the activity of MurC-F from the desired peptidoglycan intermediate products.

Liu *et al.* (2001) included glucose dehydrogenase (GDH) to recycle NADPH in their chemoenzymatic synthesis of UDP-Mur*N*Ac 5P, thus maintaining a low concentration of $NADP^+$ to alleviate product inhibition of MurB, and simplify the purification of the desired product. The method of Liu *et al.* is further discussed in Section 3.1.3. Lloyd *et al.* (2008), in addition to utilising isocitrate dehydrogenase (IDH) to recycle NADPH, included pyruvate kinase in their one-pot enzymatic synthesis reaction from UDP-Glc*N*Ac to UDP-Mur*N*Ac 5P, both to limit the starting concentration of ATP required, and to remove the ADP by-product which had complicated the purification of Reddy *et al.* (1999).

Huang *et al.* (2014) described an enzymatic Lipid II synthesis method analogous to that of Lloyd *et al.* (2008), but with differences in starting materials, MraY and MurG sources, and the cofactor recycling system. The undecaprenol kinase activity of *Streptococcus mutans* diacylglycerol kinase

(DGK) was used to generate undecaprenyl phosphate, in addition to enzymatic synthesis of UDP-Glc*N*Ac from Glc*N*Ac using *Bifidobacterium longum* NahK and *E. coli* GlmU. Purified recombinant *Bacillus subtilis* MraY and *E. coli* MurG were employed in place of a bacterial membrane preparation to provide these activities. Purified recombinant enzymes are advantageous as the impact of batch-to-batch variation can be controlled by using the specific activity of each batch to calculate the final concentration of enzyme to use in the assay. Limitations of the use of purified recombinant enzymes include the more time-intensive preparation required (in particular with specific activity determination), and the possible expense incurred by the requirement for detergent solubilisation of the enzymes. Phospholipid interactions have been found to affect the activity of enzymes in the cell wall biosynthesis pathway (Section 5.1.3.4), and so this is an additional concern for preserving the activity of purified enzymes.

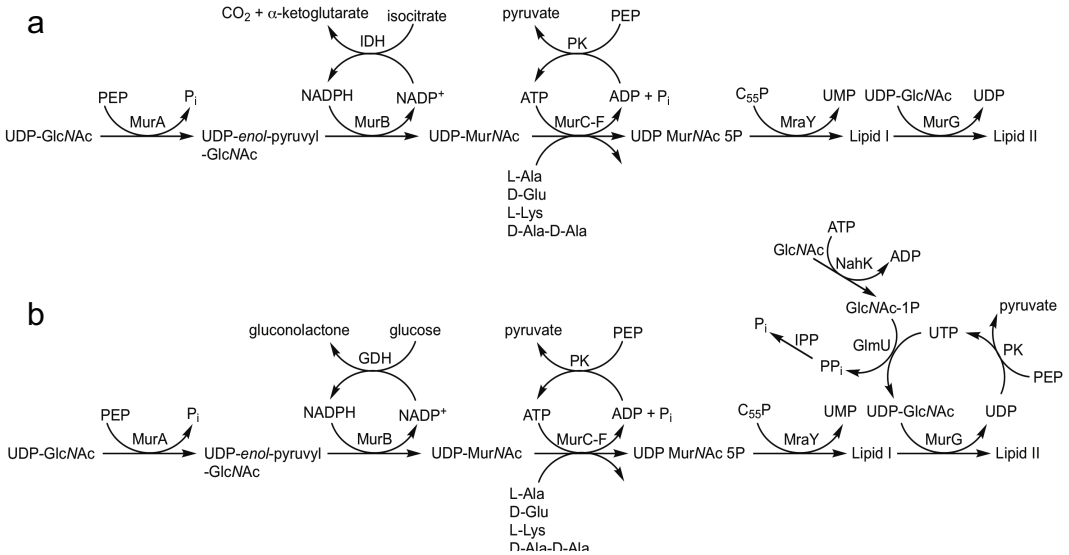

Figure 3.2: Comparison of the energy recycling systems of Lloyd *et al.* (2008) and Huang *et al.* (2014). The pathways of enzymatic biosynthesis of Lipid II published by **a)** Lloyd *et al.* (2008) and **b)** Huang *et al.* (2014) are presented to illustrate differences in the cofactor recycling enzymes used. **ADP**, Adenosine 5'-diphosphate; **ATP**, Adenosine 5'-triphosphate ; **$C_{55}P$**, undecaprenyl phosphate; **GDH**, glucose dehydrogenase; **IDH**, isocitrate dehydrogenase; **$NADP^+$**, nicotinamide adenine dinucleotide phosphate; **NADPH**, dihydronicotinamide adenine dinucleotide phosphate; **PEP**, phospho-*enol* pyruvate; **P_i**, inorganic phosphate; **PK**, pyruvate kinase; **UDP**, uridine 5'-diphosphate; **UMP**, uridine 5'-monophosphate; **UTP**, uridine 5'-triphosphate

A comparison of the reaction pathways for the Lloyd *et al.* (2008) and Huang *et al.* (2014) Lipid II syntheses, with annotation of cofactor recycling enzymes, is depicted in Figure 3.2. In both methods NADPH and ATP were recycled. Whilst both used pyruvate kinase (PK) for recycling of ATP, different enzymes were used for reduction of $NADP^+$; isocitrate dehydrogenase (IDH) by Lloyd *et al.* (2008), and glucose dehydrogenase (GDH) by Huang *et al.* (2014). In addition, Huang *et al.* (2014) used PK, NahK, GlmU and IPP to recycle UDP liberated by the activity of MurG to generate more UDP-Glc*N*Ac from Glc*N*Ac. This would be expected to significantly reduce the cost of UDP-Mur*N*Ac peptide synthesis in terms of starting materials (as of 23.10.18, UDP-Glc*N*Ac was priced at £870.00 per gram, compared to Glc*N*Ac at £16.90 per gram from Sigma-Aldrich, UK). However, the preparation of the enzymes required for the enzymatic synthesis and regeneration of UDP-Glc*N*Ac will incur its own costs.

3.1.2.3 Considerations of biosynthesis methods

Biosynthetic methods offer benefits including stereospecificity, and the potential for flexibility (although this depends upon the substrate specificity of the enzyme). Limitations can include the impact of substrate or product inhibition on yield and purity (Koeller & Wong, 2001).

Though, in general, greater flexibility in synthesis is afforded by chemical methods, there are published examples whereby enzymatic synthesis routes have been used to incorporate modifications to peptidoglycan precursors. Fonvielle *et al.* (2018) used MurE to incorporate *meso*-cystine into an enzymatically-prepared Lipid II molecule. This modified amino acid allowed subsequent functionalisation of the side chain of residue 3 in the peptide stem with an RNA moiety to mimic the acceptor arm of $tRNA^{Gly}$. The molecule generated was used to assess the impact of D-Ala-D-Lac peptide stem terminus on the activity of FemX. Whilst it may have been possible to have synthesised the intermediate chemically, as stated by Liu *et al.* (2001), enzymatic synthesis negates the requirement for handling of varied protecting groups, such as would likely be necessary here.

3.1.3 Chemical synthesis methods

Chemical synthesis has been used to generate the entire Lipid II molecule; to functionalise certain parts of Lipid II such as the peptide stem; and often in combination with enzymatic techniques where a wholly enzymatic approach would have been otherwise limited in flexibility.

3.1.3.1 Chemical synthesis of UDP-Mur*N*Ac 5P

Hitchcock *et al.* (1998) are credited with the first total chemical synthesis of UDP-Mur*N*Ac 5P. A muramyl-phosphate sugar was synthesised from *N*-acetyl glucosamine, and then coupled to a pentapeptide stem constructed by carbodiimide coupling (see further discussion of this method in Section 3.3.4.1). The Khorana-Moffatt procedure (Roseman *et al.*, 1961) was then used to couple the protected peptidomuramyl phosphate to uridine 5'-monophosphomorpholidate. Global deprotection was then achieved using sodium hydroxide.

A key limitation of the method of Hitchcock *et al.* (1998) was the time taken for the coupling of peptidomuramyl phosphate and uridine 5'-monophosphomorpholidate (14 days). Liu *et al.* (2001) addressed this issue by the inclusion of ^{1}H-tetrazole as a catalyst, achieving a reaction time of 2 days and 'nearly quantitative' yield, compared to the 32 % yield quoted by Hitchcock *et al.* (1998). The pentapeptide or depsipentapeptide (with C-terminal D-Ala-D-Lac, rather than D-Ala-D-Ala) stem was constructed by peptide coupling based on the method of Men *et al.* (1998).

Liu *et al.* (2001) also described a chemoenzymatic method for synthesis of UDP-Mur*N*Ac penta- and depsipentapeptide, whereby UDP-Mur*N*Ac was synthesised enzymatically from UDP-Glc*N*Ac using purified recombinant MurA-B, with glucose dehydrogenase to recycle the cofactor NADPH as previously discussed (Section 3.1.2). The pentapeptide or depsipentapeptide stem was synthesised and then coupled to the UDP-Mur*N*Ac as before. The authors obtained a lower yield for UDP-Mur*N*Ac 5P synthesised by the chemoenzymatic route (70 %) compared to the wholly chemical route (nearly

quantitative). No yield was quoted for the depsipentapeptide compound by the chemical route, but that quoted for the chemoenzymatic route was 56 %. The authors note, however, that the chemoenzymatic synthesis was simplified due to fewer steps in the procedure, and the need for protecting groups only in the synthesis of the peptide stems.

3.1.3.2 Chemical synthesis of Lipid-linked substrates

Men *et al.* (1998) prepared a citronelloyl-anchored Lipid I substrate analogue. The first step was synthesis of a phospho-Mur*N*Ac peptide precursor, by coupling a dibenzyl phosphate-derivatised Mur*N*Ac sugar to a protected pentapeptide. The product was then deprotected, and linked to the citronelloyl lipid by pyrophosphate exchange with diphenyl citronelloyl pyrophosphate. The authors also described biotinylation of the ε-amino group of L-lysine at the 3rd position of the peptide stem, to facilitate the downstream use of the compound in activity assays for MurG.

The Lipid I synthesis described by Men *et al.* (1998) was later used to generate starting material for Lipid II synthesis. This method used purified recombinant MurG to append Glc*N*Ac to Lipid I variants with prenyl chains of varying lengths (Ye *et al.*, 2001), necessitating a change in the coupling chemistry for Lipid I synthesis.

VanNieuwenzhe *et al.* (2001) described a similar chemical synthesis method for Lipid I to that of Men *et al.* (1998). In both methods, the phosphate moiety was first coupled to a Mur*N*Ac derivative. A peptide stem constructed by solution-phase peptide synthesis was then coupled to the Mur*N*Ac phosphate. The two pathways differed in choice of protecting groups, and in the timing of the removal of the 4,6 benzylidene moiety of the starting material in each case. VanNieuwenzhe *et al.* (2001) then generated the final product via formation of an activated phosphoimidazolidate intermediate from the phospho-Mur*N*Ac peptide, thus allowing coupling of sugar-phosphate and undecaprenyl phosphate.

Schwartz *et al.* (2001) chemically synthesised Lipid II by first assembling a disaccharyl-monopeptide, which was then phosphorylated. The remainder of the peptide stem was coupled to the phosphorylated disaccharyl-monopeptide as a tetrapeptide. Finally, the phosphoryl group was activated using 1,1′-carbonyldiimidazole (CDI) to allow coupling to undecaprenyl phosphate.

A similar synthetic route to that of Schwartz *et al.* (2001) was employed by VanNiewenzhe *et al.* (2002) to achieve total chemical synthesis of Lipid II. The starting material was the disaccharyl monopeptide moiety, synthesised using a published protocol (Saha *et al.*, 2001). The phosphate and then the tetrapeptide moieties were introduced to the molecule in similar fashion to the Lipid I synthesis protocol of the same group (VanNieuwenzhe *et al.,* 2001), in addition to the same phosphoroimidazolidate protocol for coupling of undecaprenyl phosphate to the intermediate. Despite the similar routes to synthesis employed by VanNieuwenhze *et al.* (2001) and Schwartz *et al.* (2001), the yield is much lower for the latter (24 % vs 0.7 %). However, it is unclear whether the yield calculated by VanNieuwenzhe *et al.* encompasses the steps to make the disaccharyl monopeptide, which may account for the difference.

Nakamura *et al.* (2013) generated Lipid II depsipentapeptide chemoenzymatically, though in contrast to the approach of Liu *et al.* (2001), the route to the phospho-Mur*N*Ac depsipentapeptide moiety was by linking tetradepsipeptide to phospho-Mur*N*Ac L-Ala (Schwartz *et al.*, 2001; VanNieuwenhze *et al.*, 2002). Tetradepsipeptide was synthesised by solution-phase peptide synthesis, and then coupled to protected phospho-Mur*N*Ac L-Ala. Following deprotection of the phospho-Mur*N*Ac moiety (but retaining protecting groups on the peptide stem), the phospho-sugar was activated by CDI and coupled to undecaprenyl or heptaprenyl -phosphate, followed by deprotection and purification. Heptaprenyl-Lipid II was then synthesised enzymatically from heptaprenyl Lipid I using purified recombinant MurG and UDP-[^{14}C]-Glc*N*Ac. The authors stated that undecaprenyl Lipid II synthesis was not attempted due to aggregation of undecaprenyl Lipid I in solution,

though published methods have achieved synthesis of such products by inclusion of detergent in the reaction mixture (Breukink *et al.*, 2003).

3.1.3.3 Synthesis of branched UDP-Mur*N*Ac peptides by carbodiimide coupling

A common technique throughout the chemical syntheses discussed has been peptide coupling, using activating agents such as carbodiimides, to assemble the peptide stem of peptidoglycan precursors. The chemoenzymatic method of De Pascale *et al.* (2008) utilised carbodiimide coupling to synthesise branched pneumococcal peptidoglycan precursors. UDP-Mur*N*Ac 5P was synthesised enzymatically as described by Lloyd *et al.* (2008) and the branch was then appended by coupling of N-terminally 9-fluorenylmethyloxycarbonyl (Fmoc)-protected amino acids to the ε-amino of the third position L-lysine in the stem peptide. The mechanism of this carbodiimide coupling method is further discussed in Section 3.3.4.1. *M. flavus* membranes were then used to generate branched Lipids from the UDP-Mur*N*Ac peptides according to the method described by Breukink *et al.* (2003). This chemoenzymatic method offered flexibility in the amino acids that could be incorporated into the branch, such that the pentaglycyl-Lipid II precursor of *S. aureus* could be prepared in the same way.

3.1.4 Use of variety of substrates

A variety of pneumococcal peptidoglycan intermediates were desired for this project in order to address the central research question; how does the availability of linear and branched pneumococcal peptidoglycan precursors relate to expression of resistance to β-lactam antibiotics?

Indirect cross links in the pneumococcal cell walls consist of dipeptide branches with either L-Ala or L-Ser in the first position, and an invariant L-Ala residue in the second (L-X-L-Ala) (Filipe *et al.*, 2000). The extent of indirect cross-links in pneumococcal cell walls varies by strain, as a consequence of variation in the activity level of the MurM enzyme that is responsible for branching of Lipid II (Filipe & Tomasz, 2000; Lloyd *et al.*, 2008). A range of branched PBP substrates were therefore sought to allow characterization of

the kinetics of usage for each, to shed light on how the variety in pneumococcal cell wall peptide stems affects transpeptidation, and thereby influences the β-lactam resistance mechanism.

The use of defined donor and acceptor substrates offers two main benefits in analysis of transpeptidase activity in our case; firstly, this makes possible the distinction of D,D-carboxypeptidation (the removal of the terminal D-Ala of the pentapeptide stem) from transpeptidation in assays that follow D-Ala release (Section 2.7.3). This is of particular use in the optimisation stage of assay development, as the effect of different conditions on the ratio of D,D-carboxypeptidation to transpeptidation can be assessed. Secondly, the use of defined donor and acceptor substrates allows the substrate requirements and other important chemical features of either the donor or acceptor site to be investigated independently.

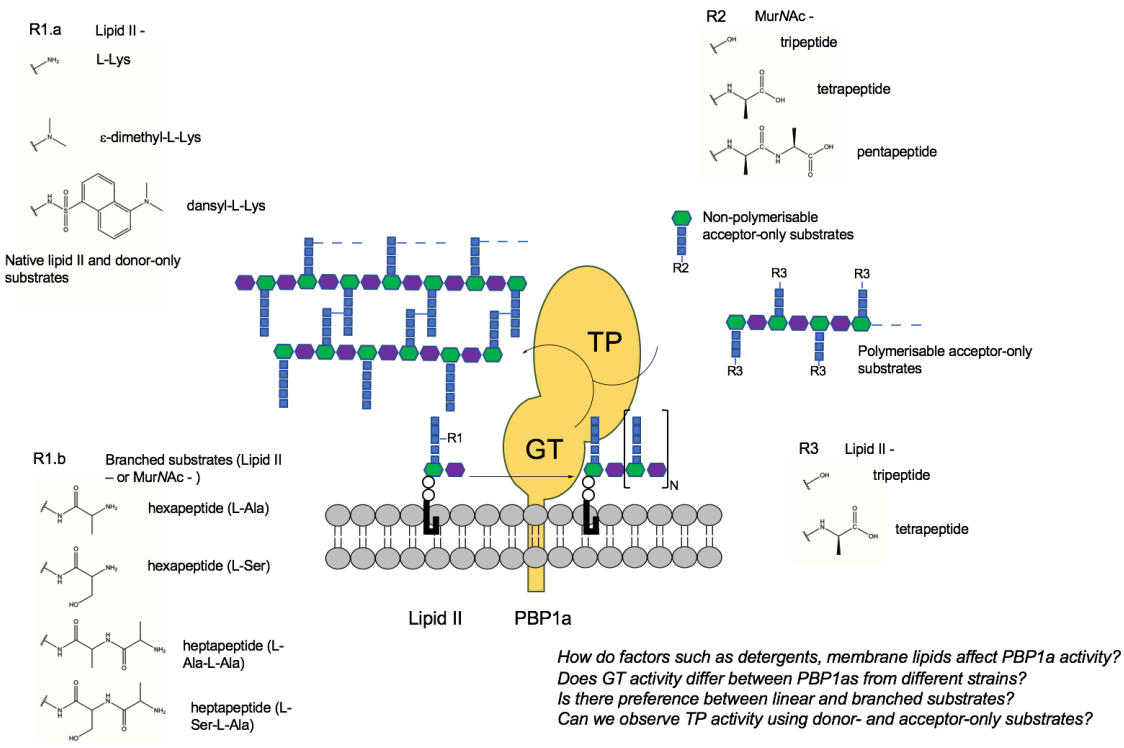

Figure 3.3 Summary of the uses for different kinds of substrates for pneumococcal PBPs.

3.2 Experimental Aims

- To synthesise UDP-Mur*N*Ac 5P (iGln) and Lipid II (iGln) using published methods
- To use the published carbodiimide synthesis method to synthesise amidated branched UDP-Mur*N*Ac peptides
- To develop a carbodiimide coupling synthesis method for synthesis of UDP-Mur*N*Ac heptapeptide intermediates
- To test the synthesis of branched Lipid II intermediates from branched UDP-Mur*N*Ac peptides
- To develop a method for synthesis of donor-only pneumococcal PBP substrates
- To synthesis a range of acceptor-only pneumococcal PBP substrates, including polymerisable and non-polymerisable variants

3.3 Results

3.3.1 Synthesis of UDP-Mur*N*Ac 5P (iGln)

The starting material for the majority of the syntheses described in this chapter was an amidated variant of the UDP-Mur*N*Ac 5P "cytoplasmic" peptidoglycan precursor, giving the peptide stem L-Ala-γ-D-iGln-L-Lys-D-Ala-D-Ala. The chosen synthesis method was by use of purified recombinant Mur ligases to assemble UDP-Mur*N*Ac 5P from UDP-Glc*N*Ac (Section 2.6.1), as described by Lloyd *et al.* (2008). The methodology has been used extensively in our group for the synthesis of a variety of native and modified peptidoglycan precursors.

The energy recycling system, as depicted in Figure 3.2, enabled ongoing supply of the ATP required for the catalytic activity of Mur ligases C to F, and also simplified the purification procedure. Byproducts of the reaction without the energy recycling enzymes would include ADP and PEP, which would coelute with UDP-Mur*N*Ac peptide at the anion exchange purification step (A.J. Lloyd, personal communication and Reddy *et al*, (1999)).

Amidated UDP-Mur*N*Ac 5P (UDP-Mur*N*Ac 5P (iGln)) was synthesized enzymatically in an overnight reaction, with UDP-Glc*N*Ac as the starting material. Amidation of the second position was achieved by inclusion of D-isoglutamine for incorporation into the peptide stem by MurD. This method ensures 100 % amidation of the final product, which is crucial if the product is to be used for Lipid II synthesis. Whilst non-amidated and amidated UDP-Mur*N*Ac pentapeptide can be resolved by the anion exchange procedure used to chromatograph the reaction (Appendix 3.1), separation of amidated and non-amidated Lipid II would likely require an additional chromatography step, with associated losses of material. A technique has been described for separation of radiolabeled amidated and non-amidated Lipid II (Siewert & Strominger, 1968). However, detection of Lipid II on HPLC in the absence of radiolabelling or a chromophore is challenging, in addition to the limited column choice owing to the difficulty in handling of C_{55} lipid. By contrast, a limitation of our method is the decreased efficiency with which MraY catalyses the linkage of the amidated substrate to undecaprenyl phosphate (Siewert & Strominger, 1968), resulting in consistent lower yields of Lipid II (iGln) in comparison to non-amidated Lipid II.

The UDP-Mur*N*Ac 5P (iGln) synthesis reaction was purified by anion exchange chromatography on Source30Q resin (GE Healthcare) as described in Section 2.6.1.3 (Figure 3.4). The chromatogram appeared as depicted in Figure 3.4.a, with peaks corresponding to (i) the desired product; (ii) PEP; and

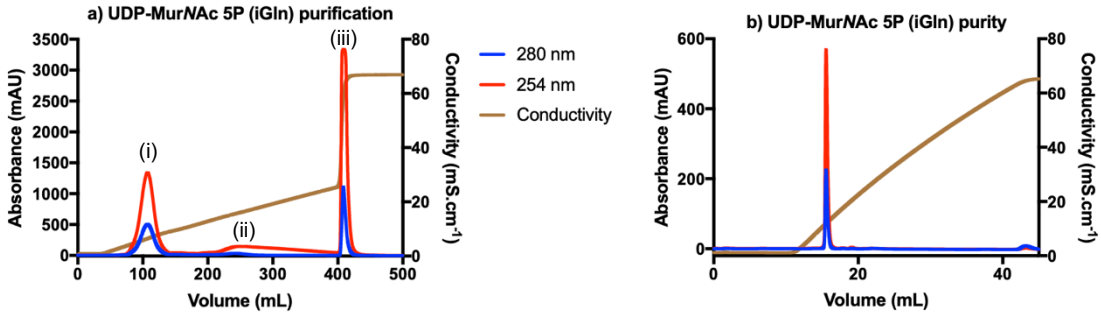

Figure 3.4 Purification of UDP-Mur*N*Ac 5P (iGln). Chromatography of the synthesis reaction **(a)** by anion exchange chromatography, and analysis of final purity **(b)** by analytical anion exchange chromatography are presented. The product peak (**i**) was resolved from PEP (**ii**) and ATP (**iii**). Analytical anion exchange indicated purity of 97 %.

(iii) ATP (Dr. A.J. Lloyd, University of Warwick, personal communication). Fractions containing the product were concentrated, and the ammonium acetate concentration reduced, by lyophilization. The final product was then quantified by A_{260nm}, purity was established by analytical anion exchange chromatography (Figure 3.4b), and the identity of the product was confirmed by mass spectrometry (Appendix 3.2 – expected (m-2)/2 573.18; observed (m-2)/2 573.18).

3.3.2 Synthesis of Lipid intermediate

Lipid intermediates were synthesized using the enzymatic method described by Breukink *et al.* (2003), wherein *M. flavus* membranes provide MraY and MurG activities. Purified recombinant MurG was used to supplement the membranes. The chromatography of such a synthesis reaction, as analysed by TLC, is presented in Figure 3.5.

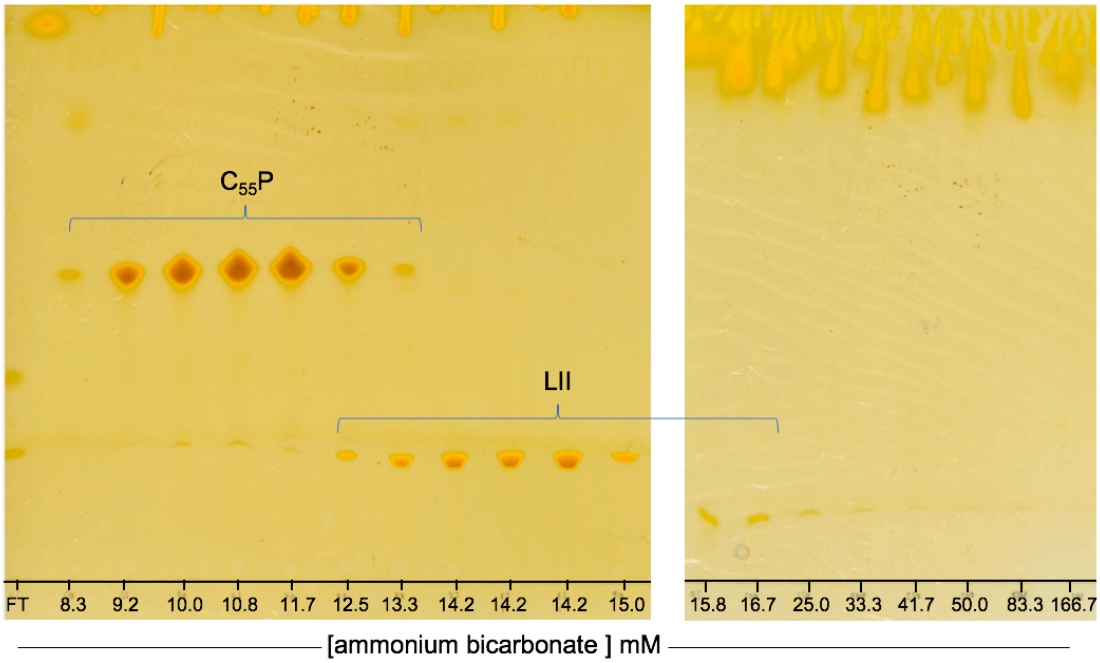

Figure 3.5 Thin-layer chromatography analysis of purification of Lipid II (iGln). The Lipid II synthesis reaction was purified by anion exchange chromatography using stepwise elution up to 166.7 mM ammonium bicarbonate in 2:3:1 chloroform:methanol:buffer. Fractions were analysed by thin-layer chromatography run in 44:88:10:1 chloroform: methanol: ammonia: water, and stained using iodine vapour. **C55P,** undecaprenyl phosphate; **LII,** Lipid II

Extensive wash steps were included between 8.3 and 16.7 mM ammonium bicarbonate, in contrast to purification of non-amidated Lipid II, whereby the wash steps across this range were 8.3, 12.5 and 100 mM only (Dr. A. York, University of Warwick, personal communication). The additional wash steps for purification of Lipid II (iGln) ensured adequate separation of the desired product from undecaprenyl phosphate (as shown in Figure 3.5), whereas non-amidated Lipid II commonly elutes from the column approximately in the 16.7 mM ammonium bicarbonate wash. The product was confirmed by mass spectrometry (expected (m-2)/2 936.03; observed (m-2)/2 936.03. See Appendix 3.3).

3.3.3 Comparison of Lipid II synthesis method to a published method

The method for synthesis of Lipid II published by Schneider *et al.* (2004) used enzymes supplied by *M. flavus* membranes. Their method was analogous to that described in this thesis, and quoted milligram yields of Lipid II, but had

Table 3.1. Comparison of the Lipid II synthesis reactions of Lloyd *et al.* (2008) and Schneider *et al.* (2004).

Reagent	Lloyd *et al.* (2008)	Schneider *et al.* (2004)
Undecaprenyl phosphate (mM)	1.4	0.067
Buffer	100 mM Tris-HCl pH 8 10 mM $MgCl_2$ 1 % (v/v) Triton X-100	60 mM Tris-HCl pH 8 5 mM $MgCl_2$ 0.5 % (v/v) Triton X-100
UDP-Mur*N*Ac 5P (mM)	4.0	0.67
UDP-Glc*N*Ac (mM)	6.0	0.67
Purified recombinant MurG ($mg.mL^{-1}$)	0.57	N/A
Incubation	Overnight at 37°C	1 hr at 30°C
***M. flavus* membranes (protein concentration – $mg.mL^{-1}$)**	2	0.4

various slight differences in composition of the synthesis reaction. A comparison of the two methods is given in Table 3.1. We sought to compare the yield of Lipid II (iGln) from the two methods, hereafter designated Lloyd *et al.* and Schneider *et al.*, to determine the best choice of method for further syntheses.

The Lloyd *et al*. Lipid II synthesis protocol was optimised to shift the equilibrium of the reversible reaction catalysed by MraY towards production of Lipid I. This was achieved using a 3:2 molar ratio of UDP-Glc*N*Ac to UDP-Mur*N*Ac pentapeptide, and by supplementing the reaction with purified recombinant MurG, to ensure that MurG forces the equilibrium position of the system towards Lipid II synthesis. By comparison, Schneider *et al.* used equimolar concentrations of UDP-Glc*N*Ac to UDP-Mur*N*Ac pentapeptide.

Table 3.2 Analytical scale reactions for comparison of Lloyd *et al.* (2008) and Schneider *et al.* (2004) Lipid II syntheses. To compare the Lipid II (iGln) yield from the synthesis methods of Lloyd *et al*. (**orange, reaction 1**) and Schneider *et al.* (**blue, reaction 2**), 200 μL reactions with combinations of these conditions as below were incubated at 37 °C overnight and analysed by silica TLC.

Reagent concentration	Reaction			
	1	2	3	4
UDP-Mur*N*Ac 5P (mM)	4	0.67	4	0.67
UDP-Glc*N*Ac (mM)	6	0.67	6	0.67
$C_{55}P$ (mM)	1.4	0.067	1.4	0.067
MurG ($mg.mL^{-1}$)	0.57	0	0.57	0
M. flavus membranes (protein mass, mg)	2	2	0.4	0.4

In the Lloyd *et al.* method, the reaction is made up to the required volume by addition of *M. flavus* membranes, and so the total protein concentration added to the reaction is over twice that quoted for the method used by Schneider *et al.*.

In order to compare the yields of Lipid II (iGln) from the methods of Schneider *et al.* and Lloyd *et al.*, analytical scale (150 μL) syntheses combining different aspects of each method were used. In addition to comparing each method as described (Lloyd *et al.*: 4 mM UDP-Mur*N*Ac 5P, 6 mM UDP-Glc*N*Ac, 1.4mM $C_{55}P$ – reaction 1, Table 3.2; Schneider *et al.*: 0.67 mM UDP-Mur*N*Ac 5P, 0.67 mM UDP-Glc*N*Ac, 0.067mM $C_{55}P$ – reaction 2, Table 3.2), the amount of *M. flavus* membranes was swapped

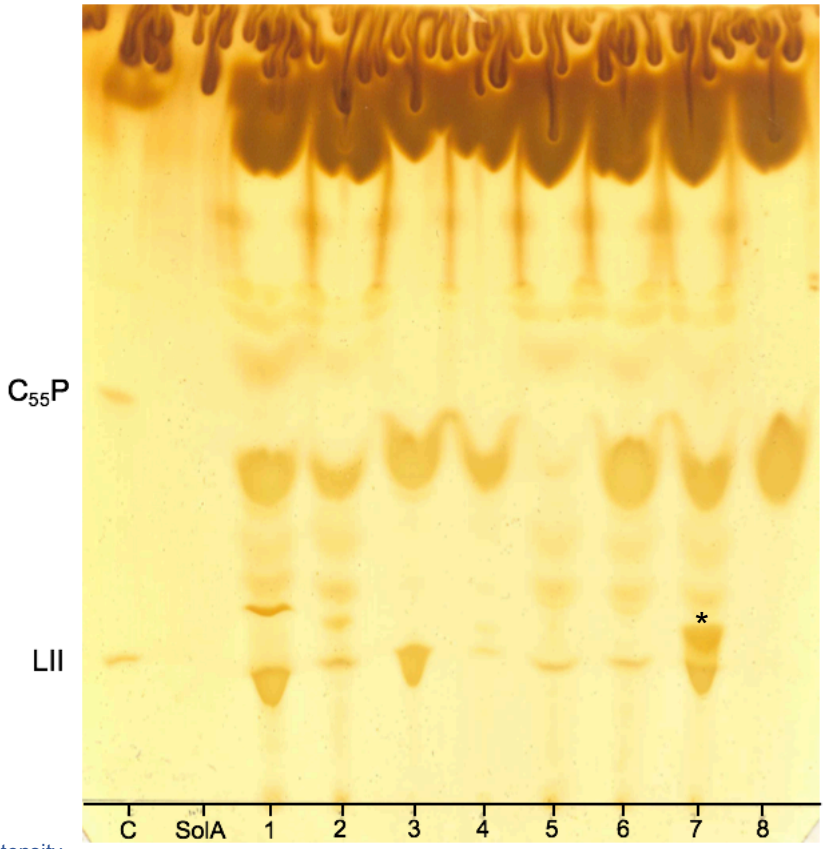

Figure 3.6. Thin-layer chromatography analysis of yield of Lipid II (iGln) from varied synthesis conditions. Reactions 1-4 correspond to the combinations set out in Table 3.2. Band intensity at the Rf expected for Lipid II was quantified using ImageJ software (Schneider *et al.*, 2012), and is presented (in blue) as values relative to the Lipid II band in the control (**C**) lane.
Reaction lanes 1-4. 1: 4 mM UDP-Mur*N*Ac 5P, 6 mM UDP-Glc*N*Ac, 1.4mM $C_{55}P$, 0.57 mg.mL^{-1} MurG, 2 mg protein from *M. flavus* membranes; **2:** 0.67 mM UDP-Mur*N*Ac 5P, 0.67 mM UDP-Glc*N*Ac, 0.067 mM $C_{55}P$, 2 mg protein from *M. flavus* membranes; **3:** 4 mM UDP-Mur*N*Ac 5P, 6 mM UDP-Glc*N*Ac, 1.4mM $C_{55}P$, 0.57 mg.mL^{-1} MurG, 0.4 mg protein from *M. flavus* membranes ; **4:** 0.67 mM UDP-Mur*N*Ac 5P, 0.67 mM UDP-Glc*N*Ac, 0.067 mM $C_{55}P$, 0.4 mg protein from *M. flavus* membranes;
Control lanes - C: Purified Lipid II and $C_{55}P$; **SolA**: Solvent A only; **5:** no 11P; **6:** no 5P; **7:** no UDP-Glc*N*Ac **8:** no *M. flavus* membranes or MurG

between the reaction schemes to reveal the impact of the amount of MraY and MurG provided by *M. flavus* membranes (Table 3.2).

Comparative analytical-scale (150 μL) syntheses were incubated at 37 °C overnight. These were then assessed by silica TLC, as presented in Figure 3.6. By this qualitative approach, there is an apparent greater yield of Lipid II with the Lloyd *et al.* synthesis protocol (Figure 3.6, Lane 1) compared to that for the protocol of Schneider *et al.* (Figure 3.6, Lane 4). Band intensities in the region of the TLC with the Lipid II bands was plotted using ImageJ software (Schneider *et al.*, 2012), and the values presented in Figure 3.6 are relative to the intensity of the Lipid II (iGln) band in the control lane.

The reactions with the same amount of C55P added, but differing in the amount of *M. flavus* membranes (Figure 3.6, Lane 1 vs 3, and Lane 2 vs 4), demonstrated similar apparent yield of Lipid II (iGln) with Lloyd *et al.* reagent concentrations (Lanes 1 and 3; band intensities 5.0 and 4.2 respectively), but greater yield with the larger amount of *M. flavus* membranes (Lane 2) with Schneider *et al.* reagent concentrations (band intensities 1.6 and 0.4 respectively for lanes 2 and 4). Altogether, these results suggest that the synthesis protocol of Lloyd *et al.* gives greater yield of Lipid II than that published by Schneider *et al*.

The double band observed running closest to the origin in lane 7 (marked *) would be expected to correspond to Lipid I, due to the omission of UDP-Glc*N*Ac from this synthesis reaction. However, the migration of this band (*) is similar to bands in lanes 1-4, and the Lipid II control. Syntheses of Lipid II described elsewhere in this Chapter were not found to contain Lipid I amongst the products, and so lanes 1-4 would be expect to correspond to Lipid II. The product in lane 7 warrants analysis by mass spectrometry, which would confirm whether the product is Lipid I.

3.3.4 Synthesis of branched peptidoglycan intermediates

Synthesis of branched peptidoglycan intermediates has been a key part of this project, to allow study of pneumococcal PBPs with relevant natural substrates. We therefore sought a reliable and flexible method for synthesis of such intermediates.

3.3.4.1 Method choice

The chosen route for synthesis of branched intermediates was by carbodiimide coupling (De Pascale *et al.*, 2008). This method was used to add the amino acids of the branch to the ε-amino group L-Lysine at residue 3 of the peptide stem in UDP-Mur*N*Ac 5P (iGln). The branched peptides thus obtained were then to be processed into Lipid intermediates as previously described (Section 3.3.2), or acid hydrolysed to generate branched acceptors for the transpeptidase reaction. The variety of branched UDP-Mur*N*Ac peptides sought (Figure 3.7) was devised to encompass the naturally occurring variation in the pneumococcal cell wall.

The mechanism of carbodiimide coupling for synthesis of branched peptide intermediates is depicted in Figure 3.8: The carboxyl-terminus of an N-

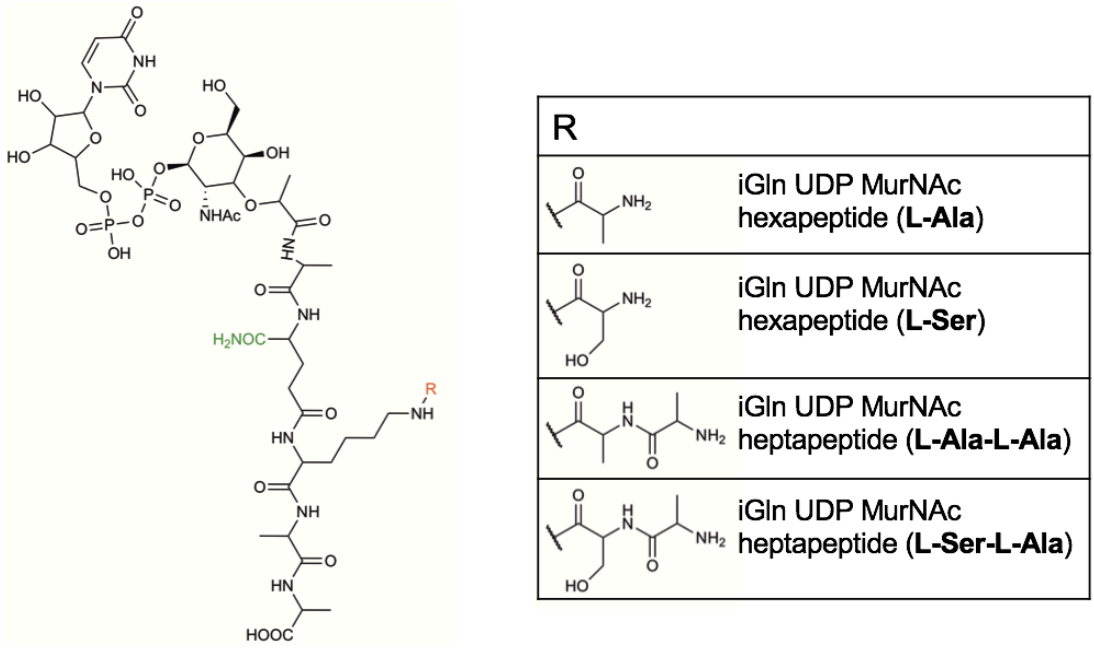

Figure 3.7 The variety of branched UDP-Mur*N*Ac pentapeptide intermediates whose synthesis has been attempted. Amidation of the stem peptide at the a-carboxyl of D-isoglutamine is highlighted in green.

terminally Fmoc-protected amino acid (1) was activated by reaction with 1-ethyl-3-(3-dimethylaminopropyl) carbodiimide (EDC, (2)), generating an O-acylisourea intermediate (3). Under the aqueous conditions necessary for handling of the UDP-Mur*N*Ac 5P starting material, the activated species is subject to hydrolysis (Staros *et al.*, 1986). The efficiency of the reaction was therefore maintained by reacting the activated species with *N*-hydroxysuccinimide (HOSu, (4)), generating a stable HOSu ester (6). Sodium bicarbonate buffer was used to adjust the pH of the solution to 10, and UDP-Mur*N*Ac pentapeptide was then added. The ε-amino group of L-lysine in the pentapeptide stem displaced HOSu by nucleophilic attack, with formation of a peptide bond (generating (8)). The reaction was then terminated by addition of ethanolamine, to quench excess HOSu esters remaining in the reaction mixture (Gestwicki *et al.*, 2001). The final compound (10) was generated after deprotection using piperidine (9). The secondary amine of piperidine removed the acidic proton (9-position of Fmoc fluorene ring), following which a β-elimination generated a dibenzofulvene intermediate (11) that formed a stable adduct with the secondary amine of piperidine (Luna *et al.*, 2016).

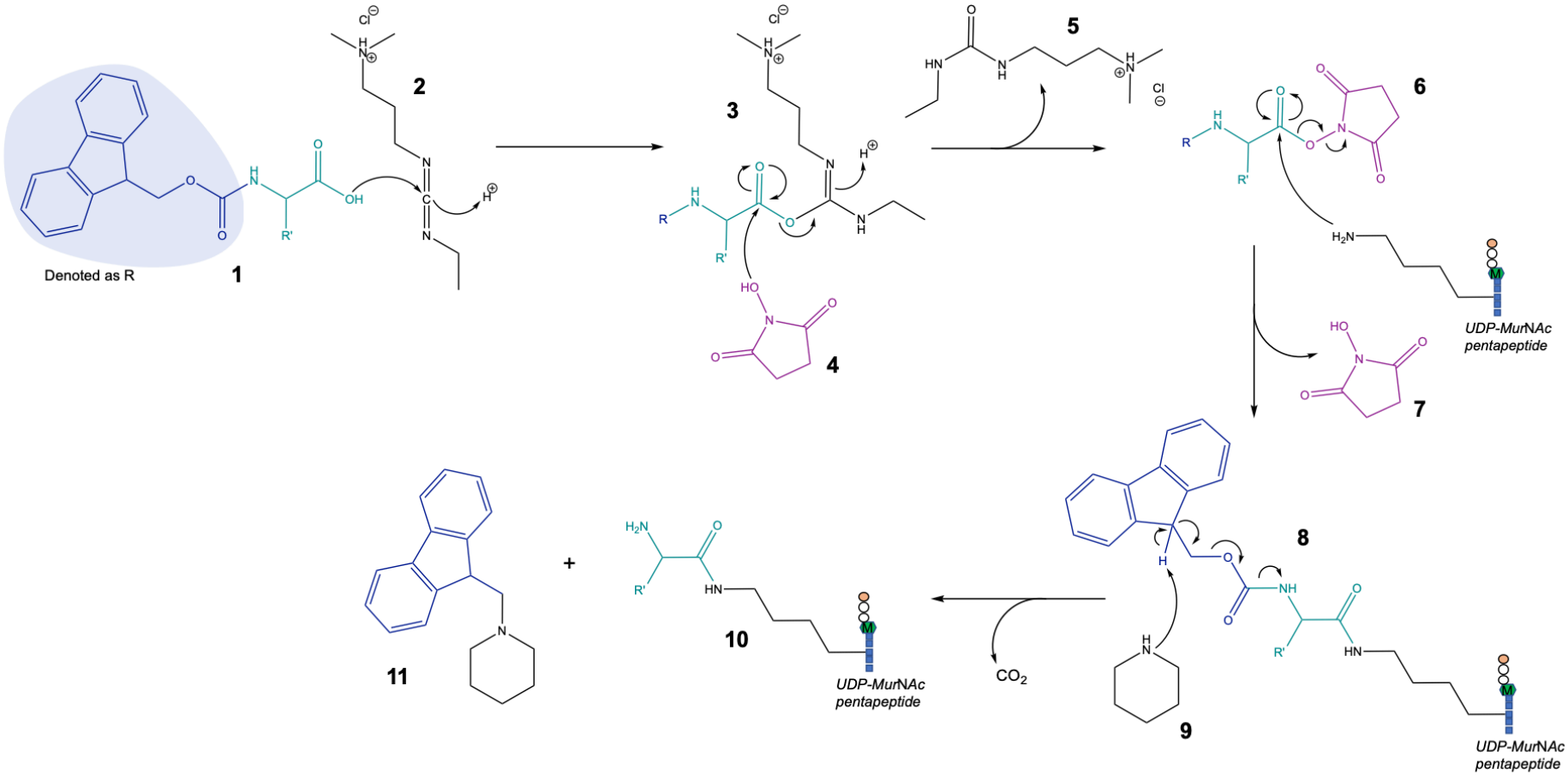

Figure 3.8 Mechanism of carbodiimide coupling for synthesis of branched intermediates. EDC (1-ethyl-3-(3-dimethylaminopropyl) carbodiimide, (**2**)) activates the carboxyl-terminus of N-terminally Fmoc-protected amino acids (**1**) generating an O-acylisourea intermediate (**3**). HOSu (*N*-hydroxysuccinimide, (**4**)) reacts with the activated species to form a stable HOSu ester (**6**). UDP-Mur*N*Ac pentapeptide was then added. The ε-amino group of L-lysine in the pentapeptide stem displaced HOSu by nucleophilic attack, with formation of a peptide bond to generate **8**. Compound **8** was deprotected using piperidine (**9**) to give the final product (**10**), with generation of an Fmoc-piperidine adduct as a by-product (**11**).

3.3.4.2 Desalting of UDP-Mur*N*Ac 5P

The UDP-Mur*N*Ac 5P (iGln) to be used as the starting material for branched peptide synthesis was first desalted by gel filtration, using a Biogel P2 column (Bio-Rad) (Section 2.6.5). This step was incorporated to remove residual ammonium acetate from the starting material, which would otherwise have decreased the coupling efficiency (by reaction with the amino acid HOSu ester formed in the coupling reaction). Those fractions containing UDP-Mur*N*Ac 5P iGln (Figure 3.9, peak (i)) eluted separately from the salt peak (peak (ii)) were concentrated by lyophilization, and the concentration of the final stock was determined by A_{260nm}.

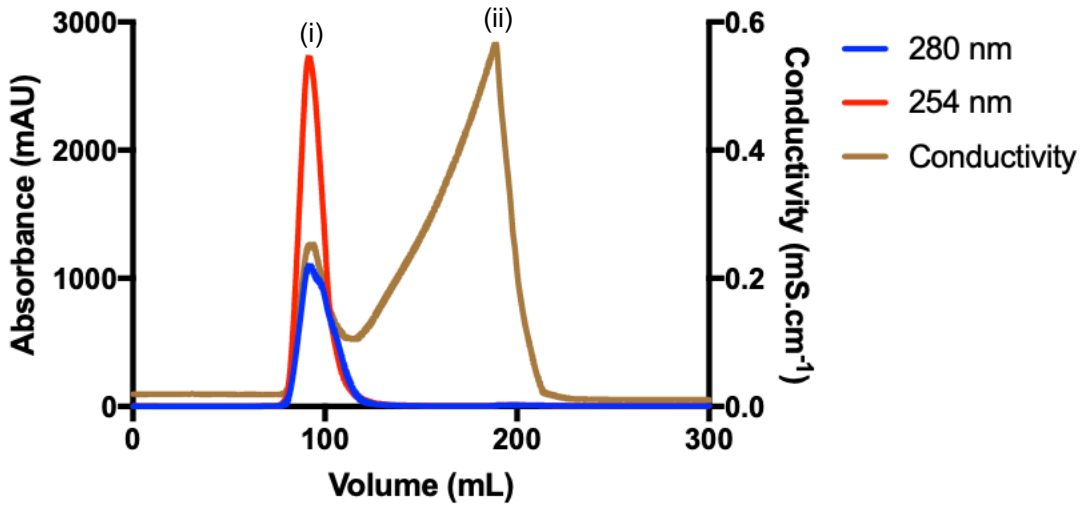

Figure 3.9 Desalting of UDP-Mur*N*Ac pentapeptide by gel filtration. UDP-Mur*N*Ac 5P (iGln) was desalted by gel filtration using a Biogel P2 column (Bio-Rad). A 500 μL sample was loaded to the column via an injection loop, and the column was then developed over 2 column volumes. UDP-MurNAc 5P (iGln) eluted (i) from the column separately from the salt peak (ii).

3.3.4.3 Synthesis of hexapeptide intermediates

A published method (De Pascale *et al.*, 2008) was initially followed for carbodiimide coupling synthesis of branched UDP-Mur*N*Ac peptides. In this protocol, ethanolamine was used to quench the reaction by consumption of excess HOSu ester, and piperidine was used to deprotect the compound. The reaction mixture was purified by anion exchange chromatography, using the same methodology as that previously described for purification of UDP-Mur*N*Ac 5P (Section 2.6.1.3).

Upon analysis by mass spectrometry of the major peak from purification of branched UDP-Mur*N*Ac peptides, we identified the occurrence of multiple additions of L-Alanine to the ε-amino group of L-Lys in the peptide stem (Table 3.3), along with loss of amidation at the second position of the peptide stem (see Appendices 3.4 to 3.7). This finding necessitated both a change in the quenching technique, and a chromatography column affording higher resolution to allow separation of products with multiple additions.

Table 3.3: Nanospray TOF mass spectrometry analysis of carbodiimide coupling reactions quenched using ethanolamine. Multiple alanylation was associated with loss of amidation of the 2nd position step peptide residue. Data collected and analysed by A.J. Lloyd.

Compound	2nd posn	Expected m/z	Observed m/z	Charge state
UDP-Mur*N*Ac 6P	iGln	608.70	608.71	(m-2)/2
	iGlu	609.19	-	
UDP-Mur*N*Ac 9P	iGln	715.25	-	
	iGlu	715.74	715.76	
UDP-Mur*N*Ac 10P	iGln	750.77	-	
	iGlu	751.26	751.28	
UDP-Mur*N*Ac 11P	iGln	786.29	-	
	iGlu	786.78	786.79	
UDP-Mur*N*Ac 12P	iGln	821.81	-	
	iGlu	822.30	822.31	

The quenching agent used in the published method, ethanolamine, has itself been employed for deprotection of Fmoc-amino acids (Carpino & Han, 1972). The presence of this compound was therefore suspected to be the cause of the multiple addition observed, by deprotecting the intended product in the presence of reactive HOSu esters, allowing additional rounds of coupling to occur. Different agents for quenching of the reaction were therefore tested. The nucleophile hydroxylamine was chosen, which is weakly basic and should therefore not cleave Fmoc.

The products of UDP-Mur*N*Ac 6P (iGln, L-Ala) syntheses that were quenched with hydroxylamine were purified by anion exchange chromatography in the ammonium acetate buffer system previously described, but utilising a preparative-scale MonoQ column (GE Healthcare), which has greater resolution than the Source30Q (GE Healthcare) column previously used. The major peak from chromatography of reactions quenched by ethanolamine (Figure 3.10a) or hydroxylamine (Figure 3.10b) eluted at conductivity of ~15 mS.cm^{-1} in each case. Based on the chromatographic analysis of reactions

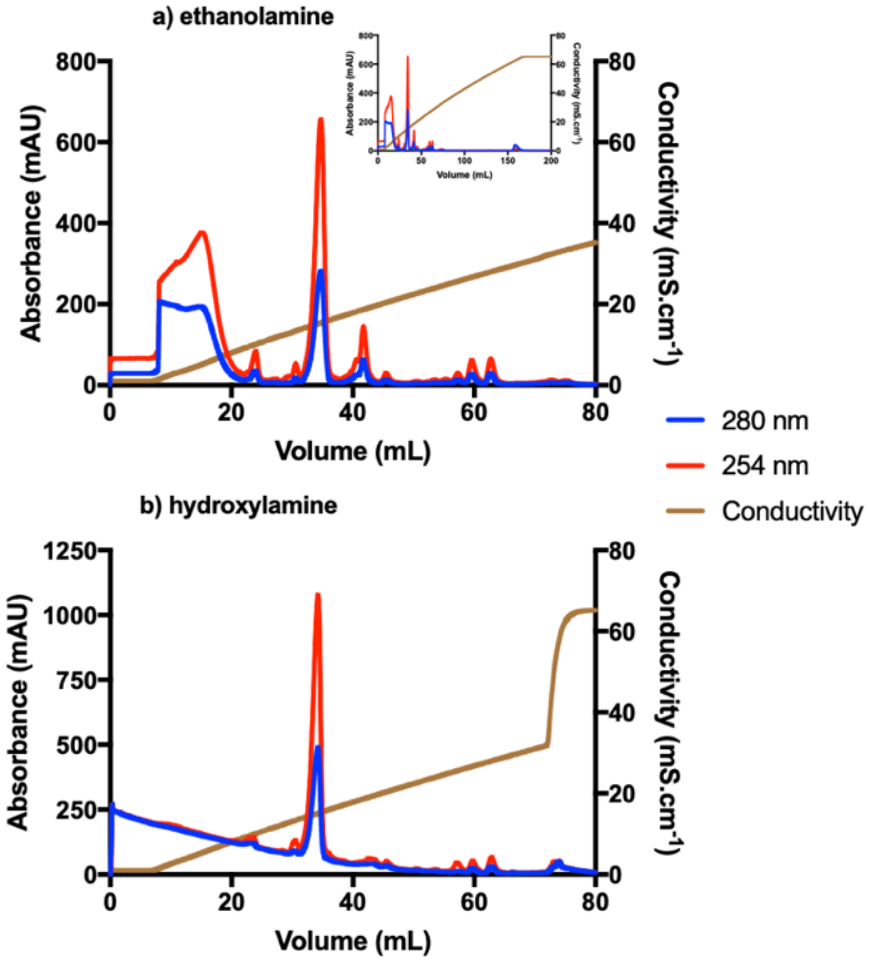

Figure 3.10. Anion exchange chromatography purification of iGln UDP-Mur*N*Ac hexapeptide (L-Ala) from reactions quenched by ethanolamine or hydroxylamine. The efficacy of **a)** ethanolamine (with inset full chromatogram) and **b)** hydroxylamine as quenching agents in the synthesis of iGln UDP-Mur*N*Ac hexapeptide (L-Ala) was compared by anion exchange chromatography.

quenched with ethanolamine or hydroxylamine, the synthesis appeared cleaner with hydroxylamine; fewer products were detected by absorbance at 280 nm and 254 nm. The major peaks from the reaction quenched with

hydroxylamine were lyophilized, and analysed by mass spectrometry (Table 3.4).

Analysis of the products by mass spectrometry confirmed the synthesis of UDP-Mur*N*Ac 6P (iGln, L-Ala) (expected (m-2)/2, 608.69; observed (m-2)/2, 608.71), but also identified minor ions corresponding to the products of multiple alanylation of UDP-Mur*N*Ac 5P (iGln). In addition, ions were detected corresponding to a loss of UMP from the molecule (Table 3.4), both co-eluting with the desired product and in a sample of the peak detected at 13.3 $mS.cm^{-1}$ (for spectra, see Appendices 3.8 to 3.11). The alternate quenching agent tested therefore did not appear to aid in improvement in yield of the desired compounds.

Table 3.4: Nanospray TOF mass spectrometry analysis of carbodiimide coupling reactions quenched using hydroxylamine. Ions detected in major peak eluting at 15.0 $mS.cm^{-1}$. Data collected and analysed by A.J. Lloyd.

Compound	Expected m/z	Observed m/z	Charge state
phospho-Mur*N*Ac 6P	912.37	912.39	(m-1)/1
UDP-Mur*N*Ac 6P	608.69	608.71	(m-2)/2
UDP-Mur*N*Ac 7P	644.21	644.23	(m-2)/2
UDP-Mur*N*Ac 8P	679.74	679.74	(m-2)/2
UDP-Mur*N*Ac 9P	715.25	715.26	(m-2)/2
UDP-Mur*N*Ac 10P	750.77	750.78	(m-2)/2

Quenching agents were therefore omitted completely from the coupling procedure. The desired UDP-Mur*N*Ac 6P (iGln, L-Ala) product was successfully synthesized under such conditions (expected (m-2)/2, 608.695; observed (m-2)/2, 608.695. See Table 3.5). A small degree of multiple alanylation was observed in the absence of quenching agent (up to UDP-Mur*N*Ac 8P (iGln, L-Ala-L-Ala-L-Ala)). However, the omission of quenching agents avoided the loss of amidation and UMP that was associated with the use of ethanolamine and hydroxylamine respectively (Appendices 3.12 and 3.13). Purification of UDP-Mur*N*Ac 6P (iGln, L-Ala) is illustrated in Figure 3.11.

3.3.4.4 Synthesis of heptapeptide intermediates

Synthesis of heptapeptide (7P) intermediates was initially attempted by multiple rounds of the liquid phase coupling described in the previous Section (3.3.4.3). This method proved unsuccessful in obtaining any measurable heptapeptide products.

An alternative method was therefore attempted whereby solid phase peptide synthesis (SPPS) (Fields & Noble, 1990) was used to generate the dipeptide 'branch', which could then be coupled to the pentapeptide in a single step. The mechanism of this peptide coupling procedure is depicted in Figure 3.12. By using the SPPS method to supply dipeptide to be coupled to UDP-Mur*N*Ac 5P as before, detectable quantities of the L-Ala-L-Ala heptapeptide was synthesized, and purified using the same method as described for the hexapeptide intermediates (Figure 3.11c).

The SPPS method had not been the first choice of method for synthesis of heptapeptide intermediates. Cyclisation of the C-terminal amino acid, forming an oxazolone, can cause racemization within the dipeptide when it is activated (Figure 3.13). A branched UDP-Mur*N*Ac peptide with a D-X-L-Ala branch could therefore be produced if this occurs during the synthesis reaction. The use of HOSu to generate an active ester as an intermediate in the coupling

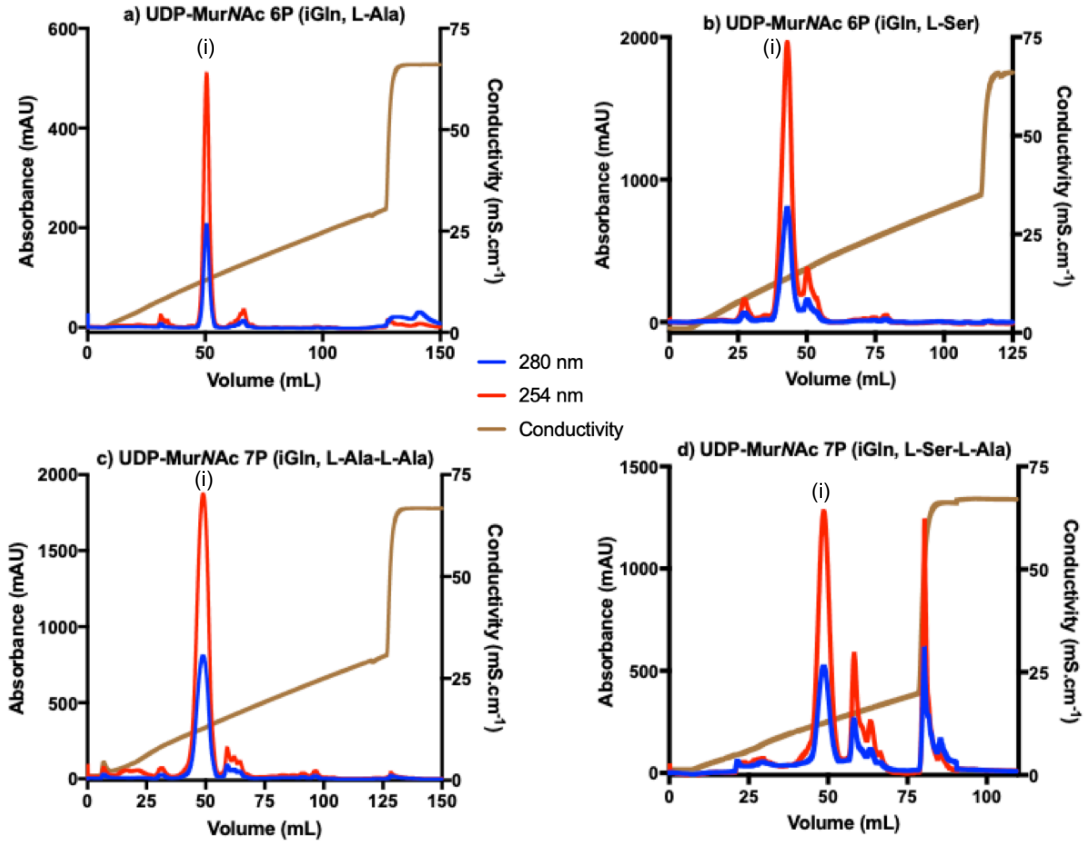

Figure 3.11 Purification of branched UDP-Mur*N*Ac peptides. Chromatograms for purification of iGln UDP-Mur*N*Ac **a)** hexapeptide (L-Ala), **b)** hexapeptide (L-Ser), **c)** heptapeptide (L-Ala-L-Ala) and **d)** heptapeptide (L-Ser-L-Ala) respectively by anion exchange chromatography on a MonoQ HR 10/10 column (GE Healthcare). Peaks corresponding to the desired (or major) product (**i**) in each case are indicated, as identified by negative ion nanospray TOF mass spectrometry (**a** – expected m/z 608.695; observed m/z 608.695; **b** – expected m/z 616.69; major ion observed m/z 644.73; **c** – expected m/z 644.213; observed m/z 644.217; **d** – expected m/z 687.73; observed m/z 652.21), though in the case of the L-Ser variants the desired product was a minor component on mass spectrometry.

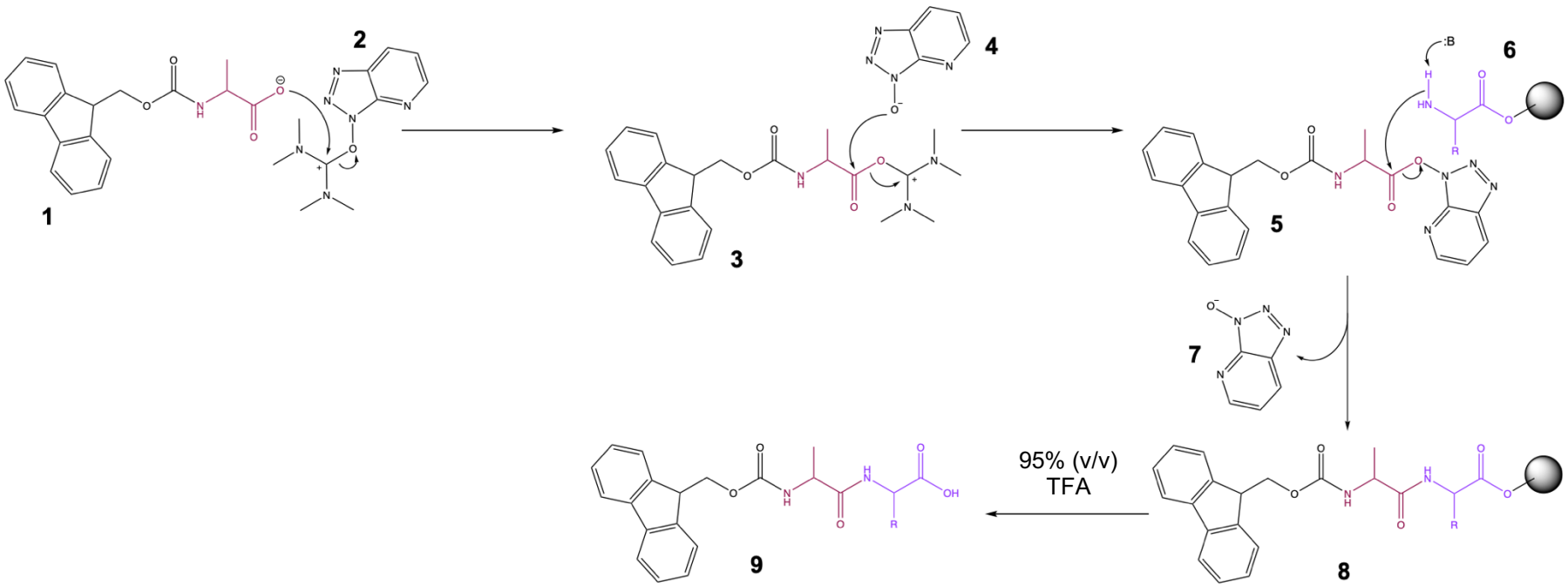

Figure 3.12 Mechanism of solid phase peptide synthesis using *N*-HATU, for synthesis of Fmoc-dipeptides. N-terminally Fmoc-protected L-Ala (**1**) was activated at the carboxyl terminus for amide coupling using HATU **(hexafluorophosphate *N*-oxide) (2). The carboxylate terminus of Fmoc-L-Ala attacks (2), generating intermediate 3 and an HOAt (1-hydroxy-7-azabenzotriazole) anion (4). 4 reacts with 3 to form an OAt-Fmoc-L-Ala activated ester (5). 5 was then subject to nucleophilic attack by the primary amine of L-Ser- or L-Ala-Wang resin (6). *N*-HATU was thus displaced (7) and the Fmoc-L-Ala coupled to the amino acid-Wang resin (8). Finally, Fmoc-dipeptide (9) was cleaved from Wang resin using trifluoroacetic acid (TFA).**

reaction has been reported to suppress racemization (Kemp *et al.*, 1970), and so this additive had been incorporated into the synthesis in original development of the method (De Pascale *et al.*, 2008).

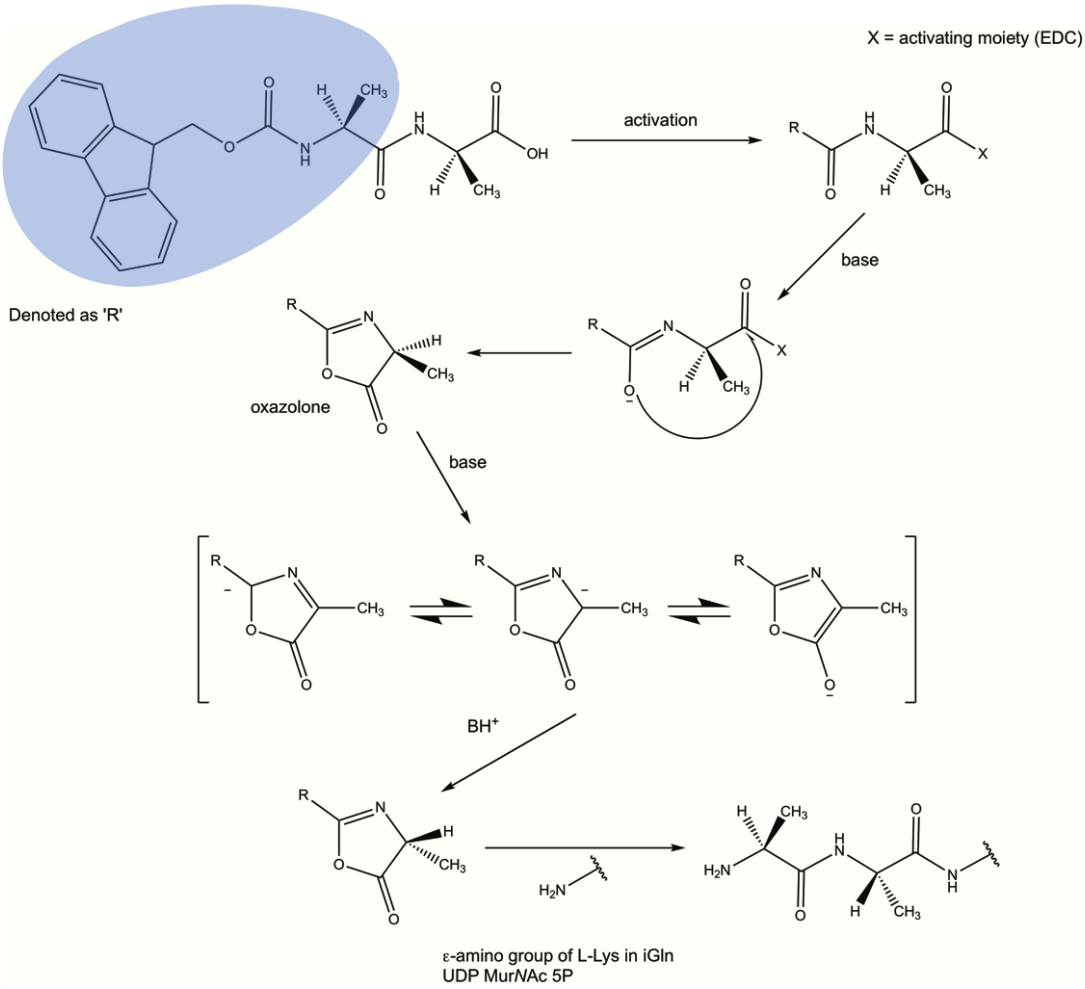

Figure 3.13 Mechanism of potential racemisation by oxazolone formation. Oxazolone formation could occur when activating Fmoc-dipeptides. The carbodiimide (EDC, denoted as 'X') provides a leaving group that allows cyclisation of the C-terminal amino acid, and upon reopening of this ring a switch in stereochemistry of this amino acid may occur. Made with reference to Scheme 2, El-Faham and Albericio (2011).

Chiral chromatography by HPLC was used to assess whether racemization had occurred in the dipeptides. The glycopeptide class of antibiotics, which bind the terminal D-Ala-D-Ala moiety of Lipid II, can be used as chirally-selective stationary phases for enantiomeric separation of amino acids, as proposed by Armstrong *et al.* (1994). In addition to this binding, other interactions between the analyte and a glycopeptide stationary phase may

include hydrophobic, electrostatic and hydrogen bonding, as determined by the structural features of the chosen stationary phase (Ilisz *et al.*, 2006). An attractive approach to generating enantiomerically pure branched muropeptides would be the enantioselective purification of Fmoc-dipeptide HOSu esters, prior to their use in the carbodiimide coupling procedure. This would give a good degree of certainty that diastereoisomerism would not be introduced into the final molecule by rearrangement during the amino acid activation. However, both vancomycin and teicoplanin, two of the antibiotics used in such columns, contain primary amines – and in the case of teicoplanin, the interaction between the ammonium group and a carboxylic acid moiety of the analytes has been demonstrated to be involved in the mechanism of separation (Ilisz *et al*., 2006). The addition of HOSu esters to such stationery phases would therefore carry a risk of covalent linkage of the analyte to these primary amines.

The method chosen was therefore to hydrolyse a sample of each Fmoc-dipeptide HOSu ester by the addition of water. These hydrolysed dipeptides, in addition to samples of the Fmoc-dipeptides before activation, were then analysed by R. Cain by chiral HPLC on a CHIROBIOTIC™ T column (Astec). The dipeptides were found by this method to be >98 % single stereoisomer. However, the analysis following hydrolysis of Fmoc-dipeptide HOSu esters proved more complicated owing to multiple peaks likely introduced by the presence of the activation reagents in the sample. In addition, this method introduced more complexity into the chromatographic resolution of pentapeptide and derivative molecules, as many more peaks were observed possibly due to the multitude of stereocenters in these molecules. Further experimentation will be required to achieve retention of the heptapeptides, to allow analysis of the stereochemistry of the dipeptide branch.

The purity of branched intermediate stocks was tested by analytical anion exchange chromatography, as depicted in Figure 3.14. Whilst L-Ala branched

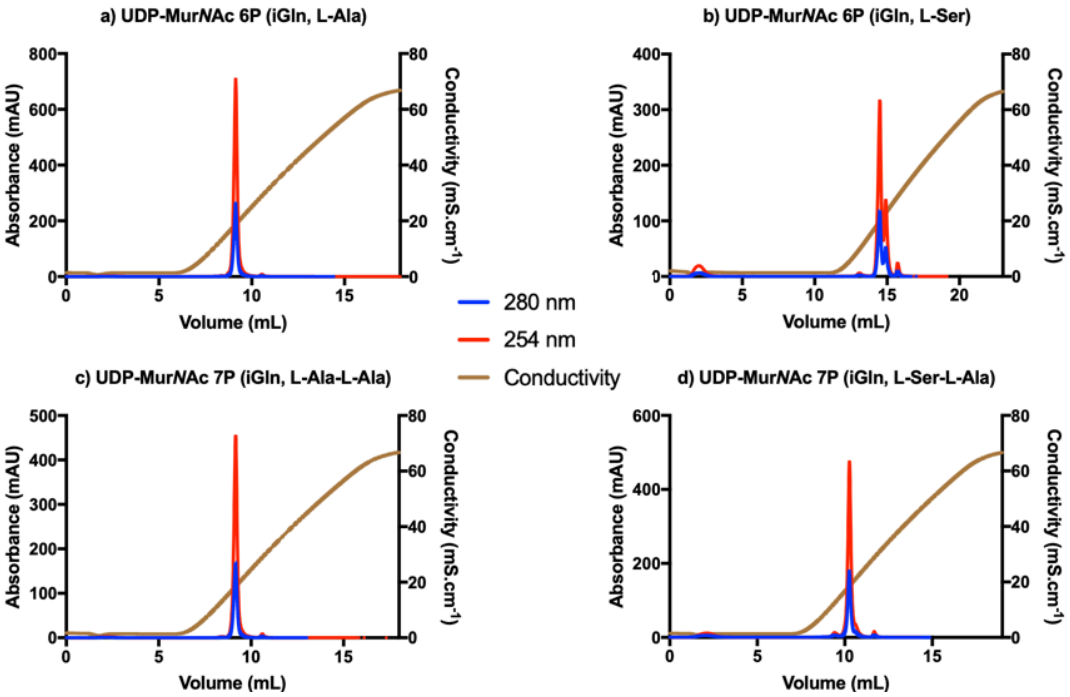

Figure 3.14 Purity assessment of branched UDP-Mur*N*Ac peptides. Samples of branched UDP-Mur*N*Ac peptides were purified by analytical exchange chromatography, with purity assessed based on the area of peaks in absorbance at 254 nm. Purities: UDP-Mur*N*Ac 6P (iGln, L-Ala), 97 %; UDP-Mur*N*Ac 6P (iGln, L-Ser), 62 %; UDP-Mur*N*Ac 7P (iGln, L-Ala-L-Ala) 95 %; UDP-Mur*N*Ac 7P (iGln, L-Ser-L-Ala), 81 %.

variants were obtained to high purity (97 % and 95 % for hexapeptide and heptapeptide respectively), the final purity of the putative L-Ser-containing variants was lower particularly for the hexapeptide (62 % and 81 % for hexapeptide and heptapeptide respectively). The final product of the Ala

Table 3.5: Nanospray TOF mass spectrometry analysis of Ala variant branched peptides. Data collected and analysed by A.J. Lloyd.

Reaction	Charge state	Expected m/z	Observed m/z	Species
UDP-Mur*N*Ac 6P (iGln, L-Ala)	(m-1)/1	1218.40	1218.40	Confirmed
	(m-2)/2	608.70	608.70	
UDP-Mur*N*Ac 7P (iGln, L-Ala-L-Ala)	(m-1)/1	1289.43	1289.44	Confirmed
	(m-2)/2	644.21	644.22	

variant syntheses was confirmed by nanospray mass spectrometry (Table 3.5). Multiple alanylation beyond the desired product was observed in reactions with coupling of dipeptides to UDP-Mur*N*Ac 5P. It was unclear how products including UDP-Mur*N*Ac 8P (iGln, L-Ala-L-Ala-L-Ala) arose from dipeptide coupling.

3.3.4.5 Challenges in synthesis of Ser-branch intermediate

Analysis of Ser variants of branched UDP-Mur*N*Ac peptides (UDP-Mur*N*Ac hexapeptide (iGln, Ser) and UDP-Mur*N*Ac heptapeptide (iGln, L-Ser-L-Ala)) revealed that the product peaks were dominated by species including the products of multiple additions, and the un-deprotected branched peptides (Table 3.6, and Appendices 3.16 to 3.19). Due to these ongoing issues, further development was focused on the Ala variants.

Table 3.6: Nanospray TOF mass spectrometry analysis of Ser variant branched peptides. Ions detected in major peaks as indicated in Figure 3.11. Data collected and analysed by A.J. Lloyd.

Reaction	Expected m/z	Observed m/z	Species	Charge state
UDP-Mur*N*Ac 6P (iGln, L-Ser)	616.69	Not detected	UDP-Mur*N*Ac 6P (iGln, L-Ser)	(m-2)/2
	644.72	644.73	UDP-Mur*N*Ac 6P (iGln, L-Ser-*tert*-Butyl)	
	680.24	680.24	UDP-Mur*N*Ac 7P (iGln, L-Ser-*tert*-Butyl-L-Ala)	
UDP-Mur*N*Ac 7P (iGln, L-Ser-L-Ala)	652.21	652.21	UDP-Mur*N*Ac 7P (iGln, L-Ser-L-Ala)	
	687.73	687.73	UDP-Mur*N*Ac 8P (iGln, L-Ser-L-Ala-L-Ala)	
	723.25	723.25	UDP-Mur*N*Ac 9P (iGln, L-Ser-L-Ala-L-Ala-L-Ala)	
	758.77	758.77	UDP-Mur*N*Ac 10P (iGln, L-Ser-L-Ala-L-Ala-L-Ala-L-Ala)	

3.3.4.6 Mass spectrometry analysis of branched UDP-Mur*N*Ac peptides

To confirm the positioning of the amino acids added to UDP-Mur*N*Ac 5P (iGln) by carbodiimide coupling, UDP-Mur*N*Ac 6P (iGln, L-Ala) and UDP Mur*N*Ac 7P (iGln, L-Ala-L-Ala) were analysed by mass spectrometry using collision-induced fragmentation. UDP-MurNAc 5P (iGln) was also fragmented to illustrate those fragments arising from the addition of the branch amino acids. For experimental details, see Appendices 3.20 to 3.23.

The fragmentation patterns of UDP-Mur*N*Ac 6P (iGln, L-Ala) and UDP-Mur*N*Ac 7P (iGln, L-Ala-L-Ala) revealed ions that were diagnostic of the

branch added to the ε-amino group of the L-Lysine in the stem peptide in each case (Figure 3.15 to Figure 3.16). Fragmentation of UDP-Mur*N*Ac 6P (iGln, L-Ala) generated Lactyl-L-Alanyl-D-isoglutaminyl-L-Lysyl-(L-Alanine)-D-Alanyl-D-Alanine, (expected (m+1)/1 631.34, observed (m+1)/1 631.34), confirming position of branch on UDP-Mur*N*Ac 6P (iGln, L-Ala). Fragmentation of UDP-Mur*N*Ac 7P (iGln, L-Ala-L-Ala) generated Lactyl-L-Alanyl-D-isoglutaminyl-L-Lysyl-(L-Alanyl-L-Alanine)-D-Alanyl-D-Alanine, (expected (m+1)/1 702.38, observed (m+1)/1 702.37), confirming position of branch on UDP-Mur*N*Ac 7P (iGln, L-Ala-L-Ala).

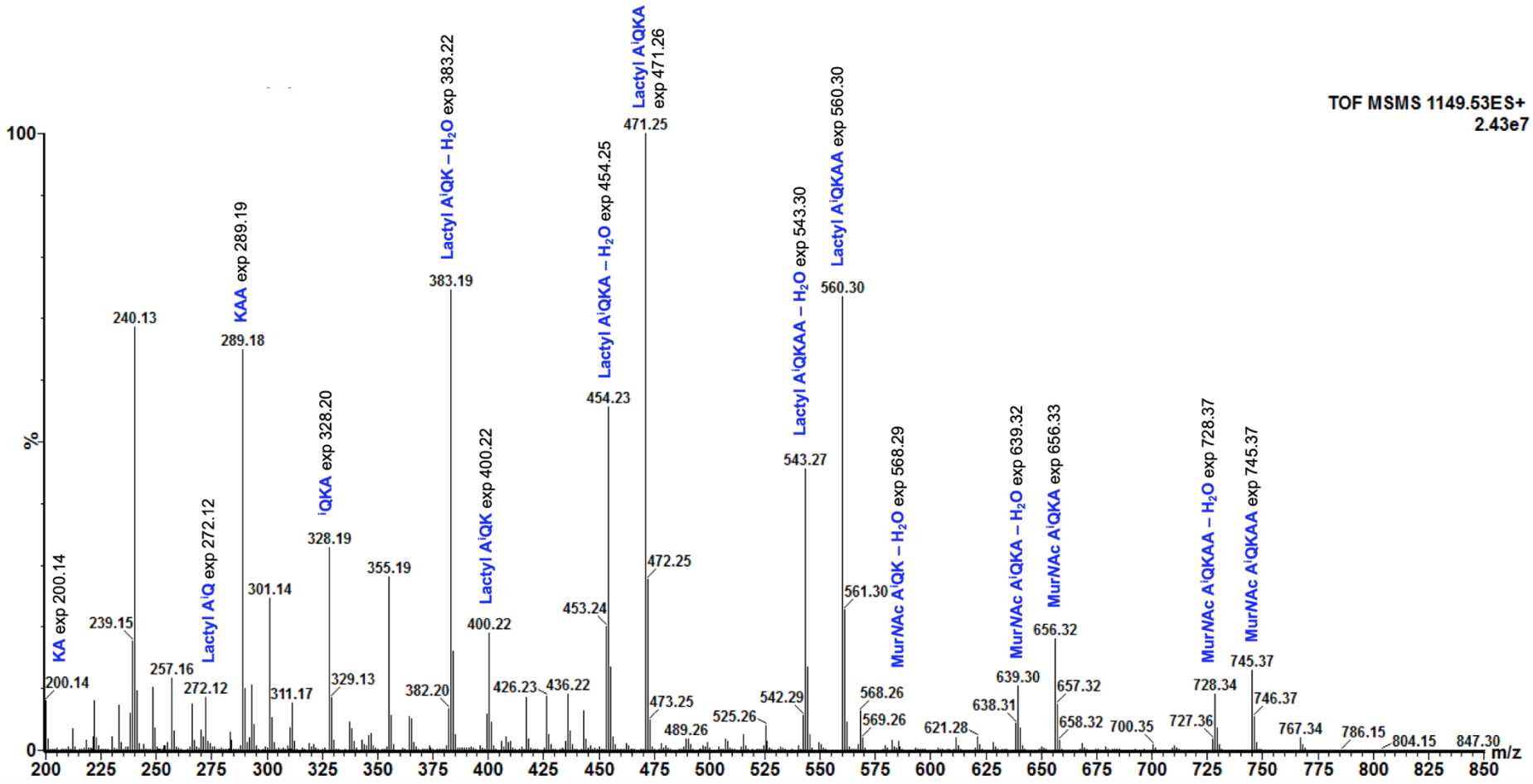

Figure 3.15 Fragmentation pattern of UDP-Mur*N*Ac 5P (iGln). UDP-Mur*N*Ac 5P (iGln) was analysed by collision-induced fragmentation. Data collected by A.J. Lloyd, and mass spectra generated using MassLynx software (Waters).

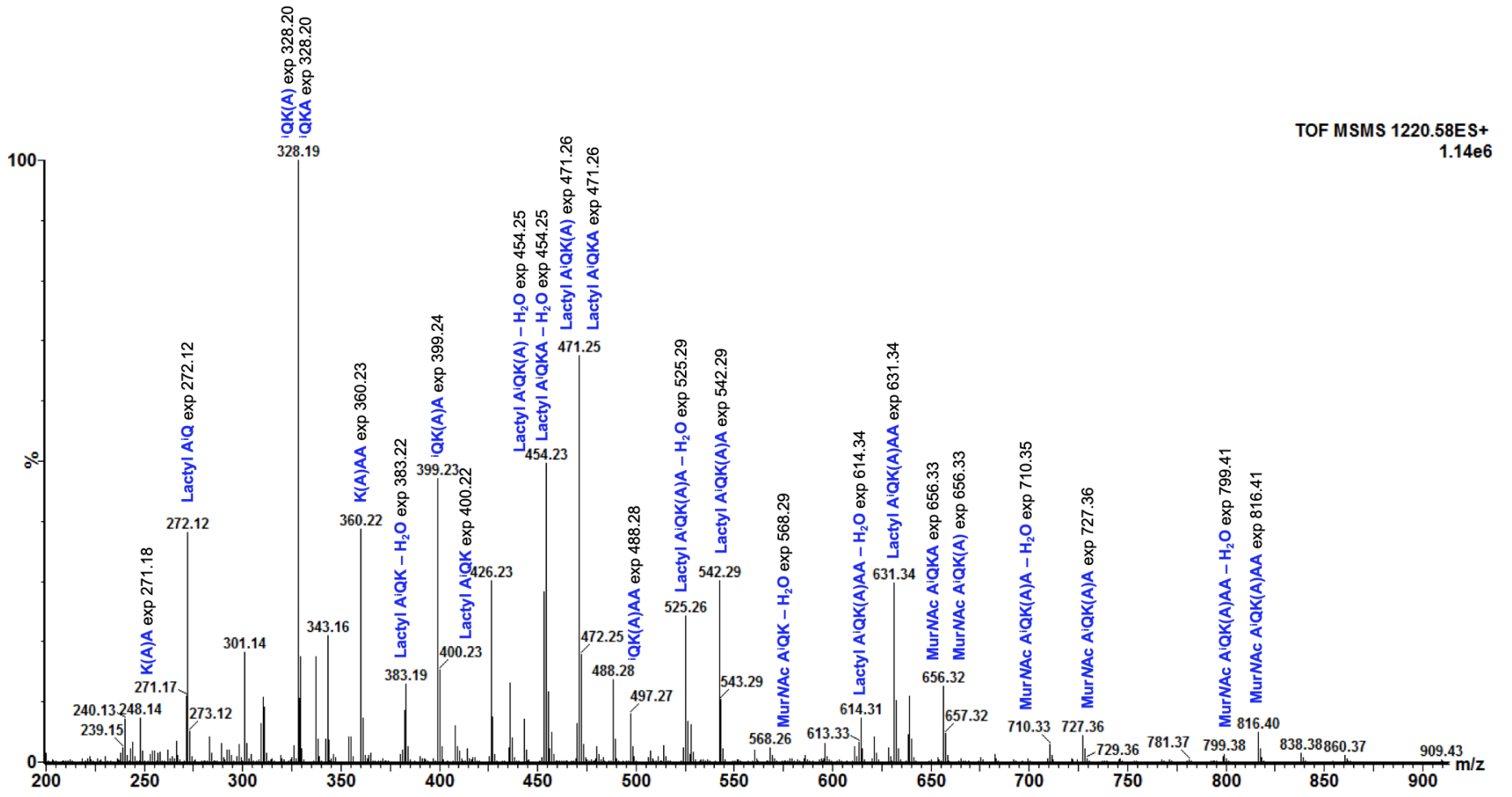

Figure 3.16 Fragmentation pattern of UDP-Mur*N*Ac 6P (iGln, L-Ala). UDP-Mur*N*Ac 6P (iGln, L-Ala) was analysed by collision-induced fragmentation. Data collected by A.J. Lloyd, and mass spectra generated using MassLynx software (Waters).

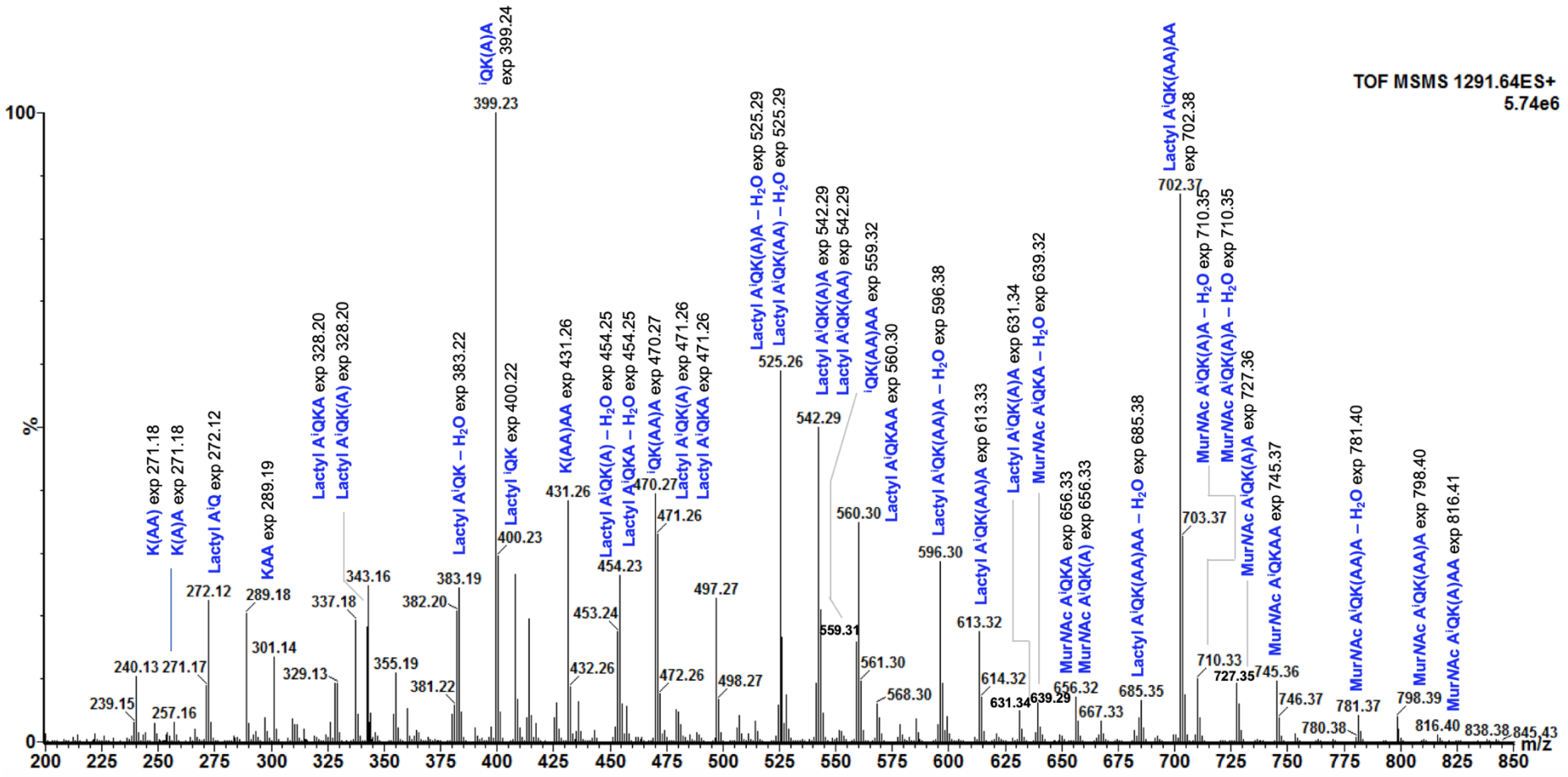

Figure 3.17 Fragmentation pattern of UDP-Mur*N*Ac 7P (iGln, L-Ala-L-Ala). UDP-Mur*N*Ac 7P (iGln, L-Ala-L-Ala) was analysed by collision-induced fragmentation. Data collected by A.J. Lloyd, and mass spectra generated using MassLynx software (Waters).

3.3.4.7 Branched lipids

Following success in obtaining branched UDP-Mur*N*Ac peptides, synthesis of lipid-linked branched intermediates was attempted by the enzymatic method previously described (Section 3.3.2). The syntheses were conducted in 400 μL reactions, in order to limit the mass of branched peptide starting material required, but provide sufficient volume for TLC and mass spectrometry analysis of the reaction products. Reactions were purified on a 400 μL bed DEAE sephacel (GE Healthcare) column by stepwise elution in increasing concentrations of ammonium bicarbonate. Fractions were then analysed by TLC (Figure 3.18). For both Lipid II 6P and Lipid II 7P, two sets of spots were observed, referred to as 'lower' and 'higher' spots. For each purification, the fractions corresponding to each were pooled, dessicated to remove solvents, and lyophilised to remove the ammonium bicarbonate. These samples were then analysed by nanospray TOF mass spectrometry. A summary of the observed masses in each sample is presented in Table 3.7 (see Appendices 3.24 to 3.27 for mass spectra).

Table 3.7 Summary of mass spectrometry data for analysis of branched lipid syntheses. Samples corresponding to the 'higher' and 'lower' spots observed on TLC analysis of the Lipid purifications were analysed by negative ion nanospray time-of-flight mass spectrometry. Data collected by A.J. Lloyd.

Sample	Charge state	Expected m/z	Observed m/z	Compound
Lipid II 6P (iGln, L-Ala) lower spot	(m-3)/3	647.36	647.45	unknown
Lipid II 6P (iGln, L-Ala) higher spot	(m-2)/2	971.55	971.56	Confirmed
Lipid II 7P (iGln, L-Ala-L-Ala) lower spot	(m-2)/2	971.55	971.55 (minor)	Lipid II 6P (iGln, L-Ala)
Lipid II 7P (iGln, L-Ala-L-Ala) higher spot	(m-2)/2	1007.07	1007.08	Confirmed

For both the Lipid II hexapeptide and Lipid II heptapeptide syntheses, a doubly-charged ion whose mass corresponded to that expected for the desired compound was detected in the 'higher' spots sample.

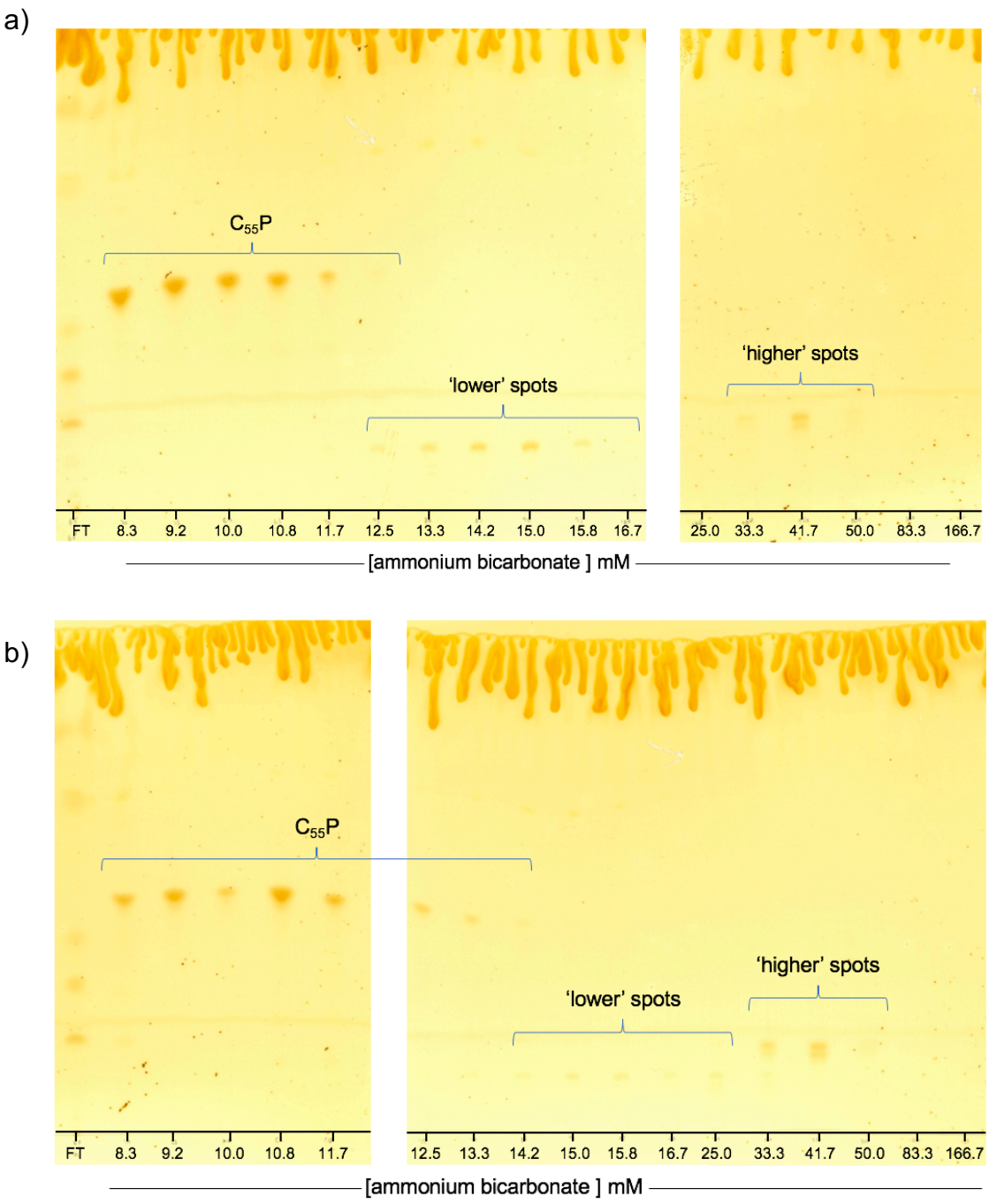

Figure 3.18 Thin-layer chromatography analysis of purification of branched lipid syntheses. Analytical scale syntheses of amidated Lipid II **a)** hexapeptide (L-Ala) and **b)** heptapeptide (L-Ala-L-Ala) were purified by anion exchange chromatography through DEAE sephacel. Elution was performed by with incrementally increasing the ammonium bicarbonate concentration as depicted, in 2:3:1 chloroform:methanol:buffer, and the fractions analysed by thin-layer chromatography run in 44:88:10:1 chloroform:methanol:water:ammonia and stained using iodine vapour. Two sets of apparent product spots were observed in each case, designated 'lower' and 'higher' spots respectively. Purer fractions containing these spots in were analysed by mass spectrometry. **FT,** flow-through **$C_{55}P$,** undecaprenyl phosphate

Lipid II hexapeptide (iGln, L-Ala) was also detected in the 'lower' spot sample for the heptapeptide purification.

3.3.5 Synthesis of donor-only PBP substrates

Transpeptidase donor- and acceptor-only substrates were sought in order to allow the composite rate observed with Lipid II (iGln, L-Lys) (with pentapeptide stem) in the Amplex Red transpeptidase assay to be resolved into the D,D-carboxypeptidation rate (as observed in the presence of the donor-only substrate alone) and the composite rate with transpeptidation (observed in the presence of both a donor-only substrate and an acceptor-only substrate). In addition, the use of defined substrates would allow the important chemical features of each substrate in the transpeptidase reaction to be investigated. Our intended methodology for synthesis of lipid-linked donor-only substrates was to first generate a modified UDP-Mur*N*Ac peptide, and to then link this precursor to undecaprenyl phosphate using *M. flavus* membranes. To render the peptide stem donor-only, the nucleophilic character of the 3rd position amino acid side chain must be lost (Figure 3.19).

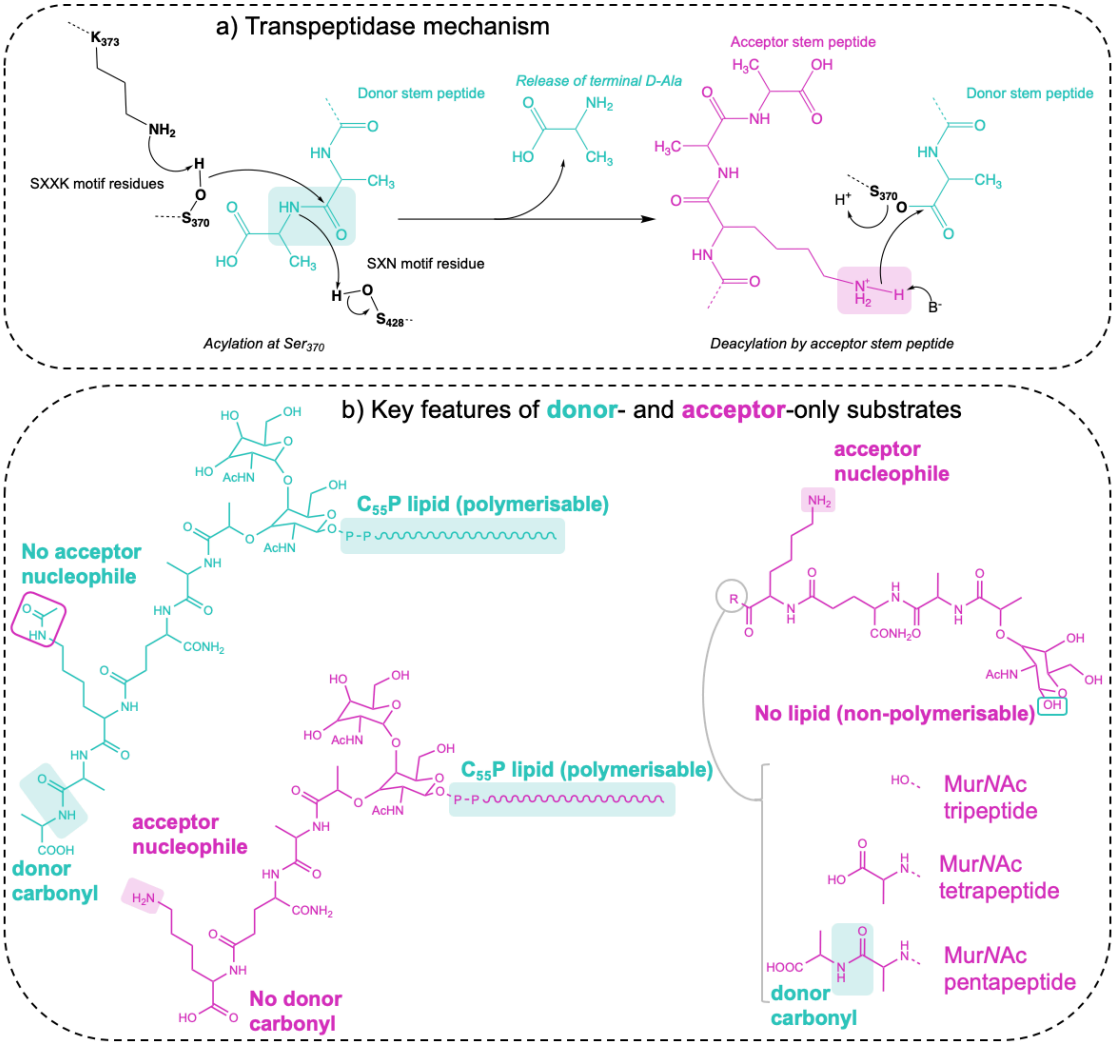

Figure 3.19 Features of donor- and acceptor-only substrates. **a)** The transpeptidase mechanism, illustrating involvement of the donor stem peptide carbonyl (green box) and the primary amine of the acceptor stem peptide (pink box). **b)** the key features determining whether particular substrate variants are donor- or acceptor-only. Donor-only substrates must be polymerisable (i.e. lipid linked) and retain the donor carbonyl. These substrates are made donor-only by loss of the acceptor nucleophile (e.g. by acetylation, as depicted). Conversely, acceptor substrates retain the acceptor nucleophile, and are made acceptor-only by loss of the lipid linker or the donor carbonyl.

3.3.5.1 Enzymatic synthesis of donor-only substrates

The first approach towards synthesis of donor-only substrate analogues for pneumococcal PBPs, was the enzymatic incorporation of non-canonical amino acids into position 3 of the pentapeptide stem by MurE. The amino acids tested for such incorporation were L-Arginine and ε-dimethyl-L-Lysine (see structures of pentapeptide stems generated in Figure 3.20). The

synthesis and purification were as described for UDP-Mur*N*Ac 5P (iGln) (Section 2.6.1) but with the relevant amino acid in place of L-Lysine (see chromatograms Figure 3.21). With both L-Arginine and ε-dimethyl-L-Lysine, the incorporation by MurE was unsuccessful, as the syntheses appeared to have halted at the stage of the dipeptide. On each chromatogram (Figure 3.21a and b), the peak (i) corresponding to a UDP-Mur*N*Ac substrate in the purification of these syntheses was freeze-dried and analysed by negative ion TOF mass spectrometry, which identified this compound as UDP-Mur*N*Ac dipeptide (iGln) (expected (m-2)/2, 438.1; observed, (m-2)/2,438.1. See Table 3.8 and Appendix 3.30).

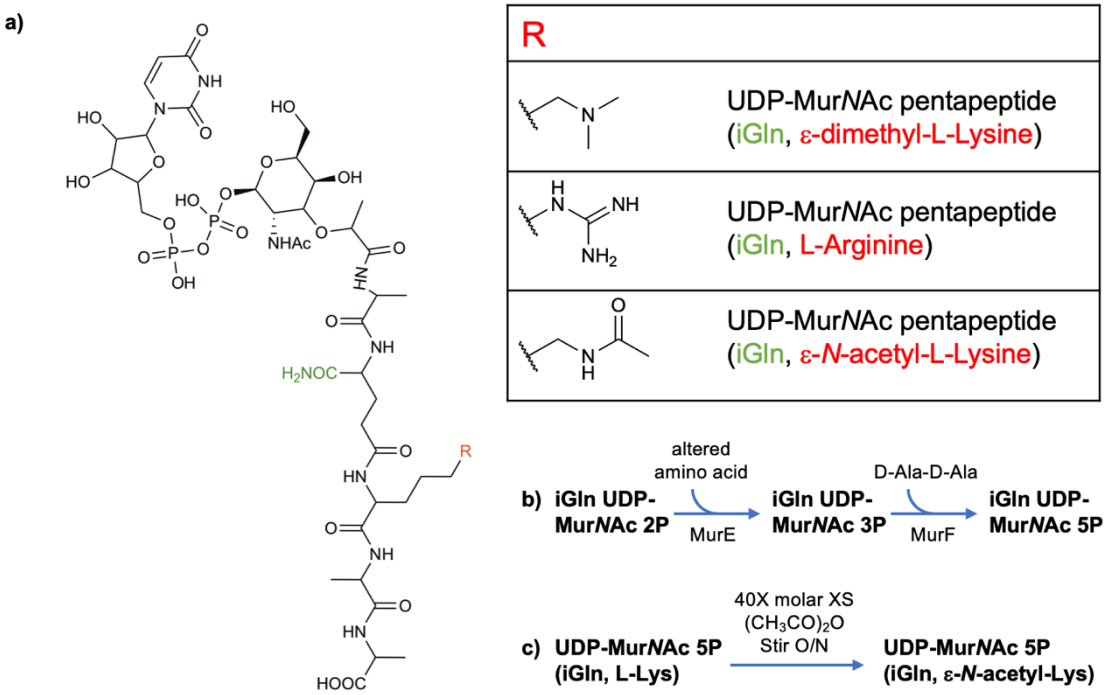

Figure 3.20. Synthesis of donor-only UDP-Mur*N*Ac pentapeptides. The pentapeptide precursors for donor-only substrates whose syntheses were attempted (**a**), with reaction schemes (**b** and **c**). For synthesis of ε-dimethyl-L-Lysine or L-Arginine -containing pentapeptides, the enzymatic biosynthesis method (**b**) was attempted, whereas acetylated pentapeptide (UDP-Mur*N*Ac 5P (iGln, ε-*N*-acetyl-L-Lysine) was synthesised by use of acetic anhydride ($(CH_3CO)_2O$) to acetylate UDP-Mur*N*Ac Lys 5P (iGln) (**c**). All precursors were amidated variants (i.e. with L-isoglutamine at the second position, site of amidation indicated in green).

The failure of incorporation of non-canonical amino acids in these experiments by MurE is likely the result of alteration of both substrates for this enzyme. The *in vivo* substrates of *S. pneumoniae* MurE would be UDP-Mur*N*Ac-L-Ala-D-Glu and L-Lysine (Barreteau *et al.*, 2008), whilst in this enzymatic synthesis, the substrates for MurE were UDP-Mur*N*Ac-L-Ala-γ-D-

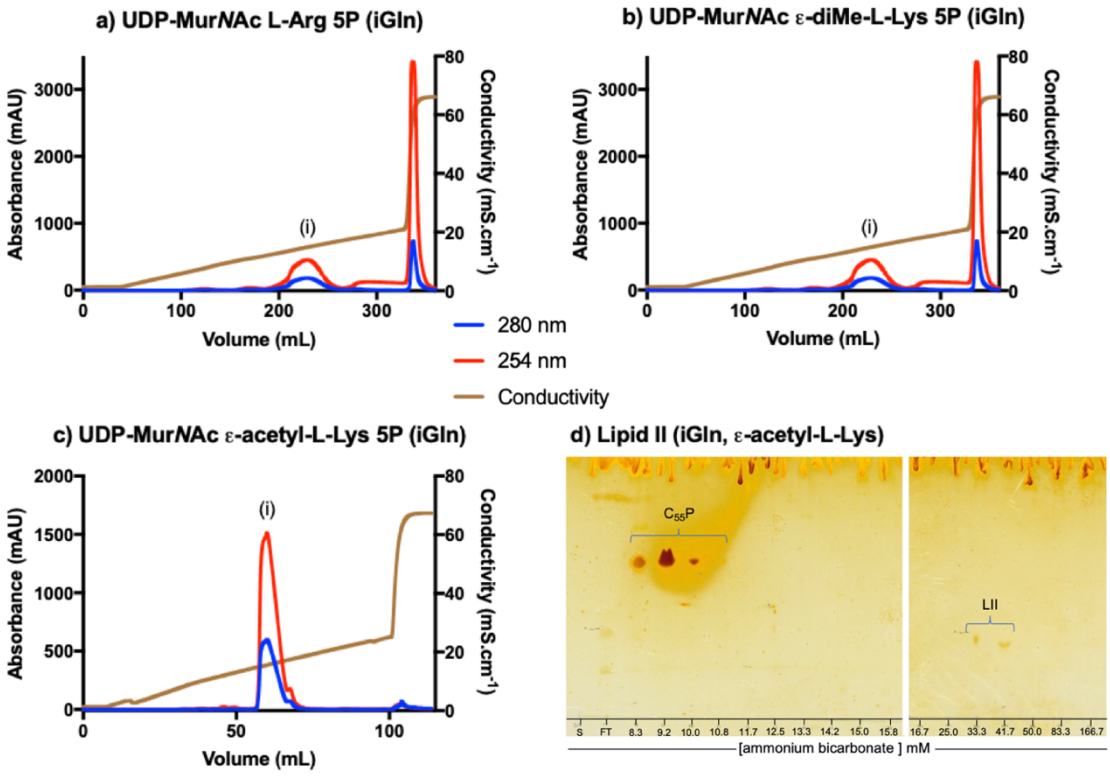

Figure 3.21. Purification of potential donor-only substrates. Pentapeptide precursors for donor-only substrates were purified by anion exchange chromatography on a Source30Q column (a-c) using ammonium acetate buffers, followed by freeze drying to concentrate the product and decrease the salt concentration. In each case, the product peak is denoted by (i). These reaction products were analysed by negative ion nano-spray TOF mass spectrometry. For the reactions to synthesise iGln UDP-Mur*N*Ac L-Arg 5P (a) and iGln UDP-Mur*N*Ac ε-diMe-L-Lysine 5P (b), peak (i) was found to contain iGln UDP-Mur*N*Ac dipeptide, indicating that the synthesis had halted at this stage. The synthesis of iGln UDP-Mur*N*Ac acetyl-L-Lys 5P (c) was successful, as peak (i) was found to contain the desired product (by analysis with negative ion nano-spray TOF mass spectrometry). This pentapeptide was therefore used to synthesise donor-only lipid (d) using *M. flavus* membranes (Breukink et al., 2003).

isoGln and ε-dimethyl-L-Lysine or L-Arginine. Both modified 3rd position amino acids can be utilized by *S. pneumoniae* MurE in an assay, but the K_m with these substrates was at least 20-fold greater than that observed with L-Lysine (Dr. A. York, unpublished, University of Warwick). The low affinity of

the MurE enzyme for both substrates in these syntheses was therefore the most likely cause of the synthesis not progressing beyond UDP-Mur*N*Ac dipeptide.

Table 3.8: Summary of MS analysis of donor-only peptide syntheses. Samples were analysed by negative mode nanospray time-of-flight mass spectrometry. Data collected by A.J. Lloyd.

Sample	Charge state	Expected m/z	Observed m/z	Compound
UDP-Mur*N*Ac 5P (iGln, ε-di-Me-Lys)	(m-2)/2	587.19	438.10	UDP-Mur*N*Ac 2P (iGln)
UDP-Mur*N*Ac 5P (iGln, L-Arg)	(m-2)/2	587.18	438.09	UDP-Mur*N*Ac 2P (iGln)
UDP-Mur*N*Ac 5P (iGln, ε-*N*-acetyl-L-Lys)	(m-2)/2	594.18	594.20	Confirmed
Lipid II (iGln, ε-*N*-acetyl-L-Lys)	(m-2)/2	957.04	957.04	Confirmed

3.3.5.2 Chemo-enzymatic synthesis of donor-only substrate

Synthesis of donor-only UDP-Mur*N*Ac peptide was next attempted by acetylation of UDP-Mur*N*Ac 5P (iGln) using acetic anhydride (Figure 3.20c, and chromatography of reaction Figure 3.21c) was therefore attempted, using a method which has proven successful for synthesis of UDP-Mur*N*Ac D,L-ε-*N*-acetyl-DAP pentapeptide (Anita Catherwood, personal communication, University of Warwick). The desired product was confirmed by negative-ion TOF mass spectrometry (expected (m-2)/2 594.18; observed (m-2)/2 594.20. See Table 3.8 and Appendix 3.28).

Donor-only lipid was then synthesized from the acetylated pentapeptide precursor using *M. flavus* membranes (Section 3.3.2). The thin-layer chromatography analysis of the fractions from the purification is shown in

Figure 3.21d. The product was confirmed by mass spectrometry (expected (m-2)/2 957.04; observed (m-2)/2 957.04. See Table 3.8 and Appendix 3.29).

3.3.6 Synthesis of acceptor-only PBP substrates

As described in Section 3.3.5, the use of defined donor- and acceptor-only substrates enables the detailed analysis of transpeptidase kinetics. The requirements for a substrate analogue to be acceptor-only appear to be that the substrate is either non-polymerisable, such as a Lipid I or Mur*N*Ac peptide compound; or that the peptide stem is lacking one or both D-Ala residues that would ordinarily terminate the stem, preventing such an intermediate from acylating the transpeptidase active site serine (Figure 3.19).

3.3.6.1 Mur*N*Ac peptide acceptors

Acceptors were synthesised by acid hydrolysis of UDP-Mur*N*Ac peptides (with the desired peptide stem), followed by purification by anion exchange chromatography. The loss of the UDP group, which would be the primary portion of the molecule providing negative charges to bind the anion exchange chromatography column, abolished binding of the product to the anion exchange column. Mur*N*Ac peptides therefore instead eluted within one column volume (peak (i), Figure 3.22) from the anion exchange column. The removed UDP (iii) group, and further degraded UMP (ii), did bind the column and can also be observed on Figure 3.22.

The Mur*N*Ac peptide compounds were collected from the column flow-through and freeze dried to remove ammonium acetate. The mass of compound was determined gravimetrically, and identity confirmed by mass spectrometry (Table 3.9). This analysis confirmed that the correct product had been synthesised (expected (m-1)/1 761.37; observed (m-1)/1 761.37; see Appendix 3.31). The acid hydrolysis method as applied to synthesis of Mur*N*Ac 5P (iGln) gave > 95 % yield.

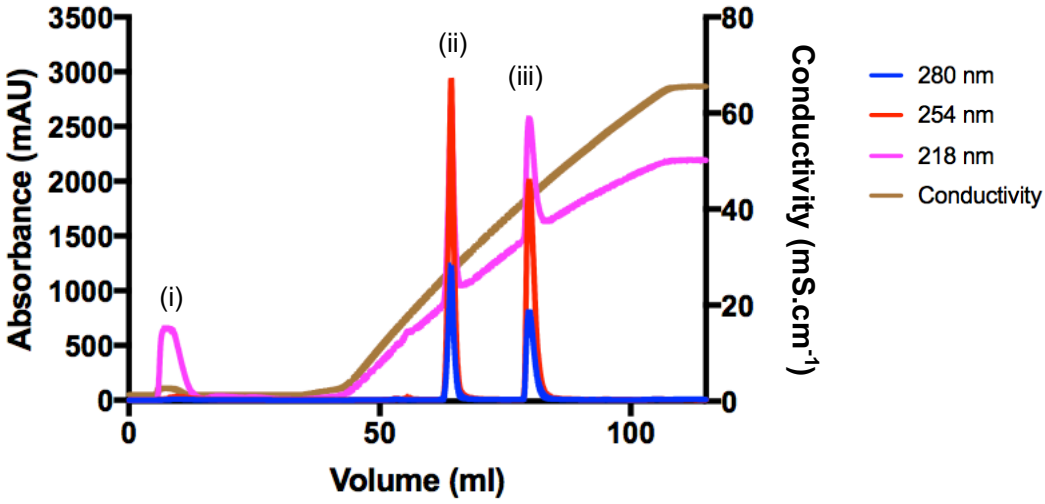

Figure 3.22 Chromatography of Mur*N*Ac 5P (iGln) synthesis. A sample of UDP-Mur*N*Ac 5P (iGln) was acid hydrolysed, neutralised and purified by anion exchange. Peaks were observed corresponding to **(i)** Mur*N*Ac 5P (iGln) **(ii)** UMP and **(iii)** UDP.

This method was then extended to other substrate variants. In addition to Mur*N*Ac peptide acceptors, acceptor-only lipid (Lipid II 3P (iGln)) was also synthesised. The variety of linear Mur*N*Ac peptide acceptor-only substrates synthesised are depicted in Figure 3.23, and summarised in Table 3.9.

Table 3.9: Summary of MS analysis of linear acceptor-only substrate syntheses. Samples were analysed by negative mode nanospray time-of-flight mass spectrometry. Data collected by A.J. Lloyd.

Sample	Charge state	Expected m/z	Observed m/z	Compound
Mur*N*Ac 5P (iGln)	(m-1)/1	761.37	761.37	Confirmed
UDP-Mur*N*Ac 4P (iGln)	(m-1)/1	1076.32	1076.33	Confirmed
	(m-2)/2	537.66	537.66	
Mur*N*Ac 4P (iGln)	(m-1)/1	690.33	690.34	Confirmed
UDP-Mur*N*Ac 3P (iGln)	(m-1)/1	1005.29	1005.30	Confirmed
	(m-2)/2	502.14	502.15	
Mur*N*Ac 3P (iGln)	(m-1)/1	619.29	619.30	Confirmed
Lipid II 3P (iGln)	(m-1)/1	1730.99	1731.00	Confirmed
	(m-2)/2	864.99	865.00	

3.3.6.1.1 Linear acceptors with truncated peptide stems

Two linear acceptors with truncated peptide stems, Mur*N*Ac 4P (iGln) and Mur*N*Ac 3P (iGln) were synthesised by distinct synthetic routes (Figure 3.23).

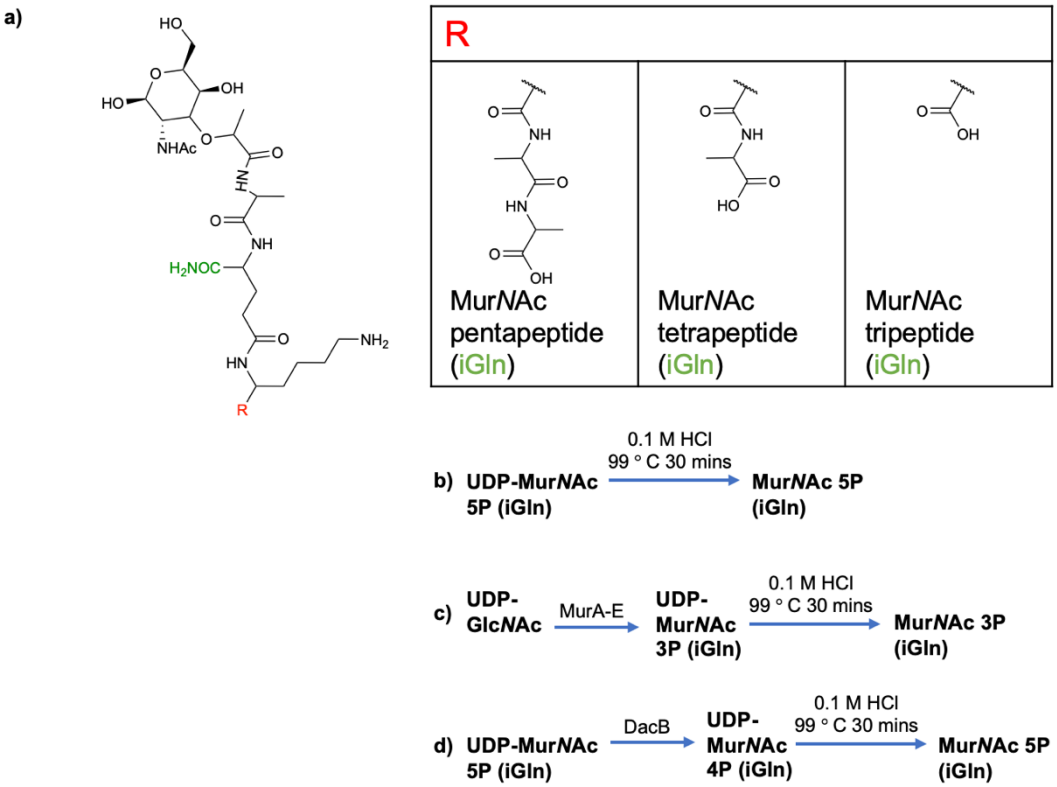

Figure 3.23. Synthesis of linear acceptor-only Mur*N*Ac pentapeptide substrates. The linear peptide acceptor-only substrates whose syntheses are described (**a**), with reaction schemes (**b** to **d**). For synthesis of Mur*N*Ac pentapeptide (**Mur*N*Ac 5P (iGln)**), UDP-Mur*N*Ac pentapeptide (UDP-Mur*N*Ac 5P (iGln) was acid hydrolysed by incubation with 0.1M hydrochloric acid at 99 °C. UDP-Mur*N*Ac tetrapeptide was synthesised from UDP-Mur*N*Ac 5P (iGln) using DacB for removal of the terminal D-Ala. UDP-Mur*N*Ac tripeptide was synthesised enzymatically. The two truncated UDP-Mur*N*Ac peptides were then acid hydrolysed as before. All precursors were amidated variants (i.e. with L-isoglutamine at the second position, site of amidation indicated in green).

Mur*N*Ac 4P (iGln) was synthesised using UDP-Mur*N*Ac 5P (iGln) as the starting material. Mur*N*Ac 4P (iGln) was made by incubating UDP-Mur*N*Ac 5P (iGln) with purified recombinant DacB. The D,D-carboxypeptidase removed the terminal D-Ala of the pentapeptide stem.

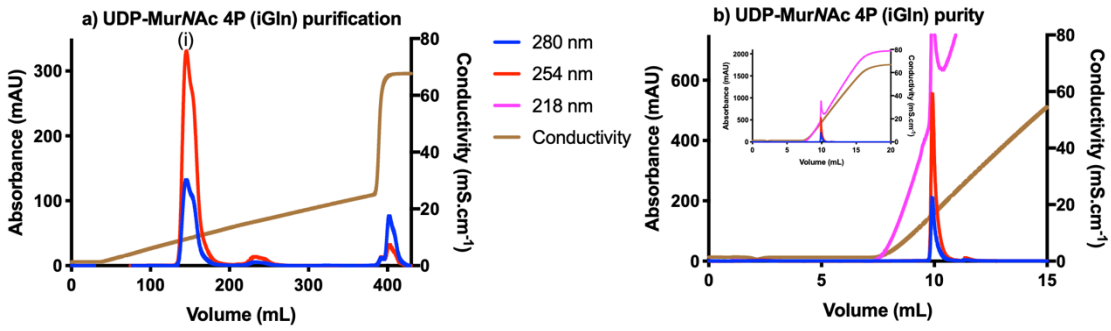

Figure 3.24 Chromatography of UDP-Mur*N*Ac 4P (iGln) synthesis. Chromatography of the synthesis reaction **(a)** by anion exchange chromatography (with product peak **(i)** indicated), and analysis of final purity **(b)** by analytical anion exchange chromatography (with full trace inset) are presented. Analytical anion exchange indicated purity of 94 %.

The reaction was purified by anion exchange (Figure 3.24a), and the product confirmed by nanospray TOF mass spectrometry (expected (m-1)/1 1076.32; observed (m-1)/1 1076.33. See Table 3.9 and Appendix 3.32). UDP-Mur*N*Ac 4P (iGln) was acid hydrolysed as before to generate Mur*N*Ac 4P (iGln)

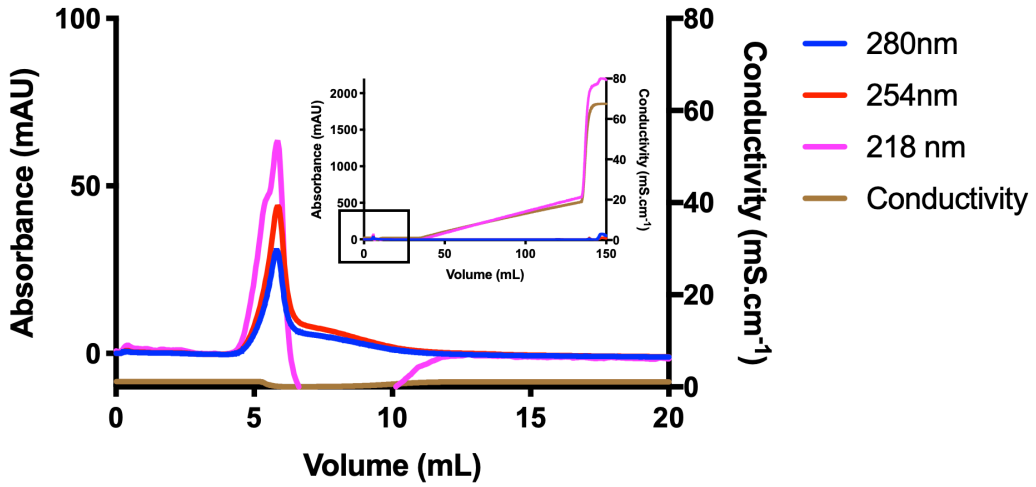

Figure 3.25 Chromatography of Mur*N*Ac 4P (iGln) synthesis. A sample of UDP-Mur*N*Ac 4P (iGln) was acid hydrolysed, neutralised and purified by anion exchange. Inset, full chromatogram with zoomed area indicated in box.

(Figure 3.25). The product was confirmed by mass spectrometry (expected

(m-1)/1, 690.33; observed (m-1)/1, 690.34) The final yield was <30% due to losses at the two steps of the procedure.

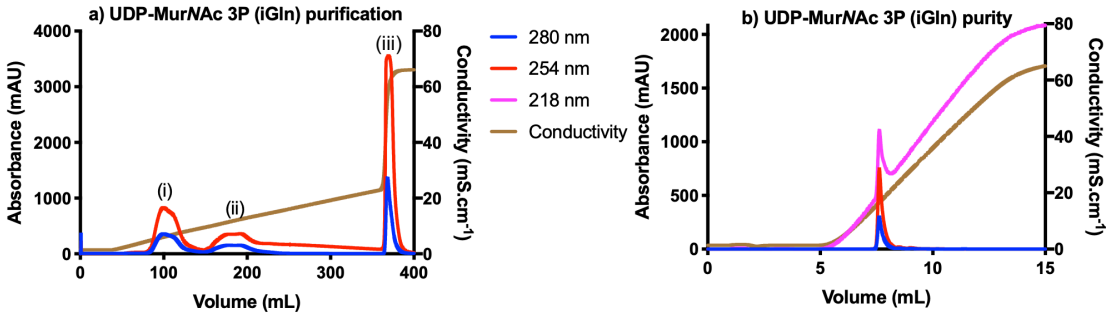

Figure 3.26 Chromatography of UDP-Mur*N*Ac 3P (iGln) synthesis. Chromatography of the synthesis reaction **(a)** by anion exchange chromatography and analysis of final purity **(b)** by analytical anion exchange chromatography are presented. The product peak (**i**) was resolved from PEP (**ii**) and ATP (**iii**). Analytical anion exchange indicated purity of 96 %.

Mur*N*Ac 3P (iGln) was synthesised by first using a modified enzymatic UDP-Mur*N*Ac peptide synthesis to generate UDP-Mur*N*Ac 3P. The synthesis of UDP-Mur*N*Ac 3P was as described for that of UDP-Mur*N*Ac 5P, but omitting MurF and D-Ala-D-Ala. The synthesis was purified by anion exchange chromatography (Figure 3.26) and the product identified by nanospray TOF mass spectrometry (expected (m-1)/1 1005.29 ; observed (m-1)/1 1005.30. See Table 3.9 and Appendix 3.34). UDP-Mur*N*Ac 3P was then hydrolysed as

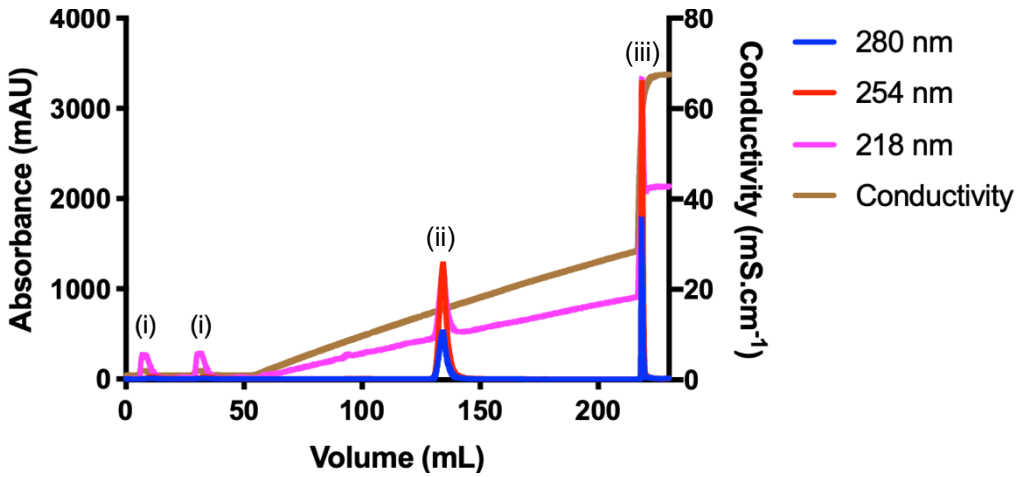

Figure 3.27 Chromatography of Mur*N*Ac 3P (iGln) synthesis. A sample of UDP-Mur*N*Ac 3P (iGln) was acid hydrolysed, neutralised and purified by anion exchange. The compound was loaded to the column in two injections, resulting in the two peaks labelled (i). Further peaks were observed corresponding to **(ii)** UMP and **(iii)** UDP.

previously to generate Mur*N*Ac 3P (iGln). Chromatography of the acid

hydrolysed sample is depicted in Figure 3.27. The acid hydrolysed sample was loaded to the column in two injection steps. The two peaks from the column flow through were collected and lyophilised, and analysed as before. The desired product was confirmed by nanospray TOF mass spectrometry (expected (m-1)/1 619.29; observed (m-)/2 619.30. See Table 3.9 and Appendix 3.35). Purities were not determined for 4P and 3P acceptors.

3.3.6.1.2 Branched acceptors

Branched acceptor-only substrates were synthesised from the UDP-Mur*N*Ac peptide stocks whose syntheses were described in Section 3.3.4. As described for synthesis of linear Mur*N*Ac peptide acceptors, aliquots of branched UDP-Mur*N*Ac peptides were acid hydrolysed using hydrochloric acid. These reactions were purified by anion exchange (Figure 3.28a and b

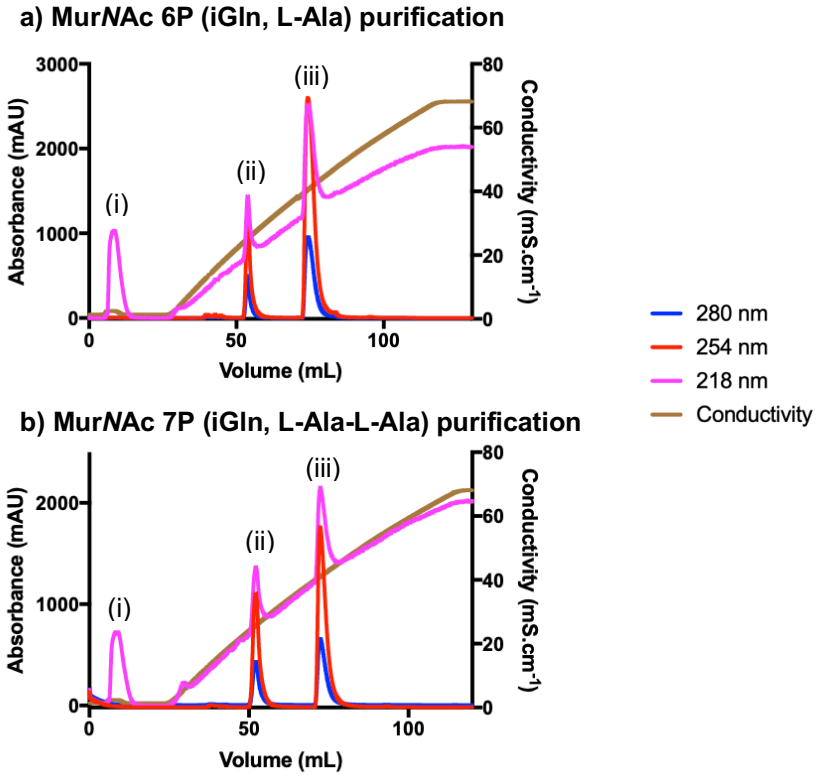

Figure 3.28 Chromatography of Mur*N*Ac 6P (iGln, L-Ala) and MurNAc 7P syntheses (iGln, L-Ala, L-Ala). Samples of **a)** UDP-Mur*N*Ac 6P (iGln, L-Ala) and **b)** UDP-Mur*N*Ac 7P (iGln, L-Ala-L-Ala) peptides were acid hydrolysed, neutralised and purified by anion exchange. Peaks were observed corresponding to **(i)** putative Mur*N*Ac peptides **(ii)** UMP and **(iii)** UDP. The putative product peaks were lyophilised in each case for analysis by mass spectrometry.

for Mur*N*Ac 6P (iGln, L-Ala) and Mur*N*Ac 7P (iGln, L-Ala-L-Ala) respectively). The profile of these purifications resembled those observed for linear peptide acid hydrolysis. The putative product peak for each of Mur*N*Ac 6P (iGln, L-Ala) and Mur*N*Ac 7P (iGln, L-Ala-L-Ala) were lyophilised and analysed by nanospray TOF mass spectrometry.

The mass spectra for both Mur*N*Ac 6P (iGln, L-Ala) and Mur*N*Ac 7P (iGln, L-Ala-L-Ala) revealed two superimposed ion series, likely corresponding to a polymeric contaminant (Figure 3.29 and Table 3.10). The origin of this contaminant was unclear. There was therefore no evidence of successful synthesis of branched Mur*N*Ac peptide substrates.

Table 3.10: Summary of MS analysis of branched acceptor-only peptide syntheses. Samples were analysed by negative mode nanospray time-of-flight mass spectrometry. Data collected by A.J. Lloyd.

Sample	Charge state	Expected m/z	Observed m/z	Compound
Mur*N*Ac 6P (iGln, L-Ala)	(m-1)/1	832.41	Polymeric ion series of $m/z+(119.96)_n$	Unknown
Mur*N*Ac 7P (iGln, L-Ala-L-Ala)	(m-1)/1	903.44	Polymeric ion series of $m/z+(119.96)_n$	Unknown

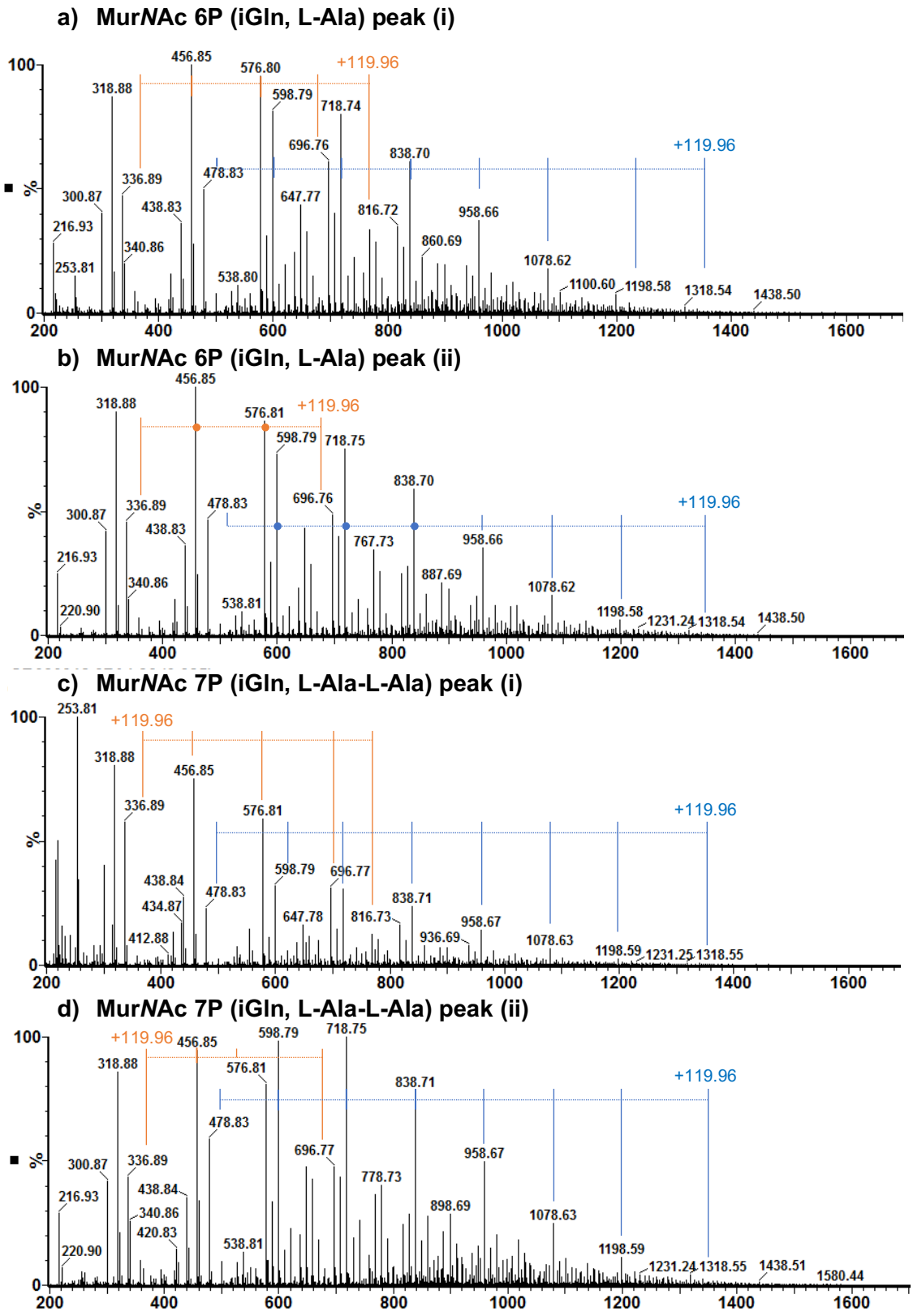

Figure 3.29 Nanospray TOF mass spectrometry of branched Mur*N*Ac peptides. Full spectra of **a)** Mur*N*Ac 6P (iGln, L-Ala) peak (i) **b)** Mur*N*Ac 6P (iGln, L-Ala) peak (ii) **c)** Mur*N*Ac 7P (iGln, L-Ala-L-Ala) peak (i) **d)** Mur*N*Ac 7P (iGln, L-Ala-L-Ala) peak (ii), showing polymeric ion series of m+(119.96)$_n$. Data collected by A.J. Lloyd, and mass spectra generated using MassLynx software (Waters).

3.3.6.2 Polymerisable acceptor – Lipid II 3P (iGln)

Polymerisable acceptor of Lipid II 3P (iGln) was synthesised by linkage of UDP-Mur*N*Ac 3P (iGln) to undecaprenyl phosphate using *M. flavus* membranes (Section 3.3.2). The reaction was purified by anion exchange as described for Lipid II (iGln), and the purification progress was analysed by TLC (Figure 3.30). The fractions containing Lipid II 3P (iGln) were pooled, lyophilised and resuspended in 2:3:1 chloroform:methanol:water for storage at -80 °C.

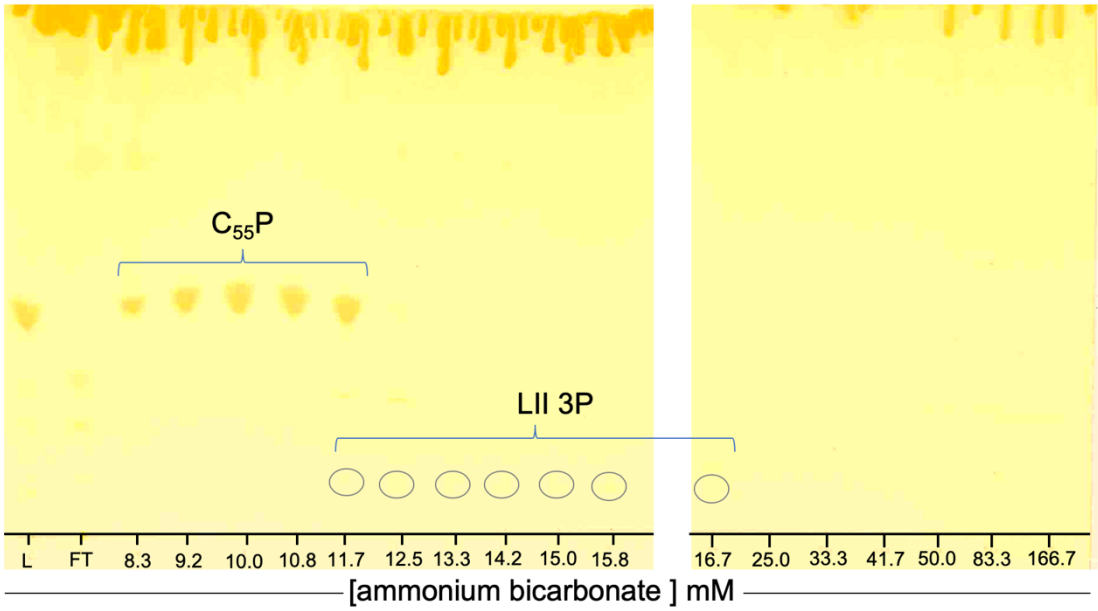

Figure 3.30 Thin-layer chromatography analysis of purification of Lipid II 3P (iGln). The Lipid II 3P (iGln) synthesis reaction was purified by anion exchange chromatography using stepwise elution up to 166.7 mM ammonium bicarbonate in 2:3:1 chloroform:methanol:buffer, and fractions were analysed by thin-layer chromatography run in 44:88:10:1 chloroform: methanol: ammonia: water, and stained using iodine vapour. Position of Lipid II 3P (iGln) spots is highlighted by circles due to poor image quality. **C55P,** undecaprenyl phosphate; **LII 3P,** Lipid II 3P (iGln); **L**, crude sample; **FT**, column flow through

The product of Lipid II 3P (iGln) synthesis was analysed by nanospray TOF mass spectrometry. Ions were detected corresponding to Lipid II 3P (iGln) (expected (m-1)/1 1730.99; observed (m-1)/1 1731.00. See Table 3.9 and Appendix 3.36). A second, unidentified compound was present in the sample, with both singly charged ((m-1)/1, 1295.90) and double charged ((m-2)/2, 647.45) series observed.

3.4 Discussion

A variety of substrates have been prepared for the study of pneumococcal PBPs by the methods described in this chapter. This is the first described synthesis of linear and branched defined substrates for pneumococcal penicillin binding proteins, and as such will allow assay of the activity of these enzymes with near-native substrates. Optimisation of the branched peptide syntheses will also pave the way for full-scale synthesis of branched lipids, further extending the capability to assay PBPs with native substrates. A chemo-enzymatic lipid synthesis for dipeptide branched lipids has also been demonstrated. From this work, larger scale lipid syntheses can be attempted, allowing the use of these substrates for pneumococcal PBP assays.

3.4.1 Limitations of the current system

Ongoing difficulties with the current methods of choice for synthesis of pneumococcal substrates include the low yield of amidated Lipid II; and the number of steps required for synthesis of branched substrates. In addition, the current work has so far not addressed the synthesis of defined donor-only branched substrates.

3.4.1.1 Amidated lipid

Studies of the importance of amidation to PBP activity have described *in vitro* amidation of Lipid II using the MurT/GatD amidase complex (Zapun *et al.*, 2013). This method allows for optimal activity of MraY in synthesising Lipid I, due to the absence of the amidation, which has very much limited the yield of lipid syntheses. This therefore may present a more optimal use of substrates for that reaction, including undecaprenyl phosphate which is expensive to buy. Several important pitfalls of enzymatic amidation using the purified GatD/MurT enzyme complex should be considered. There is the potential for incomplete amidation by the enzyme complex, thus giving rise to a mixture of amidated and non-amidated substrate. This would necessitate use of a method for separation of such a mixture, which is likely to prove difficult on the basis of such a minor chemical change in the current separation methodology. By contrast, the method currently used at Warwick

has the benefit of ensuring that all UDP-Mur*N*Ac pentapeptide will be amidated, so no such separation is necessary. Supplementation of *M. flavus* membranes with purified recombinant MraY may aid in overcoming the limited yields of this substrate.

3.4.1.2. Branched substrates

The main limitation of the procedure for synthesis of branched substrates is the number of steps taken in the procedure, and the resultant losses at each stage. Yields for the hexa- and heptapeptide syntheses were highly variable, and for both Lipid and peptide acceptor synthesis from these compounds, an additional purification step was required. Consequently, the scale of lipid synthesis that could be attempted was limited by how frequently UDP-Mur*N*Ac 5P syntheses could be carried out. In the current work, synthesis of branched Mur*N*Ac peptide acceptors could not be conclusively demonstrated, and so further pursuit of this synthesis is a key next step.

The use of N-[(Dimethlyamino)-1H-1,2,3-triazolo-[4,5-b]pyridin-1-ylmethylene]-*N*-methylmethanaminium hexafluorophosphate *N*-oxide (*N*-HATU) as the activating agent for SPPS was intended to suppress racemization in peptide synthesis (Al-Warhi *et al.*, 2012). However, *N*-HATU would hydrolyse in the aqueous buffer system used for coupling of the dipeptide to UDP-Mur*N*Ac 5P, and so there remains a risk of oxazolone formation with the EDC that is instead used as the activating agent.

Assay of the *S. aureus* Fem ligases (Schneider *et al.*, 2004) and *E. faecalis* BppA enzymes (Bouhss *et al.*, 2002) with UDP-Mur*N*Ac peptides, Lipid I and Lipid II have found that the *S. aureus* enzymes are specific for the Lipid II intermediates (with the appropriate number of glycines added in the case of FemA and FemB), whilst the *E. faecalis* enzymes will catalyse addition to the UDP-Mur*N*Ac peptides. Each of these published methods could be scaled up, allowing their use for synthesis of branched intermediates. This would be more suitable in the case of the BppA enzymes, by nature of the greater

availability of UDP-Mur*N*Ac peptides for starting material (and comparative lower impact of losses at purification steps) compared to Lipid intermediates. Challenges of ensuring full deprotection, and limiting the occurrence of multiple addition, are ongoing in the synthesis of Ser-variant branched peptides. A separate deprotection procedure is required for the *tert*-Butyl protecting group of the serine side chain, which was omitted from these procedures. Multiple addition of serine during heptapeptide syntheses may have occurred due to deprotection of this group during the SPPS procedure.

3.4.1.3 Acceptor and donor only substrates

The substrate syntheses herein described offer methodologies that will greatly support the analysis of transpeptidase activity by *S. pneumoniae* and other Gram positive bacteria exhibiting similar peptidoglycan chemistry (i.e. possessing the amidated peptide stem).

To improve the yield of Mur*N*Ac 4P (iGln) synthesis, the DacB step could be incorporated into the synthesis of UDP-Mur*N*Ac 5P (iGln), prior to anion exchange chromatography. This would decrease the number of purification steps required, and therefore mitigate the losses in this synthesis.

3.4.2. Conclusions

This work contributes to the field of peptidoglycan biosynthesis and study of antimicrobial resistance by providing methods that will facilitate the study of the activity of PBPs. This class of enzymes are a key target for antibiotics of multiple classes, and further characterization of their activity has the potential to allow identification of new factors affecting cell wall biosynthesis.

Chapter 4: Development of a transpeptidase assay for pneumococcal PBPs

4.1 Introduction

The resistance mechanism of pneumococci to β-lactams is based upon the alteration of the PBPs, and their interaction with a branched substrate. The development of a transpeptidase assay for pneumococcal PBPs using natural substrates would therefore provide insight into the resistance mechanism.

4.1.1 Published assay technologies for transpeptidases

Published assays for assessment of transpeptidation have classically relied upon substrate mimetics; the use of β-lactams as a proxy for study of acylation; and stopped assay methods involved chromatography or electrophoresis of reaction mixtures with labelled substrate.

4.1.1.1 Chromogenic thioester substrate analogues

Chromogenic thioester substrates for both D,D-transpeptidases and β-lactamases were first synthesized by Adam *et al.* (1990). Thioester substrate analogues such as S2d (*N*-benzoyl-D-alanylmercaptoacetic acid thioester) mimic the D-Alanyl-D-Ala moiety at the terminus of the donor stem peptide (Macheboeuf *et al.*, 2008). S2d can be used as a transpeptidase donor, with D-amino acid acceptors, for the study of *in vitro* transpeptidase activity. The thioester forms a covalent intermediate with the PBP (with release of thioglycolate), and upon hydrolysis the compound is released as *N*-Benzoyl-D-Ala (Macheboeuf *et al.*, 2008). Reaction of transpeptidases with thioester analogues has been followed directly by spectrophotometric assays, as well as by HPLC (Jamin *et al.*, 1993), mass spectrometry and crystallography (Macheboeuf *et al.*, 2008).

Adam *et al.* (1991) demonstrated the hydrolysis of a range of thioester substrate analogues by soluble constructs of PBPs from *E. coli*, *Enterococcus hirae* and *S. pneumoniae*. In reactions containing *E. hirae* PBP3, there was an acceleration of S2d consumption above the rate with S2d alone upon addition

of D-Ala as an acceptor, and the consumption of S2d was inhibited by addition of benzylpenicillin. Reversed-phase HPLC chromatography of the reaction products allowed Adam *et al.* (1991) to establish the ratio of hydrolysis to transpeptidation products. Certain thioester analogues were also found to inhibit labelling of *E. hirae* PBP3 by benzyl-[^{35}S]penicillin, with recovery of labelling in the presence of D-Ala as an acceptor. This was proposed to be the result of a decrease in the steady-state concentration of acyl-enzyme in the presence of acceptor (Adam *et al.*, 1991).

Macheboeuf *et al.* (2008) used crystallographic studies to reveal the structural details of the interaction of thioester analogues with *S. pneumoniae* PBP1b. As observed in PBP crystal structures in complex with β-lactams, the *N*-Benzoyl-D-Ala moiety of S2d was covalently associated with the catalytic serine, with the D-Ala moiety positioned in the oxyanion hole and stabilised by a hydrogen bonding network. Additionally, a movement of the loop between β3 and β4 was observed in the PBP1b:S2d structure as compared to the apo structure. Macheboeuf *et al.* (2008) proposed that an activation, driven by substrate recognition, was responsible for 'opening' of the active site.

Analysis of transpeptidation by the use of thioester substrate analogues has allowed the determination of acylation efficiency of transpeptidases, in addition to comparison of the ratio of hydrolysis and transfer rates in the presence of acceptors. A key limitation of the thioester substrate analogue method is the lack of coupling of transpeptidation with glycosyltransferase activity. Ongoing glycosyltransferase activity has been found to be a key requirement for *in vitro* transpeptidation of natural substrates (Section 4.1.2). The use of a substrate analogue also limits the possibility to analyse the substrate specificity of the transpeptidase donor, although a variety of amino acid and peptide acceptors have been used in thioester analogue assays (Adam *et al.*, 1991; Macheboeuf *et al.*, 2008).

4.1.1.2 HPLC methods

Reversed-phase HPLC has been extensively used to follow *in vitro* transpeptidation. Detection of reaction products by HPLC was enabled by use of radiolabelled Lipid II substrate (Bertsche *et al.*, 2005), with identification of the peaks by comparison to reference standards.

Glauner (1988) published a method for the reproducible reversed-phase HPLC separation of muropeptides. Detection of muropeptides was based on absorbance at 205 nm, or radioactivity when peptidoglycan samples were labelled with [^{3}H]-DAP. Bertsche *et al.* (2005) used the HPLC analysis described by Glauner (1988) to develop a method for following transpeptidase activity of *E. coli* PBP1b. This method has been used in applications such as determining the impact of protein interacting partners on the peptidoglycan synthesis activity of *E. coli* PBP1b (Müller *et al.*, 2007).

A distinct method for HPLC analysis of PG synthesis was described by Schwartz *et al.* (2001). This methodology involved post-reaction labelling with fluorescamine (via primary amines) to visualise glycan polymers, and to label D-Ala released by transpeptidation.

HPLC-based analyses of peptidoglycan synthesis are suited to the use of natural substrates, thereby allowing comparisons of substrate usage that are not possible with thioester substrate analogues. The sensitivity of detection of the radiolabelled substrates allows the use of very limited quantities (in the nanomolar range) of substrate. Published uses of HPLC-based analysis are unclear on the mode of identification of particular substrate peaks, and would benefit from partnered analysis by mass spectrometry. In addition, the stopped format of HPLC assays is less favourable than a continuous assay system for the determination of kinetic constants.

4.1.1.3 Tris-tricine SDS-PAGE analysis

Whilst the use of Tris-tricine SDS-PAGE has been primarily in the visualisation of glycan polymers generated by PG synthases (Section 5.1.1), the method has also been adapted to allow analysis of transpeptidase reaction products. Barrett *et al.* (2007) described the SDS-PAGE analysis of radiolabelled glycan polymers produced *in vitro.* This method was then adapted for the analysis of transpeptidase reaction products by Helassa *et al.* (2012), who used a mixture of fluorescently-labelled and unlabelled Lipid II to demonstrate putative *in vitro* synthesis of cross linked peptidoglycan by *E. coli* PBP1b. This observation was based upon the formation of high molecular weight material that was unable to enter the gel matrix, and which was not observed when penicillin was included in the reaction mixture.

The SDS-PAGE analysis of labelled PG synthesis products allows qualitative analysis of peptidoglycan synthesis, and the determination of IC50 values in certain contexts (Qiao *et al.*, 2017). However, this technique is not suited to the kinetic analysis of transpeptidation.

A key criticism of the SDS-PAGE analysis method has been the difficulty in conclusive demonstration that the high molecular weight material corresponds to cross-linked polymer. Attempts to excise the material from acrylamide gels and detect the polymer by mass spectrometry have been unsuccessful (Galley, 2015). In addition, care must be taken in analysis of transpeptidase reaction products by mass spectrometry. Zapun *et al.* (2013) assigned a 1842.743 Da product to the transpeptidase product, but this mass could also correspond to a GT dimer (see Section 4.3.2.1.1).

Qiao *et al.* (2017) validated the presence of cross-linked material using lysostaphin, which specifically hydrolyses pentaglycyl cross-links. Following lysostaphin hydrolysis, the high molecular weight material was lost, thereby illustrating that this material had been unable to enter the gel matrix due to the presence of cross-links between polymers.

4.1.1.4 BOCILLIN FL binding

BOCILLIN FL is a fluorescent β-lactam compound consisting of penicillin V with a BODIPY (boron-dipyrromethene) fluorophore conjugated to the phenyl side chain (Zhao *et al.*, 1999). BOCILLIN FL offered a more convenient labelling method for PBPs than the previously used radiolabeled penicillins, which brought issues of hazard and experimental time (Zhao *et al.*, 1999). BOCILLIN FL has been used in a variety of experiments to analyse PBPs and their interactions with other β-lactams, as reviewed by Stone *et al.* (2018).

Zhao *et al.* (1997) reported the use of BOCILLIN FL to label PBPs prior to SDS-PAGE. This method allowed detection of the PBP profiles in bacterial membrane preparations. Binding affinities of competing β-lactams could also be determined with this method. Kocaoglu *et al.* (2015) used BOCILLIN FL labelling to define the selectivity of β-lactams for particular pneumococcal PBPs.

An alternative technique for determination of binding affinities using BOCILLIN FL is based upon fluorescence anisotropy. Such assays measure the polarisation of incident light by the tumbling of BOCILLIN FL in solution, and the effect upon the signal by binding of the protein of interest (Shapiro *et al.*, 2013).

BOCILLIN FL can be used to conduct similar experiments to those historically performed using radiolabelled β-lactams, but in a safer and less time-intensive manner. Fluorescence anisotropy assays with BOCILLIN FL are limited to use with soluble PBP constructs. Detergent micelles have been found to sequester BOCILLIN FL, resulting in high anisotropy signal (Shapiro *et al.*, 2013).

4.1.1.5 Chromogenic cephalosporins: nitrocefin and CENTA

Assay systems developed for use with β-lactamases have shown utility in the study of PBPs. O'Callaghan *et al.* (1972) discovered the chromogenic properties of the cephalosporin analogue nitrocefin. Hydrolysis of nitrocefin to generate the corresponding cephalosporanoic acid could be followed

spectrophotometrically (λmax 482 nm). This phenomenon formed the basis of an extensively used assay for detection of β-lactamases (Livermore & Brown, 2001).

Nitrocefin hydrolysis has been used to analyse kinetics of PBP acylation with β-lactams. Roychoudhury *et al.* (1996) used nitrocefin to analyse the precipitation of *S. aureus* PBP2a when acylated by β-lactams.
Interestingly, nitrocefin turnover by particular PBPs has been demonstrated. Calvez *et al.* (2017) demonstrated apparent turnover of nitrocefin by *S. pneumoniae* PBP2b^{5204}, beyond the expected stoichiometric plateau. *E. coli* PBP5 has also been demonstrated to catalyse hydrolysis of the penicilloyl-enzyme complex (Josephine *et al.*, 2006).

Similarly to nitrocefin, CENTA (7-β-thien-2-yl-acetamido-3-[(4-nitro-3-carboxyphenyl)thiomethyl]-3-cephem-4-carboxylic acid) is a chromogenic cephalosporin used for the assay of β-lactamases (Jones *et al.*, 1982). In contrast to nitrocefin, assay of CENTA hydrolysis relies upon detection of the leaving group, 2-nitro-5-sulfanylbenzoic acid (λmax 405 nm) that is expelled upon opening of the lactam ring (Fast & Sutton, 2013). In comparison with nitrocefin, CENTA offers the benefit of its solubility in aqueous solutions, whilst nitrocefin is soluble in DMSO and DMF (Bebrone *et al.*, 2001). CENTA has also been used to demonstrate inhibition of PBPs (Bebrone *et al.*, 2001).

Chromogenic cephalosporins allow study of the interaction of PBPs with β-lactams. Their suitability to analysis of transpeptidation is currently limited to those examples of PBPs that catalyse rapid hydrolysis of the β-lactam ring.

4.1.1.6 Other assay technologies

Fluorescent D-amino acids (FDAAs) are chemical probes that have been used to reveal a multitude of details of the *in vivo* cell division process. Building upon this technology, Hsu *et al.* (2019) designed novel fluorogenic amino acid probes for the study of transpeptidation both *in vitro* and *in vivo*. Rotor fluorogenic D-amino acid (RfDAA) assays were based upon the principle of

fluorescent molecular rotors, whereby the steric hindrance of the environment of the probe determines the emission intensity. High hindrance environments created an 'on' state whereby the excitation energy was converted into fluorescence emission, and incorporation of RfDAAs into peptidoglycan thus resulted in fluorescence emission, with low background from free probe. Transpeptidase activity of *S. aureus* PBP4 was followed using a peptide stem mimic as the acyl donor (diacetyl-L-lysyl-D-alanyl-D-alanine), and activity was inhibited by β-lactams known to bind PBP4.

Other tool compounds for analysis of PBP activity are based on modified β-lactams, allowing the analysis of acylation and deacylation parameters. Josephine *et al.* (2006) used penicillins with stem peptide-mimicking side chains to test the *in vitro* hydrolysis and aminolysis activity against such peptides.

4.1.2 *In vitro* transpeptidase activity of pneumococcal PBPs

A variety of authors have published analyses of the kinetics of β-lactam interactions with pneumococcal PBPs (Di Guilmi *et al.*, 1998; Zhao *et al.*, 1997). Analysis of *in vitro* pneumococcal transpeptidase activity has been hindered by limited access to substrates.

Poor correlation between pneumococcal PBP activity with substrate analogues and native substrates has been observed (Helassa *et al.*, 2012). Helassa *et al.* (2012) found that whilst S2d hydrolysis could be catalysed by purified recombinant *S. pneumoniae* PBP2a, transpeptidase activity by PBP2a was not detected in the SDS-PAGE assay. However, the authors noted that this assay was performed with non-amidated Lipid II.

The first unambiguous demonstration of *in vitro* transpeptidase activity by pneumococcal PBP1a using native substrate was shown by Galley (2015), using a continuous D-Ala release assay and with confirmation of the product formed by LC-MSMS analysis. These findings formed the basis for the assay optimisation described in Section 4.3.2.

4.1.3 β-lactam resistance-linked sequences in pneumococcal PBP1a

Whilst in pneumococci the primary resistance determinants with respect to β-lactam antibiotics are PBP2x and 2b, alterations to PBP1a are also required for high level pneumococcal penicillin resistance (Barcus *et al.*, 1995; Coffey *et al.*, 1995). A variety of studies have identified particular key motifs associated with β-lactam resistance in clinical pneumococcal strains.

Smith and Klugman (1998) demonstrated the link with β-lactam resistance of the T_{371}A/S and TSQF$_{574\text{-}577}$NTGY mutations in pneumococcal PBP1a. PBP alleles originating from the resistant South African pneumococcal isolate 8303 were transformed into the susceptible strain R6. R6 transformants showed approximately 3-fold reductions in MICs when either mutation was reverted, thus illustrating the link of these amino acid changes to the resistance mechanism. Various other authors have reported the T_{371}A/S mutation in PBP1a alleles in β-lactam resistant strains (Davies *et al.*, 2008; Kosowska *et al.*, 2004; Nagai *et al.*, 2002).

The mechanistic basis of the importance of T_{371}A/S and TSQF$_{574\text{-}577}$NTGY in β-lactam resistance was analysed by Job *et al.* (2008), who compared the efficiency of acylation of PBP1a variants using intrinsic fluorescence. T_{371}A and TSQF$_{574\text{-}577}$NTGY were found individually to decrease the efficiency of acylation of PBP1a by cefotaxime and penicillin G, and an enhanced combined effect was also observed. Comparison of crystal structures from trypsinised PBP1a^{R6} and PBP1a^{5204} found that alterations to the active site in PBP1a^{5204} included the loss of a hydrogen bond between N_{430} and Y_{409}; the appearance of a hydrogen bond between K_{373} and N_{430}; rotation of the nucleophilic S_{370} to point away from the active site, with formation of an interaction with T_{560}; loss of a hydrogen bond between T_{371} (mutated to A) and W_{368}, suggested to be a factor in the 0.6 – 1.1 Å shift of the nucleophilic S_{370}; and the F_{577}Y mutation, whose modification of the properties of the hydrophobic wall at the lower portion of the active site cavity was hypothesised to be involved in changes to recognition or entrance of β-lactams (Job *et al.*, 2008).

Contreras-Martel *et al.* (2006) found that mutations in PBP1a from a penicillin and ampicillin resistant clinical pneumococcal strain, 73311, mapped mainly to loop regions of the protein. There was additionally a mutational hotspot in the catalytic cleft region. Mutations in the 'hotspot' included $TSQF_{574\text{-}577}NTGY$; $L_{606}I$, $N_{609}D$, $L_{611}F$ and $T_{612}L$ at α11; and $N_{546}G$. These modifications were suggested to alter the surface polarity at the entrance to the active site, in addition to modification of the relevant loops by alterations of residues 546 and 576. The proximity of these mutations to the interconnecting loop of β3 and β4 enhances the flexibility of this region, in a feature common to both PBP1a and PBP2x variants from penicillin resistant strains (Contreras-Martel *et al.*, 2009) and which was suggested to accommodate the branched substrates utilised in penicillin resistant strains.

The link between branched substrate synthesis and penicillin resistance of *S. pneumoniae* has been extensively documented. The mechanistic consequences of the alterations to pneumococcal PBPs, in combination with usage of branched substrates, has remained more obscure due to limitations in the available assays for transpeptidation, and supply of native substrates for these assays. Chapter 3 described efforts to address the latter issue; this Chapter focusses on experiments in pursuit of an assay for *in vitro* transpeptidation that would allow comparison of usage of linear and branched substrates.

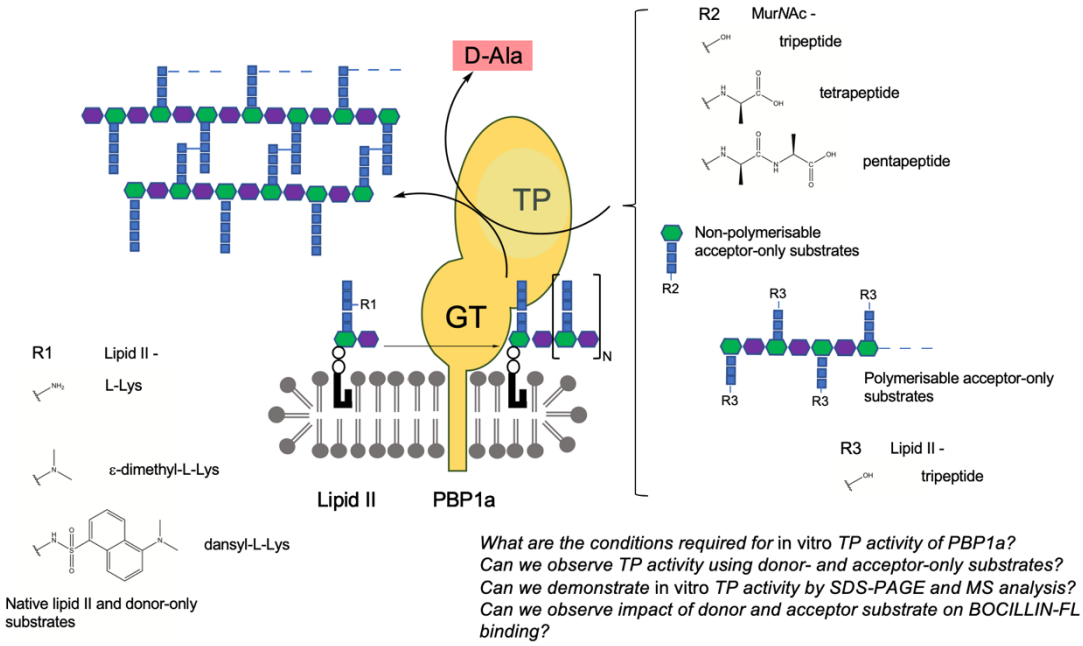

Figure 4.1 Chapter 4 experimental questions summary A visual summary of the questions to be addressed in this thesis. **GT**, glycosyltransferase; **TP**, transpeptidase

4.2 Experimental aims

- To clone PBP1a variants from *S. pneumoniae* Pn16 and 159 strains into pET46a vector
- To express and purify PBP1a variants from *S. pneumoniae* D39, Pn16 and 159 strains, and a transpeptidase active site serine mutant ($S_{370}A$) of $PBP1a^{D39}$ ($PBP1a^{D39\_S370A}$)
- To establish observation of *in-vitro* transpeptidase activity of $PBP1a^{D39}$ in the continuous D-ala release assay
- To determine the optimum concentration of E_6C_{12} detergent for *in vitro* transpeptidase activity
- To assess the contribution of transpeptidation and D,D-carboxypeptidation to the D-ala release rate, by assay of the D-ala release activity of $PBP1a^{D39}$ in the presence of donor- and acceptor-only substrates
- To assess TP activity by Tris-Tricine SDS-PAGE
- To use mutanolysin digestion followed by liquid chromatography-tandem mass spectrometry to analyse the products of putative *in-vitro* transpeptidation
- To assess whether SDS-PAGE analysis of BOCILLIN FL binding can be used to analyse donor and acceptor interactions

4.3 Results

4.3.1 Expression and purification of pneumococcal PBP1a variants

4.3.1.1 PBP1a construct progenitor strains

This work made use of expression constructs of PBP1a^{D39} and PBP1a^{D39_S370A} proteins that were generated by Abrahams (2011). Expression constructs of PBP1a variants from two clinical pneumococcal strains, Pn16 (Pen^{S}) and 159 (Pen^{R}) were made in this work, to allow comparison of activity between PBP1a variants with different modifications to the amino acid sequence, and whose progenitor strains differed in β-lactam susceptibility. These strains were chosen to complement previous studies on the activity of MurM variants (Lloyd *et al.*, 2008).

Table 4.1 Penicillin G MIC values for pneumococcal strains of interest. Penicillin G (**PenG**) MICs were obtained from the relevant publications, or determed by microbroth dilution.

Pneumococcal strain	PenG MIC (μg.mL^{-1})
D39	0.015[b]
R6	<0.016[c]
Pn16	0.012[a]
5204	6[c]
73311	8[d]
3191	16[e]
159	16[a]

Sources: a. this thesis; b. Sorg and Veening (2015); c. Job et al. *(2008); d. du Plessis* et al. *(2002); e. Smith and Klugman (2003).*

Table 4.1 compares Penicillin G minimum inhibitory concentration (MIC) values of *S. pneumoniae* strains including the progenitors of the constructs discussed in this chapter (D39, Pn16 and 159), and some strains for which amino acid changes in PBP1a have been characterized (as discussed in Section 4.1.3.2). MIC values for Pn16 and 159 were determined by microbroth dilution (Section 2.8) in accordance with CLSI guidelines (CLSI, 2014). MIC

values would ideally be determined in-house for all strains, to ensure comparability of values, but this was limited by access to the strains.

Figure 4.2 presents a comparison of the amino acid sequences of the corresponding PBP1a variants to the strains compared in Table 4.1. Notably, despite the high-level resistance of strain 159, PBP1a^{159} did not have the substitution T_{371}S/A, whose association with β-lactam resistance by several studies (Job *et al.*, 2008; Smith & Klugman, 1998) was discussed in Section 4.1.3.

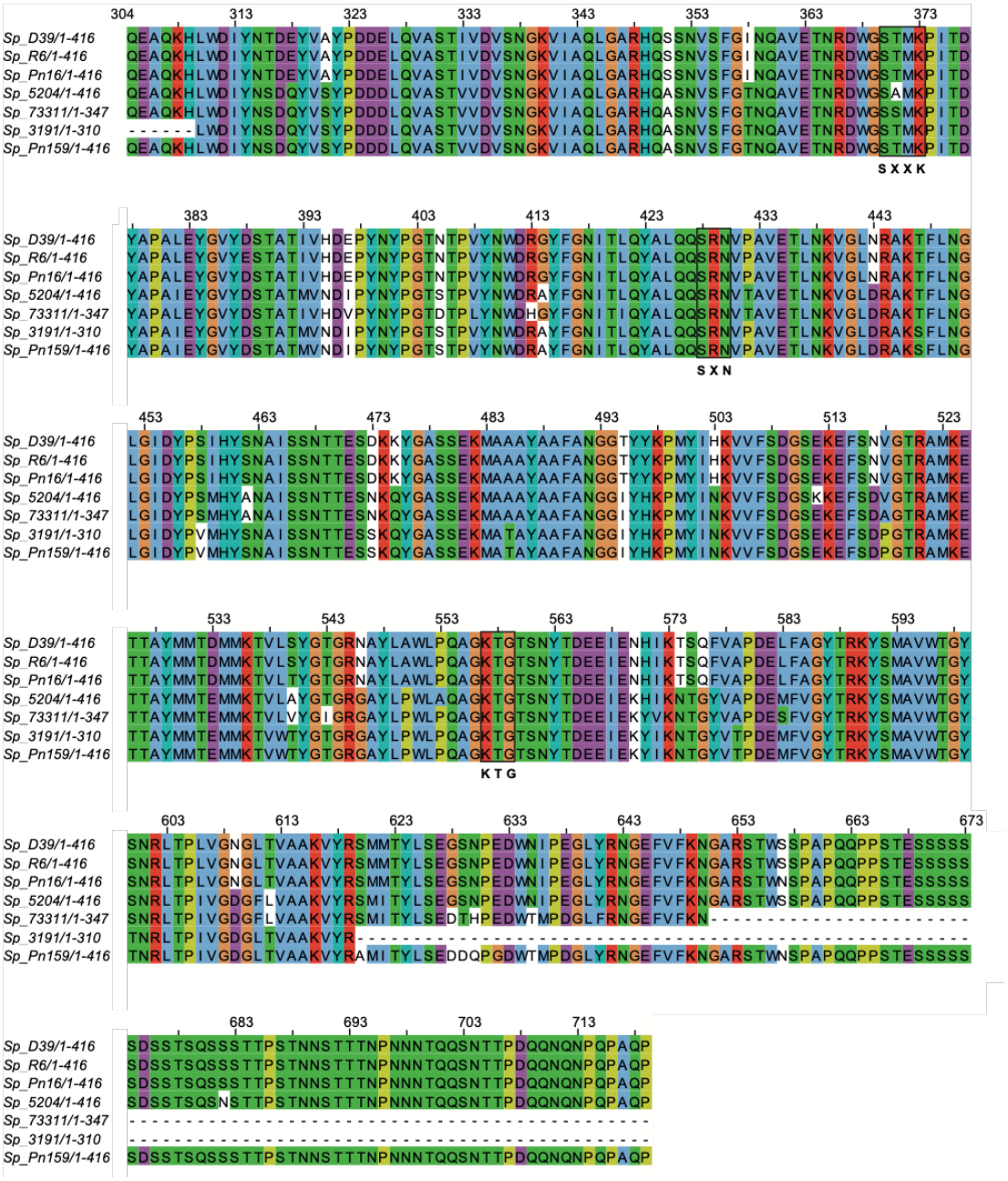

Figure 4.2 Amino acid sequence comparison of transpeptidase domains of *S. pneumoniae* PBP1a variants. Amino acids are coloured according to properties and conservation (ClustalX scheme), with unconserved positions in white. Conserved motifs $S_{370}XXK$, $S_{428}XN$ and $K_{557}TG$ are indicated by black boxes. Residue numbering corresponds to the position in the full-length protein. Alignments were performed using the Clustal Omega Multiple Sequence Alignment program (Sievers *et al.*, 2011). Only regions of the $PBP1a^{73311}$ and $PBP1a^{3191}$ available in the GenBank entries are shown.
SP_73311 Contreras Martel *et al.* (2006); **Sp_5204** Job *et al.* (2008); **Sp_3191** Smith *et al.* (2003).

4.3.1.2 Gibson cloning of Pn16 and 159 PBP1a

Expression constructs for the PBP1a variants of *S. pneumoniae* strains Pn16 and 159 in pET46a vectors were generated using cloning by Gibson Assembly® (Gibson *et al.*, 2009) (Section 2.3.5). The vector pET46a was chosen for consistency with pET46::*pbp_D39* and pET46a::*pbpa_D39_S370A* constructs, thus allowing comparison of activity between purified recombinant proteins. Vector maps are depicted in Figure 4.3. Constructs were generated in which N-terminally (N-ter.) His_{12}-tagged PBP1a from Pn16 and 159 (from

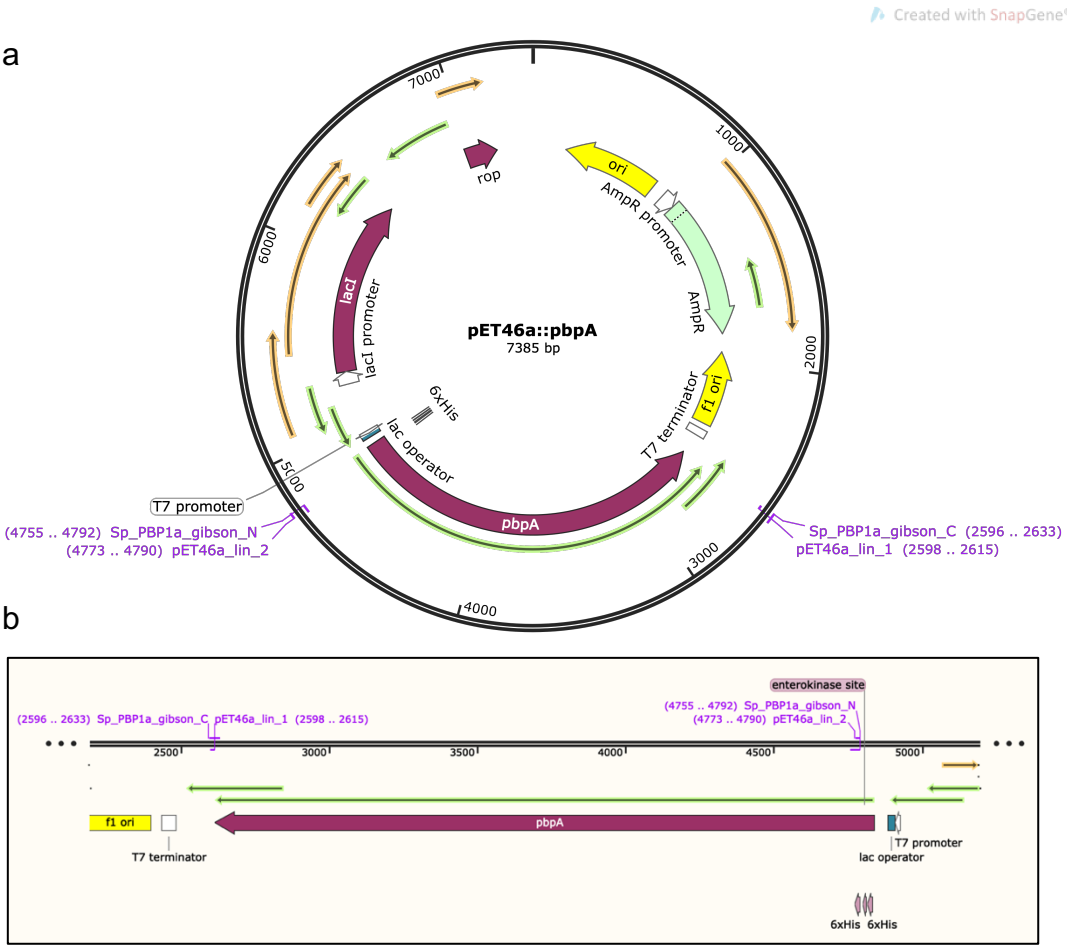

Figure 4.3 Vector map of pET46a::PBP1a constructs generated in this thesis. A) Vector map and b) diagram of the coding region. Annealing sites of Gibson primers are highlighted in purple. Also indicated is the site of the tandem His_6 tags (6xHis, pale purple arrows) Image generated using SnapGene Viewer (GSL Biotech LLC).

pET46::*pbp_Pn16* and pET46::*pbp_159* respectively) were expressed from a T7 promoter, with regulation by a lac operator. Primers spanning the inserted genes were used to sequence across the length of the insert to confirm the vector sequences. Sequence alignment of the product plasmid sequence to

the desired sequence was used to ensure that the nucleotide sequence of *pbpA_Pn16* and *pbpA_159* were inserted in frame with the N. ter. His_{12} tag. The final constructs consisted of a protein expressed full length (i.e. with the transmembrane helix) and with an N- terminal 12-Histidine tag for immobilised metal affinity chromatography. In Class A PBPs, the TM anchor is considered to act as a signal sequence, and is retained after translocation (Legaree *et al.*, 2007).

4.3.1.3 Expression and purification of PBP1a variants

The PBP1a variants presented in Table 4.2 were expressed and purified as described by Galley (2015), although with the omission of lysozyme for cell lysis (as discussed in Section 4.3.2.3.1) in later preparations.

Table 4.2 *S. pneumoniae* PBP1a variants expressed and purified for this thesis. All proteins were expressed as full length, membrane-anchored N-terminally His_{12}-tagged constructs.

PBP1a variant	Construct	Source
S. pneumoniae D39	pET46a::*pbpA_D39*	K. Abrahams (Warwick)
S. pneumoniae D39 $S_{370}A$ (TP active site serine mutant)	pET46a::*pbpA_D39_S370A*	K. Abrahams (Warwick)
S. pneumoniae Pn16	pET46a::*pbpA_Pn16*	Cloned for this project
S. pneumoniae 5204	pET46a::*pbpA_159*	Cloned for this project

PBP1a variants were expressed in cultures of BL21 (DE3) pRosetta cells by autoinduction (Section 2.4.1) at 25 °C for 22 h.

The membrane fraction was isolated from these cultures as described in Section 2.4.3.1, and membrane proteins were solubilised in phosphate-buffered saline (PBS) buffer using 1 % (w/v) sodium deoxycholate. Following buffer-exchange into PBS supplemented with 0.1 % (w/v) *N*-dodecyl β-D-maltoside (DDM), PBP1a was purified by Ni^{2+}-immobilised metal ion affinity chromatography (IMAC). The IMAC peak was then further purified by gel filtration (Figure 4.4), and the final protein stocks were frozen at – 20 °C in aliquots at 8 $mg.mL^{-1}$, in buffer containing 10 mM HEPES pH 7.5, 75 mM NaCl, 0.015 % (w/v) DDM and 50 % (v/v) glycerol. Summary SDS-PAGE gels of the purification profile of each variant are depicted in Figure 4.4, where PBP1a was observed at ~80 kDa. Similar final purity was observed for all variants of PBP1a.

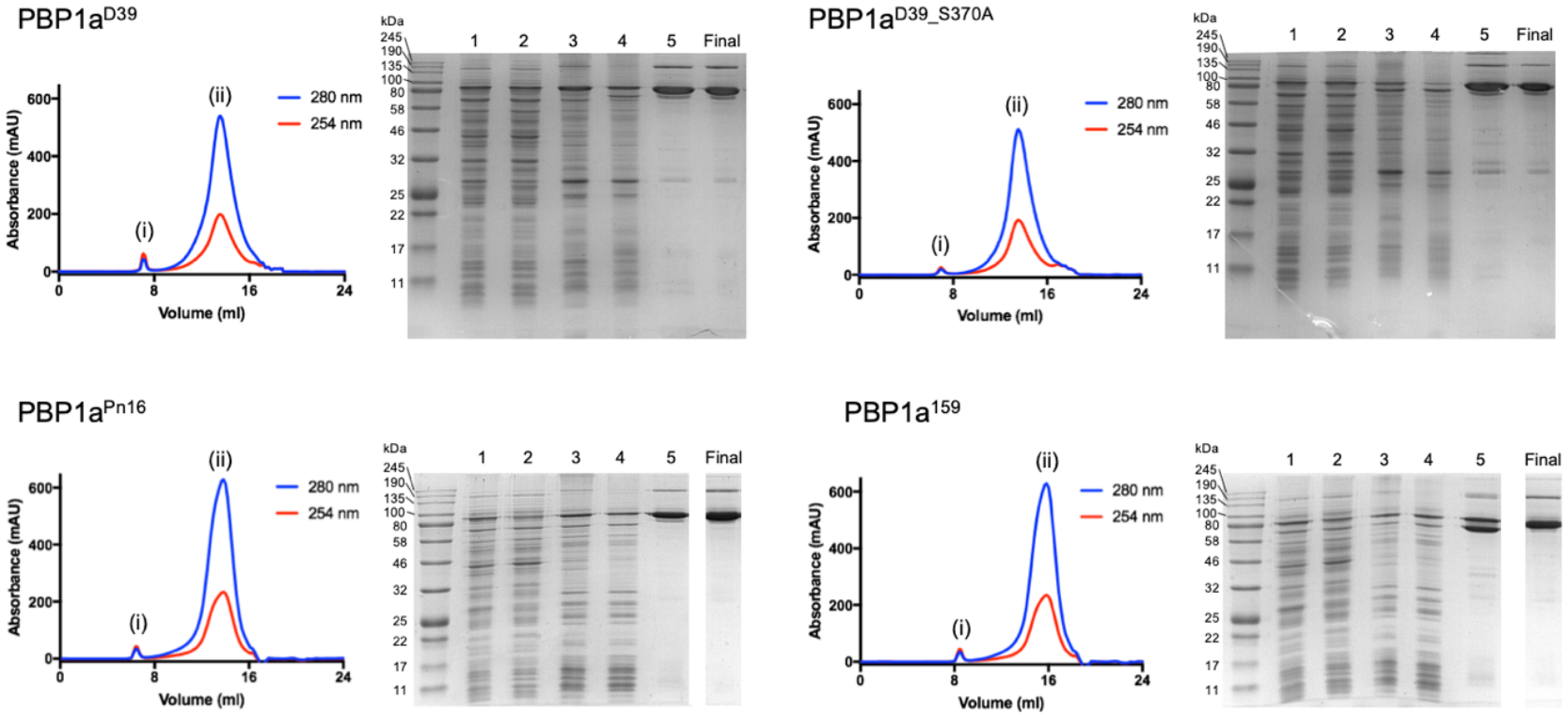

Figure 4.4 Purification of PBP1a variants from 4 *S. pneumoniae* strains. PBP1a variants from strains D39 (and an active site serine mutant, D39 S_{370}A), Pn16 and 159 were purified by immobilised metal ion affinity chromatography (**IMAC**) using TALON® Metal Affinity Resin (Clontech), followed by a gel filtration step (Superose 6 10/300 GL column (GE Healthcare)). Chromatograms illustrate the gel filtration step for each PBP1a variant. A small peak of aggregated material (**i**) was isolated from a large peak of PBP1a protein (**ii**) in each case. Summary analyses of each purification were performed by SDS-PAGE using a 12 % acrylamide gel.
Lane loading was as follows: 1, cell suspension following lysis by cell disruption; **2**, cell suspension following removal of insoluble material by centrifugation; **3**, membrane fraction; **4**, membrane proteins solubilised by 1 % (w/v) sodium deoxycholate and buffer exchanged into 0.1 (w/v) *N*-dodecyl β-D-maltoside; **5,** IMAC peak; **Final**, the final protein stock following gel filtration. **kDa,** kiloDaltons; **mAU,** milli-absorbance units; **(i),** aggregated material; **(ii),** PBP1a peak; Mr, Color Prestained Protein Standard, Broad Range (NEB) molecular weight marker.

Unless otherwise stated, the experiments in this chapter were undertaken using PBP1a^{D39}.

4.3.1.4 Protein mass spectrometry

The mass of PBP1a^{D39} was experimentally determined by mass spectrometry, in an experiment conducted and analysed by Dr. A.J. Lloyd (University of Warwick). Samples of protein before and after incubation with ampicillin were desalted and analysed by positive ion time of flight (TOF) mass spectrometry (Figure 4.5).

An increase in mass of 349.7 Da was observed in the presence of ampicillin, which was consistent with covalent modification of PBP1a^{D39} with ampicillin (expected mass change: 349.4 Da). The observed exact mass of PBP1a^{D39} was 82348.09 Da, as compared to the expected mass of 82481.48 Da (as predicted from the protein sequence, using the ExPASy ProtParam online tool (Artimo *et al.*, 2012)). This mass difference may have partially resulted from the removal of *N*-formylmethionine at the N-terminus of the protein by methionyl aminopeptidase (Ben-Bassat *et al.*, 1987). Loss of the *N*-formylmethionine would generate a polypeptide with an expected mass of 82350.29, which was within 2.2 Daltons of the experimentally determined value (Figure 4.5). This experiment demonstrated the amenability of PBP1a^{D39} to study by protein mass spectrometry.

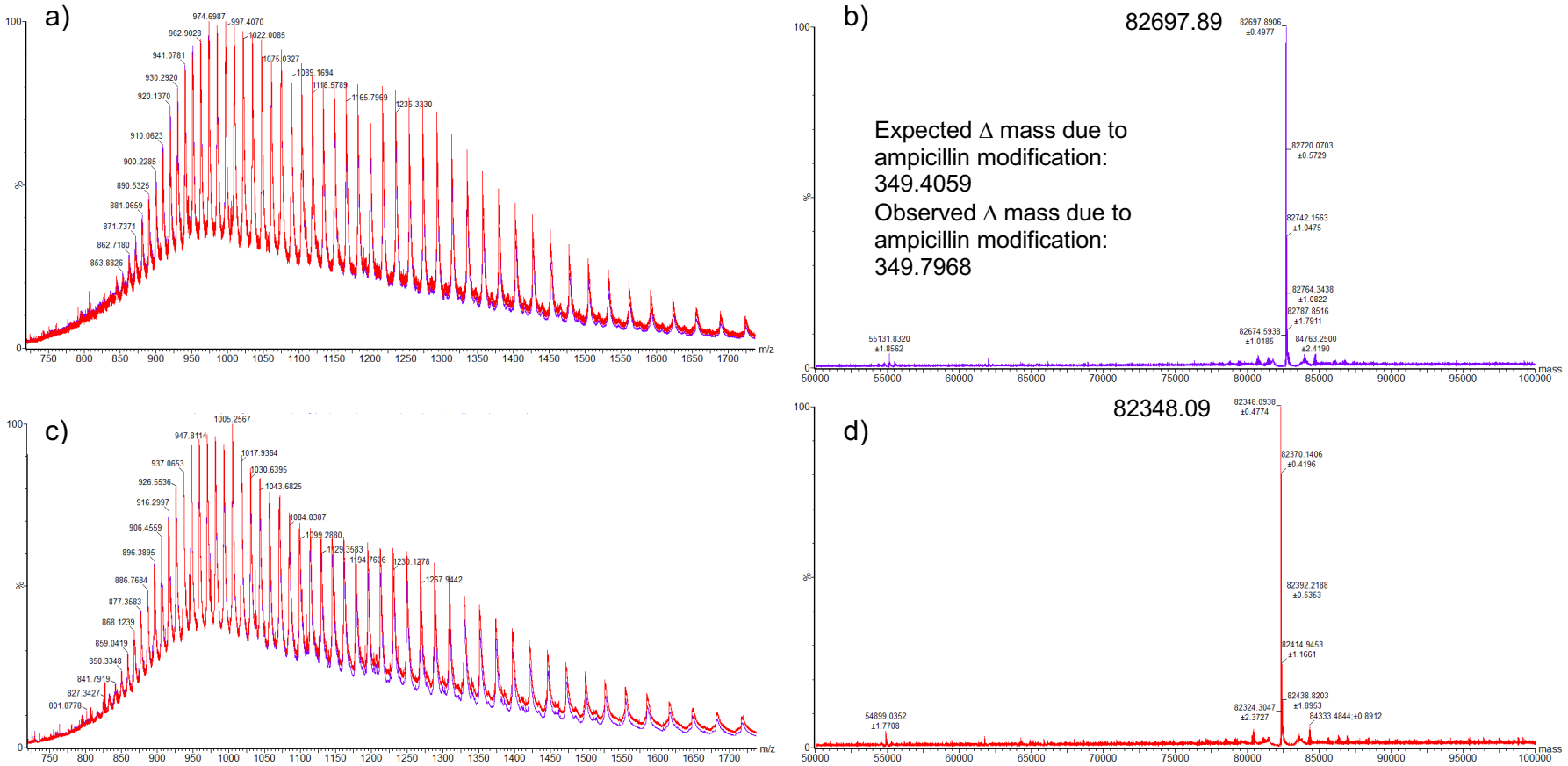

Figure 4.5 Nanospray time of flight mass spectrometry of PBP1a^{D39} and its modification by a 10:1 molar excess of ampicillin. a) Mass spectrum of ampicillin treated PBP1a (red) superimposed upon the predicted (mock) mass spectrum for the protein (purple) based on its simplest interpretation on a mass scale (b). c) Mass spectrum of untreated PBP1a (red) superimposed upon the predicted (mock) mass spectrum for the protein (purple) based on its simplest interpretation on a mass scale (d). Experiment conducted and analysed by Dr. A.J Lloyd (University of Warwick). Mass spectra were acquired using Mass Lynx software and deconvoluted to a mass scale using MaxEnt (Waters Ltd.).

4.3.2 Continuous spectrophotometric assay for transpeptidation

Purified recombinant PBP1a^{D39} was used in attempts to develop conditions for observation of *in vitro* transpeptidase activity of pneumococcal PBP1a. This work made use of the continuous assay for D-Ala release which was developed by Dr. A.J. Lloyd (University of Warwick).

In the assay system, D-Ala released by transpeptidase or D,D-carboxypeptidase activity is converted to a signal at 555 nm by the coupling enzymes, *Rhodotorula gracalis* D-amino acid oxidase (DAAO) and horseradish peroxidase (HRP). DAAO oxidises D-Ala to pyruvate, also

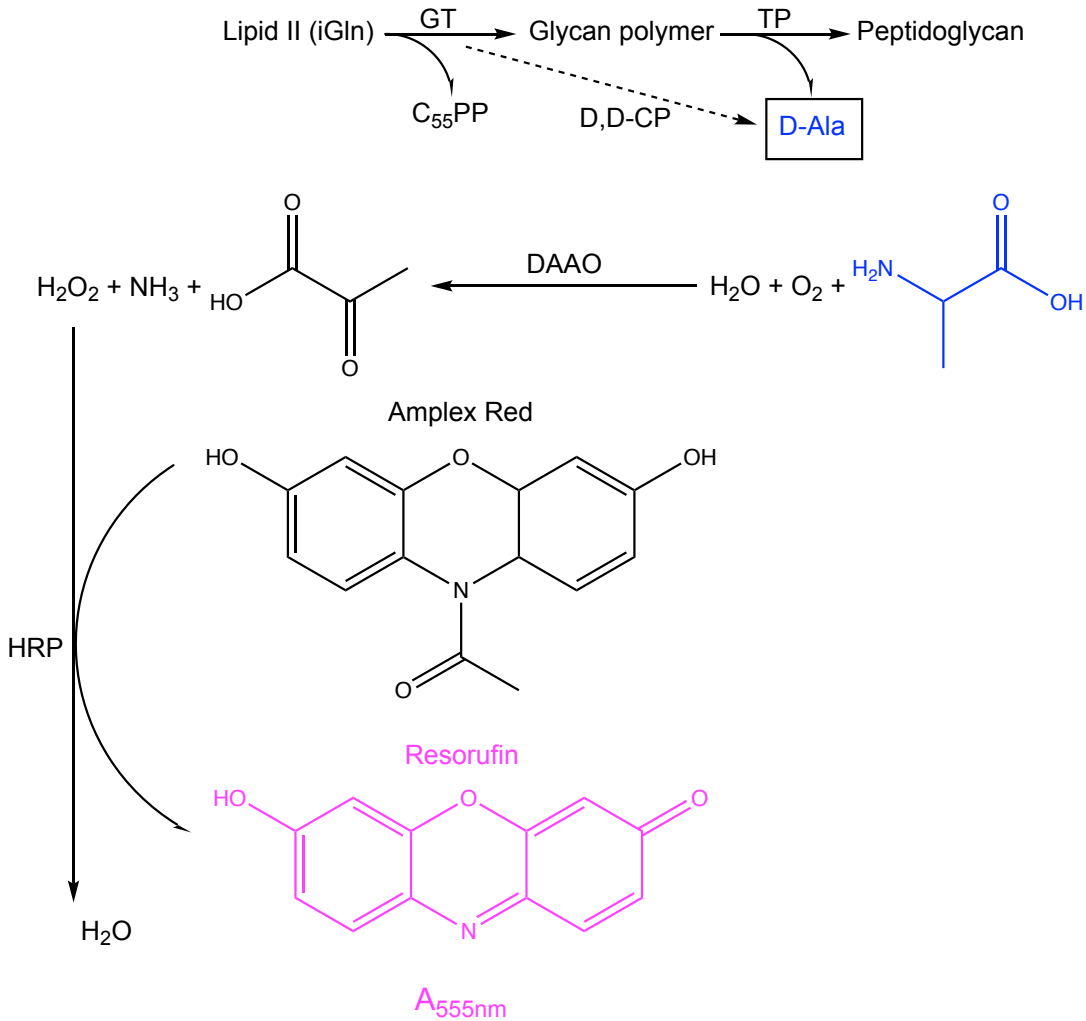

Figure 4.6 Continuous assay for D-ala release using DAAO, HRP and Amplex Red. D-Ala (blue) released by transpeptidase or D,D-carboxypeptidase activities of PBP1a^{D39} is converted to a signal at 555 nm by the coupling enzyme DAAO which oxidises D-Ala, generating hydrogen peroxide as a by-product. Horseradish peroxidase (HRP) uses hydrogen peroxide as an oxidizing agent to convert Amplex Red to Resorufin, which absorbs strongly at 555 nm.

generating hydrogen peroxide which is then used by HRP to convert Amplex Red to Resorufin, which absorbs strongly at 555 nm (Figure 4.6).

4.3.2.1 Assay with iGln LII Lys

In vitro transpeptidase activity of PBP1a^{D39} was previously observed in the D-Ala release assay (Galley, 2015). Initial attempts at observation of transpeptidase activity were made using Lipid II (iGln) as a substrate. We observed D-Ala release activity that was dependent on the presence of both enzyme and substrate, and this activity was inhibited by 50 μM moenomycin and 2 mM ampicillin (Figure 4.7).

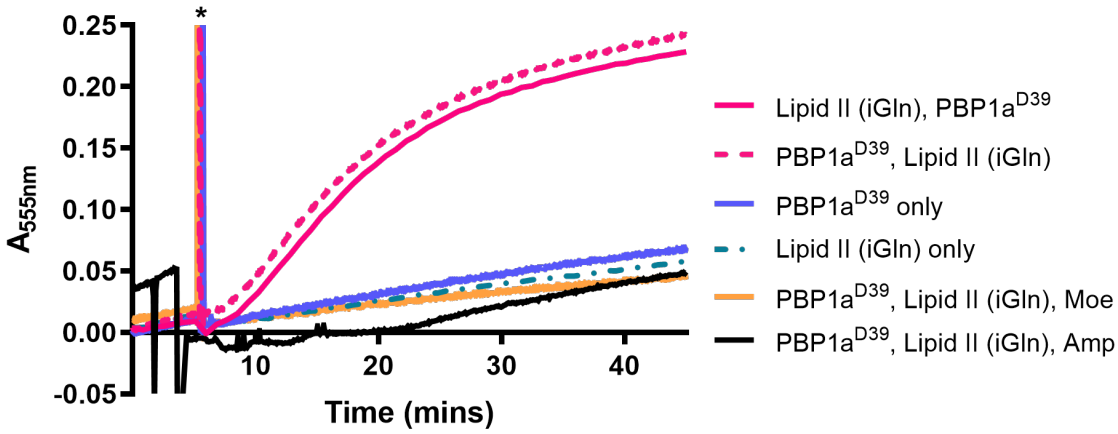

Figure 4.7 Observation of *S. pneumoniae* PBP1a^{D39}-catalysed D-alanine release in a continuous assay. Reaction mixes comprised 50 mM HEPES pH 7.6, 10 mM $MgCl_2$, 12 X CMC E_6C_{12} (0.0464%), 2 μM PBP1a^{D39}, 20 μM Lipid II (iGln), 33.51 mM.min^{-1} *R. gracalis* D-amino acid oxidase, 14.82 mM.min^{-1} horseradish peroxidase, and 50 μM Amplex Red. Reactions were initiated (*) by addition of 2 μM PBP1a^{D39} (or enzyme buffer in control reactions omitting enzyme). Controls included the glycosyltransferase (GT) inhibitor moenomycin (**Moe**), to demonstrate that D-Ala release was dependent upon GT activity; and transpeptidase inhibitor ampicillin (**Amp**) to demonstrate that the signal relied upon transpeptidation to generate D-Ala release. Reaction progress was followed by absorbance at 555 nm.
Moe, moenomycin (50 μM); **Amp,** ampicillin (2 mM); *, time point when reactions where initiated by addition of enzyme/buffer.

The relation between D-Ala release and enzyme concentration was then established to find the linear range in rate. Enzyme concentration was varied at fixed (40 μM) concentration of Lipid II (iGln) (Figure 4.8). The range over which enzyme concentration could be varied was limited by the low reaction rates (precluding use of enzyme concentrations lower than 1 μM); and the precipitation of enzyme when added to the reaction mixture at concentrations

greater than 6 μM. There is an apparent linear relationship between enzyme concentration and the rate of D-Ala release over the concentration range tested. As a full saturation curve was not generated, the relation between enzyme concentration and rate of D-Ala release cannot reliably be inferred from these data.

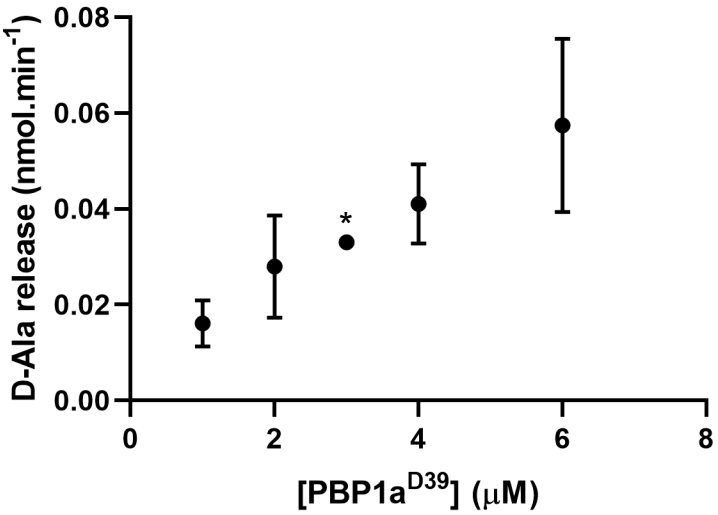

Figure 4.8 Relation between PBP1a^{D39} concentration and initial rate of D-Ala release, with Lipid II (iGln) as a substrate. Reaction mixes comprised 50 mM HEPES pH 7.6, 10 mM $MgCl_2$, 40 μM Lipid II (iGln), 33.51 mM.min^{-1} *R. gracalis* D-amino acid oxidase, 14.82 mM.min^{-1} horseradish peroxidase, 50 μM Amplex Red,12 X CMC E_6C_{12} (0.0464%), and the relevant concentration of PBP1a^{D39}. Data represent the mean rate from 3 replicates, except the 3 μM point (*) which was completed in singlicate only. Error bars indicated ± standard deviation.

4.3.2.1.1 Mass spectrometry of transpeptidase reaction products

The products of the transpeptidase reactions presented in Figure 4.7 were analysed by digesting the reaction products with *Streptomyces globisporus* mutanolysin, followed by mass spectrometry. The analysis of reaction products generated by PBP1a^{D39} when using Lipid II (iGln) as a substrate was complicated by the fact that the m/z of the transpeptidation product formed from one acceptor and one donor Lipid II (iGln) (structure (a), Figure 4.9) was identical to that if the two Lipid II (iGln) species were linked by glycosyltransfer, where one of the two pentapeptide stems had lost the C-terminal D-Alanine through D,D carboxypeptidation (structure (b), Figure 4.9). The ambiguity generated by the isobaric relationship of structures (a) and (b) in Figure 4.9 therefore necessitated MSMS fragmentation pattern analysis of the ion to

conclusively assign it as a transpeptidase product. In contrast, digestion of reaction products by mutanolysin should yield carboxypeptidase products as a Glc*N*Ac-Mur*N*Ac-tetrapeptide species (Figure 4.9c).

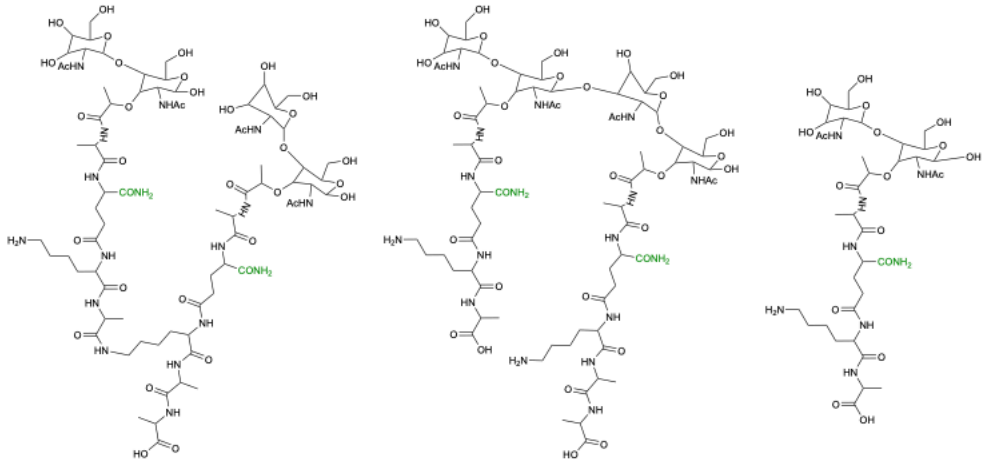

Figure 4.9 Structures of transpeptidase (TP) and D,D-carboxypeptidase (CP) products formed by *S. pneumoniae* PBP1a using Lipid II (iGln) as a substrate, following digestion by an *N*-acetylmuramidase. Products (**a**) and (**b**) are the products formed by TP and CP activities respectively of PBP1a, when using Lipid II (iGln) as a substrate and following digestion of the products by *S. globisporus* mutanolysin. Complete digestion of the CP product by mutanolysin yields product **c**).

Table 4.3 LC-MS analysis of TP reactions with Lipid II (iGln) Reactions were digested using *S. globisporus* mutanolysin and analysed by liquid chromatography-mass spectrometry (LC-MS) by positive ion electrospray time of flight mass spectrometry, to detect ions corresponding to putative TP product. Data are representative of two samples. **m/z**, mass to charge ratio. Data collected by Dr. A.J. Lloyd (University of Warwick).

Compound	Charge state	Expected m/z	Observed m/z	
			Lipid II (iGln) only	PBP1a^{D39} and Lipid II (iGln)
Putative TP product	(m+1)/1	1842.87	-	-
	(m+2)/2	921.94	-	921.41
	(m+3)/3	614.96	-	-

No species corresponding to the putative TP product was detected by positive mode LC-MS; analysis of the LC-MS chromatogram revealed only a species corresponding to the mass of the putative TP product minus 1 Da (Table 4.3, Appendices 4.1 and 4.3). There was thus no clear evidence of formation of a transpeptidase product between two Lipid II (iGln) molecules.

4.3.2.2 Effect of detergent concentration

To optimise the conditions of the D-Ala release assay of PBP1a, the impact of detergent concentration on the rate of D-Ala release activity was analysed by comparing the initial rate of D-Ala release across a range of concentrations of E_6C_{12} detergent. The starting concentration of E_6C_{12} detergent, of 12 X critical micellar concentration (CMC), was informed by the assay optimum for *E. coli* PBP1b (Dr. A.J. Lloyd, University of Warwick, personal communication). E_6C_{12} concentration was therefore varied between 12 X CMC and 1.7 X CMC (Figure 4.11). The minimum concentration was dictated by the concentration when detergent was solely contributed by the enzyme dilution and lipid resuspension buffers only. Decreasing the concentration of detergent relative to CMC was found to be associated with an increase in the rate of D-Ala release.

It appears from the trend of the data presented in Figure 4.10 that the true optimum concentration of E_6C_{12} may lie below 1.7 X CMC. However, at concentrations of detergent approaching CMC, the enzyme and its substrate may not be kept in solution. The detergent optimum for GT activity of $PBP1a^{D39}$ was similarly tested, and these data are presented in Section 5.3.1.1.

To investigate whether transpeptidation or D,D-carboxypeptidation was being

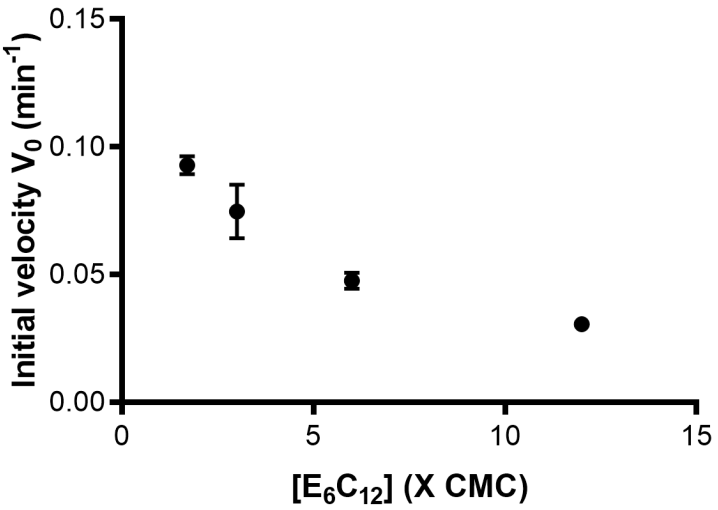

Figure 4.10 Relation between detergent concentration and initial rate of D-Ala release. The concentration of E_6C_{12} detergent was varied between 1.7 and 12 X CMC. Reaction mixes comprised 50 mM HEPES pH 7.6, 10 mM $MgCl_2$, 2 μM $PBP1a^{D39}$, 20 μM Lipid II (iGln), 33.51 mM.min^{-1} *R. gracalis* D-amino acid oxidase, 14.82 mM.min^{-1} horseradish peroxidase, 50 μM Amplex Red and the relevant concentration of E_6C_{12} Data represent the mean rate from 3 replicates.
CMC, critical micellar concentration. Error bars indicate ± standard deviation.

followed in the reactions presented in Figure 4.10, the reaction products at different concentrations of E_6C_{12} were digested using *S. globisporus* mutanolysin and analysed by positive ion LC-MS as described previously. An ion was identified in samples at all detergent concentrations (observed (m+1)/1, 1842.868) that could have corresponded to either a transpeptidase product, or Lipid IV minus D-Ala (both expected (m+1)/1, 1842.87; see Table 4.4 and Figure 4.9). This ion was not detected in control reactions from which the substrate was omitted.

To resolve the identity of this ion, we employed collision-induced fragmentation as before. However, due to the low signal for the parent ion in this fragmentation experiment, a reliable fragmentation pattern could not be determined.

Table 4.4 Summary of LC-MS analysis results from detergent titration TP reactions. Reactions were digested using mutanolysin and analysed by liquid chromatography-mass spectrometry (LC-MS) by positive ion electrospray time of flight mass spectrometry, to detect ions corresponding to putative TP product. Data are representative of two samples. **m/z**, mass to charge ratio. Data collected by Dr. A.J. Lloyd (University of Warwick).

Compound	Charge state	Expected m/z	Observed m/z at E_6C_{12} multiple of CMC (X)			
			1.7 x	3.0 x	6.0 x	12 x
TP product or CP product	(m + 1)/1	1842.87	1842.87	1842.87	1842.87	1842.87
	(m + 2)/2	921.94	921.94	921.94	921.94	-

4.3.2.3 Troubleshooting variation in rate

Difficulty was experienced in establishing reproducible activity of $PBP1a^{D39}$, with certain enzyme preparations appearing inactive. The following section discusses the factors that were considered in addressing this issue.

4.3.2.3.1 Use of lysozyme for cell lysis

The purification protocol detailed by Galley (2015) included the use of lysozyme to aid cell lysis by cleavage of peptidoglycan. As PBP1a is a bifunctional PBP, the transpeptidase donor must be provided by ongoing glycosyltransferase activity (Bertsche *et al.*, 2005). We therefore considered that lysozyme added during the purification procedure could be carried through to the final enzyme preparation, and may therefore cleave glycan polymers synthesized by $PBP1a^{D39}$ and thus prevent transpeptidase activity from occurring. Due to the use of muramidases such as lysozyme in the continuous fluorometric assay for glycosyltransferase activity to mediate the fluorescence change (Schwartz *et al.*, 2002), the impact of lysozyme carried through the purification may not have previously been detected in GT assays.

We were interested in assessing whether the omission of lysozyme from the purification procedure would improve the activity of PBP1a. Published purification procedures for preparation of PBPs such as *E. coli* PBP1b (Biboy *et al.*, 2013) do not make use of lysozyme to aid cell lysis.

We therefore assessed whether omission of lysozyme would affect the purification of PBP1a. PBP1a purified with the use of lysozyme for cell disruption was enriched in the membrane fraction (obtained by centrifugation of the lysed cell suspension at 150 000 x g). The localization of PBP1a^{D39} with and without lysozyme treatment of cultures was compared by SDS-PAGE analysis of BOCILLIN FL binding. BOCILLIN FL is a penicillin analogue fluorescently-labelled by a BODIPY label. BOCILLIN FL will therefore covalently modify the active site serine of purified recombinant PBP1a^{D39}, and allow sensitive detection of the protein throughout the purification.

Cultures with and without lysozyme treatment were lysed using a cell disruptor (Constant Systems), and samples of the insoluble (24 000 xg pellet), soluble (150 000 x g supernatant) and membrane (150 000 x g pellet) fractions were incubated with BOCILLIN FL and analysed by SDS-PAGE (Figure 4.11). A control lane (P) was included, with purified recombinant PBP1a^{D39} that was incubated with BOCILLIN FL, for comparison to fluorescent bands in the control and sample lanes. The major band in lane P was observed at 63 kDa, which was unexpected compared to the experimentally determined mass of PBP1a^{D39} at approximately 82 kDa (Section 4.3.1.4). This phenomenon was further explored in the experiments detailed in Section 4.3.3.

No fluorescent bands were observed in the control lanes, although there was some leakage of the bands from lane P (Figure 4.11a). Bands were observed in the sample lanes at 63 kDa, matching the major band of the purified PBP1a^{D39} in lane P for each gel. The fluorescent band detected in the induced samples could therefore be inferred to represent the overexpressed PBP1a^{D39}. The apparent localization of PBP1a^{D39}, based on bands observed under fluorescence detection, was unchanged by treatment of lysozyme, with the

majority of BOCILLIN FL-staining observed in the membrane fraction in each case (by comparison of Figure 4.11a, induced, lane 3; and 4.11b, induced, lane 3).

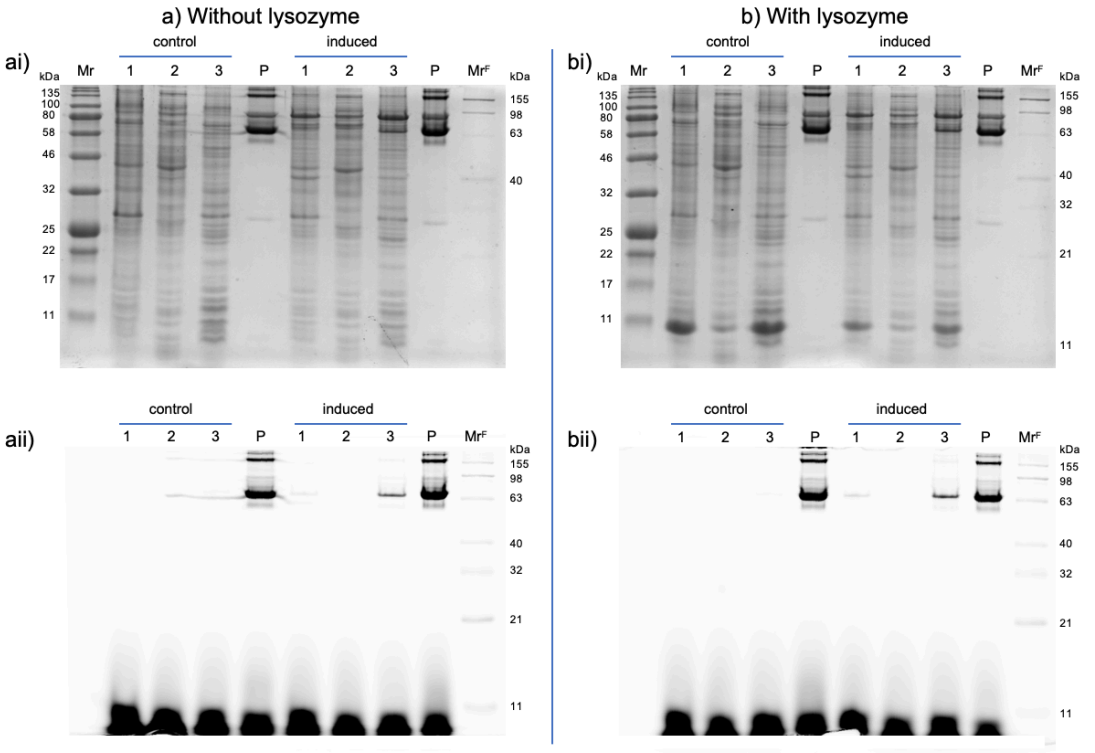

Figure 4.11 Effect of lysozyme treatment on localisation of overexpressed PBP1a^{D39}. Cultures of BL21 (DE3) pRosetta containing the plasmid pET46::*pbpa_D39*, with and without induction of expression of PBP1a^{D39}, and then with **(b)** and without **(a)** cell lysis using lysozyme, were lysed by cell disruption and then centrifugation steps at 24 000 x g and 150 000 x g were performed. Localisation of PBP1a^{D39} in each case was assessed by incubation with BOCILLIN FL, followed by analysis by SDS-PAGE. A control lane **(P)** of purified PBP1a^{D39} incubated with BOCILLIN FL, was included to allow identification of PBP1aD39 in the sample lanes. Reactions were analysed by SDS-PAGE, with equal loading of based on protein concentration, using 12 % acrylamide gels and fluorescence was imaged (gels **aii** and **bii**) using a Typhoon FLA 9500 laser scanner (GE Healthcare). Gels were then stained using InstantBlue™ Protein Stain (Expedeon) and imaged for total protein (gels ai and bi) using an ImageQuant LAS 4000 instrument (GE Healthcare).
a), without lysozyme treatment; **b),** with lysozyme treatment; **1,** insoluble (24 000 xg pellet); **2,** soluble (150 000 x g supernatant); **3,** membrane (150 000 x g pellet); **P,** purified recombinant PBP1a^{D39}; **Mr,** Color Prestained Protein Standard, Broad Range (NEB) molecular weight marker; **Mr^{F},** BenchMark™ Fluorescent Protein Standard (ThermoFisher Scientific); **kDa,** kilo-Daltons.

Despite omission of lysozyme, no transpeptidase activity of fresh preparations of PBP1a^{D39} was observed. The lack of *in vitro* activity could therefore not be ascribed to inclusion of lysozyme in the purification.

4.3.2.3.2 Variation between Lipid II (iGln) stocks

Subsequent experiments identified a variation between stocks of Lipid II (iGln), resulting in activity being detected with some batches of protein and not others. With Lipid II (iGln) from three separate synthesis (hereafter referred to as stocks 1, 2 and 3), transpeptidase activity was detected with Lipid stock 2 (with two separate batches of protein), but not with Lipid stock 1. A third Lipid stock appeared to be contaminated, as a response by the DAAO-HRP coupling enzymes was detected in the absence of PBP1a^{D39}. The purity and concentration of the three stocks was compared by thin-layer chromatography analysis, with loading of 2.5 nmol of lipid based on quantification by phosphate release assay (Section 2.6.9.4). The abundance of Lipid II (iGln) detected in stock 1 by iodine staining appeared greatly reduced in comparison to that detected in stocks 2 and 3 (Figure 4.12, '1' compared to '2' respectively). The intensity of the Lipid II (iGln) band in stock 1 relative to stock 2 was 0.3 as analysed using ImageJ software (Schneider *et al*., 2012), compared to 0.7 for stock 3. A contaminant migrating close to the solvent front was detected in stock 3 (faintly visible in Figure 4.12, '3', indicated by *). This contaminant was therefore considered as a possible cause of the stimulation of the coupling enzymes in the TP assay.

Lipid stocks 1, 2 and 3 were analysed by negative ion TOF mass spectrometry. Lipid II (iGln) was detected in stocks 1 and 2 (see Table 4.5, Appendices 4.5-6), but not in stock 3. A polymeric species was detected in stock 3, which may correspond to the species (*) observed in Figure 4.12 (see Appendix 4.7).

Figure 4.12 Analysis of quantity and purity of stocks of Lipid II (iGln). 2.5 nmol of Lipid (iGln) was loaded to a thin-layer chromatography plate and run in 88:48:10:1 chloroform:methanol:water:ammonia buffer, followed by staining in iodine vapour. Numbering of lanes refers to the stock of Lipid II (iGln), whereby transpeptidase activity of PBP1a^{D39} was observed with stock 2 only, and stock 3 gave rise to a PBP1a-independent D-Ala release signal. Band intensities of Stock 1 and 3 relative to 2 (as plotted using ImageJ software (Schneider *et al.*, 2012)) were 0.3 and 0.7 respectively.
2, Lipid II (iGln) stock 2; **1**, Lipid II (iGln) stock 1; **3**, Lipid II (iGln) stock 3; *****, contaminant observed in stock 3.

Difficulties in establishing activity of PBP1a^{D39} may therefore have resulted from variation in the lipid stocks used.

Table 4.5 Mass spectrometry data for analysis of Lipid II (iGln) stocks. Samples were analysed by negative ion time-of-flight mass spectrometry. Data collected by A. Catherwood.

Compound	Charge state	Expected m/z	Sample (response in TP assay)	Observed m/z
Lipid II (iGln)	(m-1)/1	1873.07	Stock 1 (no activity)	1873.06
			Stock 2 (activity)	1873.06
			Stock 3 (contaminant)	Polymeric species
	(m-2)/2	936.03	Stock 1 (no activity)	936.03
			Stock 2 (activity)	936.03
			Stock 3 (contaminant)	Polymeric species

4.3.2.5 *In vitro* activity of PBP1a^{D39} with donor- and acceptor-only substrates

After having established D-Ala release activity of PBP1a^{D39} with Lipid II (iGln) as the substrate, we sought to test the activity with defined donor- and acceptor-only substrates. As previously discussed in Section 3.1.4, defined donors and acceptors were sought to attempt the resolution of the transpeptidase and D,D-carboxypeptidase rates of the PBP1a. Both of these activities would contribute to the D-Ala release signal in the presence of a

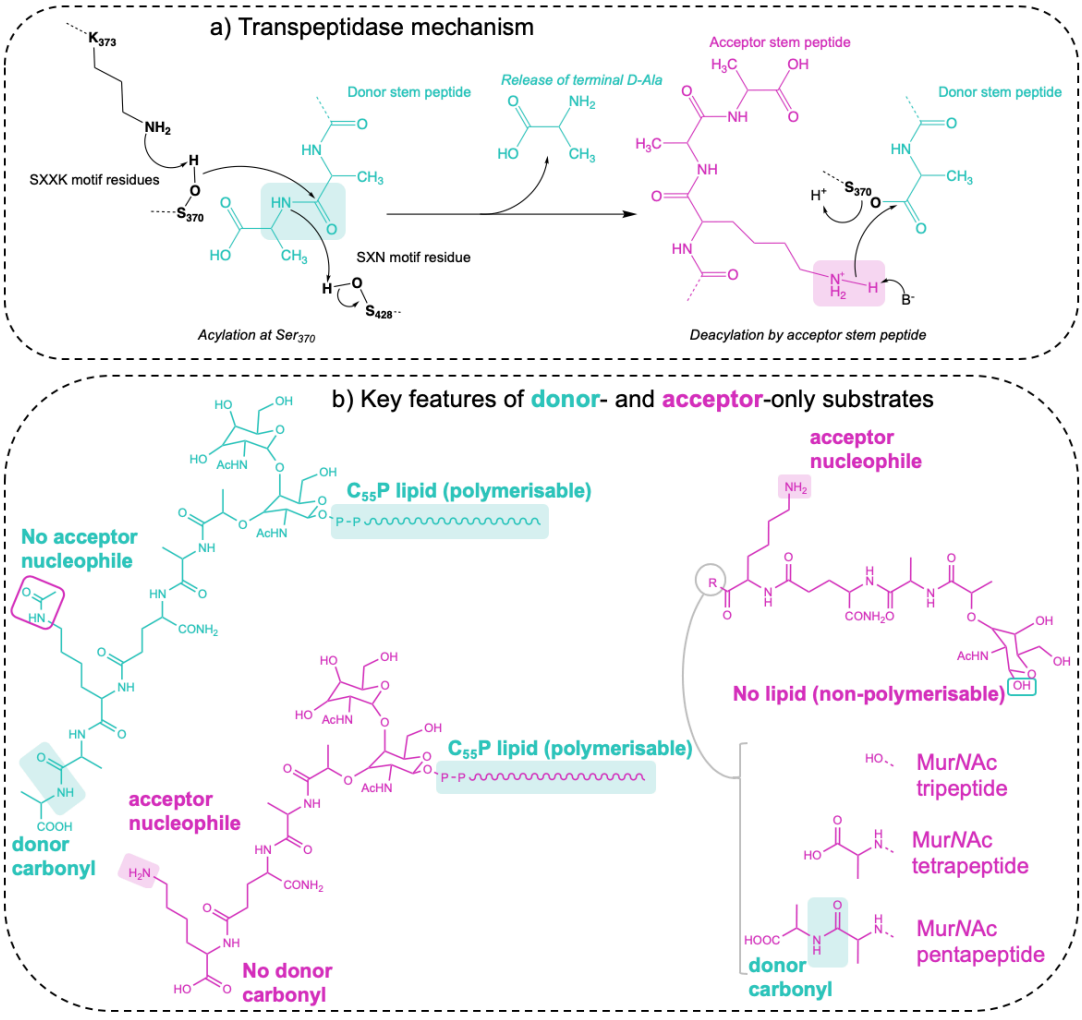

Figure 4.13 Features of donor- and acceptor-only substrates. **a)** The transpeptidase mechanism, illustrating involvement of the donor stem peptide carbonyl (green box) and the primary amine of the acceptor stem peptide (pink box). **b)** the key features determining whether particular substrate variants are donor- or acceptor-only. Donor-only substrates must be polymerisable (i.e. lipid linked) and retain the donor carbonyl. These substrates are made donor-only by loss of the acceptor nucleophile (e.g. by acetylation, as depicted). Conversely, acceptor substrates retain the acceptor nucleophile, and are made acceptor-only by loss of the lipid linker or the donor carbonyl.

single substrate such as Lipid II (iGln). The D-Ala release rate in the presence of donor-only substrate alone can be ascribed to D,D-carboxypeptidase activity. By comparison, in the presence of both donor- and acceptor only

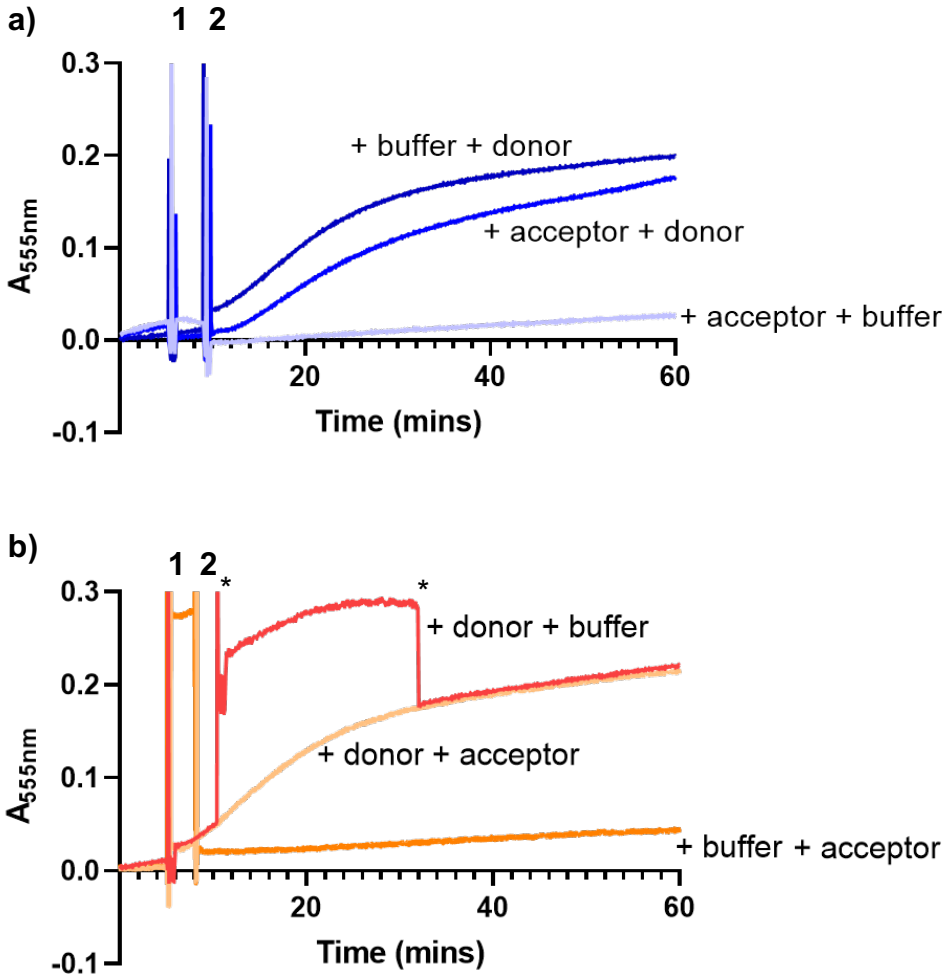

Figure 4.14 D-Ala release in the presence and absence of donor and acceptor-only substrates. The activity of PBP1a^{D39} was tested in the presence of donor-only (Lipid II (iGln, ε-*N*-acetyl-Lys)) and acceptor-only (Mur*N*Ac 5P (iGln)) substrates. Reaction mixes comprised 50 mM HEPES pH 7.6, 10 mM $MgCl_2$, 2 μM PBP1a^{D39}, 20 μM Lipid II (iGln, ε-*N*-acetyl-Lys) or buffer, 20 μM Mur*N*Ac 5P (iGln) or buffer, 33.51 mM.min^{-1} *R. gracalis* D-amino acid oxidase, 14.82 mM.min^{-1} horseradish peroxidase, 50 μM Amplex Red and 3 X CMC (0.0116 %) of E_6C_{12}. All components apart from donor and acceptor substrates were present at zero time. The subsequent addition of donor and acceptor (in the order listed in the legend) are indicated as addition **1** and **2** respectively. ***** indicates artefacts in the + donor + buffer trace due to a bubble. Absorbance at 555 nm at 30 °C was followed throughout.
donor, Lipid II (iGln, ε-*N*-acetyl-Lys); **acceptor**, Mur*N*Ac 5P (iGln).

substrates, a higher rate comprising D-Ala release originating from catalysis of both transpeptidation and D,D-carboxypeptidation would be expected.

The activity of PBP1a^{D39} was tested using Lipid II (iGln, ε-*N*-acetyl-Lys) as the donor-only substrate and Mur*N*Ac 5P (iGln) as the acceptor-only substrate (Figure 4.14). The rates of D-Ala release observed in these experiments were slow. The difference in the background-corrected rates of D-Ala release in the presence of both donor and acceptor substrate (+ acceptor + donor reaction, 0.0045 AU.min^{-1}) and donor substrate alone (+ buffer + donor reaction, 0.0072 AU.min^{-1}) was therefore likely within the error of this experiment. Irrespective of the order of addition of donor-only and acceptor-only substrate (as compared between Figures 4.14a and b), the rate of D-Ala release appeared to be independent of the presence of acceptor substrate.

The expected observation in these experiments, if *in vitro* transpeptidase activity of PBP1a^{D39} was detected, and the rate of transpeptidation was greater than that of D,D-carboxypeptidation, was that the rate would be greater in the presence of both donor and acceptor substrates compared to donor alone. The results presented in Figure 4.14 could therefore indicate either that the D-Ala release activity observed could be entirely ascribed to D,D-carboxypeptidation; or that transpeptidation was not associated with an increase in the rate of D-Ala release, which may occur if the acylation of the transpeptidase active site serine were the limiting step of the transpeptidase and D,D-carboxypeptidase reactions.

To analyse the results further, samples from the assay were digested with *S. globisporus* mutanolysin and analysed by LC-MS. Such analysis is simplified by the use of defined donor-only and acceptor-only substrates, as fragmentation analysis is not required to deconvolute the mass of D,D-carboxypeptidase and transpeptidase products (compared to when Lipid II (iGln) is the sole substrate; see Section 4.3.2.1.1). The LC-MS analyses of reactions shown in Figure 4.14a were scrutinised for the positively charged species associated with transpeptidation between the stem peptide of Lipid II

(iGln, ε-*N*-acetyl-Lys) and Mur*N*Ac 5P (iGln), or carboxypeptidation of the Lipid II (iGln, ε-*N*-acetyl-Lys), as depicted in Figure 4.15.

The LC-MS analysis of the reactions in Figure 4.14a is summarised in Table 4.6. No ions corresponding to the digested transpeptidase product was detected in any of the reaction samples. There was therefore no evidence of transpeptidase activity in these assays using donor-only and acceptor-only substrates. Based on these results, the D-Ala release rates observed in Figure 4.14 were likely representative of solely D,D-carboxypeptidase activity. An ion corresponding to the digested D,D-carboxypeptidase product (expected (m+2)/2 469.22, observed (m+2)/2 469.22) was detected only in sample a, in which both donor-only and acceptor-only substrates were included.

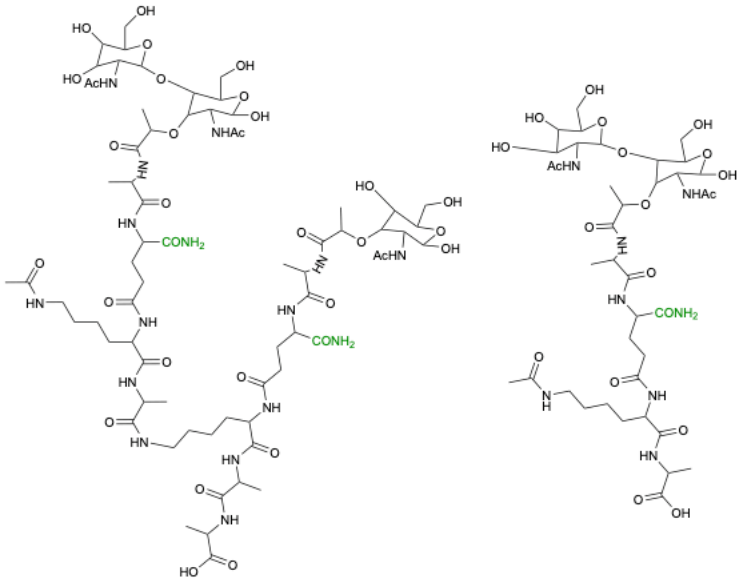

Figure 4.15 Expected products of transpeptidase and D,D-carboxypeptidase activities using Lipid II (iGln, acetyl-Lys) and Mur*N*Ac 5P (iGln) as substrates, following digestion by an *N*-acetylmuramidase. *S. globisporus* mutanolysin-digested products formed by transpeptidation (**a**) and D,D-carboxypeptidation (**b**) catalysed by PBP1a^{D39} using Lipid II (iGln, ε-*N*-acetyl-Lys and Mur*N*Ac 5P (iGln) as substrates.

Further attempts were made to establish *in vitro* transpeptidase activity in the D-Ala release assay by use of D-Lactate as a substrate, to allow greater concentrations of acceptor to be used in the assay; by testing activity at pH 9 in Bis.Tris propane buffer; and by increasing the concentration of E_6C_{12} buffer to 12 X CMC, due to the possibility that the increase in rate with decreasing

detergent concentration (Figure 4.11) may reflect an increase in the ratio of D,D-carboxypeptidase to transpeptidase activity of PBP1a^{D39}. Under each of these conditions, the rate of D-Ala release was similarly limited, and was slowed slightly in the presence of acceptor.

Table 4.6 LC-MS analysis of TP reactions with donor- and acceptor-only substrates. Assignment of CP product or TP product putative ions was based on structures in Figure 4.11. Samples were analysed by positive-ion LCMS. Data collected by Dr. A.J. Lloyd (University of Warwick).

Compound	Charge state	Expected m/z	Sample	Observed m/z
CP product	(m+2)/2	469.22	a) acceptor + donor	469.224
			b) buffer + donor	-
			c) acceptor + buffer	-
TP product	(m+2)/2	841.40	a) acceptor + donor	-
			b) buffer + donor	-
			c) acceptor + buffer	-

4.3.2.6 Analysis of TP activity under conditions of the GT assay

We considered whether the slow rates observed in the D-Ala release assay, and the apparent lack of TP activity, were the consequence of rate-limiting, slow glycosyltransferase activity by PBP1a^{D39}. Such slow GT activity would limit the supply of polymer to act as the TP donor. To test whether the apparent lack of transpeptidase activity was the result of limitation by poor GT activity, we sought to assay PBP1a^{D39}-catalysed D-Ala release under conditions known to support GT activity.

Previous results have suggested that DMSO is inhibitory to transpeptidase activity, but 25 % (v/v) DMSO was found to be optimal for *in vitro* glycosyltransferase activity in the continuous fluorometric assay with Lipid II (iGln, Dans) (Galley, 2015). Glycan polymer formation by PBP1a^{D39} using Lipid II (iGln, Dans) could be observed by Tris-tricine SDS-PAGE, and was accelerated in the presence of 25 % (v/v) DMSO (Appendix 4.9). We therefore

used Lipid II (iGln, Dans) or Lipid II (iGln, ε-*N*-acetyl-Lys) as the donor substrates in transpeptidase assays with and without 25 % (v/v) DMSO (Table 4.6).

Under conditions shown to support extensive glycan polymer formation by PBP1a^{D39} using Lipid II (iGln, Dans) as a donor substrate, no transpeptidase rate was detected in the D-Ala release assay (Table 4.7, Appendix 4.10-11). As previously (Figure 4.14), the rate of D-Ala release was slowed or unchanged in the presence of Mur*N*Ac 5P (iGln) acceptor, indicating that the rate observed was likely to be solely attributable to D,D-carboxypeptidation.

Table 4.7 D-Ala release activity under conditions suitable for GT activity. D-Ala release catalyzed by PBP1a^{D39} was followed in the presence and absence of 25 % (v/v) DMSO, and using either Lipid II (iGln, Dans) or Lipid II (iGln, ε-*N*-acetyl-L-Lys) as a donor substrate. Reaction mixes comprised 50 mM HEPES pH 7.6, 10 mM $MgCl_2$, 2 μM PBP1a^{D39}, 20 μM Lipid II (iGln, acetyl-Lys or Dans), 20 μM Mur*N*Ac 5P (iGln), 33.51 mM.min^{-1} *R. gracalis* D-amino acid oxidase, 14.82 mM.min^{-1} horseradish peroxidase, 50 μM Amplex Red and 3 X CMC (0.0116 % (w/v)) of E_6C_{12}. D-Ala release rates were ascribed to transpeptidation if an elevated rate was observed in the presence of acceptor substrate compared to donor substrate alone; and rates were ascribed to D,D-carboxypeptidation if such elevation of rate was not observed.

Lipid donor	DMSO	D,D-carboxypeptidation	Transpeptidation
Lipid II (iGln, Dans)	+	✓	×
	-	×	×
Lipid II (iGln, acetyl-Lys)	+	×	×
	-	✓	×

These results suggested that the lack of observation of TP activity in the continuous assay was not due to lack of GT activity under the conditions of the assay. No D-Ala release from Lipid II (iGln, Dans) was observed in the absence of DMSO, in agreement with the GT data. However, when Lipid II

(iGln, ε-*N*-acetyl-Lys) was supplied as the donor substrate, D-Ala release activity was only detected in the absence of DMSO. These results suggested that the requirement for DMSO for optimal GT activity in the continuous fluorometric assay was related to the dansyl fluorophore rather than being a general requirement for GT activity.

4.3.3 Analysis of TP activity by SDS-PAGE

Several published methods have used Tris-tricine gel electrophoresis to monitor transpeptidase activity, based on the inability of the cross-linked glycan polymer to enter the acrylamide gel matrix (Qiao *et al.*, 2017; Srisuknimit *et al.*, 2017; Zapun *et al.*, 2013). We therefore attempted observation of transpeptidase activity using this technique. This discontinuous technique allowed transpeptidation to be followed on a longer time scale than was possible with the D-Ala release assay. The substrates for these reactions were a 1:1 mixture of Lipid II (iGln, Dans) as the transpeptidase donor-only substrate (allowing visualisation of glycan polymers based on the Dansyl fluorophore); and Lipid II 3P (iGln) (as the acceptor substrate for transpeptidation). Glycosyltransferase assays conducted prior to this work (and described in Section 5.3.1.2) identified that among the ethylene glycol detergents tested (including E_6C_{12} used in previous work described in this Chapter), E_8C_{10} supported optimal GT activity of PBP1a^{D39}. The following experiments were therefore conducted using E_8C_{10} as the assay detergent.

4.3.3.1 Can TP activity be observed in the Tris-tricine gel system?

We used the SDS-PAGE system to attempt to establish and compare the cross-linking activity of PBP1a^{Pn16} and PBP1a^{159} (Figure 4.16). When the GT inhibitor moenomycin was included in the reaction mixture, only the Lipid II (iGln, Dans) starting material was observed, as a fluorescent band at the running front of the gel. With no inhibitor, a band at the top of the gel was

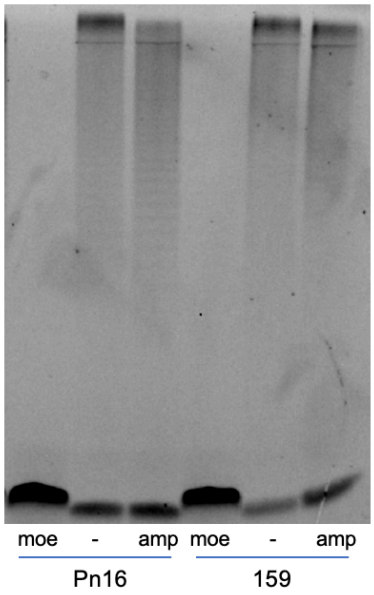

Figure 4.16 Analysis of putative transpeptidase activity of PBP1a^{Pn16} and PBP1a^{159} by Tris-tricine SDS-PAGE. Reactions comprised 50 mM HEPES pH 7.6, 10 mM $MgCl_2$, 0.5 μM PBP1a, 2.5 μM Lipid II (iGln, Dans), 2.5 μM Lipid II (iGln, tripeptide), 25 % (v/v) DMSO, 150 mM NaCl, 33.51 mM.min^{-1} *R. gracalis* D-amino acid oxidase, 14.82 mM.min^{-1} horseradish peroxidase, 50 μM Amplex Red and 3 X CMC of E_8C_{10}. Reactions without antibiotic, and control reactions incubated with 200 μM moenomycin (**moe**) to inhibit glycosyltransferase activity or 1 mM ampicillin (**amp**) to inhibit transpeptidase activity, were incubated for 30 mins. The reactions were then quenched with EDTA, mixed with loading dye and loaded to a Criterion™ 16.5 % Tris-Tricine Precast gel (Bio-Rad). The gel was run at 100 V, 50 mA for 3 h, and then imaged using an ImageQuant LAS 4000 instrument (GE Healthcare).
-, reaction with no inhibitors; **moe**, control reaction with moenomycin; **amp**, control reaction with ampicillin.

observed, as expected for putative cross-linked material. When ampicillin was included in the reaction mixture, the high molecular weight band was lost with PBP1a^{Pn16}, but the band was still observed in the reaction with PBP1a^{159}. This observation is consistent with the high molecular weight material being cross-linked polymer, based upon the likely decreased affinity of PBP1a^{159} for the ampicillin compared to PBP1a^{Pn16}. In order to assess whether transpeptidation

had occurred in these reactions, duplicate samples were digested using *S. globisporus* mutanolysin, and analysed by mass spectrometry.

The compounds queried in the LC-MS data are depicted in Figure 4.17. As both the donor and acceptor in this experiment were polymerisable, the mass of a putative TP product (Figure 4.17a) would match that of an incompletely mutanolysin-digested heterodimer (Lipid IV) species of Lipid II (iGln, Dans) and Lipid II (iGln, tripeptide) with removal of the terminal D-Ala moiety of the Dansylated stem peptide (Figure 4.17b). Ions derived from a compound of that mass would therefore require collision-induced fragmentation to discriminate between these two possibilities.

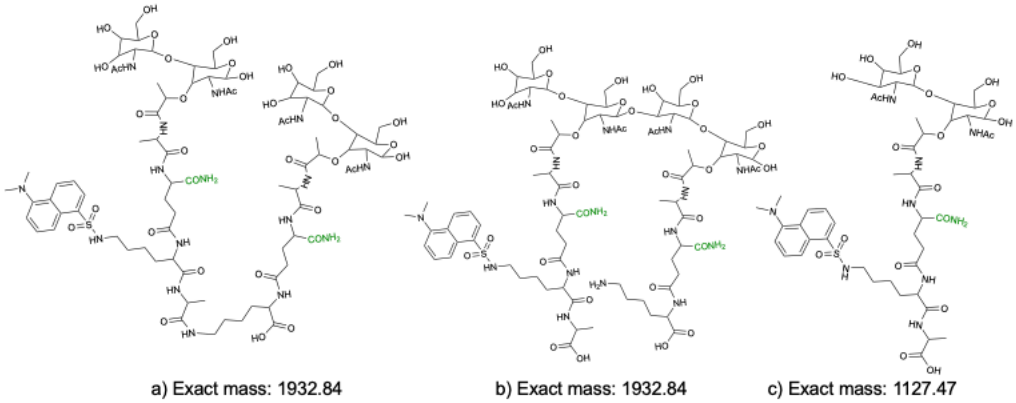

Figure 4.17 Expected products of transpeptidase and D,D-carboxypeptidase activities using Lipid II (iGln, Dans) and Lipid II (iGln, tripeptide) as substrates, following digestion by an *N*-acetylmuramidase. Diagram of the *S. globisporus* mutanolysin-digested products formed by transpeptidation (**a**) and D,D-carboxypeptidation (**b**) catalysed by PBP1a^{Pn16} or PBP1a^{159} using Lipid II (iGln, Dans) and Lipid II (iGln, tripeptide) as substrates. Full digestion of (b) by *S. globisporus* mutanolysin yields compound c).

In the LC-MS analysis of the peptidoglycan assembly reactions with PBP1a^{Pn16} and PBP1a^{159}, insufficient signal was observed for ions derived from cross-linked material. We were therefore unable to confirm whether transpeptidase activity had occurred in these reactions.

An ion associated with the D,D-carboxypeptidase product (expected (m+1)/1, 1128.48; observed (m+1)/1, 1128.48) was detected in the reactions with PBP1a^{Pn16} and no antibiotics, and PBP1a^{159} without inhibitors and with ampicillin (Table 4.8). The detection of a D,D-carboxypeptidase product in the

reaction with PBP1a^{159} and ampicillin was consistent with the result in Figure 4.16, where the high molecular weight band was still observed in the presence of ampicillin, and could be attributed to the comparative insensitivity of PBP1a^{159} to ampicillin.

Table 4.8 LC-MS analysis of peptidoglycan assembly reactions of PBP1a^{Pn16} and PBP1a^{159}. Reactions comprised 50 mM HEPES pH 7.6, 10 mM $MgCl_2$, 0.5 μM PBP1a, 2.5 μM Lipid II (iGln, Dans), 2.5 μM Lipid II (iGln, tripeptide), 25 % (v/v) DMSO, 150 mM NaCl, 33.51 mM.min^{-1} *R. gracalis* D-amino acid oxidase, 14.82 mM.min^{-1} horseradish peroxidase, 50 μM Amplex Red and 3 X CMC of E_8C_{10}. Following the reaction, samples were digested with mutanolysin and analysed by LC-MS.

Compound	Charge state	Expected m/z	Sample	Observed m/z
CP product	(m+1)/1	1128.48	Pn16	1128.48
			Pn16 amp	-
			159	1128.48
			159 amp	1128.48
			159 moe	-
TP product or GT heterodimer	(m+2)/2	967.43	Pn16	-
			Pn16 amp	-
			159	-
			159 amp	-
			159 moe	-

4.3.4 BOCILLIN FL binding to assess substrate binding

The major aim of this project was to investigate the impact of branched muropeptides on the inhibition of pneumococcal PBPs by β-lactams. As there were difficulties in establishing TP activity in the D-Ala release assay system, we looked to alternate techniques to compare the binding of β-lactams in the presence of linear and branched substrates.

We therefore sought to establish whether BOCILLIN FL binding could be used to assess the interaction of PBP1a with its substrates. We hypothesised that the substrates of PBP1a may protect the active site serine from modification

with BOCILLIN FL, and that this protection may vary depending upon whether the substrate was donor or acceptor, and linear or branched.

Interactions with BOCILLIN FL were assessed by incubating the protein with BOCILLIN FL (and any other molecules under investigation), and then analysing the samples by SDS-PAGE.

4.3.4.1 BOCILLIN FL binding by different PBP1a variants

The first step in the use of BOCILLIN FL binding for analysis of substrate interactions was to establish that each of the PBP1a variants could be modified by BOCILLIN FL. An active site serine mutant of PBP1a D39 (designated D39 $S_{370}A$) was used as a control enzyme, as the loss of the active site serine should prevent modification of this enzyme with BOCILLIN FL. For each enzyme, moenomycin and ampicillin were used in control reactions. Moenomycin binds PBP1a, but at the donor site of the glycosyltransferase active site, and as such this inhibitor should not prevent modification of PBP1a with BOCILLIN FL. Ampicillin was used to modify the active site serine of PBP1a prior to addition of BOCILLIN FL, thereby demonstrating that the modification by the latter is by interaction specifically with the active site serine. Also included was a negative control, with DMSO in place of BOCILLIN FL. As depicted in Figure 4.18, PBP1a variants from strains D39, Pn16 and 159 were all modified by BOCILLIN FL, but not $PBP1a^{D39}$ $S_{370}A$, as expected. The described control reactions were also broadly as expected, with no impact upon BOCILLIN FL binding by moenomycin, but competition of BOCILLIN FL binding by ampicillin. However, there was only partial competition of BOCILLIN FL binding of $PBP1a^{159}$ by ampicillin. This was likely the consequence of reduced affinity of $PBP1a^{159}$ for ampicillin.

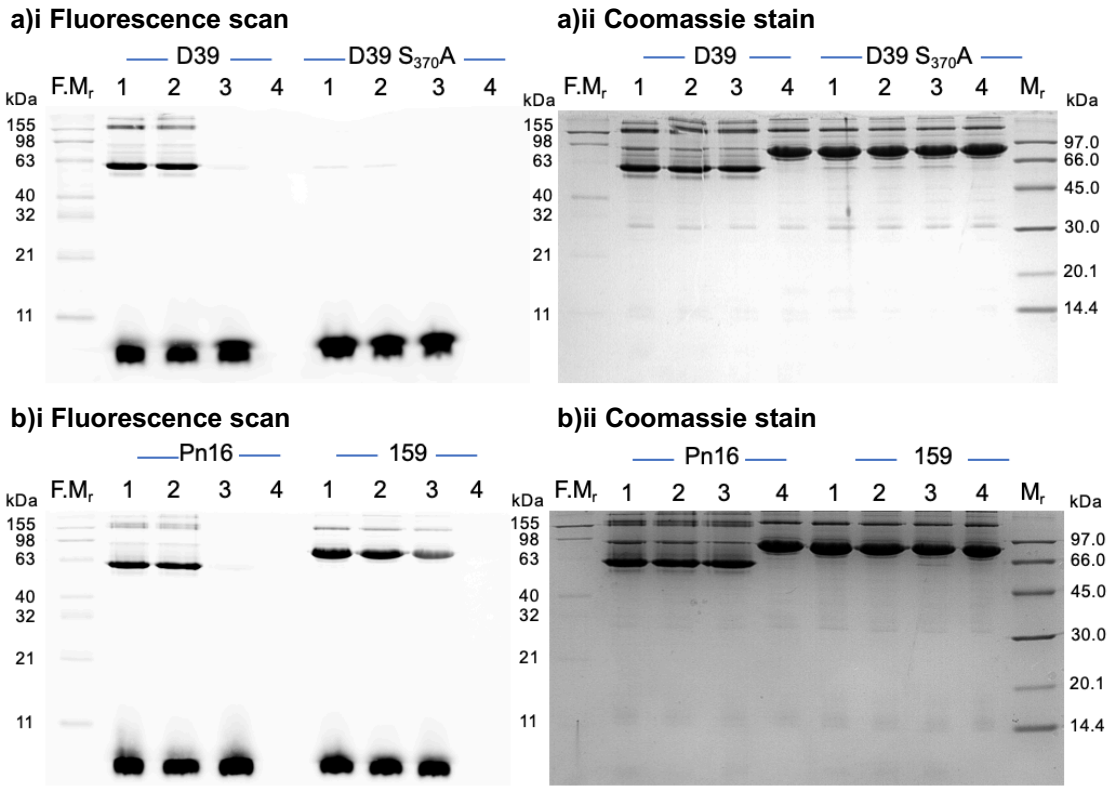

Figure 4.18 Analysis of BOCILLIN FL binding by *S. pneumoniae* PBP1a variants. Protein stocks (10 μM) were incubated with water, moenomycin (200 μM) or ampicillin (200 μM) for 30 mins at 25 °C, followed by incubation with 50 μM BOCILLIN FL or DMSO for 1 h at 37 °C. Reactions were analysed by SDS-PAGE using 12 % acrylamide gels and fluorescence was imaged (a)I and (b)i) using a Typhoon FLA 9500 laser scanner (GE Healthcare). Gels were then stained using InstantBlue Protein Stain (Expedeon) and imaged for total protein ((a)ii and (b)ii) using an ImageQuant LAS 4000 instrument (GE Healthcare).
1, PBP1a, moenomycin and BOCILLIN FL; **2**, PBP1a, water and BOCILLIN FL; **3**, PBP1a, ampicillin and BOCILLIN FL; **4**, PBP1a, water and DMSO; **F.M$_r$**, BenchMark Fluorescent Protein Standard (ThermoFisher Scientific); **M$_r$**, Color Prestained Protein Standard, Broad Range (NEB) molecular weight marker, **kDa**, kilo-Daltons.

The inclusion of the DMSO-only control allowed an additional observation from these gels; there was the shift in the bands of PBP1a^{D39} and PBP1a^{Pn16} from the expected molecular weight of ~ 82 kDa, to 63 kDa when bound to BOCILLIN FL or ampicillin. This band shift was not observed with PBP1a^{159} or the PBP1a^{D39} S_{370}A mutant, with binding of BOCILLIN FL or ampicillin. This observation was followed up in work described in Section 4.3.4.5.

4.3.4.2 Effect of donor-only substrate on BOCILLIN FL binding

Interactions with the substrates were first investigated by using the donor-only substrate, Lipid II (iGln, ε-*N*-acetyl Lys). The effect of the donor on BOCILLIN FL binding was tested by preincubating PBP1a^{D39} with Lipid, and then adding BOCILLIN FL (Figure 4.19). At the concentrations used (10:1 molar ratio of Lipid II (iGln, acetyl-Lys):PBP1a^{D39}, with 5:1 molar ratio of BOCILLIN FL: PBP1a^{D39}), no effect on BOCILLIN FL binding by the presence of Lipid II (iGln, ε-*N*-acetyl Lys) was observed.

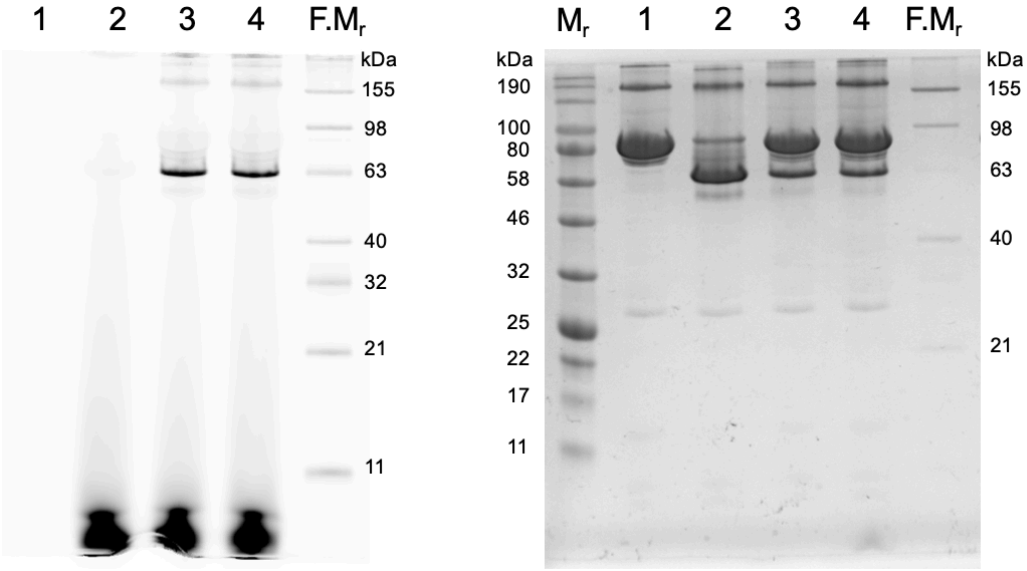

Figure 4.19 Analysis of BOCILLIN FL binding by PBP1a^{D39} in the presence of donor-only Lipid II. 6 μM PBP1a^{D39} was incubated with water, 60 μM Lipid II (iGln, acetyl-Lys) or 200 μM ampicillin for 30 mins at 25 °C, followed by incubation with 30 μM BOCILLIN FL or DMSO for 1 h at 37 °C. Reactions were analysed by SDS-PAGE using 12 % acrylamide gels and fluorescence was imaged (left-hand gel) using a Typhoon FLA 9500 laser scanner (GE Healthcare). Gels were then stained using InstantBlue Protein Stain (Expedeon) and imaged for total protein (right-hand gel) using an ImageQuant LAS 4000 instrument (GE Healthcare).
1, PBP1a^{D39}, water, DMSO; **2**, PBP1a^{D39}, ampicillin, BOCILLIN FL; **3**, PBP1a^{D39}, water, BOCILLIN FL; **4**, PBP1a^{D39}, Lipid II (iGln, acetyl-Lys), BOCILLIN FL; **F.M$_r$**, BenchMark Fluorescent Protein Standard (ThermoFisher Scientific); **M$_r$**, Color Prestained Protein Standard, Broad Range (NEB) molecular weight marker, **kDa**, kilo-Daltons.

4.3.4.3 Effect of Mur*N*Ac 5P (iGln) acceptor on BOCILLIN FL binding

Acceptor-only substrates were then tested for their ability to alter the binding of PBP1a by BOCILLIN FL. Concentrations from 1 to 1000-fold the molar

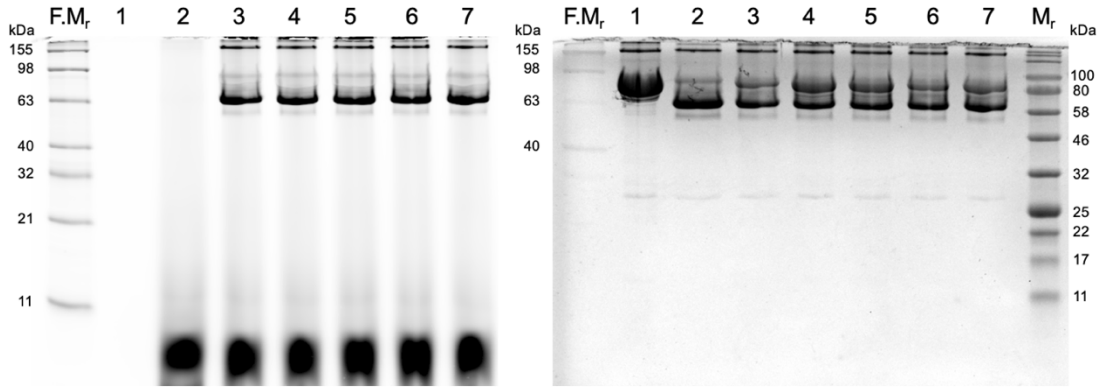

Figure 4.20 Analysis of BOCILLIN FL binding by PBP1a^{D39} in the presence of Mur*N*Ac 5P (iGln) acceptor. 6 μM PBP1a^{D39} was incubated with water, varying concentrations of Mur*N*Ac 5P (iGln) acceptor or 200 μM ampicillin for 30 mins at 25 °C, followed by incubation with 30 μM BOCILLIN FL or DMSO for 1 h at 37 °C. Reactions were analysed by SDS-PAGE using 12 % acrylamide gels and fluorescence was imaged (left-hand gel) using a Typhoon FLA 9500 laser scanner (GE Healthcare). Gels were then stained using InstantBlue Protein Stain (Expedeon) and imaged for total protein (right-hand gel) using an ImageQuant LAS 4000 instrument (GE Healthcare). **1**, PBP1a^{D39}, water, DMSO; **2**, PBP1a^{D39}, ampicillin, BOCILLIN FL; **3**, PBP1a^{D39}, water, BOCILLIN FL; **4**, 1:1 molar ratio PBP1a^{D39}:Mur*N*Ac 5P (iGln), BOCILLIN FL; **5**, 1:10 molar ratio PBP1a^{D39}:Mur*N*Ac 5P (iGln) BOCILLIN FL; **6**, 1:100 molar ratio PBP1a^{D39}:Mur*N*Ac 5P (iGln), BOCILLIN FL; **7**, 1:1000 molar ratio PBP1a^{D39}:Mur*N*Ac 5P (iGln), BOCILLIN FL; **F.M$_r$**, BenchMark Fluorescent Protein Standard (ThermoFisher Scientific); **M$_r$**, Color Prestained Protein Standard, Broad Range (NEB) molecular weight marker; **kDa**, kilo-Daltons.

concentration of enzyme were used, with 5-fold BOCILLIN FL compared to the molar concentration of enzyme. The acceptor tested was Mur*N*Ac 5P (iGln) (Figure 4.20).

No effect on BOCILLIN FL binding by the presence of Mur*N*Ac 5P (iGln) substrate was observed with PBP1a^{D39}, based on band sizes observed under fluorescence imaging. This technique, under the conditions tested, could therefore not be used to compared the impact of different substrates (both donor- and acceptor-only) on acylation by BOCILLIN FL.

4.3.4.5 Shift in migration of PBP1a bands on SDS-PAGE upon binding of β-lactams

We observed a shift in the migration of BOCILLIN FL-PBP complexes with some variants of PBP1a (Figure 4.18). We therefore sought to assess whether acylation of PBP1a by other β-lactams would give the same result. We first established whether this effect upon PBP1a^{D39} was associated with binding of ampicillin and not specific to BOCILLIN FL; and whether the effect was observed with binding of Lipid II (iGln) (Figure 4.21).

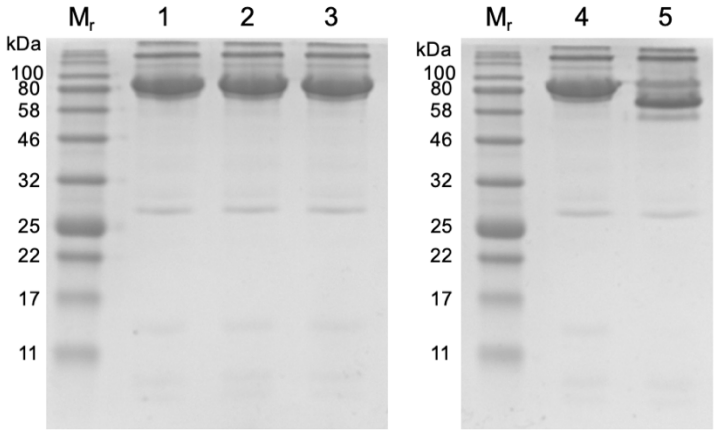

Figure 4.21 Analysis of PBP1a^{D39} band shift on SDS-PAGE in the presence of Lipid substrates and ampicillin. 6 μM PBP1a^{D39} was incubated with buffer (**1**), 60 μM Lipid II (iGln) (**2**), 60 μM Lipid II (iGln, ε-*N*-acetyl Lys) (**3**), water (**4**) or 200 μM ampicillin (**5**) for 30 mins at 25 °C. Reactions were analysed by SDS-PAGE using a 12 % acrylamide gel. The gel was then stained using InstantBlue Protein Stain (Expedeon) and imaged using an ImageQuant LAS 4000 instrument (GE Healthcare).
1, PBP1a^{D39} and buffer; **2**, PBP1a^{D39} and Lipid II (iGln, ε-*N*-acetyl Lys); **3**, PBP1a^{D39} and Lipid II (iGln); **4**, PBP1a^{D39} and water; **5**, PBP1a^{D39} and ampicillin; **M$_r$**, Color Prestained Protein Standard, Broad Range (NEB) molecular weight marker, **kDa**, kilo-Daltons.

When incubated with Lipid II buffer (Figure 4.21, lane 1) or water (lane 4), a band of PBP1a^{D39} was observed at ~80 kDa, as expected based on the experimentally determined exact mass (82.3 kDa; see Section 4.3.1.4). No change in the observed molecular weight of this band was observed in the presence of Lipid II (iGln, ε-*N*-acetyl Lys) (Figure 4.21, lane 2) or in the presence of Lipid II (iGln) (lane 3). However, as previously observed, in the presence of ampicillin the major band was observed between 58 and 80 kDa. The binding of ampicillin therefore appeared to be associated with a shift in the apparent molecular weight of PBP1a^{D39} on SDS-PAGE gels. Mass

spectrometry analysis of this complex was only consistent with a change in mass resulting from the added mass of ampicillin (Section 4.3.1.4), and so this phenomenon was likely a consequence of conformation and not a genuine decrease in mass.

We then sought to analyse whether the apparent shift in molecular weight (of PBP1a^{D39} bound to ampicillin or BOCILLIN FL) was a general property associated with acylation of PBP1a^{D39} by β-lactams.

A variety of β-lactams, to represent the variation in structure of the different generations and chemical classes, was tested for the association with the change in band migration. Of particular interest were those inhibitors

Table 4.9. Selectivity of β-lactams for pneumococcal PBPs, based on protection against labelling by BOCILLIN FL. Adapted from Kocaoglu *et al.* (2015).

Class	β-lactam	Selectivity profile (PBP)					
		1a	1b	2a	2x	2b	3
Penicillins	penicillin G				Y		Y
	ampicillin	Y			Y		Y
Cephalosporins	cephalexin						Y
	cephalothin	Y	Y				Y
	cefoxitin						Y
	cefuroxime				Y		
	cefotaxime				Y		Y
	cefsulodin						Y
	ceftriaxone				Y		Y
Monobactams	aztreonam						Y
Carbapenems	doripenem	Y			Y		Y
	meropenem	Y			Y		Y

demonstrated by Kocaoglu *et al.* (2015) to be selective for PBP1a in an unencapsulated pneumococcal D39 strain (Table 4.9). It should be noted that, surprisingly, none of the inhibitors tested were designated as selective for PBP2b, despite the importance of this PBP in the pneumococcal resistance mechanism.

Ampicillin, meropenem and cephalothin were therefore each incubated with PBP1a^{D39}, and samples analysed by SDS-PAGE to analyse the observed molecular weight. In order to confirm the binding of PBP1a^{D39} by these inhibitors, a second set of reactions were run concurrently, with subsequent addition of BOCILLIN FL to establish whether ampicillin, meropenem and cephalothin protected against acylation of the TP active site serine by BOCILLIN FL. DMSO was added to reactions without BOCILLIN FL to control for the effect of this solvent.

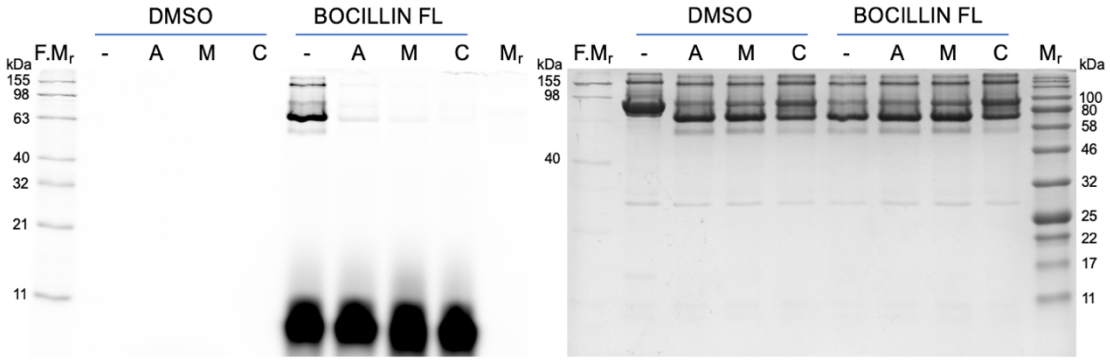

Figure 4.22 β-lactam panel for analysis of shift in migration of PBP1a^{D39}. 6 μM PBP1a^{D39} was incubated with water or 600 μM β-lactam, followed by a further incubation with DMSO or 60 μM BOCILLIN FL. Reactions were analysed by SDS-PAGE using a 12 % acrylamide gel and fluorescence was imaged (left-hand gel) using a Typhoon FLA 9500 laser scanner (GE Healthcare). The gel was then stained using InstantBlue Protein Stain (Expedeon) and imaged for total protein (right-hand gel) using an ImageQuant LAS 4000 instrument (GE Healthcare).
-, PBP1a^{D39} and water; **A**, PBP1a^{D39} and ampicillin; **M**, PBP1a^{D39} and meropenem; **C**, PBP1a^{D39} and cephalothin; **F.M$_r$**, BenchMark Fluorescent Protein Standard (ThermoFisher Scientific); **M$_r$**, Color Prestained Protein Standard, Broad Range (NEB) molecular weight marker, **kDa**, kilo-Daltons.

PBP1a^{D39} incubated with water and DMSO only migrated on SDS-PAGE as a major band at ~ 80 kDa (Figure 4.22). As previously, acylation of PBP1a^{D39} by BOCILLIN-FL was associated with a shift in the migration of the enzyme to ~ 63 kDa. Very little fluorescence was detected in samples pre-incubated with

ampicillin, meropenem or cephalothin, indicating that these inhibitors were able to acylate the active site serine and thereby prevent binding of BOCILLIN FL. Binding of PBP1a^{D39} by ampicillin, meropenem and cephalothin were all associated with a shift in the migration of the major band of PBP1a^{D39}. This phenomenon appears to therefore be a general property among this subset of PBP1a-directed β-lactams.

This experiment was then broadened to include β-lactams that were not reported to be PBP1a-selective by Kocaoglu *et al.* (2015), in addition to two peptidoglycan biosynthesis inhibitors unrelated to the β-lactams; moenomycin, as discussed previously; and vancomycin, a glycopeptide inhibitor. Vancomycin inhibits transpeptidation via binding of the D-Ala-D-Ala terminus of Lipid II, and should not therefore not be associated with the β-lactam mediated shift in band migration of PBP1a. Incubation with moenomycin or vancomycin in the absence of BOCILLIN FL was not associated with a shift in the migration of PBP1a^{D39} on an SDS-PAGE gel (Figure 4.23c), and these inhibitors did not prevent acylation of PBP1a^{D39} by BOCILLIN FL (Figure 4.23b). These observations suggest that the shift in migration requires binding of PBP1a^{D39} at the transpeptidase active site, by a β-lactam.

In agreement with the results from Figure 4.22, binding of PBP1a^{D39} by ampicillin or meropenem prevented acylation of the active site serine by BOCILLIN FL (Figure 4.23a), and was associated in a shift in the migration of the major band of protein. Such shift in migration was also observed with ceftazidime, though proportionally more protein remained at the expected molecular weight (Figure 4.23c), and protection against acylation by BOCILLIN FL (a) demonstrated acylation of the enzyme by ceftazidime. A shift in migration was observed with cephalexin, but the major band in this reaction remained at the expected molecular weight (Figure 4.23c). In addition, there was little effect on BOCILLIN FL labelling of PBP1a^{D39} when pre-incubated with cephalexin, suggesting poorer affinity of this antibiotic for the enzyme.

Whilst pre-incubation with cefoxitin preventing labelling of PBP1a with BOCILLIN FL (Figure 4.23a), indicating binding of PBP1a^{D39} by this inhibitor, there was no shift observed in the migration of the major band (Figure 4.23b

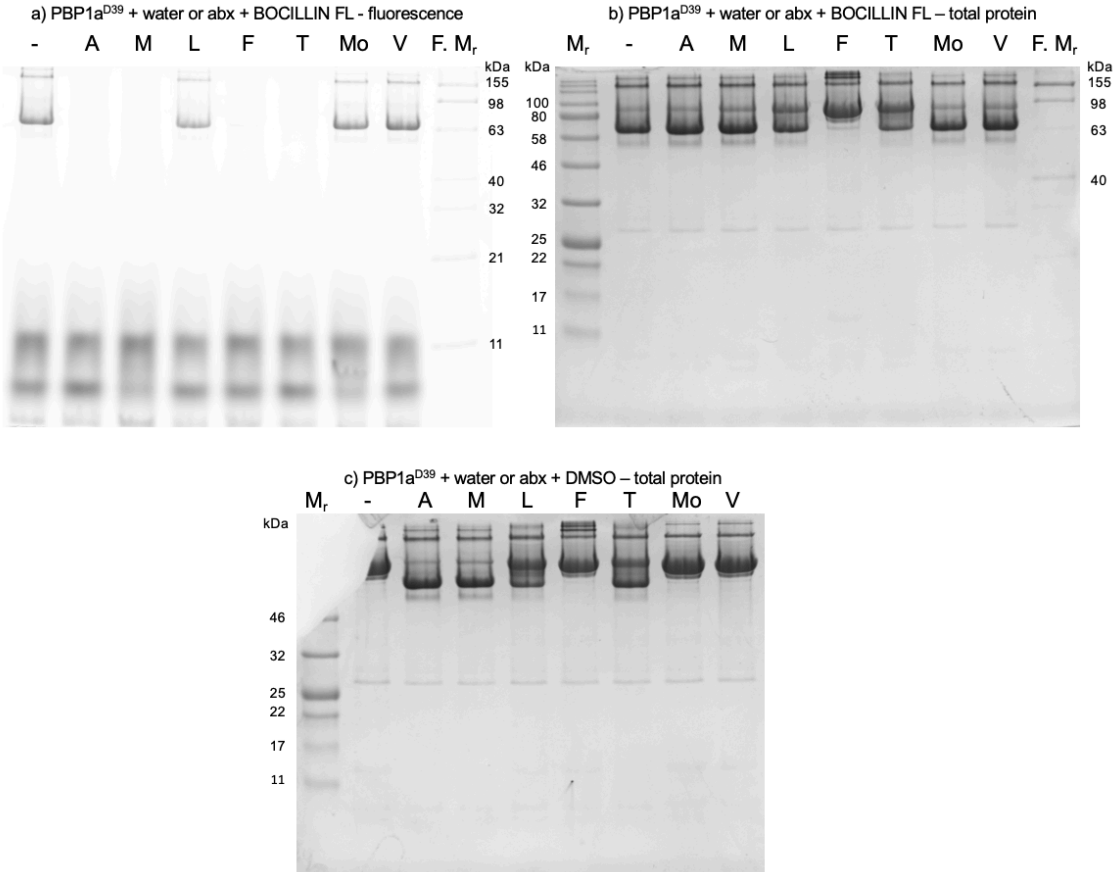

Figure 4.23 Inhibitor panel for analysis of shift in migration of PBP1a^{D39}. A range of peptidoglycan biosynthesis inhibitors (β-lactams: ampicillin (**A**), meropenem (**M**), cephalexin (**L**), cefoxitin (**F**), ceftazidime (**T**); moenomycin (**M**), a glycosyltransferase inhibitor; and vancomycin (**V**), a glycopeptide) at 600 μM or water were incubated with 6 μM PBP1a^{D39}, followed by addition of 60 μM BOCILLIN FL (gels **a**) and **b**)) or DMSO (**c**) and a further incubation step. Reactions were analysed by SDS-PAGE using a 12 % acrylamide gel and fluorescence was imaged (left-hand gel) using a Typhoon FLA 9500 laser scanner (GE Healthcare). The gel was then stained using InstantBlue Protein Stain (Expedeon) and imaged for total protein (right-hand gel) using an ImageQuant LAS 4000 instrument (GE Healthcare).
Gel a, reactions including BOCILLIN FL, and an inhibitor (**abx**) or water, and imaged for fluorescence; **Gel b**, reactions including BOCILLIN FL, and an inhibitor (**abx**) or water, and imaged for total protein; **Gel c**, reactions including DMSO, and an inhibitor (**abx**) or water, and imaged for total protein; **A**, ampicillin; **M**, meropenem; **L**, cephalexin; **F**, cefoxitin; **T**, ceftazidime; **Mo**, moenomycin; **V**, vancomycin; **F.M$_r$**, BenchMark Fluorescent Protein Standard (ThermoFisher Scientific); **M$_r$**, Color Prestained Protein Standard, Broad Range (NEB) molecular weight marker, **kDa**, kilo-Daltons.

and c). The migration-shift phenomenon was therefore not a general feature of acylation of PBP1a by β-lactams.

4.4 Discussion

4.4.1 Difficulties in establishing *in vitro* transpeptidase activity of PBP1a^{D39}

The difficulty of establishing *in vitro* transpeptidase activity has limited progress in characterisation of the pneumococcal β-lactam resistance mechanism. The data presented in this Chapter indicated that slow D,D-carboxypeptidase activity by PBP1a^{D39} could be detected, and that the rate of this activity (as measured by the rate of D-Ala release) was increased in near-CMC concentrations of E_6C_{12} assay detergent.

4.4.1.1 Low activity of PBP1a^{D39}

Activity of PBP1a^{D39} was low in comparison to purified recombinant *E. coli* PBP1b (Dr. A.J. Lloyd, University of Warwick, personal communication). D-Ala release that was detected appeared to be composed near-entirely of D,D-carboxypeptidation. This was based upon the apparent independence of D-Ala release to presence of acceptor substrate; along with lack of detection of TP products on LC-MS analysis.

Possible causes for the issues with activity that were explored included presence of lysozyme, loss of activity with storage, the choice of substrates, and insufficient GT activity under the assay conditions. Omission of lysozyme from the purification of PBP1a^{D39} did not impact the rate of transpeptidation observed. In addition, assays conducted immediately upon purification of PBP1a^{D39} did not show greater activity of the enzyme than those conducted following storage of the enzyme at – 20 °C. Finally, despite the use of both Lipid II (iGln) and donor-only and acceptor-only substrates being used for transpeptidase assays, no appreciable increase in activity of PBP1a^{D39} could be achieved. Explorations of the contribution of GT activity to the detection of TP activity are discussed in Section 4.4.1.4.

A recent publication has suggested that the role in peptidoglycan biosynthesis of Class A PBPs in the pneumococcus lies within remodelling of peptidoglycan (Straume *et al.*, 2019), which would have implications for the substrate

preference of PBP1a. Further work could encompass the use of purified peptidoglycan as a substrate to further explore this possibility. Stimulation by protein-protein interactions could also be a key component of *in vitro* activity. This is further explored in Section 4.4.5.

4.4.1.2 Detection of transpeptidation by LC-MSMS

Analysis of transpeptidation by mass spectrometry did not detect TP products from reactions with *S. pneumoniae* PBP1a^{D39}. TP products from reactions using Lipid II (iGln) as substrate have previously been detected under similar analysis conditions (Galley, 2015). The results are therefore likely to reflect lack of cross-linked product, rather than a failure of detection on LC-MS due to limited ionisation of the compound of interest.

Reactions from an experiment testing the impact of detergent titration on TP activity did result in detection of a putative TP product (Section 4.3.2.2). The low abundance of the relevant ion precluded LCMSMS analysis to determine whether TP or CP product was observed. Up to 90 % signal loss can be expected when selecting ions for diversion into the second quadrupole of the mass spectrometer. In the case of the detergent titration experiment, the signal of the ion of interest was insufficient to allow fragmentation.

In subsequent experiments, detection of TP products was attempted from samples that were in parallel analysed by Tris-tricine SDS-PAGE. Te experiment was designed to increase the amount of the putative TP product ion (and therefore hopefully the signal detected) by inclusion of longer incubation of the reactions, and concentration of the samples by lyophilization. These methods were unsuccessful in yielding detection of a TP product by mass spectrometry.

The LC-MSMS detection method warrants revisiting in combination with the further work explored in Section 4.4.5.

4.4.1.3 Variation in Lipid II (iGln) stocks

Variation in the activity of some preparations of PBP1a^{D39} could be ascribed to differences between Lipid II (iGln) stocks. Mass spectrometry, and purity analysis by TLC, revealed that a polymeric contaminant in one stock of Lipid II (iGln); and that another was apparently less concentrated than was determined using a phosphate-release assay for Lipid II concentration. In future assays using Lipid II (iGln), a master stock that has been validated for use (i.e. with which D-Ala release activity has been detected with PBP1a^{D39}) should be retained for testing of further stocks as they are made.

4.4.1.4 Potential for rate-limiting GT activity of PBP1a^{D39}

It was considered that the apparent low rate of D-Ala release may be due to slow GT activity under the conditions of the TP assay, which would prove rate-limiting to transpeptidation due to the need for supply of the TP donor from the GT site, as a polymeric species. Transpeptidase assays using Lipid II (iGln, Dans) in the presence of DMSO demonstrated similar rates of D-Ala release to those observed in assays using Lipid II (iGln). As significant and rapid GT activity could be detected using Lipid II (iGln, Dans), it was concluded that slow GT activity was unlikely to be the cause of limited D-Ala release activity.

4.4.2 The impact of detergents on D-Ala release catalysed by PBP1a^{D39}

Analysis of D-Ala release in the transpeptidase assay revealed that the rate of D-Ala release was increased with decreasing concentrations of detergent. This effect could be related to the activity of the glycosyltransferase active site, as the substrates of the GT reaction are lipid-linked (Section 1.4.1), but in the TP reaction products are not lipid linked, so it seems less likely that transpeptidation would be affect by detergent so long as the enzyme is kept in solution adequately. This impact of lipid environment on PBP1a activity was further studied in Chapter 5. The inverse relation between detergent concentration and PBP1a activity was rationalised based on surface dilution kinetics, whereby decreasing concentrations of detergent would result in less dilution of enzyme and substrate from one another.

4.4.3 Analysis of TP activity by SDS-PAGE

Tris-tricine SDS-PAGE was an alternative technique that was explored to detect transpeptidase activity, as has been shown in the literature (Qiao *et al.*, 2017; Zapun *et al.*, 2013). From the analysis of reaction products from PBP1a^{Pn16} and PBP1a^{159}, high molecular weight material was observed by Tris-tricine SDS-PAGE. However, there was no evidence of TP products by mass spectrometry. Two potential explanations for these results arise. It is possible that the high molecular weight material comprised large glycan polymers, though this would not reconcile with the loss of such material in the presence of ampicillin. Alternatively, the high molecular weight material could be cross linked peptidoglycan, but it could be that very few cross links are required to generate material that cannot enter the gel matrix. In this case, the detection of cross-linked material following mutanolysin digestion would prove difficult. There was therefore no evidence that the high molecular weight material was cross-linked product.

The most convincing example of detection of transpeptidation by Tris-tricine SDS-PAGE in the literature was that of Qiao *et al.* (2017). Qiao *et al.* (2017) used treatment with lysostaphin to demonstrate that the high-molecular weight material was cross-linked, based on the loss of this band following cleavage of the cross-links with lysostaphin. Similar analysis could be pursued with PBP1a^{D39}, in the absence of such a specific endopeptidase, by the use of Lipid II (iGln) where the materially was fluorescently labelled via the lipid chain or sugar moieties. In this case, an amidase could be used to cleave the high molecular weight material without loss of fluorescent labelling, thereby allowing a similar experiment to be conducted as that of Qiao *et al.* (2017).

4.4.4 Further work to establish *in vitro* transpeptidase activity of PBP1a^{D39}

To begin to address the resistance mechanism of *S. pneumoniae* to β-lactam antibiotics, further work is needed to establish *in vitro* transpeptidase activity.

4.4.4.1 S2d substrate analogues

One potential method for further characterising the conditions to establish PBP1a activity would be the use of S2d thioester analogues as a proxy for transpeptidase activity. These compounds could be used to establish optimum conditions for testing with Lipid II, thus decreasing the amount of this expensive reagent that need be used. In addition, previous uses of this assay have analysed the ratio of transpeptidase and D,D-carboxypeptidase activity (Adam *et al.*, 1991). Such data would be of use to corroborate the findings described in this Chapter.

4.4.4.2 Protein interactors with Class A PBPs

Another key avenue for further exploration is the interactors of *S. pneumoniae* Class A PBPs. MacP, a protein interacting partner of PBP2a, was found to be essential for *in vivo* function of PBP2a (Fenton *et al.*, 2018). By contrast, no activating partner protein of PBP1a has so far been established. A key next step would therefore be to clone and express MacP and test PG synthesis activity of PBP2a with that enzyme present. Additionally, Fenton *et al.* (2018) suggested that MacP interacted with the cytoplasmic tail or transmembrane anchor of PBP2a. It could therefore be of interest to express and analyse the activity of a PBP2a construct without the cytoplasmic domain. Studies of *E. coli* PBP1B isoforms with differing lengths of cytoplasmic tail have revealed an involvement of this region in association with PBP3 (Chalut *et al.*, 2001). Loss of the transmembrane anchor has been shown to impair GT activity of PBP2a (Galley, 2015), so this would be unlikely to yield increased activity of the protein.

4.4.5 BOCILLIN FL binding and interactions with substrates

Under the conditions tested, no impact upon BOCILLIN FL binding was observed by the presence of Lipid II variants or Mur*N*Ac 5P (iGln) acceptor.

Di Guilmi *et al.* (2003) used native PAGE to determine whether Lipid II binding to the TP domain of PBP2a could be observed on the basis of a gel-shift. Whilst binding of Lipid II to the GT domain was found to be associated with a gel-shift in the protein band, no such phenomenon was observed in the current

experiments. Native PAGE experiments could therefore be of utility in further characterisation of binding by substrates. However, this would render it difficult to distinguish between binding by the GT and TP active sites, whereas covalent interaction (as detected on SDS-PAGE) occurs only at the TP active site and not the GT active site.

To follow up on this work, a technique such as fluorescent polarisation could be employed. By this technique, the impact of donor or acceptor-only substrates on BOCILLIN FL binding could be analysed, to provide insight into how linear and branched acceptors interact. However, a limitation of this technique is its amenability to detergent; large detergent micelles such as those formed by E_6C_{12}, the detergent of choice, could themselves contribute to the anisotropy signal, and thus limit the sensitivity of the assay.

BOCILLIN FL gels revealed an experimental phenomenon of shift in migration of PBP1a upon binding of particular β-lactams. A similar shift in migration was not observed with PBP1a$_{S370A}$, which illustrated that the phenomenon was associated with β-lactam binding. In addition, the shift in migration did not appear to be a general feature of β-lactam binding, as only a subset of β-lactams caused the apparent shift, despite the use of concentrations sufficient to inhibit labelling by BOCILLIN FL.

Gel shifting has previously been observed as a phenomenon associated with membrane proteins. Rath *et al.* (2009) showed that the shift in migration of a panel of hairpin sequences from TM 3 and 4 of the human cystic fibrosis transmembrane conductance regulator (CFTR) were associated with changes in the SDS-binding capacity and hairpin helicity of these constructs. Rath *et al.* (2009) thereby suggested that some gel shifts between the constructs may be explained by replacement of protein-protein contacts by protein-detergent contacts, which thereby altered the mass to charge ratio of the proteins.
Other physical properties of proteins found associated with gel shifts included percentage of acidic amino acids, with difference between predicted and experimental molecular weight correlating with percentage of acidic amino

acids over a specific range (Guan *et al.*, 2015); post-translational modifications such as phosphorylation (Hutchison *et al.*, 1993; Lee *et al.*, 2013); particular carboxyl-terminal amino acids (Wang *et al.*, 2013); binding of Ni^{2+} ions by His-rich protein (Shelake *et al.*, 2017); and amino acid substitutions altering net charge, and therefore the number of SDS molecules bound (Shi *et al.*, 2012).

Ligand binding by proteins has been demonstrated to result in increased thermodynamic stability, and likely slower unfolding of protein (Chang *et al.*, 2012). This phenomenon was demonstrated with purified recombinant phosphoglyceromutase analysed under pulse proteolysis. Pulse proteolysis used selective digestion of unfolded proteins to provide a measure of the fraction of folded and unfolded protein in a mixture (Park & Marqusee, 2005). Chang *et al.* (2012) observed using pulse proteolysis that the transition midpoint of equilibrium unfolding (with urea as the chemical denaturant) was increased in the presence of ATP, thus indicating that binding of ATP increased the thermodynamic stability of phosphoglyceromutase.

An interesting further experiment to the BOCILLIN FL and β-lactam panels presented in this Chapter would therefore be analysis of the impact of β-lactam binding on thermodynamic stability of PBP1a, with the hypothesis that stabilisation of PBP1a by β-lactam binding may result in the shift in apparent molecular weight of PBP1a on SDS-PAGE.

4.4.6 Conclusions

Summarily, conclusive *in vitro* transpeptidase activity of $PBP1a^{D39}$ could not be established in the current work. Measurements of D-Ala release revealed optimum activity at E_6C_{12} concentrations approaching CMC. In addition, factors relating to the substrates and protein preparation have been explored for their contribution to activity of $PBP1a^{D39}$.

Chapter 5: Glycosyltransferase activity of pneumococcal PBP1a and PBP2a

5.1 Introduction

Mechanistic details of glycosyltransferase activity have been studied using techniques including thin-layer chromatography, high-pressure liquid chromatography (HPLC), continuous fluorescence-based assays and Förster resonance energy transfer (FRET)-based assays. Selected techniques are further discussed in Section 5.1.1.

5.1.1 Techniques for study of glycosyltransferase activity

The various available assays for glycosyltransferase activity are summarised in Table 5.1. A review on these techniques was published by Galley *et al.* (2014).

5.1.1.1 SDS-PAGE analysis of glycan polymers

Electrophoresis of negatively charged glycan polymers by Tricine-SDS-PAGE (Schägger & Von Jagow, 1987) has been used extensively in the literature. Whilst high molecular weight material does not enter the gel matrix, good resolution of short and intermediate chains can be achieved depending upon the choice of gel system (Barrett *et al.*, 2007). Lipid II starting material migrates just behind the dye front, and so reaction progress can be determined based on consumption of substrate.

Applications of the technique have made use of both radiolabelled (Barrett *et al.*, 2007) and fluorescently labelled (Helassa *et al.*, 2012) Lipid II as substrate, to allow visualisation of glycan polymers. Barrett *et al.* (2007) used Lipid II or Lipid IV in reactions with high enzyme:substrate ratio to generate shorter oligomers for use as molecular weight markers on SDS-PAGE gels.

Table 5.1 Summary of published techniques for observation of glycosyltransferase activity. Made with reference to Galley *et al.* (2014)

	Paper chromatography or Thin-layer chromatography (TLC)	**Polyacrylamide gel**	**HPLC**	**Continuous fluorometric assays**	**Pyrophosphate sensor assay**	**RapidFire Mass spectrometry**
Brief description	Chromatography of labelled glycan polymers on filter paper or TLC plate	Electrophoresis by Tricine-SDS-PAGE, based on the net negative charge of glycans	Chromatography of labelled glycan polymers by anion exchange or size exclusion	Monitoring of fluorescence based on change in signal depending on environment of the fluorophore	Fluorogenic anti-pyrophosphate antibody to detect undecaprenyl pyrophosphate released by GT activity	Detection of released undecaprenyl pyrophosphate from GT assays
Discontinuous or continuous	Discontinuous	Discontinuous	Discontinuous	Continuous	Continuous	Discontinuous
Example publications	Meadow *et al.* (1964) Ye *et al.* (2001)	Schagger *et al.* (1987) Barrett *et al.* (2007)	Schwartz *et al.* (2001); Schwartz *et al*. (2002)	Schwartz *et al*. (2002) Offant *et al.* (2010)	King *et al.* (2017)	Mesleh *et al.* (2016)

Although SDS-PAGE analysis is not quantitative, the technique offers the benefit of visualising the range of glycan polymers generated by a glycosyltransferase, thus allowing comparisons of enzyme processivity to be made.

5.1.1.2 HPLC analysis of glycan polymer formation

Schwartz *et al.* (2001) described a set of HPLC-based experiments to follow the GT and transpeptidase (TP) activity of *E. coli* PBP1b. Lipid II molecules in time-point samples were labelled, at the primary amine of meso-diaminopimelic acid in the peptide stem, using fluorescamine. The reaction mixture was then chromatographed by HPLC. Schwartz *et al.* (2001) were thus able to demonstrate moenomycin-sensitive consumption of Lipid II by *E. coli* PBP1b. The inclusion of muramidase in the reaction mixture then allowed both consumption of the substrate and generation of the product (Glc*N*Ac-Mur*N*Ac pentapeptide, as confirmed by mass spectrometry) to be followed from the same samples by fluorescamine labelling and HPLC as before.

Fluorescamine-labelling and HPLC also proved amenable to follow D-alanine release by transpeptidase activity, by which Schwartz *et al.* (2001) demonstrated time-dependent, penicillin G-sensitive release of D-alanine. The suitability of this HPLC technique for application to study of both GT and TP activities was beneficial as both activities could then be studied under the same reaction conditions. The detection by post-reaction labelling also allowed use of unmodified substrates for the assay, precluding the requirement for chemically labelling each substrate to be analysed prior to use in the reaction, and therefore eliminating concerns regarding the influence of chemical modification of glycosyltransferase substrates on glycosyltransferase activity.

5.1.1.3 Fluorometric assay for glycosyltransferase activity

The continuous fluorometric assay for glycosyltransferase activity measures the change in quantum yield of fluorescence of a dansyl fluorophore labelling the lipid substrate (Schwartz *et al.*, 2002). Substrate labelled with a dansyl fluorophore at the third position side chain of the peptide stem (Lipid II (Dans)) was polymerised into glycan chains by *E. coli* PBP1b, while the resulting glycan chains were digested by an *N*-acetylmuramidase included in the reaction. The dansyl group was thus transferred from a hydrophobic micellar

environment (Lipid II and glycan polymers) to an aqueous environment (soluble monomer units), with an associated decrease in the quantum yield of fluorescence (Pompliano *et al.*, 1992). The initial rate of change in fluorescence was then interpreted as the initial rate of glycosyltransfer.

The continuous fluorometric assay has been scaled down to multi-well format (Offant *et al.*, 2010), thus making it suitable for use in inhibitor screening (Derouaux *et al.*, 2011). The continuous fluorescence-based assay format allows determination of kinetic parameters such as K_m for glycosyltransferases, but limitations of this format included that the data could not be converted into units of molarity, thus allowing only relative estimates of k_{cat}; and the potential impact of the modification of substrates on the activity under observation.

Efforts towards quantitative assays of GT activity have used detection of undecaprenyl pyrophosphate release to generate the quantitative signal. Mesleh *et al.* (2016) developed a discontinuous GT assay using Rapid-Fire mass spectrometry to detect undecaprenyl pyrophosphate. Quantitative analysis was made by use of geranylgeranyl pyrophosphate (C_{20}PP) as an internal standard for normalisation of the signal, and a standard curve of C_{55}P against mass spectrometry signal. The continuous fluorescent assay for undecaprenyl pyrophosphate release of King *et al.* (2017) was based on a commercial fluorogenic anti-pyrophosphate antibody.

5.1.1.4 FRET assay

A FRET assay for glycosyltransferases was described by Huang *et al.* (2013). A FRET-based Lipid II Analogue (FBLA) formed the basis for the assay, whereby the loss of the dimethylaminoazobenzenesulfonyl quencher on the lipid moiety when FBLA was polymerised would allow detection of fluorescence, based on the Coumarin fluorophore at the third position of the peptide stem. The fluorescence signal was enhanced by inclusion of an *N*-acetylmuramidase (as described for the continuous fluorometric assay, Section 5.1.1.3). This approach was suited to enzyme kinetic analysis as well as high-throughput screening. One limitation of this technique could be the

limit in application of the substrates required; by contrast, Lipid II (Dans) is suited for use in analysis by SDS-PAGE and the continuous fluorescence assay. Additionally, the impact of both fluorophores on the ability of the glycosyltransferase to recognise its substrate remains a question.

The various assay technologies offer complimentary tools for the analysis of glycosyltransferase activities; continuous fluorescence assays have utility in the determination of kinetic parameters of glycosyltransferase activity, but did not shed light on the characteristics of the polymer made or allow application to TP analysis; HPLC assays allowed GT activity to be followed on the basis of substrate consumption or muramidase product accumulation; and SDS-PAGE analysis has limited potential for quantitative analysis but can give extensive information on the characteristics of the polymers made and the distribution of different polymer lengths, in addition to the following of time courses of the accumulation of such polymers. The continuous assay technologies also offered the benefit that there was no requirement for separation of substrates and products, as with both the continuous fluorometric assay and the FRET assay, detection was based upon the polymerization.

5.1.2 Important chemical features for glycosyltransferase activity

The majority of techniques for analysis of GT activity involve use of fluorescently- or radio-labelled Lipid II as a substrate. Appendage of a dansyl fluorescent group to the third position ε-amino moiety of the peptide stem of Lipid II prevents the substrate from acting as a transpeptidase donor (Figure 4.13). Assay techniques using Lipid II labelled in this way would therefore be specific for glycosyltransferase activity. Labelling at the side chain of position 3 of the peptide stem has been found not to greatly affect the kinetic parameters of glycosyltransferases; Schwartz *et al.* (2002) found corresponding k_{cat} values for unlabelled and dansylated Lipid II. Zhang *et al.* (2007) found that acetylation of the L-Lysine R-group amines at the third position of the peptide stem in Lipid II did not affect the use of this substrate by *E. coli* PBP1A or PBP1B.

Fraipont *et al.* (2006) used a paper chromatography assay with radiolabelled (*meso*-[^{14}C]-diaminopimelic acid-labelled Lipid II) to dissect the important

chemical characteristics of the GT donor and acceptor for *E. coli* PBP1b activity, by analysis of the impact of Lipid II analogues on GT activity. Incorporation of these unlabelled analogues appeared as GT inhibition. Among the Lipid II analogues tested, UDP-Mur*N*Ac(pentapeptide)-Glc*N*Ac inhibited GT activity by PBP1b, in a manner dependent on presence of the Glc*N*Ac and Mur*N*Ac sugars, the reactive group at the C1 of Mur*N*Ac, and a full-length pentapeptide stem. These key features of the UDP compound in inhibiting the reaction were subsequently ascribed to donor recognition. The constituent amino acids of the peptide stem were determined, by these authors and others, to not be important for recognition, as dansyl-*m*DAP (Fraipont *et al.*, 2006) and dansyl-Lysine (Chen *et al.*, 2003) could be accepted for GT activity by *E. coli* PBPs *in vitro*, and Lysine could be accepted *in vivo* (Mengin-Lecreulx *et al.*, 1999).

The use of UDP-Mur*N*Ac(pentapeptide)-Glc*N*Ac as a GT substrate was then assayed using radiolabelled UDP-Mur*N*Ac(pentapeptide)-Glc*N*Ac and fluorescently (dansyl) labelled Lipid II, by which Fraipont *et al.* (2006) showed that the radio-labelled material was incorporated into the glycan polymer, and thus the UDP-compound was used as a substrate by *E. coli* PBP1b. No glycan chain formation was detected with supply of the UDP-compound as substrate alone, from which it was inferred that either donor or acceptor required a polyprenyl moiety.

The use of UDP-Mur*N*Ac(pentapeptide)-Glc*N*Ac as donor or acceptor was further analysed by use of muramidase, to digest the reaction products of GT activity when Lipid II (Dans) and [^{14}C] UDP-Mur*N*Ac(pentapeptide)-Glc*N*Ac were supplied as substrates. Digest products included radiolabelled Mur*N*Ac(pentapeptide)-Glc*N*Ac, but not radiolabelled UDP-Mur*N*Ac(pentapeptide)-Glc*N*Ac, indicating that the UDP compound acted as a donor in the GT reaction (with resultant loss of the UDP moiety). This consequently suggested that Lipid II (Dans) participated in the reaction as an acceptor, and that the proposed requirement of a polyprenyl chain appended to one substrate was a necessary feature of the acceptor substrate. The data of Liu and Wong (2006) may also be in support of the importance of the polyprenyl chain for acceptor recognition. These authors found that when the substrate was a Lipid II analogue with the polyprenyl lipid moiety exchanged

for nitrophenol phosphate, no GT activity of enzymes including *S. pneumoniae* PBP1b was detected. This observation could be explained by the loss of an important feature (the polyprenyl moiety) of the GT acceptor, thus rendering the analogue inactive.

Crystallographic evidence also supported the proposal of Lipid II as the GT acceptor. Lovering *et al.* (2007) modelled the position of the GT substrates into the active site of their crystal structure of a soluble, truncated construct of *Staphylococcus aureus* PBP2 (in complex with moenomycin). Their data suggested that Lipid II was likely to be the acceptor in glycosyltransferase activity, with the growing glycan chain as the donor. This was corroborated by modelling of substrate interactions in the structure of *Staphylococcus aureus* monofunctional glycosyltransferase (MGT) determined by Huang *et al.* (2012).

5.1.2.1 Amidation at the second position of the peptide stem

Amidation of the second position amino acid in the peptide stem (thus giving a glutamine at that position instead of glutamate) has been identified in the peptidoglycan of Gram positive organisms including *S. pneumoniae*, *S. aureus*, and *Enterococcus faecalis.* The MurT/GatD amidase complex responsible for this modification is further discussed in Section 1.6.2.1.

The impact of amidation on pneumococcal PBP activity was analysed by Zapun *et al.* (2013), who used mixed reactions of unlabelled and dansylated Lipid II to observe PBP1a and PBP2a activity. Reactions were followed by the SDS-PAGE method previously described for analysis of GT activity (Section 5.1.1.1). In the presence of such mixtures of substrates, a high molecular weight band remaining in the wells of the gel was observed, and formation of this band did not occur in the presence of penicillin. The use of this technique to assay transpeptidation is discussed in Section 4.1.1.3.

A vast decrease in the amount of high molecular weight material was seen when the substrate was unamidated Lipid II (Lipid II (Glu)) compared to amidated Lipid II (Lipid II (Gln)), in addition to an apparent reduction in the glycan chain lengths formed. These data suggested that Lipid II (Glu) was a poorer substrate for pneumococcal PBPs than Lipid II (Gln). The activity of PBP2a appeared to be more sensitive to amidation of the substrate than that

of PBP1a, as residual formation of the high molecular mass material was observed with PBP1a, but to a lesser extent with PBP2a.

Galley (2015) compared the usage of dansylated amidated (Gln, Dans) and dansylated unamidated (Glu, Dans) substrate by PBP1a and PBP2a by SDS-PAGE and in the continuous fluorometric assay for glycosyltransferase activity. Time course experiments over 24 h, analysed by SDS-PAGE, demonstrated faster consumption of Lipid II (Gln, Dans) substrate by both PBP1a and PBP2a. Kinetic parameters derived from the continuous assay illustrated that the differential substrate usage was manifested in significantly tighter binding and catalytic efficiency with Lipid II (Gln, Dans) in comparison to Lipid II (Glu, Dans), and for both PBP1a and PBP2a.

5.1.3 Lipid environment and PBP GT activity

Both the bifunctional PBPs and their Lipid substrate are associated *in vivo* with the cell membrane, and so both require detergents for solubility under aqueous assay conditions. Assay systems have been described whereby soluble PBP constructs and alternative prenyl moieties on the lipid substrate facilitate the study of GT activity under aqueous conditions (Zhang *et al.*, 2007). However, previous study of pneumococcal PBPs has made use of full-length enzymes and undecaprenyl-linked substrates (Galley, 2015; Helassa *et al.*, 2012; Zapun *et al.*, 2013). Consequently, it was of interest in the current work to further study how the components of the lipid environment of the glycosyltransferase reaction affected the activity of PBPs.

5.1.3.1 Membrane anchors and PBP activity

Helassa *et al.* (2012) characterised the reaction conditions required for observation of glycosyltransferase activity of PBP2a in the SDS-PAGE gel assay system. The authors found that no activity was observed using tagged variants of PBP2a. Helassa *et al.* (2012) determined that the specific activity of soluble and full-length PBP2a (i.e. without and with the membrane anchor respectively) constructs in the continuous fluorometric assay were similar, but demonstrated a decrease in processivity of the periplasmic construct, thus suggesting a role for the membrane anchor in this factor of enzyme activity. Galley (2015) also found that truncated, soluble constructs of PBP1a and

PBP2a demonstrated impaired processivity in comparison to full length constructs. Truncation of *E. coli* PBP1b to remove the transmembrane domain has also been found to impair both activity and inhibition by moenomycin (Sung *et al.*, 2009).

Berg *et al.* (2014) showed that exchange of the membrane anchor of PBP2x resulted in loss of *in vivo* function, and exchange of the PBP2b membrane anchor resulted in a phenotype resembling PBP2b depletion.

5.1.3.2 Lipid moiety of substrates and PBP activity

Chen *et al.* (2003), working with *E. coli* PBP1b, showed that kinetic parameters of GT activity (k_{cat} and k_{cat}/K_m) were unaffected by the modification of the lipid substrate to include a betulaheptaprenyl (C35) lipid moiety in place of undecaprenyl. By contrast, Zhang *et al.* (2007) determined in their assay of *E. coli* PBP1b that betulaheptaprenyl Lipid II was a better substrate for glycosyltransferase activity as compared to undecaprenyl Lipid II.

Liu *et al.* (2010) synthesized a Lipid substrate whereby the dansyl fluorophore was positioned on the lipid moiety, in comparison to other syntheses where the label was positioned on the peptide stem (Schwartz *et al.*, 2002). Although the fluorophore remained attached to the glycan polymer at the reducing end of the glycan strand at each catalytic cycle, only one unit was retained per polymer strand (compared to one fluorophore per disaccharide when peptide-labelled substrate was used). This appears to have prevented detection of polymer upon subsequent HPLC analysis. Though Liu *et al.* (2010) suggested that positioning of the fluorophore at the lipid moeity may not have impacted upon substrate recognition by glycosyltransferases, there was no direct evidence in support of this. As discussed in Section 5.1.2, other studies have suggested the importance of the lipid moiety in recognition of acceptors.

5.1.3.3 DMSO and lipid environment

Glycosyltransferase assays using dansylated substrates have reported inclusion of 5 - 30 % (v/v) dimethylsulfoxide (DMSO) in the reaction mixture for optimal enzyme activity (Helassa *et al.*, 2012; Offant *et al.*, 2010; Schwartz *et al.*, 2002). The contribution of DMSO may be explained by the impact of DMSO on micelle dynamics. Bruckdorfer and Sherry (1984) found that the impact of DMSO on micelle dynamics was an increase in the exchange of radiolabelled cholesterol from liposomes with unlabelled cholesterol from

erythrocytes. In addition, 1.5 M DMSO was found to increase the CMC of cholesterol.

Schwartz *et al.* (2002) analysed the impact of DMSO on glycosyltransferase activity using HPLC assays. The impact of DMSO on *in vitro* glycosyltransferase activity was to increase the steady-state rate, and further kinetic characterisation demonstrated that DMSO impacted catalysis, as k_{cat} was increased in the presence of DMSO. The authors suggested that this effect was through enhanced solubility of Lipid II, in addition to the effect of DMSO on micelle dynamics.

5.1.3.4 Phospholipids and enzyme activity

The phospholipid components of the cytoplasmic membrane interact with transmembrane domains of proteins to anchor them and satisfy hydrophobic interactions. A growing body of evidence suggests that beyond serving as an attachment point for membrane proteins, the membrane itself influences, and is influenced by, the activity of the membrane proteins that coordinate cell division. Multiple such proteins have been found to interact with the membrane phospholipid, cardiolipin. Cardiolipin has been observed to accumulate at the poles of rod-shaped cells (Wood, 2018). The interaction of cardiolipin with one partner protein was shown to occur through ionic interactions with the lipid head groups, and van der Waals interactions between the lipid tails and intramembrane surface of the protein (McAuley *et al.*, 1999).

MurG overexpression was associated with increase of cellular cardiolipin, and cardiolipin was found to be enriched in the lipids copurified with the overexpressed protein (van den Brink-van der Laan *et al.*, 2003). In addition, the activity of MurG on Lipid I was greater in vesicles containing cardiolipin than in those containing phosphatidylglycerol.

Phospholipids had been suggested to be involved in the Lipid II flippase mechanism, as inhibition of phospholipid synthesis inhibited O-antigen synthesis, which shares in common the lipid carrier undecaprenyl phosphate (Ehlert & Höltje, 1996). This was supported by the study of the flippase enzyme MurJ by Bolla *et al.* (2018). Bolla *et al.* (2018) used native protein mass spectrometry to analyse the interactions of MurJ and FtsW with Lipid II. These

experiments revealed that cardiolipin decreased the binding of Lipid II by MurJ, such that the authors proposed that interaction with this phospholipid may play a role in the flippase mechanism. In addition, similarly to with MurG, the authors found that cardiolipin was enriched under overexpression of MurJ, and that a range of cardiolipins copurified with MurJ.

Of particular importance is the established link between phospholipid synthesis and penicillin susceptibility in *E. coli.* Inhibition of phospholipid synthesis was associated with inhibition of PG synthesis, which the authors suggested was the result of involvement of phospholipids in the assembly of the PG synthesis machinery (Rodionov & Ishiguro, 1996). The impact of cardiolipin and phosphatidylglycerol on pneumococcal MurM activity has also been demonstrated. Cardiolipin was found to stimulate the *in vitro* activity of MurM, whilst strain-dependent impact of phosphatidylglycerol on MurM activity was observed (A.J. Lloyd, unpublished).

There remains to be explored the impact of membrane environment on PBP1a GT activity (and therefore indirectly TP activity), to rationalise the observed importance of the detergent choice and membrane anchor on glycosyltransfer.

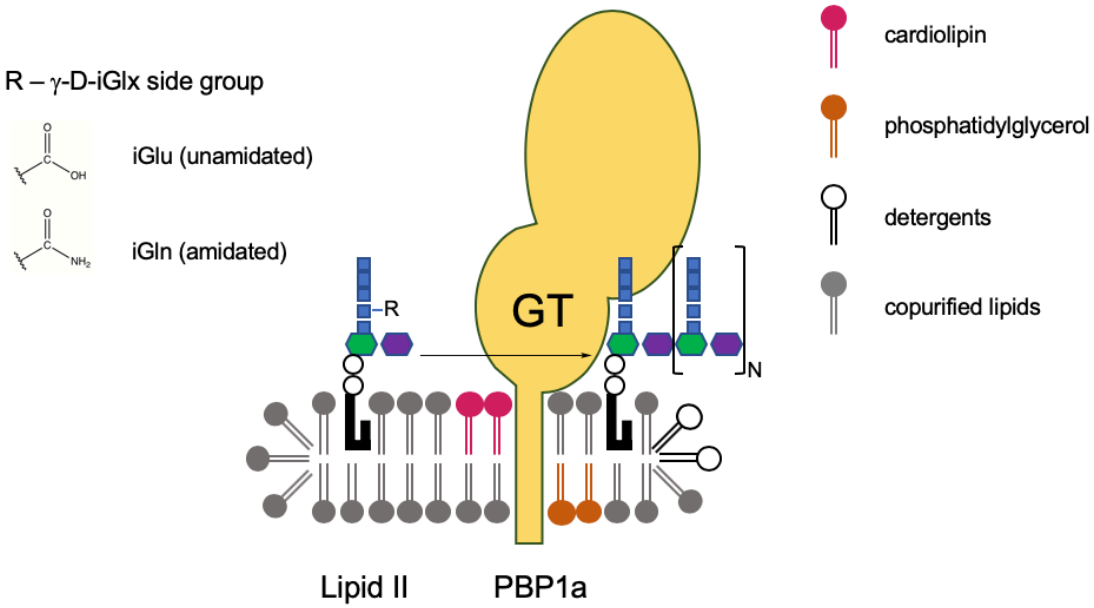

How do factors such as detergents, membrane lipids affect PBP1a GT activity?
Does GT activity differ between PBP1as from different strains?
Does the formation of glycan polymer over time differ depending upon whether the lipid substrate is amidated?

Figure 5.1 Chapter 5 experimental questions summary A visual summary of the questions to be addressed in this thesis. **GT**, glycosyltransferase

PBP1a variants may differ in their response to the micellar environment, as has been observed for MurM. Additionally, the characterisation of GT activity is a necessary first step to study of *in vitro* TP activity in relation to β-lactam resistance. GT activity of a bifunctional enzyme must be analysed to confirm whether any variation in activity is manifested in changes to transpeptidation. Finally, detailed analysis of glycan polymer assembly over early time points was of interest to further probe the impact of amidation on GT activity.

5.2 Experimental Aims

- To establish glycosyltransferase activity of PBP1a expressed from constructs using genes from pneumococcal D39, Pn16 and 159 strains
- To find the optimum concentration of a detergent known to support TP activity (E_6C_{12}) for assay of glycosyltransferase activity of PBP1a
- To test a range of ethylene glycol detergents for their ability to support PBP1a glycosyltransferase activity
- To characterise the impact of pneumococcal phospholipids on formation of glycan polymers by PBP1a from D39, Pn16 and 159 pneumococcal strains
- To compare the formation of glycan polymers by PBP1a and PBP2a over 3 h with Lipid II (Gln, Dans) and Lipid II (Glu, Dans) substrates

5.3 Results

The activity of bifunctional penicillin-binding proteins has been considered to occur such that PBP1a GT activity supplies the donor substrate for transpeptidation. Reaction conditions that support GT activity can guide establishment of the conditions required for TP activity. Analysis of GT activity was therefore conducted with transfer to TP analysis in mind. For this reason, some conditions such as the starting detergent of E_6C_{12} and the concentration used (12 x CMC) were informed by the conditions conducive to a previous observation of D-Ala release in the TP assay (Galley, 2015). Conditions of the GT assay were otherwise informed by optima determined by Galley (2015), including 25 % (v/v) DMSO and 150 mM NaCl.

5.3.1 The effect of detergent on GT activity

Rapid GT activity of *S. pneumoniae* D39 PBP1a was previously observed with Triton X-100 as the assay detergent (Galley, 2015). However, E_6C_{12} assay detergent was demonstrated to support observation of transpeptidase activity, whilst the Triton X-100 assay detergent did not support transpeptidase activity (Galley, 2015). We therefore looked to further characterise the optimum

concentrations and detergent choice of PBP1a GT activity, to identify a detergent that may support *in vitro* TP activity.

5.3.1.1 Detergent concentration and PBP1a activity

The concentration of E_6C_{12} in the GT assay mixture was contributed by the enzyme dilution buffer, the lipid resuspension buffer and the assay buffer. The optimum concentration of E_6C_{12} detergent for GT activity in reactions containing 2 μM *S. pneumoniae* D39 PBP1a and 20 μM Lipid II (Gln, Dans) was determined by analysis of glycan polymer accumulation over 30 mins by SDS-PAGE (Figure 5.2). Concentrations from 12 x CMC to 1.7 x CMC were tested. The minimum concentration tested was based upon contribution of E_6C_{12} from the Lipid resuspension buffer and enzyme dilution buffers only.

Concentrations of E_6C_{12} approaching the CMC were associated with formation of longer glycan polymers over 30 mins, with higher concentrations associated with apparent inhibition of polymer accumulation. This result was in agreement with observations of the impact of detergent concentration on the rate of D-Ala release by PBP1a (Section 4.3.2.2).

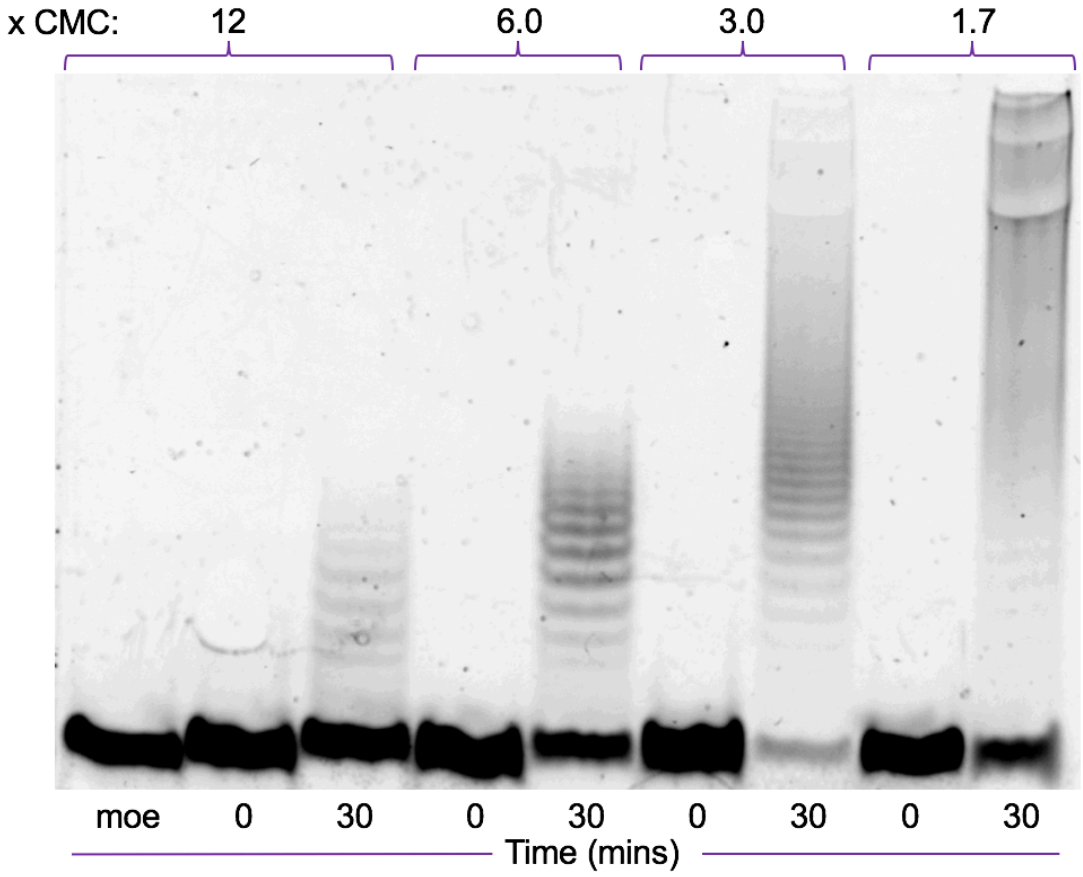

Figure 5.2 Effect of E_6C_{12} detergent concentration on glycan polymer formation over 30 mins with 2 μM PBP1a and 20 μM Lipid II (Gln, Dans). Reactions comprised 50 mM HEPES, 10 mM $MgCl_2$, 25 % (v/v) DMSO, 150 mM NaCl, 2 μM PBP1a and 20 μM Lipid II (Gln, Dans). The E_6C_{12} concentration was varied by addition of assay buffer at the appropriate concentration, with the exception of the reaction with 1.7 x CMC, in which E_6C_{12} was solely contributed by the enzyme dilution and Lipid resuspension buffers. Samples were taken at the stated timepoints and the reactions quenched with 0.3 mM moenomycin and 50 mM EDTA. A control was included (**moe**) in which moenomycin was added to the reaction prior to initiation, and the reaction incubated for 30 mins. Samples were analysed by electrophoresis on a 9 % Tris-Tricine gel, which was subsequently visualised using an ImageQuant LAS 4000 imager with transmitted light at 312 nm and a 605 nm filter. **CMC**, critical micellar concentration; **mins**, minutes; **moe**, moenomycin

To confirm the relation between E_6C_{12} concentration and glycan polymer formation, the experiment was repeated using concentrations of 0.5 μM PBP1a and 5 μM Lipid II (Gln, Dans). As depicted in Figure 5.3, the equivalent relationship between concentration of E_6C_{12} detergent and formation of glycan polymer was observed under these conditions.

For subsequent optimisation experiments, a detergent concentration of 3 x

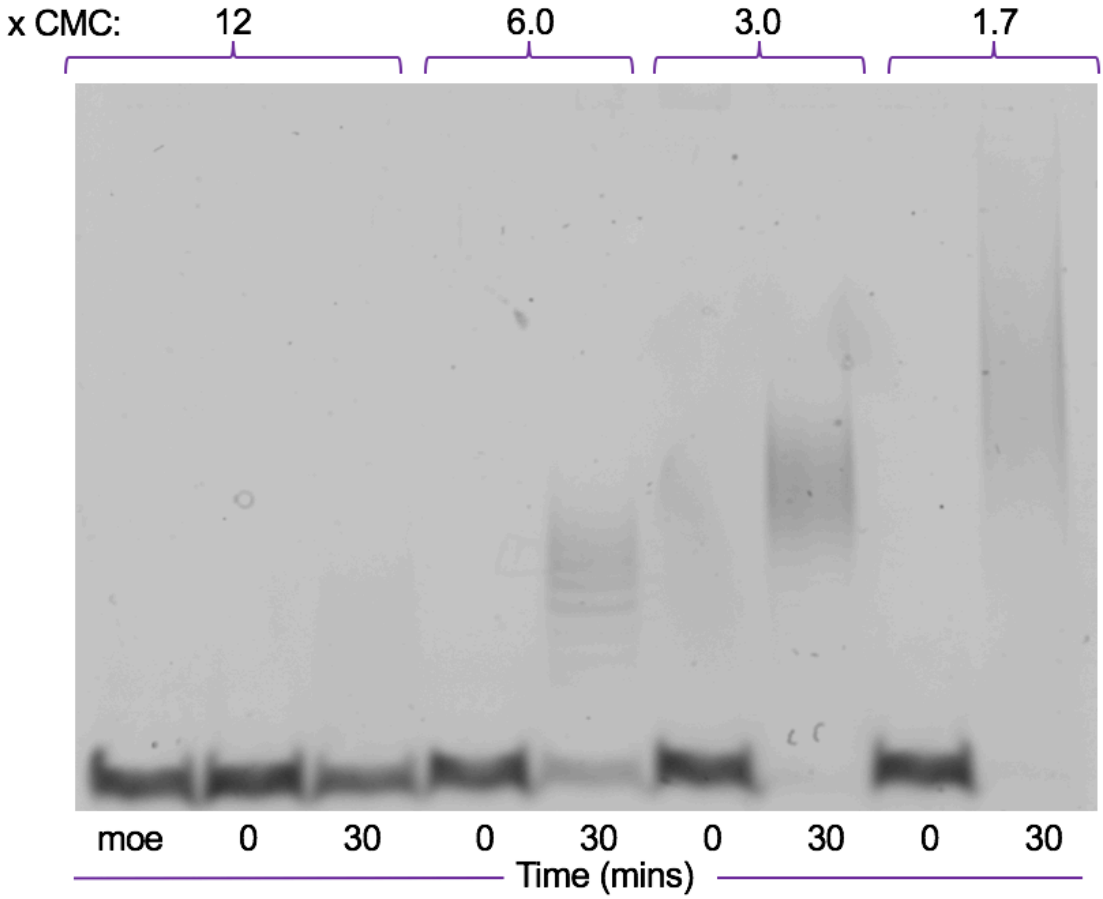

Figure 5.3 Effect of E_6C_{12} detergent concentration on glycan polymer formation over 30 mins with 0.5 μM PBP1a and 5 μM Lipid II (Gln, Dans). Reactions comprised 50 mM HEPES, 10 mM $MgCl_2$, 25 % (v/v) DMSO, 150 mM NaCl, 0.5 μM PBP1a and 5 μM Lipid II (Gln, Dans). The E_6C_{12} concentration was varied by addition of assay buffer at the appropriate concentration, with the exception of the reaction with 1.7 x CMC, in which E_6C_{12} was solely contributed by the enzyme dilution and lipid resuspension buffers. Samples were taken at the stated timepoints and the reactions quenched with 0.3 mM moenomycin and 50 mM EDTA. A control was included (**moe**) in which moenomycin was added to the reaction prior to initiation, and the reaction incubated for 30 mins. Samples were analysed by electrophoresis on a 9 % Tris-Tricine gel which was subsequently visualised using an ImageQuant LAS 4000 imager with transmitted light at 312 nm and a 605 nm filter. **CMC**, critical micellar concentration; **mins**, minutes; **moe**, moenomycin

CMC was chosen, as this would allow both an increase and a decrease in GT

activity to be detected. By comparison, the rapid activity in the presence of 1.7 x CMC detergent may be expected to reduce the sensitivity towards detection of any increase in activity.

5.3.1.2 The effect of assay detergent on GT activity

A variety of ethylene glycol detergents was next investigated for their impact on GT activity on PBP1a^{D39}. These covered a variety in both in the number of ethylene glycol moieties and the alkyl chain length. Lipid II (Gln, Dans) was delivered in CHAPS detergent for the initial screening. This allowed the Lipid to be delivered from the same master stock to all reactions. Consistency was also then achieved in that all reactions would occur within mixed micelles, as the use of E_6C_{12} as the delivery detergent may otherwise have favoured activity in E_6C_{12} assay buffer. GT activity in different detergents was analysed by SDS-PAGE as previously described.

Some detergents, such as E_5C_8, did not support GT activity, as no glycan polymer formation was observed over 30 mins (Figure 5.4, lanes 7-8). Stimulation of PBP1a activity was observed in the presence of E_8C_{10} (lanes 13-14) and E_4C_{12} (lanes 5-6) assay detergent, though the distribution of glycan chain length appeared shifted slightly towards longer polymers in the presence of E_8C_{10}. High concentration of CHAPS detergent was interpreted to be incompatible with the Tris-tricine gel system used for this experiment, as the Lipid II (Gln, Dans) substrate did not form a uniform band at the running front (lanes 1-2).

The apparent optimum detergent from these experiments, E_8C_{10}, was taken forward to an additional experiment in which either CHAPS or E_6C_{12} was the lipid delivery detergent, to confirm the apparent faster activity of PBP1a in E_8C_{10} as the assay detergent. Activity was monitored as before by SDS-PAGE gel (Figure 5.5).

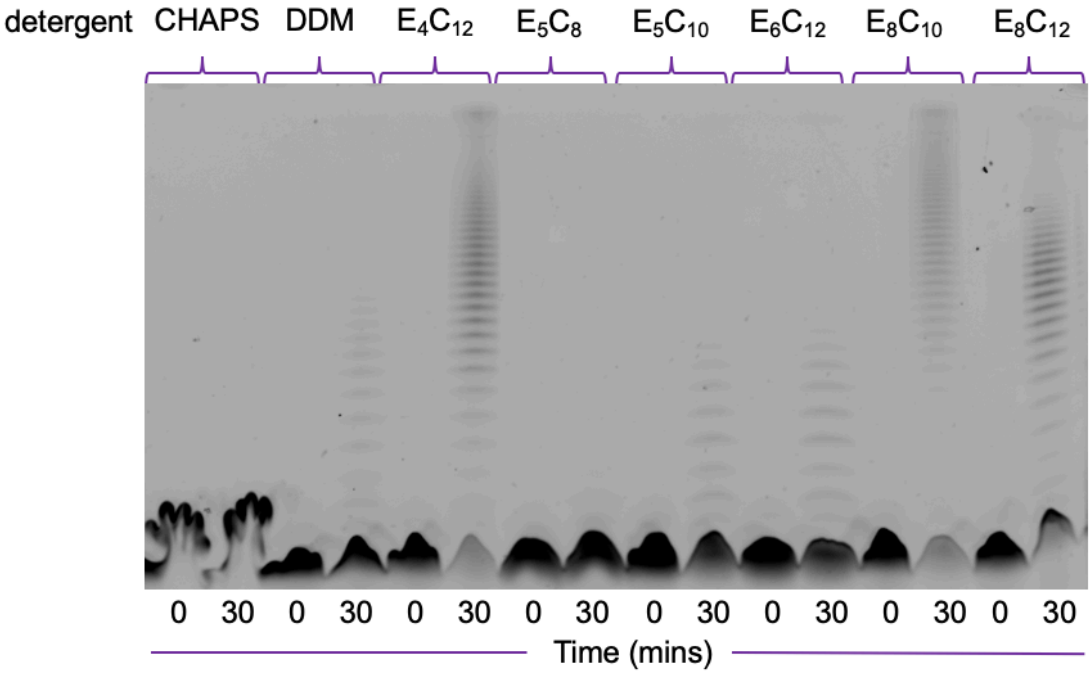

Figure 5.4 Effect of assay detergent on glycan polymer formation over 30 mins with 0.5 μM PBP1a and 5 μM Lipid II (Gln, Dans). Reactions comprised 50 mM HEPES, 10 mM $MgCl_2$, 25 % (v/v) DMSO, 150 mM NaCl, 0.5 μM PBP1a and 5 μM Lipid II (Gln, Dans), 3 x CMC of the stated detergent, and 0.33 x CMC CHAPS detergent (contributed by Lipid II (Gln, Dans) delivery buffer). Samples were taken at the stated timepoints and the reactions quenched with 0.3 mM moenomycin and 50 mM EDTA. Samples were analysed by electrophoresis on a precast 16.5 % Tris-Tricine gel which was subsequently visualised using an ImageQuant LAS 4000 imager with transmitted light at 312 nm and a 605 nm filter. **CMC**, critical micellar concentration; **mins**, minutes

When Lipid was delivered in CHAPS detergent (Figure 5.5, lanes 2-5), PBP1a formed larger glycan polymers within 30 mins with E_8C_{10} assay detergent compared to E_6C_{12}, in agreement with the observation from Figure 5.4. The same relationship was observed when E_6C_{12} was used as the lipid delivery detergent (Fig. 5.5, lanes 6-9). This experiment further supported the observation of more rapid formation of large polymers in E_8C_{10} assay detergent, independent of the choice of Lipid II delivery detergent. The impact

of the Lipid II delivery detergent itself on GT activity cannot be inferred from Figure 5.5, as there appears to be more Lipid II (Gln, Dans) present in those reactions to which Lipid II (Gln, Dans) was delivered in E_6C_{12} detergent.

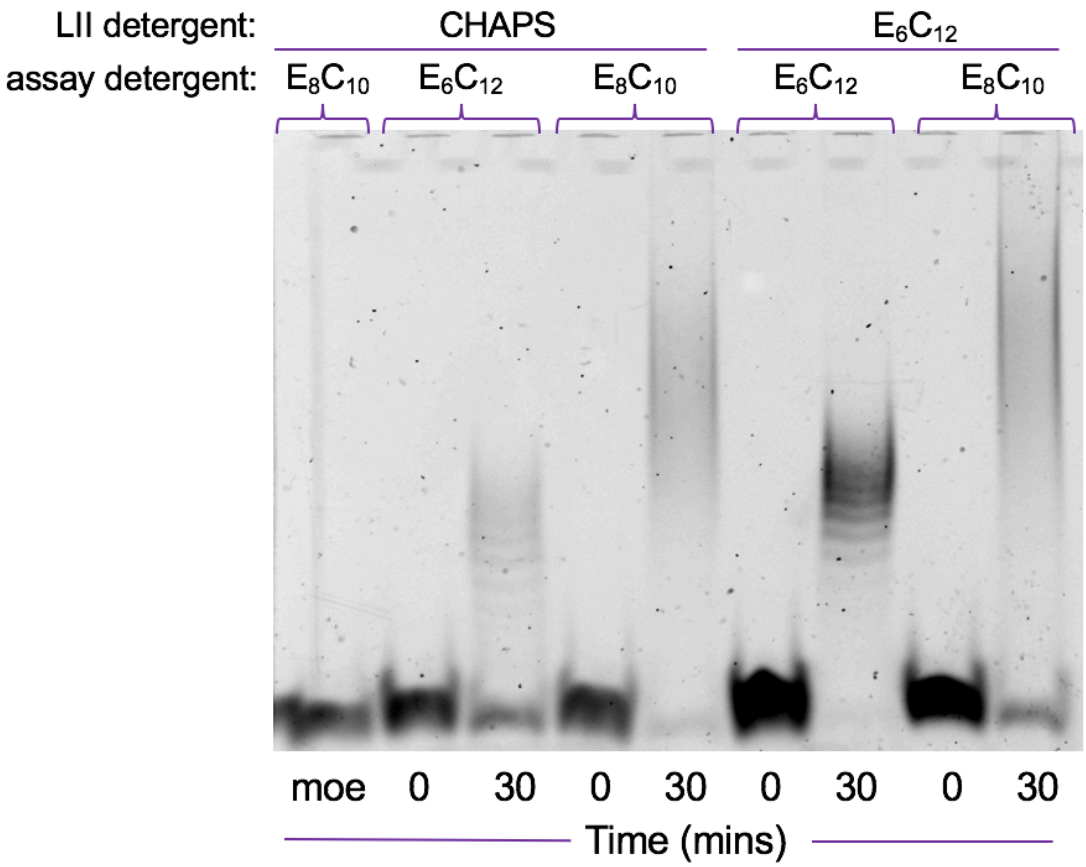

Figure 5.5 Comparison of E_6C_{12} and E_8C_{10} as the assay detergent for analysis of glycan polymer assembly. Reactions comprised 50 mM HEPES, 10 mM $MgCl_2$, 25 % (v/v) DMSO, 150 mM NaCl, 0.5 μM PBP1a and 5 μM Lipid II (Gln, Dans) resuspended in CHAPS or E_6C_{12}, and either E_6C_{12} or E_8C_{10} as the major assay detergent, at 3 x CMC. Samples were taken at the stated timepoints and the reactions were quenched with 0.3 mM moenomycin and 50 mM EDTA. A control was included (**moe**) in which moenomycin was added to the reaction prior to initiation, and the reaction incubated for 30 mins. Samples were analysed by electrophoresis on a 9 % Tris-Tricine gel, which was subsequently visualised using an ImageQuant LAS 4000 imager with transmitted light at 312 nm and a 605 nm filter. **CMC**, critical micellar concentration; **mins**, minutes; **moe**, moenomycin

5.3.2 GT activity of pneumococcal strain D39, Pn16 and 159 PBP1a variants

A key aim of this thesis was to compare activity across PBP1a variants from different pneumococcal strains. The activity of different PBP1a constructs was therefore compared under the basic GT activity conditions, to establish whether similar activity was seen with each. There is 100% sequence identity in the GT domain between the PBP1a amino acid sequences of the enzymes of pneumococcal strains D39, Pn16 and 159 (Appendix 5.2) and so equivalent GT activity may be expected between different variants expressed and purified in the same way. We therefore sought to compare the GT activity of these proteins, to enable exclusion of variation in GT activity from subsequent comparison of TP activity.

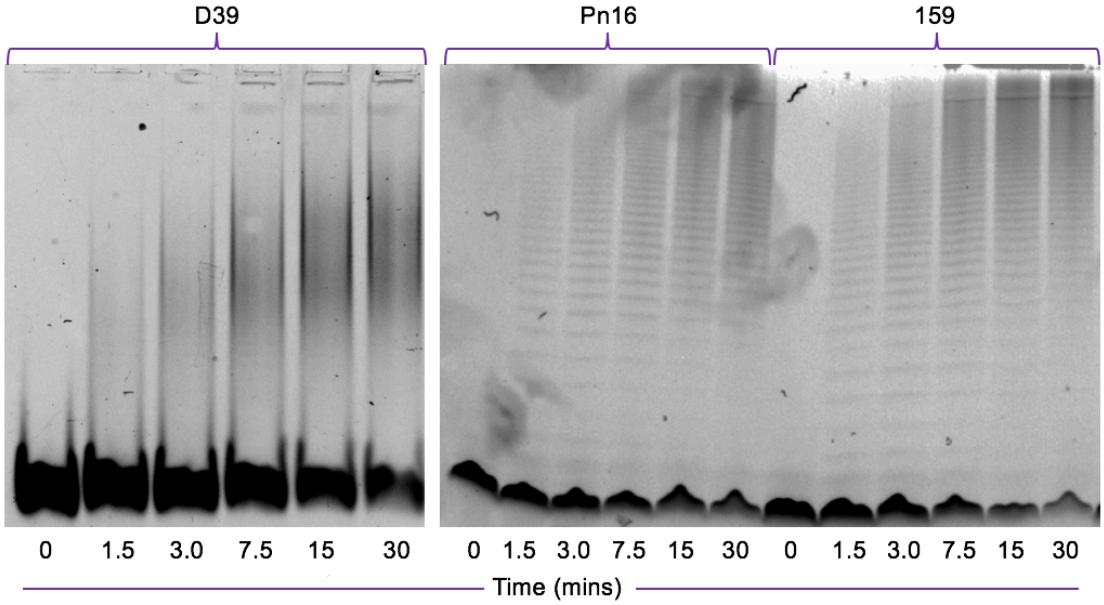

Figure 5.6 Comparison of glycan polymer assembly over 30 mins by PBP1a variants from *S. pneumoniae* strains D39, Pn16 and 159. Reactions comprised 50 mM HEPES, 10 mM $MgCl_2$, 25 % (v/v) DMSO, 150 mM NaCl, 0.0136 % (w/v) E_8C_{10}, 0.5 μM PBP1a and 5 μM Lipid II (Gln, Dans). Samples were taken at the stated timepoints and quenched with 0.3 mM moenomycin and 50 mM EDTA. Samples were analysed by electrophoresis on a 9 % Tris-Tricine gel (D39) or precast 16.5 % Tris-Tricine gel, which was subsequently visualised using an ImageQuant LAS 4000 imager with transmitted light at 312 nm and a 605 nm filter. **mins**, minutes

PBP1a variants were expressed and purified as described in Section 4.3.1. Formation of glycan polymers over 30 mins was followed by SDS-PAGE time course experiments (Figure 5.6). Similar activity was observed under these

conditions for the D39, Pn16 and 159 strain PBP1a variants. In all cases, polymer formation could be detected within 1.5 mins. High molecular weight material was observed at the top of each gel within 7.5 minutes, though the 159 variant appears to have assembled such polymers slightly faster in this respect (by comparison of the 7.5 and 15 minute time points for the three variants). The resolution of low molecular weight polymers was comparably poorer on the gel depicting $PBP1a^{D39}$ GT activity. This is due to the use of precast 16.5 % Tris-Tricine gels for analysis of $PBP1a^{Pn16}$ and $PBP1a^{159}$ GT polymers.

The rate of GT activity was then compared for each enzyme using the continuous fluorescence assay for GT activity, to more precisely quantitate the catalytic activity of D39, Pn16 and 159 PBP1a with respect to GT activity. Initial rates were measured under the same reaction conditions as were used for the Tris-tricine gels (50 mM HEPES, 10 mM $MgCl_2$, 25 % (v/v) DMSO, 150 mM NaCl, 0.5 μM enzyme, and 5 μM Lipid II (Gln, Dans)). In place of E_8C_{10}

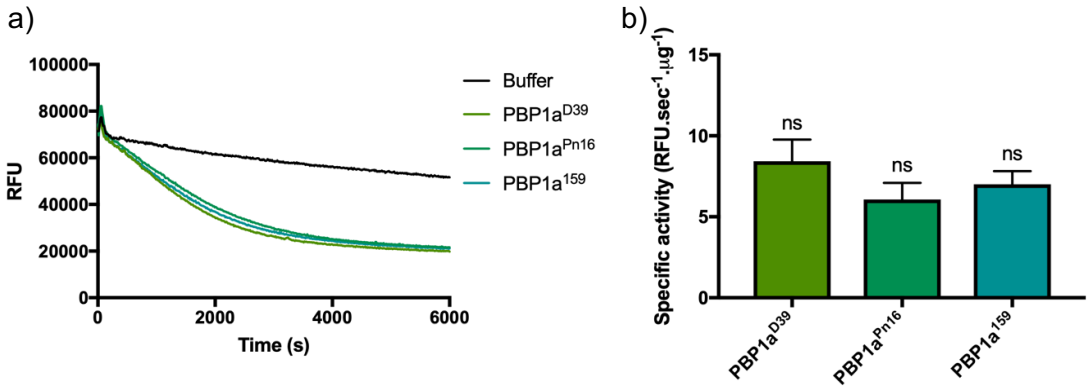

Figure 5.7 Specific activity of PBP1a variants from *S. pneumoniae* strains D39, Pn16 and 159 in the continuous fluorometric assay. Reactions comprised 50 mM HEPES, 10 mM $MgCl_2$, 25 % (v/v) DMSO, 150 mM NaCl, 0.0116 % (w/v) E_6C_{12}, 0.5 μM PBP1a, 5 μM Lipid II (Gln, Dans), and 0.1 $mg.mL^{-1}$ lysozyme. Reactions were initiated with enzyme and monitored for 100 mins. Blank measurements were taken with reactions in which enzyme buffer was added in place of enzyme. Results were graphed in GraphPad Prism to determine the initial rate (a). The mean specific activity (n = 3) for each PBP1a variant was compared by one-way ANOVA, which indicated no significant difference **(ns)** between any of these mean values. **$RFU.sec^{-1}.\mu g^{-1}$,** relative fluorescence units per second per μg of PBP1a.

detergent, 3 x CMC E_6C_{12} detergent was used, to facilitate subsequent testing of reaction conditions in the continuous fluorometric assay.

The mean specific activities (Figure 5.7) of the three enzymes were determined by one-way ANOVA to not be significantly different. $PBP1a^{D39}$, $PBP1a^{Pn16}$ and $PBP1a^{159}$ were therefore concluded to exhibit comparable GT activity under the conditions tested.

5.3.3 The effect of phospholipids on GT activity

As previously discussed (Section 5.1.3.4), reconstitution of the *in vivo* lipid environment of cell wall synthesis enzymes has been demonstrated to influence their activity. In particular, cardiolipin has been observed to be involved in supporting the activity of enzymes including MurM, which is linked to PBP1a by supply of branched substrates and thus involved in the β-lactam resistance mechanism (Dr. A.J. Lloyd, University of Warwick, unpublished).

Pneumococcal membranes contain two phospholipids; cardiolipin and phosphatidylglycerol (Brundish *et al.*, 1967), in a ratio between 1:1 and 3:1 (Trombe *et al.*, 1979). We sought to test the effect upon PBP1a activity of adding pneumococcal membrane phospholipids to the GT assay system. We tested the effect of cardiolipin on the extent of Lipid II polymerisation over 30 mins. Cardiolipin was dissolved in a solution of the assay buffer, E_6C_{12}, with the overall concentration of the detergent in the assay was fixed at 3 x CMC as previous.

5.3.3.1 The effect of cardiolipin on GT activity

The activity of PBP1a constructs from pneumococcal strains D39, Pn16 and 159 was tested in the presence of 10, 1.0 and 0.1 μM cardiolipin, and these were compared to controls with E_6C_{12} assay detergent only (Figure 5.8). We observed that there was a reproducible dose-dependent stimulation of GT activity by cardiolipin, as larger glycan polymers were assembled over 30 mins in the presence of higher concentrations of cardiolipin in the assay. The effect on GT activity was consistent across the three PBP1a variants.

We surmised that mimicry of the *in vivo* lipid environment of PBP1a could underlie the detergent preference observed in Section 5.3.1.2. We thus titrated cardiolipin against PBP1a^{D39} activity in reactions where the assay detergent was either E_8C_{10} or E_5C_8. We hypothesised that cardiolipin may offer no stimulatory effect in reactions where the beneficial physical properties of this phospholipid were provided by the assay detergent (e.g. with a detergent with which greater activity was observed - E_8C_{10}), whilst cardiolipin may be able to rescue PBP1a GT activity in reactions with a comparably 'poor' assay detergent (E_5C_8), as the detergent alone in this case was not able to

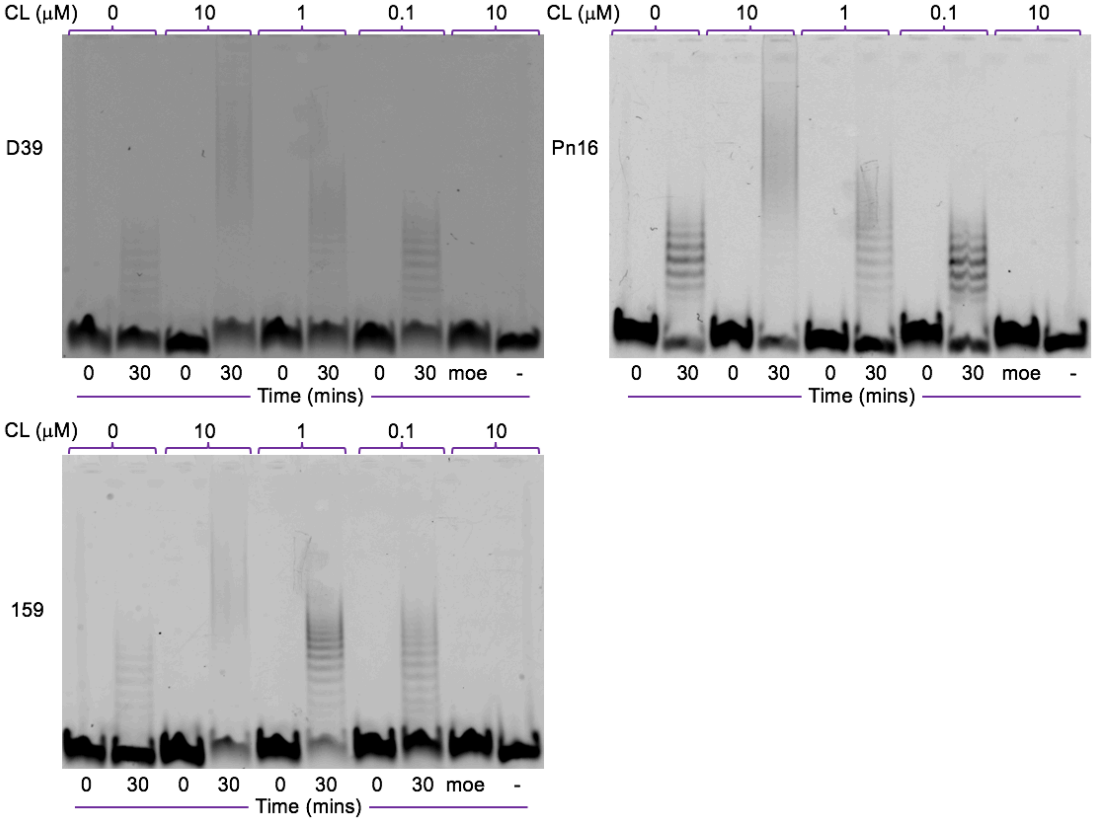

Figure 5.8 Effect of cardiolipin on glycan polymer assembly over 30 mins by PBP1a variants from *S. pneumoniae* strains D39, Pn16 and 159. Reactions comprised 50 mM HEPES, 10 mM $MgCl_2$, 25 % (v/v) DMSO, 150 mM NaCl, 0.0116 % (w/v) E_6C_{12}, 0.5 μM PBP1a, 5 μM Lipid II (Gln, Dans), and varying concentrations of cardiolipin. Samples were taken at the stated timepoints and quenched with 0.3 mM moenomycin and 50 mM EDTA. A control was included (moe) in which moenomycin was added to the reaction prior to initiation, and the reaction incubated for 30 mins, in addition to a no enzyme control (-) to which the equivalent volume of enzyme dilution buffer was added. Samples were analysed by electrophoresis on a 9 % Tris-Tricine gel, which was subsequently visualised using an ImageQuant LAS 4000 imager with transmitted light at 312 nm and a 605 nm filter. **CL**, cardiolipin; **mins**, minutes; **moe**, moenomycin

adequately recreate the important physical properties of the *in vivo* lipid environment.

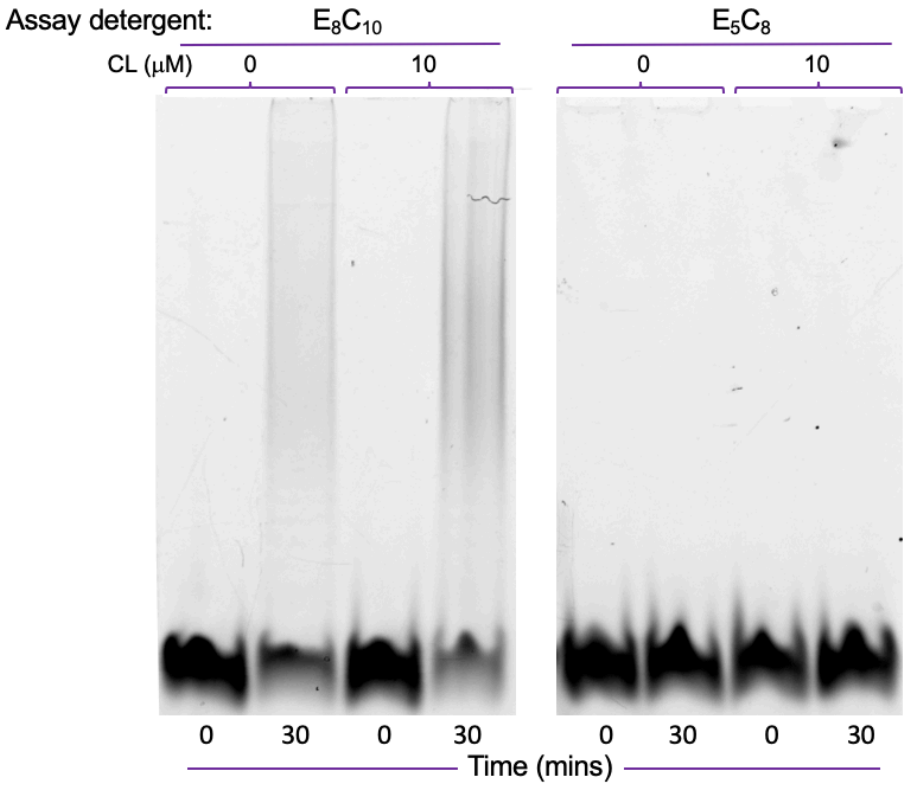

Figure 5.9 Effect of cardiolipin on glycan polymer assembly over 30 mins by *S. pneumoniae* PBP1a^{D39} in varying assay detergents. Reactions comprised 50 mM HEPES, 10 mM $MgCl_2$, 25 % (v/v) DMSO, 150 mM NaCl, 3 x CMC E_8C_{10} or E_5C_8, 0.5 μM PBP1a, 5 μM Lipid II (Gln, Dans), and ± 10 μM cardiolipin. Samples were taken at the stated timepoints and quenched with 0.3 mM moenomycin and 50 mM EDTA. Samples were analysed by electrophoresis on a 9 % Tris-Tricine gel, which was subsequently visualised using an ImageQuant LAS 4000 imager with transmitted light at 312 nm and a 605 nm filter. **CL**, cardiolipin; **mins**, minutes

.

We observed (Figure 5.9) that there was no striking impact of cardiolipin on GT activity when the assay detergent was E_8C_{10} (as determined by the similar extent of glycan polymer formation), and that the presence of cardiolipin did not rescue GT activity with E_5C_8 under the conditions tested (Figure 5.9).

The effect of cardiolipin on the rate of GT activity was then compared for PBP1a^{Pn16} using the continuous fluorescence assay for GT activity, to more precisely analyse the impact of the phospholipid on PBP1a^{D39}, PBP1a^{Pn16} and PBP1a^{159} GT activity. The dose-response experiment presented in Figure 5.8

was repeated in the continuous fluorometric assay to find the maximal response from cardiolipin on the initial rate of fluorescence change.

Rate of GT activity appears to increase with cardiolipin concentration until 50 μM, where there is a drop in the rate at 100 μM cardiolipin. This apparent 'hook effect' may result from a dilution of the hydrophobic environment of the assay,

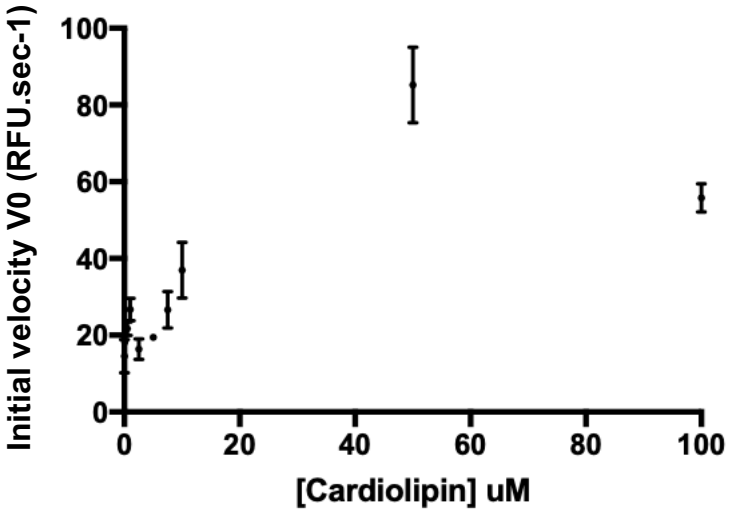

Figure 5.10 Dose-response analysis of the effect of cardiolipin on GT activity of PBP1a^{Pn16} in the continuous fluorometric assay. Reactions comprised 50 mM HEPES, 10 mM $MgCl_2$, 25 % (v/v) DMSO, 150 mM NaCl, 3 X CMC E_6C_{12} (0.0116 % (w/v)), 0.5 μM PBP1a, 0.1 mg.mL^{-1} lysozyme and a range of concentrations of Lipid II (iGln, Dans). Reactions were initiated with enzyme and monitored for 100 mins. Results were graphed in GraphPad Prism to determine the initial rate.
RFU.sec^{-1} relative fluorescence units per second.

thus decreasing the likelihood of productive contact between enzyme and substrate. The 50 μM cardiolipin condition was taken forward for further studies of the impact on kinetics of GT activity.

5.3.3.1.2 Kinetics of cardiolipin impact on GT activity

The kinetics of cardiolipin usage were established by conducting GT assays where substrate concentration was titrated in the presence and absence of 50 μM cardiolipin. The data were fit to a kinetic model (equation 1) incorporating cooperativity in activity (Copeland, 2004);

Equation 1:
$$V_0 = \frac{V_{max}[S]^h}{S_{0.5} + [S]^h}$$

Whilst insufficient Lipid II concentrations were reached to capture the full curve of the detergent-only condition, the profiles shown in Figure 5.11 for both PBP1a^{Pn16} and PBP1a^{159} suggest that affinity of the enzymes for Lipid II (iGln, Dans) is enhanced in the presence of cardiolipin. The kinetic parameters extracted from these curve fits are presented in Table 5.2.

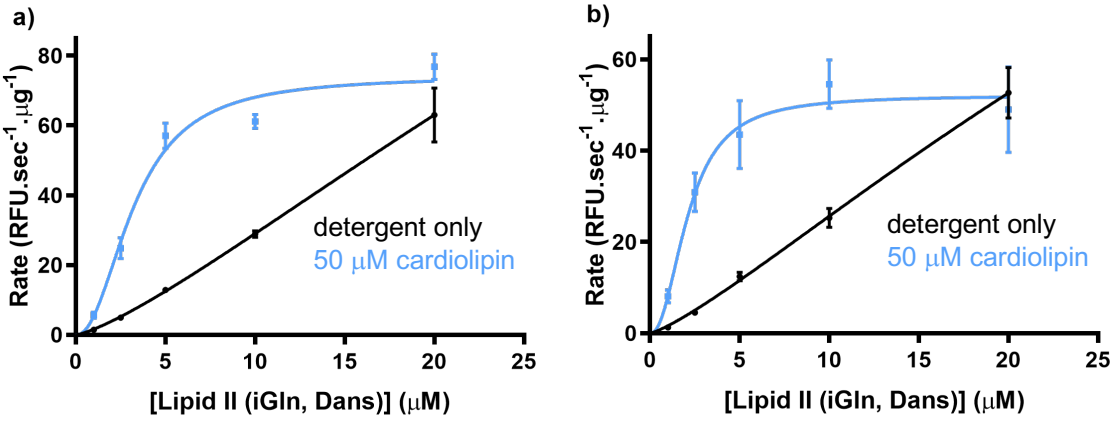

Figure 5.11: Kinetics of Lipid II (iGln, Dans) usage in the presence and absence of 50 μM cardiolipin. The kinetics of Lipid II (iGln, Dans) usage in glycosyltransferase reactions by **a)** PBP1a^{Pn16} and **b)** PBP1a^{159} were determined using the continuous fluorometric assay. Reactions comprised 50 mM HEPES, 10 mM $MgCl_2$, 25 % (v/v) DMSO, 150 mM NaCl, 0.0116 % (w/v) E_6C_{12}, 0.5 μM PBP1a, varied concentrations of Lipid II (Gln, Dans), and 0.1 mg.mL^{-1} lysozyme. Reactions were initiated with enzyme and monitored for 100 mins. Results were graphed in GraphPad Prism to determine the initial rate. Error bars: standard deviation.
RFU.sec^{-1}.μg^{-1}, relative fluorescence units per second per μg PBP1a.

No kinetic parameters were determined for the detergent-only reactions due to the full curves not being captured. However, the curve profiles suggest an $S_{0.5}$ value greater than those calculated for the cardiolipin reactions in each case.

The estimates of $S_{0.5}$ appear high in comparison to the profile of the curves. This may indicate poor fit to the proposed model, or be the consequence of few data points in the linear region of the curve.

Table 5.2: Kinetic parameters for PBP1a^{Pn16} and PBP1a^{159} glycosyltransferase activity in the presence of 50 μM cardiolipin. Values for Vmax, S0.5 and the Hill coefficient for cooperativity (h) were extracted from the fits shown in Figure 5.11.

Enzyme	Condition	Vmax (RFU.sec^{-1}.μg^{-1})	$S_{0.5}$ (μM)	Vmax/$S_{0.5}$	Hill coefficient	R^2
PBP1a^{Pn16}	detergent	-	-	-	-	0.98
	cardiolipin	74.15 ± 3.38	12.95 ± 4.82	5.73	2.16 ± 0.35	0.97
PBP1a^{159}	detergent	-	-	-	-	0.99
	cardiolipin	52.08 ±3.05	5.44 ± 2.53	9.57	2.23 ± 0.56	0.90

It was unclear from the data presented in Figure 5.8 whether the assembly of larger glycan polymers over 30 mins in the presence of cardiolipin could be entirely ascribed to the enhanced rate of GT activity (as illustrated in Figure 5.10), or whether cardiolipin also altered the processivity of PBP1a to contribute to assembly of longer glycan polymers. Time course experiments were therefore conducted in the presence and absence of 50 μM cardiolipin, to allow comparison of the size of the glycan polymers assembled in each condition (Figure 5.12). This experiment illustrated that in the presence of 50 μM cardiolipin, longer glycan polymers were assembled within 2 mins of initiating the reaction than the maximum polymer length synthesised in 30 mins in the absence of cardiolipin. An apparent maximum polymer length was attained within 15 mins in the absence of cardiolipin. These data illustrate that

cardiolipin increased the processivity of PBP1a, in addition to the enhancement of GT rate.

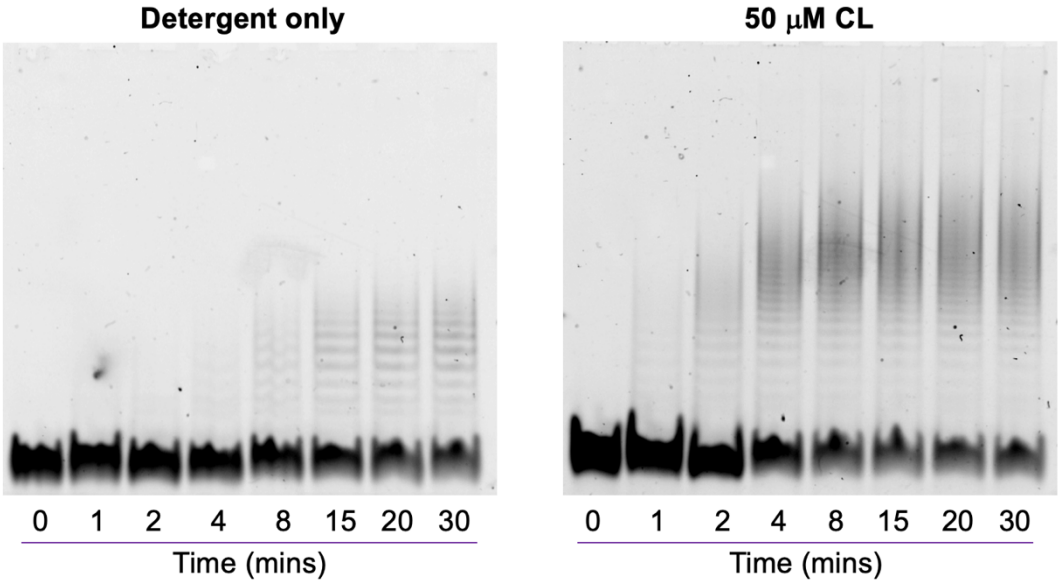

Figure 5.12 Time course of glycan polymer assembly over 30 mins by *S. pneumoniae* PBP1a^{Pn16} in the presence and absence of 50 μM cardiolipin. Reactions comprised 50 mM HEPES, 10 mM $MgCl_2$, 25 % (v/v) DMSO, 150 mM NaCl, 3 x CMC E_6C_{12}, 0.25 μM PBP1a, and 5 μM Lipid II (Gln, Dans). Samples were taken at the stated timepoints and quenched with 0.3 mM moenomycin and 50 mM EDTA. Samples were analysed by electrophoresis on a 9 % Tris-Tricine gel, which was subsequently visualised using an ImageQuant LAS 4000 imager with transmitted light at 312 nm and a 605 nm filter. **CL**, cardiolipin; **mins**, minutes

5.3.3.2 The effect of phosphatidylglycerol on GT activity

The approach to testing of cardiolipin impact on PBP1a GT activity was similarly employed to analyse whether phosphatidylglycerol would affect GT activity of PBP1a from strains D39, Pn16 or 159. As before, phosphatidylglycerol was dissolved in a stock of E_6C_{12} assay buffer and the effect on glycan polymer assembly was tested at concentrations of 10, 1.0 and 0.1 μM phosphatidylglycerol (Figure 5.11). Under the conditions tested, no

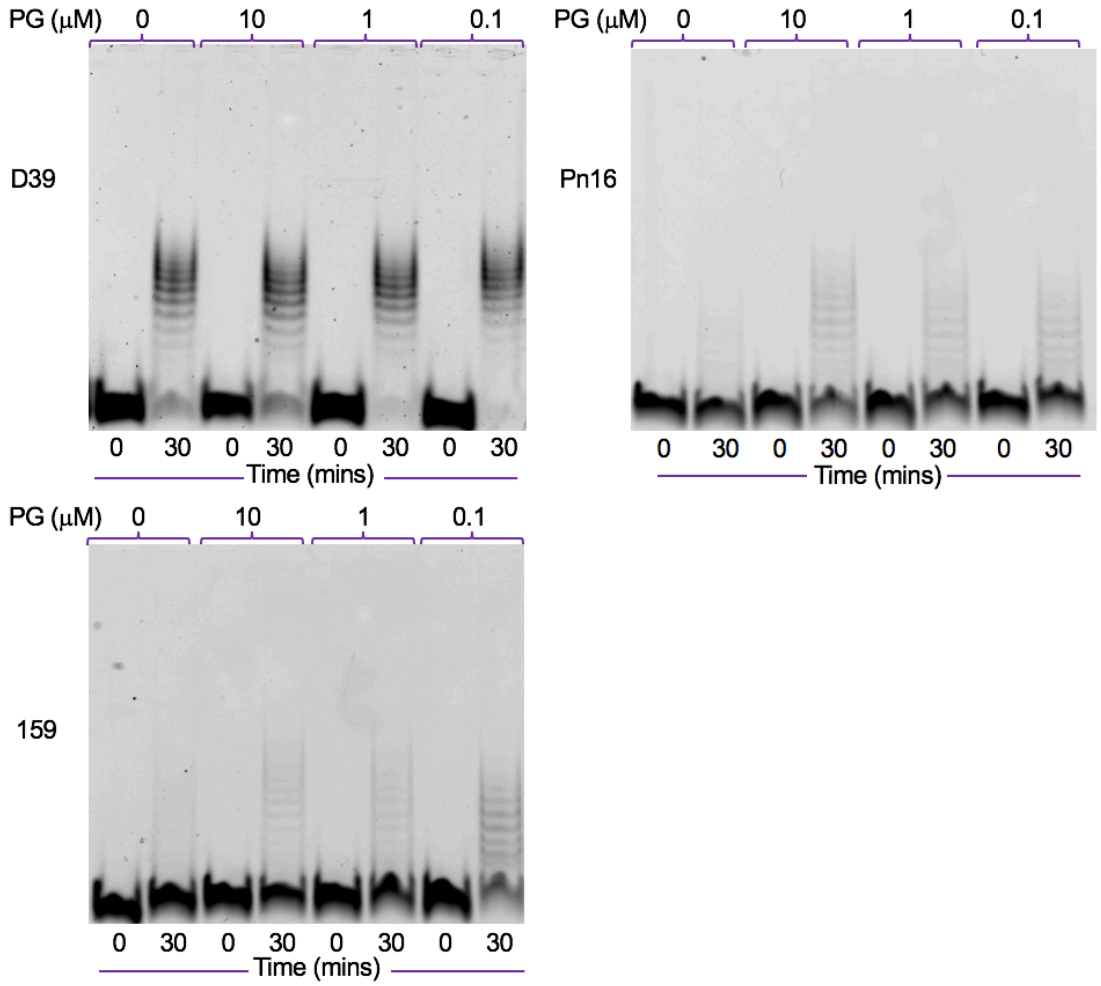

Figure 5.13 Effect of phosphatidylglycerol on glycan polymer assembly over 30 mins by PBP1a variants from *S. pneumoniae* strains D39, Pn16 and 159. Reactions comprised 50 mM HEPES, 10 mM $MgCl_2$, 25 % (v/v) DMSO, 150 mM NaCl, 3 x CMC E_6C_{12}, 0.5 μM PBP1a, 5 μM Lipid II (Gln, Dans), and varying concentrations of phosphatidylglycerol. Samples were taken at the stated timepoints and quenched with 0.3 mM moenomycin and 50 mM EDTA. Samples were analysed by electrophoresis on a 9 % Tris-Tricine gel, which was subsequently visualised using an ImageQuant LAS 4000 imager with transmitted light at 312 nm and a 605 nm filter. **PG**, phosphatidylglycerol; **mins**, minutes

impact was observed on GT activity over 30 mins, with any of the three PBP1a variants.

The effect of phosphatidylglycerol on the rate of GT activity was then compared for each enzyme using the continuous fluorescence assay for GT activity. Whilst no effect of phosphatidylglycerol was observed in the gel-based assay, with 50 μM phosphatidylglycerol an increase in rate was observed. This indicates that the stimulation of GT activity by phosphatidylglycerol requires higher concentrations of the phospholipid.

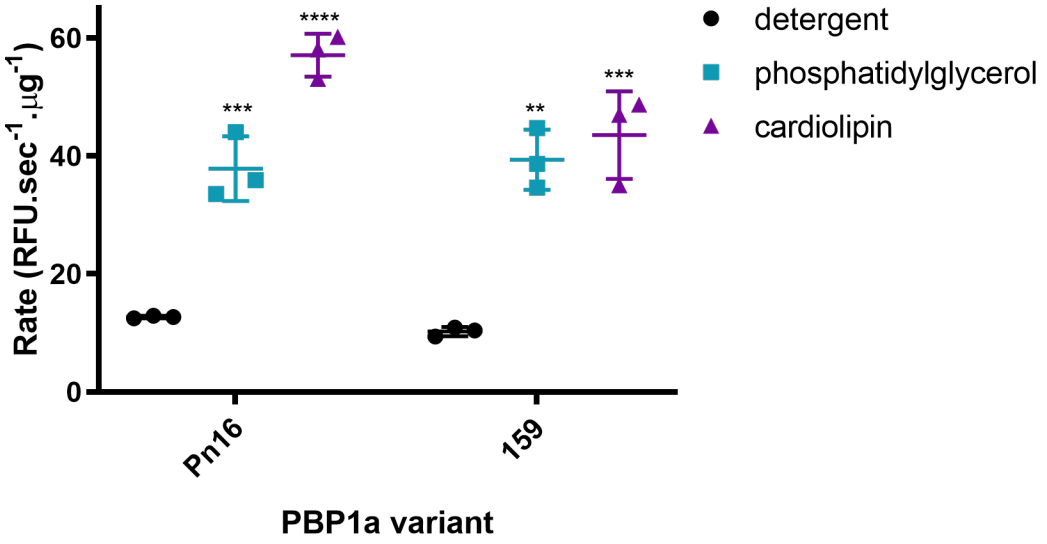

Figure 5.14 Comparison of the effect of 50 μM cardiolipin and 50 μM phosphatidylglycerol on the initial rate of glycosyltransferase activity of PBP1a^{Pn16} and PBP1a^{159}. Reactions comprised 50 mM HEPES, 10 mM $MgCl_2$, 25 % (v/v) DMSO, 150 mM NaCl, 3 X CMC E_6C_{12} (0.0116 % (w/v)), 0.5 μM PBP1a, 0.1 mg.mL^{-1} lysozyme and 5 μM Lipid II (iGln, Dans), ± 50 μM cardiolipin or 50 μM phosphatidylglycerol. Reactions were initiated with enzyme and monitored for 100 mins. Results were graphed in GraphPad Prism to determine the initial rate. The mean specific activity (n = 3) for each PBP1a variant in each condition was compared by one-way ANOVA, which indicated a significant difference between the mean values with phosphatidylglycerol and cardiolipin in each case.
RFU.sec^{-1}.μg^{-1}, relative fluorescence units per second per μg PBP1a.

The mean specific activities (Figure 5.14) of the two enzymes in each of the three conditions were determined by one-way ANOVA to show a significant difference in the presence of phosphatidylglycerol or cardiolipin. These data indicate that both of these phospholipids stimulate activity of PBP1a.

5.3.4 The effect of amidation on GT activity by PBP1a^{D39} and PBP2a^{D39}

We sought to extend the observations on the importance of amidation in GT activity by pneumococcal PBP1a and PBP2a, made by Galley (2015). The previous work demonstrated impact of amidation on the kinetic parameters of GT activity; this work aimed to demonstrate the difference in accumulation of glycan polymers over a similar time course to that in the continuous fluorometric assay.

5.3.4.1 Expression of PBP2a

Expression of untagged PBP2a from the construct pET30::*pbp2a* was attempted as described by Helassa *et al.* (2012). The expression under these conditions failed, and so different conditions were trialled to achieve sufficient expression for purification of PBP2a. The published method expressed PBP2a in BL21 (DE3) cells.

Table 5.3 Rare codon analysis of D39 *pbp2a*. Those codons for which tRNAs are provided by pRosetta (as found in BL21 (DE3) pRosetta cell line) are highlighted in bold. Analysis was completed using Rare Codon Caltor (http://people.mbi.ucla.edu/sumchan/caltor.html).

Amino acid	Arg				Gly		Ile	Leu	Pro	Thr
Rare codon	CGA	CGG	**AGG**	**AGA**	**GGA**	GGG	**AUA**	**CUA**	**CCC**	ACG
Frequency	4	5	1	4	18	8	3	11	2	3

Rare codon analysis of the D39 *pbp2a* gene sequence identified multiple rare codons (Table 5.3). Expression of PBP2a from pET30::*pbp2a* was therefore undertaken using BL21:: pRosetta cells, to supply tRNAs for a selection of those rare codons from the pRosetta plasmid. In this cell line, sufficient PBP2a^{D39} was expressed to allow purification of the enzyme.

Purification was by cation and then anion exchange, made possible by the pI of certain defined areas of the PBP2a structure; and made necessary by lack of activity of tagged full-length PBP2a constructs (Helassa *et al.*, 2012) .The purification protocol was altered such that the solubilisation step was earlier in the procedure, followed by pelleting of insoluble material by centrifugation at 20 000 x g. This modification to the procedure shortened the overall process to allow more rapid storage of the final enzyme stock. The column steps were as described by Helassa *et al.* (2012) (Methods 2.4.5.2). Chromatograms from the two purification steps, along with a summary analysis of the purification by

SDS-PAGE, are presented in Figure 5.15. PBP2a was stored at a final concentration of 8 mg.mL^{-1}.

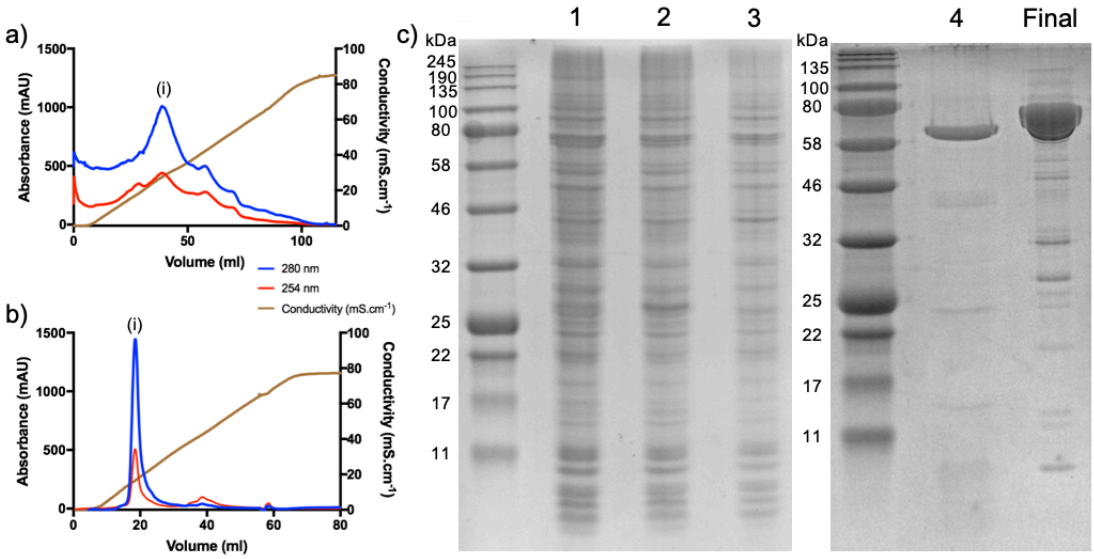

Figure 5.15 Purification of *S. pneumoniae* PBP2a^{D39}. Untagged PBP2a^{D39} was purified by **(a)** cation exchange using a HiTrap SP HP column; and **(b)** anion exchange using a 6 mL RESOURCE™ Q column. **(i)** indicates the peaks corresponding to PBP2a^{D39}. **(c)** illustrates the purification as analysed by SDS-PAGE using a 12 % acrylamide gel (with 5 μg protein loaded per sample). **1**, cell suspension following lysis by cell disruption; **2**, cell suspension following solubilisation of membrane proteins with 1 % (w/v) Triton X-100; **3**, cell suspension following removal of insoluble material by centrifugation; **4**, cation exchange peak; **Final**, the final protein stock following anion exchange. **kDa**, kilodaltons; **mAU**, milli-absorbance units.

To demonstrate penicillin-binding activity of the purified PBP2a, BOCILLIN FL binding was analysed using the electrophoresis assay presented in Chapter 5. The protein band was stained by BOCILLIN FL fluorescence in this experiment, and this staining was lost under preincubation with ampicillin (Figure 5.16). This demonstrated that the purified protein binds penicillin and therefore is likely PBP2a.

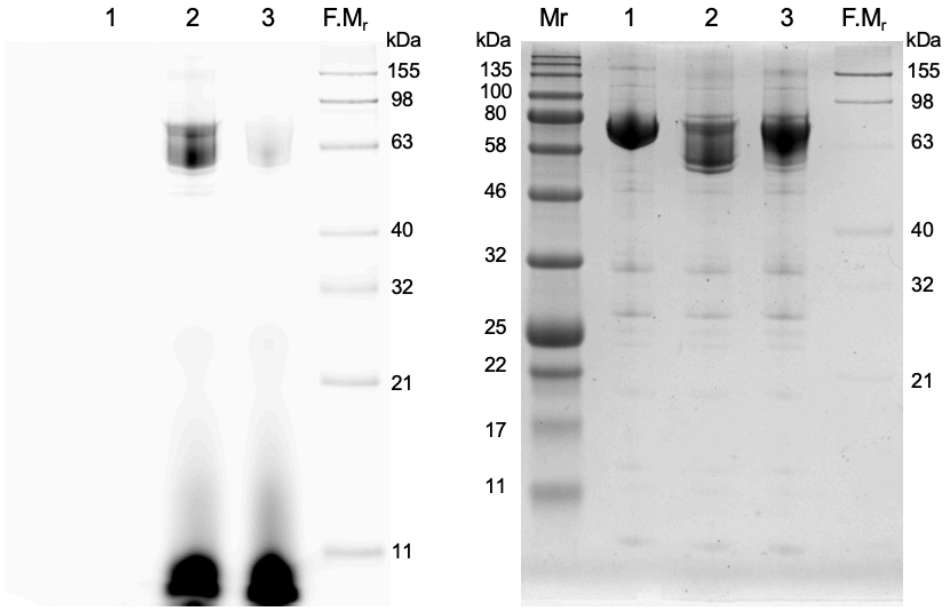

Figure 5.16 Analysis of BOCILLIN FL binding by PBP2a^{D39}. Protein stocks were incubated with water or ampicillin for 30 mins at 25 °C, followed by incubation with BOCILLIN FL or DMSO for 1 h at 37 °C. Reactions were analysed by SDS-PAGE using 12 % acrylamide gels, and fluorescence was imaged (left-hand gel) using a Typhoon FLA 9500 laser scanner (GE Healthcare). Gels were then stained using InstantBlue™ Protein Stain (Expedeon) and imaged for total protein (right-hand gel) using an ImageQuant LAS 4000 instrument (GE Healthcare).
1, PBP2a^{D39} only; **2,** PBP2a^{D39} and BOCILLIN FL; **3,** PBP2a^{D39}, ampicillin and BOCILLIN FL; **F.M$_r$**, BenchMark™ Fluorescent Protein Standard (ThermoFisher Scientific); **M$_r$**, Color Prestained Protein Standard, Broad Range (NEB) molecular weight marker, **kDa**, kilo-Daltons.

5.3.4.2 Time course of GT activity with Lipid II (Gln, Dans) and Lipid II (Glu, Dans)

The impact of amidation on the kinetics of GT activity was previously analysed by use of the continuous fluorometric assay (Galley, 2015), which demonstrated greater catalytic efficiency with and affinity for Lipid II (Gln, Dans), for both PBP1a and PBP2a.

To complement the kinetic analysis of usage of Lipid II (Gln, Dans) and Lipid II (Glu, Dans), we sought to characterise how the formation of glycan polymers by PBP1a or PBP2a compared between these two substrates by SDS-PAGE analysis over a 3 h time course. The experiments presented in Figures 5.17 and 5.18 were completed in collaboration with Dr. Ricky Cain, who quenched

and loaded to gels the samples taken from the Lipid II (Glu, Dans) reactions in each Figure.

Based upon the findings of (Galley, 2015), different time points were chosen to establish the polymerisation of Lipid II (Gln, Dans) and Lipid II (Glu, Dans) substrates. More frequent early time points were used for Lipid II (Gln, Dans), compared to the first time point at 15 minutes for Lipid II (Glu, Dans). This was informed by the slowed rate of GT activity by both PBP1a and PBP2a with the Lipid II (Glu, Dans) substrate previously observed by Galley (2015).

With both PBP1a and PBP2a, high molecular weight polymers were formed

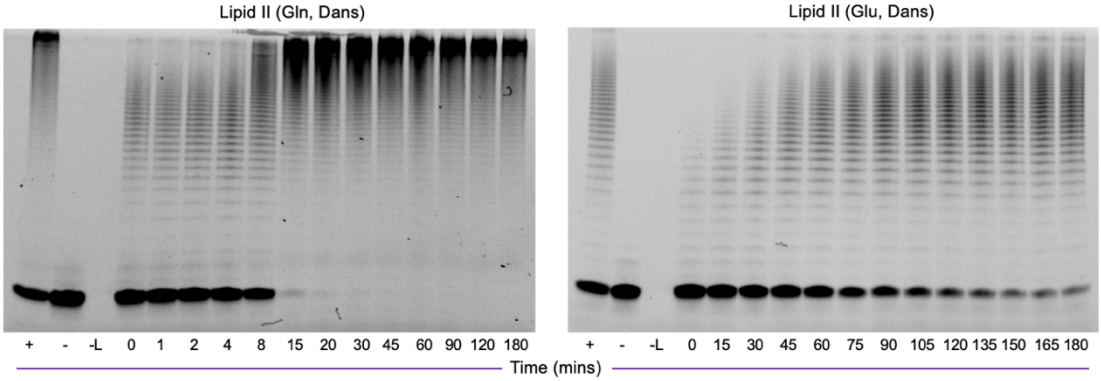

Figure 5.17 Time course of assembly of glycan polymer by *S. pneumoniae* D39 PBP1a with Lipid II (Gln, Dans) or Lipid II (Glu, Dans). Reactions comprised 50 mM HEPES, 10 mM $MgCl_2$, 25 % (v/v) DMSO, 150 mM NaCl, 0.02 % (w/v) Triton X-100, 0.5 μM PBP1a, and 10 μM Lipid II (Gln, Dans) or Lipid II (Glu, Dans). Samples were taken at the stated timepoints and quenched with 0.3 mM moenomycin and 50 mM EDTA. Controls were included with (**-**) no enzyme, (**-L**) no lipid, and (**+**) both enzyme and lipid present, all of which were incubated for the full 180 mins. Samples were analysed by electrophoresis on a precast 16.5 % Tris-Tricine gel (Criterion), which was subsequently visualised using an ImageQuant LAS 4000 imager with transmitted light at 312 nm and a 605 nm filter. **mins**, minutes

.

more rapidly using Lipid II (Gln, Dans) than Lipid II (Glu, Dans), as expected from the fluorometric assay data. In PBP1a reactions, high molecular weight material was formed within 15 minutes with Lipid II (Gln, Dans) (Figure 5.17), whereas similarly sized material did not accumulate to the same extent in Lipid II (Glu, Dans) substrate reactions through the entire time course. A similar pattern was observed with PBP2a (Figure 5.18). The processivity of PBP2a appeared lower with Lipid II (Glu, Dans), as little increase in the polymer length synthesized was observed beyond 135 mins. These results corresponded well with previous observations on the effect of amidation on GT activity.

The positive control lanes of Figures 5.17 and 5.18 did not correspond with the 180 min reactions. This may have resulted from insufficient moenomycin added to these reactions. However, by comparison of each positive lane

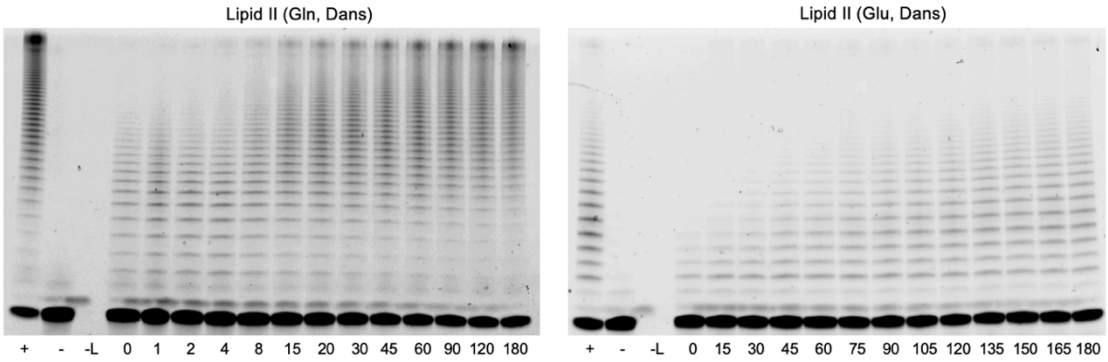

Figure 5.18 Time course of assembly of glycan polymer by *S. pneumoniae* D39 PBP2a with Lipid II (Gln, Dans) or Lipid II (Glu, Dans). Reactions comprised 50 mM HEPES, 10 mM $MgCl_2$, 25 % (v/v) DMSO, 150 mM NaCl, 0.02 % (w/v) Triton X-100, 0.5 μM PBP1a, and 10 μM Lipid II (Gln, Dans) or Lipid II (Glu, Dans). Samples were taken at the stated timepoints and quenched with 0.3 mM moenomycin and 50 mM EDTA. Controls were included with (**-**) no enzyme, (**-L**) no lipid, and (**+**) both enzyme and lipid present, all of which were incubated for the full 180 mins. Samples were analysed by electrophoresis on a precast 16.5 % Tris-Tricine gel (Criterion), which was subsequently visualised using an ImageQuant LAS 4000 imager with transmitted light at 312 nm and a 605 nm filter. **mins**, minutes

between usage of Lipid II (iGln, Dans) and Lipid II (Glu, Dans), the polymer length showed a clear shift to longer polymers under usage of Lipid II (iGln, Dans).

5.4 Discussion

5.4.1 Activity of PBP1a from different pneumococcal strains

The aim of the investigation of pneumococcal PBP1a is to progress to comparison of TP activity between different constructs. As it has been observed that the GT activity of each protein was not significantly different, the GT specific activity of each construct could be a useful scaling factor for different PBP1a variants, and as a controlling factor for any batch-to-batch variation in activity. Zapun *et al.* (2013) used Bocillin-FL binding for this purpose. Bocillin FL binding as a scaling factor is limited as it only offers a measure of TP active site concentration, but does not necessarily prove that the TP active site is properly folded.

5.4.2 Effect of detergent identity and concentration on PBP1a GT activity

Detergent concentration can be considered to control the volume in which the GT reaction could occur, by virtue of the requirement of the enzyme and its substrate for a lipidic environment for solubilisation in aqueous solution.

SDS-PAGE analyses demonstrated inhibition of PBP1a activity by detergent concentrations greater than 3 x CMC. These observations are in agreement with the data of Schwartz *et al.* (2002), who demonstrated that decyl-PEG detergent in concentrations above the CMC behaved as a reversible inhibitor of the activity of *E. coli* PBP1b. The effect of high concentrations of detergent compared to CMC is likely the result of decreasing probability of productive contact between micelles containing enzyme and those containing substrate (Schwartz *et al.*, 2002), known as surface dilution kinetics (Carman *et al.*, 1995). In addition, Helassa *et al.* (2012) suggested that the high CMC typically associated with shorter detergents would decrease the likelihood of contact between enzyme and substrate-containing micelles.

Full analysis of the relationship between detergent concentration and enzyme activity could involve a titration of enzyme concentration against detergent concentration, to analyse the impact on kinetics of glycosyltransfer. Such analysis was performed by Stein *et al.* (2000), who characterised the effect of Triton X-100 concentration on *E. coli* signal peptidase I (SPase I). Stein *et al.* (2000) found that the catalytic efficiency (kcat/Km) decreased with increasing concentration of Triton X-100 above the CMC. This effect was manifested in both increases in K_m and decreases in k_{cat} as the Triton X-100 concentration was increased.

Rapid GT activity of *S. pneumoniae* PBP1a has previously been observed in Triton X-100 as the assay detergent (Galley, 2015). This detergent constitutes a mixture of ethylene glycol moieties, amongst which there may be species inhibitory to the activity of the enzyme. We therefore screened a set of defined ethylene glycol detergents to identify those offering the greatest activity of PBP1a. Such defined ethylene glycol detergents are also beneficial in

facilitating downstream analysis of PBP1a activity assays, for example by liquid chromatography-mass spectrometry (LC-MS). Triton X-100 is ill-suited to LC-MS analysis as it ionises in a polymeric series, thus obscuring any other ions of interest (Dr. A.J. Lloyd, University of Warwick, personal communication).

Some studies have used liposomes to create the lipid environment necessary to maintain membrane proteins in a folded state and reconstitute the enzymatic activity (Hernández-Rocamora *et al.*, 2018). The use of membrane lipid extracts from the originating bacterial species may be expected to best reconstitute the activity of a given enzyme. Use of liposomes instead of detergents to solubilise enzymes for assays would require prior identification of the preferred lipids of the enzyme in question, or use of an uncharacterised mixture. By contrast, detergents are beneficial in that their compatibility with various biochemical applications is known (Linke, 2009).

5.4.3 Phospholipids and PBP1a

Cardiolipin was found to stimulate GT activity, with a dose-dependent response, whilst no impact of phosphatidylglycerol on GT activity was observed under the conditions tested.

The observation of stimulation of PBP1a activity by cardiolipin is in accordance with previous findings on the impact of cardiolipin on pneumococcal MurM (Dr. A.J. Lloyd, University of Warwick, unpublished). A growing body of evidence supports a role for cardiolipin in stimulation of enzymes of the cell wall biosynthetic pathway, with possible links to localisation of the cell wall synthesis machinery.

A limitation of the current work is that cardiolipin was obtained from bovine heart preparations, and so differences in fatty acid moieties would be expected as compared to cardiolipin found in cell membrane of *S. pneumoniae*. In addition, phospholipid asymmetry is an important consideration for these results; it is difficult to determine the proportion of cardiolipin at the intracellular and extracellular faces of the cytoplasmic membrane. This factor is important to determine the relevance of inferred relationships between phospholipids and membrane proteins. Mukhopadhyay *et al.* (2007) used nonacrydyl-orange

(NAO) staining to analyse to phospholipid composition between the inner and outer leaflets of the *S. aureus* cytoplasmic membrane. The authors demonstrated that a large proportion of the total cardiolipin content of the membrane was found at the outer leaflet of the cytoplasmic membrane.

A key further area of experimentation would therefore be the isolation of membrane lipids from relevant strains of *S. pneumoniae*, to allow comparison of the relative concentrations of particular phospholipids. Such extracts could also be used to create liposomes for reconstitution of PBP1a activity, and provide the source material from which those membrane components that did impact GT activity could be isolated.

The mechanism of the stimulatory interaction between cardiolipin and PBP1a also remains to be determined. The interaction appears to be specific to cardiolipin, as the same stimulatory effect was not observed with phosphatidylglycerol at similar Lipid II concentrations.

In light of the demonstrable importance of phospholipids in the activity of cell division proteins, a move away from the use of detergents for solubilisation would be a positive step in the ability to characterise the activities of cell division proteins. Alternative methods to detergents for solubilisation include nanodiscs, amphipols and reconstitution in liposomes.

Among nanodisc technologies, styrene maleic acid (SMA) particles have been a successful technology for the reconstitution and study of membrane proteins. SMA lipid particles (SMALP). Mass spectrometry has been used to analyse the lipids co-extracted in SMALP, through which the lipid profiles associated with particular proteins have been analysed (Teo *et al.*, 2019).

5.4.4 Amidation and GT activity

The results of our time course analysis are in agreement with previous data demonstrating an impact of amidation on the activity of bifunctional pneumococcal PBPs (Zapun *et al.*, 2013). Both PBP1a and PBP2a demonstrated preference for amidation, with greater processivity confirmed in the current work. A remaining question surrounding the impact of amidation on PBP activity is whether amidation is also recognised by the TP active site. Zapun *et al.* (2013) demonstrated poorer accumulation of high-molecular

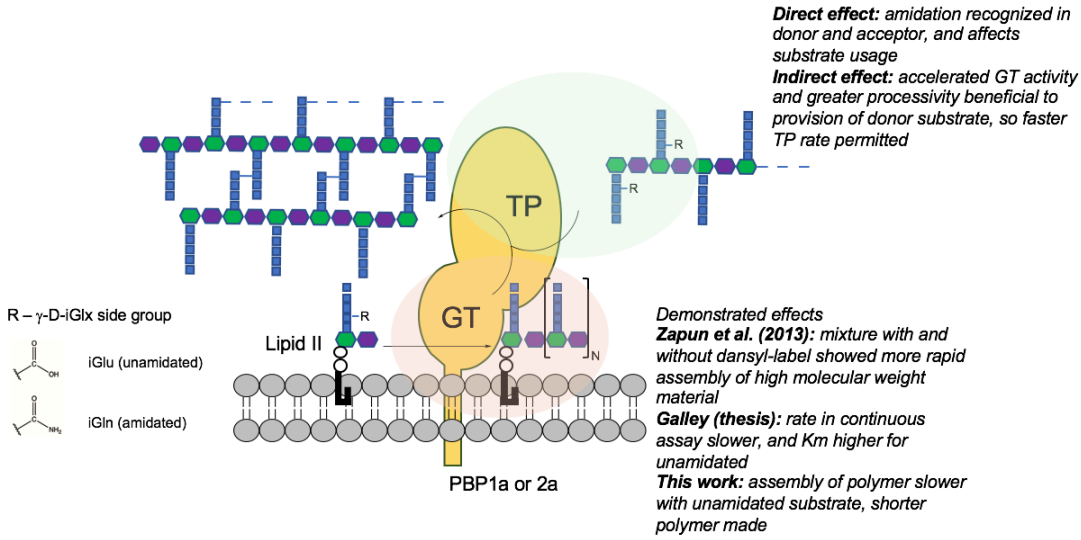

Figure 5.19 Summary of understanding to date on the impact of amidation on *S. pneumoniae* PBP1a and PBP2a function.

weight material in the presence of Lipid II (Glu) on SDS-PAGE analysis, inferring slower transpeptidation. However, this observation could be the result of an indirect effect, in that activity of the GT site is boosted and thus provides donor substrate more efficiently; or could be a direct effect, with the transpeptidase active site recognising the second position amino acid, in the donor and/or acceptor substrate.

In addition, the residues of the GT active site that are responsible for recognition of amidation remain to be determined. The data to date and some remaining experimental questions are summarised in Figure 5.19.

5.4.5 Conclusions

This work offers the first demonstration of the impact of phospholipids on PBP activity. Key areas for further characterisation include determination of the

mechanism of the interaction between phospholipids and PBP1a, and investigation of the link between phospholipid synthesis and β-lactam resistance.

Chapter 6: General Discussion and Conclusions

Antibiotic resistance poses a major threat to healthcare and economies worldwide. To prevent the current projected death toll of 10 million per year worldwide by 2050 due to resistant infections, it is important that alongside education and sanitation initiatives, that we strengthen the antibiotic pipeline with promising new drug candidates. Better understanding and tools for study of key bacterial processes including cell wall biosynthesis can make a significant contribution to the delivery of new inhibitors. Cell wall biosynthesis is a crucial process for bacterial growth and a well-validated target for existing antimicrobials, and there remains much to be understood about cell wall biosynthesis, not least with regards to the PBPs themselves.

This thesis aimed to contribute by deepening our knowledge of the penicillin-binding proteins of *Streptococcus pneumoniae*, a key pathogen in terms of its healthcare burden and the prevalence of resistance to β-lactams. We aimed to develop methods in synthesis of pneumococcal peptidoglycan precursors, and assay of pneumococcal PBPs, in order to analyse the pneumococcal β-lactam resistance mechanism.

6.1 Synthesis of pneumococcal peptidoglycan precursors

Methods for the synthesis of pneumococcal peptidoglycan intermediates have revolutionised our ability to assay peptidoglycan synthases, where progress was historically limited by availability of native substrate. We present the first synthesis of molecules that could in principle act as defined donor-only and acceptor-only substrates for transpeptidation by pneumococcal PBPs. These substrates will provide valuable tools for the understanding of these enzymes and how they function with natural substrates, which is key for addressing the biochemical details of pneumococcal β-lactam resistance.

The methods for synthesis of these defined donor-only and acceptor-only pneumococcal peptidoglycan substrates can be extended to synthesis of the branched substrates key to the β-lactam resistance mechanism. Synthesis of acceptor-only branched substrates was attempted, but could not be confirmed by mass spectrometry due to the presence of a contaminating ion series, but

the origin of this contaminant is unconfirmed and may have been unrelated to the specific processes of the experiment.

Synthesis of lipid linked, branched PG intermediates was demonstrated at analytical scale. These syntheses could now be scaled up to generate potential donor substrates for biochemical assays. It would also be of interest to exploit recently published methods for purification of lipid-linked, branched precursors from bacterial cultures (Qiao *et al.*, 2017). Such purifications from pneumococcal cultures would be challenging due to the autolysis of pneumococcal cultures in stationary phase by the action of the autolysin LytA (Mellroth *et al.*, 2012), necessitating careful monitoring of the cultures. Also, there is strain-by-strain variation in the extent and composition of indirect cross-links in peptidoglycan, likely reflecting variation in the peptidoglycan precursor pool (Filipe *et al.*, 2000; Filipe *et al.*, 2001). Purification of Lipid II directly from pneumococcal cultures would therefore be expected to generate a mixed product of linear and branched Lipid II. One could envision experiments whereby these mixed samples were incubated with PBP1a or PBP2a, and the products muramidase-digested analysed by LC-MS to determine whether transpeptidation had occurred, and the relative use of different substrates in this process. Such experiments would require internal standards for mass spectrometry to render them quantitative. This mass spectrometry approach could be an alternative for analysis of the results described here with use of linear Lipid II variants in the D-Ala release assay, where there was detection of D,D-carboxypeptidase activity only. HPLC analysis of the mixtures of substrates generated from cultures would also allow comparison of the substrate pools of the pneumococcal strains of interest in this work.

In addition to use in assays of PBPs, pneumococcal peptidoglycan precursors are a useful research tool for applications such as study of immune responses to infection, as peptidoglycan fragments are bound by innate immune receptors (Koppe *et al.*, 2011; Wolf & Underhill, 2018); and biophysical characterisations of proteins that bind peptidoglycan (Righino *et al.*, 2018). The library of pneumococcal precursors could therefore be applied to answer

a variety of questions surrounding cell wall biosynthesis and the interaction of pneumococci with their environment.

6.2 Development of Assay for Pneumococcal Transpeptidase Activity

A variety of methods were explored to establish *in vitro* transpeptidase activity of pneumococcal PBP1a, but mass spectrometry detected only D,D-carboxypeptidase activity. The results of SDS-PAGE-based analysis of PBP1a transpeptidase activity were similarly equivocal.

Several key recent publications could inform further work to establish *in vitro* transpeptidase activity of pneumococcal PBPs. Class A PBPs have been suggested to remodel peptidoglycan synthesised by the FtsW/PBP2x peptidoglycan synthesis complex. This work was based on analysis of phases in resistance of pneumococcal cultures to the CbpD hydrolase under titration of oxacillin. Further work could focus on using purified PG from pneumococci as an acceptor or donor to reconstitute PG biosynthesis, or use of FtsW/PBP2x to generate polymeric substrate for PBP1a *in vitro*.

Further work could also encompass the recently reported interactors with Class A pneumococcal PBPs (Fenton *et al.*, 2018; Fenton *et al.*, 2016), which may activate the activity of their partner proteins *in vitro* in a manner analogous to that described by lipoprotein activators of *E. coli* and *P. aeruginosa* Class A PBPs. Peptidoglycan synthesis by pneumococcal PBP2a has been demonstrated to be activated by MacP (Fenton *et al.*, 2018), and so testing of the D-Ala release activity by this enzyme in the presence of the activating partner would be a key further experiment to the work presented in this thesis.

Alternative techniques to analyse the usage by PBP1a of the substrate variants generated in this work could include assays with S2d thioester analogues as the transpeptidase donor, or techniques such as surface plasmon resonance or mass spectrometry to compare the binding of different substrates.

6.3 The Impact of Lipid Environment on Pneumococcal Glycosyltransferase Activity

There is growing recognition of the importance of lipids in divisome activity. Interactions of cardiolipin with proteins at the lipid-linked stages of the peptidoglycan synthesis pathway have been described, with data indicating modulation of the Lipid II flippase MurJ by cardiolipin (Bolla *et al.*, 2018) and stimulation of catalytic activity of MurG in the presence of cardiolipin (van den Brink-van der Laan *et al.*, 2003). In this thesis, comparison of GT activity has identified a novel link between the phospholipids of the pneumococcal membrane, and the activity of the PBPs from both β-lactam sensitive and resistant strains. Cardiolipin was shown to accelerate GT activity in a dose-dependent manner, via reduction of apparent K_m for the Lipid II (iGln, Dans) substrate. This is the first observation of the impact of cardiolipin on the activity of a PBP, and corresponds with growing evidence in support of a role of cardiolipin in regulation of cell division proteins. These observations warrant extension of the studies to other pneumococcal peptidoglycan synthases, not least the SEDS glycosyltransferases which are integral membrane proteins.

The observation of the impact of cardiolipin suggests some interesting further work to characterise the nature of the beneficial effect upon PBP1a activity. The transmembrane anchor of PBPs has been shown to be important for GT activity, with involvement in the formation of oligomeric states (Galley, 2015). This process, and the configuration of the substrate and enzyme, could be investigated using molecular dynamics simulation of the interaction of PBP1a and the lipid substrate in the presence of cardiolipin. Recent studies using molecular dynamics simulations have suggested a role for cardiolipin, in combination with AcrZ, in modulating the activity of the multidrug efflux pump AcrB (Du *et al.*, 2019). Alternatively, interactions could be studied using ion mobility mass spectrometry, as applied to show modulation of *E. coli* aquaporin Z by cardiolipin (Laganowsky *et al.*, 2014); or by non-denaturing mass spectrometry to analyse oligomeric state of protein (Gupta *et al.*, 2017).

6.4 Conclusion

This thesis describes progress towards the establishment of *in vitro* transpeptidase activity of pneumococcal PBPs, with the provision of a range of natural substrates; a study of the impact of lipid environment on PBP1a GT activity; and studies focussing on the use of a D-Ala release assay for transpeptidation by PBP1a. Further work is required to establish *in vitro* transpeptidase activity, but with recent advances in knowledge of the pneumococcal cell division machinery (Massidda *et al.*, 2013; Vollmer *et al.*, 2019), several opportunities arise to test protein-protein interactions that may stimulate pneumococcal transpeptidase activity *in vitro*.

Through deepening of our understanding of the mechanisms that underlie resistance to current antibiotics, we will build the knowledge base required for the design of new inhibitors that may bypass these mechanisms or restore activity.

The importance of antibiotic resistance as a research and global healthcare challenge can be summed up by the words of Aminov (2010), who noted that “In fact, [antibiotic resistance] should be of everyone’s concern, because, in the end, there is always a probability for any of us at some stage to get infected with a pathogen that is resistant to antibiotic treatment.”.

Bibliography

Abrahams, K. A. (2011). The enzymology of Streptococcus pneumoniae peptidoglycan polymerisation. (Doctoral dissertation, University of Warwick).

Adam, M., Damblon, C., Jamin, M., Zorzi, W., Dusart, V., Galleni, M., . . . Keck, W. (1991). Acyltransferase activities of the high-molecular-mass essential penicillin-binding proteins. *Biochemical Journal, 279*(2), 601-604.

Adam, M., Damblon, C., Plaitin, B., Christiaens, L., & Frere, J. M. (1990). Chromogenic depsipeptide substrates for β-lactamases and penicillin-sensitive DD-peptidases. *Biochemical Journal 270*(2), 525-529.

Adams, D. W., & Errington, J. (2009). Bacterial cell division: assembly, maintenance and disassembly of the Z ring. *Nature Reviews Microbiology, 7*(9), 642.

Al-Warhi, T. I., Al-Hazimi, H. M. A., & El-Faham, A. (2012). Recent development in peptide coupling reagents. *Journal of Saudi Chemical Society, 16*(2), 97-116.

American Academy of Pediatrics Committee on Infectious Diseases. (2010). Recommendations for the prevention of Streptococcus pneumoniae infections in infants and children: use of 13-valent pneumococcal conjugate vaccine (PCV13) and pneumococcal polysaccharide vaccine (PPSV23). *Pediatrics, 126*(1), 186-190.

Aminov, R. (2010). A brief history of the antibiotic era: lessons learned and challenges for the future. *Frontiers in Microbiology, 1*, 134.

Anderson, J. S., Matsuhashi, M., Haskin, M. A., & Strominger, J. L. (1965). Lipid-phosphoacetylmuramyl-pentapeptide and lipid-phosphodisaccharide-pentapeptide: presumed membrane transport intermediates in cell wall synthesis. *Proceedings of the National Academy of Sciences, 53*(4), 881-889.

Anderson, J. S., Matsuhashi, M., Haskin, M. A., & Strominger, J. L. (1967). Biosynthesis of the peptidoglycan of bacterial cell walls II. Phospholipid carriers in the reaction sequence. *Journal of Biological Chemistry, 242*(13), 3180-3190.

Arbeloa, A., Segal, H., Hugonnet, J.E., Josseaume, N., Dubost, L., Brouard, . . . & Arthur, M. (2004). Role of Class A Penicillin-Binding Proteins in PBP5-Mediated β-Lactam Resistance in Enterococcus faecalis. *Journal of Bacteriology, 186*(5), 1221-1228.

Armstrong, D. W., Tang, Y., Chen, S., Zhou, Y., Bagwill, C., & Chen, J.-R. (1994). Macrocyclic antibiotics as a new class of chiral selectors for liquid chromatography. *Analytical Chemistry, 66*(9), 1473-1484.

Artimo, P., Jonnalagedda, M., Arnold, K., Baratin, D., Csardi, G., De Castro, E., . . . Gasteiger, E. (2012). ExPASy: SIB bioinformatics resource portal. *Nucleic acids research, 40*(W1), W597-W603.

Barcus, V. A., Ghanekar, K., Yeo, M., Coffey, T. J., & Dowson, C. G. (1995). Genetics of high level penicillin resistance in clinical isolates of Streptococcus pneumoniae. *FEMS Microbiology Letters, 126*(3), 299-303.

Barreteau, H., Kovač, A., Boniface, A., Sova, M., Gobec, S., & Blanot, D. (2008). Cytoplasmic steps of peptidoglycan biosynthesis. *FEMS Microbiology Reviews, 32*(2), 168-207.

Barrett, D., Wang, T.-S. A., Yuan, Y., Zhang, Y., Kahne, D., & Walker, S. (2007). Analysis of glycan polymers produced by peptidoglycan glycosyltransferases. *Journal of Biological Chemistry, 282*(44), 31964-31971.

Bättig, P., & Mühlemann, K. (2008). Influence of the spxB gene on competence in Streptococcus pneumoniae. *Journal of Bacteriology, 190*(4), 1184-1189.

Bebrone, C., Moali, C., Mahy, F., Rival, S., Docquier, J. D., Rossolini, G. M., . . . Galleni, M. (2001). CENTA as a chromogenic substrate for studying β-lactamases. *Antimicrobial Agents and Chemotherapy, 45*(6), 1868-1871.

Ben-Bassat, A., Bauer, K., Chang, S.-Y., Myambo, K., Boosman, A., & Chang, S. (1987). Processing of the initiation methionine from proteins: properties of the Escherichia coli methionine aminopeptidase and its gene structure. *Journal of Bacteriology, 169*(2), 751-757.

Berg, K. H., Straume, D., & Håvarstein, L. S. (2014). The function of the transmembrane and cytoplasmic domains of pneumococcal penicillin-binding proteins 2x and 2b extends beyond that of simple anchoring devices. *Microbiology, 160*(8), 1585-1598.

Bertani, G. (1951). Studies on lysogenesis i.: The mode of phage liberation by lysogenic escherichia coli1. *Journal of Bacteriology, 62*(3), 293.

Bertsche, U., Breukink, E., Kast, T., & Vollmer, W. (2005). In Vitro Murein (Peptidoglycan) Synthesis by Dimers of the Bifunctional Transglycosylase-Transpeptidase PBP1B from Escherichia coli. *Journal of Biological Chemistry, 280*(45), 38096-38101.

Biarrotte-Sorin, S., Hugonnet, J.-E., Delfosse, V., Mainardi, J.-L., Gutmann, L., Arthur, M., & Mayer, C. (2006). Crystal Structure of a Novel β-Lactam-insensitive Peptidoglycan Transpeptidase. *Journal of Molecular Biology, 359*(3), 533-538.

Biboy, J., Bui, N. K., & Vollmer, W. (2013). In vitro peptidoglycan synthesis assay with lipid II substrate. In *Bacterial Cell Surfaces* (pp. 273-288): Springer.

Blewett, A. M., Lloyd, A. J., Echalier, A., Fülöp, V., Dowson, C. G., Bugg, T. D., & Roper, D. I. (2004). Expression, purification, crystallization and preliminary characterization of uridine 5′-diphospho-N-acetylmuramoyl l-alanyl-d-glutamate: lysine ligase (MurE) from Streptococcus pneumoniae 110K/70. *Acta Crystallographica Section D: Biological Crystallography, 60*(2), 359-361.

Bogaert, D., van Belkum, A., Sluijter, M., Luijendijk, A., de Groot, R., Rümke, H. C., ... & Hermans, P. W. M. (2004). Colonisation by Streptococcus pneumoniae and Staphylococcus aureus in healthy children. *The Lancet, 363*(9424), 1871-1872.

Bolla, J. R., Sauer, J. B., Wu, D., Mehmood, S., Allison, T. M., & Robinson, C. V. (2018). Direct observation of the influence of cardiolipin and antibiotics on lipid II binding to MurJ. *Nature Chemistry, 10*, 363.

Boucher, H. W., Talbot, G. H., Bradley, J. S., Edwards, J. E., Gilbert, D., Rice, L. B., . . . Bartlett, J. (2009). Bad Bugs, No Drugs: No ESKAPE! An

Update from the Infectious Diseases Society of America. *Clinical Infectious Diseases, 48*(1), 1-12.

Bouhss, A., Josseaume, N., Allanic, D., Crouvoisier, M., Gutmann, L., Mainardi, J.-L., . . . Arthur, M. (2001). Identification of the UDP-MurNAc-Pentapeptide:l-Alanine Ligase for Synthesis of Branched Peptidoglycan Precursors in Enterococcus faecalis. *Journal of Bacteriology, 183*(17), 5122-5127.

Bouhss, A., Josseaume, N., Severin, A., Tabei, K., Hugonnet, J.-E., Shlaes, D., . . . Arthur, M. (2002). Synthesis of the L-alanyl-L-alanine cross-bridge of Enterococcus faecalis peptidoglycan. *Journal of Biological Chemistry, 277*(48), 45935-45941.

Bowler, L. D., Spratt, B. G., Smith, J. M., Zhang, Q.-Y., & Zhou, J. (1992). Role of interspecies transfer of chromosomal genes in the evolution of penicillin resistance in pathogenic and commensal Neisseria species. *Journal of Molecular Evolution, 34*(2), 115-125.

Breukink, E., van Heusden, H. E., Vollmerhaus, P. J., Swiezewska, E., Brunner, L., Walker, S., . . . de Kruijff, B. (2003). Lipid II is an intrinsic component of the pore induced by nisin in bacterial membranes. *J Biol Chem, 278*(22), 19898-19903.

Bruckdorfer, K. R., & Sherry, M. K. (1984). The solubility of cholesterol and its exchange between membranes. *Biochimica et Biophysica Acta (BBA)-Biomembranes, 769*(1), 187-196.

Brundish, D., Shaw, N., & Baddiley, J. (1967). The phospholipids of Pneumococcus I-192R, ATCC 12213: Some structural rearrangements occurring under mild conditions. *Biochemical Journal, 104*(1), 205.

Bugg, T. D. H., Braddick, D., Dowson, C. G., & Roper, D. I. (2011). Bacterial cell wall assembly: still an attractive antibacterial target. *Trends in Biotechnology, 29*(4), 167-173.

Cabeen, M. T., & Jacobs-Wagner, C. (2005). Bacterial cell shape. *Nature Reviews Microbiology, 3*(8), 601.

Calvez, P., Breukink, E., Roper, D. I., Dib, M., Contreras-Martel, C., & Zapun, A. (2017). Substitutions in PBP2b from β-Lactam-resistant Streptococcus pneumoniae Have Different Effects on Enzymatic Activity and Drug Reactivity. *Journal of Biological Chemistry, 292*(7), 2854-2865.

Carattoli, A. (2013). Plasmids and the spread of resistance. *International Journal of Medical Microbiology, 303*(6-7), 298-304.

Carman, G. M., Deems, R. A., & Dennis, E. A. (1995). Lipid signaling enzymes and surface dilution kinetics. *Journal of Biological Chemistry, 270*(32), 18711-18714.

Carpino, L. A., & Han, G. Y. (1972). 9-Fluorenylmethoxycarbonyl amino-protecting group. *The Journal of Organic Chemistry, 37*(22), 3404-3409.

Carroll, B., O'Rourke, B., & Ward, A. (1982). The kinetics of solubilization of single component non-polar oils by a non-ionic surfactant. *Journal of Pharmacy and Pharmacology, 34*(5), 287-292.

Cartwright, K. (2002). Pneumococcal disease in western Europe: burden of disease, antibiotic resistance and management. *European journal of pediatrics, 161*(4), 188-195.

Centers for Disease Control and Prevention (US) (2013). *Antibiotic resistance threats in the United States, 2013*: Centers for Disease Control and Prevention, US Department of Health and Human Services.

Chain, E., Florey, H.W., Gardner, A.D., Heatley, N.G., Jennings, M.A., Orr-Ewing, J. and Sanders, A.G. (1940). Penicillin as a chemotherapeutic agent. *The Lancet, 236*(6104), 226-228.

Chalut, C., Charpentier, X., Remy, M.-H., & Masson, J.-M. (2001). Differential responses of Escherichia coli cells expressing cytoplasmic domain mutants of penicillin-binding protein 1b after impairment of penicillin-binding proteins 1a and 3. *Journal of Bacteriology, 183*(1), 200-206.

Chambers, H. F. (1997). Methicillin resistance in staphylococci: molecular and biochemical basis and clinical implications. *Clin Microbiol Rev, 10*(4), 781-791.

Chang, Y., Schlebach, J. P., VerHeul, R. A., & Park, C. (2012). Simplified proteomics approach to discover protein–ligand interactions. *Protein Science, 21*(9), 1280-1287.

Chen, L., Walker, D., Sun, B., Hu, Y., Walker, S., & Kahne, D. (2003). Vancomycin analogues active against vanA-resistant strains inhibit bacterial transglycosylase without binding substrate. *Proceedings of the National Academy of Sciences, 100*(10), 5658-5663.

Chewapreecha, C., Marttinen, P., Croucher, N. J., Salter, S. J., Harris, S. R., Mather, A. E., ... & Turner, P. (2014). Comprehensive identification of single nucleotide polymorphisms associated with beta-lactam resistance within pneumococcal mosaic genes. *PLoS genetics, 10*(8), e1004547.

Chi, F., Nolte, O., Bergmann, C., Ip, M., & Hakenbeck, R. (2007). Crossing the barrier: evolution and spread of a major class of mosaic pbp2x in Streptococcus pneumoniae, S. mitis and S. oralis. *International Journal of Medical Microbiology, 297*(7-8), 503-512.

CLSI. (2014). Clinical and Laboratory Standards Institute: Performance standards for antimicrobial susceptibility testing: Twenty-fourth informational supplement, M100-S24. *34*(1).

Coffey, T. J., Daniels, M., McDougal, L. K., Dowson, C. G., Tenover, F. C., & Spratt, B. G. (1995). Genetic analysis of clinical isolates of Streptococcus pneumoniae with high-level resistance to expanded-spectrum cephalosporins. *Antimicrobial Agents and Chemotherapy, 39*(6), 1306-1313.

Contreras-Martel, C., Dahout-Gonzalez, C., Martins, A. D. S., Kotnik, M., & Dessen, A. (2009). PBP active site flexibility as the key mechanism for β-lactam resistance in pneumococci. *Journal of Molecular Biology, 387*(4), 899-909.

Contreras-Martel, C., Job, V., Di Guilmi, A. M., Vernet, T., Dideberg, O., & Dessen, A. (2006). Crystal structure of penicillin-binding protein 1a (PBP1a) reveals a mutational hotspot implicated in β-lactam resistance in Streptococcus pneumoniae. *Journal of Molecular Biology, 355*(4), 684-696.

Copeland, R. A. (2004). *Enzymes: a practical introduction to structure, mechanism, and data analysis*: John Wiley & Sons.

Croucher, N. J., Løchen, A., & Bentley, S. D. (2018). Pneumococcal Vaccines: Host Interactions, Population Dynamics, and Design Principles. *Annual Review of Microbiology, 72*, 521-549.

Dagan, R., Leibovitz, E., Greenberg, D., Yagupsky, P., Fliss, D. M., & Leiberman, A. (1998). Dynamics of pneumococcal nasopharyngeal colonization during the first days of antibiotic treatment in pediatric patients. *The Pediatric infectious disease journal, 17*(10), 880-885.

Davies, T. A., Shang, W., Bush, K., & Flamm, R. K. (2008). Activity of doripenem and comparator β-lactams against US clinical isolates of Streptococcus pneumoniae with defined mutations in the penicillin-binding domains of pbp1a, pbp2b and pbp2x. *Journal of Antimicrobial Chemotherapy, 61*(3), 751-753.

Dawson, R. M. C., Elliott, D. C., Elliott, W. H., & Jones, K. M. (1969). *Data for biochemical research* (Vol. 316): Clarendon Press Oxford.

de Kraker, M. E., Stewardson, A. J., & Harbarth, S. (2016). Will 10 million people die a year due to antimicrobial resistance by 2050?. *PLoS medicine, 13*(11), e1002184.

De Pascale, G., Lloyd, A. J., Schouten, J. A., Gilbey, A. M., Roper, D. I., Dowson, C. G., & Bugg, T. D. H. (2008). Kinetic Characterization of Lipid II-Ala:Alanyl-tRNA Ligase (MurN) from Streptococcus pneumoniae using Semisynthetic Aminoacyl-lipid II Substrates. *Journal of Biological Chemistry, 283*(50), 34571-34579.

Den Blaauwen, T., de Pedro, M. A., Nguyen-Distèche, M., & Ayala, J. A. (2008). Morphogenesis of rod-shaped sacculi. *FEMS Microbiology Reviews, 32*(2), 321-344.

Derouaux, A., Turk, S., Olrichs, N. K., Gobec, S., Breukink, E., Amoroso, A., . . . Chopra, I. (2011). Small molecule inhibitors of peptidoglycan synthesis targeting the lipid II precursor. *Biochemical Pharmacology, 81*(9), 1098-1105.

Di Guilmi, A. M., Dessen, A., Dideberg, O., & Vernet, T. (2003). The glycosyltransferase domain of penicillin-binding protein 2a from Streptococcus pneumoniae catalyzes the polymerization of murein glycan chains. *Journal of Bacteriology, 185*(15), 4418-4423.

Di Guilmi, A. M., Mouz, N., Andrieu, J.-P., Hoskins, J., Jaskunas, S. R., Gagnon, J., . . . Vernet, T. (1998). Identification, purification, and characterization of transpeptidase and glycosyltransferase domains of Streptococcus pneumoniae penicillin-binding protein 1a. *Journal of Bacteriology, 180*(21), 5652-5659.

Dirienzo, J. M., Nakamura, K., & Inouye, M. (1978). The outer membrane proteins of Gram-negative bacteria: biosynthesis, assembly, and functions. *Annual Review of Biochemistry, 47*(1), 481-532.

Dowson, C. G., Coffey, T. J., Kell, C., & Whiley, R. A. (1993). Evolution of penicillin resistance in Streptococcus pneumoniae; the role of Streptococcus mitis in the formation of a low affinity PBP2B in S. pneumoniae. *Molecular Microbiology, 9*(3), 635-643.

Dowson, C. G., Hutchison, A., Brannigan, J. A., George, R. C., Hansman, D., Liñares, J., . . . Spratt, B. G. (1989). Horizontal transfer of penicillin-binding protein genes in penicillin-resistant clinical isolates of Streptococcus pneumoniae. *Proceedings of the National Academy of Sciences, 86*(22), 8842-8846.

Du, D., Neuberger, A., Orr, M. W., Newman, C. E., Hsu, P. C., Samsudin, F., ... & Storz, G. (2019). Interactions of a bacterial RND transporter with a transmembrane small protein in a lipid environment. *bioRxiv*, 813394.

Duchesne, E. (1897). Contribution à l'étude de la concurrence vitale chez les microorganismes: antagonisme entre les moisissures et les microbes. Alexandre Rey, imprimeur de la faculté de médecine.

Ealand, C. S., Machowski, E. E., & Kana, B. D. (2018). β-lactam resistance: The role of low molecular weight penicillin binding proteins, β-lactamases and ld-transpeptidases in bacteria associated with respiratory tract infections. *IUBMB life, 70*(9), 855-868.

Egan, A. J., Biboy, J., van't Veer, I., Breukink, E., & Vollmer, W. (2015). Activities and regulation of peptidoglycan synthases. *Phil. Trans. R. Soc. B, 370*(1679), 20150031.

Ehlert, K., & Höltje, J. V. (1996). Role of precursor translocation in coordination of murein and phospholipid synthesis in Escherichia coli. *Journal of bacteriology, 178*(23), 6766-6771.

El Khoury, J. Y., Boucher, N., Bergeron, M. G., Leprohon, P., & Ouellette, M. (2017). Penicillin induces alterations in glutamine metabolism in Streptococcus pneumoniae. *Scientific Reports, 7*(1), 14587.

El Zoeiby, A., Sanschagrin, F., Havugimana, P. C., Garnier, A., & Levesque, R. C. (2001). In vitro reconstruction of the biosynthetic pathway of peptidoglycan cytoplasmic precursor in Pseudomonas aeruginosa. *FEMS Microbiology Letters, 201*(2), 229-235.

El Zoeiby, A., Sanschagrin, F., Lamoureux, J., Darveau, A., & Levesque, R. C. (2000). Cloning, over-expression and purification of Pseudomonas aeruginosa murC encoding uridine diphosphate N-acetylmuramate: L-alanine ligase. *FEMS Microbiology Letters, 183*(2), 281-288.

El-Faham, A., & Albericio, F. (2011). Peptide coupling reagents, more than a letter soup. *Chemical reviews, 111*(11), 6557-6602.

Emami, K., Guyet, A., Kawai, Y., Devi, J., Wu, L. J., Allenby, N., . . . Errington, J. (2017). RodA as the missing glycosyltransferase in Bacillus subtilis and antibiotic discovery for the peptidoglycan polymerase pathway. *Nature Microbiology, 2*(3), 16253.

EUCAST (2018). Breakpoint tables for interpretation of MICs and zone diameters. Version 8.1. Available from: http://www.eucast.org. Accessed 22nd October, 2019

Farber, B. F., Eliopoulos, G. M., Ward, J. I., Ruoff, K. L., Syriopoulou, V., & Moellering, R. C. (1983). Multiply resistant viridans streptococci: susceptibility to beta-lactam antibiotics and comparison of penicillin-binding protein patterns. *Antimicrobial agents and chemotherapy, 24*(5), 702-705.

Faruki, H., & Sparling, P. (1986). Genetics of resistance in a non-beta-lactamase-producing gonococcus with relatively high-level penicillin resistance. *Antimicrobial Agents and Chemotherapy, 30*(6), 856-860.

Fast, W., & Sutton, L. D. (2013). Metallo-β-lactamase: inhibitors and reporter substrates. *Biochimica et Biophysica Acta (BBA)-Proteins and Proteomics, 1834*(8), 1648-1659.

Felmingham, D., Cantón, R., & Jenkins, S. G. (2007). Regional trends in β-lactam, macrolide, fluoroquinolone and telithromycin resistance among

Streptococcus pneumoniae isolates 2001–2004. *Journal of Infection, 55*(2), 111-118.

Fenton, A. K., Manuse, S., Flores-Kim, J., Garcia, P. S., Mercy, C., Grangeasse, C., . . . Rudner, D. Z. (2018). Phosphorylation-dependent activation of the cell wall synthase PBP2a in Streptococcus pneumoniae by MacP. *Proceedings of the National Academy of Sciences, 115*(11), 2812-2817.

Fenton, A. K., Mortaji, L. E., Lau, D. T. C., Rudner, D. Z., & Bernhardt, T. G. (2016). CozE is a member of the MreCD complex that directs cell elongation in Streptococcus pneumoniae. *Nature Microbiology, 2*, 16237.

Fields, G. B., & Noble, R. L. (1990). Solid phase peptide synthesis utilizing 9-fluorenylmethoxycarbonyl amino acids. *International journal of peptide and protein research, 35*(3), 161-214.

Figueiredo, T. A., Sobral, R. G., Ludovice, A. M., de Almeida, J. M. F., Bui, N. K., Vollmer, W., . . . Tomasz, A. (2012). Identification of genetic determinants and enzymes involved with the amidation of glutamic acid residues in the peptidoglycan of Staphylococcus aureus. *PLoS pathogens, 8*(1), e1002508.

Filipe, S. R., Pinho, M. G., & Tomasz, A. (2000). Characterization of the murMN Operon Involved in the Synthesis of Branched Peptidoglycan Peptides in Streptococcus pneumoniae. *Journal of Biological Chemistry*.

Filipe, S. R., Severina, E., & Tomasz, A. (2001). Functional analysis of Streptococcus pneumoniae MurM reveals the region responsible for its specificity in the synthesis of branched cell wall peptides. Journal of Biological Chemistry, 276(43), 39618-39628.

Filipe, S. R., & Tomasz, A. (2000). Inhibition of the expression of penicillin resistance in Streptococcus pneumoniae by inactivation of cell wall muropeptide branching genes. *Proceedings of the National Academy of Sciences, 97*(9), 4891-4896.

Fisher, J. F., Meroueh, S. O., & Mobashery, S. (2005). Bacterial resistance to β-lactam antibiotics: compelling opportunism, compelling opportunity. *Chemical reviews, 105*(2), 395-424.

Fleming, A. (1929). On the antibacterial action of cultures of a penicillium, with special reference to their use in the isolation of *B. influenzae*. *British Journal of Experimental Pathology, 10*(3), 226-236.

Fonvielle, M., Bouhss, A., Hoareau, C., Patin, D., Mengin-Lecreulx, D., Iannazzo, L., . . . Ethève-Quelquejeu, M. (2018). Synthesis of lipid-carbohydrate-peptidyl-RNA conjugates to explore the limits imposed by the substrate specificity of cell wall enzymes on the acquisition of drug resistance. *Chemistry–A European Journal*.

Fraipont, C., Sapunaric, F., Zervosen, A., Auger, G., Devreese, B., Lioux, T., . . . Van Beeumen, J. (2006). Glycosyl transferase activity of the Escherichia coli penicillin-binding protein 1b: specificity profile for the substrate. *Biochemistry, 45*(12), 4007-4013.

Galley, N. F. (2015). *The role of species-specific modifications in peptidoglycan biosynthesis.* (Doctororal dissertation, University of Warwick).

Galley, N. F., O'Reilly, A. M., & Roper, D. I. (2014). Prospects for novel inhibitors of peptidoglycan transglycosylases. *Bioorganic chemistry, 55*, 16-26.

Garcia-Bustos, J., Chait, B. T., & Tomasz, A. (1987). Structure of the peptide network of pneumococcal peptidoglycan. *Journal of Biological Chemistry, 262*(32), 15400-15405.

Garcia-Bustos, J., & Tomasz, A. (1990). A biological price of antibiotic resistance: major changes in the peptidoglycan structure of penicillin-resistant pneumococci. *Proceedings of the National Academy of Sciences of the United States of America, 87*(14), 5415-5419.

Gestwicki, J. E., Hsieh, H. V., & Pitner, J. B. (2001). Using receptor conformational change to detect low molecular weight analytes by surface plasmon resonance. *Analytical Chemistry, 73*(23), 5732-5737.

Gibson, D. G., Young, L., Chuang, R.-Y., Venter, J. C., Hutchison III, C. A., & Smith, H. O. (2009). Enzymatic assembly of DNA molecules up to several hundred kilobases. *Nature methods, 6*(5), 343.

Glauner, B. (1988). Separation and quantification of muropeptides with high-performance liquid chromatography. *Anal Biochem, 172*(2), 451-464.

Goodell, E. W., Markiewicz, Z., & Schwarz, U. (1983). Absence of oligomeric murein intermediates in Escherichia coli. *Journal of Bacteriology, 156*(1), 130-135.

Gram, C. (1884). The differential staining of Schizomycetes in tissue sections and in dried preparations. *Fortschitte der Medicin, 2*, 185-189.

Gray, B. M., Converse III, G. M., & Dillon Jr, H. C. (1980). Epidemiologic studies of Streptococcus pneumoniae in infants: acquisition, carriage, and infection during the first 24 months of life. *Journal of Infectious Diseases, 142*(6), 923-933.

Greene, N. G., Fumeaux, C., & Bernhardt, T. G. (2018). Conserved mechanism of cell-wall synthase regulation revealed by the identification of a new PBP activator in Pseudomonas aeruginosa. *Proceedings of the National Academy of Sciences, 115*(12), 3150-3155.

Greene, N. G., Narciso, A. R., Filipe, S. R., & Camilli, A. (2015). Peptidoglycan Branched Stem Peptides Contribute to Streptococcus pneumoniae Virulence by Inhibiting Pneumolysin Release. *PLoS Pathog, 11*(6), e1004996.

Guan, Y., Zhu, Q., Huang, D., Zhao, S., Lo, L. J., & Peng, J. (2015). An equation to estimate the difference between theoretically predicted and SDS PAGE-displayed molecular weights for an acidic peptide. *Scientific reports, 5*, 13370.

Guan, Z., Breazeale, S. D., & Raetz, C. R. (2005). Extraction and identification by mass spectrometry of undecaprenyl diphosphate-MurNAc-pentapeptide-GlcNAc from Escherichia coli. *Anal Biochem, 345*(2), 336-339.

Gupta, K., Donlan, J. A., Hopper, J. T., Uzdavinys, P., Landreh, M., Struwe, W. B., ... & Robinson, C. V. (2017). The role of interfacial lipids in stabilizing membrane protein oligomers. *Nature, 541*(7637), 421.

Hakenbeck, R., Grebe, T., Zähner, D., & Stock, J. B. (1999). β-Lactam resistance in Streptococcus pneumoniae: penicillin-binding proteins

and non-penicillin-binding proteins. *Molecular microbiology, 33*(4), 673-678.

Hammes, W. P., & Neuhaus, F. C. (1974). On the Specificity of Phospho-N-acetylmuramyl-pentapeptide Translocase: The Peptide Subunit Of Uridine Diphosphate-N-Acetylmuramyl-Pentapeptide. *Journal of Biological Chemistry, 249*(10), 3140-3150.

Helassa, N., Vollmer, W., Breukink, E., Vernet, T., & Zapun, A. (2012). The membrane anchor of penicillin-binding protein PBP2a from Streptococcus pneumoniae influences peptidoglycan chain length. *FEBS Journal, 279*(11), 2071-2081.

Henrichfreise, B., Brunke, M., & Viollier, P. H. J. C. B. (2016). Bacterial surfaces: the wall that SEDS built. *26*(21), R1158-R1160.

Henrichsen, J. (1995). Six newly recognized types of Streptococcus pneumoniae. *Journal of clinical microbiology, 33*(10), 2759.

Hernández-Rocamora, V. M., Otten, C. F., Radkov, A., Simorre, J.-P., Breukink, E., VanNieuwenhze, M., & Vollmer, W. (2018). Coupling of polymerase and carrier lipid phosphatase prevents product inhibition in peptidoglycan synthesis. *The Cell Surface, 2*, 1-13.

Hiller, N. L., Ahmed, A., Powell, E., Martin, D. P., Eutsey, R., Earl, J., ... & Sampath, R. (2010). Generation of genic diversity among Streptococcus pneumoniae strains via horizontal gene transfer during a chronic polyclonal pediatric infection. *PLoS pathogens, 6*(9), e1001108.

Hirst, R. A., Sikand, K. S., Rutman, A., Mitchell, T. J., Andrew, P. W., & O'Callaghan, C. (2000). Relative roles of pneumolysin and hydrogen peroxide from Streptococcus pneumoniae in inhibition of ependymal ciliary beat frequency. *Infection and immunity, 68*(3), 1557-1562.

Hitchcock, S. A., Eid, C. N., Aikins, J. A., Zia-Ebrahimi, M., & Blaszczak, L. C. (1998). The First Total Synthesis of Bacterial Cell Wall Precursor UDP−N-Acetylmuramyl-Pentapeptide (Park Nucleotide). *Journal of the American Chemical Society, 120*(8), 1916-1917.

Hjelmeland, L. M., Nebert, D. W., & Osborne Jr, J. C. (1983). Sulfobetaine derivatives of bile acids: Nondenaturing surfactants for membrane biochemistry. *Anal Biochem, 130*(1), 72-82.

Hoskins, J., Matsushima, P., Mullen, D. L., Tang, J., Zhao, G., Meier, T. I., . . . Jaskunas, S. R. (1999). Gene disruption studies of penicillin-binding proteins 1a, 1b, and 2a in Streptococcus pneumoniae. *Journal of Bacteriology, 181*(20), 6552-6555.

Hsu, Y.-P., Hall, E., Booher, G., Murphy, B., Radkov, A. D., Yablonowski, J., . . . Brun, Y. V. (2019). Fluorogenic d-amino acids enable real-time monitoring of peptidoglycan biosynthesis and high-throughput transpeptidation assays. *Nature Chemistry*, *11*(4), 335.

Huang, C.-Y., Shih, H.-W., Lin, L.-Y., Tien, Y.-W., Cheng, T.-J. R., Cheng, W.-C., . . . Ma, C. (2012). Crystal structure of Staphylococcus aureus transglycosylase in complex with a lipid II analog and elucidation of peptidoglycan synthesis mechanism. *Proceedings of the National Academy of Sciences, 109*(17), 6496-6501.

Huang, L. Y., Huang, S. H., Chang, Y. C., Cheng, W. C., Cheng, T. J. R., & Wong, C. H. (2014). Enzymatic synthesis of lipid II and analogues. *Angewandte Chemie International Edition, 53*(31), 8060-8065.

Huang, S.-H., Wu, W.-S., Huang, L.-Y., Huang, W.-F., Fu, W.-C., Chen, P.-T., . . . Wong, C.-H. (2013). New continuous fluorometric assay for bacterial transglycosylase using Forster resonance energy transfer. *Journal of the American Chemical Society, 135*(45), 17078-17089.

Hutchison, K. A., Dalman, F. C., Hoeck, W., Groner, B., & Pratt, W. B. (1993). Localization of the~ 12 kDa Mr discrepancy in gel migration of the mouse glucocorticoid receptor to the major phosphorylated cyanogen bromide fragment in the transactivating domain. The Journal of steroid biochemistry and molecular biology, 46(6), 681-686.

Hyams, C., Camberlein, E., Cohen, J. M., Bax, K., & Brown, J. S. (2010). The Streptococcus pneumoniae capsule inhibits complement activity and neutrophil phagocytosis by multiple mechanisms. *Infection and Immunity, 78*(2), 704-715.

Ilisz, I., Berkecz, R., & Peter, A. (2006). HPLC separation of amino acid enantiomers and small peptides on macrocyclic antibiotic-based chiral stationary phases: a review. *J Sep Sci, 29*(10), 1305-1321.

Ishiguro, E., & Ramey, W. (1978). Involvement of the relA gene product and feedback inhibition in the regulation of DUP-N-acetylmuramyl-peptide synthesis in Escherichia coli. *Journal of Bacteriology, 135*(3), 766-774.

Izaki, K., Matsuhashi, M., & Strominger, J. L. (1968). Biosynthesis of the Peptidoglycan of Bacterial Cell Walls XIII. Peptidoglycan Transpeptidase And D-Alanine Carboxypeptidase: Penicillin-Sensitive Enzymatic Reaction In Strains Of Escherichia Coli. *Journal of Biological Chemistry, 243*(11), 3180-3192.

Jamin, M., Damblon, C., Millier, S., Hakenbeck, R., & Frère, J.-M. (1993). Penicillin-binding protein 2x of Streptococcus pneumoniae: enzymic activities and interactions with β-lactams. *Biochemical Journal, 292*(3), 735-741.

Job, V., Carapito, R., Vernet, T., Dessen, A., & Zapun, A. (2008). Common Alterations in PBP1a from Resistant Streptococcus pneumoniae Decrease Its Reactivity toward β-Lactams STRUCTURAL INSIGHTS. *Journal of Biological Chemistry, 283*(8), 4886-4894.

Jones, R. N., Wilson, H., Novick, W., Barry, A., & Thornsberry, C. (1982). In vitro evaluation of CENTA, a new beta-lactamase-susceptible chromogenic cephalosporin reagent. *Journal of clinical microbiology, 15*(5), 954-958.

Josephine, H. R., Charlier, P., Davies, C., Nicholas, R. A., & Pratt, R. (2006). Reactivity of penicillin-binding proteins with peptidoglycan-mimetic β-lactams: what's wrong with these enzymes? *Biochemistry, 45*(51), 15873-15883.

Kahan, F. M., Kahan, J. S., Cassidy, P. J., & Kropp, H. (1974). The mechanism of action of fosfomycin (phosphonomycin). *Annals of the New York Academy of Sciences, 235*(1), 364-386.

Kardos, N., & Demain, A. (2011). Penicillin: the medicine with the greatest impact on therapeutic outcomes. *Applied Microbiology and Biotechnology, 92*(4), 677-687.

Kemp, D. S., Bernstein, Z., & Rebek Jr, J. (1970). Racemization during peptide couplings using the mixed anhydride, N-hydroxysuccinimide ester, 8-hydroxyquinoline ester, and acyl azide methods. *Journal of the American Chemical Society, 92*(15), 4756-4757.

Kern, T., Giffard, M., Hediger, S., Amoroso, A., Giustini, C., Bui, N. K., . . . Simorre, J.-P. (2010). Dynamics characterization of fully hydrated bacterial cell walls by solid-state NMR: evidence for cooperative binding of metal ions. *Journal of the American Chemical Society, 132*(31), 10911-10919.

King, D. T., Wasney, G. A., Nosella, M., Fong, A., & Strynadka, N. C. J. J. o. B. C. (2017). Structural insights into inhibition of Escherichia coli penicillin-binding protein 1B. *292*(3), 979-993.

Kocaoglu, O., Tsui, H.-C. T., Winkler, M. E., & Carlson, E. E. (2015). Profiling of β-lactam selectivity for penicillin-binding proteins in Streptococcus pneumoniae D39. *Antimicrobial Agents and Chemotherapy*, AAC. 05142-05114.

Koeller, K. M., & Wong, C.-H. (2001). Enzymes for chemical synthesis. *Nature, 409*(6817), 232.

Köhler, T., Michea-Hamzehpour, M., Epp, S. F., & Pechere, J. C. (1999). Carbapenem activities against Pseudomonas aeruginosa: respective contributions of OprD and efflux systems. *Antimicrobial agents and chemotherapy, 43*(2), 424-427.

Kohlrausch, U., & Höltje, J.-V. (1991). One-step purification procedure for UDP-N-acetylmuramyl-peptide murein precursors from Bacillus cereus. *FEMS Microbiology Letters, 78*(2-3), 253-257.

Koppe, U., Suttorp, N., & Opitz, B. (2012). Recognition of Streptococcus pneumoniae by the innate immune system. *Cellular microbiology, 14*(4), 460-466.

Kosowska, K., Jacobs, M., Bajaksouzian, S., Koeth, L., & Appelbaum, P. (2004). Alterations of penicillin-binding proteins 1A, 2X, and 2B in Streptococcus pneumoniae isolates for which amoxicillin MICs are higher than penicillin MICs. *Antimicrobial Agents and Chemotherapy, 48*(10), 4020-4022.

KPMG (2014). The Global Economic Impact of Anti-microbial Resistance. KPMG LLP.

Laddomada, F., Miyachiro, M. M., & Dessen, A. (2016). Structural Insights into Protein-Protein Interactions Involved in Bacterial Cell Wall Biogenesis. *Antibiotics, 5*(2), 14.

Lambert, M. P., & Neuhaus, F. C. (1972). Mechanism of D-cycloserine action: alanine racemase from Escherichia coli W. *Journal of Bacteriology, 110*(3), 978-987.

Lazar, K., & Walker, S. (2002). Substrate analogues to study cell-wall biosynthesis and its inhibition. *Current Opinion in Chemical Biology, 6*(6), 786-793.

le Maire, M., Champeil, P., & MÖller, J. V. (2000). Interaction of membrane proteins and lipids with solubilizing detergents. *Biochimica et Biophysica Acta (BBA)-Biomembranes, 1508*(1), 86-111.

le Maire, M., Kwee, S., Andersen, J. P., & Møller, J. V. (1983). Mode of interaction of polyoxyethyleneglycol detergents with membrane proteins. *European Journal of Biochemistry, 129*(3), 525-532.

Lee, C. R., Park, Y. H., Kim, Y. R., Peterkofsky, A., & Seok, Y. J. (2013). Phosphorylation-dependent mobility shift of proteins on SDS-PAGE is due to decreased binding of SDS. *Bulletin of the Korean Chemical Society, 34*(7), 2063-2066.

Lee, L., Gu, X.-X., & Nahm, M. (2014). Towards new broader spectrum pneumococcal vaccines: the future of pneumococcal disease prevention. *Vaccines, 2*(1), 112-128.

Lee, S. H., Jarantow, L. W., Wang, H., Sillaots, S., Cheng, H., Meredith, T. C., . . . Roemer, T. (2011). Antagonism of chemical genetic interaction networks resensitize MRSA to β-lactam antibiotics. *Chemistry & Biology, 18*(11), 1379-1389.

Legaree, B. A., Daniels, K., Weadge, J. T., Cockburn, D., & Clarke, A. J. (2007). Function of penicillin-binding protein 2 in viability and morphology of Pseudomonas aeruginosa. *Journal of antimicrobial chemotherapy, 59*(3), 411-424.

Lim, D., & Strynadka, N. C. (2002). Structural basis for the β lactam resistance of PBP2a from methicillin-resistant Staphylococcus aureus. *Nature Structural & Molecular Biology, 9*(11), 870.

Linares, J., Ardanuy, C., Pallares, R., & Fenoll, A. (2010). Changes in antimicrobial resistance, serotypes and genotypes in Streptococcus pneumoniae over a 30-year period. *Clinical Microbiology and Infection, 16*(5), 402-410.

Linke, D. (2009). Detergents: an overview. In *Methods in enzymology* (Vol. 463, pp. 603-617): Elsevier.

Liu, C.-Y., Guo, C.-W., Chang, Y.-F., Wang, J.-T., Shih, H.-W., Hsu, Y.-F., . . . Cheng, T.-J. R. (2010). Synthesis and evaluation of a new fluorescent transglycosylase substrate: Lipid II-based molecule possessing a dansyl-C20 polyprenyl moiety. *Organic letters, 12*(7), 1608-1611.

Liu, H., Sadamoto, R., Sears, P. S., & Wong, C.-H. (2001). An efficient chemoenzymatic strategy for the synthesis of wild-type and vancomycin-resistant bacterial cell-wall precursors: UDP-N-acetylmuramyl-peptides. *Journal of the American Chemical Society, 123*(40), 9916-9917.

Liu, H., & Wong, C.-H. (2006). Characterization of a transglycosylase domain of Streptococcus pneumoniae PBP1b. *Bioorganic & Medicinal Chemistry, 14*(21), 7187-7195.

Livermore, D. M., & Brown, D. F. (2001). Detection of β-lactamase-mediated resistance. *Journal of Antimicrobial Chemotherapy, 48*(suppl_1), 59-64.

Lloyd, A. J., Gilbey, A. M., Blewett, A. M., De Pascale, G., El Zoeiby, A., Levesque, R. C., . . . Dowson, C. G. (2008). Characterization of tRNA-dependent Peptide Bond Formation by MurM in the Synthesis of Streptococcus pneumoniae Peptidoglycan. *Journal of Biological Chemistry, 283*(10), 6402-6417.

Lovering, A. L., De Castro, L. H., Lim, D., & Strynadka, N. C. (2007). Structural insight into the transglycosylation step of bacterial cell-wall biosynthesis. *Science, 315*(5817), 1402-1405.

Lovering, A. L., Gretes, M., & Strynadka, N. C. (2008). Structural details of the glycosyltransferase step of peptidoglycan assembly. *Current Opinion in Structural Biology, 18*(5), 534-543.

Luna, O. F., Gomez, J., Cárdenas, C., Albericio, F., Marshall, S. H., & Guzmán, F. (2016). Deprotection reagents in Fmoc solid phase peptide synthesis: moving away from piperidine? *Molecules, 21*(11), 1542.

Lutkenhaus, J., Pichoff, S., & Du, S. (2012). Bacterial cytokinesis: from Z ring to divisome. *Cytoskeleton, 69*(10), 778-790.

MacGowan, A.P. and Wise, R. (2001). Establishing MIC breakpoints and the interpretation of in vitro susceptibility tests. *Journal of Antimicrobial Chemotherapy, 48*(Suppl. S1), 17-28.

Macheboeuf, P., Contreras-Martel, C., Job, V., Dideberg, O., & Dessen, A. (2006). Penicillin Binding Proteins: key players in bacterial cell cycle and drug resistance processes. *FEMS Microbiology Reviews, 30*(5), 673-691.

Macheboeuf, P., Di Guilmi, A. M., Job, V., Vernet, T., Dideberg, O., & Dessen, A. (2005). Active site restructuring regulates ligand recognition in class A penicillin-binding proteins. *Proceedings of the National Academy of Sciences, 102*(3), 577-582.

Macheboeuf, P., Lemaire, D., Martins, A. D. S., Dideberg, O., Jamin, M., & Dessen, A. (2008). Trapping of an acyl–enzyme intermediate in a penicillin-binding protein (PBP)-catalyzed reaction. *Journal of Molecular Biology, 376*(2), 405-413.

Mainardi, J.-L., Fourgeaud, M., Hugonnet, J.-E., Dubost, L., Brouard, J.-P., Ouazzani, J., . . . Arthur, M. (2005). A novel peptidoglycan cross-linking enzyme for a β-lactam-resistant transpeptidation pathway. *Journal of Biological Chemistry, 280*(46), 38146-38152.

Mainardi, J.-L., Legrand, R., Arthur, M., Schoot, B., van Heijenoort, J., & Gutmann, L. (2000). Novel mechanism of β-lactam resistance due to bypass of DD-transpeptidation in Enterococcus faecium. *Journal of Biological Chemistry, 275*(22), 16490-16496.

Manat, G., Roure, S., Auger, R., Bouhss, A., Barreteau, H., Mengin-Lecreulx, D., & Touzé, T. (2014). Deciphering the metabolism of undecaprenyl-phosphate: the bacterial cell-wall unit carrier at the membrane frontier. *Microbial Drug Resistance, 20*(3), 199-214.

Margolis, E. (2009). Hydrogen peroxide-mediated interference competition by Streptococcus pneumoniae has no significant effect on Staphylococcus aureus nasal colonization of neonatal rats. *Journal of Bacteriology, 191*(2), 571-575.

Massidda, O., Nováková, L., & Vollmer, W. (2013). From models to pathogens: how much have we learned about S treptococcus pneumoniae cell division? *Environmental microbiology, 15*(12), 3133-3157.

McAuley, K. E., Fyfe, P. K., Ridge, J. P., Isaacs, N. W., Cogdell, R. J., & Jones, M. R. (1999). Structural details of an interaction between cardiolipin and an integral membrane protein. *Proceedings of the National Academy of Sciences, 96*(26), 14706-14711.

McLeod, J. W., & J. Gordon. 1922. Production of hydrogen peroxide by bacteria. *Biochem. J. 16*, 499–506.

McPherson, D. C., & Popham, D. L. (2003). Peptidoglycan synthesis in the absence of class A penicillin-binding proteins in Bacillus subtilis. *185*(4), 1423-1431.

Meadow, P. M., Anderson, J. S., & Strominger, J. L. (1964). Enzymatic polymerization of UDP-acetylmuramyl. L-ala. D-glu. L-lys. D-ala. D-ala and UDP-acetylglucosamine by a particulate enzyme from Staphylococcus aureus and its inhibition by antibiotics. *Biochemical and biophysical research communications, 14*, 382.

Meeske, A. J., Riley, E. P., Robins, W. P., Uehara, T., Mekelanos, J. J., Kahne, D., . . . Rudner, D. Z. (2016). SEDS proteins are a widespread family of bacterial cell wall polymerases. *Nature, 537*(7622), 634.

Mellroth, P., Daniels, R., Eberhardt, A., Rönnlund, D., Blom, H., Widengren, J., ... & Henriques-Normark, B. (2012). LytA, major autolysin of Streptococcus pneumoniae, requires access to nascent peptidoglycan. *Journal of Biological Chemistry, 287*(14), 11018-11029.

Men, H., Park, P., Ge Mellroth, P., Daniels, R., Eberhardt, A., Rönnlund, D., Blom, H., Widengren, J., ... & Henriques-Normark, B. (2012). LytA, major autolysin of Streptococcus pneumoniae, requires access to nascent peptidoglycan. Journal of Biological Chemistry, 287(14), 11018-11029., M., & Walker, S. (1998). Substrate synthesis and activity assay for MurG. *Journal of the American Chemical Society, 120*(10), 2484-2485.

Mengin-Lecreulx, D., Falla, T., Blanot, D., van Heijenoort, J., Adams, D. J., & Chopra, I. (1999). Expression of the Staphylococcus aureusUDP-N-Acetylmuramoyl-l-Alanyl-d-Glutamate: l-Lysine Ligase in Escherichia coli and Effects on Peptidoglycan Biosynthesis and Cell Growth. *Journal of Bacteriology, 181*(19), 5909-5914.

Mesleh, M. F., Rajaratnam, P., Conrad, M., Chandrasekaran, V., Liu, C. M., Pandya, B. A., . . . Becker, B. (2016). Targeting bacterial cell wall peptidoglycan synthesis by inhibition of glycosyltransferase activity. *Chemical biology & drug design, 87*(2), 190-199.

Mohammadi, T., van Dam, V., Sijbrandi, R., Vernet, T., Zapun, A., Bouhss, A., . . . Breukink, E. (2011). Identification of FtsW as a transporter of lipid-linked cell wall precursors across the membrane. *Embo j, 30*(8), 1425-1432.

Mohr, K. I. (2016). History of antibiotics research. In *How to Overcome the Antibiotic Crisis* (pp. 237-272): Springer.

Morlot, C., Straume, D., Peters, K., Hegnar, O. A., Simon, N., Villard, A.-M., . . . Gravier-Pelletier, C. (2018). Structure of the essential peptidoglycan amidotransferase MurT/GatD complex from Streptococcus pneumoniae. *Nature Communications, 9*(1), 3180.

Mueller, J. H., Hinton, J. (1941). A protein-free medium for primary isolation of the gonococcus and meningococcus. *Proceedings of the Society for Experimental Biology and Medicine, 48*(1), 330-333.

Mukhopadhyay, K., Whitmire, W., Xiong, Y. Q., Molden, J., Jones, T., Peschel, A., . . . Bayer, A. S. (2007). In vitro susceptibility of Staphylococcus aureus to thrombin-induced platelet microbicidal protein-1 (tPMP-1) is influenced by cell membrane phospholipid composition and asymmetry. *Microbiology, 153*(4), 1187-1197.

Müller, P., Ewers, C., Bertsche, U., Anstett, M., Kallis, T., Breukink, E., . . . Vollmer, W. (2007). The essential cell division protein FtsN interacts with the murein (peptidoglycan) synthase PBP1B in Escherichia coli. *Journal of Biological Chemistry, 282*(50), 36394-36402.

Mullis, K., Faloona, F., Scharf, S., Saiki, R., Horn, G., & Erlich, H. (1986). *Specific enzymatic amplification of DNA in vitro: the polymerase chain reaction.* In Cold Spring Harbor symposia on quantitative biology (Vol. 51, pp. 263-273). Cold Spring Harbor Laboratory Press.

Münch, D., Roemer, T., Lee, S. H., Engeser, M., Sahl, H. G., & Schneider, T. (2012). Identification and in vitro analysis of the GatD/MurT enzyme-complex catalyzing lipid II amidation in Staphylococcus aureus. *PLoS Pathog, 8*(1), e1002509.

Nagai, K., Davies, T. A., Jacobs, M. R., & Appelbaum, P. C. (2002). Effects of amino acid alterations in penicillin-binding proteins (PBPs) 1a, 2b, and 2x on PBP affinities of penicillin, ampicillin, amoxicillin, cefditoren, cefuroxime, cefprozil, and cefaclor in 18 clinical isolates of penicillin-susceptible,-intermediate, and-resistant pneumococci. *Antimicrobial Agents and Chemotherapy, 46*(5), 1273-1280.

Nakamura, J., Yamashiro, H., Miya, H., Nishiguchi, K., Maki, H., & Arimoto, H. (2013). Staphylococcus aureus Penicillin-Binding Protein 2 Can Use Depsi-Lipid II Derived from Vancomycin-Resistant Strains for Cell Wall Synthesis. *Chemistry–A European Journal, 19*(36), 12104-12112.

Narayan, R. S., & VanNieuwenhze, M. S. (2007). Synthesis of substrates and biochemical probes for study of the peptidoglycan biosynthetic pathway. *European journal of organic chemistry, 2007*(9), 1399-1414.

Neuhaus, F. C., & Lynch, J. L. (1964). The enzymatic synthesis of D-alanyl-D-alanine. III. On the inhibition of D-alanyl-D-alanine synthetase by the antibiotic D-cycloserine. *Biochemistry, 3*(4), 471-480.

Neuhaus, F. C., & Struve, W. G. (1965). Enzymatic synthesis of analogs of the cell-wall precursor. I. Kinetics and specificity of uridine diphospho-N-acetylmuramyl-L-alanyl-D-glutamyl-L-lysine: D-alanyl-D-alanine ligase (adenosine diphosphate) from Streptococcus faecalis R. *Biochemistry, 4*(1), 120-131.

Nuorti, J. P., & Whitney, C. G. (2010). Updated recommendations for prevention of invasive pneumococcal disease among adults using the 23-valent pneumococcal polysaccharide vaccine (PPSV23). Morbidity and mortality weekly report, 59(34), 1102-1106.

O'Callaghan, C. H., Morris, A., Kirby, S. M., & Shingler, A. (1972). Novel method for detection of β-lactamases by using a chromogenic cephalosporin substrate. *Antimicrobial Agents and Chemotherapy, 1*(4), 283-288.

Offant, J., Terrak, M., Derouaux, A., Breukink, E., Nguyen-Distèche, M., Zapun, A., & Vernet, T. (2010). Optimization of conditions for the glycosyltransferase activity of penicillin-binding protein 1a from Thermotoga maritima. *The FEBS journal, 277*(20), 4290-4298.

Osborn, M. (1969). Structure and biosynthesis of the bacterial cell wall. *Annual Review of Biochemistry, 38*(1), 501-538.

Ottolenghi-Nightingale, E. (1972). Competence of pneumococcal isolates and bacterial transformations in man. *Infection and immunity, 6*(5), 785-792.

Pai, H., Kim, J.-W., Kim, J., Lee, J. H., Choe, K. W., & Gotoh, N. (2001). Carbapenem resistance mechanisms in Pseudomonas aeruginosa clinical isolates. *Antimicrobial Agents and Chemotherapy, 45*(2), 480-484.

Paik, J., Kern, I., Lurz, R., & Hakenbeck, R. (1999). Mutational analysis of the Streptococcus pneumoniae bimodular class A penicillin-binding proteins. *Journal of Bacteriology, 181*(12), 3852-3856.

Paradis-Bleau, C., Markovski, M., Uehara, T., Lupoli, T. J., Walker, S., Kahne, D. E., & Bernhardt, T. G. (2010). Lipoprotein cofactors located in the

outer membrane activate bacterial cell wall polymerases. *Cell, 143*(7), 1110-1120.

Park, J. T. (1952). Uridine-5'-Pyrophosphate Derivatives I. Isolation From Staphylococcus Aureus. *Journal of Biological Chemistry, 194*(2), 877-884.

Park, J. T., & Uehara, T. (2008). How Bacteria Consume Their Own Exoskeletons (Turnover and Recycling of Cell Wall Peptidoglycan). *Microbiology and Molecular Biology Reviews : MMBR, 72*(2), 211-227.

Park, C., & Marqusee, S. (2005). Pulse proteolysis: a simple method for quantitative determination of protein stability and ligand binding. *Nature methods, 2*(3), 207.

Park, B., Nizet, V., & Liu, G. Y. (2008). Role of Staphylococcus aureus catalase in niche competition against Streptococcus pneumoniae. *Journal of Bacteriology, 190*(7), 2275-2278.

Park, W., Seto, H., Hakenbeck, R., & Matsuhashi, M. (1985). Major peptidoglycan transglycosylase activity in Streptococcus pneumoniae that is not a penicillin-binding protein. *FEMS Microbiology Letters, 27*(1), 45-48.

Pericone, C. D., Overweg, K., Hermans, P. W., & Weiser, J. N. (2000). Inhibitory and bactericidal effects of hydrogen peroxide production by Streptococcus pneumoniae on other inhabitants of the upper respiratory tract. *Infection and immunity, 68*(7), 3990-3997.

Perlstein, D. L., Zhang, Y., Wang, T.-S., Kahne, D. E., & Walker, S. (2007). The direction of glycan chain elongation by peptidoglycan glycosyltransferases. *Journal of the American Chemical Society, 129*(42), 12674-12675.

Pesakhov, S., Benisty, R., Sikron, N., Cohen, Z., Gomelsky, P., Khozin-Goldberg, I., . . . Porat, N. (2007). Effect of hydrogen peroxide production and the Fenton reaction on membrane composition of Streptococcus pneumoniae. *Biochimica et Biophysica Acta (BBA) - Biomembranes, 1768*(3), 590-597.

Pinho, M. G., Kjos, M., & Veening, J.-W. (2013). How to get (a) round: mechanisms controlling growth and division of coccoid bacteria. *Nature Reviews Microbiology, 11*(9), 601.

Pompliano, D. L., Gomez, R. P., & Anthony, N. J. (1992). Intramolecular fluorescence enhancement: a continuous assay of Ras farnesyl: protein transferase. *Journal of the American Chemical Society, 114*(20), 7945-7946.

Pons, R., Valiente, M., & Montalvo, G. (2010). Structure of Aggregates in Diluted Aqueous Octyl Glucoside/Tetraethylene Glycol Monododecyl Ether Mixtures with Different Alkanols. *Langmuir, 26*(4), 2256-2262.

Poole, K. (2004). Resistance to β-lactam antibiotics. *Cellular and Molecular Life Sciences CMLS, 61*(17), 2200-2223.

Poole, K. (2005). Efflux-mediated antimicrobial resistance. *Journal of Antimicrobial Chemotherapy, 56*(1), 20-51.

Prudhomme, M., Attaiech, L., Sanchez, G., Martin, B., & Claverys, J.-P. J. S. (2006). Antibiotic stress induces genetic transformability in the human pathogen Streptococcus pneumoniae. *313*(5783), 89-92.

Punekar, A. S., Samsudin, F., Lloyd, A. J., Dowson, C. G., Scott, D. J., Khalid, S., & Roper, D. I. (2018). The role of the jaw subdomain of

peptidoglycan glycosyltransferases for lipid II polymerization. *The Cell Surface, 2*, 54-66.

Qiao, Y., Srisuknimit, V., Rubino, F., Schaefer, K., Ruiz, N., Walker, S., & Kahne, D. (2017). Lipid II overproduction allows direct assay of transpeptidase inhibition by β-lactams. *Nature chemical biology, 13*(7), 793.

Rai, P., Parrish, M., Tay, I. J. J., Li, N., Ackerman, S., He, F., ... & Engelward, B. P. (2015). Streptococcus pneumoniae secretes hydrogen peroxide leading to DNA damage and apoptosis in lung cells. *Proceedings of the National Academy of Sciences, 112*(26), E3421-E3430.

Randle, E., Ninis, N., & Inwald, D. (2011). Invasive pneumococcal disease. *Archives of Disease in Childhood-Education and Practice, 96*(5), 183-190.

Rath, A., Glibowicka, M., Nadeau, V.G., Chen, G. and Deber, C.M., 2009. Detergent binding explains anomalous SDS-PAGE migration of membrane proteins. *Proceedings of the National Academy of Sciences, 106*(6), pp.1760-1765.

Reddy, S. G., Waddell, S. T., Kuo, D. W., Wong, K. K., & Pompliano, D. L. (1999). Preparative enzymatic synthesis and characterization of the cytoplasmic intermediates of murein biosynthesis. *Journal of the American Chemical Society, 121*(6), 1175-1178.

Regev-Yochay, G., Dagan, R., Raz, M., Carmeli, Y., Shainberg, B., Derazne, E., ... & Rubinstein, E. (2004). Association between carriage of Streptococcus pneumoniae and Staphylococcus aureus in children. *Jama, 292*(6), 716-720.

Regev-Yochay, G., Raz, M., Dagan, R., Porat, N., Shainberg, B., Pinco, E., . . . Rubinstein, E. (2004). Nasopharyngeal carriage of Streptococcus pneumoniae by adults and children in community and family settings. *Clinical Infectious Diseases, 38*(5), 632-639.

Regev-Yochay, G., Trzciński, K., Thompson, C. M., Malley, R., & Lipsitch, M. (2006). Interference between Streptococcus pneumoniae and Staphylococcus aureus: in vitro hydrogen peroxide-mediated killing by Streptococcus pneumoniae. *Journal of Bacteriology, 188*(13), 4996-5001.

Reichmann, P., König, A., Linares, J., Alcaide, F., Tenover, F. C., Swidsinski, S., & Hakenbeck, R. (1997). A global gene pool for high-level cephalosporin resistance in commensal Streptococcus species and Streptococcus pneumoniae. *Journal of Infectious Diseases, 176*(4), 1001-1012.

Reynolds, P. (1961). Studies on the mode of action of vancomycin. *Biochim Biophys Acta, 52*, 403.

Righino, B., Galisson, F., Pirolli, D., Vitale, S., Réty, S., Gouet, P., & De Rosa, M. C. (2018). Structural model of the full-length Ser/Thr protein kinase StkP from S. pneumoniae and its recognition of peptidoglycan fragments. *Journal of Biomolecular Structure and Dynamics, 36*(14), 3666-3679.

Rodionov, D. G., & Ishiguro, E. E. (1996). Dependence of peptidoglycan metabolism on phospholipid synthesis during growth of Escherichia coli. *Microbiology, 142*(10), 2871-2877.

Rohrer, S., Ehlert, K., Tschierske, M., Labischinski, H., & Berger-Bächi, B. (1999). The essential Staphylococcus aureus gene fmhB is involved in the first step of peptidoglycan pentaglycine interpeptide formation. *Proceedings of the National Academy of Sciences, 96*(16), 9351-9356.

Roseman, S., Distler, J., Moffatt, J., & Khorana, H. (1961). Nucleoside polyphosphates. XI. 1 An improved general method for the synthesis of nucleotide coenzymes. Syntheses of uridine-5', cytidine-5'and guanosine-5'diphosphate derivatives. *Journal of the American Chemical Society, 83*(3), 659-663.

Roychoudhury, S., Kaiser, R. E., Brems, D. N., & Yeh, W.-K. (1996). Specific interaction between beta-lactams and soluble penicillin-binding protein 2a from methicillin-resistant Staphylococcus aureus: development of a chromogenic assay. *Antimicrobial Agents and Chemotherapy, 40*(9), 2075-2079.

Saha, S. L., Van Nieuwenhze, M. S., Hornback, W. J., Aikins, J. A., & Blaszczak, L. C. (2001). Synthesis of an orthogonally protected precursor to the glycan repeating unit of the bacterial cell wall. *Organic letters, 3*(22), 3575-3577.

Sauvage, E., Kerff, F., Terrak, M., Ayala, J. A., & Charlier, P. (2008). The penicillin-binding proteins: structure and role in peptidoglycan biosynthesis. *FEMS Microbiology Reviews, 32*(2), 234-258.

Schägger, H., & Von Jagow, G. (1987). Tricine-sodium dodecyl sulfate-polyacrylamide gel electrophoresis for the separation of proteins in the range from 1 to 100 kDa. *Anal Biochem, 166*(2), 368-379.

Schleifer, K. H., & Kandler, O. (1972). Peptidoglycan types of bacterial cell walls and their taxonomic implications. *Bacteriological reviews, 36*(4), 407.

Schneider, T., & Sahl, H.-G. (2010). An oldie but a goodie – cell wall biosynthesis as antibiotic target pathway. *International Journal of Medical Microbiology, 300*(2–3), 161-169.

Schneider, T., Senn, M. M., Berger-Bächi, B., Tossi, A., Sahl, H. G., & Wiedemann, I. (2004). In vitro assembly of a complete, pentaglycine interpeptide bridge containing cell wall precursor (lipid II-Gly5) of Staphylococcus aureus. *Mol Microbiol, 53*(2), 675-685.

Schwartz, B., Markwalder, J. A., Seitz, S. P., Wang, Y., & Stein, R. L. (2002). A kinetic characterization of the glycosyltransferase activity of Eschericia coli PBP1b and development of a continuous fluorescence assay. *Biochemistry, 41*(41), 12552-12561.

Schwartz, B., Markwalder, J. A., & Wang, Y. (2001). Lipid II: Total Synthesis of the Bacterial Cell Wall Precursor and Utilization as a Substrate for Glycosyltransfer and Transpeptidation by Penicillin Binding Protein (PBP) 1b of Eschericia c oli. *Journal of the American Chemical Society, 123*(47), 11638-11643.

Sham, L.-T., Butler, E. K., Lebar, M. D., Kahne, D., Bernhardt, T. G., & Ruiz, N. (2014). MurJ is the flippase of lipid-linked precursors for peptidoglycan biogenesis. *Science, 345*(6193), 220-222.

Shapiro, A. B., Gu, R.-F., Gao, N., Livchak, S., & Thresher, J. (2013). Continuous fluorescence anisotropy-based assay of BOCILLIN FL penicillin reaction with penicillin binding protein 3. *Anal Biochem, 439*(1), 37-43.

Shelake, R. M., Ito, Y., Masumoto, J., Morita, E. H., & Hayashi, H. (2017). A novel mechanism of “metal gel-shift” by histidine-rich Ni2+-binding Hpn protein from Helicobacter pylori strain SS1. *PloS one, 12*(2), e0172182.

Shi, Y., Mowery, R. A., Ashley, J., Hentz, M., Ramirez, A. J., Bilgicer, B., ... & Shaw, B. F. (2012). Abnormal SDS-PAGE migration of cytosolic proteins can identify domains and mechanisms that control surfactant binding. *Protein Science, 21*(8), 1197-1209.

Shockman, G. D., & Barren, J. F. (1983). Structure, function, and assembly of cell walls of gram-positive bacteria. *Annual Review of Microbiology, 37*(1), 501-527.

Sievers, F., Wilm, A., Dineen, D., Gibson, T. J., Karplus, K., Li, W., . . . Söding, J. (2011). Fast, scalable generation of high-quality protein multiple sequence alignments using Clustal Omega. *Molecular systems biology, 7*(1), 539.

Siewert, G., & Strominger, J. L. (1968). Biosynthesis of the Peptidoglycan of Bacterial Cell Walls: XI. Formation Of The Isoglutamine Amide Group In The Cell Walls Of Staphylococcus Aureus. *Journal of Biological Chemistry, 243*(4), 783-790.

Smith, A. M., & Klugman, K. P. (1998). Alterations in PBP 1A Essential for High-Level Penicillin Resistance in Streptococcus pneumoniae. *Antimicrobial Agents and Chemotherapy, 42*(6), 1329-1333.

Smith, A. M., & Klugman, K. P. (2000). Non-penicillin-binding protein mediated high-level penicillin and cephalosporin resistance in a Hungarian clone of Streptococcus pneumoniae. *Microbial Drug Resistance, 6*(2), 105-110.

Sobhanifar, S., King, D. T., & Strynadka, N. C. (2013). Fortifying the wall: synthesis, regulation and degradation of bacterial peptidoglycan. *Current Opinion in Structural Biology, 23*(5), 695-703.

Srisuknimit, V., Qiao, Y., Schaefer, K., Kahne, D., & Walker, S. (2017). Peptidoglycan cross-linking preferences of Staphylococcus aureus penicillin-binding proteins have implications for treating MRSA infections. *Journal of the American Chemical Society, 139*(29), 9791-9794.

Staros, J. V., Wright, R. W., & Swingle, D. M. (1986). Enhancement by N-hydroxysulfosuccinimide of water-soluble carbodiimide-mediated coupling reactions. *Anal Biochem, 156*(1), 220-222.

Stein, R. L., Barbosa, M. D., & Bruckner, R. (2000). Kinetic and mechanistic studies of signal peptidase I from Escherichia coli. *Biochemistry, 39*(27), 7973-7983.

Stone, M. R. L., Butler, M. S., Phetsang, W., Cooper, M. A., & Blaskovich, M. A. (2018). Fluorescent antibiotics: new research tools to fight antibiotic resistance. *Trends in Biotechnology, 36*(5), 523-536.

Straume, D., Piechowiak, K. W., Olsen, S., Stamsås, G. A., Berg, K. H., Kjos, M., . . . Håvarstein, L. S. (2019). Class A PBPs have a distinct and unique role in the construction of the pneumococcal cell wall. *bioRxiv*, 665463.

Studier, F. W. (2005). Protein production by auto-induction in high-density shaking cultures. *Protein Expression and Purification, 41*(1), 207-234.

Studier, F. W., & Moffatt, B. A. (1986). Use of bacteriophage T7 RNA polymerase to direct selective high-level expression of cloned genes. *Journal of Molecular Biology, 189*(1), 113-130.

Sung, M.-T., Lai, Y.-T., Huang, C.-Y., Chou, L.-Y., Shih, H.-W., Cheng, W.-C., . . . Ma, C. (2009). Crystal structure of the membrane-bound bifunctional transglycosylase PBP1b from Escherichia coli. *Proceedings of the National Academy of Sciences, 106*(22), 8824-8829.

Swoboda, J. G., Campbell, J., Meredith, T. C., & Walker, S. (2010). Wall teichoic acid function, biosynthesis, and inhibition. *Chembiochem, 11*(1), 35-45.

Tacconelli, E., Carrara, E., Savoldi, A., Harbarth, S., Mendelson, M., Monnet, D. L., . . . Carmeli, Y. J. T. L. I. D. (2018). Discovery, research, and development of new antibiotics: the WHO priority list of antibiotic-resistant bacteria and tuberculosis. *18*(3), 318-327.

Taguchi, A., Welsh, M. A., Marmont, L. S., Lee, W., Kahne, D., Bernhardt, T. G., & Walker, S. (2018). FtsW is a peptidoglycan polymerase that is activated by its cognate penicillin-binding protein. *bioRxiv*, 358663.

Taylor, J., Hafner, M., Yerushalmi, E., Smith, R., Bellasio, J., Vardavas, R., ... & Rubin, J. (2014). Estimating the economic costs of antimicrobial resistance. Model and Results. RAND Corporation, Cambridge, UK.

Teo, A. C., Lee, S. C., Pollock, N. L., Stroud, Z., Hall, S., Thakker, A., . . . Roper, D. I. (2019). Analysis of SMALP co-extracted phospholipids shows distinct membrane environments for three classes of bacterial membrane protein. *Scientific Reports, 9*(1), 1813.

Terrak, M., Ghosh, T. K., van Heijenoort, J., Van Beeumen, J., Lampilas, M., Aszodi, J., . . . Nguyen-Disteche, M. (1999). The catalytic, glycosyl transferase and acyl transferase modules of the cell wall peptidoglycan-polymerizing penicillin-binding protein 1b of Escherichia coli. *Mol Microbiol, 34*(2), 350-364.

Trombe, M.-C., Lanéelle, M.-A., & Lanéelle, G. (1979). Lipid composition of aminopterin-resistant and sensitive strains of Streptococcus pneumoniae. Effect of aminopterin inhibition. *Biochimica et Biophysica Acta (BBA) - Lipids and Lipid Metabolism, 574*(2), 290-300.

Turnidge, J. and Paterson, D.L. (2007). Setting and revising antibacterial susceptibility breakpoints. *Clinical Microbiology Reviews, 20*(3), 391-408.

Typas, A., Banzhaf, M., Gross, C. A., & Vollmer, W. (2012). From the regulation of peptidoglycan synthesis to bacterial growth and morphology. *Nat Rev Micro, 10*(2), 123-136.

Typas, A., Banzhaf, M., van den Berg van Saparoea, B., Verheul, J., Biboy, J., Nichols, R. J., . . . Vollmer, W. (2010). Regulation of Peptidoglycan Synthesis by Outer-Membrane Proteins. *Cell, 143*(7), 1097-1109.

Umbreit, J. N., & Strominger, J. L. (1972). Isolation of the lipid intermediate in peptidoglycan biosynthesis from Escherichia coli. *Journal of Bacteriology, 112*(3), 1306.

van den Brink-van der Laan, E., Boots, J.-W. P., Spelbrink, R. E. J., Kool, G. M., Breukink, E., Killian, J. A., & de Kruijff, B. (2003). Membrane Interaction of the Glycosyltransferase MurG: a Special Role for Cardiolipin. *Journal of Bacteriology, 185*(13), 3773-3779.

Van Heijenoort, Y., Gómez, M., Derrien, M., Ayala, J., & Van Heijenoort, J. (1992). Membrane intermediates in the peptidoglycan metabolism of Escherichia coli: possible roles of PBP 1b and PBP 3. *Journal of Bacteriology, 174*(11), 3549-3557.

VanAken, T., Foxall-VanAken, S., Castleman, S., & Ferguson-Miller, S. (1986). Alkyl glycoside detergents: Synthesis and applications to the study of membrane proteins. In *Methods in enzymology* (Vol. 125, pp. 27-35): Elsevier.

VanNieuwenhze, M. S., Mauldin, S. C., Zia-Ebrahimi, M., Aikins, J. A., & Blaszczak, L. C. (2001). The total synthesis of lipid I. *Journal of the American Chemical Society, 123*(29), 6983-6988.

VanNieuwenhze, M. S., Mauldin, S. C., Zia-Ebrahimi, M., Winger, B. E., Hornback, W. J., Saha, S. L., . . . Blaszczak, L. C. (2002). The First Total Synthesis of Lipid II: The Final Monomeric Intermediate in Bacterial Cell Wall Biosynthesis. *Journal of the American Chemical Society, 124*(14), 3656-3660.

Vollmer, W., Blanot, D., & De Pedro, M. A. (2008). Peptidoglycan structure and architecture. *FEMS Microbiology Reviews, 32*(2), 149-167.

Vollmer, W., Joris, B., Charlier, P., & Foster, S. (2008). Bacterial peptidoglycan (murein) hydrolases. *FEMS Microbiology Reviews, 32*(2), 259-286.

Vollmer, W., Massidda, O., & Tomasz, A. (2019). The Cell Wall of Streptococcus pneumoniae. *Microbiology spectrum, 7*(3).

Wahl, B., O'Brien, K. L., Greenbaum, A., Majumder, A., Liu, L., Chu, Y., . . . Campbell, H. (2018). Burden of Streptococcus pneumoniae and Haemophilus influenzae type b disease in children in the era of conjugate vaccines: global, regional, and national estimates for 2000–15. *The Lancet Global Health, 6*(7), e744-e757.

Walsh, T. R., Toleman, M. A., Poirel, L., & Nordmann, P. (2005). Metallo-β-lactamases: the quiet before the storm? *Clin Microbiol Rev, 18*(2), 306-325.

Wang, Q. M., Peery, R. B., Johnson, R. B., Alborn, W. E., Yeh, W.-K., & Skatrud, P. L. (2001). Identification and characterization of a monofunctional glycosyltransferase from Staphylococcus aureus. *Journal of Bacteriology, 183*(16), 4779-4785.

Wang, T.-S. A., Manning, S. A., Walker, S., & Kahne, D. (2008). Isolated peptidoglycan glycosyltransferases from different organisms produce different glycan chain lengths. *Journal of the American Chemical Society, 130*(43), 14068-14069.

Wang, W., Chen, Z., Billiar, T. R., Stang, M. T., & Gao, W. (2013). The carboxyl-terminal amino acids render pro-human LC3B migration similar to lipidated LC3B in SDS-PAGE. *PloS one, 8*(9), e74222

Ward, J. B., & Perkins, H. R. (1973). The direction of glycan synthesis in a bacterial peptidoglycan. *Biochemical Journal, 135*(4), 721-728.

Weidenmaier, C., & Peschel, A. (2008). Teichoic acids and related cell-wall glycopolymers in Gram-positive physiology and host interactions. *Nat Rev Micro, 6*(4), 276-287.

Weinstein, M. P., Klugman, K. P., & Jones, R. N. (2009). Rationale for revised penicillin susceptibility breakpoints versus Streptococcus pneumoniae: coping with antimicrobial susceptibility in an era of resistance. *Clinical infectious diseases, 48*(11), 1596-1600.

Weiser, J. N. (2010). The pneumococcus: why a commensal misbehaves. *Journal of molecular medicine, 88*(2), 97-102.
Welzel, P. (2005). Syntheses around the transglycosylation step in peptidoglycan biosynthesis. *Chemical reviews, 105*(12), 4610-4660.
Weston, A., Ward, J., & Perkins, H. (1977). Biosynthesis of peptidoglycan in wall plus membrane preparations from Micrococcus luteus: direction of chain extension, length of chains and effect of penicillin on cross-linking. *Microbiology, 99*(1), 171-181.
Wilke, M. S., Lovering, A. L., & Strynadka, N. C. J. (2005). β-Lactam antibiotic resistance: a current structural perspective. *Current Opinion in Microbiology, 8*(5), 525-533.
Winkelman, W., & Gratton, D. (1989). Topical antibacterials. *Clinics in dermatology, 7*(3), 156-162.
Wolf, A. J., & Underhill, D. M. (2018). Peptidoglycan recognition by the innate immune system. *Nature Reviews Immunology, 18*(4), 243.
Wood, J. M. (2018). Perspective: challenges and opportunities for the study of cardiolipin, a key player in bacterial cell structure and function. *Current genetics, 64*(4), 795-798.
World Health Organisation. (2018). Antimicrobial Resistance Fact Sheet. *Fact Sheets.* Retrieved from https://www.who.int/en/news-room/fact-sheets/detail/antimicrobial-resistance
Yagupsky, P., Porat, N., Fraser, D., Prajgrod, F., Merires, M., McGee, L., ... & Dagan, R. (1998). Acquisition, carriage, and transmission of pneumococci with decreased antibiotic susceptibility in young children attending a day care facility in southern Israel. *Journal of Infectious Diseases, 177*(4), 1003-1012.
Ye, X.-Y., Lo, M.-C., Brunner, L., Walker, D., Kahne, D., & Walker, S. (2001). Better substrates for bacterial transglycosylases. *Journal of the American Chemical Society, 123*(13), 3155-3156.
Yuan, Y., Barrett, D., Zhang, Y., Kahne, D., Sliz, P., & Walker, S. (2007). Crystal structure of a peptidoglycan glycosyltransferase suggests a model for processive glycan chain synthesis. *Proceedings of the National Academy of Sciences, 104*(13), 5348-5353.
Zapun, A., Philippe, J., Abrahams, K. A., Signor, L., Roper, D. I., Breukink, E., & Vernet, T. (2013). In vitro Reconstitution of Peptidoglycan Assembly from the Gram-Positive Pathogen Streptococcus pneumoniae. *ACS Chemical Biology, 8*(12), 2688-2696.
Zapun, A., Vernet, T., & Pinho, M. G. (2008). The different shapes of cocci. *FEMS Microbiology Reviews, 32*(2), 345-360.
Zhang, Y., Fechter, E. J., Wang, T.-S. A., Barrett, D., Walker, S., & Kahne, D. E. (2007). Synthesis of Heptaprenyl− Lipid IV to Analyze Peptidoglycan Glycosyltransferases. *J. Am. Chem. Soc, 129*(11), 3080-3081.
Zhao, G., Meier, T. I., Kahl, S. D., Gee, K. R., & Blaszczak, L. C. (1999). BOCILLIN FL, a sensitive and commercially available reagent for detection of penicillin-binding proteins. *Antimicrobial Agents and Chemotherapy, 43*(5), 1124-1128.
Zhao, G., Yeh, W.-K., Carnahan, R. H., Flokowitsch, J., Meier, T. I., Alborn, W., . . . Jaskunas, S. R. J. J. o. b. (1997). Biochemical characterization of penicillin-resistant and-sensitive penicillin-binding protein 2x transpeptidase activities of Streptococcus pneumoniae and

mechanistic implications in bacterial resistance to beta-lactam antibiotics. *179*(15), 4901-4908.
Zhao, H., Patel, V., Helmann, J. D., & Dörr, T. (2017). Don’t let sleeping dogmas lie: new views of peptidoglycan synthesis and its regulation. *Mol Microbiol, 106*(6), 847-860.

Appendices

Appendices to Chapter 3

Appendix 3.1: Ease of separation of UDP-Mur*N*Ac peptides with and without amidation

Appendix 3.1 compares the elution profiles of amidated (UDP-Mur*N*Ac 5P (iGln)) and non-amidated (UDP-Mur*N*Ac 5P (Glu)). When purified by anion exchange on the same gradient of ammonium acetate, the peak elution of each substrate was separated by ~75 mL. This distinct elution would allow separation of un-amidated substrate arising from the UDP-Mur*N*Ac peptide synthesis.

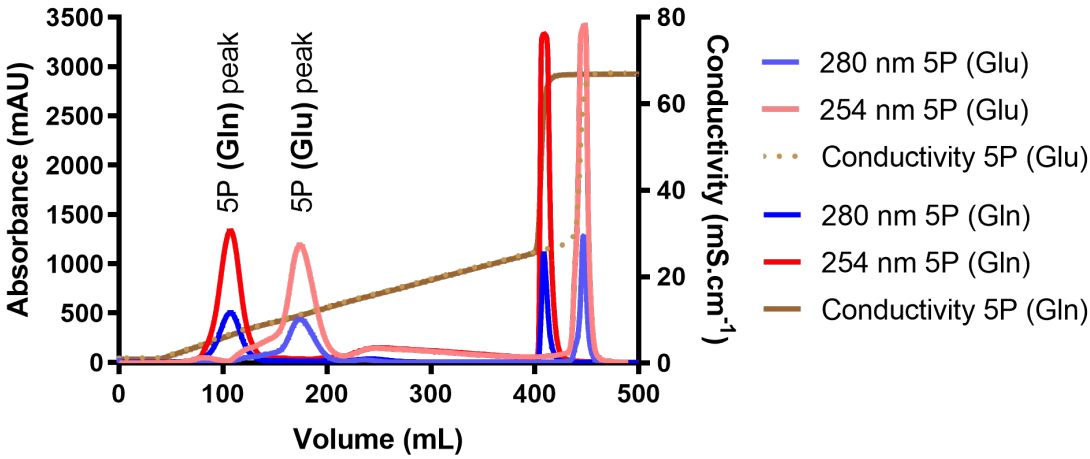

Appendix 3.1 Comparison of elution profiles UDP-Mur*N*Ac 5P (iGln) and UDP-Mur*N*Ac 5P (Glu). Synthesis reactions of UDP-Mur*N*Ac 5P were chromatographed by anion exchange. The position of the product peak is indicated for each reaction (as verified by nanospray TOF mass spectrometry). **5P (Glu)**, UDP-Mur*N*Ac 5P (Glu); **5P (Gln)**, UDP-Mur*N*Ac 5P (iGln).

Appendices 3.2 and 3.3: Mass spectral analysis of UDP-Mur*N*Ac 5P (iGln) and Lipid II (iGln)

Synthesis of UDP-MurNAc 5P (iGln) and Lipid II (iGln) was verified by nanospray TOF mass spectrometry.

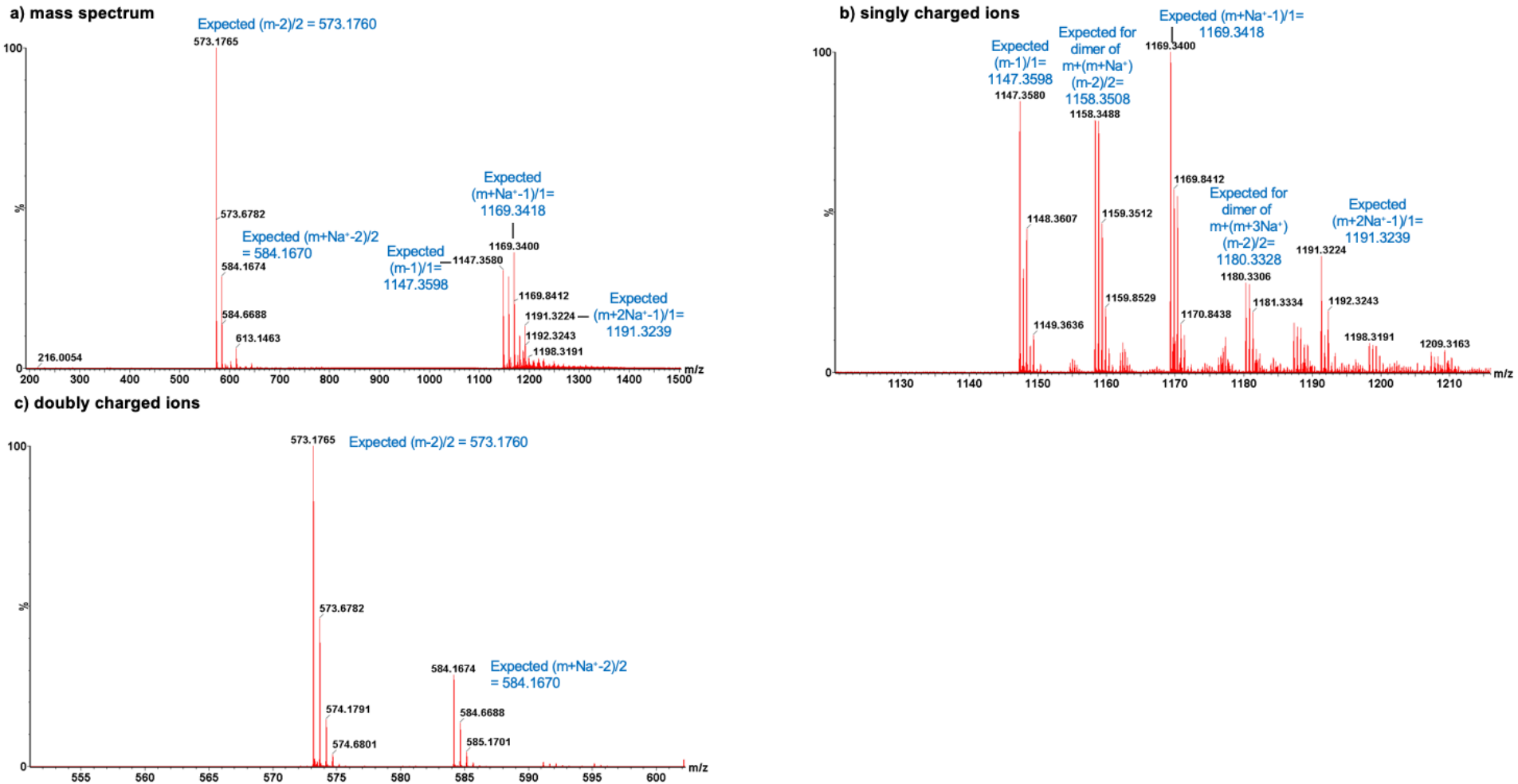

Appendix 3.2 Nanospray TOF mass spectrum of UDP-Mur*N*Ac 5P (iGln). Samples were analysed by negative ion nanospray TOF mass spectrometry. The full spectrum **(a)**, along with focused views of the singly charged **(b)** and doubly charged **(c)** ions are presented. Data collected and analysed by A.J. Lloyd, and mass spectra generated using MassLynx software (Waters).

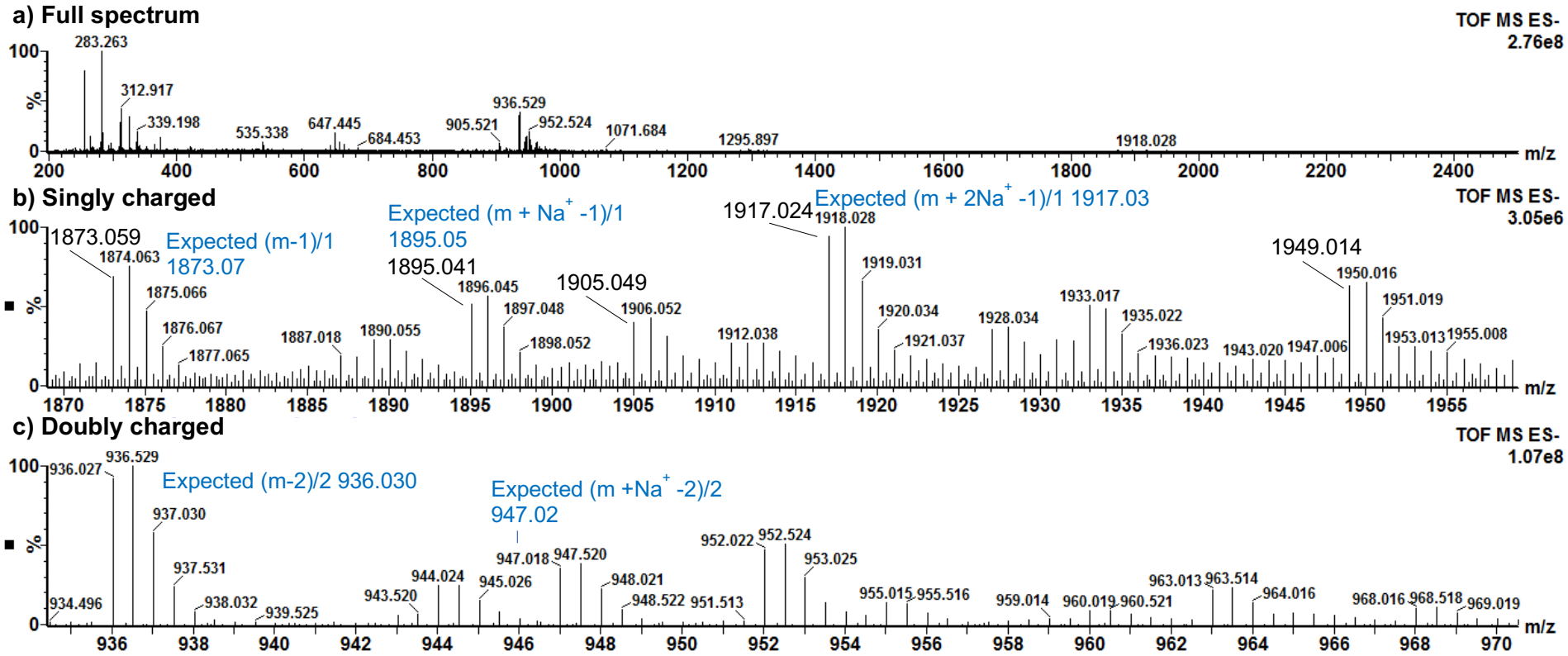

Appendix 3.3 Nanospray TOF mass spectrum of Lipid II (iGln). Samples were analysed by negative ion nanospray TOF mass spectrometry. The full spectrum **(a)**, along with focused views of the singly charged **(b)** and doubly charged **(c)** ions, are presented. Data collected and analysed by A.J. Lloyd, and mass spectra generated using MassLynx software (Waters).

Appendices 3.4 – 3.11: Mass spectrometry analysis of carbodiimide coupling syntheses quenched with ethanolamine or hydroxylamine

Carbodiimide coupling reactions were quenched with ethanolamine or hydroxylamine. The products were analysed by nanospray TOF mass spectrometry to determine the extent of multiple alanylation under each condition.

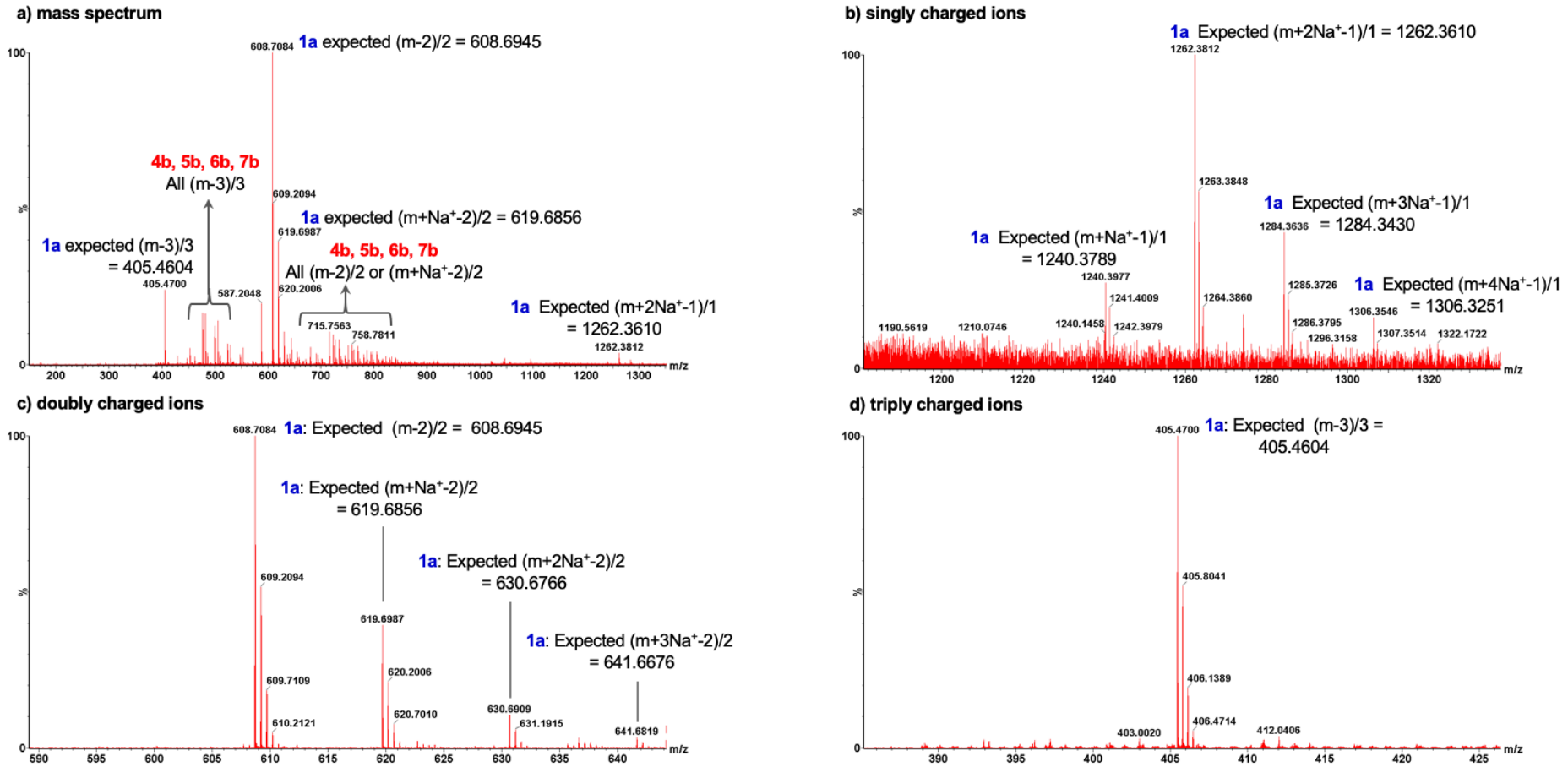

Appendix 3.4 Nanospray TOF mass spectrometry analysis of carbodiimide coupling reactions quenched using ethanolamine. Samples were analysed by negative ion nanospray TOF mass spectrometry. These mass spectra were generated from a sample of the 'eth 18.7' peak upon anion exchange chromatography of the reaction. The full mass spectrum (**a**) and spectra depicted singly (**b**), doubly (**c**) and triply (**d**) charged ions related to the desired product, UDP-Mur*N*Ac 6P (iGln, L-Ala) are given. See Appendix 3.6 for spectra depicting products of multiple alanylation. Data collected and analysed by A.J. Lloyd, and mass spectra generated using MassLynx software (Waters). **1a**, UDP-Mur*N*Ac 6P (iGln, L-Ala); **4b**, UDP-Mur*N*Ac 9P (iGln, $(L\text{-}Ala)_4$; **5b**, UDP-Mur*N*Ac 10P (iGln, $(L\text{-}Ala)_5$; **6b**, UDP-Mur*N*Ac 11P (iGln, $(L\text{-}Ala)_6$; **7b**, UDP-Mur*N*Ac 12P (iGln, $(L\text{-}Ala)_7$.

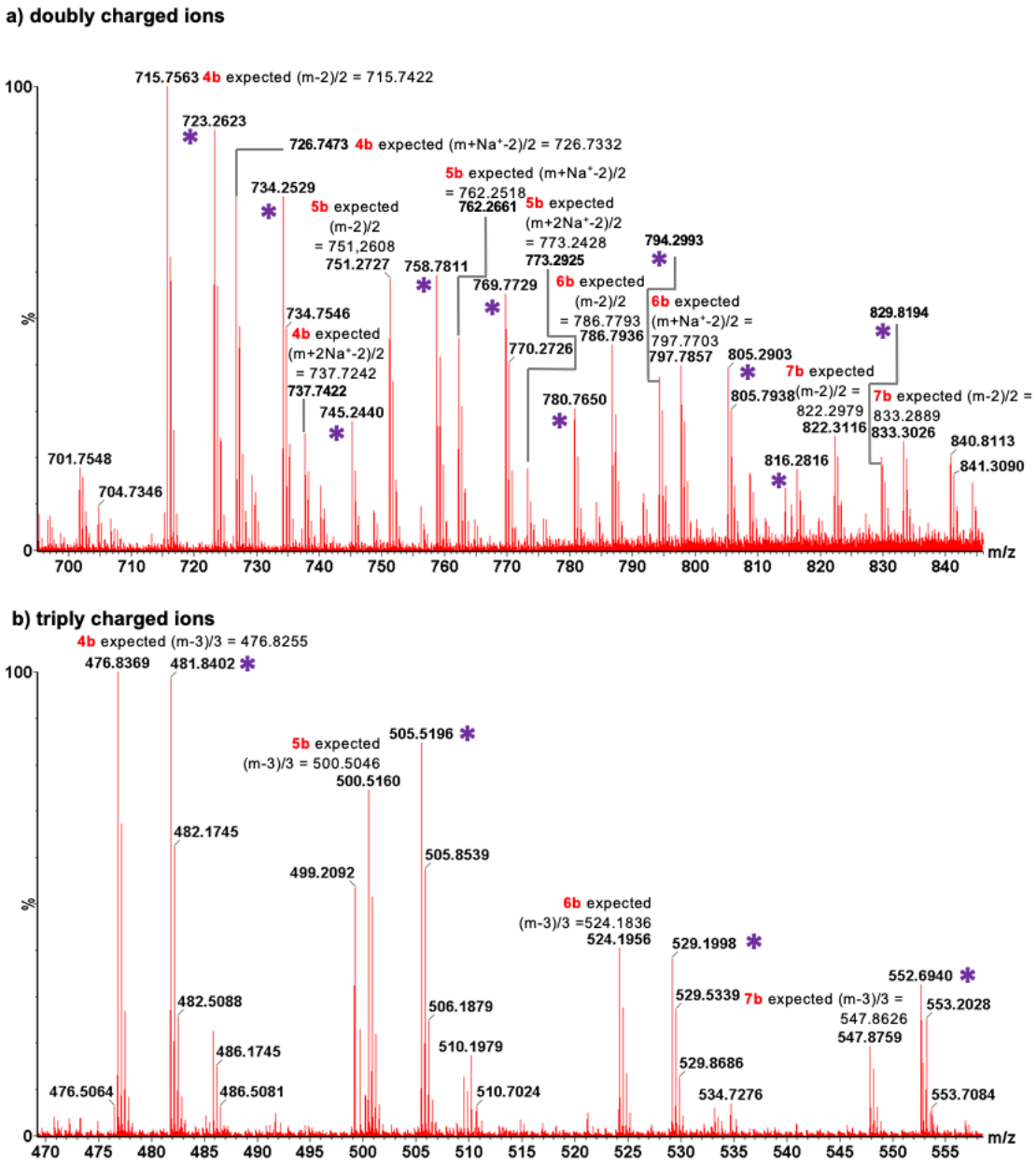

Appendix 3.5 Nanospray TOF mass spectrometry analysis of carbodiimide coupling reactions quenched using ethanolamine – doubly and triply charged ions corresponding to products of multiple alanylation. Samples were analysed by negative ion nanospray TOF mass spectrometry. These mass spectra were generated from a sample of the 'eth 18.7' peak upon anion exchange chromatography of the reaction. Data collected and analysed by A.J. Lloyd, and mass spectra generated using MassLynx software (Waters). **4b**, UDP-Mur*N*Ac 9P (iGln, (L-Ala)$_4$; **5b**, UDP-Mur*N*Ac 10P (iGln, (L-Ala)$_5$; **6b**, UDP-Mur*N*Ac 11P (iGln, (L-Ala)$_6$; **7b**, UDP-Mur*N*Ac 12P (iGln, (L-Ala)$_7$; *, unknown ion series.

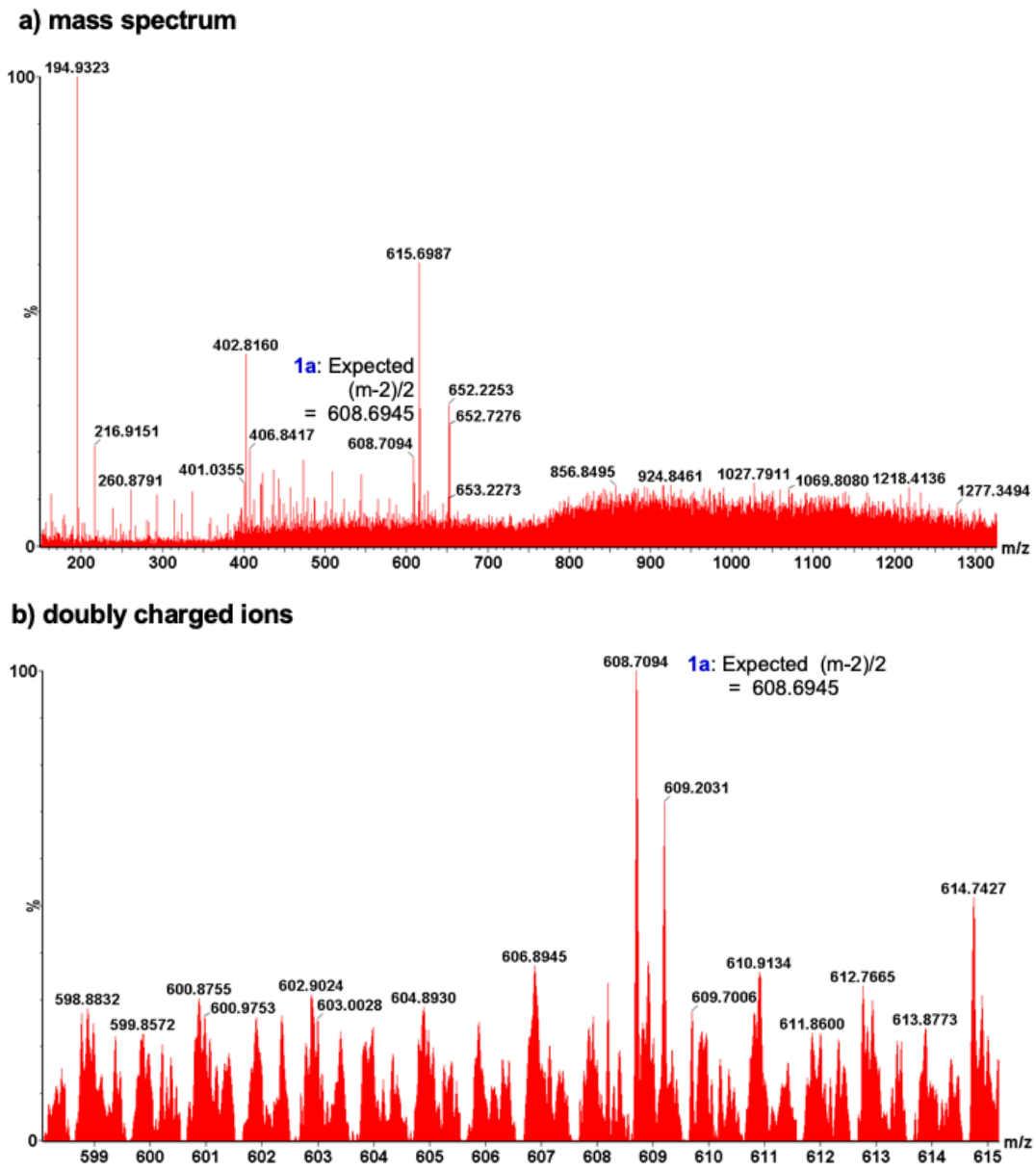

Appendix 3.6 Nanospray TOF mass spectrometry analysis of carbodiimide coupling reactions quenched using ethanolamine. Samples were analysed by negative ion nanospray TOF mass spectrometry. These mass spectra were generated from a sample of the 'eth 20.4' peak upon anion exchange chromatography of the reaction. The full mass spectrum (**a**), and the spectrum displaying the doubly charged series (**b**) corresponding to the ion of interest are displayed. Data collected and analysed by A.J. Lloyd, and mass spectra generated using MassLynx software (Waters). **1a**, UDP-Mur*N*Ac 6P (iGln, L-Ala).

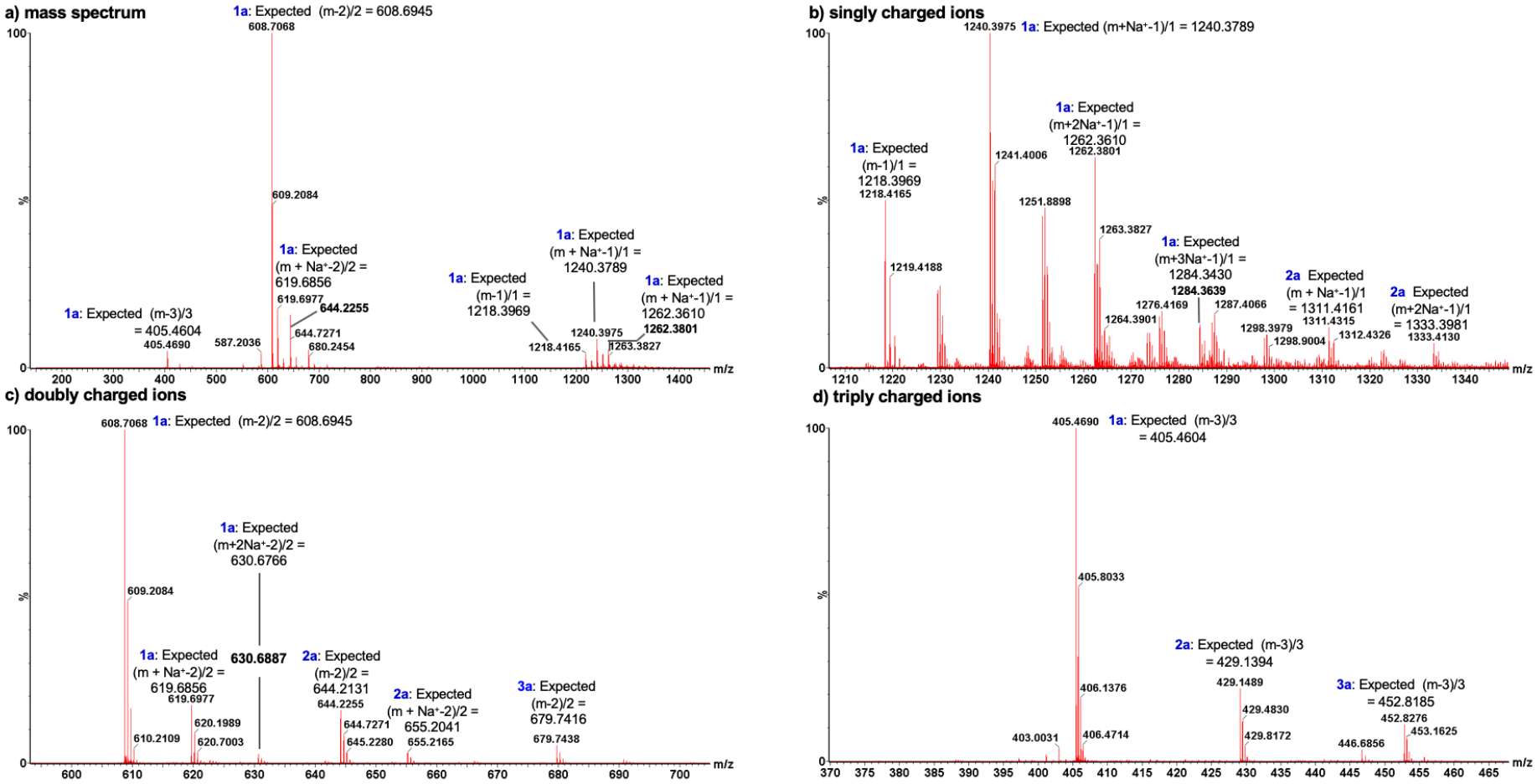

Appendix 3.7 Nanospray TOF mass spectrometry analysis of carbodiimide coupling reactions quenched using hydroxylamine – doubly and triply charged ions corresponding to products of multiple alanylation. See legend following page.

(previous page) Appendix 3.7 Nanospray TOF mass spectrometry analysis of carbodiimide coupling reactions quenched using hydroxylamine – doubly and triply charged ions corresponding to products of multiple alanylation. Samples were analysed by negative ion nanospray TOF mass spectrometry. These mass spectra were generated from a sample of the 'hyx 15.0' peak upon anion exchange chromatography of the reaction. The full mass spectrum (**a**), and spectra corresponding to the singly charged (**b**), doubly charged (**c**) and triply charged (**d**) ions are displayed. Data collected and analysed by A.J. Lloyd, and mass spectra generated using MassLynx software (Waters).. **1a**, UDP-Mur*N*Ac 6P (iGln, L-Ala); **2a**, UDP-Mur*N*Ac 7P (iGln, $(L\text{-}Ala)_2$); **3a**, UDP-Mur*N*Ac 8P (iGln, $(L\text{-}Ala)_3$).

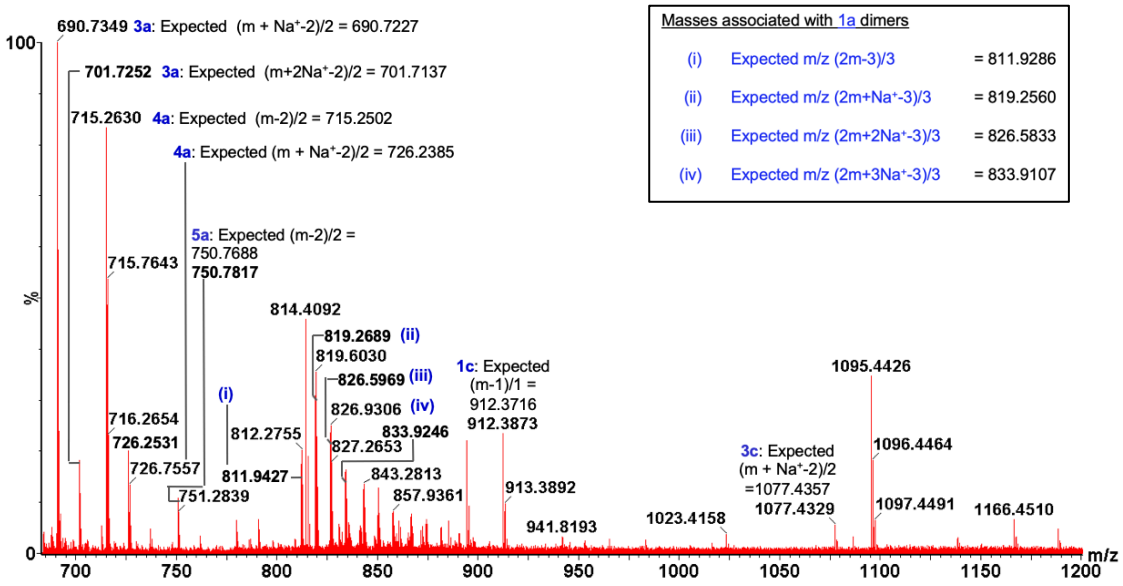

Appendix 3.8 Nanospray TOF mass spectrometry analysis of carbodiimide coupling reactions quenched using hydroxylamine – minor ions between doubly and singly charged ions. Samples were analysed by negative ion nanospray TOF mass spectrometry. These mass spectra were generated from a sample of the 'hyx 15.0' peak upon anion exchange chromatography of the reaction. Triply charged dimers, with and without sodiation, of ion **1c**, were observed at **(i)**, **(ii)**, **(iii)** and **(iv)**. Data collected and analysed by A.J. Lloyd, and mass spectra generated using MassLynx software (Waters). **1c**, phospho-Mur*N*Ac 6P (iGln, L-Ala); **3a**, UDP-Mur*N*Ac 8P (iGln, $(L\text{-}Ala)_3$); **3c**, phospho-Mur*N*Ac 8P (iGln, $(L\text{-}Ala)_3$); **4a**, UDP-Mur*N*Ac 9P (iGln, $(L\text{-}Ala)_4$); **5a**, UDP-Mur*N*Ac 10P (iGln, $(L\text{-}Ala)_5$).

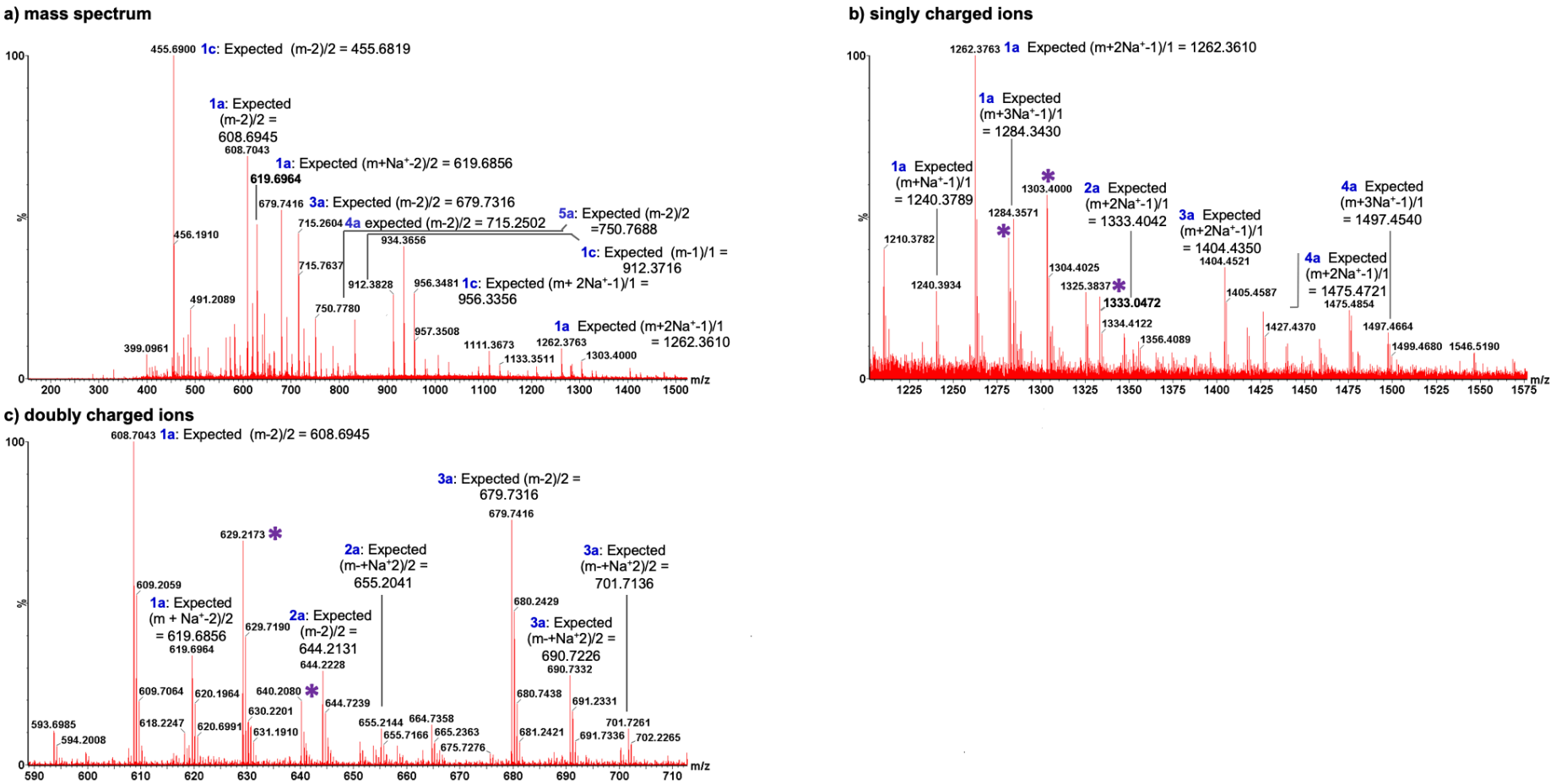

Appendix 3.9 Nanospray TOF mass spectrometry analysis of carbodiimide coupling reactions quenched using hydroxylamine – doubly and triply charged ions corresponding to products of multiple alanylation. See legend following page.

(previous page) Appendix 3.9 Nanospray TOF mass spectrometry analysis of carbodiimide coupling reactions quenched using hydroxylamine – doubly and triply charged ions corresponding to products of multiple alanylation. Samples were analysed by negative ion nanospray TOF mass spectrometry. These mass spectra were generated from a sample of the 'hyx 13.3' peak upon anion exchange chromatography of the reaction. Data collected and analysed by A.J. Lloyd, and mass spectra generated using MassLynx software (Waters). **1a**, UDP-Mur*N*Ac 6P (iGln, L-Ala); **1c**, phospho-Mur*N*Ac 6P (iGln, L-Ala); **2c**, phospho-Mur*N*Ac 7P (iGln, $(L\text{-}Ala)_2$); **4a**, UDP-Mur*N*Ac 9P (iGln, $(L\text{-}Ala)_4$); **5a**, UDP-Mur*N*Ac 10P (iGln, $(L\text{-}Ala)_5$); **6a**, UDP-Mur*N*Ac 11P (iGln, $(L\text{-}Ala)_6$); **7a**, UDP-Mur*N*Ac 12P (iGln, $(L\text{-}Ala)_7$).

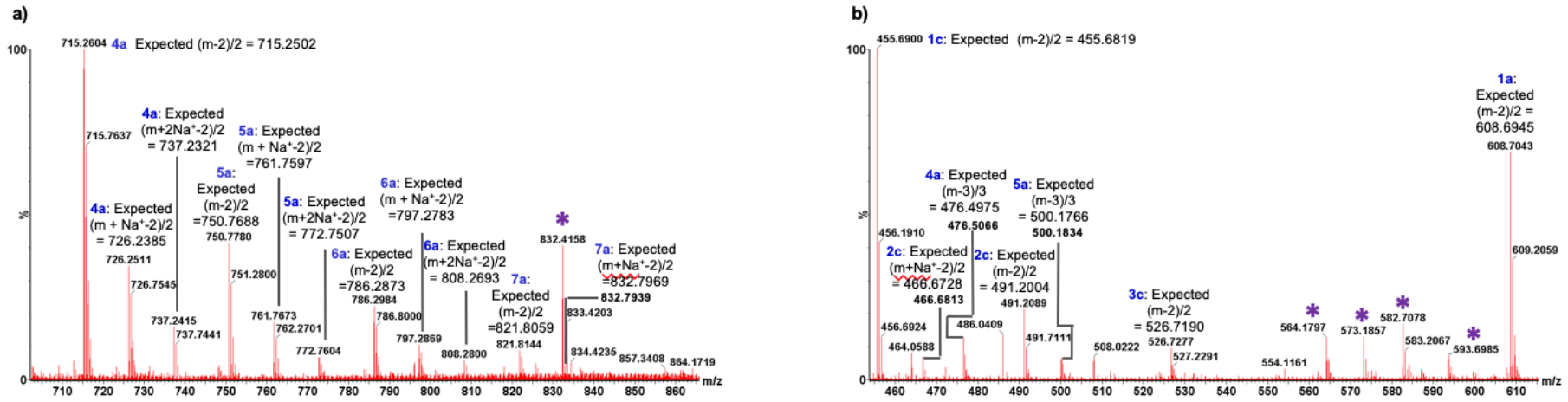

Appendix 3.10 Nanospray TOF mass spectrometry analysis of carbodiimide coupling reactions quenched using hydroxylamine – products of multiple alanylation and cleavage. Samples were analysed by negative ion nanospray TOF mass spectrometry. These mass spectra were generated from a sample of the 'hyx 13.3' peak upon anion exchange chromatography of the reaction. Data collected and analysed by A.J. Lloyd, and mass spectra generated using MassLynx software (Waters). **1a**, UDP-Mur*N*Ac 6P (iGln, L-Ala); **1c**, phospho-Mur*N*Ac 6P (iGln, L-Ala); **2c**, phospho-Mur*N*Ac 77P (iGln, $(L\text{-}Ala)_2$); **4a**, UDP-Mur*N*Ac 9P (iGln, $(L\text{-}Ala)_4$); **5a**, UDP-Mur*N*Ac 10P (iGln, $(L\text{-}Ala)_5$); **6a**, UDP-Mur*N*Ac 11P (iGln, $(L\text{-}Ala)_6$); **7a**, UDP-Mur*N*Ac 12P (iGln, $(L\text{-}Ala)_7$).

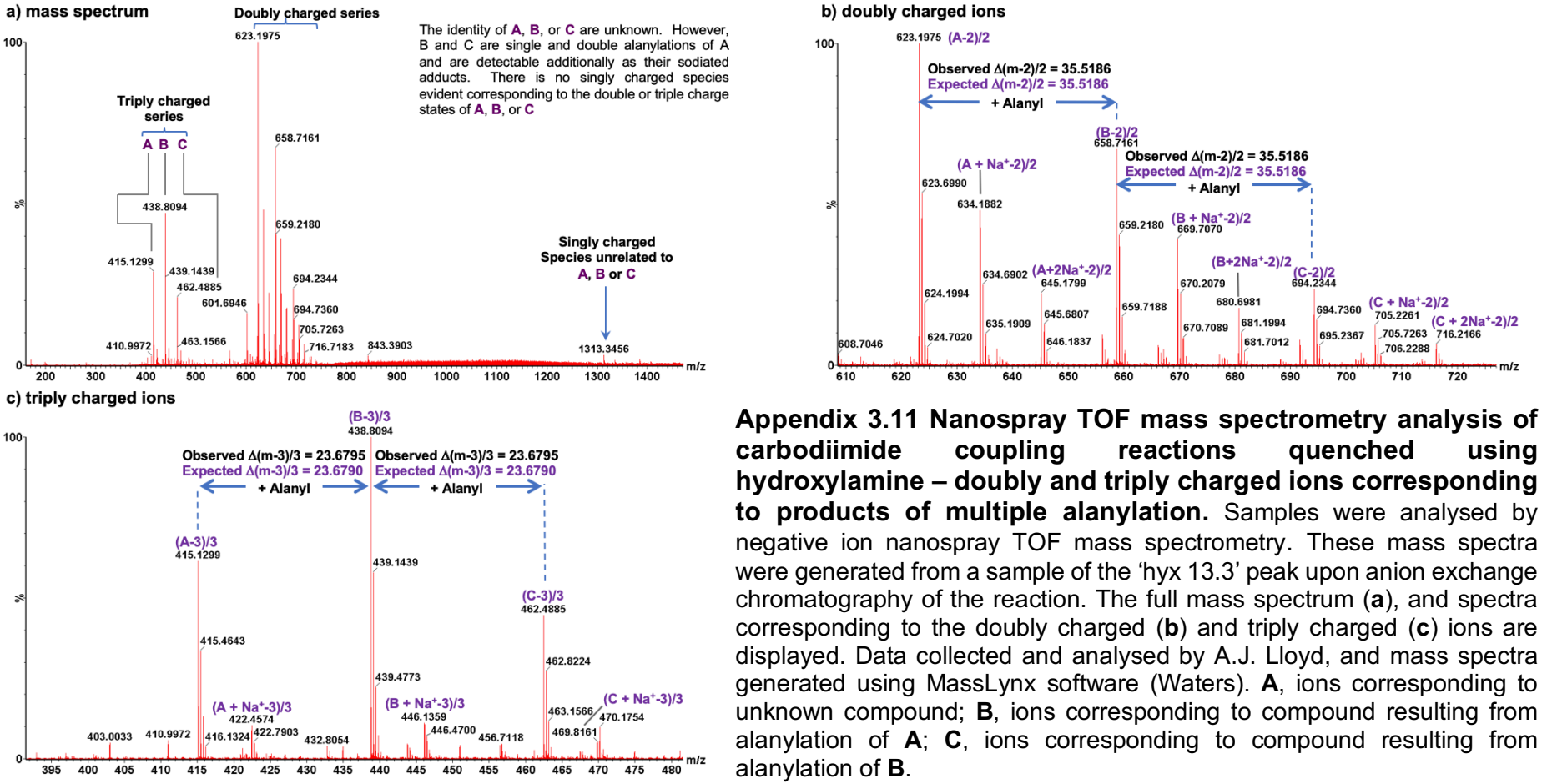

Appendix 3.11 Nanospray TOF mass spectrometry analysis of carbodiimide coupling reactions quenched using hydroxylamine – doubly and triply charged ions corresponding to products of multiple alanylation. Samples were analysed by negative ion nanospray TOF mass spectrometry. These mass spectra were generated from a sample of the 'hyx 13.3' peak upon anion exchange chromatography of the reaction. The full mass spectrum (**a**), and spectra corresponding to the doubly charged (**b**) and triply charged (**c**) ions are displayed. Data collected and analysed by A.J. Lloyd, and mass spectra generated using MassLynx software (Waters). **A**, ions corresponding to unknown compound; **B**, ions corresponding to compound resulting from alanylation of **A**; **C**, ions corresponding to compound resulting from alanylation of **B**.

Appendix 3.12 – 3.19: Mass spectrometry analysis of carbodiimide coupling syntheses omitting quenching agent

Carbodiimide coupling reactions omitting the quenching agent were analysed by nanospray TOF mass spectrometry, to determine the extent of multiple alanylation.

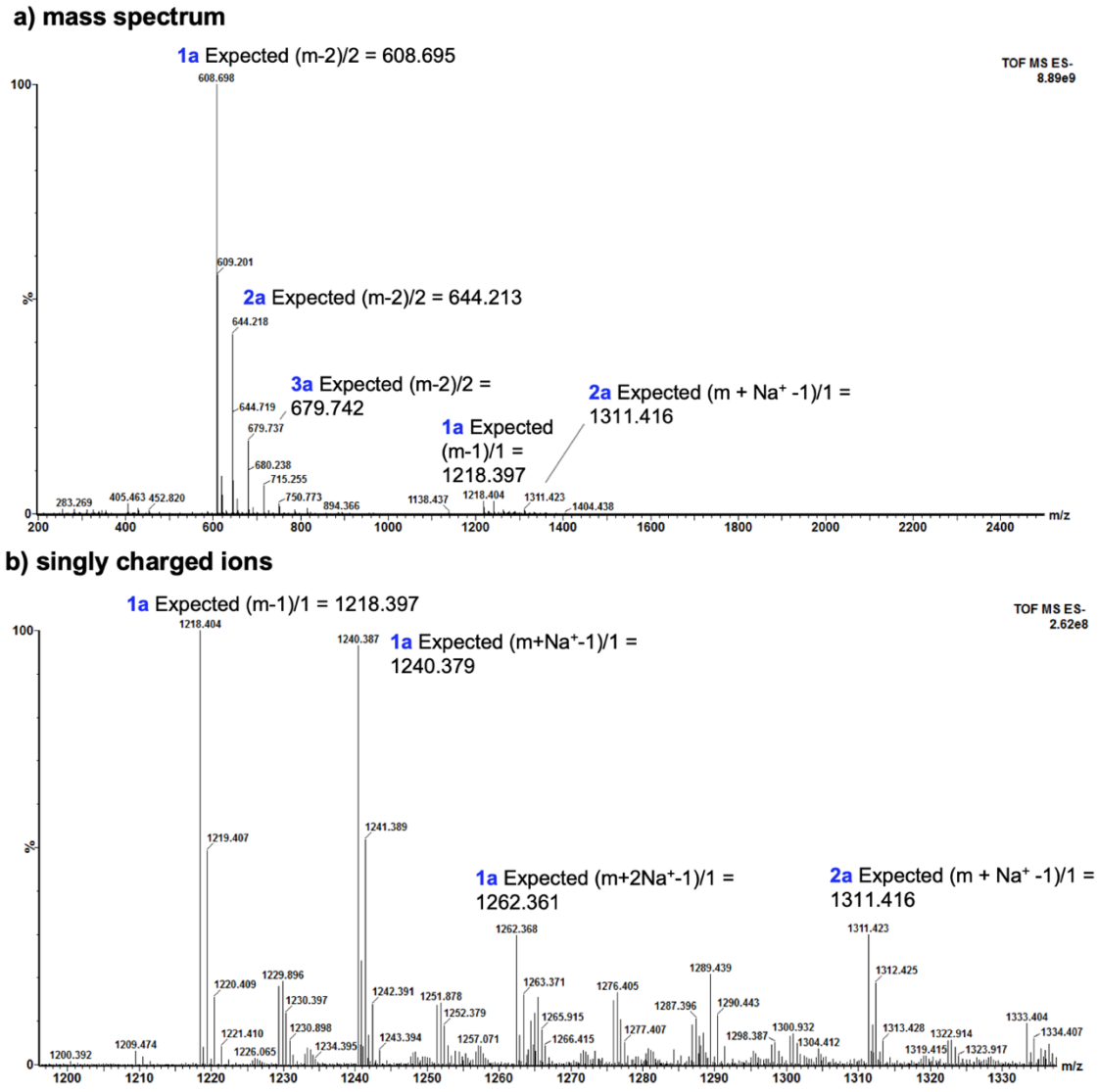

Appendix 3.12 Nanospray TOF mass spectrometry analysis of carbodiimide coupling reactions for synthesis of UDP-Mur*N*Ac 6P (iGln, L-Ala), omitting the quenching agent – full spectrum and singly charged spectrum. Samples were analysed by negative ion nanospray TOF mass spectrometry. The full mass spectrum (**a**), and a spectrum corresponding to the singly charged (**b**) ions are displayed. Data collected and analysed by A.J. Lloyd, and mass spectra generated using MassLynx software (Waters). **1a**, UDP-Mur*N*Ac 6P (iGln, L-Ala); **2a**, UDP-Mur*N*Ac 7P (iGln, $(L\text{-}Ala)_2$); **3a**, UDP-Mur*N*Ac 8P (iGln, $(L\text{-}Ala)_3$).

a) doubly charged ions

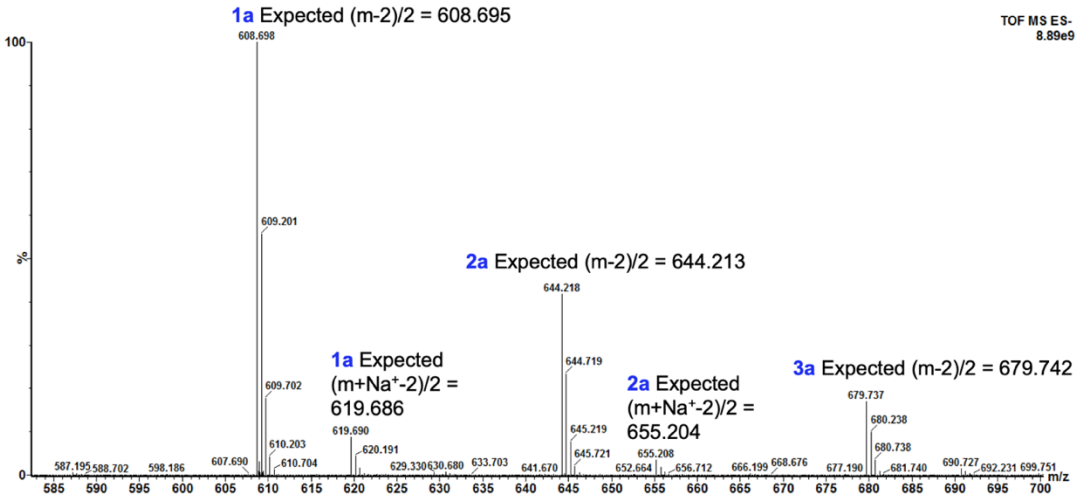

b) triply charged ions

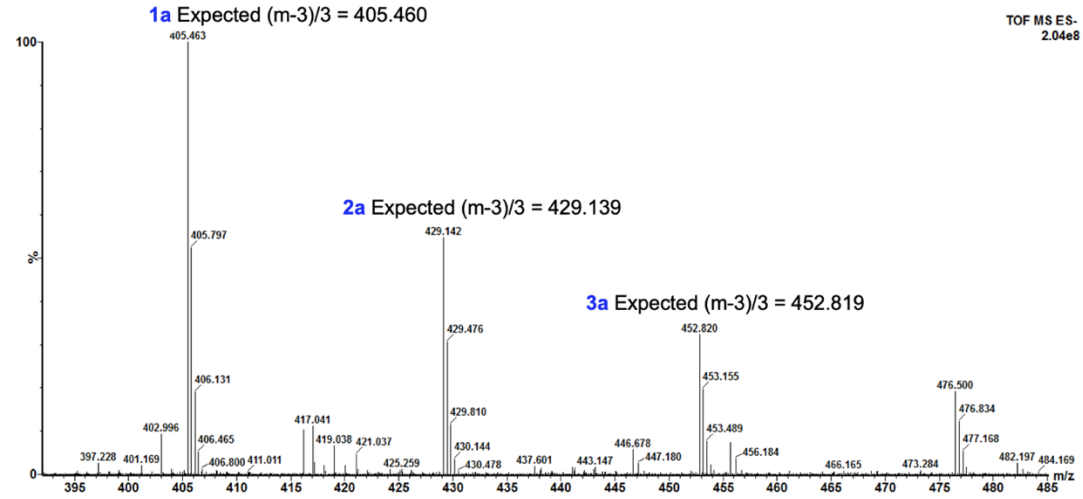

Appendix 3.13 Nanospray TOF mass spectrometry analysis of carbodiimide coupling reactions for synthesis of UDP-Mur*N*Ac 6P (iGln, L-Ala), omitting the quenching agent – doubly and triply charged ions corresponding to products of multiple alanylation. Samples were analysed by negative ion nanospray TOF mass spectrometry. Spectra corresponding to the doubly charged (**a**) and triply charged (**b**) ions are displayed. Data collected and analysed by A.J. Lloyd, and mass spectra generated using MassLynx software (Waters). **1a**, UDP-Mur*N*Ac 6P (iGln, L-Ala); **2a**, UDP-Mur*N*Ac 7P (iGln, $(L\text{-}Ala)_2$); **3a**, UDP-Mur*N*Ac 8P (iGln, $(L\text{-}Ala)_3$).

a) mass spectrum

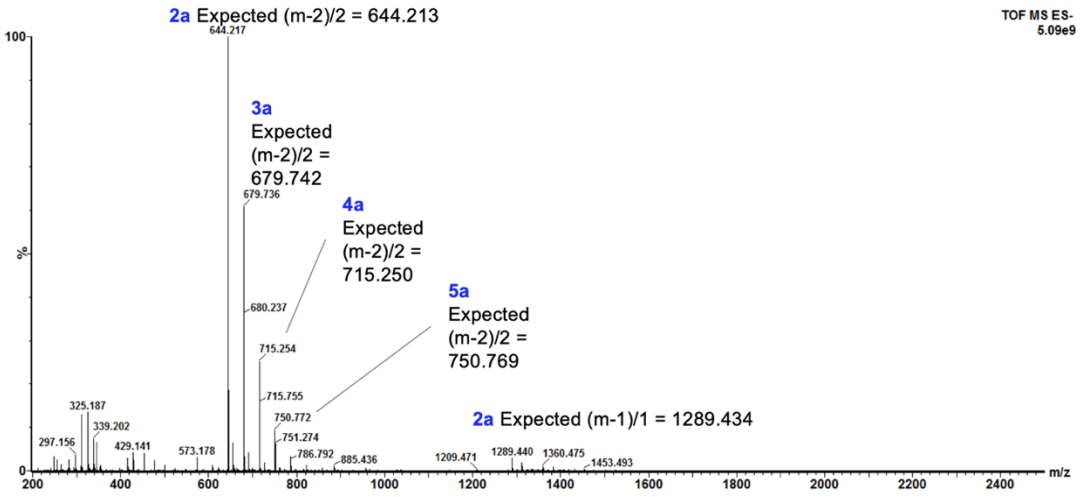

b) singly charged ions

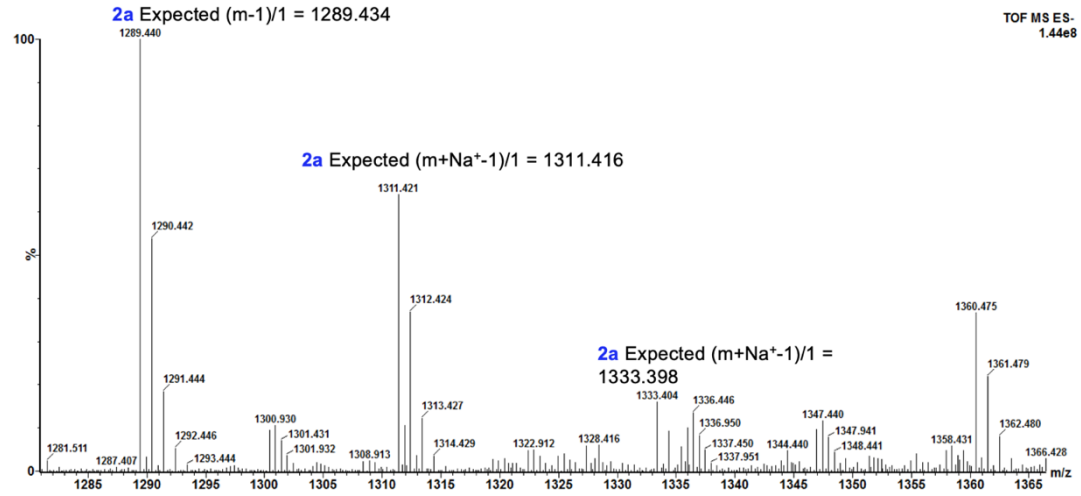

Appendix 3.14 Nanospray TOF mass spectrometry analysis of carbodiimide coupling reactions for synthesis of UDP-Mur*N*Ac 7P (iGln, L-Ala-L-Ala), omitting the quenching agent – full spectrum and singly charged spectrum. Samples were analysed by negative ion nanospray TOF mass spectrometry. The full mass spectrum (**a**), and a spectrum corresponding to the singly charged (**b**) ions are displayed. Data collected and analysed by A.J. Lloyd, and mass spectra generated using MassLynx software (Waters). **2a**, UDP-Mur*N*Ac 7P (iGln, $(L\text{-Ala})_2$); **3a**, UDP-Mur*N*Ac 8P (iGln, $(L\text{-Ala})_3$); **4a**, UDP-Mur*N*Ac 9P (iGln, $L\text{-Ala})_4$; **5a**, UDP-Mur*N*Ac 10P (iGln, $(L\text{-Ala})_5$).

a) doubly charged ions

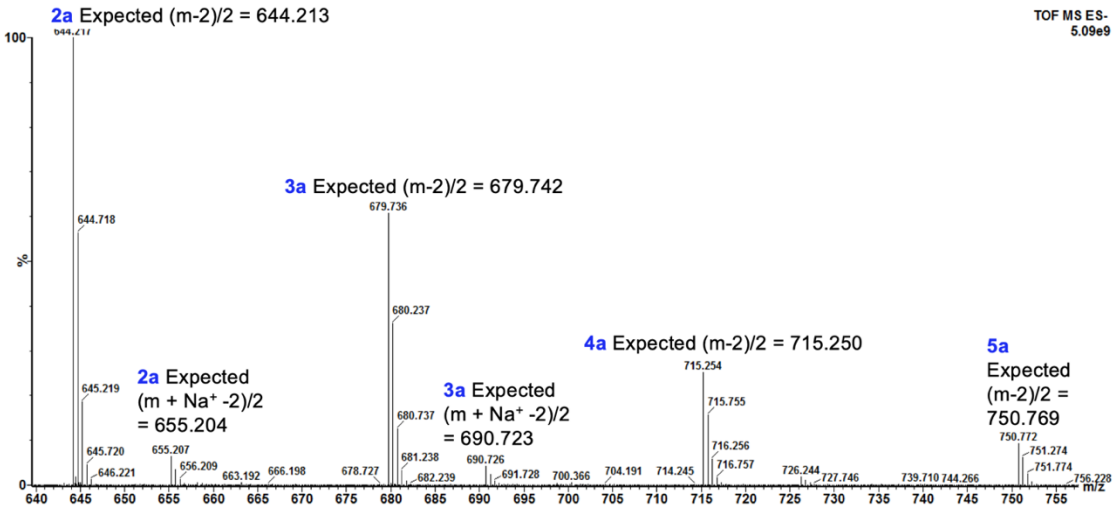

b) triply charged ions

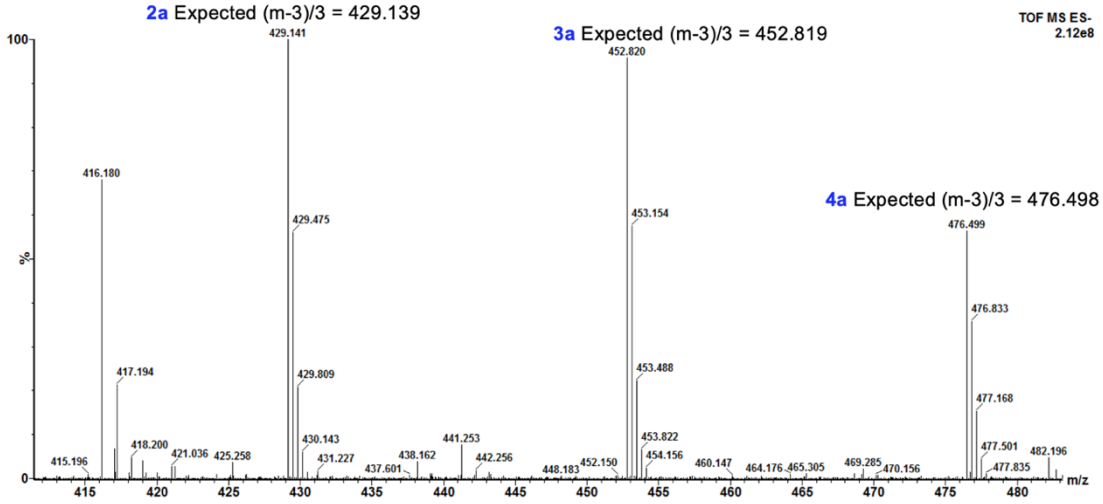

Appendix 3.15 Nanospray TOF mass spectrometry analysis of carbodiimide coupling reactions for synthesis of UDP-Mur*N*Ac 7P (iGln, L-Ala-L-Ala), omitting the quenching agent – doubly and triply charged spectra. Samples were analysed by negative ion nanospray TOF mass spectrometry. Spectra corresponding to the doubly charged (**a**) and triply charged (**b**) ions are displayed. Data collected and analysed by A.J. Lloyd, and mass spectra generated using MassLynx software (Waters). **2a**, UDP-Mur*N*Ac 7P (iGln, $(L\text{-}Ala)_2$); **3a**, UDP-Mur*N*Ac 8P (iGln, $(L\text{-}Ala)_3$); **4a**, UDP-Mur*N*Ac 9P (iGln, $L\text{-}Ala)_4$; **5a**, UDP-Mur*N*Ac 10P (iGln, $(L\text{-}Ala)_5$).

a) mass spectrum

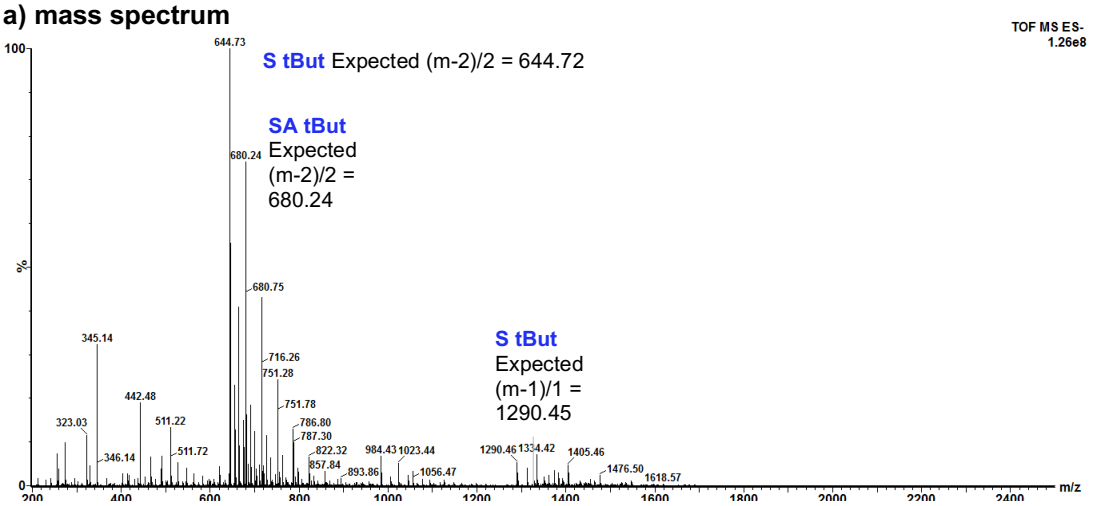

b) singly charged

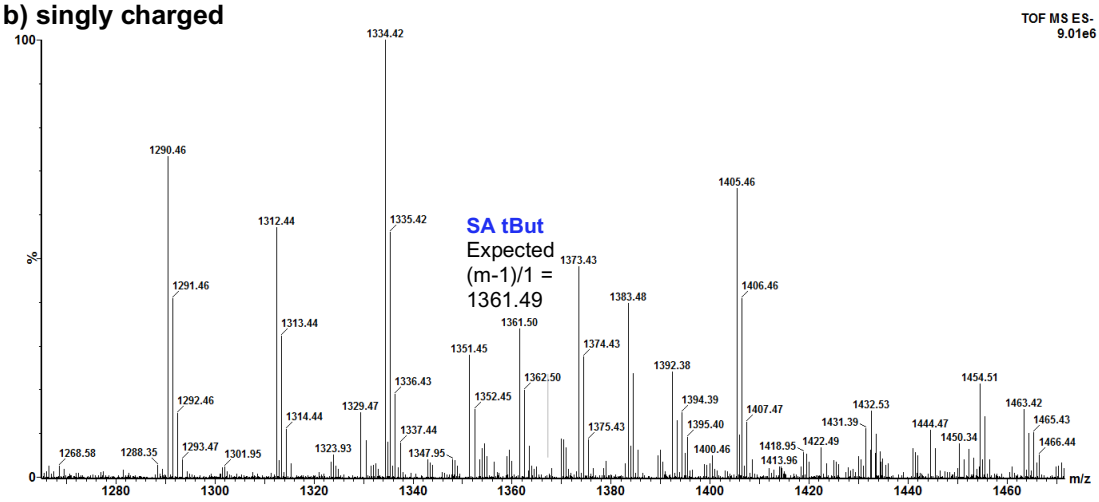

Appendix 3.16 Nanospray TOF mass spectrometry analysis of carbodiimide coupling reactions for synthesis of UDP-Mur*N*Ac 6P (iGln, L-Ser) – full and singly charged spectra. Samples were analysed by negative ion nanospray TOF mass spectrometry. Spectra corresponding to the full spectrum (**a**) and singly charged (**b**) ions are displayed. Data collected and analysed by A.J. Lloyd, and mass spectra generated using MassLynx software (Waters).

a) doubly charged ions

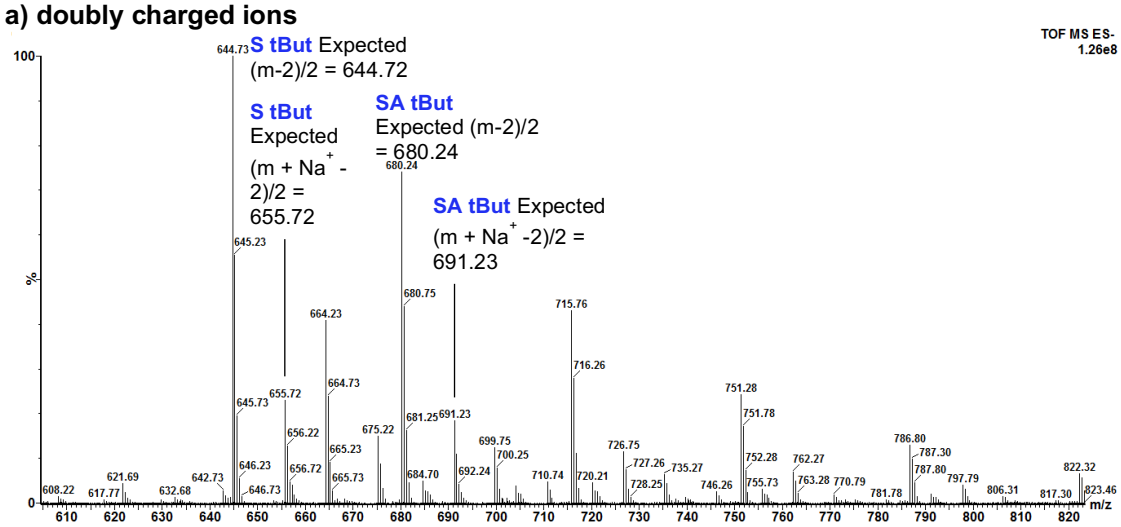

b) triply charged ions

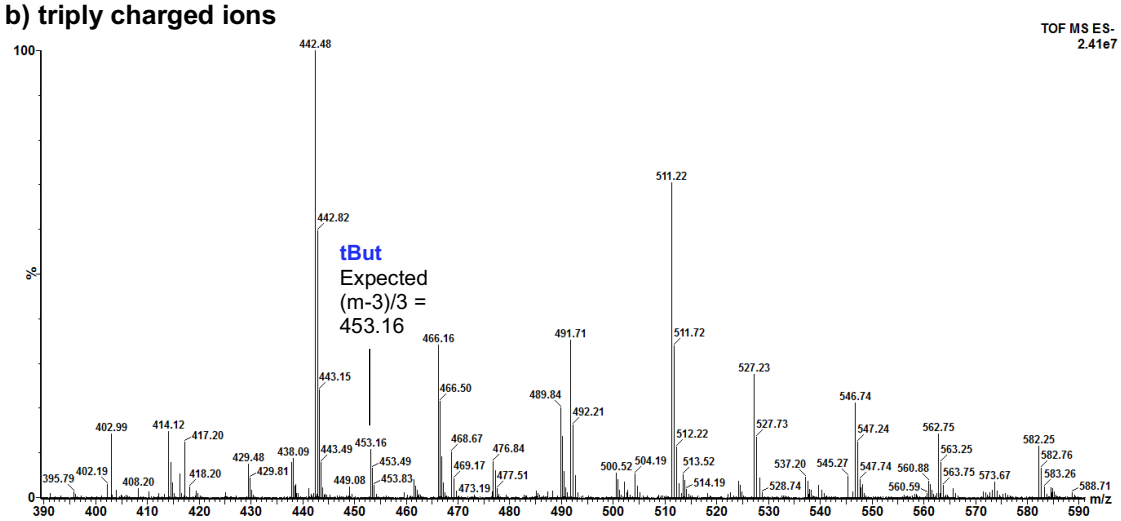

Appendix 3.17 Nanospray TOF mass spectrometry analysis of carbodiimide coupling reactions for synthesis of UDP-Mur*N*Ac 6P (iGln, L-Ser) – doubly and triply charged spectra. Samples were analysed by negative ion nanospray TOF mass spectrometry. Spectra corresponding to the doubly (**a**) and triply charged (**b**) ions are displayed. Data collected and analysed by A.J. Lloyd, and mass spectra generated using MassLynx software (Waters).

a) mass spectrum

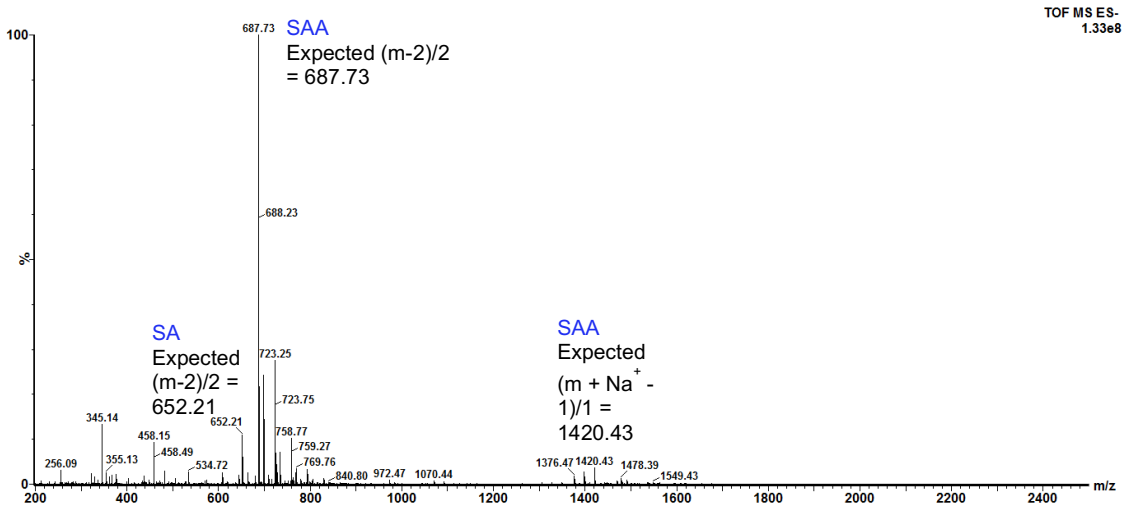

b) singly charged ions

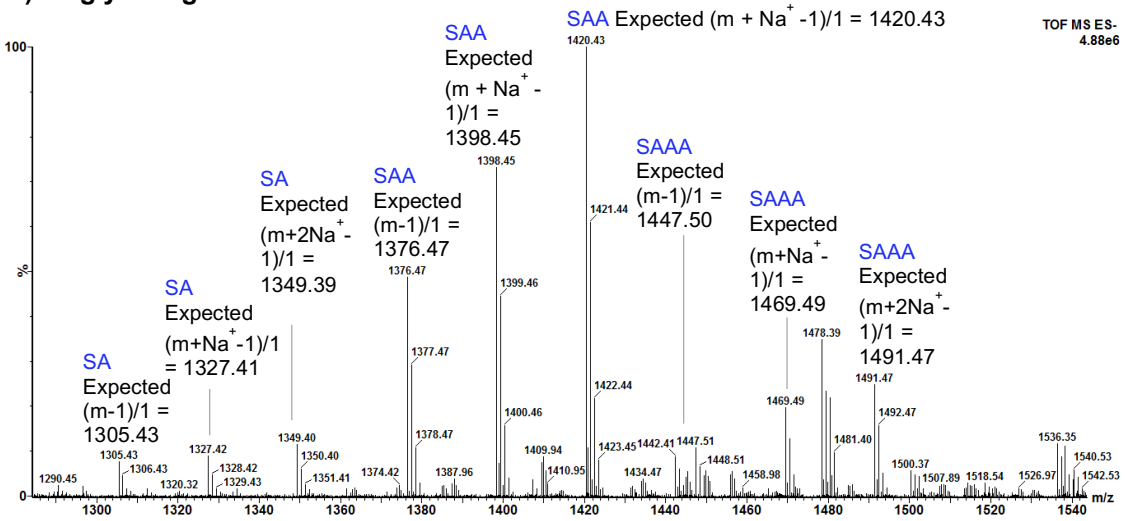

Appendix 3.18 Nanospray TOF mass spectrometry analysis of carbodiimide coupling reactions for synthesis of UDP-Mur*N*Ac 7P (iGln, L-Ser-L-Ala) – full and singly charged spectra. Samples were analysed by negative ion nanospray TOF mass spectrometry. Spectra corresponding to the full (**a**) and singly charged (**b**) ions are displayed. Data collected by A.J. Lloyd, and mass spectra generated using MassLynx software (Waters).

a) doubly charged ions

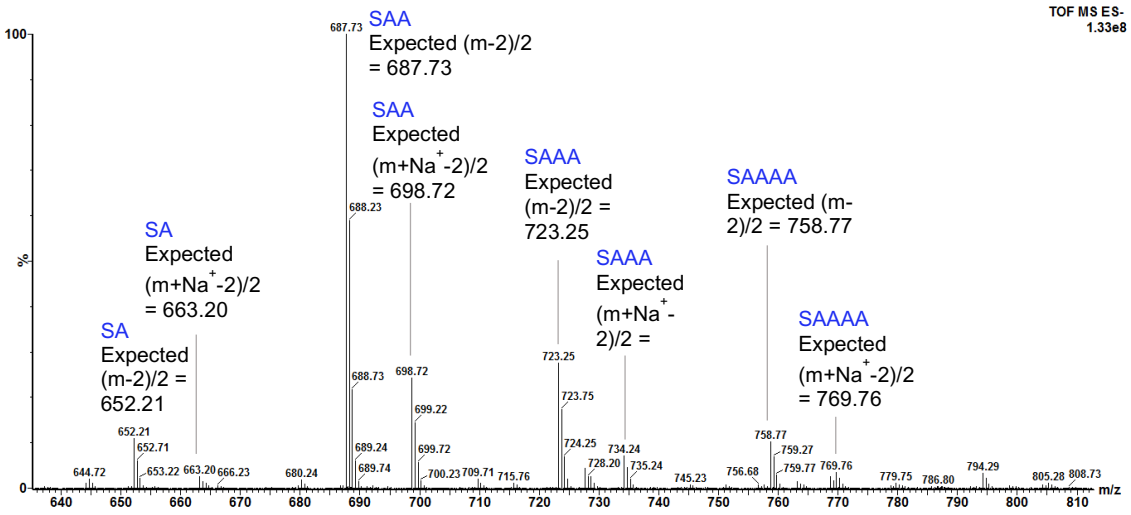

b) triply charged ions

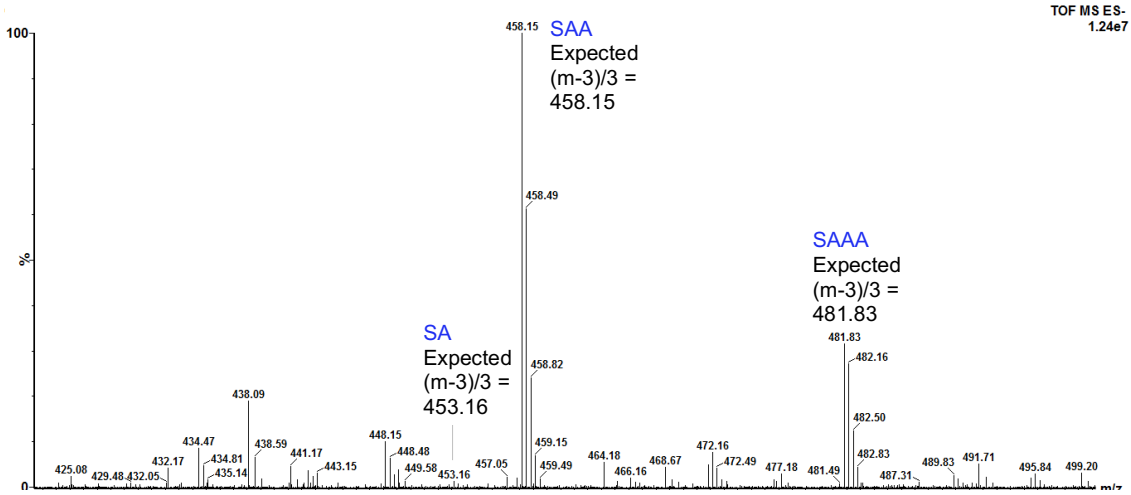

Appendix 3.19 Nanospray TOF mass spectrometry analysis of carbodiimide coupling reactions for synthesis of UDP-Mur*N*Ac 7P (iGln, L-Ser-L-Ala) – doubly and triply charged spectra. Samples were analysed by negative ion nanospray TOF mass spectrometry Spectra corresponding to the doubly (**a**) and triply charged (**b**) ions are displayed. Data collected by A.J. Lloyd, and mass spectra generated using MassLynx software (Waters).

Appendix 3.20 - 3.23: Collision-induced fragmentation of UDP-Mur*N*Ac 5P (iGln), UDP-Mur*N*Ac 6P (iGln, L-Ala) and UDP-Mur*N*Ac 7P (iGln, (L-Ala)$_2$)

Mass spectrometry was used to confirm the correct positioning of the branch on UDP-Mur*N*Ac 6P (iGln, L-Ala) and UDP-Mur*N*Ac 7P (iGln, (L-Ala)$_2$). Sample of the two substrates, and the starting material (UDP-Mur*N*Ac 5P (iGln)) were subjected to increasing collision energies until the parent ion was lost. The resultant ions were then assigned to fragmentation patterns of the parent ion to determine the positioning of the branch amino acids.

The fragmentation patterns are presented in Section 3.3.4.6.

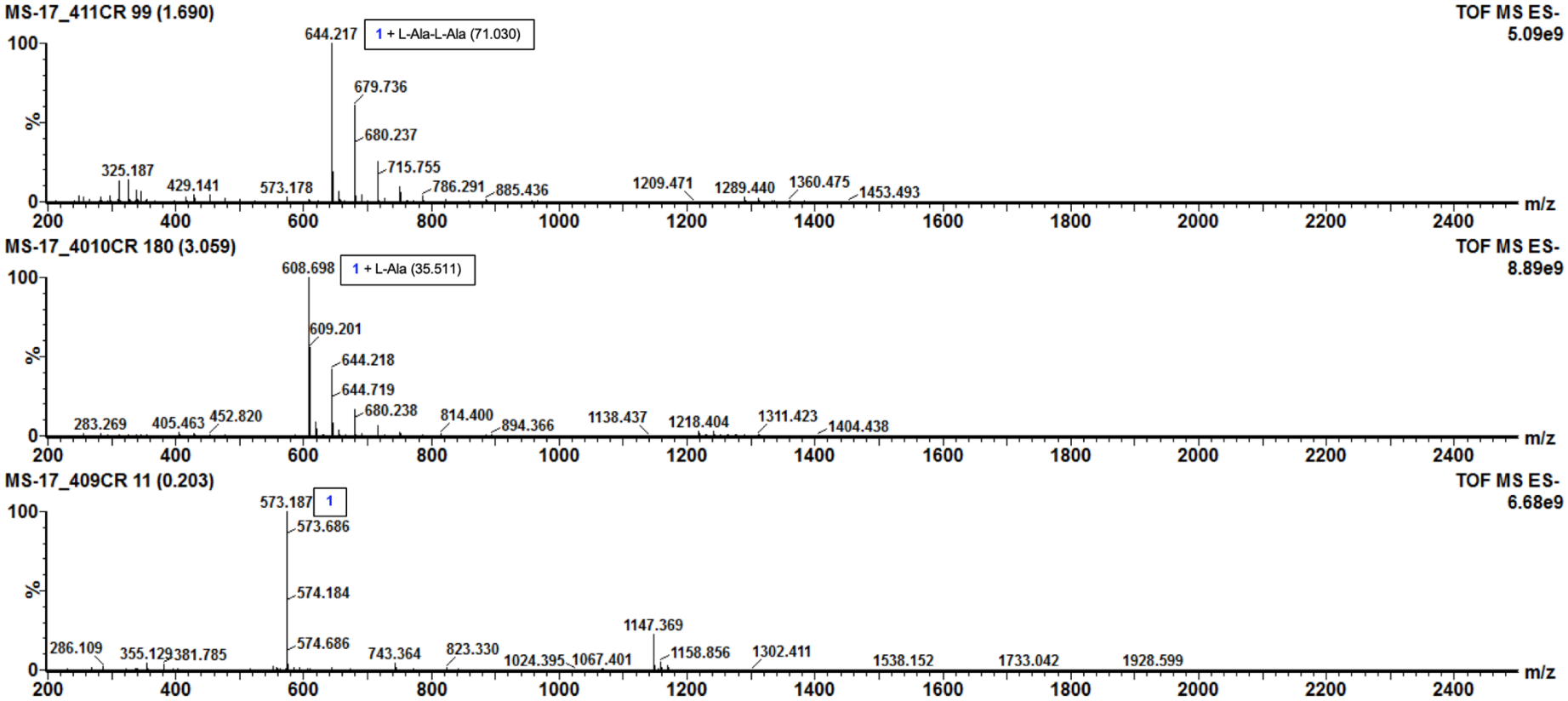

Figure 3.20 Mass spectrometry analysis of UDP-Mur*N*Ac -5P (iGln), -6P (iGln, L-Ala), and -7P (iGln, L-Ala-L-Ala). Samples for analysis of fragmentation pattern were analysed by negative ion nanospray TOF mass spectrometry. Data collected by A.J. Lloyd, and mass spectra generated using MassLynx software (Waters).

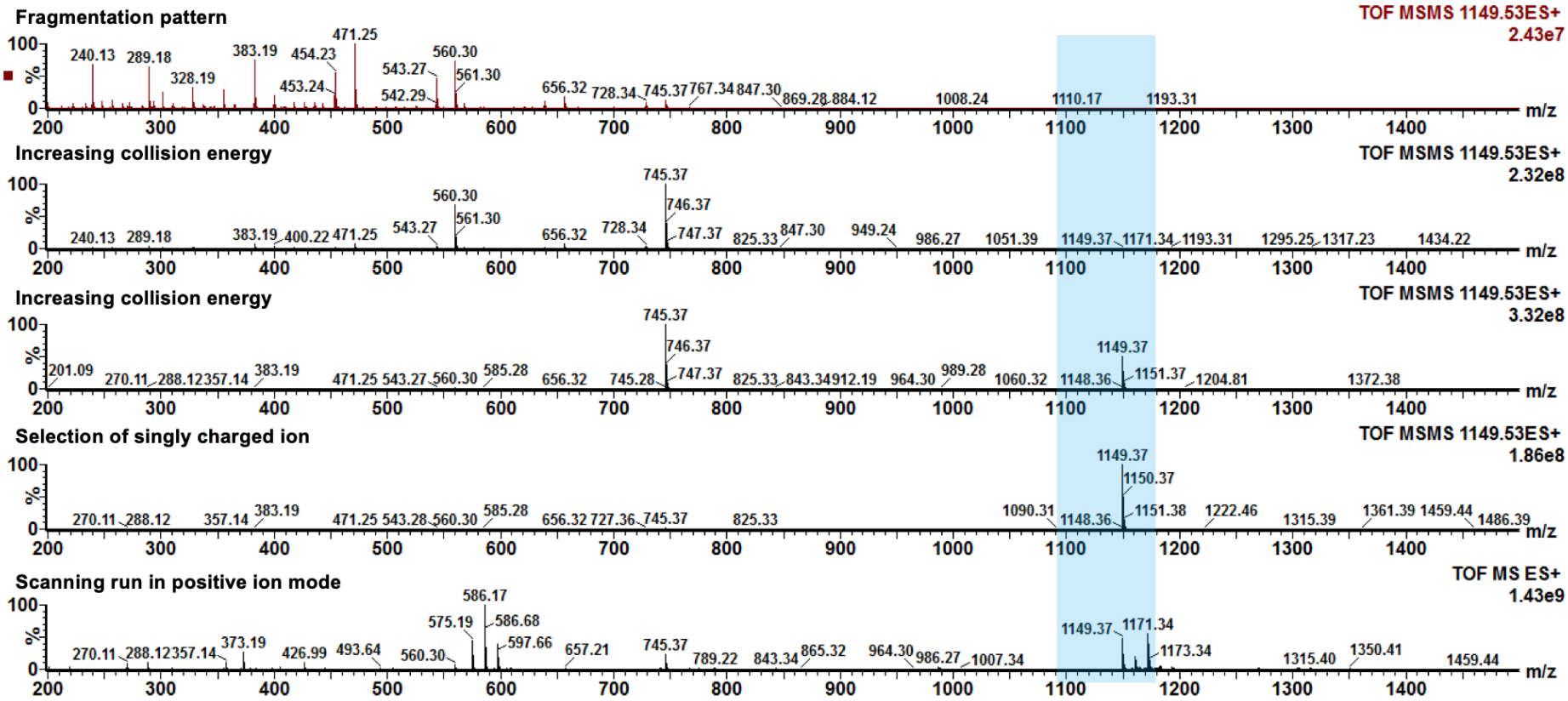

Appendix 3.21 Mass spectrometry experiment for collision-induced fragmentation of UDP-Mur*N*Ac 5P (iGln). Samples were analysed by positive ion nanospray TOF mass spectrometry. The parent ion was selected for fragmentation (blue panel), and then subjected to increasing collision energies, until loss of the parent ion to generate a fragmentation pattern. Data collected and analysed by A.J. Lloyd, and mass spectra generated using MassLynx software (Waters).

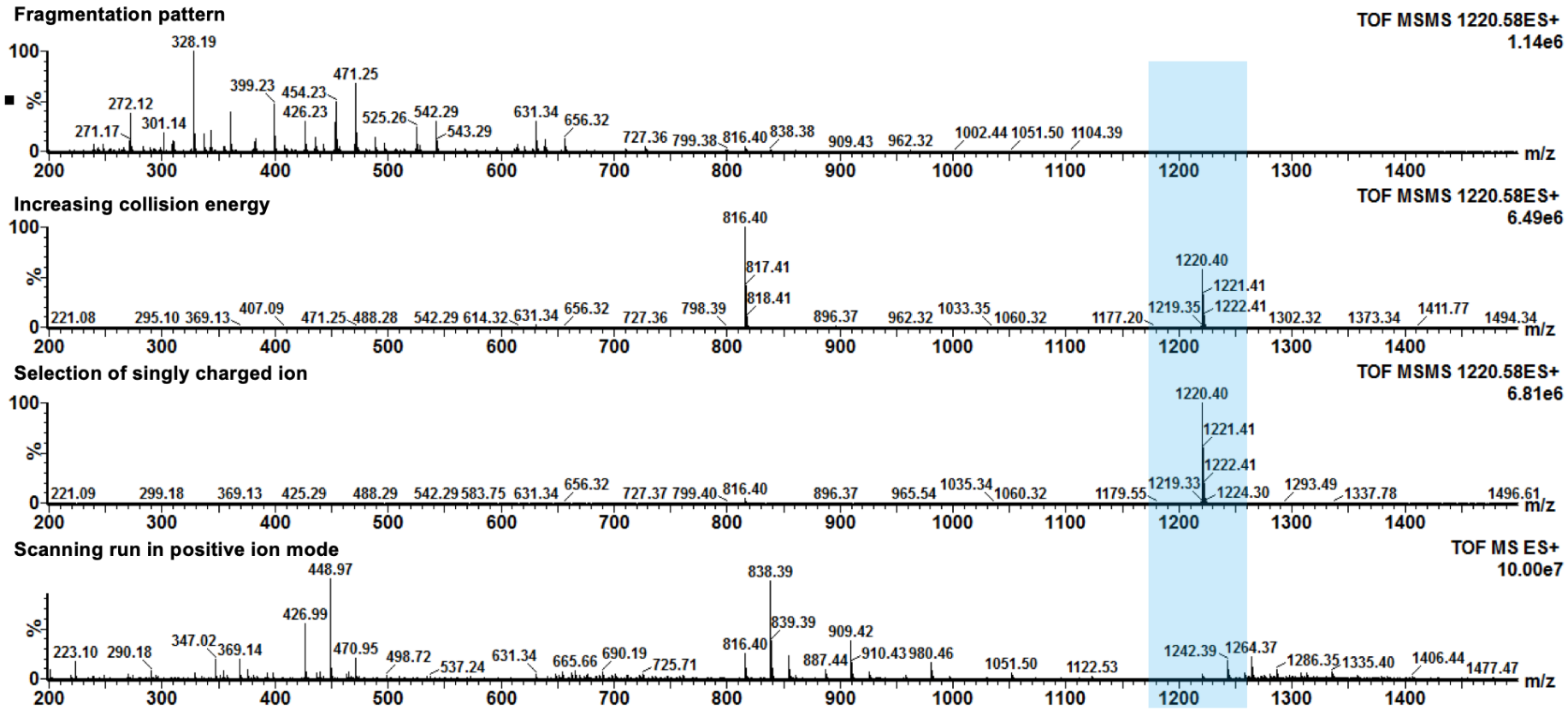

Appendix 3.22 Mass spectrometry experiment for collision-induced fragmentation of UDP-Mur*N*Ac 6P (iGln, L-Ala). Samples were analysed by positive ion nanospray TOF mass spectrometry. The parent ion was selected for fragmentation (blue panel), and then subjected to increasing collision energies, until loss of the parent ion to generate a fragmentation pattern. Data collected and analysed by A.J. Lloyd, and mass spectra generated using MassLynx software (Waters).

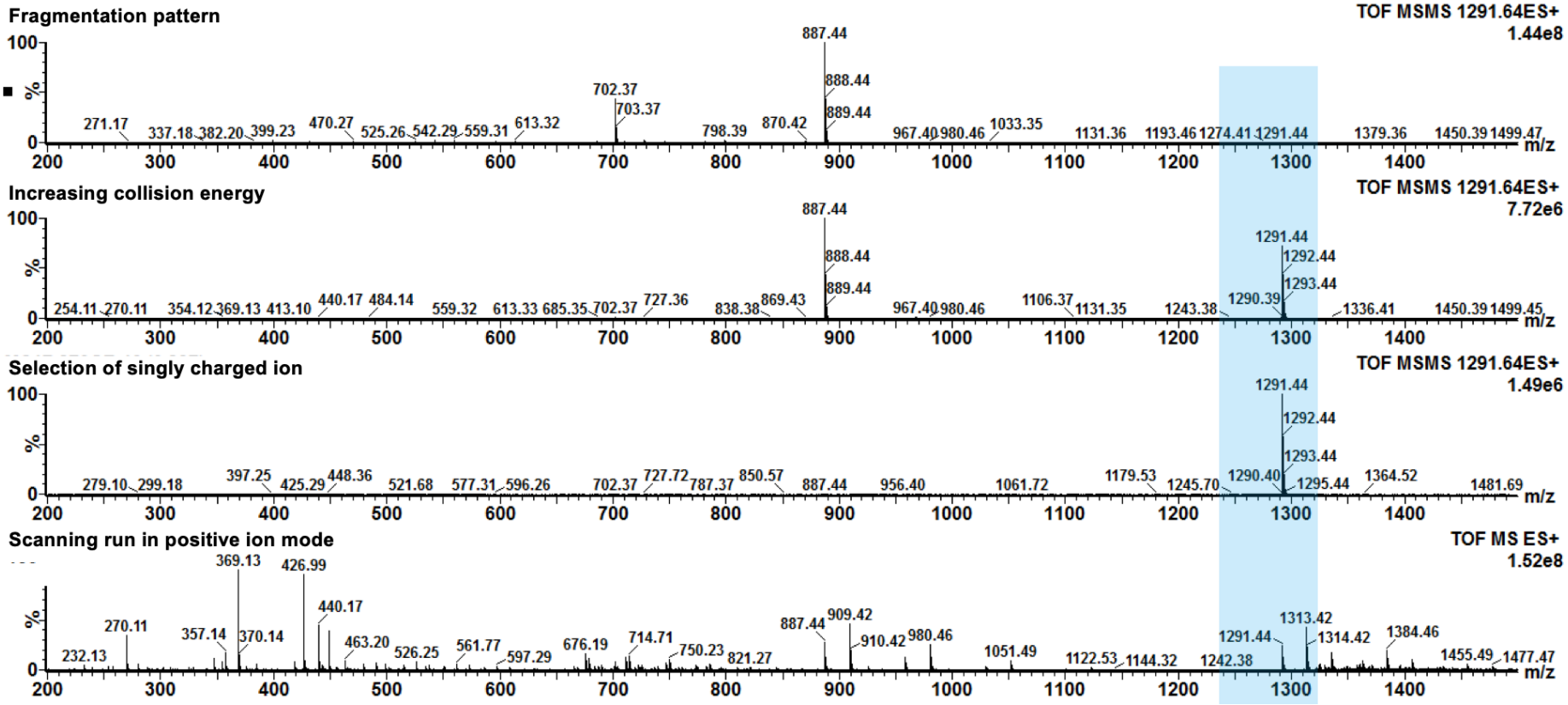

Appendix 3.23 Mass spectrometry experiment for collision-induced fragmentation of UDP-Mur*N*Ac 7P (iGln, L-Ala-L-Ala). Samples were analysed by positive ion nanospray TOF mass spectrometry. The parent ion was selected for fragmentation (blue panel), and then subjected to increasing collision energies, until loss of the parent ion to generate a fragmentation pattern. Data collected and analysed by A.J. Lloyd, and mass spectra generated using MassLynx software (Waters).

Appendix 3.24 - 3.27: Analysis of branched Lipid II (iGln) purifications

Purifications of branched Lipid II (iGln) syntheses (Lipid II 6P (iGln, L-Ala) and Lipid II 7P (iGln, L-Ala-L-Ala)) showed two sets of spots on TLC analysis, eluting at different times. These are hereafter referred to as the ‘lower’ and ‘higher’ spots. Samples were pooled and analysed by mass spectrometry to identify the spot corresponding to the desired product.

a) 6P lower spots full

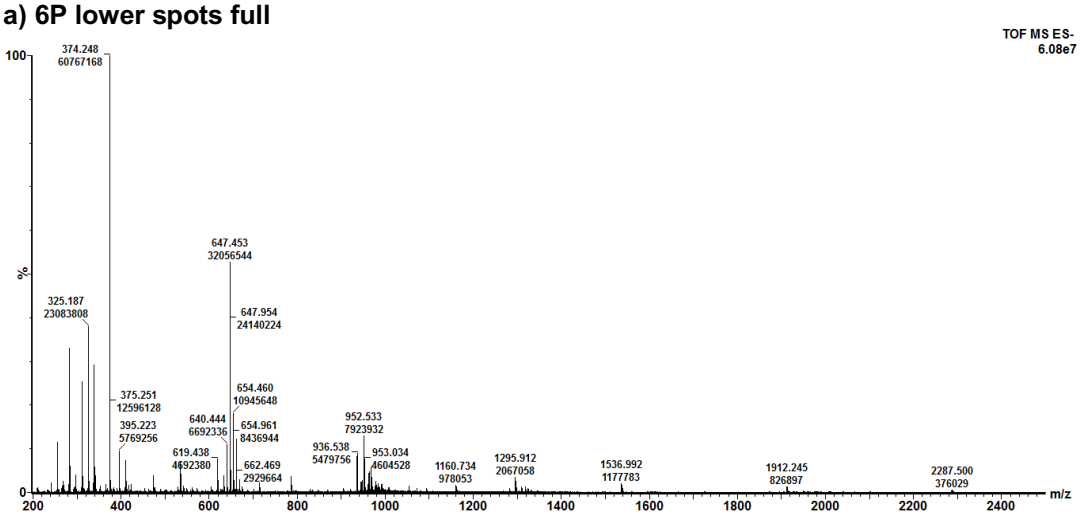

b) Doubly and triply charged

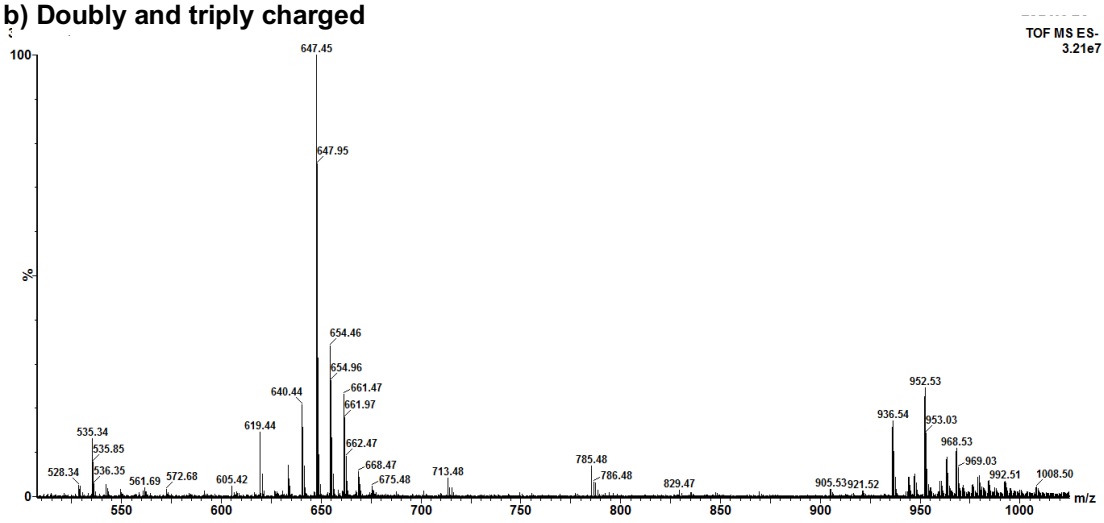

c) Triply charged spectrum

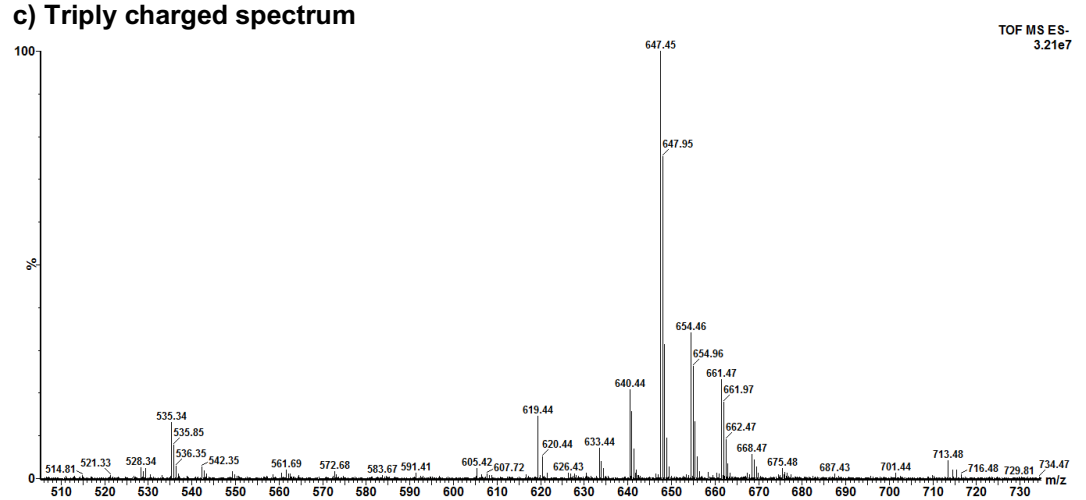

Appendix 3.24 Nanospray TOF mass spectrometry of Lipid II 6P (iGln, L-Ala) 'lower spot' from purification. Samples were analysed by negative ion nanospray TOF mass spectrometry. The full spectrum **(a)**, and double and triply (**b** and **c**) charged spectra are presented. Data collected by A.J. Lloyd, and mass spectra generated using MassLynx software (Waters).

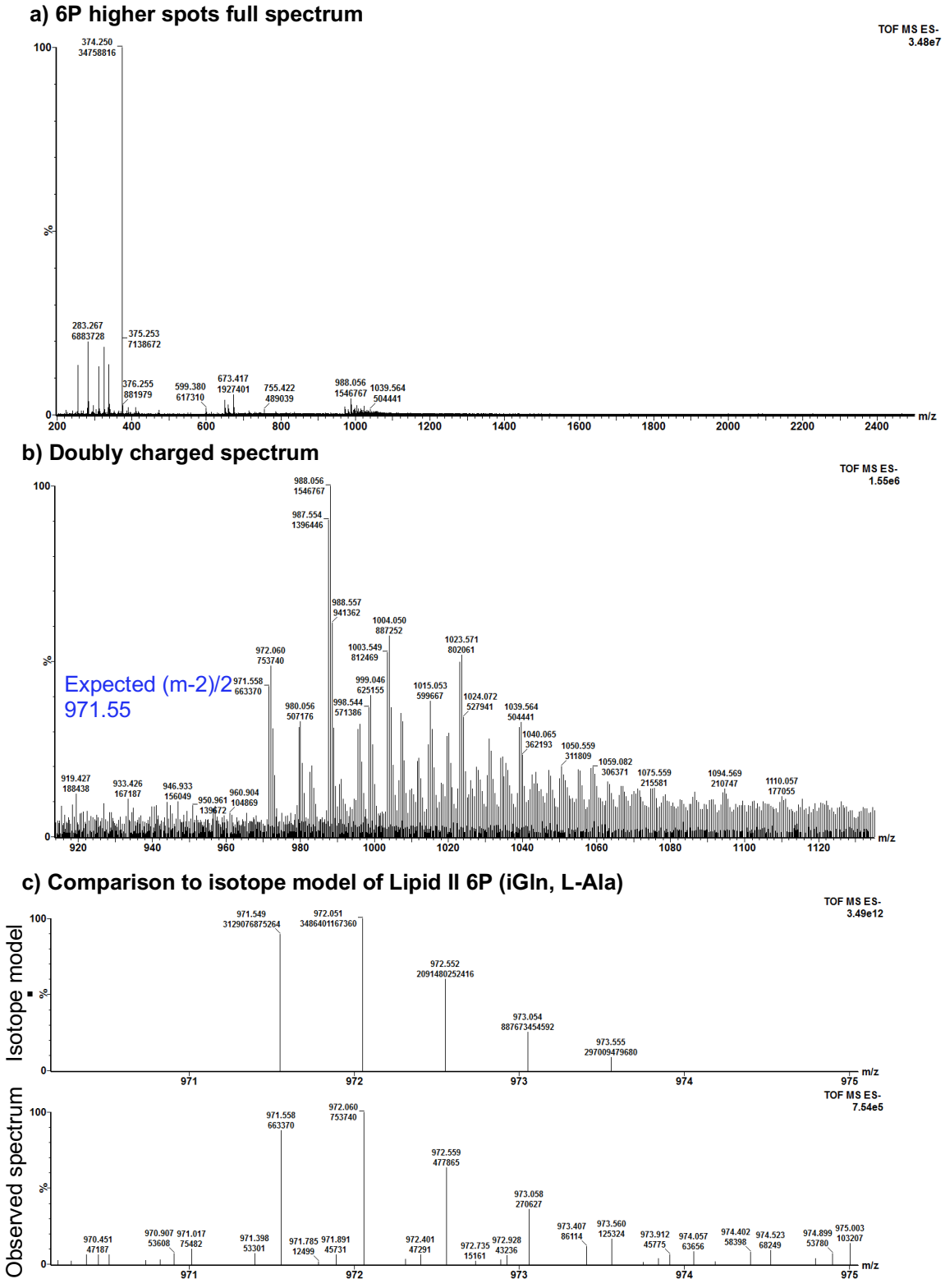

Appendix 3.25 Nanospray TOF mass spectrometry of Lipid II 6P (iGln, L-Ala) 'higher spot' from purification. Samples were analysed by negative ion nanospray TOF mass spectrometry. The full spectrum **(a)**, and doubly charged spectrum **(b)** are presented, alongside **(c)** a comparison to an isotope model for Lipid II 6P (iGln, L-Ala). Data collected by A.J. Lloyd, and mass spectra generated using MassLynx software (Waters).

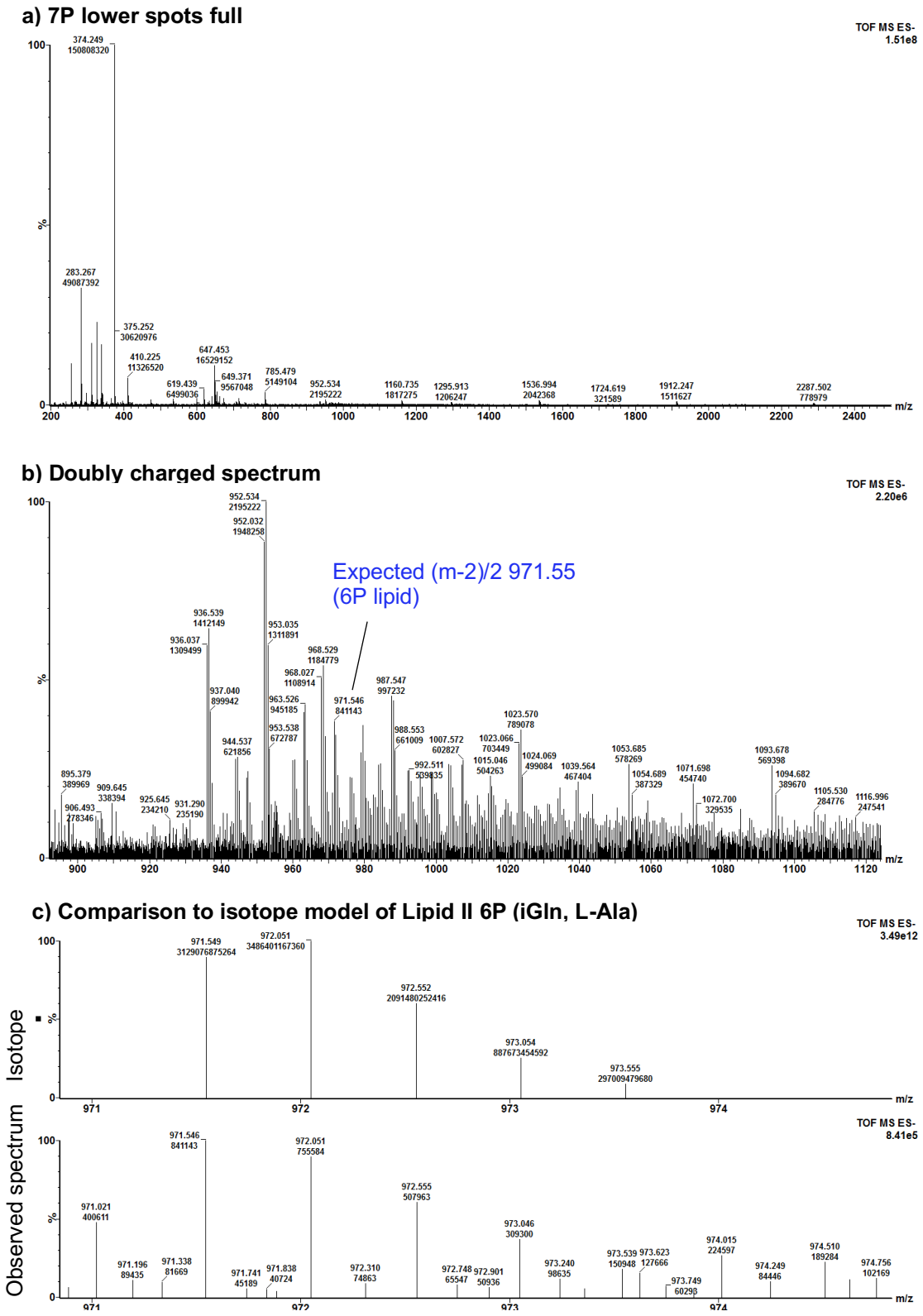

Appendix 3.26 Nanospray TOF mass spectrometry of Lipid II 7P (iGln, L-Ala-L-Ala) 'lower spot' from purification. Samples were analysed by negative ion nanospray TOF mass spectrometry. The full spectrum **(a)**, and doubly charged spectrum **(b)** are presented, alongside **(c)** a comparison to an isotope model for Lipid II 6P (iGln, L-Ala). Data collected by A.J. Lloyd, and mass spectra generated using MassLynx software (Waters).

a) 7P higher spots full spectrum

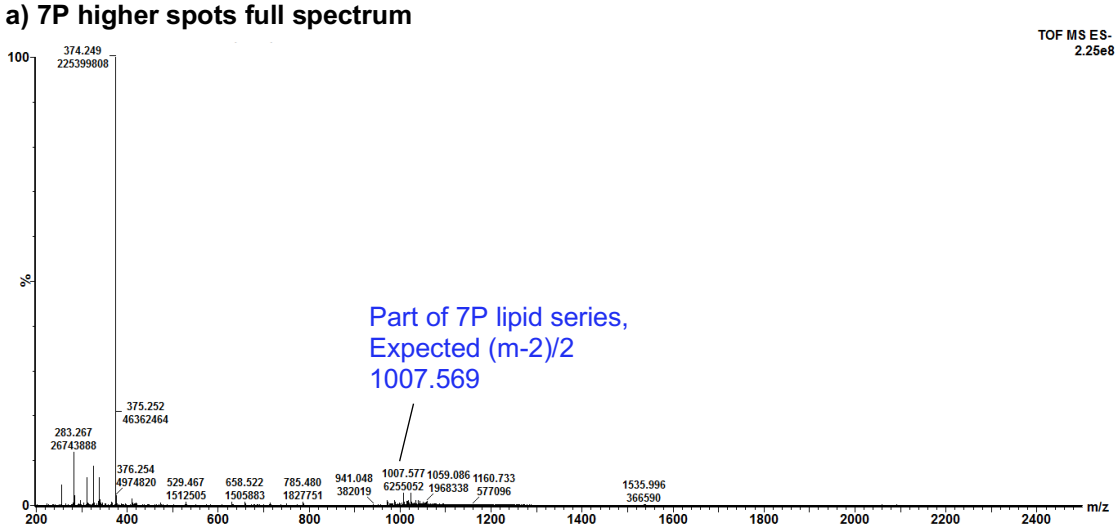

b) Doubly charged spectrum with Lipid II 6P (iGln, L-Ala)

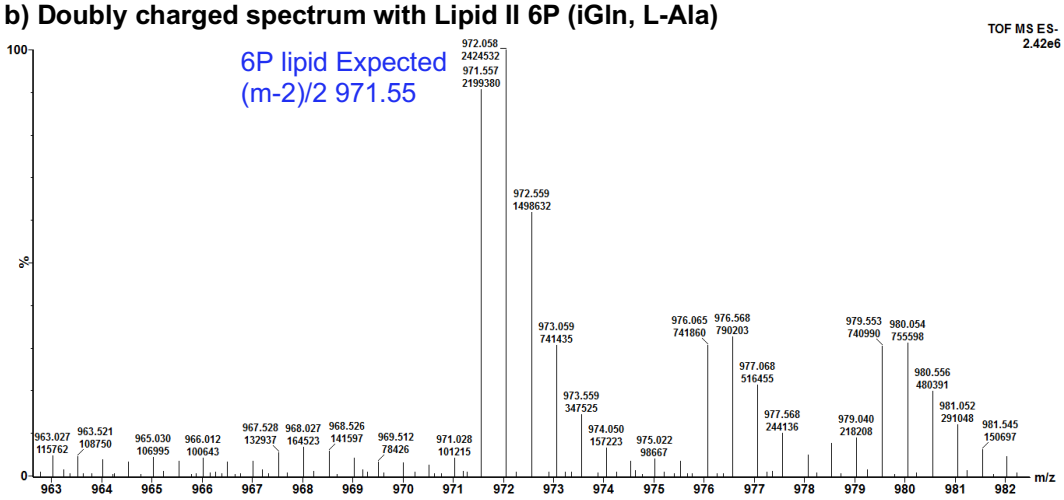

c) Comparison to isotope model of Lipid II 7P (iGln, L-Ala-L-Ala)

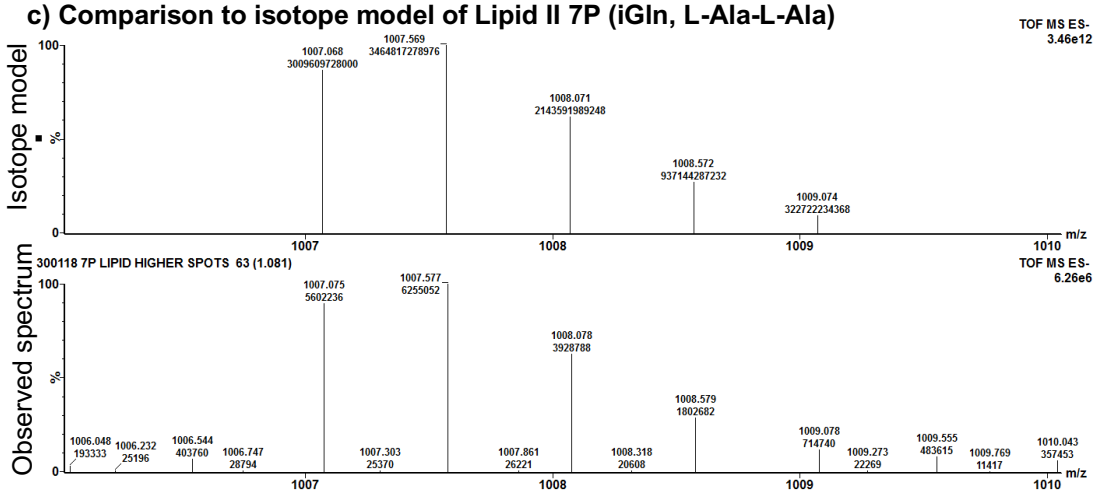

Appendix 3.27 Nanospray TOF mass spectrometry of Lipid II 7P (iGln, L-Ala-L-Ala) 'higher spot' from purification. See legend following page.

(previous page) Appendix 3.27 Nanospray TOF mass spectrometry of Lipid II 7P (iGln, L-Ala-L-Ala) 'higher spot' from purification. Samples were analysed by negative ion nanospray TOF mass spectrometry. The full spectrum **(a)**, and doubly charged spectrum **(b)** are presented, alongside a comparison to an isotope model for Lipid II 7P (iGln, L-Ala). Data collected by A.J. Lloyd, and mass spectra generated using MassLynx software (Waters).

Appendix 3.28 – 3.30: Mass spectrometry analysis of putative donor-only substrates

To provide starting material for synthesis of donor-only Lipid II substrates, UDP-Mur*N*Ac pentapeptide variants were synthesised with altered groups at the side chain of the third position in the peptide stem. Negative ion nanospray TOF mass spectrometry was used to confirm the synthesis of these intermediates.

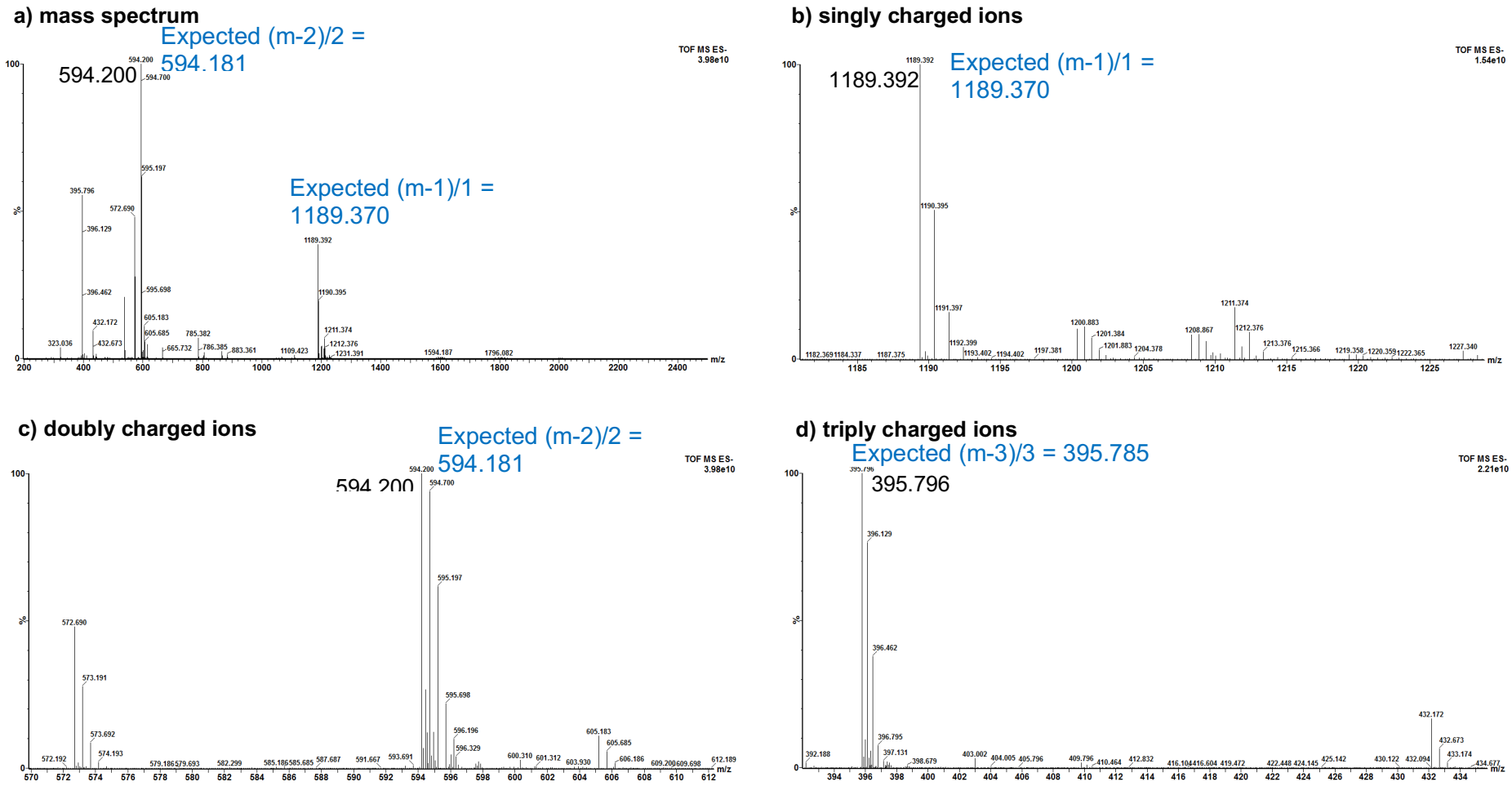

Appendix 3.28 Nanospray TOF mass spectrometry of UDP-Mur*N*Ac 5P (iGln, ε-*N*-acetyl-L-Lys). Samples were analysed by negative ion nanospray TOF mass spectrometry. The full spectrum **(a)** along with singly **(b)**, doubly charged **(c)** and triply **(b)** charged ions are presented. Data collected by A.J. Lloyd, and mass spectra generated using MassLynx software (Waters).

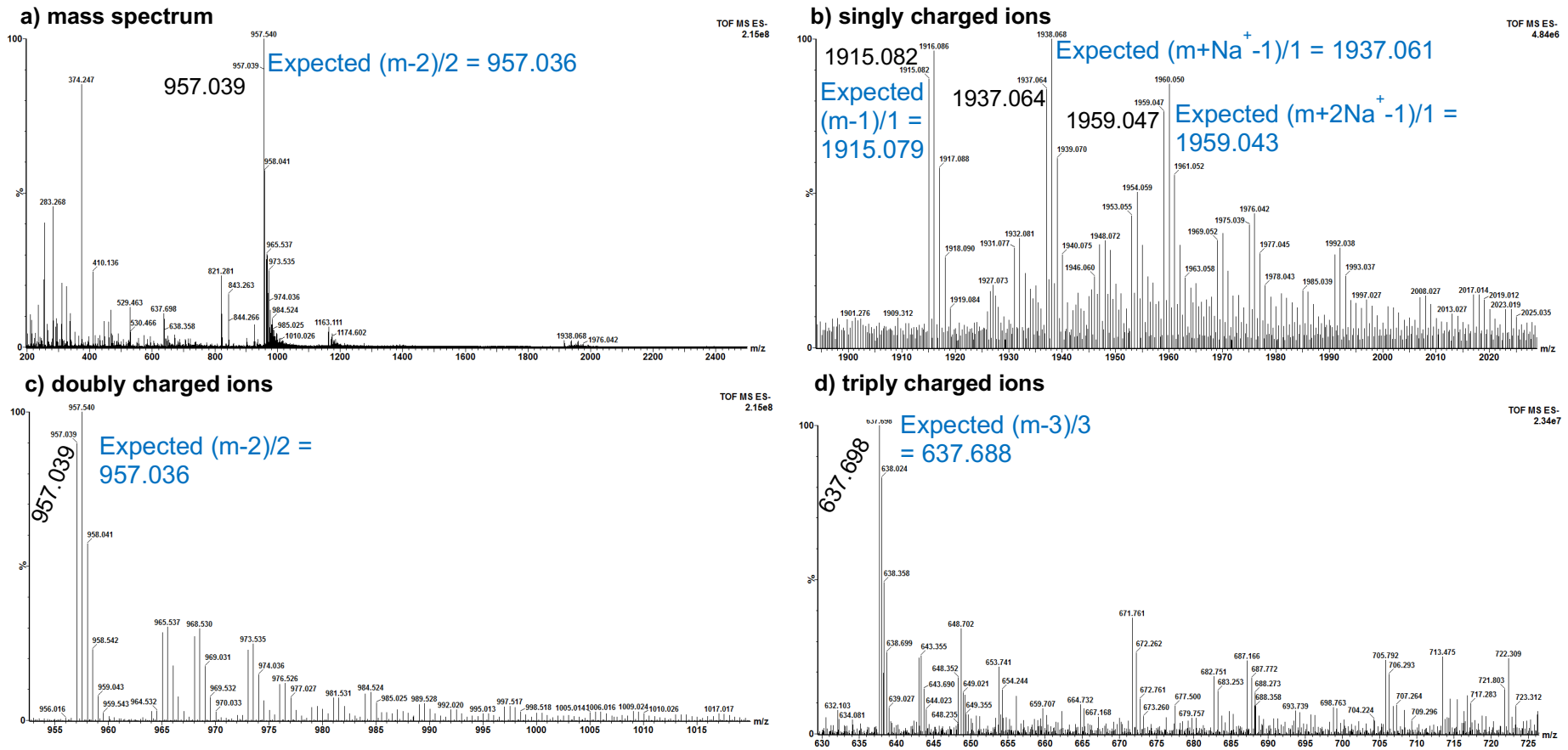

Appendix 3.29 Nanospray TOF mass spectrometry of Lipid II (iGln, ε-*N*-acetyl-L-Lys). Samples were analysed by negative ion nanospray TOF mass spectrometry. The full spectrum **(a)** along with singly **(b)**, doubly charged **(c)** and triply **(b)** charged ions are presented. Data collected by A.J. Lloyd, and mass spectra generated using MassLynx software (Waters).

a) Full spectra

i) Mur*N*Ac 2P (iGln) isotope model

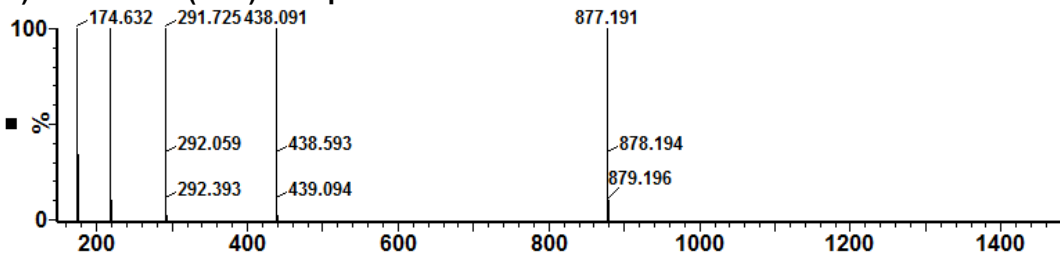

ii) UDP-Mur*N*Ac 5P (iGln, ε-diMe-Lys)

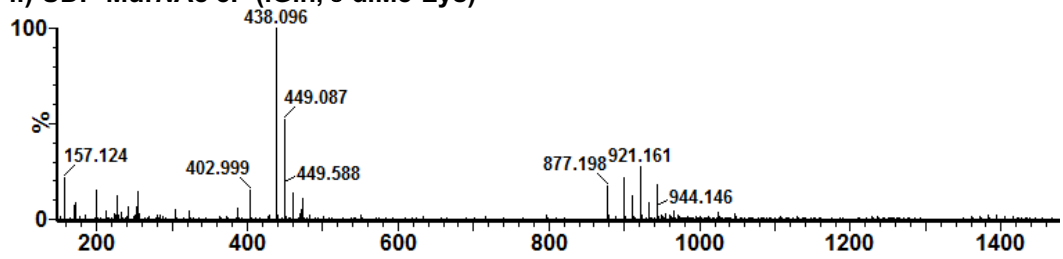

iii) UDP-Mur*N*Ac 5P (iGln, L-Arg)

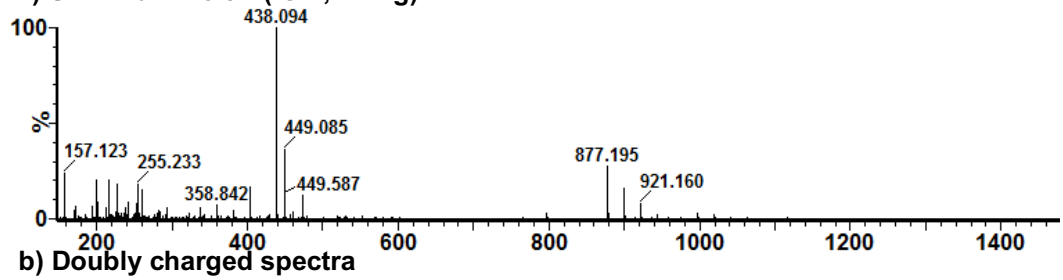

b) Doubly charged spectra

i) Mur*N*Ac 2P (iGln) isotope model

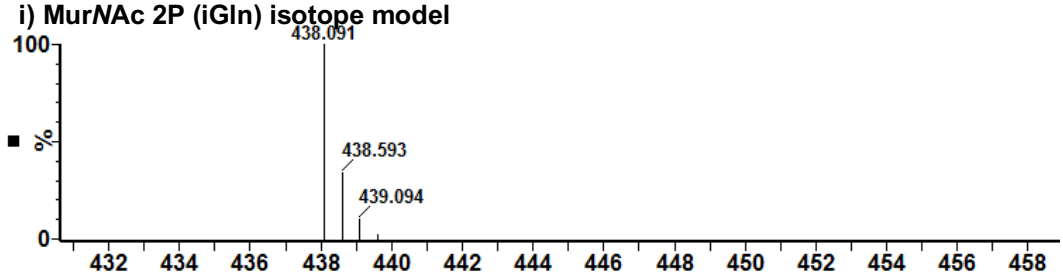

ii) UDP-Mur*N*Ac 5P (iGln, ε-diMe-Lys)

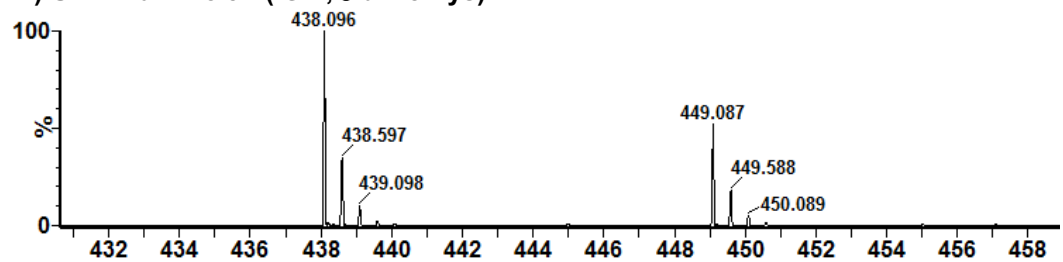

iii) UDP-Mur*N*Ac 5P (iGln, L-Arg)

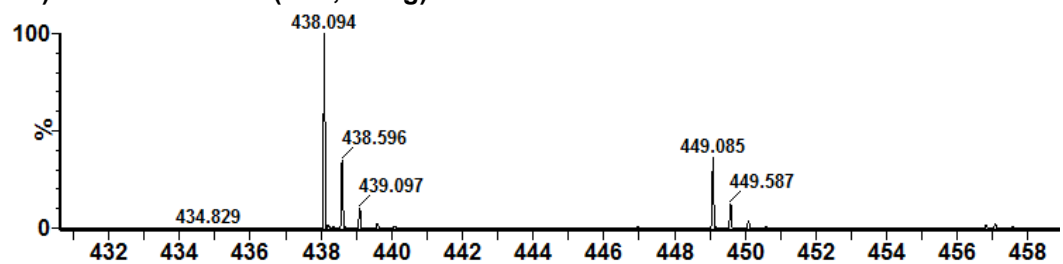

(previous page) Appendix 3.30 Nanospray TOF mass spectrometry of putative donor-only peptides. Samples were analysed by negative ion nanospray TOF mass spectrometry. **a)** Full spectra for (**i**) isotope model of UDP-Mur*N*Ac dipeptide (iGln); (**ii**) UDP-Mur*N*Ac 5P (iGln, ε-diMe-Lys) synthesis; (**iii**) UDP-Mur*N*Ac 5P (iGln, L-Arg) synthesis. **b**) Doubly charged spectra for (**i**) isotope model of UDP-Mur*N*Ac dipeptide (iGln); (**ii**) UDP-Mur*N*Ac 5P (iGln, ε-diMe-Lys) synthesis; (**iii**) UDP-Mur*N*Ac 5P (iGln, L-Arg) synthesis. Data collected by A.J. Lloyd, and mass spectra generated using MassLynx software (Waters).

Appendix 3.31 - 3.36: Mass spectrometry of acceptor-only substrate syntheses

The substrates and starting material for acceptor-only substrates were analysed by negative ion nanospray TOF mass spectrometry to confirm the syntheses.

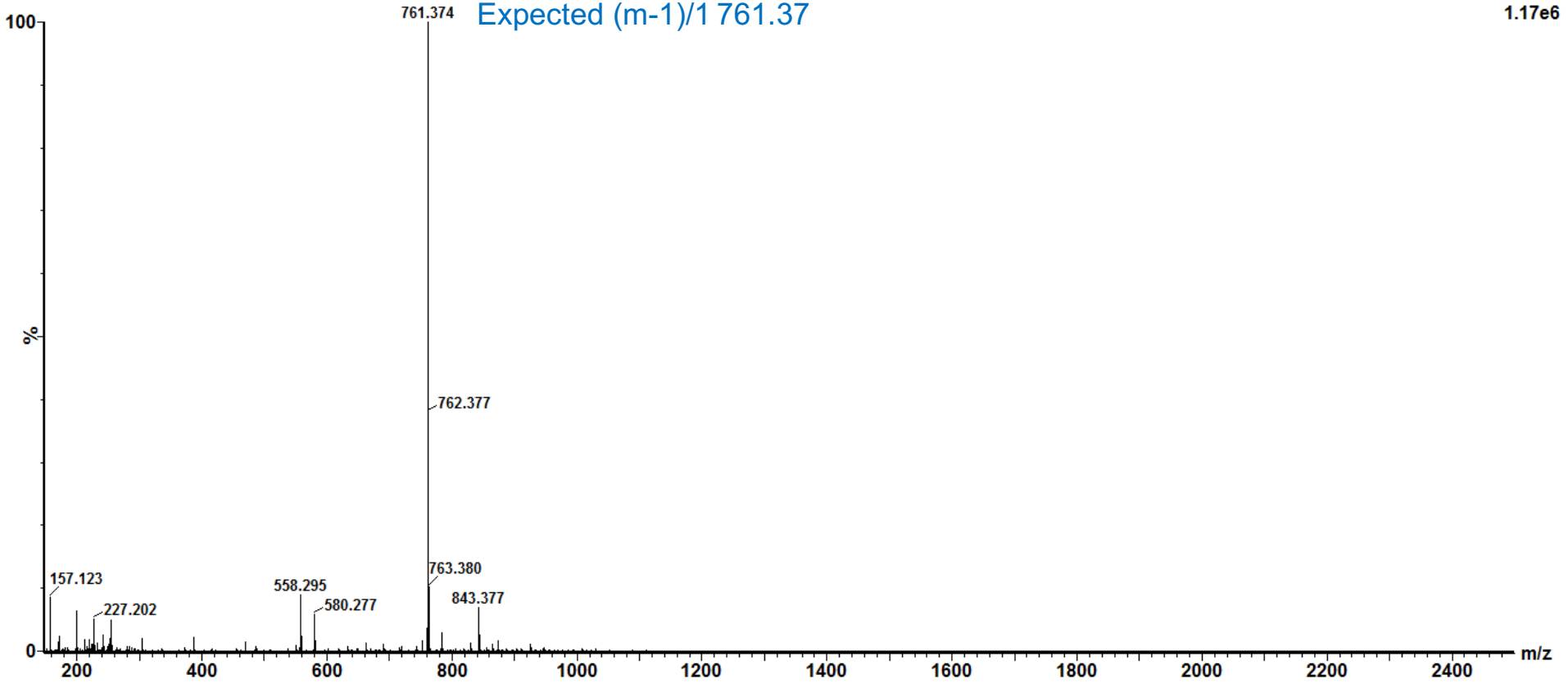

Appendix 3.31 Nanospray TOF mass spectrometry of Mur*N*Ac 5P(iGln). The sample was analysed by negative ion nanospray TOF mass spectrometry. Data collected by A.J. Lloyd, and mass spectra generated using MassLynx software (Waters).

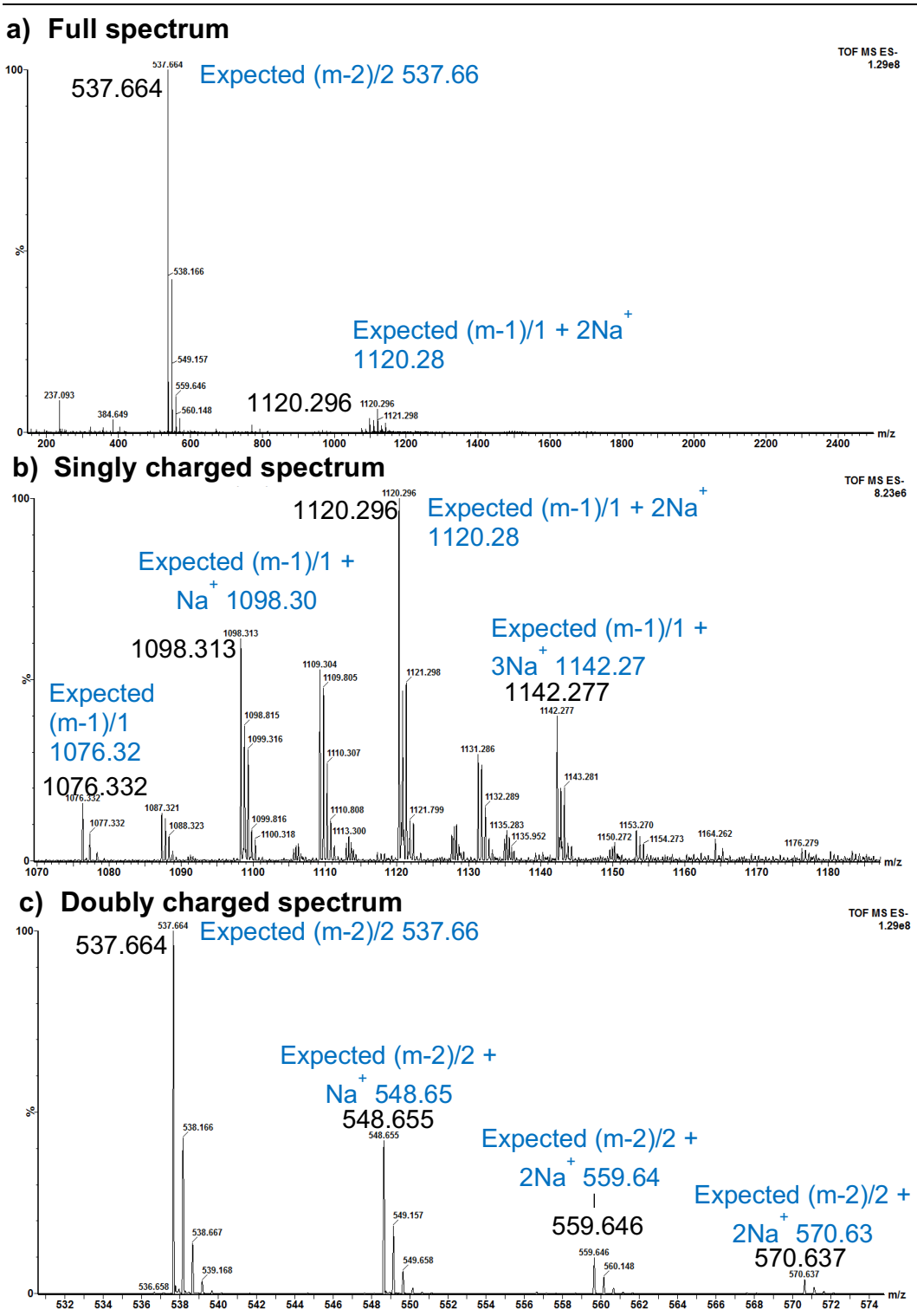

Appendix 3.32 Nanospray TOF mass spectrometry of UDP-Mur*N*Ac 4P (iGln) Samples were analysed by negative ion nanospray TOF mass spectrometry **a)** Full spectrum **b**) Singly charged spectrum and **c**) doubly charged spectrum. Data collected by A.J. Lloyd, and mass spectra generated using MassLynx software (Waters).

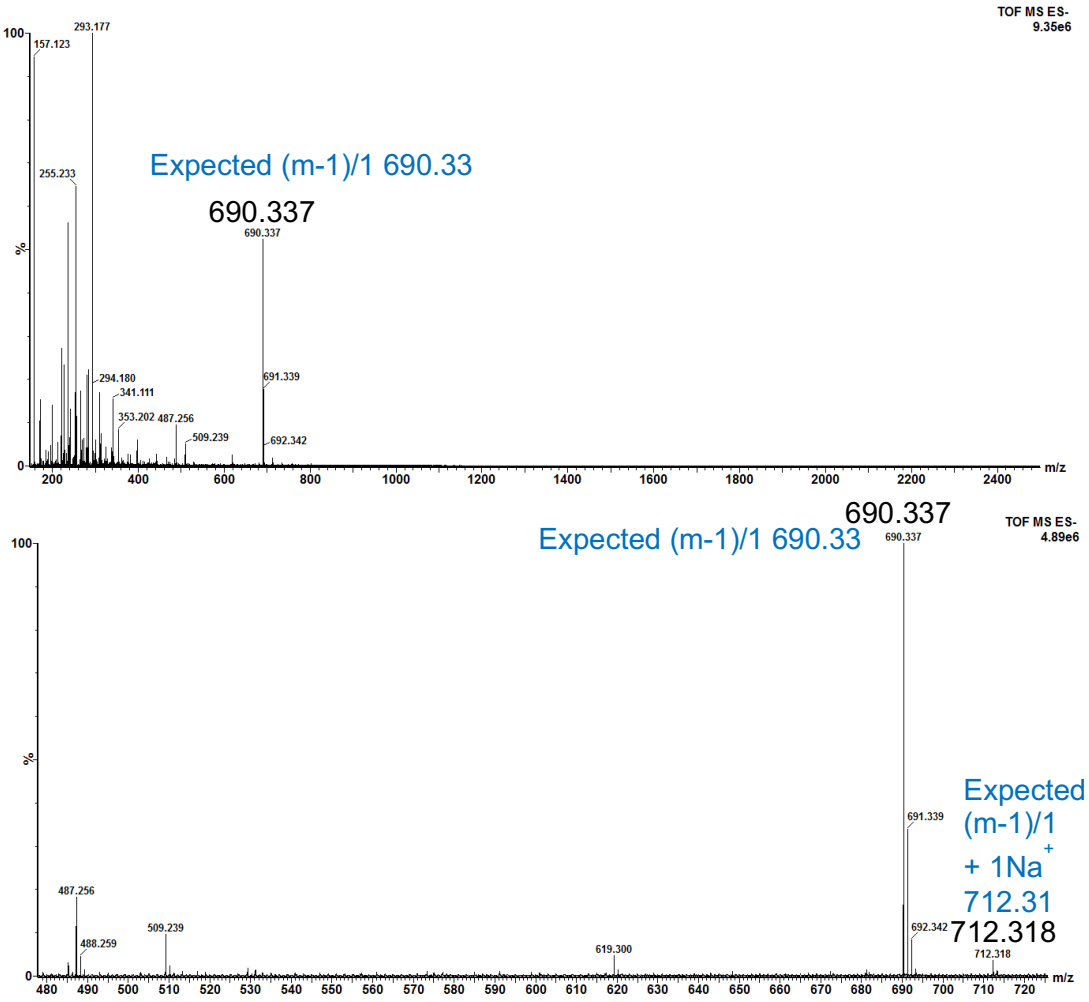

Appendix 3.33 Nanospray TOF mass spectrometry of Mur*N*Ac 4P (iGln)
Samples were analysed by negative ion nanospray TOF mass spectrometry. **a)** Full spectrum and **b**) Singly charged spectrum. Data collected by A.J. Lloyd, and mass spectra generated using MassLynx software (Waters).

a) Full spectrum

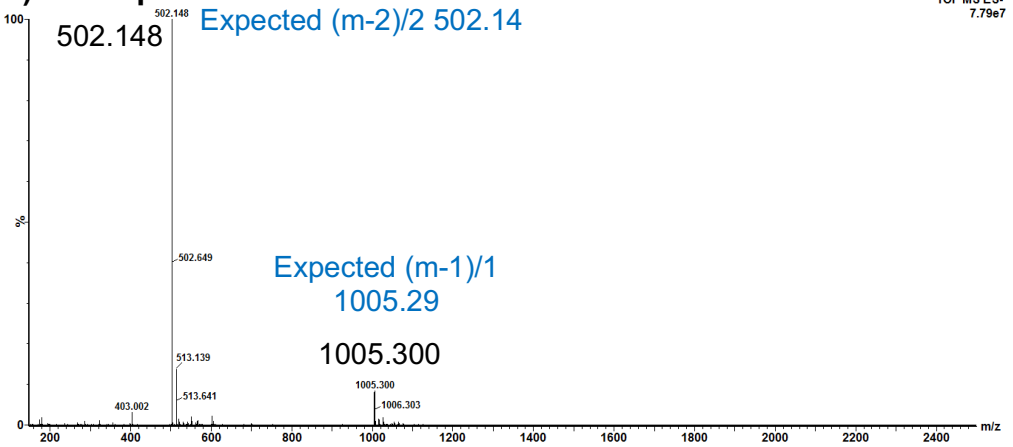

b) Singly charged spectrum

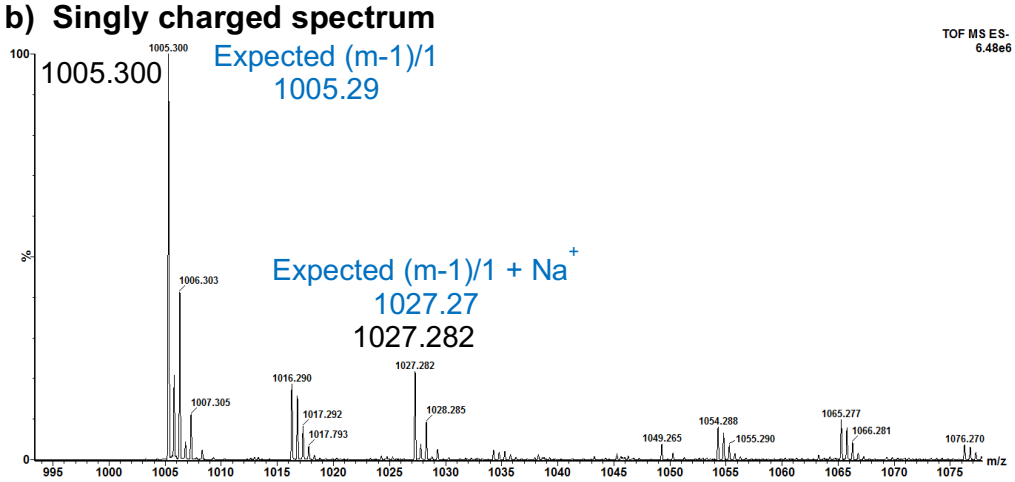

c) Singly charged spectrum

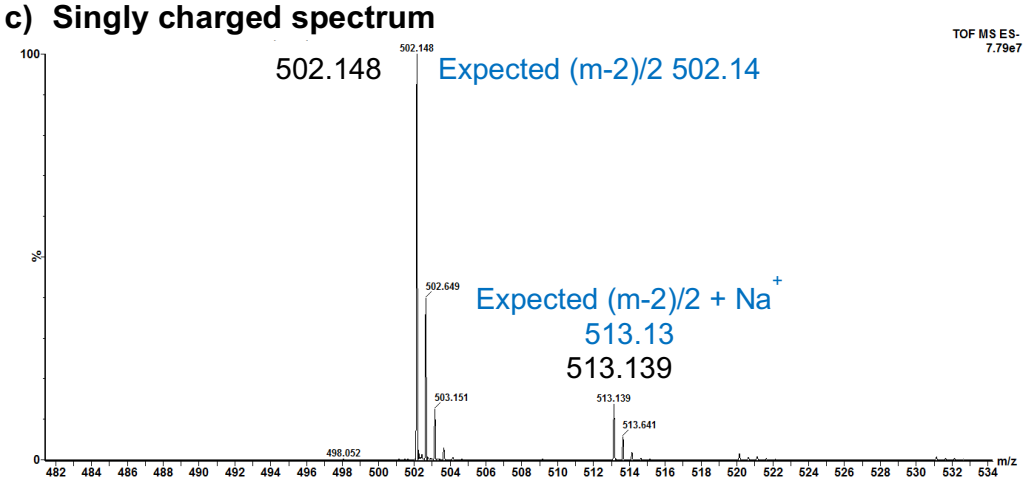

Appendix 3.34 Nanospray TOF mass spectrometry of UDP-Mur*N*Ac 3P (iGln) Samples were analysed by negative ion nanospray TOF mass spectrometry. **a)** Full spectrum **b**) Singly charged spectrum and **c**) Doubly charged spectrum. Data collected by A.J. Lloyd, and mass spectra generated using MassLynx software (Waters).

a) Full spectrum

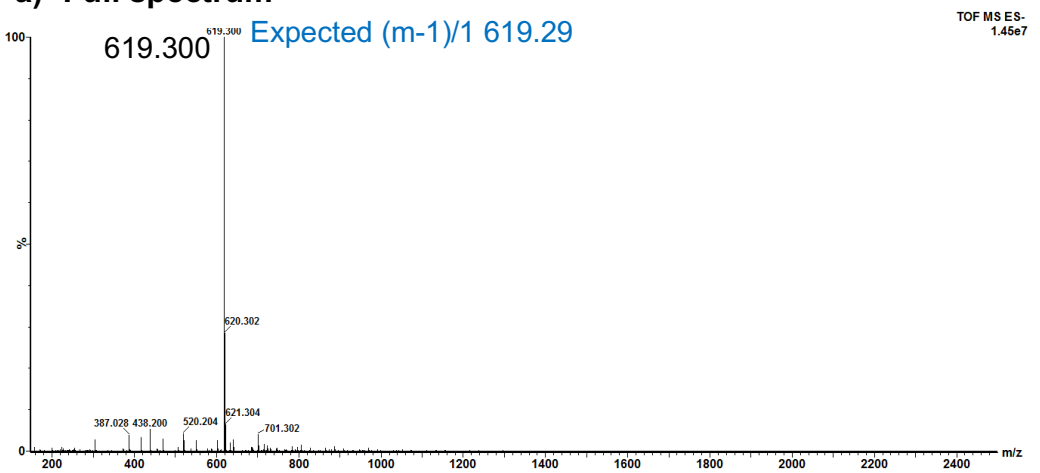

b) Singly charged spectrum

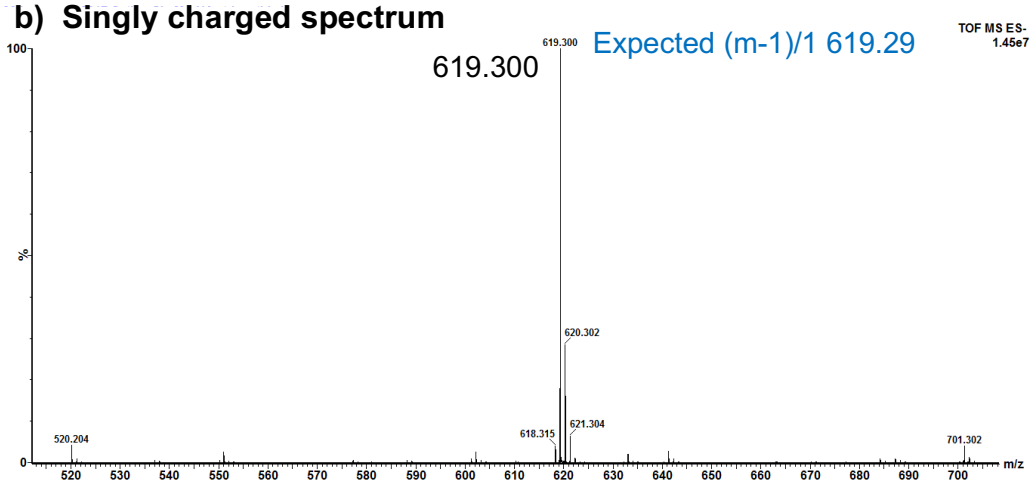

Appendix 3.35 Nanospray TOF mass spectrometry of Mur*N*Ac 3P (iGln) Samples were analysed by negative ion nanospray TOF mass spectrometry. **a)** Full spectrum and **b**) Singly charged spectrum. Data collected by A.J. Lloyd, and mass spectra generated using MassLynx software (Waters).

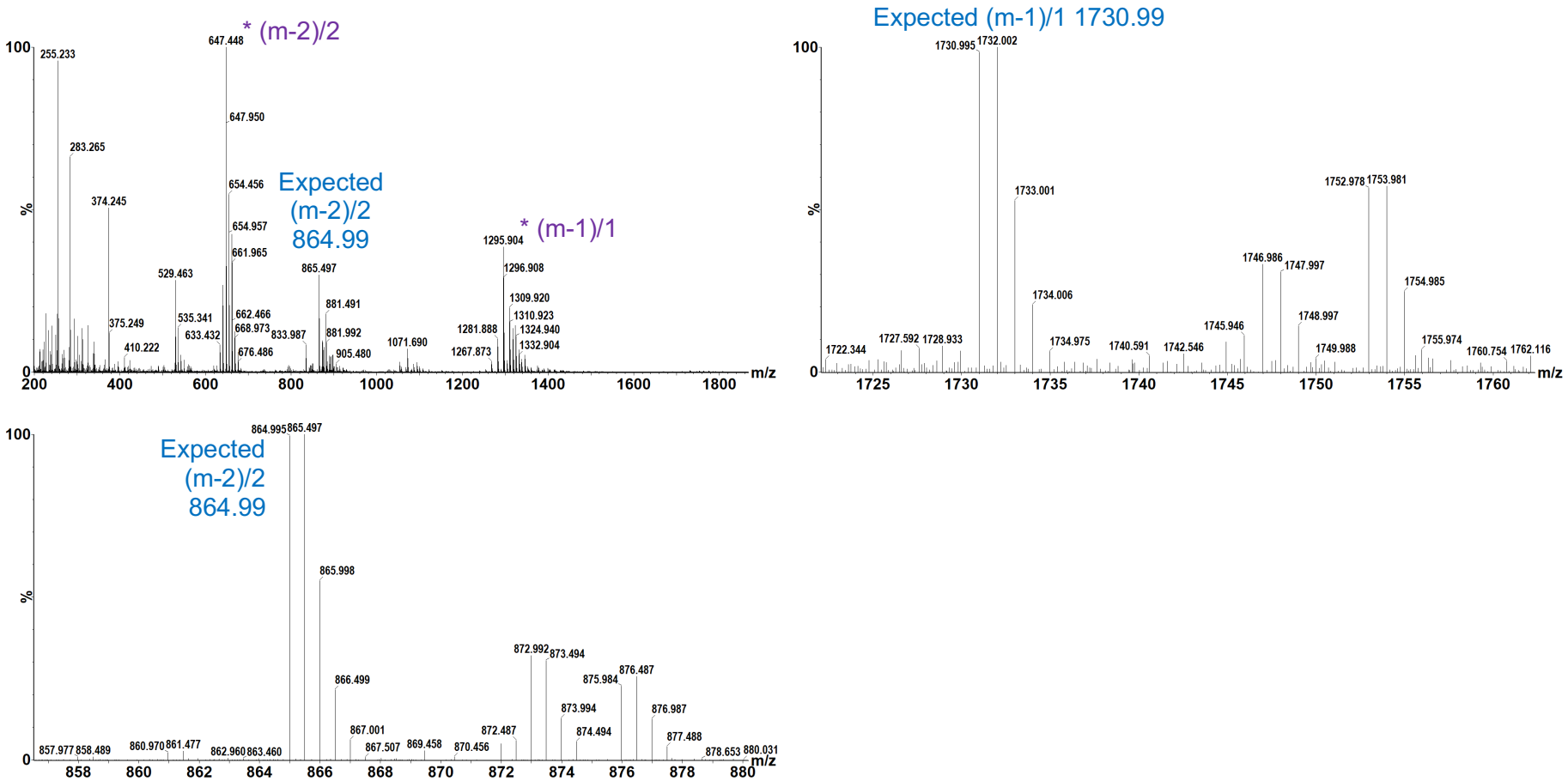

Appendix 3.36 Nanospray TOF mass spectrometry of Lipid II 3P (iGln) Samples were analysed by negative ion nanospray TOF mass spectrometry. **a)** Full spectrum and **b**) Singly charged spectrum. Data collected by J. Tod, and mass spectra generated using MassLynx software (Waters).

Appendices to Chapter 4

Appendix 4.1 – 4.3: Mass spectrometry analysis of mutanolysin-digested TP products

Mass spectrometry was used to detect transpeptidation products formed by PBP1a^{D39}. Transpeptidase reactions of PBP1a^{D39} using Lipid II (iGln) as a substrate were digested using mutanolysin and analysed by liquid chromatography-mass spectrometry (LC-MS). Two independent samples were analysed in this way (spectra illustrated for one sample).

(next page) Appendix 4.1 LC-MS analysis of TP reactions with PBP1a^{D39} and Lipid II (iGln) (C) or Lipid II (iGln) only. The total ion chromatograms (Ai and Bi) were queried for mass to charge ratios corresponding to the triply (iv), doubly (ii) and singly (i) charged ions that would correspond to the putative TP product. The blue box highlights the peak of interest in sample A, and the corresponding timepoint in sample B. Data collected by A.J. Lloyd, and mass spectra generated using MassLynx software (Waters).

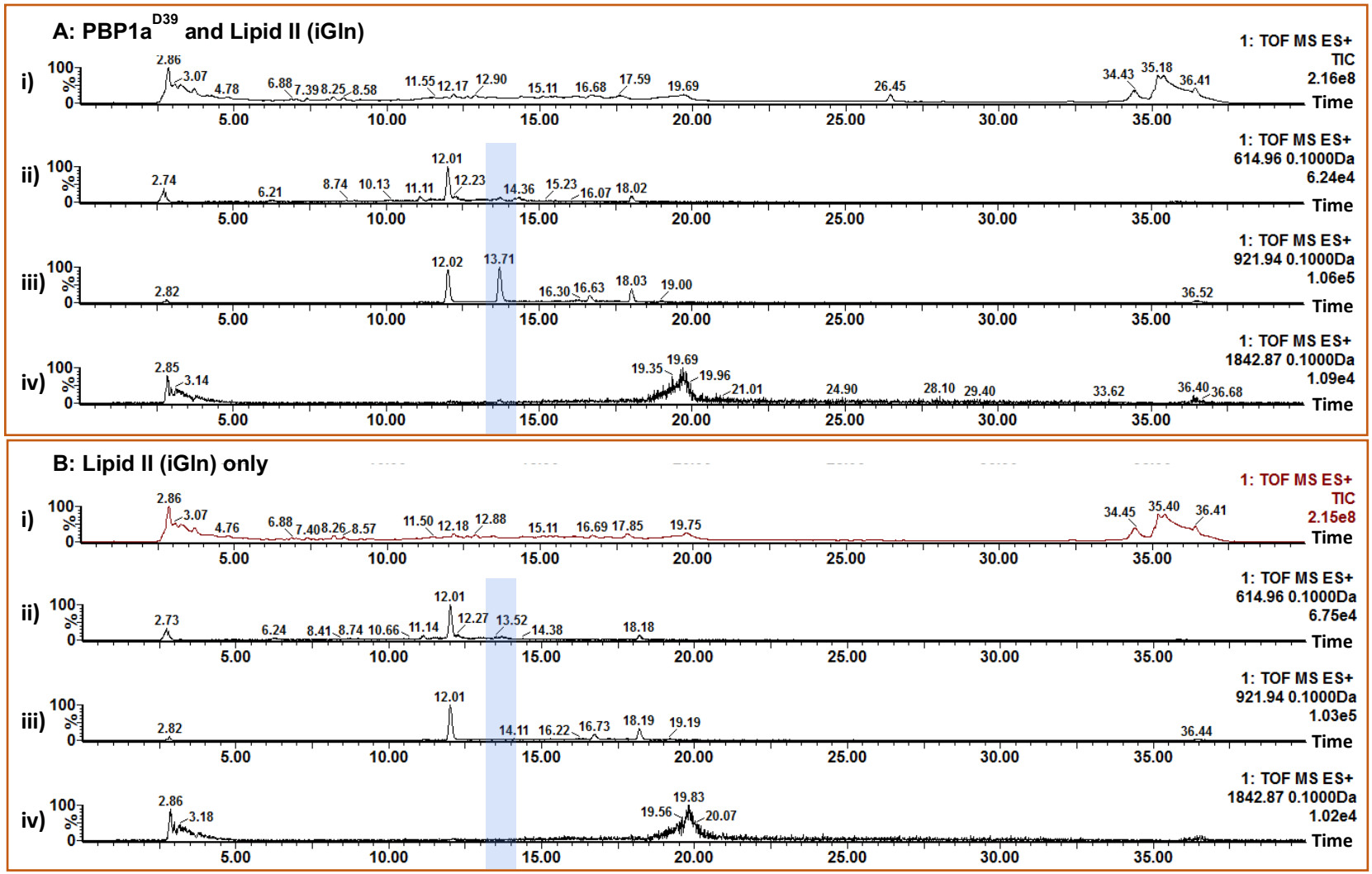
A: PBP1a D39 and Lipid II (iGln)
i)
1: TOF MS ES+
TIC
2.16e8
2.86
3.07
4.78
6.88
7.39
8.25
8.58
11.55
12.17
12.90
15.11
16.68
17.59
19.69
26.45
34.43
35.18
36.41
Time
ii)
1: TOF MS ES+
614.96 0.1000Da
6.24e4
2.74
6.21
8.74
10.13
11.11
12.01
12.23
14.36
15.23
16.07
18.02
Time
iii)
1: TOF MS ES+
921.94 0.1000Da
1.06e5
2.82
12.02
13.71
16.30
16.63
18.03
19.00
36.52
Time
iv)
1: TOF MS ES+
1842.87 0.1000Da
1.09e4
2.85
3.14
19.35
19.69
19.96
21.01
24.90
28.10
29.40
33.62
36.40
36.68
Time
B: Lipid II (iGln) only
i)
1: TOF MS ES+
TIC
2.15e8
2.86
3.07
4.76
6.88
7.40
8.26
8.57
11.50
12.18
12.88
15.11
16.69
17.85
19.75
34.45
35.40
36.41
Time
ii)
1: TOF MS ES+
614.96 0.1000Da
6.75e4
2.73
6.24
8.41
8.74
10.66
11.14
12.01
12.27
13.52
14.38
18.18
Time
iii)
1: TOF MS ES+
921.94 0.1000Da
1.03e5
2.82
12.01
14.11
16.22
16.73
18.19
19.19
36.44
Time
iv)
1: TOF MS ES+
1842.87 0.1000Da
1.02e4
2.86
3.18
19.56
19.83
20.07
Time

a) Full mass spectrum

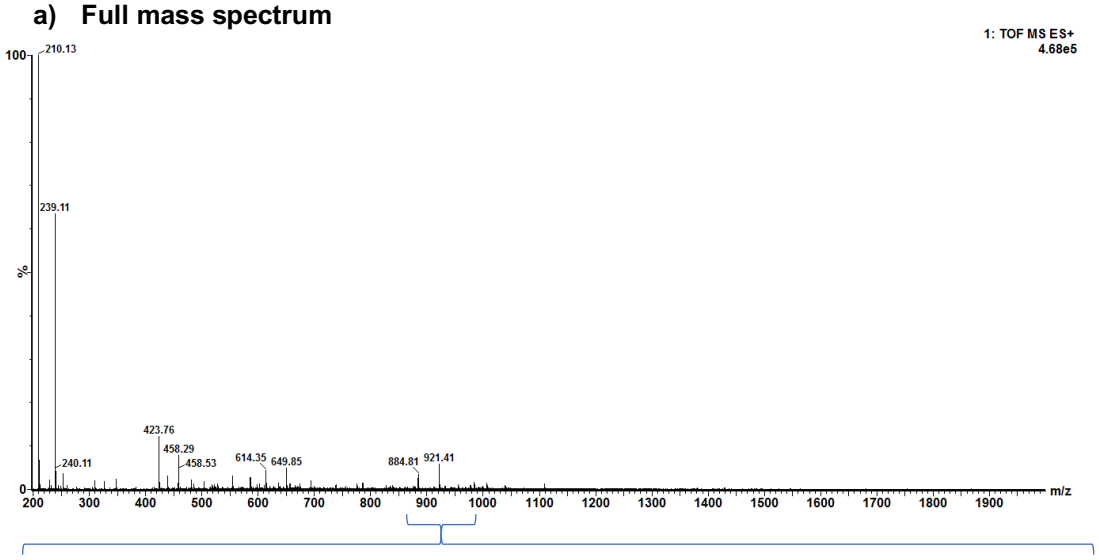

b) Doubly charged series

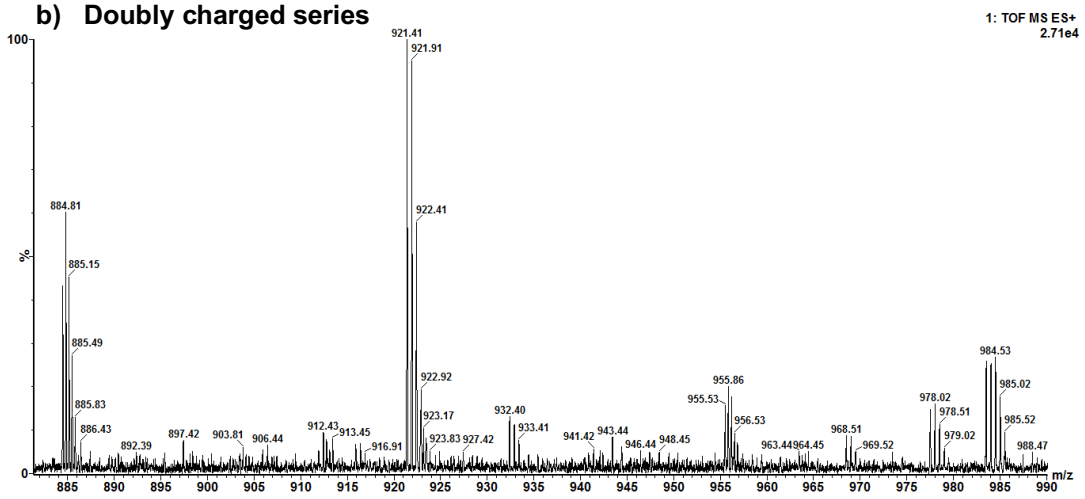

c) Theoretical mass spectrum of TP product from Lipid II

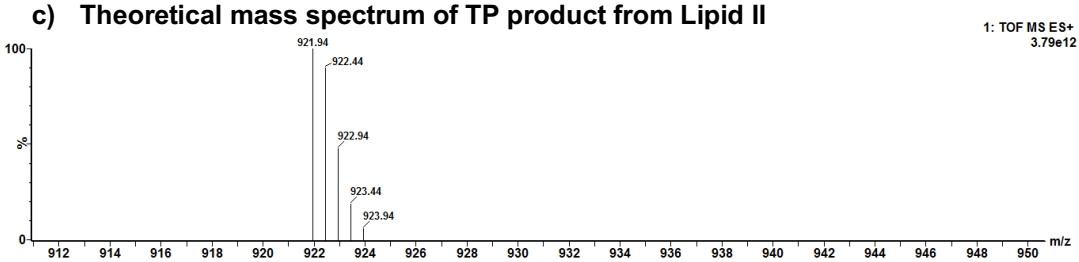

d) Observed doubly charged series

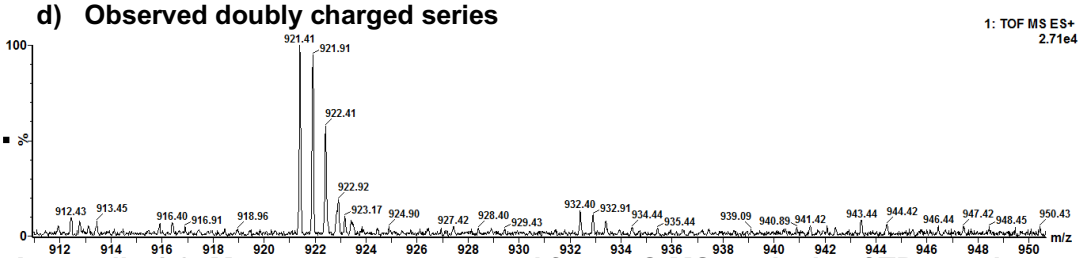

Appendix 4.2: Mass spectra generated from LC-MS analysis of TP reactions with PBP1a^{D39} and Lipid II (iGln). See legend following page.

(previous page) Appendix 4.2: Mass spectra generated from LC-MS analysis of TP reactions with PBP1a^{D39} and Lipid II (iGln). From a peak in the total ion chromatogram containing an ion of interest, a full mass spectrum **(a)** was generated. The doubly charged series **(b)** identified in the LC-MSMS analysis was compared (d) to the theoretical mass spectrum (c) of the putative TP product. Data collected by A.J. Lloyd, and mass spectra generated using MassLynx software (Waters).

Appendix 4.3 LC-MS analysis of TP reactions with Lipid II (iGln) Reactions were digested using mutanolysin and analysed by liquid chromatography-mass spectrometry (LC-MS) by positive ion electrospray time of flight mass spectrometry, to detect ions corresponding to putative TP product. **m/z**, mass to charge ratio. Data collected by A.J. Lloyd, and mass spectra generated using MassLynx software (Waters).

Compound	**Charge state**	**Expected m/z**	**Observed m/z**			
			A: PBP1a^{D39} and Lipid II (iGln)	**B:** Lipid II (iGln)	**C:** PBP1a^{D39} and Lipid II (iGln)	**D:** Lipid II (iGln)
TP or CP product	(m + 1)/1	1842.87	-	-	-	-
	(m + 2)/2	921.94	921.41 921.91 922.41	-	921.41 921.91 922.41	-
	(m + 3)/3	614.96	-	-	-	-

Appendix 4.4 – 4.5: Mass spectrometry analysis of mutanolysin-digested TP products from detergent titration experiments

Mass spectrometry was used to detect transpeptidation products formed by PBP1a^{D39} in reactions containing varied concentrations of E_6C_{12} detergent. Transpeptidase reactions of PBP1a^{D39} using Lipid II (iGln) as a substrate were digested using mutanolysin and analysed by liquid chromatography-mass spectrometry (LC-MS). Two independent samples were analysed in this way (spectra illustrated for one sample).

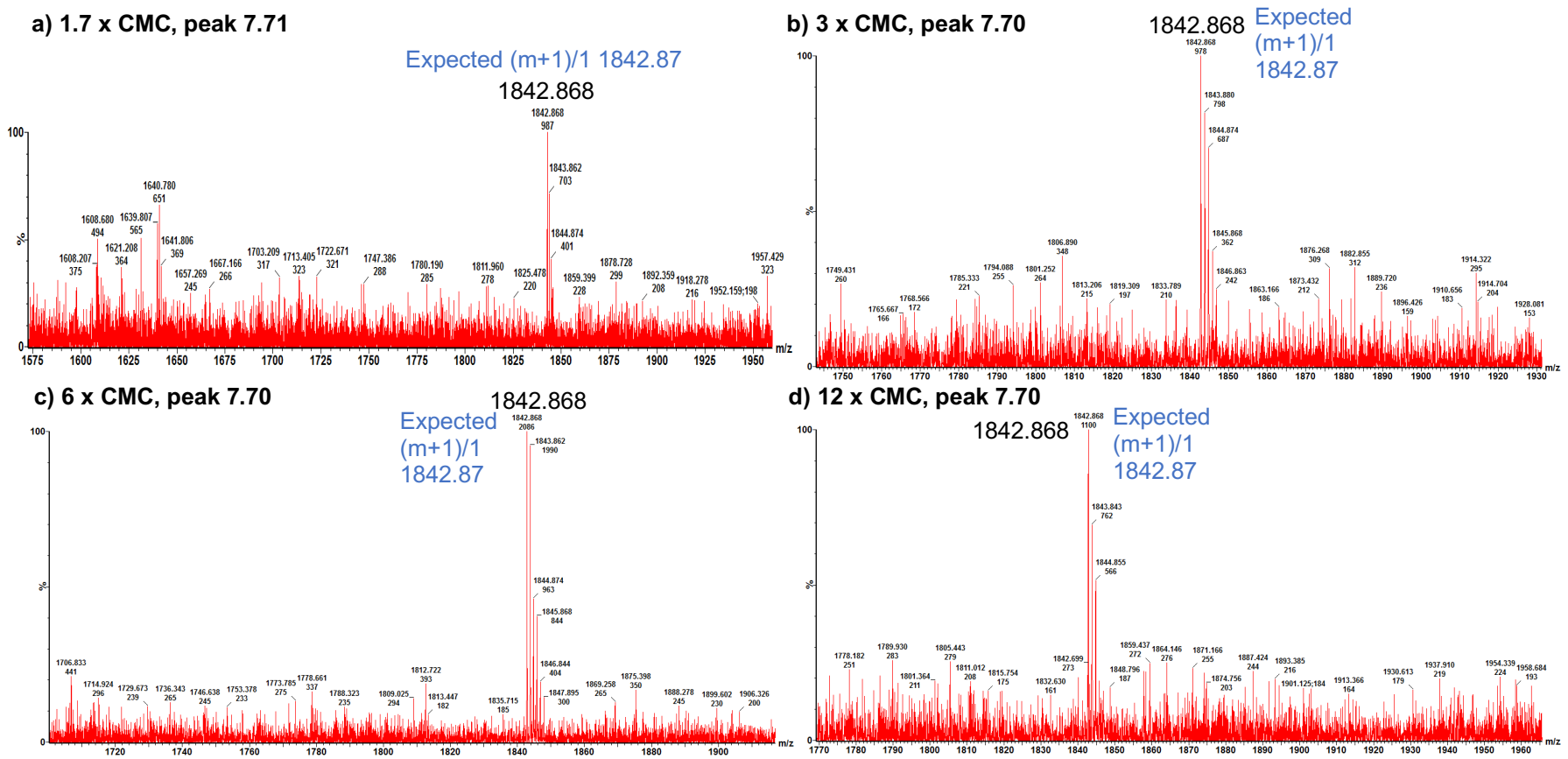

Appendix 4.4 LC-MS analysis of TP reactions with varied concentrations of E_6C_{12} detergent – singly charged spectra. Samples were analysed by positive ion nanospray TOF mass spectrometry. The total ion chromatogram for each reaction was queried for mass to charge ratios corresponding to the singly charged ions of putative transpeptidase or carboxypeptidase products, generating mass spectra for peaks containing those ions **(a-d)**. Mass spectra are labelled according to the reaction of origin (multiple of CMC), and the peak in the total ion chromatogram. Data collected by A.J. Lloyd, and mass spectra generated using MassLynx software (Waters).

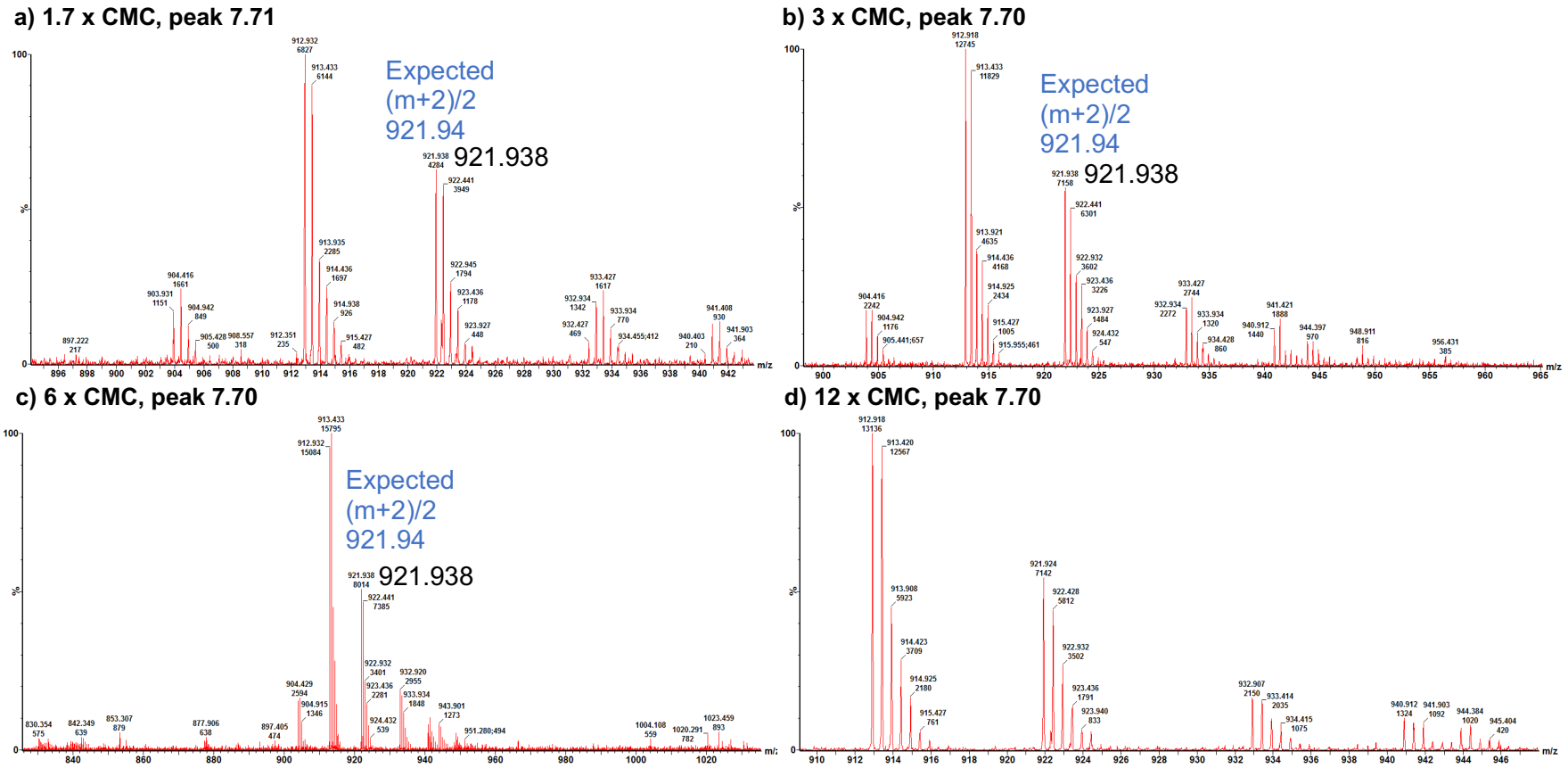

Appendix 4.5 LC-MS analysis of TP reactions with varied concentrations of E_6C_{12} detergent – doubly charged spectra. Samples were analysed by positive ion nanospray TOF mass spectrometry. The total ion chromatogram for each reaction was queried for mass to charge ratios corresponding to the doubly charged ions of putative transpeptidase or carboxypeptidase products, generating mass spectra for peaks containing those ions **(a-d)**. Mass spectra are labelled according to the reaction of origin (multiple of CMC), and the peak in the total ion chromatogram. Data collected by A.J. Lloyd, and mass spectra generated using MassLynx software (Waters).

Appendix 4.5 – 4.8: Mass spectrometry of Lipid II (iGln) stocks

Transpeptidase assays identified variation between stocks of Lipid II (iGln), where one stock supported activity (stock 2), another did not (1), and another (3) appeared to have a contaminant that was reactive with the coupling system. These three stocks of Lipid II (iGln) were analysed by negative ion TOF mass spectrometry to analyse the variation between the three stocks.

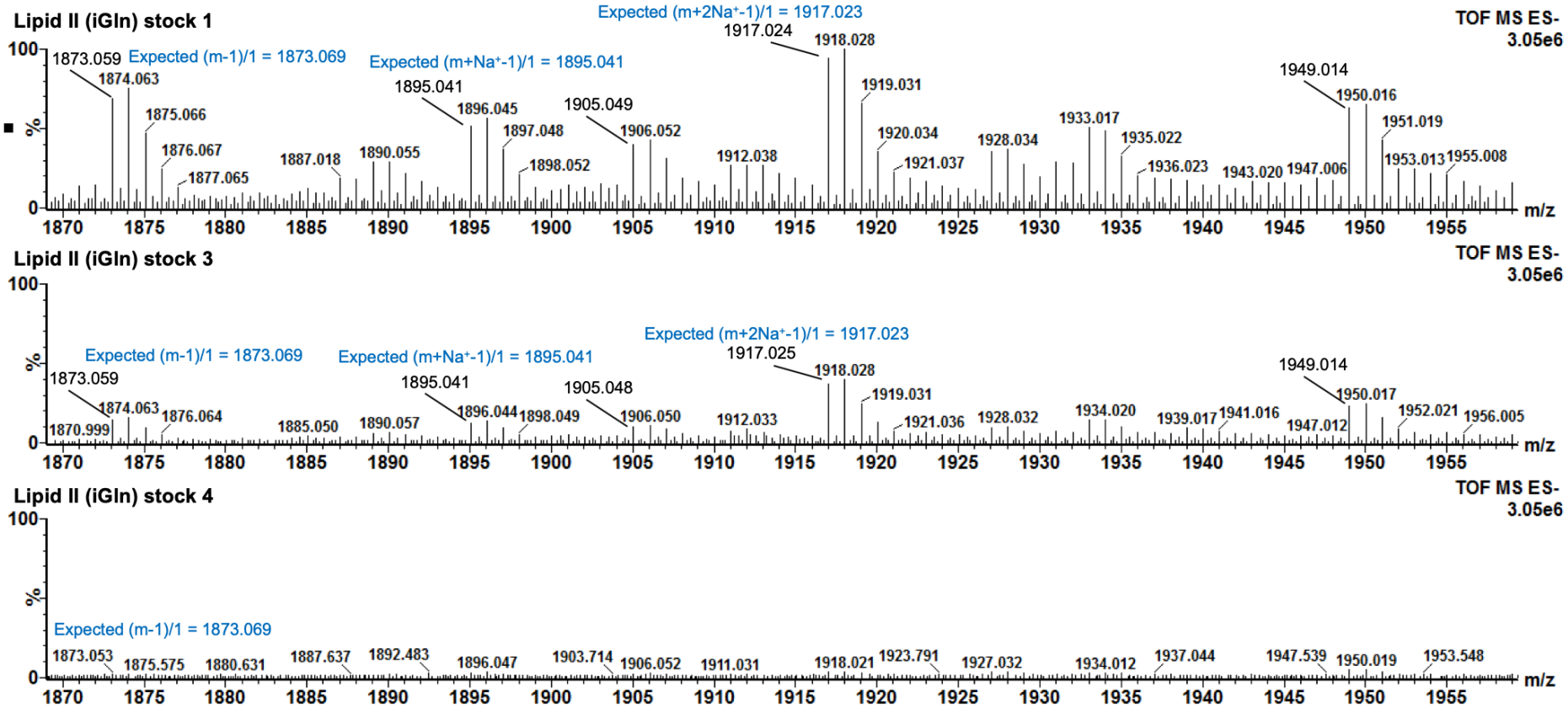

Appendix 4.6 Nanospray TOF mass spectra of Lipid II (iGln) stocks – singly charged spectra. Samples were analysed by negative ion nanospray TOF mass spectrometry. Singly charged spectra for each stock are shown. Data collected and analysed by A. Catherwood, and mass spectra generated using MassLynx software (Waters).

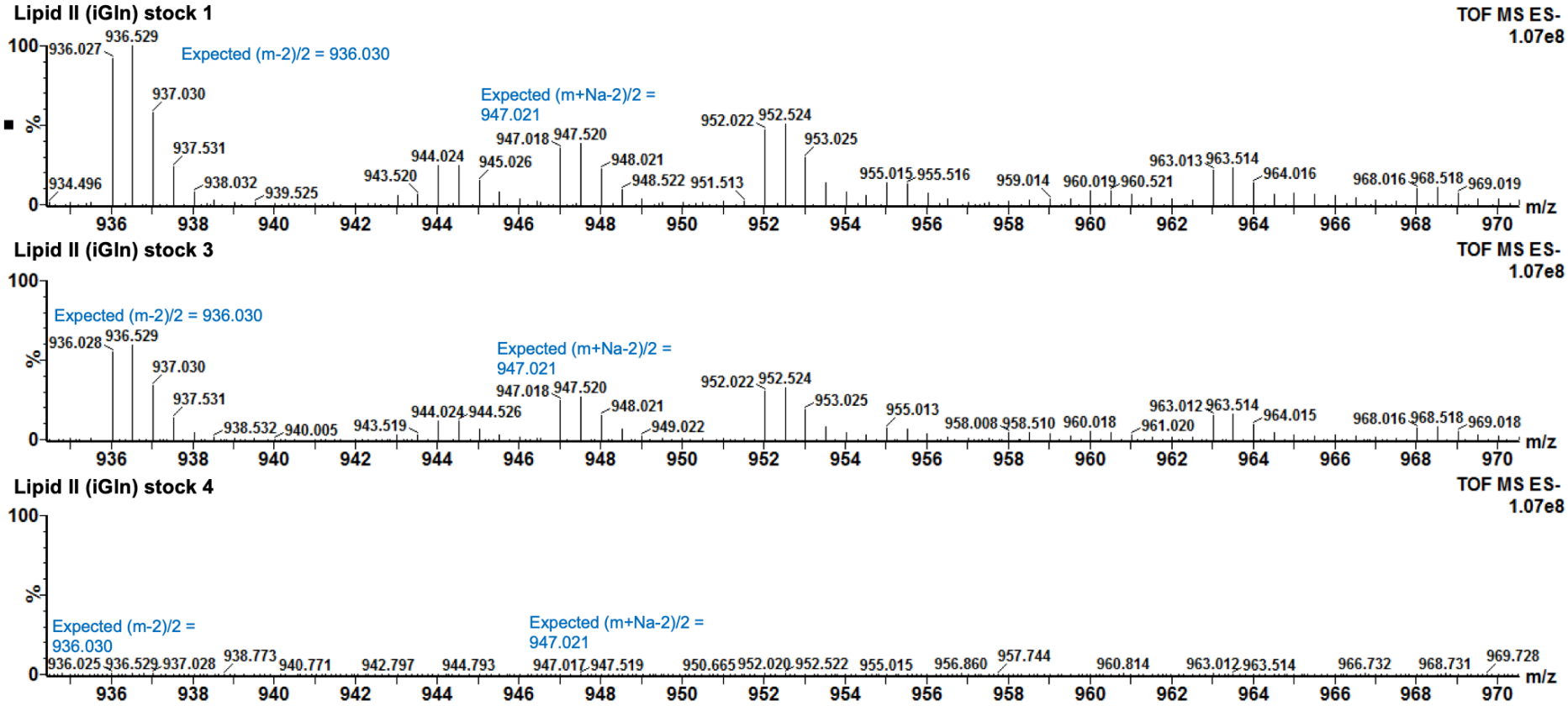

Appendix 4.7 Nanospray TOF mass spectra of Lipid II (iGln) stocks – doubly charged spectra. Samples were analysed by negative ion nanospray TOF mass spectrometry. Doubly charged spectra for each stock are shown. Data collected and analysed by A. Catherwood, and mass spectra generated using MassLynx software (Waters).

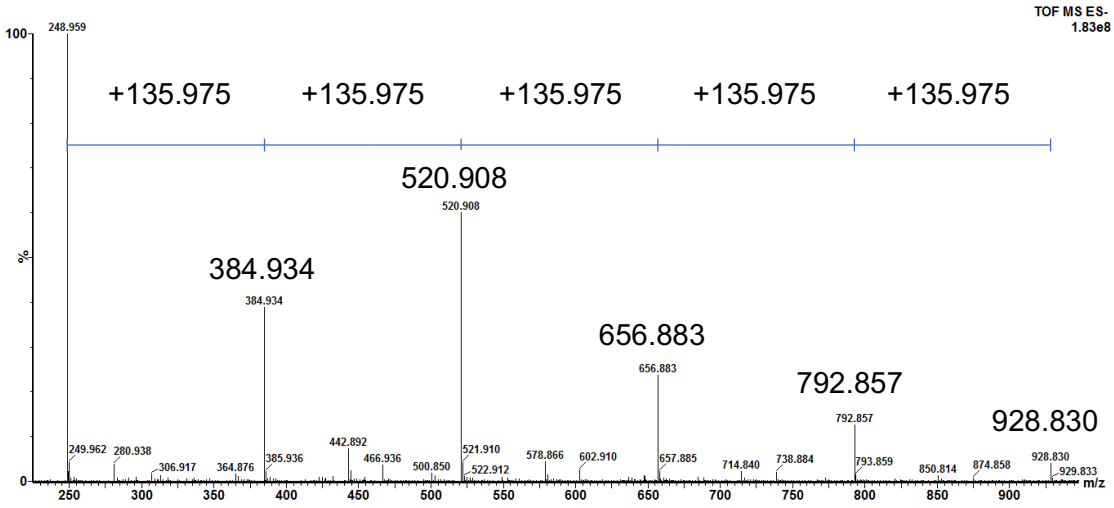

Appendix 4.8 Nanospray TOF mass spectrum of Lipid II (iGln) stock 3, illustrating polymeric contaminant. Sample was analysed by negative ion nanospray TOF mass spectrometry. Data collected and analysed by A. Catherwood, and mass spectra generated using MassLynx software (Waters).

Appendix 4.9: Mass spectrometry analysis of mutanolysin-digested TP products from donor-only and acceptor-only substrates

Mass spectrometry was used to detect transpeptidation products formed by PBP1a^{D39} in reactions using donor-only and acceptor-only substrates. Transpeptidase reactions were digested using mutanolysin and analysed by liquid chromatography-mass spectrometry (LC-MS).

a) Full mass spectrum from chromatogram peak of interest

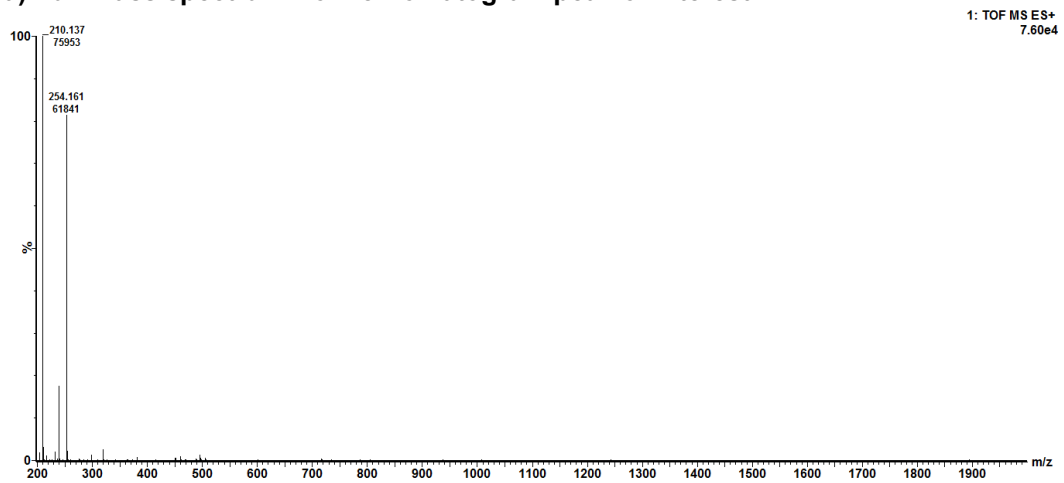

b) Lipid II (iGln, acLys) CP product, TP359

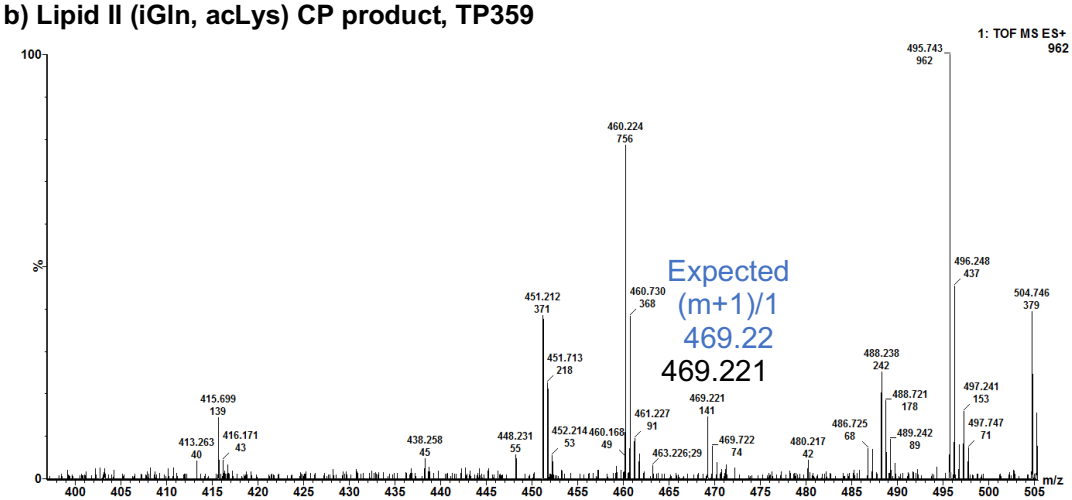

Appendix 4.9 LC-MS analysis of TP reactions with PBP1a^{D39} and donor-only and acceptor-only substrates. The total ion chromatogram for a reaction containing acceptor-only (Mur*N*Ac 5P (iGln)) and donor-only (Lipid II (iGln, ε-*N*-acetyl-Lys)) substrates was queried for mass to charge ratios corresponding to the doubly charged ions of putative transpeptidase and carboxypeptidase **(CP)** products, generating mass spectra for peaks containing those ions **(a)**. Only ions corresponding to the CP product of Lipid II (iGln, acLys) were identified **(b)**. Data collected by A.J. Lloyd and mass spectra generated using MassLynx software (Waters).

Appendix 4.10 – 4.11: Glycan polymer assembly under the conditions of the TP assay plus DMSO

Whilst GT activity of PBP1a^{D39} had been demonstrated *in vitro* using both continuous fluorescence and SDS-PAGE assays, no TP activity by this enzyme was observed using the D-Ala release assay. We questioned whether this was the consequence of lack of GT activity under the conditions of the D-Ala release assay. Glycan polymer assembly under the conditions of the D-Ala release assay (50 mM HEPES, 10 mM $MgCl_2$, 0.0116 % (w/v) E_6C_{12}; PBP1a^{D39} and Lipid II substrate as required) plus 25 % (v/v) DMSO was therefore analysed by Tris-Tricine SDS-PAGE. DMSO appeared to be required for glycan chain assembly using Lipid II (iGln, Dans). Transpeptidase assays were then conducted with donor substrate consisting of either Lipid II (iGln, Dans) or Lipid II (iGln, ε-*N*-acetyl-L-Lys), in the presence and absence

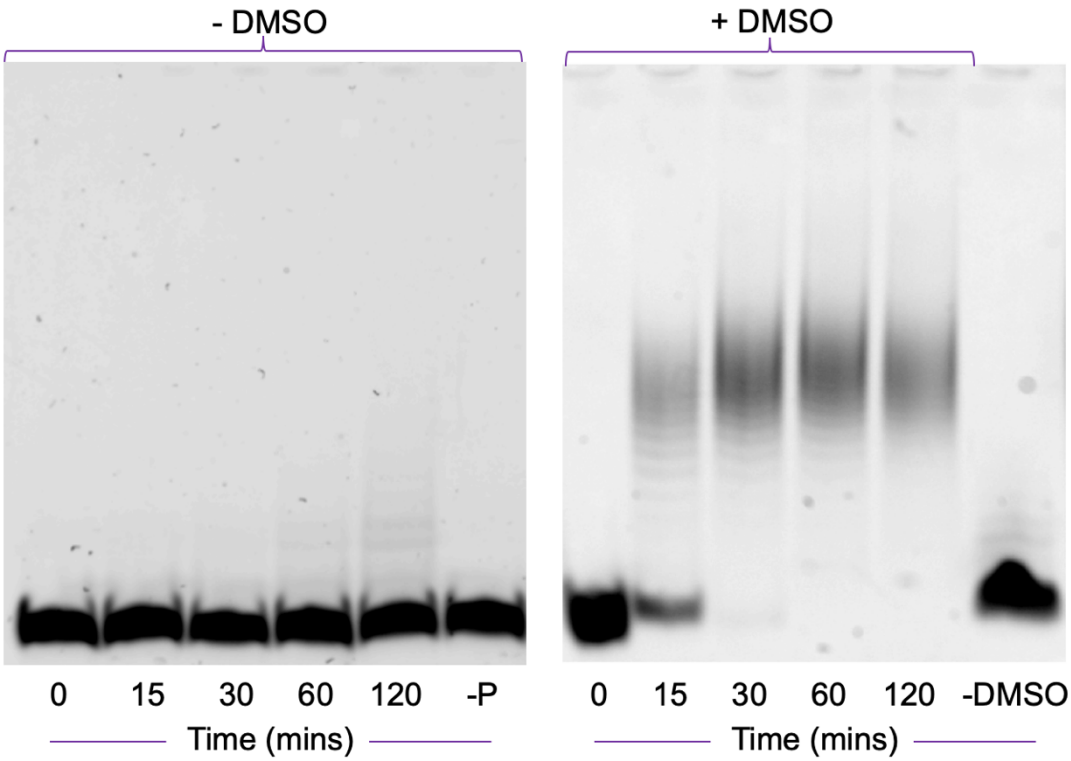

Appendix 4.10 Glycan polymer assembly under conditions for the TP assay, with and without DMSO. Reactions comprised 50 mM HEPES, 10 mM $MgCl_2$, ± 25 % (v/v) DMSO, 0.0116 % (w/v) E_6C_{12}, 2 μM PBP1a^{D39} and 20 μM Lipid II (Gln, Dans). Samples were taken at the stated timepoints and the reactions quenched with 0.3 mM moenomycin and 50 mM EDTA. Samples were analysed by electrophoresis on a 9 % Tris-Tricine gel, which was subsequently visualised using an ImageQuant LAS 4000 imager with transmitted light at 312 nm and a 605 nm filter. **mins**, minutes; **-DMSO control**, reaction without DMSO, incubated for 120 mins; -P; reaction without protein, incubated for 120 mins.

of DMSO. This allowed analysis of the need for DMSO for transpeptidation; and also for transpeptidase activity to be analysed under conditions known to support glycan chain formation.

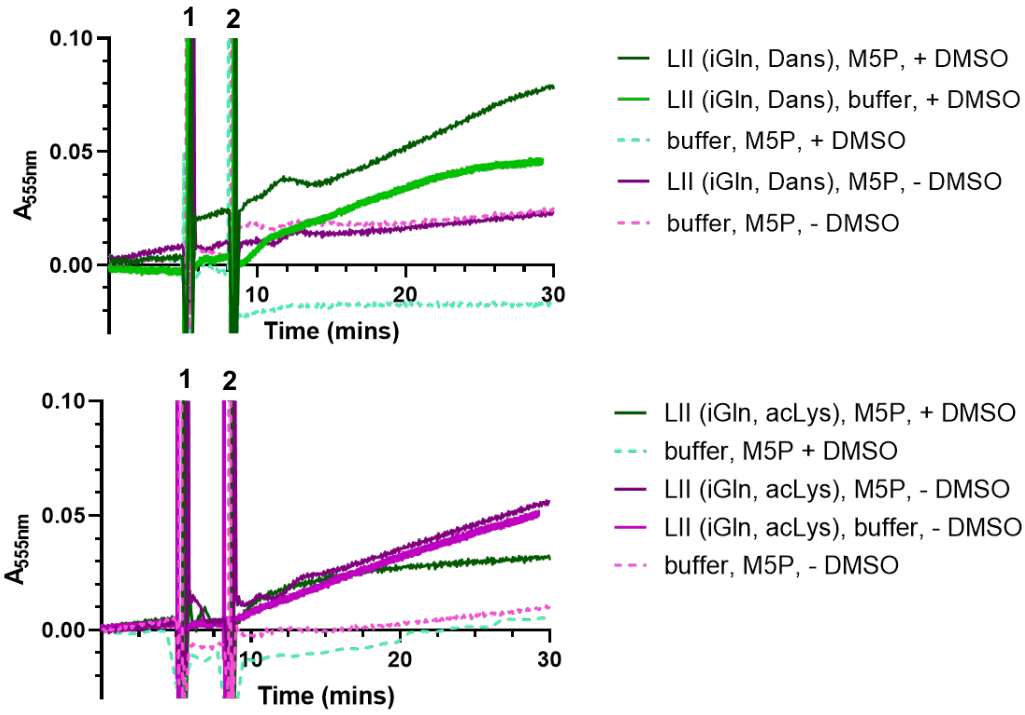

Appendix 4.11 Transpeptidase activity of PBP1a^{D39} ± DMSO. D-Ala release catalyzed by PBP1a^{D39} was followed in the presence and absence of 25 % (v/v) DMSO, and using either Lipid II (iGln, Dans) or Lipid II (iGln, ε-*N*-acetyl-L-Lys) as a donor substrate. Reaction mixes comprised 50 mM HEPES pH 7.6, 10 mM $MgCl_2$, 2 μM PBP1a^{D39}, 20 μM Lipid II (iGln, acetyl-Lys or Dans), 20 μM Mur*N*Ac 5P (iGln), 33.51 mM.min^{-1} *R. gracalis* D-amino acid oxidase, 14.82 mM.min^{-1} horseradish peroxidase, 50 μM Amplex Red and 3 X CMC (0.0116 % (w/v)) of E_6C_{12}. Reactions are labelled in the order of addition of the substrates (or buffer). **mins,** minutes; **LII**, Lipid II; **M5P**, Mur*N*Ac 5P (iGln); **1**, addition of substrate 1; **2**, addition of substrate 2.

Appendix 4.12: Mass spectrometry analysis of mutanolysin-digested TP products from reactions followed by SDS-PAGE

Mass spectrometry was used to detect transpeptidation products formed by PBP1a^{D39} in reactions using Lipid II (iGln, Dans) and Lipid II (iGln, tripeptide). Transpeptidase reactions were digested using mutanolysin and analysed by liquid chromatography-mass spectrometry (LC-MS).

(next page) Appendix 4.12 LC-MS analysis of TP reactions with Lipid II (iGln, Dans) and Lipid II (iGln, 3P) Reactions were digested using mutanolysin and analysed by liquid chromatography-mass spectrometry (LC-MS) by positive ion electrospray time of flight mass spectrometry, to detect ions corresponding to putative TP product. Data are representative of two samples.. **m/z**, mass to charge ratio; **amp**, reaction performed in the presence of 2 uM ampicillin. Data collected by A.J. Lloyd and mass spectra generated using MassLynx software (Waters).

b) PBP1a^{Pn16} only

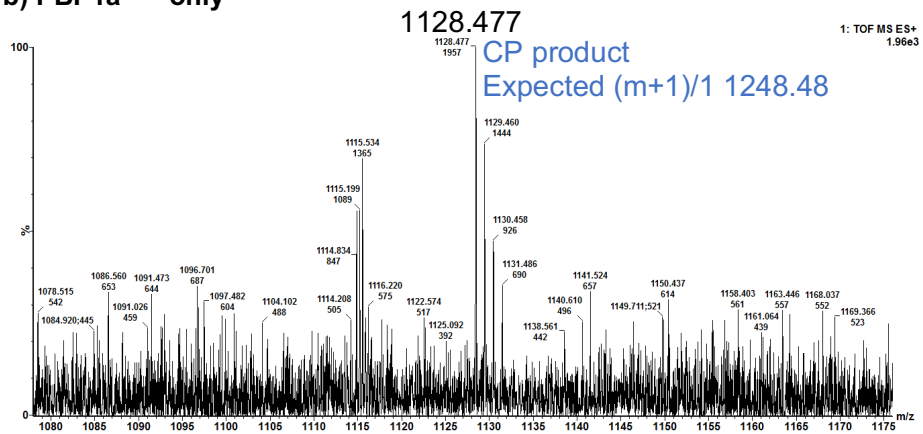

b) PBP1a^{159} only

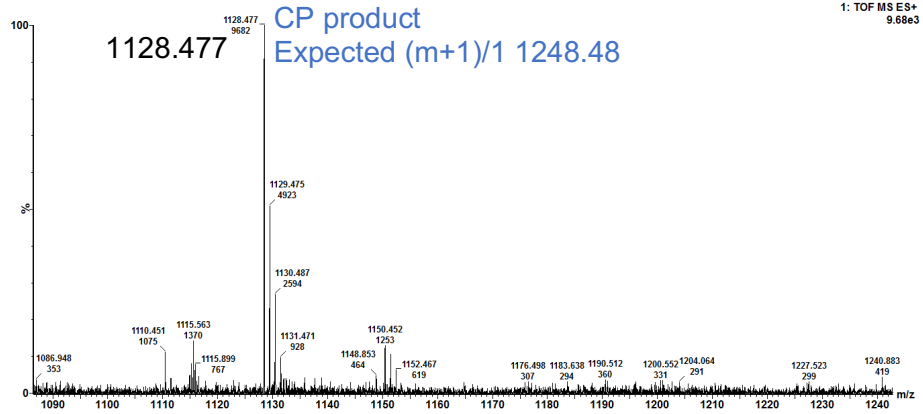

c) PBP1a^{159} amp

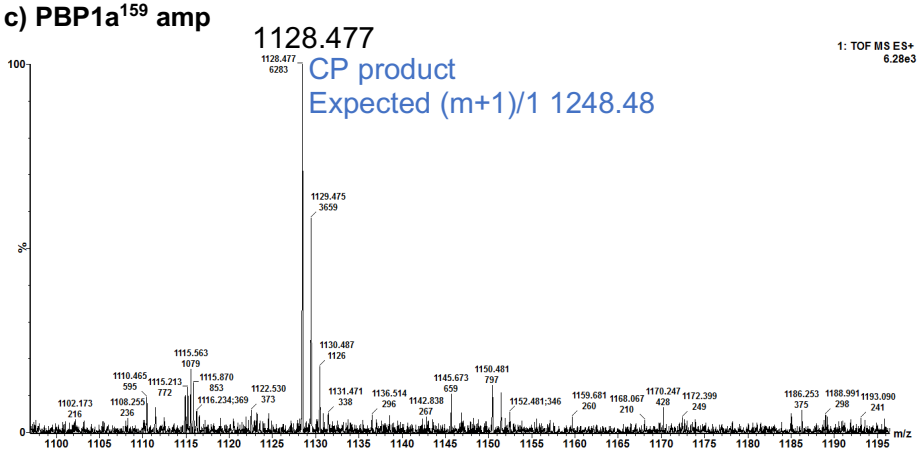

Appendices to Chapter 5

Appendix 5.1: CMC of detergents used in biochemical assays

In development of the GT assay for PBP1a^{D39}, a variety of detergents were tested for optimum activity, at a defined multiple of their critical micellar concentration (CMC). The values used for these experiments are given in Appendix 5.1.

Appendix 5.1: CMC of detergents used in biochemical assays.

Detergent	(CMC) % (w/v)	Source
TX-100 *(Triton X-100)*	0.010 - 0.015	le Maire *et al.* (2000)
CHAPS *(3-((3-cholamidopropyl) dimethylammonio)-1-propanesulfonate)*	0.49	Hjelmeland *et al.* (1983)
DDM *(n-dodecyl-β-D-maltoside)*	0.0087	VanAken *et al.* (1986)
E_4C_{12} *(Tetraethylene glycol monododecyl ether)*	0.0026	Pons *et al.* (2010)
E_5C_8 *(Pentaethylene glycol monooctylether)*	0.25	Anatrace catalogue no. P350
E_5C_{10} *(Pentaethylene glycol monodecylether)*	0.031	Anatrace catalogue no. P340
E_6C_{12} *(Hexaethylene glycol monododecylether)*	0.0044	Carroll *et al.* (1982)
E_8C_{10} *(Octaethylene glycol monodecylether)*	0.0048*	Approximate based on CMC of E_8C_{12}
E_8C_{12} *(Octaethylene glycol monododecylether)*	0.0048	le Maire *et al.* (1983); le Maire *et al.* (2000)

Appendix 5.2: Amino acid sequence alignment over GT domain of PBP1a^{D39}, PBP1a^{Pn16} and PBP1a^{159}.

To support comparison of the activity of PBP1a variants from different pneumococcal strains, the amino acid sequence over the N terminal protein of the proteins of interest was aligned to analyse the sequence identity. This analysis revealed 100 % sequence identity over the GT domains of PBP1a^{D39}, PBP1a^{Pn16} and PBP1a^{159}.

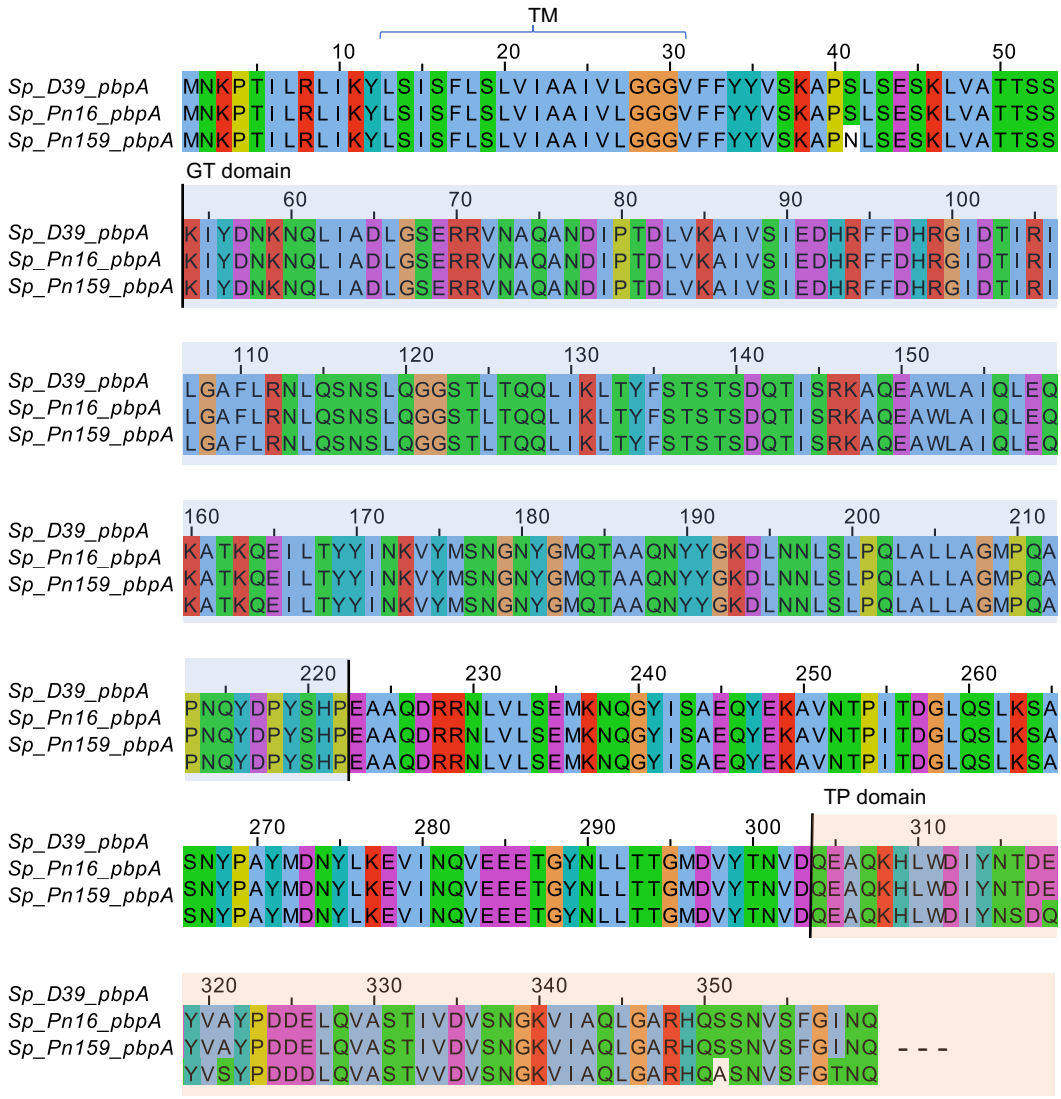

Appendix 5.2 Amino acid sequence comparison of the glycosyltransferase domains of the PBP1a variants used in this project. The three proteins show 100 % sequence identity over the glycosyltransferase (**GT**) domain. Sequences were aligned using Clustal Omega. The GT domain is highlighted in blue, and the N-terminal portion of the transpeptidase (**TP**) domain in orange. The transmembrane (**TM**) segment is also highlighted.

Bibliography for Appendices

Carroll, B., O'ROURKE, B., & Ward, A. (1982). The kinetics of solubilization of single component non-polar oils by a non-ionic surfactant. *Journal of Pharmacy and Pharmacology, 34*(5), 287-292.

Hjelmeland, L. M., Nebert, D. W., & Osborne Jr, J. C. (1983). Sulfobetaine derivatives of bile acids: Nondenaturing surfactants for membrane biochemistry. *Anal Biochem, 130*(1), 72-82.

le Maire, M., Champeil, P., & MÖller, J. V. (2000). Interaction of membrane proteins and lipids with solubilizing detergents. *Biochimica et Biophysica Acta (BBA)-Biomembranes, 1508*(1), 86-111.

le Maire, M., Kwee, S., Andersen, J. P., & Møller, J. V. (1983). Mode of interaction of polyoxyethyleneglycol detergents with membrane proteins. *European Journal of Biochemistry, 129*(3), 525-532.

Pons, R., Valiente, M., & Montalvo, G. (2010). Structure of Aggregates in Diluted Aqueous Octyl Glucoside/Tetraethylene Glycol Monododecyl Ether Mixtures with Different Alkanols. *Langmuir, 26*(4), 2256-2262.

VanAken, T., Foxall-VanAken, S., Castleman, S., & Ferguson-Miller, S. (1986). Alkyl glycoside detergents: Synthesis and applications to the study of membrane proteins. In *Methods in enzymology* (Vol. 125, pp. 27-35): Elsevier.